frontiers | Research Topics

Role of non-coding RNAs, metabolites and extracellular vesicles in disease regulation and health

Edited by
Olanrewaju B. Morenikeji, Naseer A. Kutchy and Nadeem Shabir

Published in
Frontiers in Genetics

ISSN 1664-8714
ISBN 978-2-8325-2801-3
DOI 10.3389/978-2-8325-2801-3

About Frontiers

Frontiers is more than just an open access publisher of scholarly articles: it is a pioneering approach to the world of academia, radically improving the way scholarly research is managed. The grand vision of Frontiers is a world where all people have an equal opportunity to seek, share and generate knowledge. Frontiers provides immediate and permanent online open access to all its publications, but this alone is not enough to realize our grand goals.

Frontiers journal series

The Frontiers journal series is a multi-tier and interdisciplinary set of open-access, online journals, promising a paradigm shift from the current review, selection and dissemination processes in academic publishing. All Frontiers journals are driven by researchers for researchers; therefore, they constitute a service to the scholarly community. At the same time, the *Frontiers journal series* operates on a revolutionary invention, the tiered publishing system, initially addressing specific communities of scholars, and gradually climbing up to broader public understanding, thus serving the interests of the lay society, too.

Dedication to quality

Each Frontiers article is a landmark of the highest quality, thanks to genuinely collaborative interactions between authors and review editors, who include some of the world's best academicians. Research must be certified by peers before entering a stream of knowledge that may eventually reach the public - and shape society; therefore, Frontiers only applies the most rigorous and unbiased reviews. Frontiers revolutionizes research publishing by freely delivering the most outstanding research, evaluated with no bias from both the academic and social point of view. By applying the most advanced information technologies, Frontiers is catapulting scholarly publishing into a new generation.

What are Frontiers Research Topics?

Frontiers Research Topics are very popular trademarks of the *Frontiers journals series*: they are collections of at least ten articles, all centered on a particular subject. With their unique mix of varied contributions from Original Research to Review Articles, Frontiers Research Topics unify the most influential researchers, the latest key findings and historical advances in a hot research area.

Find out more on how to host your own Frontiers Research Topic or contribute to one as an author by contacting the Frontiers editorial office: frontiersin.org/about/contact

Role of non-coding RNAs, metabolites and extracellular vesicles in disease regulation and health

Topic editors

Olanrewaju B. Morenikeji — University of Pittsburgh at Bradford, United States
Naseer A. Kutchy — The State University of New Jersey, United States
Nadeem Shabir — Sher-e-Kashmir University of Agricultural Sciences and Technology, India

Citation

Morenikeji, O. B., Kutchy, N. A., Shabir, N., eds. (2023). *Role of non-coding RNAs, metabolites and extracellular vesicles in disease regulation and health*. Lausanne: Frontiers Media SA. doi: 10.3389/978-2-8325-2801-3

Table of contents

frontiers | Frontiers in Genetics

TYPE Editorial
PUBLISHED 09 June 2023
DOI 10.3389/fgene.2023.1206569

OPEN ACCESS

EDITED BY
William C. Cho,
QEH, Hong Kong SAR, China

REVIEWED BY
Xavier Lucas,
Monte Rosa Therapeutics, Switzerland

*CORRESPONDENCE
Olanrewaju B. Morenikeji,
obm3@pitt.edu

RECEIVED 16 April 2023
ACCEPTED 01 June 2023
PUBLISHED 09 June 2023

CITATION
Morenikeji OB and Kutchy NA (2023), Editorial: Role of non-coding RNAs, metabolites, and extracellular vesicles in disease regulation and health.
Front. Genet. 14:1206569.
doi: 10.3389/fgene.2023.1206569

Editorial: Role of non-coding RNAs, metabolites, and extracellular vesicles in disease regulation and health

Olanrewaju B. Morenikeji[1]* and Naseer A. Kutchy[2]

[1]Division of Biological and Health Sciences, University of Pittsburgh at Bradford, Bradford, PA, United States, [2]Department of Animal Sciences, Rutgers, The State University of New Jersey, New Brunswick, NJ, United States

KEYWORDS

non-coding RNAs, extracellular vesicles, disease, gene regulation, health

Editorial on the Research Topic
Role of non-coding RNAs, metabolites, and extracellular vesicles in disease regulation and health

Non-coding ribonucleic acids (small or large ncRNAs) are involved in epigenetic regulations and could mediate pre- or post-transcriptional gene silencing. These molecules are opening new avenues for therapeutic purposes with putative consequences for immunity. Similarly, emerging studies have demonstrated that extracellular vesicles (EVs) are involved in many immune response dysregulations and diseases. EVs, such as apoptotic bodies, exosomes, and microvesicles, are membrane-bound vesicles ranging in size from 30 to 1,000 nm in diameter. During pathological conditions, the number, size, and content of EVs are found to be altered and have been shown to play crucial roles in disease progression. Likewise, bacteria or a host can produce EVs containing ncRNAs that can mediate intercellular communication with epithelial and immune cells, potentially regulating the expression of genes involved in resistance to pathologies.

This Research Topic brought together various articles, including primary research articles, reviews, methods, and systematic reviews, that focus on elucidating the role of ncRNAs and EVs in molecular immunotherapy and cross talk with genetic or epigenetic mechanisms in controlling cellular function in disease biology as potential therapeutic tools.

Nie et al. discussed the lack of early diagnosis of hepatocellular carcinoma (HCC), which results in poor prognosis for patients. The authors mentioned that early HCC diagnosis currently depends on the level of serum alpha-fetoprotein (AFP) and imaging technologies which are not optimal. Through meta-analysis, Nie et al. identified key circular RNAs in exosomes for screening and diagnosing HCC. According to the authors, HCC is rated the fourth highest cause of death worldwide but lacks accurate biomarkers for early detection. The authors emphasized the role of the unique expression of circular RNAs in HCC including circ_0000798, circSATD3, hsa_circ_0007750, and cMTO1 in suppressing HCC progression with their possible use in diagnosis or treatment.

Yousuf et al. used a panel of three miRNAs (miR-221, miR-222, and Let-7a) to detect HCC in the early stage. The authors reported a correlation between the expression of the three miRNAs and AFP in the serum and tissues, indicating promises for early diagnosis of HCC. Therefore, they proposed the use of these miRNAs in combination with AFP as

biomarkers for early diagnosis of HCC and on a large cohort of HCC patients. Lu et al.'s study is similar to that of Yousuf et al. because it identified the use of miRNAs for the diagnosis and prognosis of HCC. However, the fundamental difference was that Lu et al.'s study was based on a meta-analysis. The authors cataloged different studies from PubMed, Embase, and Wan Fang databases and identified the miR-17–92 cluster in context of diagnosis and prognosis of HCC. Lu et al. determined the sensitivity, specificity, and diagnostic odds ratio (DOR) on the miR-17–92 cluster for disease diagnosis. They found that the sensitivity of the diagnosis of HCC using the miR-17–92 cluster was 0.75 [at 95% confidence interval (CI)], with a specificity of 0.73 at 95% CI and a DOR of 7.87. Based on their results, Lu et al. finally suggested that the miR-17–92 cluster could be used as a diagnostic and prognostic biomarker for HCC.

A mini-review by Ruiz-Manriquez et al. discussed miRNA-mediated regulation in key signaling pathways during hepatocellular carcinoma development. The authors emphasized that microRNAs are directly or indirectly involved in cellular signaling, and manipulating those miRNAs can potentially affect key signaling pathways resulting in carcinogenesis. In addition, Ruiz-Manriquez et al. suggested that miRNA-media/ted PI3K/Akt/mTOR, Hippo-YAP/TAZ, and Wnt/β-catenin signaling pathways could lead to HCC development. This perspective could help for a better understanding of diagnosis and management of HCC.

Knowing that long non-coding RNAs (lncRNAs) could act as epigenetic regulators in diverse cellular processes including ferroptosis and iron metabolism, Hong-Bin et al. used RNA sequencing analysis and clinical information to decipher an iron metabolic-related lncRNA signature that could be used to determine osteosarcoma (OS) survival and the immune landscape. The authors identified a total of 302 iron metabolism-related lncRNAs including lncRNA GAS5, UNC5B-AS1, PARD6G-AS1, and LINC01060 that are capable of regulating cell proliferation, migration, and invasion during osteosarcoma. The authors concluded that iron metabolism-related lncRNA signatures had good performance in predicting survival outcomes and the immune landscape for OS patients.

Zhao et al. showed the importance of 11 autophagy-related lncRNAs for esophageal squamous cell carcinoma (ESCC). They analyzed the immune function and tumor mutational burden between two groups with varying sensitivity to chemotherapy and immunotherapy. Overall, Zhao et al. reported the signature expression of some lncRNAs, including AL078604.2, BDNF-AS, HAND2-AS1, and ZEB1-AS1, among others, to be co-expressed with autophagy genes. Importantly, the authors provided an lncRNA risk model that could be used as a tool for the prognosis and treatment of patients with ESCC.

As described by Peeples et al., neonatal hypoxic–ischemic brain injury (HIBI) is reported to present varying phenotypes, posing difficult diagnosis and increased morbidity and mortality despite available therapy. This calls for an alternative novel therapy to safeguard the life of infants. Peeples et al. elucidated the role of miRNAs in gene regulation during HIBI as a promising therapeutic target for miRNA-based therapy. Overall, they found 61 unique miRNAs being differentially expressed in various regions of the brain including miR-410-5p, -1264-3p, 1298-5p, -5,126, and -34b-3p. These miRNAs targeted pathways associated with inflammation, metabolism, and cell death.

Zhang et al. highlighted the importance of miRNAs in coronary artery disease (CAD) from microarray datasets using various bioinformatics tools. The authors defined CAD as a cardiovascular disease associated with low-density lipoprotein cholesterol and categorized it as a major source of death worldwide. They also observed a correlation between miRNA expression pattern and CAD, although the role of many of the miRNAs in CAD is still unclear. Zhang et al. reported that miR-22-3p interacted with eight transcription factors in the cardiovascular system and suggested it as a better predictor for CAD, making it a potential biomarker for disease diagnosis.

It is noteworthy that host ncRNAs also play a significant role in modulating viral replication during host–pathogen interactomes. Morenikeji et al. identified important miRNAs that could target RNA-dependent RNA polymerase (RdRp), an enzyme necessary for coronavirus replication inside the host. Due to frequent mutations in coronavirus, several disease control measures, such as vaccines and antiviral drugs, are less effective in completely controlling viral replication. Since the RdRp is conserved among coronavirus variants, the authors found it to be an important target for miRNAs in controlling virus replication. Ultimately, the authors reported the ability of hsa-miR-1283, hsa-miR-579-3p, and hsa-miR-664b-3p to block virus replication through binding to their RdRp target and noted their potential use as a broad-spectrum antiviral.

Li et al. shed light on the role of melatonin and its interactions with ncRNAs in regulating osteoarthritis (OA). OA is a slowly progressive and irreversible disease of joints and lacks early treatments. Therefore, the authors gathered substantial knowledge about the melatonin-mediated modulation of ncRNAs in the early stage of OA. In addition, the authors proposed that the interaction between ncRNAs and target genes constitutes a complex network of OA regulation. In conclusion, they suggested that a combination of ncRNAs or their regulators with melatonin may be a new approach for the treatment of OA in the future.

A review by Liu et al. examined the role of circRNA E3 ubiquitin–protein ligase (circRNA ITCH) in clinical applications during tumor and non-tumor diseases. circRNA is a closed-loop RNA capable of up- or down-regulating gene expression at different levels. They have been implicated in cellular processes, including inhibiting cell proliferation, migration, and invasion and promoting apoptosis. Due to their molecular function and other involvement in biological processes, circ-ITCH could be used as a marker to monitor disease progression.

The uterine environment is important for a successful pregnancy, especially during the peri-implantation stage. Hitit et al. highlighted the role of miRNAs during embryo implantation. They also provided an understanding of circulating miRNA in maternal plasma as a biomarker for early detection of pregnancy in sheep. They found that 22 miRNA expression patterns were associated with the estrous cycle and early pregnancy, of which two were oar-miR-218a- and oar-miR-1185-3p-targeted genes related to embryonic morphogenesis and developmental process. The authors concluded that circulating miRNAs from plasma hold a promise for early detection of pregnancy in sheep.

Body fluids carrying small extracellular vesicles (sEVs) have been isolated from blood, pleural fluids, saliva, and urine as biomarkers. These sEVs could be carrying cargoes with exosomal miRNAs (exomiRs), which have been found responsible for cancer pathogenesis. Some exomiR expressions could indicate cancer progression, cancer growth, and drug response/resistance. Furthermore, Alotabi described the use of exomiRs as biomarkers for cancer diagnosis, treatment response, metastasis, and promotion of T cell anti-tumor immunity via activation of immune checkpoint molecules. The author pinpointed how exomiRs could better regulate the expression of immune checkpoint molecules, leading to activation of T cell anti-tumor immunity. Alotabi reviewed multiple literature records to underscore the importance of sEVs, especially in patients with immune rejection.

The article by Luo et al. also discussed the role of sEVs carrying ncRNA cargoes and summarized their impact on kidney diseases. The authors found that sEVs could be produced by all cell types in the kidney, including neighboring cells like renal tubular epithelial cells, podocytes, collecting duct cells, and leap cells. These sEVs could then be loaded with aberrant ncRNAs that could be responsible for many kidney diseases. Luo et al. concluded that the sEV-ncRNAs could play a fundamental role in the early detection and prognosis of kidney diseases.

Singh et al. identified estrus biomarkers through biofluid, such as saliva, using proteomic profiling of buffaloes in different stages of the estrus cycle. They used both label-free quantitation (LFQ) and labeled (TMT) quantitation and mass spectrometry analysis. The authors reported an over-expression of proteins such as SERPINB1, HSPA1A, VMO1, SDF4, LCN1, OBP, and ENO3 in buffalo saliva estrus, depicting a novel method for estrus detection. The markers were functionally classified to be over-represented in several ontologies, including glycolysis, pyruvate metabolism, endopeptidase inhibitor activity, salivary secretion, innate immune response, calcium–ion binding, oocyte meiosis, and estrogen signaling. Singh et al. concluded by generating an array panel of candidate proteins that may be considered buffalo estrus biomarkers, applied in the development of a diagnostic kit for estrus detection in buffaloes.

Finally, our editorial summarizes various articles on the role of non-coding ribonucleic acids and extracellular vesicles to understand epigenetic mechanisms that control cellular functions in different diseases. We believe that various findings in this research topic would be of much help in expanding the basic knowledge in disease studies and as potential therapeutic tools. We appreciate all contributors to this research article, including the authors, reviewers, and the editorial team, Frontiers in Genetics.

Author contributions

OM conceptualized the topic. OM and NK drafted and revised the editorial. All authors contributed to the article and approved the submitted version.

Conflict of interest

The authors declare that the research was conducted in the absence of any commercial or financial relationships that could be construed as a potential conflict of interest.

Publisher's note

frontiers in Genetics

SYSTEMATIC REVIEW
published: 21 December 2021
doi: 10.3389/fgene.2021.794105

Diagnostic Accuracy of Circular RNAs in Different Types of Samples for Detecting Hepatocellular Carcinoma: A Meta-Analysis

*Guilin Nie†, Dingzhong Peng†, Bei Li, Jiong Lu and Xianze Xiong**

Department of Biliary Surgery, West China Hospital of Sichuan University, Chengdu, China

The lack of accurate biomarkers impeded the screening, diagnosis and early treatment of hepatocellular carcinoma (HCC). As a result of the development of high-throughput transcriptome analysis techniques, circular RNAs, a newly discovered class of noncoding RNAs, were recognized as potential novel biomarkers. This meta-analysis was performed to update the diagnostic roles of circular RNAs for HCC. We acquired 23 articles from PubMed, Web of Science, EMBASE, and Cochrane Library databases up to September 2021. The overall sensitivity was 0.80 (95% CI: 0.77–0.84), and the specificity was 0.83 (95% CI: 0.79–0.85), with an AUC of 0.88 (0.85–0.91). Considering of the significant heterogeneity, studies were divided into four groups based on the control types. The circular RNAs in exosomes had a sensitivity of 0.69 (95% CI: 0.61–0.75), and a highest specificity of 0.91 (95% CI: 0.83–0.96). The pooled sensitivity of circular RNAs in serum/plasma was 0.84 (95% CI: 0.81–0.87), and the pooled specificity was 0.83 (95% CI: 0.79–0.86). The pooled sensitivity of circular RNAs distinguishing tumor tissue from chronic hepatitis/cirrhosis tissues was 0.56 (95% CI: 0.48–0.64), and specificity was 0.76 (95% CI: 0.67–0.82). When the controls were adjacent tissues, the sensitivity was 0.78 (95% CI: 0.70–0.84), and the specificity was 0.78 (95% CI: 0.71–0.85). Hsa_circ_0001445 with a pooled sensitivity of 0.81, a specificity of 0.76 and an AUC of 0.85 in two studies, might be a suitable diagnostic blood biomarker for HCC. Relying on function in HCC, the AUC of subgroups were 0.88 (95%CI: 0.84–0.90) (function group) and 0.87 (95%CI: 0.84–0.90) (unknown function group). As for only reported in HCC or not, these circular RNAs had an AUC of 0.89 (95%CI: 0.86–0.91) (only in HCC) and 0.85 (95%CI: 0.82–0.88) (not only in HCC). In conclusion, the results suggested that circular RNAs were acceptable biomarkers for detecting HCC, especially those circular RNAs existing in exosomes or serum/plasma.

Keywords: circular RNAs, exosome, serum/plasma, hepatocellular carcinoma, diagnosis, meta-analysis

OPEN ACCESS

Edited by:
Naseer Ahmad Kutchy, St. George's University, Grenada

Reviewed by:
Nicola Mosca, Fondazione Policlinico Universitario A. Gemelli IRCCS, Italy
Waseem Lone, University of Nebraska Medical Center, United States

****Correspondence:***
Xianze Xiong
xiongxianze163@163.com

†These authors have contributed equally to this work and share first authorship

Specialty section:
This article was submitted to RNA, a section of the journal Frontiers in Genetics

Received: *13 October 2021*
Accepted: *30 November 2021*
Published: *21 December 2021*

Citation:
Nie G, Peng D, Li B, Lu J and Xiong X (2021) Diagnostic Accuracy of Circular RNAs in Different Types of Samples for Detecting Hepatocellular Carcinoma: A Meta-Analysis. Front. Genet. 12:794105. doi: 10.3389/fgene.2021.794105

1 INTRODUCTION

Hepatocellular carcinoma (HCC) is the fourth leading cause of cancer-related death worldwide. In 2020, 905,677 new cases and 830,180 deaths from HCC were reported, which accounted for 75–85% of cases of primary liver cancer (Sung et al., 2021). Furthermore, it is the fourth most common malignancy and the second leading cause of tumor-related death in China (Chen et al., 2016). According to the

recommendation of guidelines (European Association for the Study of the Liver, 2018; Marrero et al., 2018), HCC will be treated more efficaciously if it is diagnosed early. Aside from alpha-fetoprotein (AFP), a biomarker whose sensitivity and specificity for detecting HCC ranges from 39 to 64% and 76–91% (Oka et al., 1994; Okuda et al., 2000; Marrero and Lok, 2004), and complex ultrasound, respectively, a class of more sensitive and specific diagnostic markers of HCC are urged to improve the accuracy of early diagnosis.

Endogenous circular RNAs are characterized by covalently closed-loop noncoding RNAs (Jeck et al., 2013), giving the circular RNAs higher stability than their linear counterparts, which prevents exonuclease-mediated degradation (Jeck et al., 2013). Circular RNAs are expressed widely in all human tissues, but their functions may be specific to cells and tissues (Salzman et al., 2013). Since the recent discovery of circular RNAs, interest in their clinical characteristics and pathologic mechanisms (especially in solid tumors) has increased. Despite their widespread existence, only a minor fraction of circular RNAs possessing biological functions has been identified. Nevertheless, this limitation cannot prevent circular RNAs from becoming efficacious therapeutic targets for tumors. Most circular RNAs reportedly act as microRNA (miRNA) "sponges" (Hansen et al., 2013), whereas others interact with proteins to regulate the function of proteins (Li Z. et al., 2015), change the stability of mRNAs (Chen et al., 2019), or to code proteins (Zhang M. et al., 2018).

Moreover, the stability and wide existence of circular RNAs in tissues and blood suggest that they may be effective diagnostic biomarkers of HCC (Shen et al., 2021). Recent studies have found their existence not only in tumor and blood, but also in exosomes, saliva, urine and bile (Li Y. et al., 2015; Bahn et al., 2015; Kölling et al., 2019; Wen et al., 2020; Xu et al., 2021), making them ideal noninvasive biopsy biomarker candidates. Exosome-derived circular RNAs (Wang et al., 2019) or multi-circular RNAs diagnostic models (Yu et al., 2020) have been created to improve the diagnostic accuracy of circular RNAs. Also, a sensitive, selective, and stable integrated electrochemical point-of-care (POCT) platform for detection of circular RNAs has been invented to achieve the rapid screening and detection of HCC (Zhang et al., 2021). The development and application of new detection technologies of circular RNAs provides a bright future in circular RNAs field. We undertook a meta-analysis to summarize the latest advances of diagnostic values and characteristics of circular RNAs in HCC and process a deeper exploration centered on the roles of circular RNAs in blood and exosomes, and different diagnostic values from different tissues (cirrhosis, hepatitis, and adjacent tumor tissues). Meanwhile, the problem if it would be different in diagnostic accuracy of functional circular RNAs or not and special-expression circular RNAs in HCC or not were involved in our analysis.

2 METHODS

2.1 Search Strategy

Two investigators (Dingzhong Peng and Bei Li) searched relevant studies in PubMed, Web of Science, Cochrane Library, and EMBASE up to September 2, 2021, following the Preferred Reporting Items for Systematic reviews and Meta-Analyses (PRISMA) (Page et al., 2021) protocols. We used the following keywords: "circRNA or circular RNA" and "liver cancer or liver carcinoma or hepatocellular carcinoma or HCC". We also searched the reference lists of selected articles or contacted the authors to obtain more details.

2.2 Criteria for Study Selection

The inclusion criteria were: 1) the study explored the relationship between circular RNAs and HCC; 2) the diagnosis of HCC was made on the basis of histopathology; 3) detection method for ncRNA profiling was clearly defined in the article; 4) case–control study or cohort study; 5) the study contained adequate information so that the prevalence of true-positives (TPs), true-negatives (TNs), false-positives (FPs), and false-negatives (FNs) could be calculated for the diagnosis.

The exclusion criteria were: 1) letters, case reports, meta-analysis, review articles, or animal studies; 2) studies not relevant to circular RNAs or HCC; 3) unavailable/incomplete data or missing researchers; 4) the studies written in a language other than English.

2.3 Extraction and Quality Assessment of Data

Two investigators extracted relevant data for analyses independently. The information extracted was: 1) first author; 2) publication year; 3) type of cancer and circular RNAs; 4) type and size of specimen; 5) assay method for circular RNAs; 6) cutoff value of circular RNAs; 7) study location; 8) TP, TN, FP, FN, and AUC for diagnostic analyses; 9) circular RNAs expression. The quality of included diagnostic studies was evaluated using Quality Assessment of Diagnostic Accuracy Studies 2 (QUADAS-2) (Whiting et al., 2011) and showed in **Supplementary Figure S1**. A third investigator participated in the process if problems arose.

2.4 Statistical Analysis

Data were analyzed using the "midas" plugin of STATA 15.0 (STATA, College Station, TX, United States) and Review Manager 5.4 (https://training.cochrane.org/online-learning/core-software-cochrane-reviews/revman/). The pooled sensitivity and specificity (with 95% confidence intervals (CIs)) were calculated to determine the diagnostic value of parameters. The threshold effect between included studies was assessed by the correlation coefficient and p-value. $p < 0.05$ indicated the existence of a threshold effect. The hierarchical summary receiver operating characteristics (HSROC) model was used to ameliorate the threshold effect and plot SROC in midas (Rutter and Gatsonis, 2001). Heterogeneity was estimated using Cochran's Q test and I^2 (Higgins et al., 2003). A random-effects model was adopted if I^2 >50% or $p < 0.10$. The pooled diagnostic odds ratio (DOR), positive likelihood ratio (+LR), and negative likelihood ratio (−LR) were calculated for deeper analyses of heterogeneity. Then, subgroup analyses were conducted if high heterogeneity was present. We used Fagan's

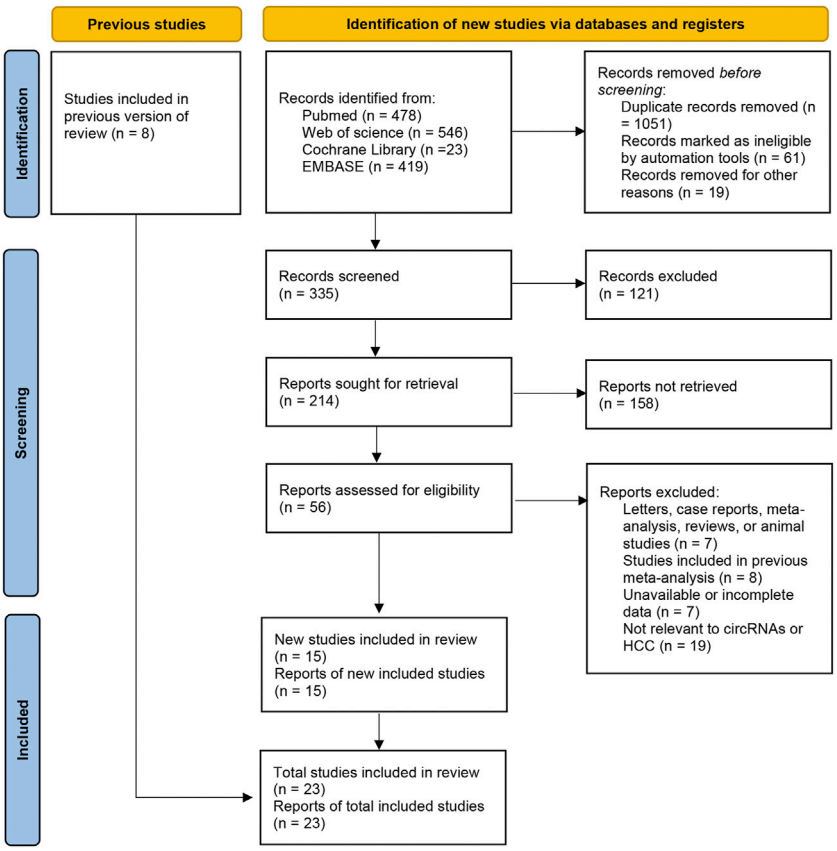

FIGURE 1 | Flow-process diagram of the study selection process.

nomogram plot analysis to evaluate the changes between pre-test probability and post-test probability (the probability of having the disease after the result of the index test had been obtained). A potential publication bias of articles related to HCC diagnosis was evaluated using Deeks' funnel-plot asymmetry test. $p < 0.10$ indicated significant asymmetry and a publication bias.

3 RESULTS

3.1 Included Studies

Twenty-three studies were included in our meta-analysis (Qin et al., 2016; Shang et al., 2016; Yao et al., 2017; Zhang et al., 2018b; Chen et al., 2018; Zhang et al., 2018c; Fu et al., 2018; Matboli et al., 2018; Yao et al., 2018; Li Z. et al., 2019; Jiang et al., 2019; Qiao et al., 2019; Sun S. et al., 2020; Sun X.-H. et al., 2020; Chen et al., 2020; Gao et al., 2020; Wei et al., 2020; Wu et al., 2020; Yu et al., 2020; Zhu et al., 2020; Guo et al., 2021; Liu et al., 2021; Wang et al., 2021). The types of clinical samples were tumor tissue, adjacent tissue, tissue from cirrhosis patients, tissue from hepatitis patients, serum/plasma, and exosome. All studies focused on circular RNAs and measured the levels of circular RNAs by real time reverse-transcription-quantitative polymerase chain reaction. The number of samples ranged from 72 to 278. Sufficient data were selected from the articles for calculation of pooled sensitivity, specificity, and other statistical indicators. The details and process are shown in **Supplementary Table S1** and **Figure 1**.

3.2 Primary meta-Analysis

The pooled sensitivity was 0.80 (95%CI: 0.77–0.84). The pooled specificity was 0.83 (95%CI: 0.79–0.85) (**Figure 2**). The pooled DOR, +LR, and −LR was 19 (95%CI: 14–27), 4.6 (95%CI: 3.8–5.5), and 0.24 (95%CI: 0.20–0.29), respectively (**Table 1**). The correlation coefficient of the threshold effect of circular RNAs was 0.28 ($p < 0.08$): a threshold effect was absent. The pooled AUC arising from the HSROC model was 0.88 (0.85–0.91). Cochran's Q was 125.75 ($p < 0.001$), and I^2 was 98%, which showed considerable heterogeneity (**Figure 3A**). Thus, a subgroup analysis for the types of samples was processed. With a pre-test probability of a positive circular RNAs of 20%, the post-test probability of positive circular RNAs giving positive and negative results was 54 and 6%, respectively (**Figure 3B**).

3.3 Subgroup Analysis

The significant heterogeneity that we encountered prompted us to undertake subgroup analyses. Four groups were created: sample type of exosomes; serum/plasma; HCC tissue *vs* tissue from cirrhosis cases or tissue from cases with chronic hepatitis;

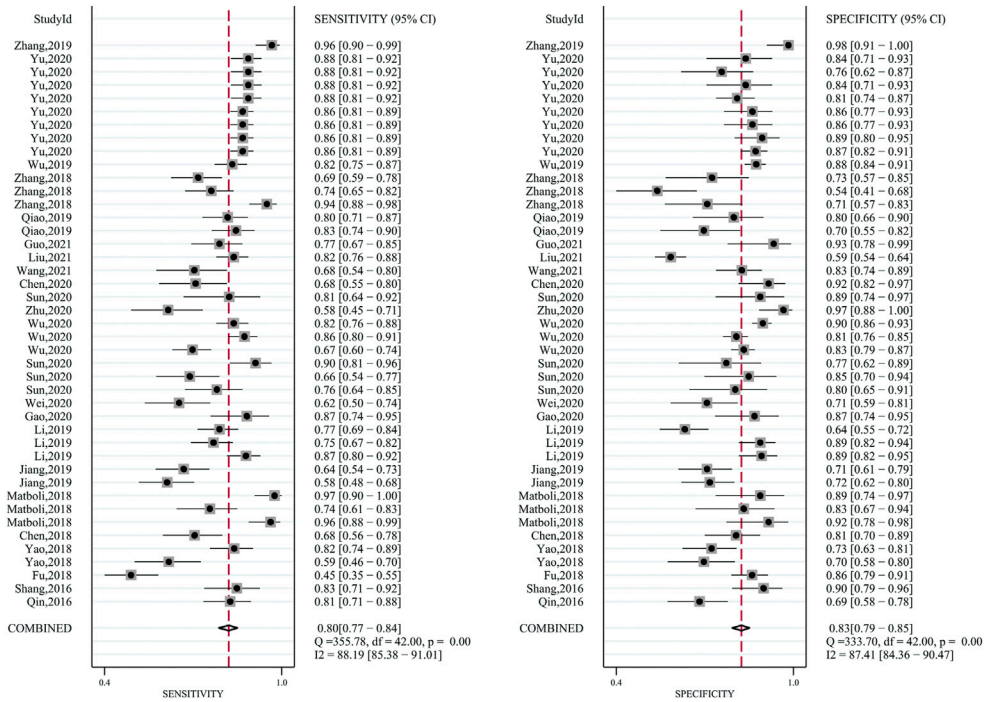

FIGURE 2 | Forest plots for diagnostic accuracy of circular RNAs in hepatocellular carcinoma (HCC).

TABLE 1 | Subgroup analysis of diagnostic accuracy of circular RNAs in HCC.

	Sen	Spe	PLR	NLR	DOR	AUC	heterogeneity	
	95%CI	95%CI	95%CI	95%CI	95%CI	95%CI	I^2	P
Type of sample								
Exosomes	0.69 (0.61,0.75)	0.91 (0.83,0.96)	7.8 (4.0,15.2)	0.34 (0.28,0.43)	23 (11,47)	0.82 (0.78,0.85)	32%	0.115
Serum/plasma	0.84 (0.81,0.87)	0.83 (0.79,0.86)	4.9 (4.0,6.1)	0.19 (0.16,0.23)	26 (18,38)	0.90 (0.87,0.93)	97%	< 0.001
HCC vs adjacent tissues	0.79 (0.72,0.85)	0.79 (0.72,0.84)	3.7 (2.7,5.0)	0.27 (0.19,0.37)	14 (8,25)	0.86 (0.82,0.88)	21%	0.181
HCC vs hepatitis tissues	0.56 (0.49,0.64)	0.76 (0.67,0.82)	2.1 (1.8,2.6)	0.58 (0.50,0.66)	4 (3,6)	0.70 (0.66,0.74)	80%	0.004
Function								
Yes	0.82 (0.77,0.86)	0.80 (0.73,0.86)	4.1 (2.9,5.8)	0.23 (0.18,0.30)	18 (10,31)	0.88 (0.84,0.90)	95%	< 0.001
No	0.75 (0.67,0.82)	0.84 (0.80,0.87)	4.6 (3.5,6.0)	0.30 (0.21,0.41)	15 (9,27)	0.87 (0.84,0.90)	95%	< 0.001
Only in HCC								
Yes	0.79 (0.71,0.84)	0.84 (0.80,0.88)	4.9 (3.7,6.7)	0.25 (0.18,0.35)	19 (11,35)	0.89 (0.86,0.91)	98%	< 0.001
No	0.79 (0.73,0.83)	0.78 (0.70,0.85)	3.6 (2.6,5.0)<	0.27 (0.21,0.35)	13 (8,21)	0.85 (0.82,0.88)	95%	< 0.001
Overall	0.80 (0.79,0.85)	0.83 (0.79,0.85)	4.6 (3.8,5.5)	0.24 (0.20,0.29)	19 (14,27)	0.88 (0.85,0.91)	98%	< 0.001

Abbreviations: Sen: sensitivity; Spe: specificity; +LR: positive likelihood ratio; -LR: negative likelihood ratio; DOR: diagnostic OR; AUC: area under the curve; HCC: hepatocellular carcinoma.

HCC tissue *vs* adjacent tissue. The sensitivity, specificity, AUC, and other statistical indicators were calculated and compared (**Table 1**). Besides that, we also divided all of them into other kind of subgroups, based on function in HCC or not and only studied in HCC or not. The same analysis methods were possessed.

3.3.1 Types of Samples

3.3.1.1 Exosomes

Four studies focused on the diagnostic value of exosome-derived circular RNAs. All of those studies were published in 2020–2021. The pooled sensitivity was 0.69 (95%CI: 0.61–0.75). The pooled specificity was 0.91 (95%CI: 0.83–0.96). The pooled DOR, +LR, and −LR was 23 (95%CI: 11–47), 7.8 (95%CI: 4.0–15.2), and 0.34 (95%CI: 0.28–0.43), respectively. Fagan's nomogram plot analysis revealed values of 66% (positive) and 8% (negative) (**Supplementary Figure S2A**). The correlation coefficient of the threshold effect was −0.73 (p = 0.53): the threshold effect was absent. The pooled AUC was 0.82 (0.78–0.85) (**Figure 4A**). Cochran's Q was 2.942 (p = 0.115) and I^2 was 32%, which indicated low heterogeneity.

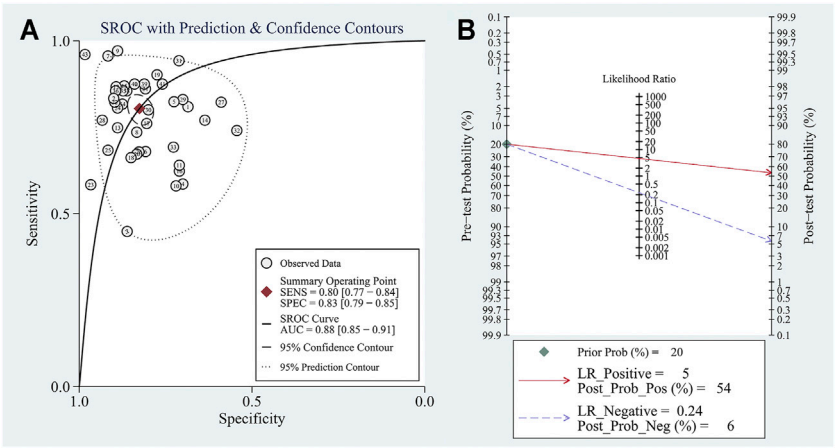

FIGURE 3 | (A) The summary receiver operator characteristic (SROC) for circular RNAs in hepatocellular carcinoma; **(B)** Fagan plot analysis to evaluate the clinical utility of circular RNAs.

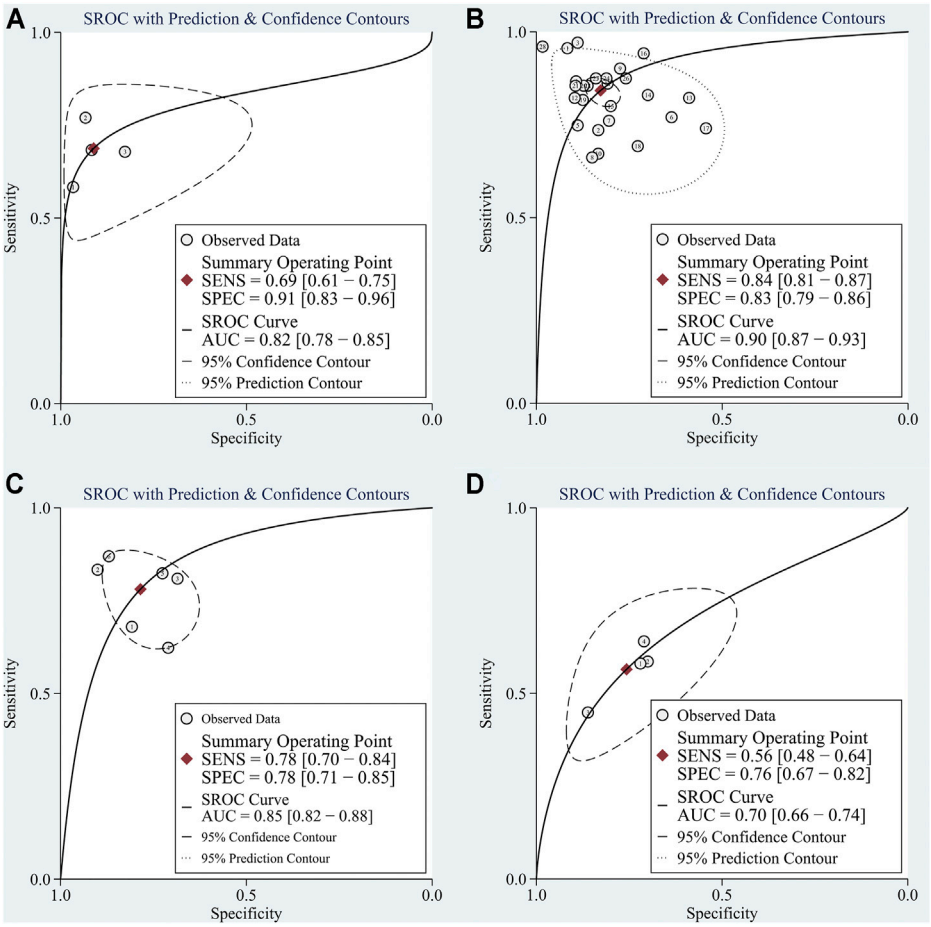

FIGURE 4 | The summary receiver operator characteristic (SROC) for circular RNAs in **(A)** exosomes; **(B)** serum/plasma; **(C)** HCC tissue vs adjacent tissue; **(D)** HCC tissues vs tissues from cirrhosis or chronic hepatitis cases.

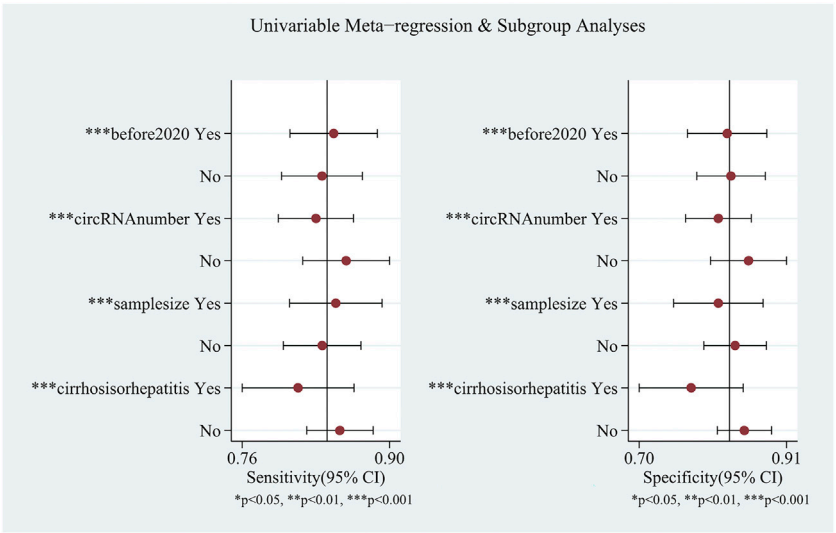

FIGURE 5 | Meta-regression for the heterogeneity existing in circular RNAs in plasma/serum.

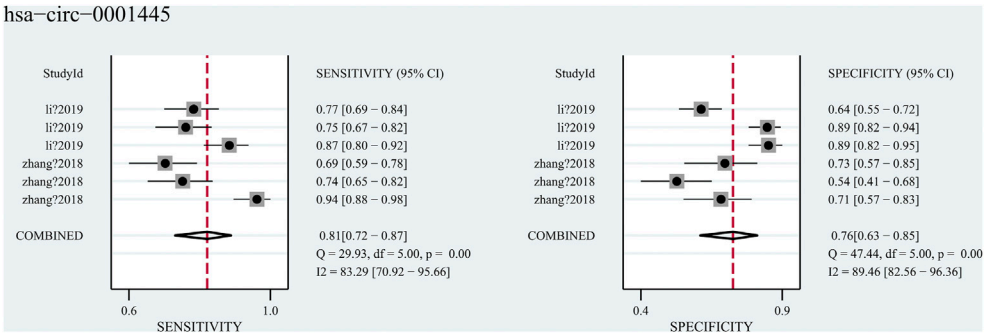

FIGURE 6 | Forest plots for diagnostic accuracy of hsa_circ_0001445 in hepatocellular carcinoma (HCC).

3.3.1.2 Serum/Plasma

Ten studies explored the diagnostic accuracy of circular RNAs in serum/plasma. Most of these studies were published in 2020–2021. The pooled sensitivity was 0.84 (95%CI: 0.81–0.87). The pooled specificity was 0.83 (95%CI: 0.79–0.86). The pooled DOR, +LR, and −LR was 26 (95%CI: 18–38), 4.9 (95% CI: 4.0–6.1), and 0.19 (95%CI: 0.16–0.23), respectively. Fagan's nomogram plot analysis revealed values of 55% (positive) and 5% (negative) (**Supplementary Figure S2B**). The correlation coefficient of the threshold effect was 0.44 (p = 0.20): the threshold effect was considered absent. The pooled AUC was 0.90 (0.87–0.93) (**Figure 4B**). Cochran's Q was 59.459 ($p < 0.001$), and I^2 was 97%, which indicated high heterogeneity. To solve the heterogeneity, we processed a meta-regression based on publication year (before 2020 or not), circular RNAs numbers (single or multiple), high risk patients (with cirrhosis or hepatitis or not), and sample size (< 200 or ≥200). We found that all of these could influence the heterogeneity (**Figure 5**).

Hsa_circ_0001445, was researched in two studies (Zhang et al. and Li et al.), which contained diagnose-related data and both focused on the diagnostic role of hsa_circ_0001445 in blood. A total of 755 blood samples (from 239 HCC patients, 200 cirrhosis patients, 161 hepatitis patients and 155 health subjects) were included in the two studies. The pooled sensitivity was 0.81 (95% CI: 0.72–0.87), and the pooled specificity was 0.76 (95%CI: 0.63–0.85) (**Figure 6**) with an AUC of 0.85 (95%CI: 0.82–0.88). However, significant heterogeneity (I^2 = 88%, $p <$ 0.001) existed in these data. Considering that the diagnostic accuracy of hsa_circ_0001445 might be various in different groups of people, we divided them into three subgroups-HCC vs cirrhosis, HCC vs hepatitis, and HCC vs health. The results of subgroup analysis were showed in **Table 2**. We found that the group HCC vs health has the highest sensitivity (0.90), specificity (0.82) and AUC (0.91), with no heterogeneity ($I^2 = 0$, $p = 0.554$). Regrettably, the reliability of our results was limited by the sparse studies.

TABLE 2 | The subgroup analysis of the diagnostic accuracy of hsa_circ_0001445.

Group	Sen	95%CI	Spe	95%CI	DOR	95%CI	AUC	95%CI	heterogeneity	
									I^2	P
HCC vs hepatitis	0.75	0.69–0.80	0.76	0.45–0.92	9	1–60	0.80	0.76–0.84	88%	0.003
HCC vs cirrhosis	0.74	0.68–0.79	0.66	0.59–0.72	6	4–9	0.76	0.71–0.80	81%	0.023
HCC vs health	0.90	0.84–0.95	0.82	0.66–0.92	48	26–91	0.91	0.82–1.00	0	0.554
Overall	0.81	0.72–0.87	0.76	0.63–0.85	13	6–30	0.85	0.82–0.88	88%	< 0.000

Abbreviations: Sen: sensitivity; Spe: specificity; DOR: diagnostic OR; AUC: area under the curve; HCC: hepatocellular carcinoma.

3.3.1.3 HCC Tissues vs Adjacent Tissues

Six studies explored the diagnostic role of circular RNAs from the comparisons between tissues adjacent to cancerous tissues and cancerous tissues. All seven studies were published before 2021. The pooled sensitivity was 0.78 (95% CI: 0.70–0.84). The pooled specificity was 0.78 (95%CI: 0.71–0.85). The pooled DOR, +LR, and −LR was 13 (95%CI: 7–25), 3.6 (95%CI: 2.5–5.2), and 0.28 (95%CI: 0.20–0.40), respectively. The Fagan's nomogram plot analysis revealed values of 48% (positive) and 6% (negative) (**Supplementary Figure S2C**). The correlation coefficient of the threshold effect was 0.49 (p = 0.29): a threshold effect was absent. The pooled AUC was 0.85 (0.82–0.88). Cochran's Q was 2.000 (p = 0.140) and I^2 was 21%, which indicated low heterogeneity (**Figure 4C**).

3.3.1.4 HCC Tissues vs Tissues From Patients With Cirrhosis or Hepatitis

Three studies explored the diagnostic accuracy of circular RNAs extracted from HCC tissues and the tissues of patients suffering from cirrhosis or hepatitis. All three studies were published before 2020. The pooled sensitivity was 0.56 (95%CI: 0.49–0.64). The pooled specificity was 0.76 (95%CI: 0.67–0.82). The pooled DOR, +LR, and −LR was 4 (95%CI: 3–6), 2.3 (95%CI: 1.8–3.0), and 0.58 (95%CI: 0.50–0.66), respectively. The Fagan's nomogram plot analysis revealed values of 37% (positive) and 13% (negative) (**Supplementary Figure S2D**). The correlation coefficient of the threshold effect was −1.00 (p = 1): a threshold effect was absent. The pooled AUC was 0.70 (0.66–0.74). Cochran's Q was 9.881 (p = 0.004) and I^2 was 80%, which indicated moderate heterogeneity (**Figure 4D**).

3.3.2 Function in HCC

After searching for target circular RNAs in related databases, we listed the circular RNAs related to the pathological mechanism of hepatocellular carcinoma, including hsa_circ_0001649, hsa_circ_0005075, CircZKSCAN1, hsa_circ_0001445, hsa_circ_0003998, Circ-104075, Circ-TCF4.85, Circ-CDYL, hsa_circ_0027345, hsa_circ_0051443, hsa_circ_0005397. Most of them worked as a miRNA sponge, except hsa_circ_0027345, forming a ternary complex with EZH2 and STAT3. Moreover, circ-104075, circ-TCF4.85, has-circ-0027345, and has-circ-5397 were only reported to be pathologically functional in HCC. Others were just focused on their clinic values. The results were showed in **Supplementary Table S2**. Their target genes consisted of SHPRH, DLC1, TIMP3, PCBP1, YAP-1, HDFG, HIF1AN, STAT3, RNF38, BAK1 and PDK2. Only hsa_circ_0001649 can activate its parental gene, SHPRH, to inhibit HCC progression *via* sponging miR-127–5p/miR-612/miR-4688. We also calculated the pooled sensitivity, specificity and AUC for two groups, function or not (**Table 1**). The pooled sensitivities were 0.82 (95%CI: 0.77–0.86) (function group) and 0.75 (95%CI: 0.67–0.82) (unknown function group), when the specificities were 0.80 (95%CI: 0.73–0.86) and 0.84 (95%CI: 0.80–0.87). As for AUC, they were 0.88 (95%CI: 0.84–0.90) (function group) and 0.87 (95%CI: 0.84–0.90) (unknown function group). As we knew, there was a tiny difference in AUC between two groups.

3.3.3 Only in HCC or Not

We extracted several circular RNAs that only were reported to work in HCC, including hsa_circ_0003570, hsa_circ_0068669, hsa_circ_0128298, hsa_circ_000224, hsa_circ_00156, hsa_circ_000520, hsa_circ_0028502, hsa_circ_0076251, hsa_circ_0004001, hsa_circ_0004123, hsa_circ_0075792, hsa_circ_0009582, hsa_circ_0037120, hsa_circ_0140117, hsa_circ_0027345, hsa_circ_0051443, hsa_circ_0005397, hsa_circ_0006602, hsa_circ_0028861. Others were found that played some roles in other cancers, such as gastric cancer, colorectal cancer, glioma, bladder cancer and so on (**Supplementary Table S2**). In addition, circ-104075, circ-TCF4.85, hsa_circ_0027345, hsa_circ_0051443 and hsa_circ_0005397 could regulate specific target genes through sponging microRNAs or binding to proteins only in HCC. Similarly, the same statistical treatment happened in both of two groups-only in HCC or not. The pooled sensitivities were 0.79 (95%CI: 0.71–0.84) and 0.79 (95%CI: 0.73–0.83), equally in two groups, and the specificities were 0.84 (95%CI: 0.80–0.88) (only in HCC) and 0.78 (95%CI: 0.70–0.85) (not only in HCC). As for AUC, they were 0.89 (95%CI: 0.86–0.91) and 0.85 (95%CI: 0.82–0.88) (**Table 1**). Consequently, these circular RNAs only reported in HCC had a higher pooled specificity and an AUC.

3.3.4 Quality Assessment and Publication Bias

The included articles were judged by QUADSA-2. The details were shown in **Supplementary Figure S1**. All articles were acceptable. Deeks' funnel-plot asymmetry test was processed to ascertain if a publication bias was present in our analysis. The results, p-value of exosomes group, plasma/serum group, adjacent tissues group and tissues from patients with cirrhosis or hepatitis group were 0.16, 0.42, 0.25 and 0.21, demonstrating a low likelihood of the publication bias (**Figure 7**).

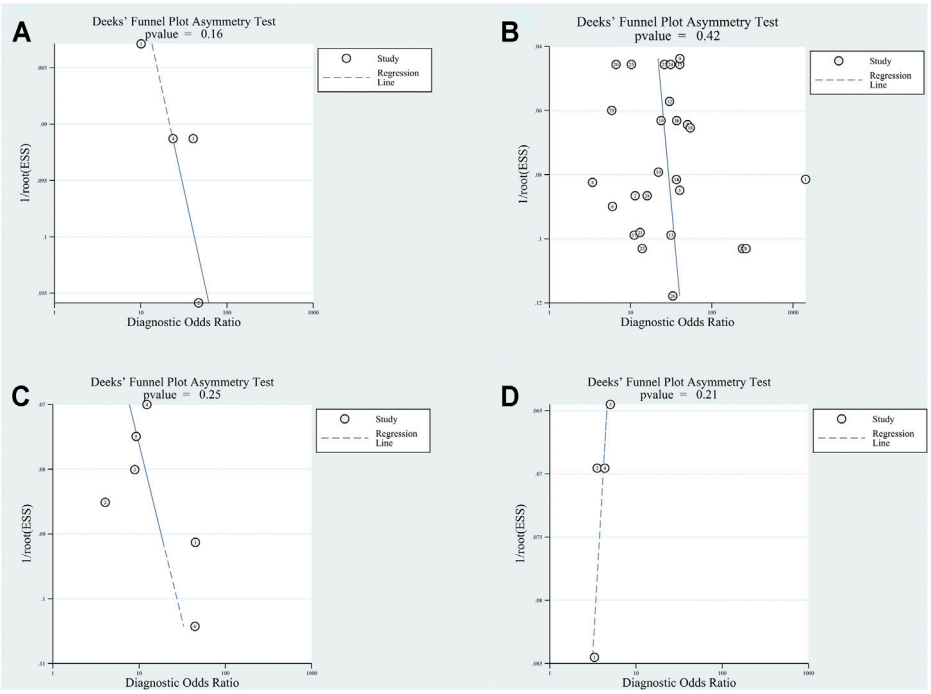

FIGURE 7 | Deek's Funnel test for circular RNAs in **(A)** exosomes; **(B)** serum/plasma; **(C)** HCC tissue vs adjacent tissue; **(D)** HCC tissues vs tissues from cirrhosis or chronic hepatitis cases.

4 DISCUSSION

Compared to radioactive or expensive imaging methods, biomarkers are easier to be evaluated because the measurements are objective and can be obtained in real time using a relatively innocuous and low-cost venipuncture procedure (Öberg et al., 2020). The potential biomarkers that could be used to detect HCC are AFP, glypican-3 (GPC3), des-gamma-carboxy prothrombin (DCP), miRNAs, and circular RNAs(Yu et al., 2020). The sensitivity and specificity of AFP for detecting HCC has been reported to be 39–64% and 76–91% (Oka et al., 1994; Okuda et al., 2000; Marrero and Lok, 2004), respectively. The sensitivity and specificity of the serum GPC3 level to detect HCC was reported to be 68 and 92%, but the results were influenced by the threshold effect and significant heterogeneity (Xu et al., 2019). According to a meta-analysis in 2014, the sensitivity and specificity of DCP to detect HCC was 71 and 84%, respectively (Zhu et al., 2014). However, those protein biomarkers relied on inconvenient enzyme-linked immunosorbent assays for rapid detection, taking serval hours.

We included 23 articles (5,135 persons) from 2016 to 2021 to explore the diagnostic role of circular RNAs in HCC detection. The pooled sensitivity and specificity were 0.80 and 0.83, respectively, with an AUC of 0.88. The result of Fagan test means circular RNAs could be used to diagnose HCC (when the pre-test probability is 20%), with 54% probability of correctly diagnosing HCC following a "positive" measurement and 6% probability of wrong diagnosing HCC following a "negative" result. These data suggested that circular RNAs were suitable biomarkers for HCC detection. An electrochemical detection assay of circular RNAs based on a combination of back-splice junctions and duplex-specific nucleases was first reported in 2019 (Jiao et al., 2020). Currently, application of an electrochemical POCT platform for DNA and glucose has been expanded to circular RNAs. This electrochemical POCT platform can be integrated readily with a smartphone using limited sample volumes to achieve a sensitive, accurate, real-time, and rapid analysis (Zhang et al., 2021).

Exosomes are nanoscale (30–150 nm) extracellular vesicles of endocytic origin shed by most types of cells. Exosomes circulate in interstitial fluid, blood, urine, saliva, and breast milk (Boriachek et al., 2018) and function in mediating intercellular communication, tumor microenvironment (Zhang and Wang, 2015), immune system (Yu et al., 2018), development and differentiation, cell signaling and viral replication (Alenquer and Amorim, 2015). In 2015, Li and coworkers firstly reported exosome-derived circular RNAs, and explored their potential diagnostic value (Li Y. et al., 2015). They identified 137,696 circular RNAs in the exosomes presenting in human serum, and >90% of the circular RNAs overlapped with known genes, including 82,892 multiexon circular RNAs, 27728 exon–intron circular RNAs, 6,709 intronic circular RNAs, 3,961 single-exon circular RNAs. Those data suggested that circular RNAs could be transferred actively from cells to exosomes, and indicated the underlying possibility of using circular RNAs as diagnostic markers for tumors (Wang et al., 2019).

Our meta-analysis showed that exosome-derived circular RNAs had a specificity of 0.91 and post-test probability of

66% (positive) and 8% (negative) as the low sensitivity (0.69) and AUC (0.82). Such relatively low sensitivity and AUC might result from included studies about hepatitis-related exosomes in blood, and a model using single circular RNA. Extracellular vesicle long RNAs (eight RNAs diagnostic model) have been reported to have an AUC of 0.98 with 89% sensitivity and 91% specificity for detecting HCC(Li Y. et al., 2019). According to a study focusing on miRNA, single miR-251–5p was 0.72 (AUC), when combination of three exo-miRNAs had a 0.95 AUC(Cho et al., 2020). Combination with traditional biomarkers was another way. As shown in Wang and others' research, hsa_circ_0028861 plus AFP had an impressive development in sensitivity (0.67–0.76) (Wang et al., 2021).

Circular RNAs existing in blood or other bodily fluids are stable and can be used as biomarkers. Different from previous Jiang's meta-analyses, in our meta-analysis, the serum/plasma group had a higher sensitivity (0.84 *vs*. 0.78) and specificity (0.83 *vs*. 0.78) compared with those from the adjacent-tissue group, and the AUC was similar (0.90 *vs*. 0.85). The diagnostic value from Fagan analysis similarly proved this (55–5% vs 48–6%). Hence, circular RNAs from serum/plasma or tissues were suitable diagnostic biomarkers for HCC. Besides, the relationship between expression in serum/plasma and that in HCC tissues from HCC patients required deeper exploration. The heterogeneity observed in the serum/plasma group might have been caused by diverse blood samples (healthy people, individuals suffering from cirrhosis or chronic hepatitis, or people not suffering from HCC) from our former meta-analysis (Nie et al., 2021). In addition, the heterogeneity also was caused by different publication years, single or multiple circular RNAs diagnostic models and sample size.

As for hsa_circ_0001445, a circular RNA with a sensitivity (0.81), specificity (0.76) and an AUC (0.85) in combining two studies, might be a suitable diagnostic blood biomarker for HCC. Following development of liver cirrhosis in patients with chronic hepatitis, liver disease may continue to progress and evolve into hepatocellular carcinoma. Some circular RNAs have been proved to participate in this process. Circular RNA cMTO1 was reported to suppress liver fibrosis and hepatocellular carcinoma progression by acting as a sponge of microRNA (Han et al., 2017; Jin et al., 2020). This might explain the worse diagnostic efficiency of circular RNA happening in hepatitis or cirrhosis patients and HCC patients. Otherwise, the abundance of hsa_circ_0001445 changed gradually in HCC, cirrhosis, hepatitis patients and healthy subjects in both of studies. We could conjecture that hsa_circ_0001445 functioned in the process of hepatitis-cirrhosis-hepatocellular carcinoma, which required deeper researches to prove.

Multi-circular RNAs models had a higher diagnostic accuracy. To improve the accuracy of detection of HCC using serum/plasma circular RNAs, a preferable strategy may be to combine several circular RNAs with conventional biomarkers. For example, in a large-scale multicenter study, the AUC of hsa_circ_0000976 was 0.70. Upon combining hsa_circ_0000976 with two other circular RNAs (hsa_circ_0007750 and hsa_circ_0139,897), the AUC became 0.86. With a combination of those three circular RNAs and AFP, the AUC reached 0.87 (Sun X.-H. et al., 2020). Besides serum/plasma circular RNAs, circ_0000798 extracted from peripheral blood mononuclear cells had an AUC of 0.70 for distinguishing HCC patients from healthy controls (Lei et al., 2019). Wang and collaborators reported that circSATD3 in peripheral venous blood could predict microvascular invasion with an AUC of 0.637 (Wang et al., 2020). Moreover, in a meta-analysis about the diagnostic accuracy of combination of circular RNAs and AFP in detecting HCC, their combination showed a higher clinic application value (Nie et al., 2021). Thus, the diagnostic value of circular RNAs in different components of blood merits further investigation.

In the subgroups of cirrhosis and hepatitis, sensitivity (0.56) and specificity (0.76) were lowest in all groups. The post-test possibility was in the same condition. This result was similar to our previous study on serum/plasma circular RNAs, and indicates the limitation of using circular RNAs to distinguish HCC patients from patients suffering from cirrhosis or chronic hepatitis. Therefore, more studies are required to ascertain the more effective circular RNAs for detection of cirrhosis and chronic hepatitis.

Circular RNAs from exosomes or serum/plasma shared more clinical diagnostic value than circular RNAs from tissues. Circular RNAs are ideal candidates as biomarkers in "liquid biopsies" because they are expressed in tissue- and developmental stage-specific manners, and are also found stable existence in bodily fluids (Arnaiz et al., 2019). Liquid biopsy is a non-invasive method that uses body fluids (e.g., blood, plasma, serum, urine, gastric juice) to reflect the disease state (Reimers and Pantel, 2019). This method could be used to detect HCC at an early stage before insensitive and expensive imaging examinations. Seventy percent of HCC patients detected at an early stage can achieve 5-years survival with suitable therapies (Padhya et al., 2013). In addition, the detection of circular RNAs in blood or in exosomes has been widely explored. A virus-mimicking vesicle (Vir-FV) method was reported that enabled rapid, efficient, and high-throughput detection of exosome-derived miRNAs within 2 h (Gao et al., 2019). Getulio et al. detected extracellular vesicle RNAs using molecular beacons, which was fast, simple and specific (Oliveira et al., 2020). Thus, self-testing has become available with POCT platforms and similar technologies.

The group function and group non-function seemed no difference in diagnostic value. Maybe this result could be explained by that some non-function circular RNAs just were not found out their mechanism in HCC at present. Obviously, most studies paid their close attention to the role of circular RNAs in the growth and metastasis of HCC. Just like included studies in our meta-analysis, most of circular RNAs were found to regulate the growth and metastasis, except hsa_circ_0003998, which could promote epithelial to mesenchymal transition, and circ-CDYL, which could cause stem-like characteristics. Several researchers have explored how circular RNAs influenced resistance. For example, circ-SORE and circ-FN1 were reported to induce HCC sorafenib

resistance (Xu et al., 2020; Yang et al., 2020). However, regulation mechanisms of circular RNAs in immunity escape, metabolism, cancer stem cell or other areas were lacking.

Analysis of circular RNAs reported only in HCC or not, we found that these circular RNAs only reported in HCC had a higher pooled specificity and AUC, which meant they might have a more ideal diagnostic accuracy. Obviously, the characteristics of circular RNAs still stayed unknown. The same circular RNA possessed varied regulation mechanisms in different cancers, known or unknown. Hsa_circ_0001445 could regulate VEGFA mRNA through binding to SRSF1 in glioblastoma, while in HCC, it sponged miR-17–3p and miR-181b-5p to induce the expression of TIMP3 in order to inhibit growth and metastasis. Not only in cancers, it also inhibited ox-LDL-induced HUVECs inflammation by regulating miR-640 (Cai et al., 2020). In a word, the mechanisms of circular RNAs were complex and unexplainable. Thus, this area needed more attention and researches.

Our meta-analysis had four main limitations. First, most studies were carried out in China, which limited the generalizability of our findings. This phenomenon is due (at least in part) to the high incidence of HCC-related deaths in China. Second, the comparatively poor performance of circular RNAs for identifying patients with HCC from patients with cirrhosis or hepatitis weakened the goal of HCC surveillance (which is to diagnose and treat HCC early in high-risk individuals to improve long-term outcomes) (Yang and Kim, 2012). Hence, more suitable circular RNAs or models must be developed for screening, especially in high-risk individuals. The American Association for the Study of Liver Diseases and Asian Pacific Association for the Study of the Liver define "high-risk individuals" as Asian men (age >40 years ears) or Asian women (age >50 years), individuals with a family history of HCC, and African or African–American individuals, all with hepatitis-B-virus infection or individuals with cirrhosis (Omata et al., 2017; Marrero et al., 2018). Third, the level of evidence was low as a result of the lack of randomized controlled trials or prospective studies. Fourth, high heterogeneity remained in some subgroups (e.g., circular RNAs from serum/plasma).

5 CONCLUSION

Our meta-analysis suggested the marked diagnostic accuracy of circular RNAs for detecting HCC. The diagnostic accuracy varied among subgroups. The circular RNAs in exosomes and serum/plasma were suitable for liquid biopsies. In addition, more high-quality, multiple-central and multiple-circular-RNAs studies were needed to explore the value of circular RNAs for detecting HCC.

DATA AVAILABILITY STATEMENT

The original contributions presented in the study are included in the article/**Supplementary Material**, further inquiries can be directed to the corresponding author.

AUTHOR CONTRIBUTIONS

Conception and design: XX; Administrative support: XX; Collection and assembly of data: BL, DP; Data analysis and interpretation: GN; Manuscript writing: GN, JL; Final approval of manuscript: All authors.

FUNDING

This work was Supported by 1·3·5 project for disciplines of excellence–Clinical Research Incubation Project, West China Hospital, Sichuan University (20HXFH021), National Natural Science Foundation of China (Grant No. 81900516), and Science and Technology Support Project of Sichuan Province (Grant No. 2020YSF0238 and No. 2019YFS0041)

SUPPLEMENTARY MATERIAL

The Supplementary Material for this article can be found online at: https://www.frontiersin.org/articles/10.3389/fgene.2021.794105/full#supplementary-material

REFERENCES

Alenquer, M., and Amorim, M. (2015). Exosome Biogenesis, Regulation, and Function in Viral Infection. *Viruses* 7 (9), 5066–5083. doi:10.3390/v7092862

Arnaiz, E., Sole, C., Manterola, L., Iparraguirre, L., Otaegui, D., and Lawrie, C. H. (2019). CircRNAs and Cancer: Biomarkers and Master Regulators. *Semin. Cancer Biol.* 58, 90–99. doi:10.1016/j.semcancer.2018.12.002

Bahn, J. H., Zhang, Q., Li, F., Chan, T.-M., Lin, X., Kim, Y., et al. (2015). The Landscape of microRNA, Piwi-Interacting RNA, and Circular RNA in Human Saliva. *Clin. Chem.* 61 (1), 221–230. doi:10.1373/clinchem.2014.230433

Boriachek, K., Islam, M. N., Möller, A., Salomon, C., Nguyen, N. T., Hossain, M. S. A., et al. (2018). Biological Functions and Current Advances in Isolation and Detection Strategies for Exosome Nanovesicles. *Small* 14 (6), 1702153. doi:10.1002/smll.201702153

Cai, Y., Xu, L., Xu, C., Wang, Y., and Fan, C. (2020). Hsa_circ_0001445 Inhibits Ox-LDL-Induced HUVECs Inflammation, Oxidative Stress and Apoptosis by Regulating miRNA-640. *Perfusion*, 26765912097947. doi:10.1177/0267659120979472

Chen, D., Zhang, C., Lin, J., Song, X., and Wang, H. (2018). Screening Differential Circular RNA Expression Profiles Reveal that Hsa_circ_0128298 Is a Biomarker in the Diagnosis and Prognosis of Hepatocellular Carcinoma. *Cmar* 10, 1275–1283. doi:10.2147/CMAR.S166740

Chen, R.-X., Chen, X., Xia, L.-P., Zhang, J.-X., Pan, Z.-Z., Ma, X.-D., et al. (2019). N6-methyladenosine Modification of circNSUN2 Facilitates Cytoplasmic export and Stabilizes HMGA2 to Promote Colorectal Liver Metastasis. *Nat. Commun.* 10 (1), 4695. doi:10.1038/s41467-019-12651-2

Chen, W., Quan, Y., Fan, S., Wang, H., Liang, J., Huang, L., et al. (2020). Exosome-transmitted Circular RNA Hsa_circ_0051443 Suppresses Hepatocellular Carcinoma Progression. *Cancer Lett.* 475, 119–128. doi:10.1016/j.canlet.2020.01.022

Chen, W., Zheng, R., Baade, P. D., Zhang, S., Zeng, H., Bray, F., et al. (2016). Cancer Statistics in China, 2015. *CA: A Cancer J. Clinicians* 66 (2), 115–132. doi:10.3322/caac.21338

Cho, H., Eun, J., Baek, G., Seo, C., Ahn, H., Kim, S., et al. (2020). Serum Exosomal MicroRNA, miR-10b-5p, as a Potential Diagnostic Biomarker for Early-Stage Hepatocellular Carcinoma. *Jcm* 9 (1), 281. doi:10.3390/jcm9010281

European Association for the Study of the Liver (2018). EASL Clinical Practice Guidelines: Management of Hepatocellular Carcinoma. *J. Hepatol.* 69 (1), 182–236. doi:10.1016/j.jhep.2018.03.019

Fu, L., Wu, S., Yao, T., Chen, Q., Xie, Y., Ying, S., et al. (2018). Decreased Expression of Hsa_circ_0003570 in Hepatocellular Carcinoma and its Clinical Significance. *J. Clin. Lab. Anal.* 32, e22239. doi:10.1002/jcla.22239

Gao, J., Dai, C., Yu, X., Yin, X. B., and Zhou, F. (2020). Circ-TCF4.85 Silencing Inhibits Cancer Progression through microRNA-486-5p-targeted Inhibition of ABCF2 in Hepatocellular Carcinoma. *Mol. Oncol.* 14 (2), 447–461. doi:10.1002/1878-0261.12603

Gao, X., Li, S., Ding, F., Fan, H., Shi, L., Zhu, L., et al. (2019). Rapid Detection of Exosomal MicroRNAs Using Virus-Mimicking Fusogenic Vesicles. *Angew. Chem. Int. Ed.* 58 (26), 8719–8723. doi:10.1002/anie.201901997

Guo, S., Hu, C., Zhai, X., and Sun, D. (2021). Circular RNA 0006602 in Plasma Exosomes: a New Potential Diagnostic Biomarker for Hepatocellular Carcinoma. *Am. J. Transl Res.* 13 (6), 6001–6015.

Han, D., Li, J., Wang, H., Su, X., Hou, J., Gu, Y., et al. (2017). Circular RNA circMTO1 Acts as the Sponge of microRNA-9 to Suppress Hepatocellular Carcinoma Progression. *Hepatology* 66 (4), 1151–1164. doi:10.1002/hep.29270

Hansen, T. B., Jensen, T. I., Clausen, B. H., Bramsen, J. B., Finsen, B., Damgaard, C. K., et al. (2013). Natural RNA Circles Function as Efficient microRNA Sponges. *Nature* 495 (7441), 384–388. doi:10.1038/nature11993

Higgins, J. P. T., Thompson, S. G., Deeks, J. J., and Altman, D. G. (2003). Measuring Inconsistency in Meta-Analyses. *Bmj* 327 (7414), 557–560. doi:10.1136/bmj.327.7414.557

Jeck, W. R., Sorrentino, J. A., Wang, K., Slevin, M. K., Burd, C. E., Liu, J., et al. (2013). Circular RNAs Are Abundant, Conserved, and Associated with ALU Repeats. *Rna* 19 (2), 141–157. doi:10.1261/rna.035667.112

Jiang, Z., Shen, L., Wang, S., Wu, S., Hu, Y., Guo, J., et al. (2019). Hsa_circ_0028502 and Hsa_circ_0076251 Are Potential Novel Biomarkers for Hepatocellular Carcinoma. *Cancer Med.* 8 (17), 7278–7287. doi:10.1002/cam4.2584

Jiao, J., Li, C., Ning, L., Shi, L., Wang, L., Xiang, Y., et al. (2020). Electrochemical Detection of circRNAs Based on the Combination of Back-Splice junction and Duplex-specific Nuclease. *Sensors Actuators B: Chem.* 302, 127166. doi:10.1016/j.snb.2019.127166

Jin, H., Li, C., Dong, P., Huang, J., Yu, J., and Zheng, J. (2020). Circular RNA cMTO1 Promotes PTEN Expression through Sponging miR-181b-5p in Liver Fibrosis. *Front. Cel Dev. Biol.* 8, 714. doi:10.3389/fcell.2020.00714

Kölling, M., Haddad, G., Wegmann, U., Kistler, A., Bosakova, A., Seeger, H., et al. (2019). Circular RNAs in Urine of Kidney Transplant Patients with Acute T Cell-Mediated Allograft Rejection. *Clin. Chem.* 65 (10), 1287–1294. doi:10.1373/clinchem.2019.305854

Lei, B., Zhou, J., Xuan, X., Tian, Z., Zhang, M., Gao, W., et al. (2019). Circular RNA Expression Profiles of Peripheral Blood Mononuclear Cells in Hepatocellular Carcinoma Patients by Sequence Analysis. *Cancer Med.* 8 (4), 1423–1433. doi:10.1002/cam4.2010

Li, Y., Zhao, J., Yu, S., Wang, Z., He, X., Su, Y., et al. (2019a). Extracellular Vesicles Long RNA Sequencing Reveals Abundant mRNA, circRNA, and lncRNA in Human Blood as Potential Biomarkers for Cancer Diagnosis. *Clin. Chem.* 65 (6), 798–808. doi:10.1373/clinchem.2018.301291

Li, Y., Zheng, Q., Bao, C., Li, S., Guo, W., Zhao, J., et al. (2015a). Circular RNA Is Enriched and Stable in Exosomes: a Promising Biomarker for Cancer Diagnosis. *Cell Res* 25 (8), 981–984. doi:10.1038/cr.2015.82

Li, Z., Huang, C., Bao, C., Chen, L., Lin, M., Wang, X., et al. (2015b). Exon-intron Circular RNAs Regulate Transcription in the Nucleus. *Nat. Struct. Mol. Biol.* 22 (3), 256–264. doi:10.1038/nsmb.2959

Li, Z., Zhou, Y., Yang, G., He, S., Qiu, X., Zhang, L., et al. (2019b). Using Circular RNA SMARCA5 as a Potential Novel Biomarker for Hepatocellular Carcinoma. *Clinica Chim. Acta* 492, 37–44. doi:10.1016/j.cca.2019.02.001

Liu, R., Li, Y., Wu, A., Kong, M., Ding, W., Hu, Z., et al. (2021). Identification of Plasma Hsa_circ_0005397 and Combined with Serum AFP, AFP-L3 as Potential Biomarkers for Hepatocellular Carcinoma. *Front. Pharmacol.* 12, 639963. doi:10.3389/fphar.2021.639963

Marrero, J. A., Kulik, L. M., Sirlin, C. B., Zhu, A. X., Finn, R. S., Abecassis, M. M., et al. (2018). Diagnosis, Staging, and Management of Hepatocellular Carcinoma: 2018 Practice Guidance by the American Association for the Study of Liver Diseases. *Hepatology* 68 (2), 723–750. doi:10.1002/hep.29913

Marrero, J. A., and Lok, A. S. F. (2004). Newer Markers for Hepatocellular Carcinoma. *Gastroenterology* 127 (5 Suppl. 1), S113–S119. doi:10.1053/j.gastro.2004.09.024

Matboli, M., Shafei, A. E., Ali, M. A., Ashry, A. M., Kamal, K. M., Agag, M. A., et al. (2018). circRNAs (Hsa_circ_00156, Hsa_circ _000224, and Hsa_circ _000520) Are Novel Potential Biomarkers in Hepatocellular Carcinoma. *J. Cel Biochem* 120, 7711–7724. doi:10.1002/jcb.28045

Nie, G., Peng, D., Li, B., Lu, J., Cai, Y., Xiong, X., et al. (2021). Diagnostic Accuracy of Serum/Plasma Circular RNAs and the Combination of Circular RNAs and α-Fetoprotein for Detecting Hepatocellular Carcinoma: A Meta-Analysis. *Front. Genet.* 12 (1684), 722208. doi:10.3389/fgene.2021.722208

Öberg, K., Califano, A., Strosberg, J. R., Ma, S., Pape, U., Bodei, L., et al. (2020). A Meta-Analysis of the Accuracy of a Neuroendocrine Tumor mRNA Genomic Biomarker (NETest) in Blood. *Ann. Oncol.* 31 (2), 202–212. doi:10.1016/j.annonc.2019.11.003

Oka, H., Tamori, A., Kuroki, T., Kobayashi, K., and Yamamoto, S. (1994). Prospective Study of α-fetoprotein in Cirrhotic Patients Monitored for Development of Hepatocellular Carcinoma. *Hepatology* 19 (1), 61–66. doi:10.1002/hep.1840190111

Okuda, H., Nakanishi, T., Takatsu, K., Saito, A., Hayashi, N., Takasaki, K., et al. (2000). Serum Levels of Des-?-Carboxy Prothrombin Measured Using the Revised Enzyme Immunoassay Kit with Increased Sensitivity in Relation to Clinicopathologic Features of Solitary Hepatocellular Carcinoma. *Cancer* 88 (3), 544–549. doi:10.1002/(sici)1097-0142(20000201)88:3<544:aid-cncr8>3.0.co;2-f

Oliveira, G. P. d., Jr., Zigon, E., Rogers, G., Davodian, D., Lu, S., Jovanovic-Talisman, T., et al. (2020). Detection of Extracellular Vesicle RNA Using Molecular Beacons. *iScience* 23 (1), 100782. doi:10.1016/j.isci.2019.100782

Omata, M., Cheng, A.-L., Kokudo, N., Kudo, M., Lee, J. M., Jia, J., et al. (2017). Asia-Pacific Clinical Practice Guidelines on the Management of Hepatocellular Carcinoma: a 2017 Update. *Hepatol. Int.* 11 (4), 317–370. doi:10.1007/s12072-017-9799-9

Padhya, K. T., Marrero, J. A., and Singal, A. G. (2013). Recent Advances in the Treatment of Hepatocellular Carcinoma. *Curr. Opin. Gastroenterol.* 29 (3), 285–292. doi:10.1097/MOG.0b013e32835ff1cf

Page, M. J., McKenzie, J. E., Bossuyt, P. M., Boutron, I., Hoffmann, T. C., Mulrow, C. D., et al. (2021). The PRISMA 2020 Statement: an Updated Guideline for Reporting Systematic Reviews. *Bmj* 372, n71. doi:10.1136/bmj.n71

Qiao, G.-L., Chen, L., Jiang, W.-H., Yang, C., Yang, C.-M., Song, L.-N., et al. (2019). Hsa_circ_0003998 May Be Used as a New Biomarker for the Diagnosis and Prognosis of Hepatocellular Carcinoma. *Ott* 12, 5849–5860. doi:10.2147/ott.S210363

Qin, M., Liu, G., Huo, X., Tao, X., Sun, X., Ge, Z., et al. (2016). Hsa_circ_0001649: A Circular RNA and Potential Novel Biomarker for Hepatocellular Carcinoma. *Cbm* 16 (1), 161–169. doi:10.3233/CBM-150552

Reimers, N., and Pantel, K. (2019). Liquid Biopsy: Novel Technologies and Clinical Applications. *Clin. Chem. Lab. Med.* 57 (3), 312–316. doi:10.1515/cclm-2018-0610

Rutter, C. M., and Gatsonis, C. A. (2001). A Hierarchical Regression Approach to Meta-Analysis of Diagnostic Test Accuracy Evaluations. *Statist. Med.* 20 (19), 2865–2884. doi:10.1002/sim.942

Salzman, J., Chen, R. E., Olsen, M. N., Wang, P. L., and Brown, P. O. (2013). Cell-type Specific Features of Circular RNA Expression. *Plos Genet.* 9 (9), e1003777. doi:10.1371/journal.pgen.1003777

Shang, X., Li, G., Liu, H., Li, T., Liu, J., Zhao, Q., et al. (2016). Comprehensive Circular RNA Profiling Reveals that Hsa_circ_0005075, a New Circular RNA Biomarker, Is Involved in Hepatocellular Crcinoma Development. *Medicine (Baltimore)* 95 (22), e3811. doi:10.1097/MD.0000000000003811

Shen, H., Liu, B., Xu, J., Zhang, B., Wang, Y., Shi, L., et al. (2021). Circular RNAs: Characteristics, Biogenesis, Mechanisms and Functions in Liver Cancer. *J. Hematol. Oncol.* 14 (1), 134. doi:10.1186/s13045-021-01145-8

Sun, S., Gao, J., Zhou, S., Li, Y., Wang, Y., Jin, L., et al. (2020a). A Novel Circular RNA Circ-LRIG3 Facilitates the Malignant Progression of Hepatocellular Carcinoma by Modulating the EZH2/STAT3 Signaling. *J. Exp. Clin. Cancer Res.* 39 (1), 252. doi:10.1186/s13046-020-01779-5

Sun, X.-H., Wang, Y.-T., Li, G.-F., Zhang, N., and Fan, L. (2020b). Serum-derived Three-circRNA Signature as a Diagnostic Biomarker for Hepatocellular Carcinoma. *Cancer Cel Int* 20, 226. doi:10.1186/s12935-020-01302-y

Sung, H., Ferlay, J., Siegel, R. L., Laversanne, M., Soerjomataram, I., Jemal, A., et al. (2021). Global Cancer Statistics 2020: GLOBOCAN Estimates of Incidence and Mortality Worldwide for 36 Cancers in 185 Countries. *CA A. Cancer J. Clin.* 71, 209–249. doi:10.3322/caac.21660

Wang, P., Xu, L.-L., Zheng, X.-B., Hu, Y.-T., Zhang, J.-F., Ren, S.-S., et al. (2020). Correlation between the Expressions of Circular RNAs in Peripheral Venous Blood and Clinicopathological Features in Hepatocellular Carcinoma. *Ann. Transl Med.* 8 (6), 338. doi:10.21037/atm.2020.02.134

Wang, Y., Liu, J., Ma, J., Sun, T., Zhou, Q., Wang, W., et al. (2019). Exosomal circRNAs: Biogenesis, Effect and Application in Human Diseases. *Mol. Cancer* 18 (1), 116. doi:10.1186/s12943-019-1041-z

Wang, Y., Pei, L., Yue, Z., Jia, M., Wang, H., and Cao, L.-L. (2021). The Potential of Serum Exosomal Hsa_circ_0028861 as the Novel Diagnostic Biomarker of HBV-Derived Hepatocellular Cancer. *Front. Genet.* 12, 703205. doi:10.3389/fgene.2021.703205

Wei, Y., Chen, X., Liang, C., Ling, Y., Yang, X., Ye, X., et al. (2020). A Noncoding Regulatory RNAs Network Driven by Circ-CDYL Acts Specifically in the Early Stages Hepatocellular Carcinoma. *Hepatology* 71 (1), 130–147. doi:10.1002/hep.30795

Wen, G., Zhou, T., and Gu, W. (2020). The Potential of Using Blood Circular RNA as Liquid Biopsy Biomarker for Human Diseases. *Protein Cell*. doi:10.1007/s13238-020-00799-3

Whiting, P. F., Rutjes, A. W., Westwood, M. E., Mallett, S., Deeks, J. J., Reitsma, J. B., et al. (2011). QUADAS-2: a Revised Tool for the Quality Assessment of Diagnostic Accuracy Studies. *Ann. Intern. Med.* 155 (8), 529–536. doi:10.7326/0003-4819-155-8-201110180-00009

Wu, C., Deng, L., Zhuo, H., Chen, X., Tan, Z., Han, S., et al. (2020). Circulating circRNA Predicting the Occurrence of Hepatocellular Carcinoma in Patients with HBV Infection. *J. Cel Mol Med* 24 (17), 10216–10222. doi:10.1111/jcmm.15635

Xu, D., Su, C., Sun, L., Gao, Y., and Li, Y. (2019). Performance of Serum Glypican 3 in Diagnosis of Hepatocellular Carcinoma: A Meta-Analysis. *Ann. Hepatol.* 18 (1), 58–67. doi:10.5604/01.3001.0012.7863

Xu, J., Wan, Z., Tang, M., Lin, Z., Jiang, S., Ji, L., et al. (2020). N6-methyladenosine-modified CircRNA-SORE Sustains Sorafenib Resistance in Hepatocellular Carcinoma by Regulating β-catenin Signaling. *Mol. Cancer* 19 (1), 163. doi:10.1186/s12943-020-01281-8

Xu, Y., Leng, K., Yao, Y., Kang, P., Liao, G., Han, Y., et al. (2021). A Circular RNA, Cholangiocarcinoma-Associated Circular RNA 1, Contributes to Cholangiocarcinoma Progression, Induces Angiogenesis, and Disrupts Vascular Endothelial Barriers. *Hepatology* 73 (4), 1419–1435. doi:10.1002/hep.31493

Yang, C., Dong, Z., Hong, H., Dai, B., Song, F., Geng, L., et al. (2020). circFN1 Mediates Sorafenib Resistance of Hepatocellular Carcinoma Cells by Sponging miR-1205 and Regulating E2F1 Expression. *Mol. Ther. - Nucleic Acids* 22, 421–433. doi:10.1016/j.omtn.2020.08.039

Yang, J. D., and Kim, W. R. (2012). Surveillance for Hepatocellular Carcinoma in Patients with Cirrhosis. *Clin. Gastroenterol. Hepatol.* 10 (1), 16–21. doi:10.1016/j.cgh.2011.06.004

Yao, T., Chen, Q., Shao, Z., Song, Z., Fu, L., and Xiao, B. (2018). Circular RNA 0068669 as a New Biomarker for Hepatocellular Carcinoma Metastasis. *J. Clin. Lab. Anal.* 32 (8), e22572. doi:10.1002/jcla.22572

Yao, Z., Luo, J., Hu, K., Lin, J., Huang, H., Wang, Q., et al. (2017). ZKSCAN1gene and its Related Circular RNA (circZKSCAN1) Both Inhibit Hepatocellular Carcinoma Cell Growth, Migration, and Invasion but through Different Signaling Pathways. *Mol. Oncol.* 11 (4), 422–437. doi:10.1002/1878-0261.12045

Yu, G., Jung, H., Kang, Y. Y., and Mok, H. (2018). Comparative Evaluation of Cell- and Serum-Derived Exosomes to Deliver Immune Stimulators to Lymph Nodes. *Biomaterials* 162, 71–81. doi:10.1016/j.biomaterials.2018.02.003

Yu, J., Ding, W. b., Wang, M. c., Guo, X. g., Xu, J., Xu, Q. g., et al. (2020). Plasma Circular RNA Panel to Diagnose Hepatitis B Virus-related Hepatocellular Carcinoma: A Large-scale, Multicenter Study. *Int. J. Cancer* 146 (6), 1754–1763. doi:10.1002/ijc.32647

Zhang, B., Chen, M., Cao, J., Liang, Y., Tu, T., Hu, J., et al. (2021). An Integrated Electrochemical POCT Platform for Ultrasensitive circRNA Detection towards Hepatocellular Carcinoma Diagnosis. *Biosens. Bioelectron.* 192, 113500. doi:10.1016/j.bios.2021.113500

Zhang, M., Huang, N., Yang, X., Luo, J., Yan, S., Xiao, F., et al. (2018a). A Novel Protein Encoded by the Circular Form of the SHPRH Gene Suppresses Glioma Tumorigenesis. *Oncogene* 37 (13), 1805–1814. doi:10.1038/s41388-017-0019-9

Zhang, X., Xu, Y., Qian, Z., Zheng, W., Wu, Q., Chen, Y., et al. (2018b). circRNA_104075 Stimulates YAP-dependent Tumorigenesis through the Regulation of HNF4a and May Serve as a Diagnostic Marker in Hepatocellular Carcinoma. *Cell Death Dis* 9 (11), 1091. doi:10.1038/s41419-018-1132-6

Zhang, X., Zhou, H., Jing, W., Luo, P., Qiu, S., Liu, X., et al. (2018c). The Circular RNA Hsa_circ_0001445 Regulates the Proliferation and Migration of Hepatocellular Carcinoma and May Serve as a Diagnostic Biomarker. *Dis. Markers* 2018, 1–9. doi:10.1155/2018/3073467

Zhang, Y., and Wang, X.-F. (2015). A Niche Role for Cancer Exosomes in Metastasis. *Nat. Cel Biol* 17 (6), 709–711. doi:10.1038/ncb3181

Zhu, C., Su, Y., Liu, L., Wang, S., Liu, Y., and Wu, J. (2020). Circular RNA Hsa_circ_0004277 Stimulates Malignant Phenotype of Hepatocellular Carcinoma and Epithelial-Mesenchymal Transition of Peripheral Cells. *Front. Cel Dev. Biol.* 8, 585565. doi:10.3389/fcell.2020.585565

Zhu, R., Yang, J., Xu, L., Dai, W., Wang, F., Shen, M., et al. (2014). Diagnostic Performance of Des-γ-Carboxy Prothrombin for Hepatocellular Carcinoma: A Meta-Analysis. *Gastroenterol. Res. Pract.* 2014, 1–9. doi:10.1155/2014/529314

Conflict of Interest: The authors declare that the research was conducted in the absence of any commercial or financial relationships that could be construed as a potential conflict of interest.

Publisher's Note: All claims expressed in this article are solely those of the authors and do not necessarily represent those of their affiliated organizations, or those of the publisher, the editors, and the reviewers. Any product that may be evaluated in this article, or claim that may be made by its manufacturer, is not guaranteed or endorsed by the publisher.

frontiers in Genetics

ORIGINAL RESEARCH
published: 16 February 2022
doi: 10.3389/fgene.2022.841043

Early Brain microRNA/mRNA Expression is Region-Specific After Neonatal Hypoxic-Ischemic Injury in a Mouse Model

Eric S. Peeples[1,2,3]*, *Namood-e Sahar*[1,3], *William Snyder*[1,3] and *Karoly Mirnics*[3,4,5,6]

[1]Department of Pediatrics, University of Nebraska Medical Center, Omaha, NE, United States, [2]Department of Pediatrics, Children's Hospital & Medical Center, Omaha, NE, United States, [3]Child Health Research Institute, Omaha, NE, United States, [4]Department of Biochemistry and Molecular Biology, University of Nebraska Medical Center, Omaha, NE, United States, [5]Department of Pharmacology and Experimental Neuroscience, University of Nebraska Medical Center, Omaha, NE, United States, [6]Munroe-Meyer Institute for Genetics and Rehabilitation, University of Nebraska Medical Center, Omaha, NE, United States

OPEN ACCESS

Edited by:
Olanrewaju B. Morenikeji,
University of Pittsburgh at Bradford, United States

Reviewed by:
Thomas Ragnar Wood,
University of Washington, United States
Jie Qiu,
Nanjing Children's Hospital, China

***Correspondence:**
Eric S. Peeples
epeeples@childrensomaha.org

Specialty section:
This article was submitted to RNA, a section of the journal Frontiers in Genetics

Received: 21 December 2021
Accepted: 25 January 2022
Published: 16 February 2022

Citation:
Peeples ES, Sahar NE, Snyder W and Mirnics K (2022) Early Brain microRNA/mRNA Expression is Region-Specific After Neonatal Hypoxic-Ischemic Injury in a Mouse Model. Front. Genet. 13:841043. doi: 10.3389/fgene.2022.841043

Background: MicroRNAs (miRNAs) may be promising therapeutic targets for neonatal hypoxic-ischemic brain injury (HIBI) but targeting miRNA-based therapy will require more precise understanding of endogenous brain miRNA expression.

Methods: Postnatal day 9 mouse pups underwent HIBI by unilateral carotid ligation + hypoxia or sham surgery. Next-generation miRNA sequencing and mRNA Neuroinflammation panels were performed on ipsilateral cortex, striatum/thalamus, and cerebellum of each group at 30 min after injury. Targeted canonical pathways were predicted by KEGG analysis.

Results: Sixty-one unique miRNAs showed differential expression (DE) in at least one region; nine in more than one region, including miR-410-5p, -1264-3p, 1298-5p, -5,126, and -34b-3p. Forty-four mRNAs showed DE in at least one region; 16 in more than one region. MiRNAs showing DE primarily targeted metabolic pathways, while mRNAs targeted inflammatory and cell death pathways. Minimal miRNA-mRNA interactions were seen at 30 min after HIBI.

Conclusion: This study identified miRNAs that deserve future study to assess their potential as therapeutic targets in neonatal HIBI. Additionally, the differences in miRNA expression between regions suggest that future studies assessing brain miRNA expression to guide therapy development should consider evaluating individual brain regions rather than whole brain to ensure the sensitivity needed for the development of targeted therapies.

Keywords: encephalopathy, cerebellum, next-generation sequencing, striatum, cortex

INTRODUCTION

Neonatal hypoxic-ischemic encephalopathy (HIE), which is the clinical phenotype resulting from perinatal hypoxic-ischemic brain injury (HIBI), is a devastating neurological injury resulting from decreased oxygen and blood flow to the brain around the time of birth. Despite widespread use of therapeutic hypothermia, nearly half of infants with moderate to severe HIE die or suffer from significant developmental disability (Jacobs et al., 2013). Given the continued high morbidity and mortality despite available therapy, novel supplemental therapies are desperately needed. One promising target that has shown potential in *in vivo* studies of HIBI is the modulation of microRNA (miRNA) expression (Li et al., 2019; Xiong et al., 2020).

MiRNAs are small non-coding RNAs that modulate gene expression through post-transcription silencing of messenger RNAs. One significant hurdle to designing miRNA-based therapies for neonatal HIBI is a lack of data describing the endogenous miRNA expression after neonatal HIBI. To date, there have been two studies that have profiled the serum miRNA changes in human newborns with HIE using high-throughput analyses using the same cohort but two different miRNA detection techniques (Looney et al., 2015; Casey et al., 2020). Between the two studies, the investigators identified at least 107 miRNAs that were significantly up- or downregulated in newborns diagnosed with HIE. The human studies, however, are understandably limited to only circulating blood levels and therefore may vary considerably based on the amount of systemic organ (heart, liver, kidney, etc.) injury that results from the hypoxic-ischemic injury (Michniewicz et al., 2020). Our group recently profiled the temporal changes in brain miRNA expression at 24 and 72 h after neonatal HIBI (Peeples et al., 2022); however, no study to date has assessed brain region-specific miRNA changes after injury.

The brain has been shown to have a unique baseline miRNA profile compared to other tissues, and each brain region also has a specific expression signature (Hua et al., 2009). These baseline differences may result in significantly different regional miRNA responses in disease processes, such as neonatal HIBI, that tend to preferentially affect certain regions of the brain more than others. Although all regions of the brain are exposed to the systemic hypoxia that is introduced in the unilateral carotid artery ligation HIBI model, the reduction in blood flow resulting in the ischemic injury does not affect all brain regions equally. In one of the initial descriptions of this model by Dr. Vannucci, his group described the most significant reductions in regional blood flow as occurring in the striatum and thalamus (2–3 times the reduction seen in areas such as the subcortical white matter), which correlated closely with the distribution and extent of ischemic neuronal necrosis that was primarily seen in the striatum, thalamus, and posterior cortical regions (Vannucci et al., 1988). At the same time, Dr. Vannucci's group noted no change or increased blood flow to the cerebellum and brainstem after HIBI in this model, consistent with an injury produced by occluding only the anterior cerebral circulation (carotid artery). Injury to the thalamus and basal ganglia have been consistently associated with poorer outcomes after HIBI (Martinez-Biarge et al., 2011; Cheong et al., 2012); thus, assessing miRNA expression in different regions may provide further insight into the development of adverse outcomes after HIBI.

Based on this knowledge of the variable blood flow distribution and injury, the goal of the current study was to evaluate the brain region-specific miRNA changes after neonatal HIBI in a mouse model. The primary regions of interest were chosen as the cortex, striatum/thalamus, and cerebellum. We hypothesized that the miRNA profile would differ between the cortex and striatum/thalamus and that the cerebellar miRNA expression would be distinct from both of the other regions given its relative protection from ischemic injury in this model. As described above, all of the human studies were obtained immediately after delivery (i.e., cord blood) (Looney et al., 2015; Casey et al., 2020), but previous studies in the piglet model of neonatal HIBI have demonstrated that many miRNAs do not reach peak dysregulation until around 1 h after injury (Garberg et al., 2017; Casey et al., 2020). As such, to allow for comparison with the previous clinical studies (of cord blood at 0 min after injury) but also ensure time for miRNA dysregulation to occur (peak at 60 min after injury), the region-specific miRNA levels assessed in this study were all obtained at 30 min after injury, consistent with the timing used in other similar studies (Yuan et al., 2010; Garberg et al., 2017).

MATERIALS AND METHODS

This study protocol was reviewed and approved by the University of Nebraska Medical Center Institutional Animal Care and Use Committee. Timed pregnant CD1 mouse dams were obtained from Charles River Laboratory (Wilmington, MA). The CD1 strain was chosen due to the high rate of moderate-to-severe injury and low mortality after HIBI (Sheldon et al., 1998). Because the overall goal of this research was to identify potential miRNA targets for therapeutic intervention rather than the identification of biomarkers that can differentiate between hypoxia and HIBI or between levels of HIBI severity, the study was not powered to stratify by severity and a hypoxia-only group was not used. After delivery, pups were maintained in a 12-h light and 12-h dark environment with the dam and littermates. At postnatal day 9, pups of both sexes were randomized to HIBI or control (4 pups/group). The HIBI groups were induced with 5% isoflurane and then were anesthetized with 2.5% isoflurane. Analgesia was provided by injection of 2 mg/kg bupivacaine at the incision site. A small vertical incision was made in the midline of the ventral neck and the neck was dissected in order to identify, isolate, and cauterize the right common carotid artery (Sheldon et al., 1998). Surgeries took no longer than 5 min. The control group underwent the same anesthesia, analgesia, and dissection, but the neck was closed without vessel ligation. Pups were maintained at normothermia (34–36°C skin temperature with infrared thermometry (Goodrich, 1977; Mei et al., 2018)) throughout surgery and recovery. Once the pups were fully recovered, they were returned to the dam and littermates for a 2-h recovery period. After recovery, groups were again separated,

TABLE 1 | Sequences for each messenger RNA (mRNA) quantitative polymerase chain reaction primer.

mRNA	
ATF3 Forward	CCAGGTCTCTGCCTCAGAAG
ATF3 Reverse	CAAAGGGTGTCAGGTTAGCAA
BDNF Forward	ATTAGCGAGTGGGTCACAGC
BDNF Reverse	TCAGTTGGCCTTTGGATACC
EGR1 Forward	GAGCACCTGACCACAGAGTC
EGR1 Reverse	CGAGTCGTTTGGCTGGGATA
FOS Forward	GGTGAAGACCGTGTCAGGAG
FOS Reverse	CCTTCGGATTCTCCGTTTCT
NFKB2 Forward	GGCCGGAAGACCTATCCTAC
NFKB2 Reverse	AGGTGGGTCACTGTGTGTCA
SOCS3 Forward	GGTCACCCACAGCAAGTTTC
SOCS3 Reverse	GGTACTCGCTTTTGGAGCTG
SRXN1 Forward	ATGTACCTGGGAGCATCCAC
SRXN1 Reverse	GCTGCATGTGTCTTCTGAGC

and the HIBI group underwent 30 min at 8% oxygen in a hypoxia chamber (BioSpherix, Parish, NY) at normothermia while the sham control group spent the same 30 min separated from the dam but in a warm normoxic environment.

At 30 min after injury, pups were euthanized, the brain extracted quickly and the hemispheres separated. Each hemisphere was further dissected into three regions—cortex, striatum/thalamus, and cerebellum—and then immediately frozen on dry ice and stored at −80°C until analysis. The entire cortex was used for these analyses. The hippocampus was also dissected out but was not able to be analyzed due to low miRNA yield. Regional brain tissue was then homogenized using a dounce homogenizer with Qiazol Lysis Reagent (Qiagen, Hilden, Germany) and the RNA extracted using the RNeasy Lipid Tissue Mini kit (Qiagen) per the manufacturer instructions. The RNA concentration and integrity was determined through spectrophotometry (DeNovix DS-11, Wilmington, DE). Only samples with ratios of 260/280 nm absorbance >1.9 were used for analyses.

The RNA samples then underwent further quality confirmation through parallel capillary electrophoresis on a Fragment Analyzer (Agilent, Santa Clara, CA) and then were processed for high-throughput sequencing. For miRNA-Seq, libraries were prepared from 200 ng RNA per sample with the NEXTFLEX Small RNA Kit (PerkinElmer, Waltham, MA) per the manufacturer's instructions. The libraries were then sequenced on the Illumina NextSeq 550 platform (San Diego, CA). For the mRNA analyses, RNA samples underwent the CodeSet Hybridization protocol with the nCounter Mouse Neuroinflammation probes (Nanostring, Seattle, WA) overnight and then transferred to the nCounter MAX/FLEX (Nanostring) device for analysis.

mRNA panel findings were validated by qPCR for the mRNAs that were highly differentially expressed and/or were previously reported to have biological relevance in neonatal HIBI. The High-Capacity cDNA Reverse Transcription Kit (Applied Biosystems) was used to generate cDNA from 1 μg of RNA. qPCR was performed using the PowerUp SYBR Green Master Mix (Applied Biosystems, Waltham, MA) with specific primers for each of the target mRNAs (shown in **Table 1**). The expression of four housekeeping genes (GAPDH, HPRT1, PGK1 and RPLPO) and the efficiency of the primer pairs were examined in samples from HIBI and controls. HPRT1, PGK1 and RPLPO were uniformly expressed between the different experiment conditions but the PGK1 primer pair had the best percent efficiency of 104%, so cycle threshold (Ct) values were normalized to the housekeeping gene PGK1 and expression levels were calculated by the ΔΔCt method (Livak and Schmittgen, 2001). For validation of miRNA-Seq findings, we performed qPCR on five miRNAs: mmu-miR-128-2-5p, mmu-miR-155-5p, mmu-miR-1969, mmu-miR-335-5p, and mmu-miR-6240. We performed qPCR on eight brains per group. miRCURY LNA Reverse Transcription Kit (Qiagen) was used to generate cDNA from 200 ng of RNA. We performed qPCR using the miRCURY LNA SYBR Green qPCR kit (Qiagen) with manufacturer generated primers for each of the target mature miRNAs. Values were normalized to U6 as an endogenous control. Expression fold-change in the HIBI group compared to controls was reported after $\log_2$ transformation. All qPCR samples were run in triplicate.

For miRNA sequencing, results were aligned to mature mouse miRNA from miRBase using bowtie2 alignment, and differential expression analysis performed using EdgeR. A false discovery rate <0.05 or p-value < .05 was considered significant. Those miRNAs with inverse differential expression in the cortex and striatum/thalamus compared to cerebellum suggested specificity for ischemia, given that the cerebellum undergoes hypoxia but not ischemia in this model. Those with similar direction of differential expression in all three regions were suggested to be primarily affected by the systemic hypoxic injury. For Nanostring mRNA analyses, data were uploaded to nSolver for normalization and analysis. Expression pattern relationships between the three regions were assessed using unsupervised two-way (gene vs. sample) hierarchical clustering based on Euclidian distance using the Morpheus program (Broad Institute, Cambridge, MA). Correlation between Nanostring high-throughput results and qPCR were performed using linear regression with Prism version 9.2.0 (GraphPad, La Jolla, CA). Goodness of fit was determined using the R^2 value.

The miRNA KEGG pathway analyses were performed using Diana Tools (Vlachos et al., 2015) using Tarbase annotations, a p-value threshold of .05, and enrichment analysis by Fisher's exact test with hypergeometric distribution. The mRNA KEGG pathway analyses were performed using Ingenuity Pathway Analysis (Qiagen). For both analyses, pathway data were stratified by -log (p-value). Network visualization of mRNA-mRNA and miRNA-mRNA networks were obtained using Cytoscape (Institute for Systems Biology, Seattle, WA). The mRNAs demonstrating significant differential expression in each region were mapped to the BioGRID *Mus musculus* interactions archive (version 4.4.200). The nodes from the significant mRNAs were selected, and networks were generated using two degrees of connection (undirected) between those mRNA and the other mRNA included in the Nanostring Neuroinflammation panel. Those mRNAs with less than two connections were excluded from the network. Node fill

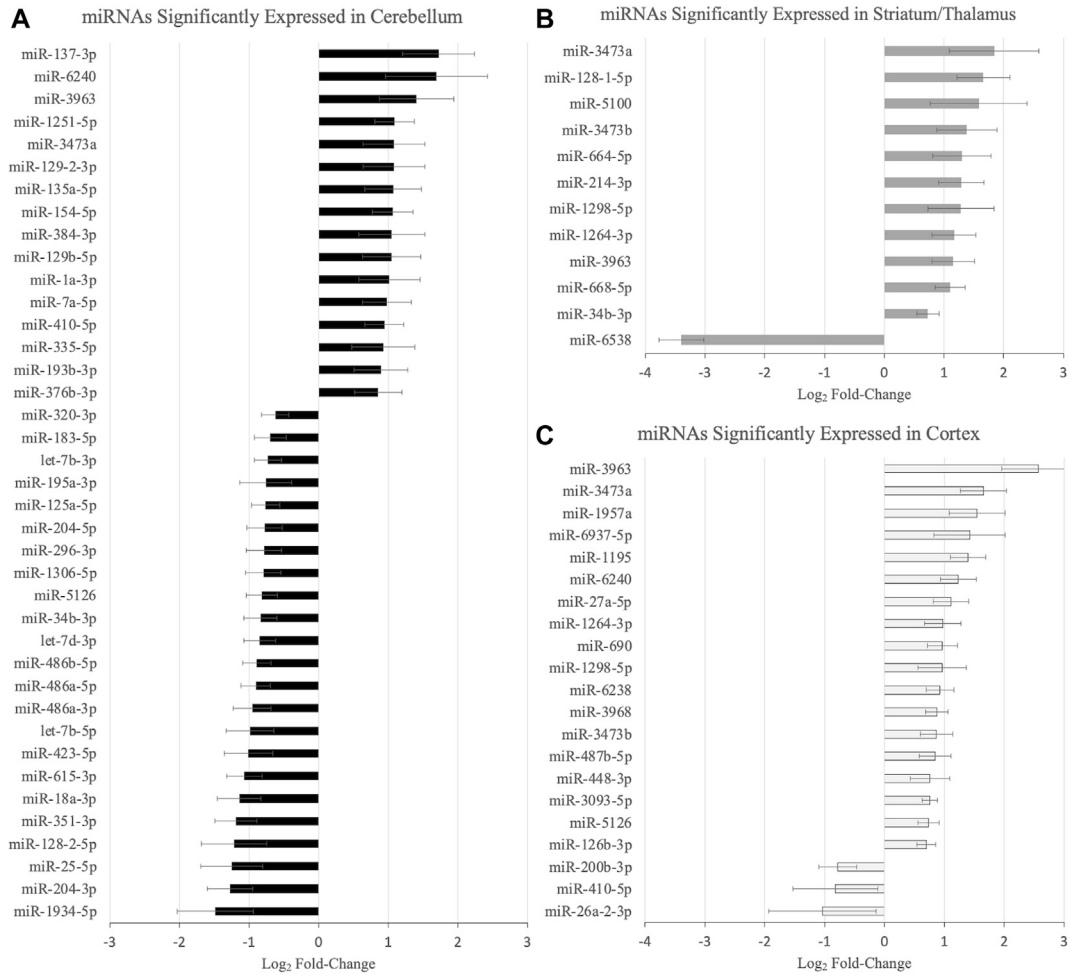

FIGURE 1 | MicroRNAs with significant differential expression at 30 min after hypoxic-ischemic brain injury in the **(A)** cerebellum, **(B)** striatum/thalamus, and **(C)** cortex (n = 4/group for each region). Significance defined by fold-change > 1.5, p value and/or false discovery rate < .05, and average count per million reads >10. Error bars represent standard error of the mean.

color relates to the log fold change of mRNA in hypoxic-ischemic brain injury compared to controls. The same process was used for the miRNA-mRNA networks, with the following exception: starting with the miRNAs that demonstrated significant differential expression, the miR2Gene pathway analysis (Qiu et al., 2011) was used to predict miRNA-mRNA interactions.

RESULTS

Figure 1 demonstrates the miRNAs with significant differential expression after neonatal HIBI compared to controls in each region. There were 39 miRNAs that were differentially expressed in the cerebellum (16 upregulated; 23 downregulated), 12 in the striatum/thalamus (11 upregulated; 1 downregulated), and 21 in the cortex (18 upregulated; 3 downregulated). In all, 61 unique miRNAs demonstrated significant differential expression in one or more region studied (shown in **Figure 2A**); nine of which had significant differential expression in more than one region. Of those miRNAs affected in multiple regions, miR-410-5p, -1264-3p, -1298-5p, -5,126, and -34b-3p all had inverse differential expression in the cortex and striatum/thalamus compared to the cerebellum. MiR-6240, -3,963, -3473a, and -3473b all had differential expression in the same direction for the three regions (shown in **Figure 2B**). The differentiation between cerebellar miRNA signaling and that of the cortex and striatum/thalamus was confirmed by two-way unsupervised clustering (shown in **Figure 2C**) demonstrating a clear separation of three of the four cerebellum samples from those of the other two regions.

Further assessment of the canonical pathways that are predicted to be affected by the miRNAs that were upregulated at 30 min after HIBI was performed by KEGG pathway analysis (shown in **Figure 2D**). The KEGG analysis demonstrated that the miRNAs with altered regulation in this study primarily alter metabolic pathways, including that of fatty acid metabolism and biosynthesis, lysine metabolism, steroid biosynthesis, AMPK signaling, and sphingolipid metabolism. Many of the

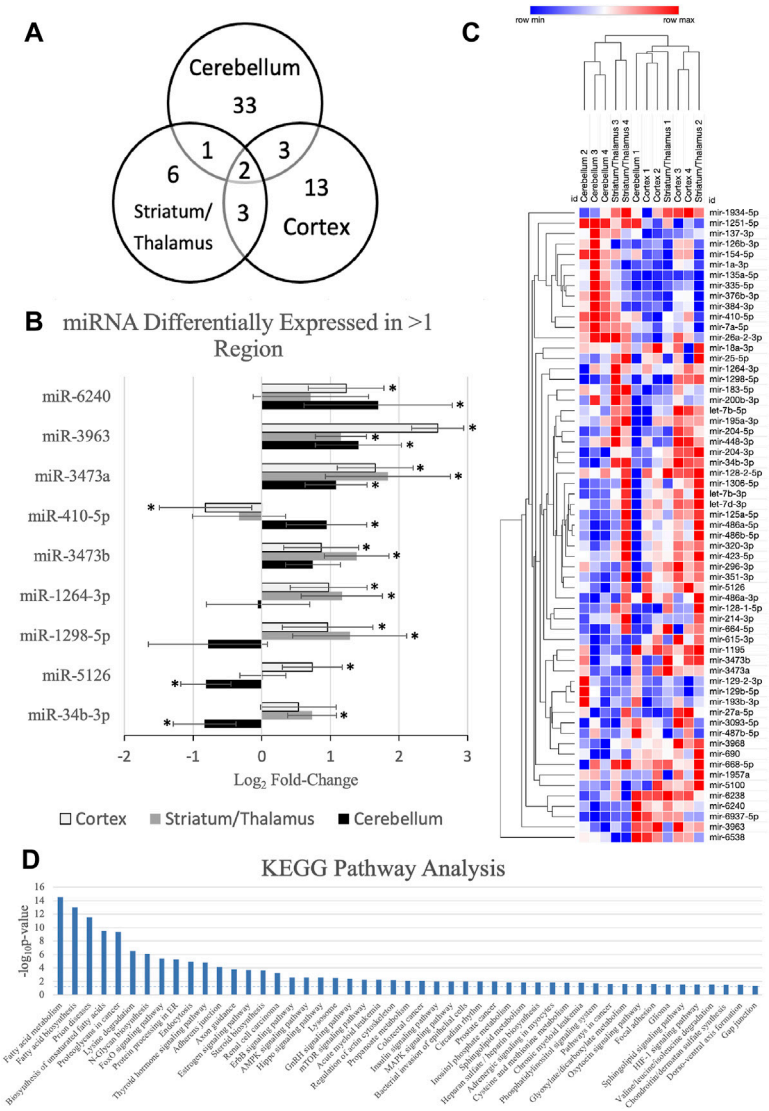

FIGURE 2 | MicroRNAs (miRNA) with significant differential expression in more than one region. **(A)** Venn diagram demonstrating the number of miRNAs with significant differential expression and the overlap between each region; **(B)** differential expression of the nine miRNAs with significant differential expression in more than one region (*regional expression significant, as defined by fold-change > 1.5, p value < .05, and average count per million reads >10); **(C)** two-way unsupervised clustering of differentially expressed microRNAs demonstrating separation of the majority of the cerebellum samples from the cortex and striatum/thalamus samples. Rows represent microRNA species and columns represent samples. Each square represents expression in a single sample, color-coded for magnitude of change relative to controls; and **(D)** KEGG pathway analysis of the miRNAs with significant differential expression. Error bars represent standard error of the mean.

traditional hypoxia and cell death pathways, including mTOR, MAPK, and HIF-1 were also included in the KEGG analysis, but had a lower -log (p-value).

In order to further evaluate the effects of miRNA alterations on mRNA levels in the early period after HIBI, mRNA levels were also assessed at 30 min after injury using the Nanostring Neuroinflammation Panel. **Figure 3** shows the 44 mRNAs that were differentially expressed in at least one region; 16 demonstrating significant differential expression in two or more regions (shown in **Figure 3A**). Of note, all mRNAs that had significant differential expression demonstrated increased expression after HIBI relative to controls (shown in **Figure 3B**). Only a few mRNAs in the figure showed downregulation in any of the three regions (for instance, Eomes in the cerebellum and cortex); however, in each case this downregulation did not reach statistical significance.

KEGG mRNA pathway analysis demonstrated that the mRNAs that are upregulated at 30 min after HIBI are largely involved in inflammatory and cell death pathways, including interleukin (IL-3, -8, -10, -17A), TNF receptor, HIF1α, and PI3K

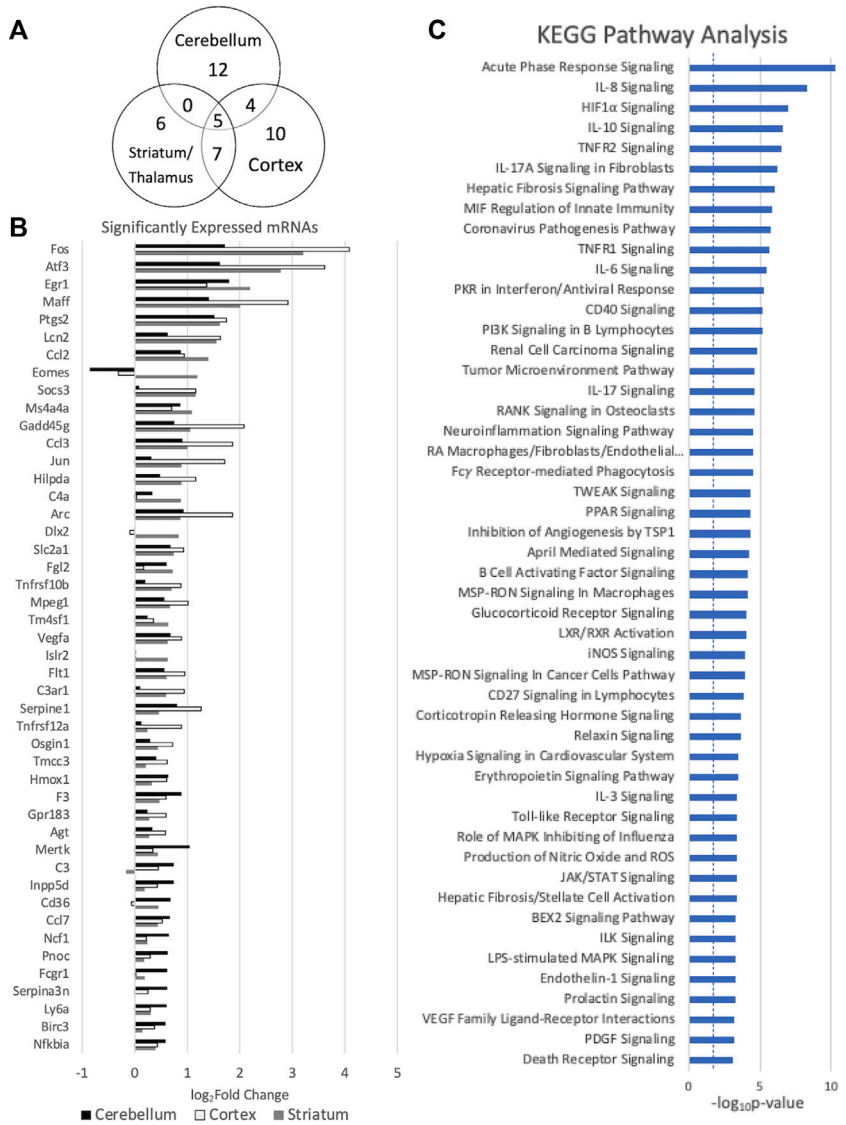

FIGURE 3 | Messenger RNAs (mRNA) with significant differential expression in more than one region. **(A)** Venn diagram demonstrating the number of mRNAs with significant differential expression and the overlap between each region; **(B)** differential expression of the mRNAs with significant differential expression in at least one region (significance defined by fold-change > 1.5 and *p* value and/or false discovery rate < .05), *n* = 4/group for each region; and **(C)** KEGG analysis demonstrating the canonical pathways affected by all of the mRNAs demonstrating significant differential expression. Error bars represent standard error of the mean.

signaling (shown in **Figure 3C**). For the mRNA KEGG analysis, 335 pathways were identified as significant; the top 50 were included in the figure.

Figure 4 demonstrates the mRNA-mRNA network connections between those mRNAs with significant differential expression 30 min after HIBI and up to two degrees of connection with the other mRNAs analyzed in this study. The differentially regulated genes that were consistently demonstrated to be highly integrated into all three regional networks included Atf3, Fos, Arc, Jun, and Tlr. Two miRNA species that were significantly differentially expressed in the cortex were closely associated with mRNAs that were also found to have significant differential expression: miR-1195 and -690 (shown in **Figure 5**). MiR-1195 was associated with Tnfsf10b and miR-690 with Egr1. There were no significant miRNA-mRNA networks in either the striatum/thalamus or the cerebellum.

For validation of high-throughput mRNA data, qPCR was performed on each of the samples for seven of the mRNAs with significant differential expression. **Figure 6** shows very strong correlation ($R^2 = 0.894$) between the Nanostring values and the qPCR values for all three regions and all seven mRNA species. Four miRNAs also demonstrated consistent directional

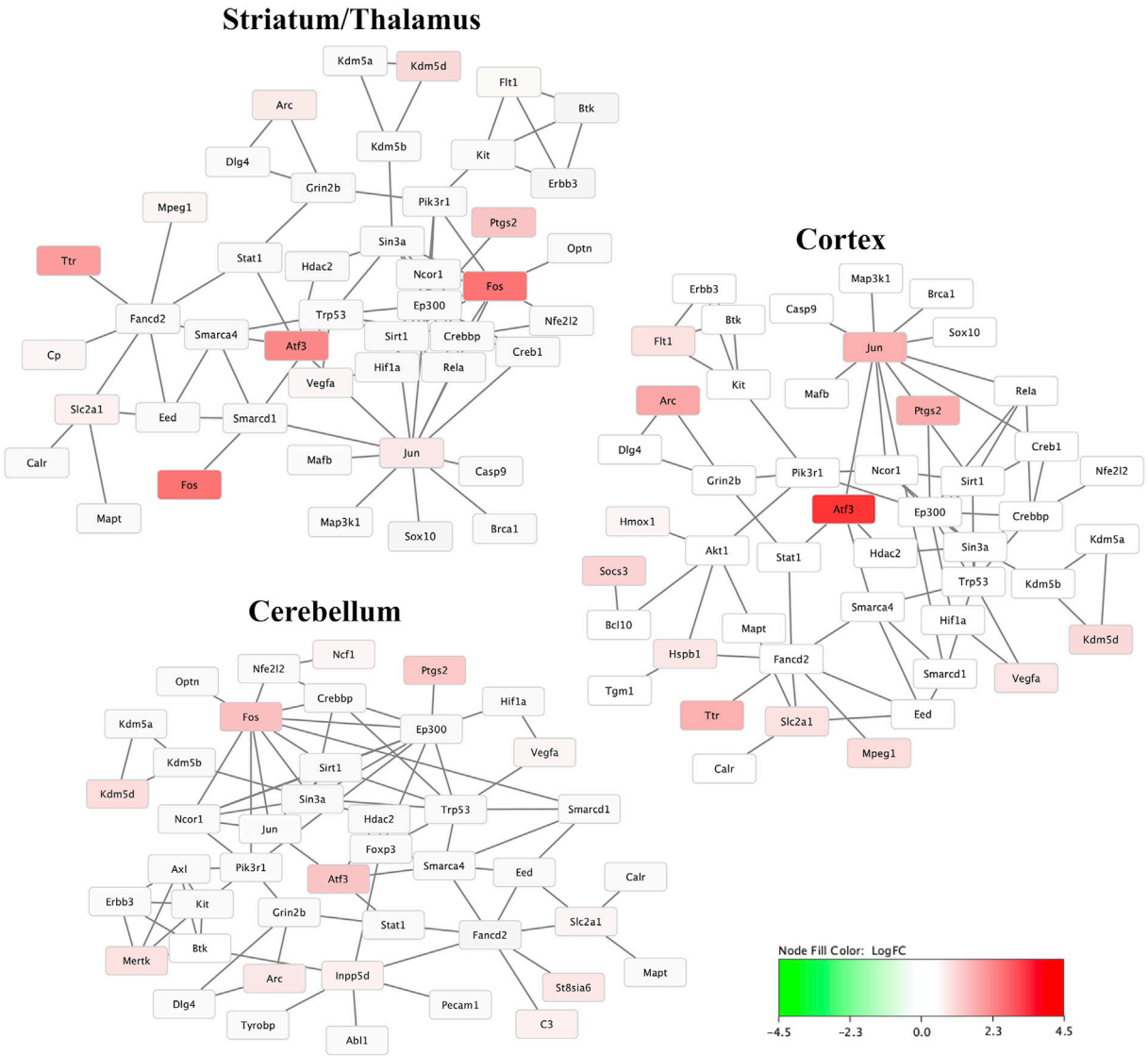

FIGURE 4 | Messenger RNA (mRNA) networks in each region representing the mRNA with significant differential expression after hypoxic-ischemic brain injury versus controls and two degrees of connection between those mRNA and the other mRNA analyzed in this study. Not shown are any mRNAs with no, or only one, connection. Node fill color relates to the log fold change of mRNA in hypoxic-ischemic brain injury compared to controls.

differential expression in striatum/thalamus qPCR compared to miRNA Seq: miR-128-2-5p (log_2FC -0.36 vs -0.28), miR-155-5p (log_2FC -0.50 vs. -0.98), miR-1969 (log_2FC 0.07 vs. 0.44), and miR-335-5p (log_2FC -0.54 vs. -2.35). One miRNA had inverse direction: miR-6240 (log_2FC 0.10 in miRNA-Seq vs. -0.98 in qPCR).

DISCUSSION

This study represents the first brain region-specific profiling of miRNA expression after neonatal HIBI, finding 61 unique miRNAs with significant differential expression in at least one of the three regions studied. Additionally, Nanostring mRNA panel analyses were performed in order to attempt to link the miRNA changes that were seen to alterations in relevant mRNA pathways. Only two miRNAs were found to have direct pathway links to the mRNAs with significant differential expression, underscoring the differences in pathway targeting that were seen between the mRNAs and miRNAs. While the altered mRNAs were mostly made up of immediate early genes (IEG) such as Fos, Jun, and Arc that were associated with downstream inflammatory and apoptotic pathways on KEGG analysis, the miRNAs that demonstrated significant differential expression were mostly associated with pathways of metabolism and synthesis. Although any conclusions regarding pathway analyses must take into consideration the limited scope of the mRNA analyses (using a specific panel rather than whole genome

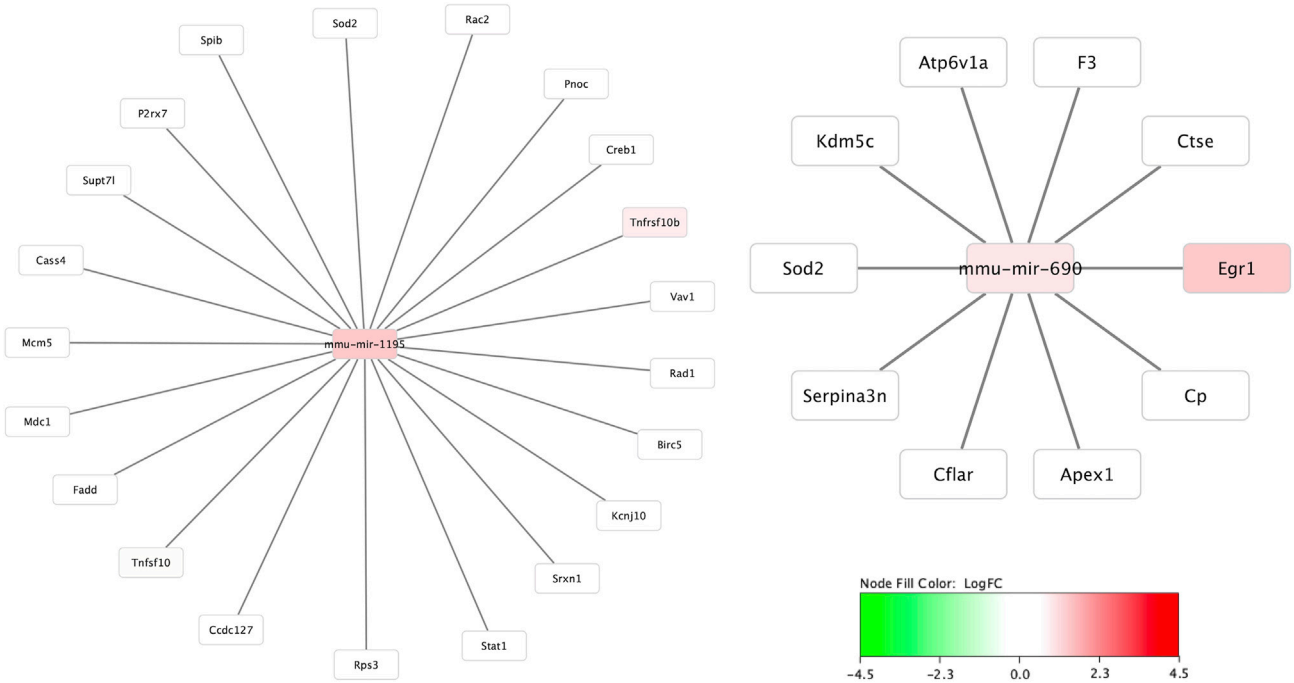

FIGURE 5 | MicroRNA to messenger RNA (miRNA-mRNA) networks in the cortex. The only two miRNAs that demonstrated significant differential expression at 30 min and were closely linked to mRNAs also significantly altered at 30 min after injury were miR-1195 and -690. Neither the striatum/thalamus nor cerebellum expression data resulted in significant miRNA-mRNA networks.

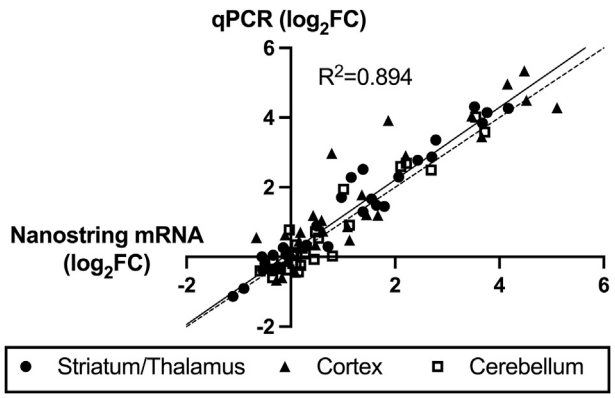

FIGURE 6 | Correlation between Nanostring RNA sequencing and quantitative polymerase chain reaction (qPCR) validation of seven highly expressed mRNAs. The *x*-axis values are Nanostring $\log_2$ fold-change (FC, hypoxic-ischemic brain injury versus control) values and *y*-axis are qPCR $\Delta\Delta$Ct $\log_2$FC values. The solid line represents the best-fit regression of the data points with strong correlation ($R^2 = 0.894$) and the dashed line represents the ideal correlation line (x = y).

analyses), these data suggest differing roles of mRNAs versus miRNAs in the first 30 min after neonatal hypoxic-ischemic brain injury.

Most of the mRNAs that demonstrated significant differential expression at 30 min after HIBI were IEGs, including Atf3, Fos, Arc, Jun, and Tlr; IEGs that are largely involved in inflammatory and cell death pathways, including interleukin (IL-3, -8, -10, -17A), TNF receptor, HIF1α, and PI3K signaling. IEGs are genes that are rapidly transcribed in response to positive (e.g., neuronal activity) or negative (e.g., injury) stimuli and often act as transcription factors and DNA-binding proteins (Minatohara et al., 2016). The regulation of the IEGs is complex but, of importance for the current study, is closely tied with miRNA expression. IEGs can directly regulate the expression of various miRNAs (Avraham et al., 2010). Specifically, Atf3 expression has been shown by multiple investigator groups to be regulated largely by a negative miRNA-based feedback loop (Tindall and Clerk, 2014; Aitken et al., 2015). Stimulating IEG expression briefly inhibits production of the negative feedback miRNAs (Tindall and Clerk, 2014; Aitken et al., 2015). This feedback relationship is a likely cause of the lack of predicted miRNA-mRNA interaction seen in the current study; when IEGs are highly expressed, their associated miRNAs are repressed, and vice versa. Additional studies will be necessary to further investigate the mechanisms for early miRNA- and mRNA-mediated changes (e.g., it is possible that miRNAs do not interact in a typical way with the RNA-induced silencing complex during the acute phase of injury) and to assess miRNA-mRNA interactions at later time points after injury.

Compared to the IEG mRNA expression, the miRNA KEGG analysis demonstrated that the miRNAs with altered regulation were primarily associated with metabolic pathways, which is consistent with the understanding that one of the primary deficiencies in neonatal HIBI is metabolic

failure (Sánchez-Illana et al., 2017). The targeted pathways include the ceramide and glycosphingolipid synthetic pathways which are known to be altered by HIBI, with decreased ceramide and sphingomyelin levels present for up to 7 days after preterm HIBI (Vlassaks et al., 2013). The glycosphingolipid pathways are predicted to be altered by miR-6240 (which inhibits Fut1) as well as miR-1264-3p (which inhibits Fut9) (Kanehisa and Goto, 2000). Sterol synthesis and metabolism has also been found to be altered after neonatal HIBI (Dave and Peeples, 2021). One of the primary genes in sterol synthesis is 3-hydroxy-3-methylglutaryl-CoA reductase (HMGCR) may be altered by several of the miRNAs in the current study—including miR-6240, -410-5p, -3473a, -3473b, -1264-3p, and -1298-5p—through the AMPK pathway (Hardie, 2011).

Neonatal HIBI is a triphasic injury. The primary phase starts with the initial hypoxic-ischemic insult leading to primary energy failure and hypoperfusion and continues for the first minutes to few hours after injury. While the secondary phase is primarily characterized by apoptotic cell death, the primary phase consists mainly of necrotic and necroptotic cell death (Hassell et al., 2015). Necroptosis, also termed programmed necrosis, can occur through several pathways and has been shown to be activated by the ErbB (Hu et al., 2021), mTOR (Liu et al., 2014), and HIF1α (Yang et al., 2017) pathways, which were all predicted targets by the differentially expressed miRNAs in our study (shown in **Figure 2D**). Additionally, miR-214, which demonstrated increased expression in the striatum/thalamus after HIBI in our data has also been associated with necroptosis regulation in other inflammatory diseases (Ou et al., 2019).

To date, there have been very few confirmatory studies of the *in silico* predicted effects of some of the miRNAs with altered expression in multiple regions, including miR-1298, -6240, and -5126. Similarly, although miR-3963 has been found to be highly upregulated in microglia in the developing brain (Varol et al., 2017), it has not otherwise been well studied and it's conservation between mammalian species is not known. Several of the other promising miRNA targets, however, have demonstrated some potential for neuroprotection in previous studies. For instance, miR-3473a, which was upregulated in all three regions in the current study, was one of the miRNAs found to be downregulated in the brain after preconditioning, suggesting that the relative decrease in expression may play a role in the neuroprotective effects of preconditioning (Miao et al., 2020). Additionally, miR-34b, which demonstrated increased expression in the striatum and thalamus, has been shown to increase cell apoptosis through increased p53 and Bax and decreased BCL2 (Zhang et al., 2020).

Other miRNAs that were differentially expressed in multiple regions include miR-1264, which demonstrated increased expression in the cortex, striatum, and thalamus. Similar to our findings, in adult stroke, upregulated miR-1264 expression was noted immediately after injury, peaking around 3 h after injury (Uhlmann et al., 2017). Inhibition of miR-1264 attenuates apoptosis through targeting WNT/β-catenin signaling (Zou et al., 2021). Lastly, miR-410 was found in the current study to be downregulated in the cortex and upregulated in the cerebellum at 30 min after injury. It was also downregulated in umbilical cord blood (Looney et al., 2015) as well as in circulating blood within 6 h after delivery (Meng et al., 2021) in infants diagnosed with HIE. Overexpression of miR-410 attenuated apoptosis and inflammation in OGD models using both PC12 and SH-SY5Y cell lines (Meng et al., 2021). Furthermore, mesenchymal stem cell derived extracellular vesicles that were neuroprotective when injected intraperitoneally after neonatal HIBI lost their positive effects on cerebral edema and infarct size after treatment with miR-410 antagonist (Han et al., 2021).

When considering the development of miRNA-targeted therapies, it is important to consider timing of intervention. While intervention for neonatal hypoxic-ischemic encephalopathy at 30 min after injury is unlikely to be clinically feasible, the results of the current study can be taken in combination with our previous results (Peeples et al., 2022) to identify those miRNAs that are persistently altered throughout the first few days after injury. For instance, miR-3473b demonstrated increased expression in both the striatum/thalamus and cortex at 30 min after injury and remained elevated at 72 h after injury in our previous study. Consistent with the multiphasic miRNA response that we previously described, however, many of the miRNAs either demonstrated altered regulation early at 30 min without differences at 24 or 72 h (e.g., miR-125a, -410, and -1264) or were altered later at 24 and/or 72 h but did not demonstrate regional differences at 30 min (e.g., miR-182, -2137, and -342). These data further support the importance of taking into account the timing after injury when considering miRNA-based interventions.

In addition to providing insight into potential miRNA targets early after neonatal HIBI, this study also demonstrated that the cerebellum had a unique miRNA profile from either of the other two regions (shown in **Figure 2C**), likely due to its sparing from the ischemic injury induced by the carotid artery ligation (Vannucci et al., 1988). Our previous study suggested that the contralateral brain is not an appropriate internal control for miRNA studies, at least in the subacute phase after neonatal HIBI (Peeples et al., 2022). Although this study only assessed the miRNA profiles at 30 min after injury, the findings here suggest that contrary the contralateral hemisphere at 24 h after injury, the cerebellum has a distinct miRNA expression profile, at least in the first hour after injury.

There are a few limitations to this study that warrant discussion. Even though the inclusive expression cutoffs (FDR < 0.05 or $p < .05$) in this study minimized type II error in the setting of this exploratory study, this methodology could increase the risk for type I error. Although the goal of the current study was to seek out potential therapeutic miRNA targets for HIBI, the lack of a hypoxia-only control group to allow for better mechanistic understanding could be considered a limitation. Though it may be reasonable to consider the cerebellum group as a hypoxia-only group, in comparing the cortex and striatum/thalamus data to the cerebellum it is not possible to separate whether differences are related to the inter-region differences or due to differences between hypoxia only and HIBI. Additionally, the mRNA analyses in this study were limited to only those

mRNAs included in the Nanostring Neuroinflammation panel. Although this panel contains 770 genes relevant to neuroinflammation and brain injury, the network analyses performed were restricted to only those genes in the panel. Also, although all HIBI-injured brains demonstrated visible injury, this study did not include the sample size necessary to stratify results based on characteristics such as severity of brain injury or sex. Though the sample size was limited and therefore may not detect small differences between groups, based on the highly differentially expressed miRNA data (such as miR-2137) from our previous work (Peeples et al., 2022), four animals per group provides 80% power at an alpha level of 0.05 to detect similar differences. Future larger studies would be needed to define whether injury severity or sex affect miRNA expression after HIBI. Lastly, we were unable to study individual hippocampal sections due to low miRNA yield. Future studies assessing hippocampal RNA signaling in this model could consider pooling samples.

In conclusion, this study demonstrated that miRNA expression varies by brain region after neonatal HIBI, and that the cerebellar miRNA profile is clearly distinct from those of the striatum/thalamus and cortex. Although miRNA-mRNA interactions may play more significant roles outside of the immediate period after HIBI, most of the mRNAs with significant differential expression in this study were IEGs associated with downstream inflammatory and cell death pathways that were mostly distinct from the miRNA-targeted metabolic pathways. Future studies assessing brain miRNA expression to guide therapy development should consider evaluating individual brain regions rather than whole brain to ensure the sensitivity needed for the development of targeted therapies.

DATA AVAILABILITY STATEMENT

The datasets presented in this study can be found in online repositories. The names of the repository/repositories and accession number(s) can be found below: https://www.ncbi.nlm.nih.gov/geo/, GSE184997.

ETHICS STATEMENT

The animal study was reviewed and approved by University of Nebraska Medical Center Institutional Animal Care and Use Committee.

AUTHOR CONTRIBUTIONS

EP participated in the conception and design, acquisition of data, interpretation of data, and drafting and critical revision of the manuscript. NES and WS participated in the acquisition of data, analysis of data and critical revision of the manuscript. KM participated in the interpretation of data and critical revision of the manuscript. All authors provided final approval of the version to be published.

FUNDING

Research reported in this manuscript was supported by the Child Health Research Institute at Children's Hospital & Medical Center and the University of Nebraska Medical Center.

ACKNOWLEDGMENTS

The authors wish to thank Dr. Zeljka Korade for her support and mentorship throughout the course of this project, as well as the University of Nebraska DNA Sequencing Core which receives partial support from the NIGMS (INBRE P20GM103427-14 and COBRE 1P30GM110768-01) grants and The Fred & Pamela Buffett Cancer Center Support Grant (P30CA036727) for performing the miRNA sequencing. We also thank the Bioinformatics and Systems Biology Core at UNMC, which receives support from Nebraska Research Initiative and NIH (2P20GM103427 and 5P30CA036727) grants, for providing data analysis services.

REFERENCES

Aitken, S., Magi, S., Alhendi, A. M. N., Itoh, M., Kawaji, H., Lassmann, T., et al. (2015). Transcriptional Dynamics Reveal Critical Roles for Non-coding RNAs in the Immediate-Early Response. *Plos Comput. Biol.* 11 (4), e1004217. doi:10.1371/journal.pcbi.1004217

Avraham, R., Sas-Chen, A., Manor, O., Steinfeld, I., Shalgi, R., Tarcic, G., et al. (2010). EGF Decreases the Abundance of microRNAs that Restrain Oncogenic Transcription Factors. *Sci. Signal.* 3 (124), ra43. doi:10.1126/scisignal.2000876

Casey, S., Goasdoue, K., Miller, S. M., Brennan, G. P., Cowin, G., O'Mahony, A. G., et al. (2020). Temporally Altered miRNA Expression in a Piglet Model of Hypoxic Ischemic Brain Injury. *Mol. Neurobiol.* 57 (10), 4322–4344. doi:10.1007/s12035-020-02018-w

Cheong, J. L., Coleman, L., Hunt, R. W., Lee, K. J., Doyle, L. W., Inder, T. E., et al. (2012). Prognostic Utility of Magnetic Resonance Imaging in Neonatal Hypoxic-Ischemic Encephalopathy: Substudy of a Randomized Trial. *Arch. Pediatr. Adolesc. Med.* 166 (7), 634–640. doi:10.1001/archpediatrics.2012.284

Dave, A. M., and Peeples, E. S. (2021). Cholesterol Metabolism and Brain Injury in Neonatal Encephalopathy. *Pediatr. Res.* 90, 37–44. doi:10.1038/s41390-020-01218-3

Garberg, H. T., Huun, M. U., Baumbusch, L. O., Åsegg-Atneosen, M., Solberg, R., and Saugstad, O. D. (2017). Temporal Profile of Circulating microRNAs after Global Hypoxia-Ischemia in Newborn Piglets. *Neonatology* 111 (2), 133–139. doi:10.1159/000449032

Goodrich, C. A. (1977). Measurement of Body Temperature in Neonatal Mice. *J. Appl. Physiol.* 43 (6), 1102–1105. doi:10.1152/jappl.1977.43.6.1102

Han, J., Yang, S., Hao, X., Zhang, B., Zhang, H., Xin, C., et al. (2021). Extracellular Vesicle-Derived microRNA-410 from Mesenchymal Stem Cells Protects against Neonatal Hypoxia-Ischemia Brain Damage through an HDAC1-dependent EGR2/Bcl2 Axis. *Front. Cel Dev. Biol.* 8, 579236. doi:10.3389/fcell.2020.579236

Hardie, D. G. (2011). AMP-activated Protein Kinase: a Cellular Energy Sensor with a Key Role in Metabolic Disorders and in Cancer. *Biochem. Soc. Trans.* 39 (1), 1–13. doi:10.1042/bst0390001

Hassell, K. J., Ezzati, M., Alonso-Alconada, D., Hausenloy, D. J., and Robertson, N. J. (2015). New Horizons for Newborn Brain protection: Enhancing Endogenous

Neuroprotection. *Arch. Dis. Child. Fetal Neonatal. Ed.* 100 (6), F541–F552. doi:10.1136/archdischild-2014-306284

Hu, X., Xiao, G., He, L., Niu, X., Li, H., Lou, T., et al. (2021). Sustained ErbB Activation Causes Demyelination and Hypomyelination by Driving Necroptosis of Mature Oligodendrocytes and Apoptosis of Oligodendrocyte Precursor Cells. *J. Neurosci.* 41, 9872. doi:10.1523/jneurosci.2922-20.2021

Hua, Y. J., Tang, Z. Y., Tu, K., Zhu, L., Li, Y. X., Xie, L., et al. (2009). Identification and Target Prediction of miRNAs Specifically Expressed in Rat Neural Tissue. *BMC genomics* 10 (1), 214. doi:10.1186/1471-2164-10-214

Jacobs, S. E., Berg, M., Hunt, R., Tarnow-Mordi, W. O., Inder, T. E., and Davis, P. G. (2013). Cooling for Newborns with Hypoxic Ischaemic Encephalopathy. *Cochrane Database Syst. Rev.* (1), CD003311. doi:10.1002/14651858.CD003311.pub3

Kanehisa, M., and Goto, S. (2000). KEGG: Kyoto Encyclopedia of Genes and Genomes. *Nucleic Acids Res.* 28 (1), 27–30. doi:10.1093/nar/28.1.27

Li, B., Dasgupta, C., Huang, L., Meng, X., and Zhang, L. (2019). MiRNA-210 Induces Microglial Activation and Regulates Microglia-Mediated Neuroinflammation in Neonatal Hypoxic-Ischemic Encephalopathy. *Cell Mol. Immunol.* 17, 976. doi:10.1038/s41423-019-0257-6

Liu, Q., Qiu, J., Liang, M., Golinski, J., van Leyen, K., Jung, J. E., et al. (2014). Akt and mTOR Mediate Programmed Necrosis in Neurons. *Cell Death Dis.* 5 (2), e1084. doi:10.1038/cddis.2014.69

Livak, K. J., and Schmittgen, T. D. (2001). Analysis of Relative Gene Expression Data Using Real-Time Quantitative PCR and the 2−ΔΔCT Method. *Methods* 25 (4), 402–408. doi:10.1006/meth.2001.1262

Looney, A.-M., Walsh, B. H., Moloney, G., Grenham, S., Fagan, A., O'Keeffe, G. W., et al. (2015). Downregulation of Umbilical Cord Blood Levels of miR-374a in Neonatal Hypoxic Ischemic Encephalopathy. *J. Pediatr.* 167 (2), 269–273. doi:10.1016/j.jpeds.2015.04.060

Martinez-Biarge, M., Diez-Sebastian, J., Kapellou, O., Gindner, D., Allsop, J. M., Rutherford, M. A., et al. (2011). Predicting Motor Outcome and Death in Term Hypoxic-Ischemic Encephalopathy. *Neurology* 76 (24), 2055–2061. doi:10.1212/wnl.0b013e31821f442d

Mei, J., Riedel, N., Grittner, U., Endres, M., Banneke, S., and Emmrich, J. V. (2018). Body Temperature Measurement in Mice during Acute Illness: Implantable Temperature Transponder versus Surface Infrared Thermometry. *Sci. Rep.* 8 (1), 3526. doi:10.1038/s41598-018-22020-6

Meng, Q., Yang, P., and Lu, Y. (2021). MicroRNA-410 Serves as a Candidate Biomarker in Hypoxic-Ischemic Encephalopathy Newborns and Provides Neuroprotection in Oxygen-Glucose Deprivation-Injured PC12 and SH-Sy5y Cells. *Brain Behav.* 11 (8), e2293. doi:10.1002/brb3.2293

Miao, W., Yan, Y., Bao, T.-h., Jia, W.-j., Yang, F., Wang, Y., et al. (2020). Ischemic Postconditioning Exerts Neuroprotective Effect through Negatively Regulating PI3K/Akt2 Signaling Pathway by microRNA-124. *Biomed. Pharmacother.* 126, 109786. doi:10.1016/j.biopha.2019.109786

Michniewicz, B., Szpecht, D., Sowińska, A., Sibiak, R., Szymankiewicz, M., and Gadzinowski, J. (2020). Biomarkers in Newborns with Hypoxic-Ischemic Encephalopathy Treated with Therapeutic Hypothermia. *Childs Nerv Syst.* 36 (12), 2981–2988. doi:10.1007/s00381-020-04645-z

Minatohara, K., Akiyoshi, M., and Okuno, H. (2016). Role of Immediate-Early Genes in Synaptic Plasticity and Neuronal Ensembles Underlying the Memory Trace. *Front. Mol. Neurosci.* 8 (78), 78. doi:10.3389/fnmol.2015.00078

Ou, L., Sun, T., Cheng, Y., Huang, L., Zhan, X., Zhang, P., et al. (2019). MicroRNA-214 Contributes to Regulation of Necroptosis via Targeting ATF4 in Diabetes-associated Periodontitis. *J. Cel Biochem* 120 (9), 14791–14803. doi:10.1002/jcb.28740

Peeples, E. S., Sahar, N. E., Snyder, W., and Mirnics, K. (2022). Temporal Brain microRNA Expression Changes in a Mouse Model of Neonatal Hypoxic–Ischemic Injury. *Pediatr. Res.* 91 (1), 92–100. doi:10.1038/s41390-021-01701-5

Qiu, C., Wang, J., and Cui, Q. (2011). miR2Gene: Pattern Discovery of Single Gene, Multiple Genes, and Pathways by Enrichment Analysis of Their microRNA Regulators. *BMC Syst. Biol.* 5, S9 (Springer). doi:10.1186/1752-0509-5-S2-S9

Sánchez-Illana, Á., Núñez-Ramiro, A., Cernada, M., Parra-Llorca, A., Valverde, E., Blanco, D., et al. (2017). Evolution of Energy Related Metabolites in Plasma from Newborns with Hypoxic-Ischemic Encephalopathy during Hypothermia Treatment. *Scientific Rep.* 7 (1), 17039. doi:10.1038/s41598-017-17202-7

Sheldon, R. A., Sedik, C., and Ferriero, D. M. (1998). Strain-related Brain Injury in Neonatal Mice Subjected to Hypoxia-Ischemia. *Brain Res.* 810 (1-2), 114–122. doi:10.1016/s0006-8993(98)00892-0

Tindall, M. J., and Clerk, A. (2014). Modelling Negative Feedback Networks for Activating Transcription Factor 3 Predicts a Dominant Role for miRNAs in Immediate Early Gene Regulation. *Plos Comput. Biol.* 10 (5), e1003597. doi:10.1371/journal.pcbi.1003597

Uhlmann, S., Mracsko, E., Javidi, E., Lamble, S., Teixeira, A., Hotz-Wagenblatt, A., et al. (2017). Genome-Wide Analysis of the Circulating miRNome after Cerebral Ischemia Reveals a Reperfusion-Induced MicroRNA Cluster. *Stroke* 48 (3), 762–769. doi:10.1161/strokeaha.116.013942

Vannucci, R. C., Lyons, D. T., and Vasta, F. (1988). Regional Cerebral Blood Flow during Hypoxia-Ischemia in Immature Rats. *Stroke* 19 (2), 245–250. doi:10.1161/01.str.19.2.245

Varol, D., Mildner, A., Blank, T., Shemer, A., Barashi, N., Yona, S., et al. (2017). Dicer Deficiency Differentially Impacts Microglia of the Developing and Adult Brain. *Immunity* 46 (6), 1030–1044. doi:10.1016/j.immuni.2017.05.003

Vlachos, I. S., Zagganas, K., Paraskevopoulou, M. D., Georgakilas, G., Karagkouni, D., Vergoulis, T., et al. (2015). DIANA-miRPath v3.0: Deciphering microRNA Function with Experimental Support. *Nucleic Acids Res.* 43 (W1), W460–W466. doi:10.1093/nar/gkv403

Vlassaks, E., Mencarelli, C., Nikiforou, M., Strackx, E., Ferraz, M. J., Aerts, J. M., et al. (2013). Fetal Asphyxia Induces Acute and Persisting Changes in the Ceramide Metabolism in Rat Brain. *J. Lipid Res.* 54 (7), 1825–1833. doi:10.1194/jlr.m034447

Xiong, L., Zhou, H., Zhao, Q., Xue, L., Al-Hawwas, M., He, J., et al. (2020). Overexpression of miR-124 Protects against Neurological Dysfunction Induced by Neonatal Hypoxic-Ischemic Brain Injury. *Cell Mol Neurobiol* 40 (5), 737–750. doi:10.1007/s10571-019-00769-2

Yang, X.-S., Yi, T.-L., Zhang, S., Xu, Z.-W., Yu, Z.-Q., Sun, H.-T., et al. (2017). Hypoxia-inducible Factor-1 Alpha Is Involved in RIP-Induced Necroptosis Caused by *In Vitro* and *In Vivo* Ischemic Brain Injury. *Sci. Rep.* 7 (1), 5818. doi:10.1038/s41598-017-06088-0

Yuan, Y., Wang, J. Y., Xu, L. Y., Cai, R., Chen, Z., and Luo, B. Y. (2010). MicroRNA Expression Changes in the Hippocampi of Rats Subjected to Global Ischemia. *J. Clin. Neurosci.* 17 (6), 774–778. doi:10.1016/j.jocn.2009.10.009

Zhang, L., Ma, T., Tao, Q., Tan, W., Chen, H., Liu, W., et al. (2020). Bta-miR-34b Inhibits Proliferation and Promotes Apoptosis via the MEK/ERK Pathway by Targeting MAP2K1 in Bovine Primary Sertoli Cells. *J. Anim. Sci.* 98 (10), skaa313. doi:10.1093/jas/skaa313

Zou, L., Xia, P. F., Chen, L., and Hou, Y. Y. (2021). XIST Knockdown Suppresses Vascular Smooth Muscle Cell Proliferation and Induces Apoptosis by Regulating miR-1264/wnt5a/β-Catenin Signaling in Aneurysm. *Biosci. Rep.* 41 (3), BSR20201810. doi:10.1042/BSR20201810

Conflict of Interest: The authors declare that the research was conducted in the absence of any commercial or financial relationships that could be construed as a potential conflict of interest.

Publisher's Note: All claims expressed in this article are solely those of the authors and do not necessarily represent those of their affiliated organizations, or those of the publisher, the editors, and the reviewers. Any product that may be evaluated in this article, or claim that may be made by its manufacturer, is not guaranteed or endorsed by the publisher.

frontiers in Genetics

ORIGINAL RESEARCH
published: 11 March 2022
doi: 10.3389/fgene.2022.816460

Identification of an Iron Metabolism-Related lncRNA Signature for Predicting Osteosarcoma Survival and Immune Landscape

Shao Hong-bin[1†], *Yang Wan-jun*[2†], *Dong Chen-hui*[1†], *Yang Xiao-jie*[1†], *Li Shen-song*[1] *and Zhou Peng*[1*]

[1]Department of Joint Surgery, The 940 Hospital of PLA Joint Logistics Support Force, Lanzhou, China, [2]The Second Affiliated Hospital of Xi'an Medical College, Xi'an, China

OPEN ACCESS

Edited by:
Nadeem Shabir,
Sher-e-Kashmir University of Agricultural Sciences and Technology, India

Reviewed by:
Raja Ishaq Nabi Khan,
Indian Veterinary Research Institute (IVRI), India
Peerzada Tajamul Mumtaz,
University of Nebraska-Lincoln, United States

***Correspondence:**
Zhou Peng
zhoup940@163.com

[†]These authors have contributed equally to this work

Specialty section:
This article was submitted to RNA, a section of the journal Frontiers in Genetics

Received: 16 November 2021
Accepted: 21 February 2022
Published: 11 March 2022

Citation:
Hong-bin S, Wan-jun Y, Chen-hui D, Xiao-jie Y, Shen-song L and Peng Z (2022) Identification of an Iron Metabolism-Related lncRNA Signature for Predicting Osteosarcoma Survival and Immune Landscape. Front. Genet. 13:816460. doi: 10.3389/fgene.2022.816460

Background: Long noncoding RNAs (lncRNAs) act as epigenetic regulators in the process of ferroptosis and iron metabolism. This study aimed to identify an iron metabolism-related lncRNA signature to predict osteosarcoma (OS) survival and the immune landscape.

Methods: RNA-sequencing data and clinical information were obtained from the TARGET dataset. Univariate Cox regression and LASSO Cox analysis were used to develop an iron metabolism-related lncRNA signature. Consensus clustering analysis was applied to identify subtype-based prognosis-related lncRNAs. CIBERSORT was used to analyze the difference in immune infiltration and the immune microenvironment in the two clusters.

Results: We identified 302 iron metabolism-related lncRNAs based on 515 iron metabolism-related genes. The results of consensus clustering showed the differences in immune infiltration and the immune microenvironment in the two clusters. Through univariate Cox regression and LASSO Cox regression analysis, we constructed an iron metabolism-related lncRNA signature that included seven iron metabolism-related lncRNAs. The signature was verified to have good performance in predicting the overall survival, immune-related functions, and immunotherapy response of OS patients between the high- and low-risk groups.

Conclusion: We identified an iron metabolism-related lncRNA signature that had good performance in predicting survival outcomes and showing the immune landscape for OS patients. Furthermore, our study will provide valuable information to further develop immunotherapies of OS.

Keywords: osteosarcoma, iron metabolism, lncRNA, immune landscape, signature

INTRODUCTION

Osteosarcoma (OS) is the most common primary solid malignancy of the bone in children and adolescents, and the overall incidence is ~4.8 per million worldwide (Lancia et al., 2019; Pingping et al., 2019). The 5-year survival rate of patients with nonmetastatic disease reaches 70–75%; however, the long-term survival rate of metastatic OS is <25% (Anwar et al., 2020). In addition, resistance to chemotherapy or radiation treatments is a common problem for OS treatment (Strauss et al., 2010). Thus, there is an urgent need to identify more efficient targets and novel biomarkers for therapeutic treatment.

Iron is an indispensable element involved in many cellular processes, such as DNA synthesis, ATP production, and oxygen transport (Brown et al., 2020; Forciniti et al., 2020). Iron metabolism is usually divided into distinct processes, including iron acquisition, efflux, storage, and regulation, which is regulated by a set of iron-dependent proteins (Torti & Torti, 2013). Moreover, increasing evidence suggests that dysregulated iron homeostasis and excess iron are crucial risks for cancer development (Morales & Xue, 2021). Ferroptosis is an iron-dependent form of regulated cell death caused by excess levels of reactive oxygen species (ROS) and lipid peroxidation products (Stockwell et al., 2017; Chen et al., 2021). Emerging evidence shows that triggering ferroptosis has anticancer potential for cancer therapy (Liang et al., 2019; Xu et al., 2019).

As a type of noncoding RNA with a length of more than 200 nucleotides, long noncoding RNA (lncRNA) plays important roles in transcriptional regulation and epigenetic gene regulation (Mercer et al., 2009; Kumar & Goyal, 2017). In addition, accumulating evidence shows that lncRNAs act as epigenetic regulators to promote the process of ferroptosis and are involved in iron metabolism (Wu et al., 2020). For example, the report showed that lncRNA RP11-89 promoted tumorigenesis of bladder cancer and inhibited ferroptosis through PROM2-activated iron export (Luo et al., 2021). Another study suggested that lncRNA MT1DP improved the sensitivity of erastin-induced ferroptosis and increased the intracellular ferrous iron concentration in non-small-cell lung cancer (NSCLC) (Gai et al., 2020). However, there is still a lack of reports on the iron metabolism-related lncRNAs in osteosarcoma. Hence, there is an urgent need to develop novel iron metabolism-related lncRNA signatures for the diagnosis and prognosis of OS.

In this study, we downloaded RNA-sequencing and clinical data from Therapeutically Applicable Research to Generate Effective Treatments (TARGET) and obtained iron metabolism-related gene sets from the Molecular Signatures database v7.4 (MSigDB). Through univariate Cox regression and consensus clustering analysis, we estimated immune infiltration and clinical features in two prognosis-related lncRNAs and molecular subtypes. Then, we applied least absolute shrinkage and selection operator (LASSO) regression analysis to construct an iron metabolism-related lncRNA signature. Finally, we established nomograms to predict prognosis and developed a treatment strategy for OS patients. The workflow of the study is shown in **Figure 1**.

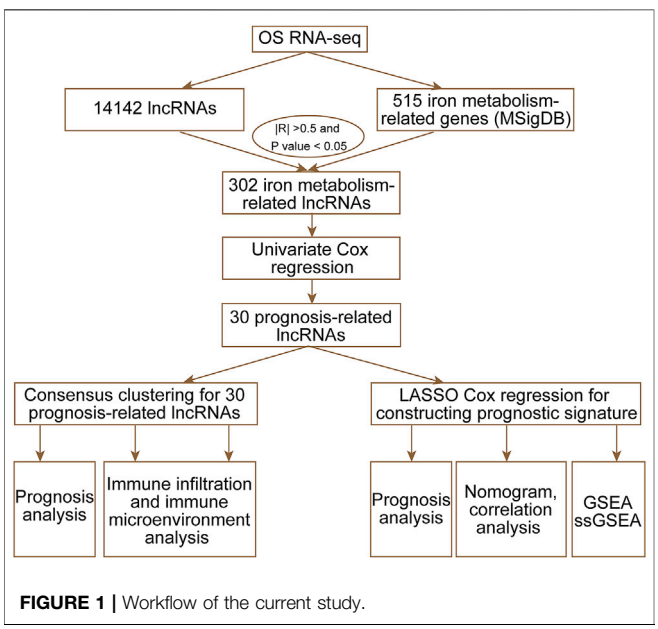

FIGURE 1 | Workflow of the current study.

METHODS

Data Collection and Preprocessing

RNA-seq data and clinical information of OS patients were downloaded from Therapeutically Applicable Research to Generate Effective Treatments (TARGET; https://ocg.cancer.gov/programs/target). Finally, we obtained 84 patients' RNA-seq data and clinical information. From the Molecular Signatures database v7.4 (MSigDB) (Liberzon et al., 2015), we extracted 515 iron metabolism-related genes from 15 iron metabolism-related gene sets.

Identification of Iron Metabolism-Related lncRNAs and Prognosis-Related lncRNAs

The Perl programming language was used to obtain the expression matrix of iron metabolism-related genes and lncRNAs from the TARGET dataset. The 302 iron metabolism-related lncRNAs were selected based on the criteria that the absolute value of the correlation coefficient was greater than 0.5 ($|R|>0.5$) and the p-value was less than 0.05 ($p < 0.05$). Through univariate Cox regression analysis, we identified 30 iron metabolism-related lncRNAs whose expression levels were significantly associated ($p < 0.05$) with the overall survival of OS patients.

Consensus Clustering

ConsensusCluster usually generates a consensus matrix heatmap and a log of selected features that distinguish each pair of clusters. Based on 30 prognosis-related lncRNAs, we applied the "ConsensusClusterPlus" software package (Wilkerson & Hayes, 2010) to perform consensus clustering analysis. Meanwhile, we

also obtained unbiased and unsupervised outcomes for approximately 84 OS patients. According to two different regulation patterns, we visualized the expression of 30 prognosis-related lncRNAs by using the R package "pheatmap" (Kolde, 2015).

Estimation of the Immune Microenvironment and Immune Infiltration

We estimated the parameters of the immune microenvironment (stromal score, immune score, and ESTIMATE score) through the "estimate" software package (Yoshihara et al., 2013) in Cluster 1 and Cluster 2. Moreover, we applied CIBERSORT (Newman et al., 2019) to analyze the expression matrix of immune cell subtypes between Cluster 1 and Cluster 2.

Construction and Evaluation of an Iron Metabolism-Related lncRNA Signature

LASSO Cox analysis was used to obtain an optimal iron metabolism-related lncRNA signature by using the R package "glmnet" (Friedman et al., 2010). Based on the best lambda value and coefficients, the risk score of each OS case could be obtained by the following algorithm:

$$\text{Risk Score} = \sum_{i=1}^{n} \text{Coef}_i * \text{E}_i,$$

where n, Coef_i, and E_i represent the number of signature genes, coefficient of a gene, and expression of a gene, respectively. The Kaplan–Meier survival curve was used to assess the overall survival of the high- and low-risk groups by using the R package "survival" (Lorent et al., 2014). Principal component analysis (PCA) was used to evaluate distribution patterns between high- and low-risk groups based on an iron metabolism-related lncRNA signature through the "ggplot2" software package (Gómez-Rubio, 2017). Moreover, the receiver-operating characteristic (ROC) curves were applied to evaluate the diagnostic efficacy of each clinicopathological characteristic and the prognostic signature through the "survivalROC" software package (Heagerty et al., 2000). Finally, we applied multivariate Cox regression analyses to evaluate the independent prognostic value between the risk score and other clinical variables, such as age, sex, and the prognosis stage by using the "forestplot" package (Gordon & Lumley, 2016).

Nomogram Construction

A nomogram was constructed to analyze the probable 1-, 3-, and 5-year overall survival of the OS patients by using the R package "rms" (Bandos et al., 2009). 3- and 5-year calibration curve analyses were used to evaluate the suitability of our nomogram.

Gene Set Enrichment Analysis

The "ConsensusClusterPlus" software package was used for enrichment. GSEA (http://www.broadinstitute.org/gsea/index.jsp) was used to evaluate the differentially enriched genes between the high- and low-risk groups. "c2. cp. kegg.v7.2. symbols. gmt" and "c5. go. v7.4. symbols. gmt" were used as the reference gene sets. The criterion of statistically significant enrichment was $|\text{NES}| > 1$ and p-value < 0.05.

TABLE 1 | Clinical features of all patients.

Feature	Group	TARGET dataset (n = 84)
		Number of patients (%)
Age	<16	48 (57.1)
	≥16	36 (42.9)
Gender	Female	36 (42.9)
	Male	48 (57.1)
Metastatic	Metastatic	21 (25.0)
	Non-metastatic	63 (75.0)
Histologic response	Stage 1/2	18 (21.4)
	Stage 3/4	16 (19.0)
Vital status	Alive	55 (65.5)
	Dead	29 (34.5)

Statistical Analysis

R software (version 4.0.2; https://cran.r-project.org/bin/windows/base/) and various R packages were used for all statistical analyses and visualization in this study. Perl (version 5.8.3; https://www.perl.org/get.html) was applied to integrate RNA-seq data and clinical information for screening prognosis-related genes. The criterion of statistical significance was p-value < 0.05.

RESULTS

Identification of Iron Metabolism-Related lncRNAs and Prognosis-Related lncRNAs

To identify iron metabolism-related lncRNAs, we first extracted 515 iron metabolism-related genes from 15 iron metabolism-related gene sets (**Supplementary Table S1**). Moreover, we obtained an expression matrix of 14,142 lncRNAs from RNA-sequencing data. According to the criteria $|R| > 0.5$ and p-value < 0.05, 302 lncRNAs were regarded as iron metabolism-related lncRNAs. Then, we combined the expression of 302 iron metabolism-related lncRNAs and clinical information to screen prognosis-related lncRNAs (**Table 1**). Univariate Cox regression analysis showed that 30 iron metabolism-related lncRNAs significantly correlated with the overall survival of OS patients (**Figure 2A**). Meanwhile, we found that the expression levels of 10 prognosis-related lncRNAs were negatively related to the survival rate, while 20 other lncRNA prognosis-related lncRNAs were positively associated with the survival rate.

Consensus Clustering by Prognosis-Related lncRNAs

To gain insight into the function of iron metabolism-related lncRNAs, we applied unsupervised consensus analysis to the expression levels of 30 prognosis-related lncRNAs. The results

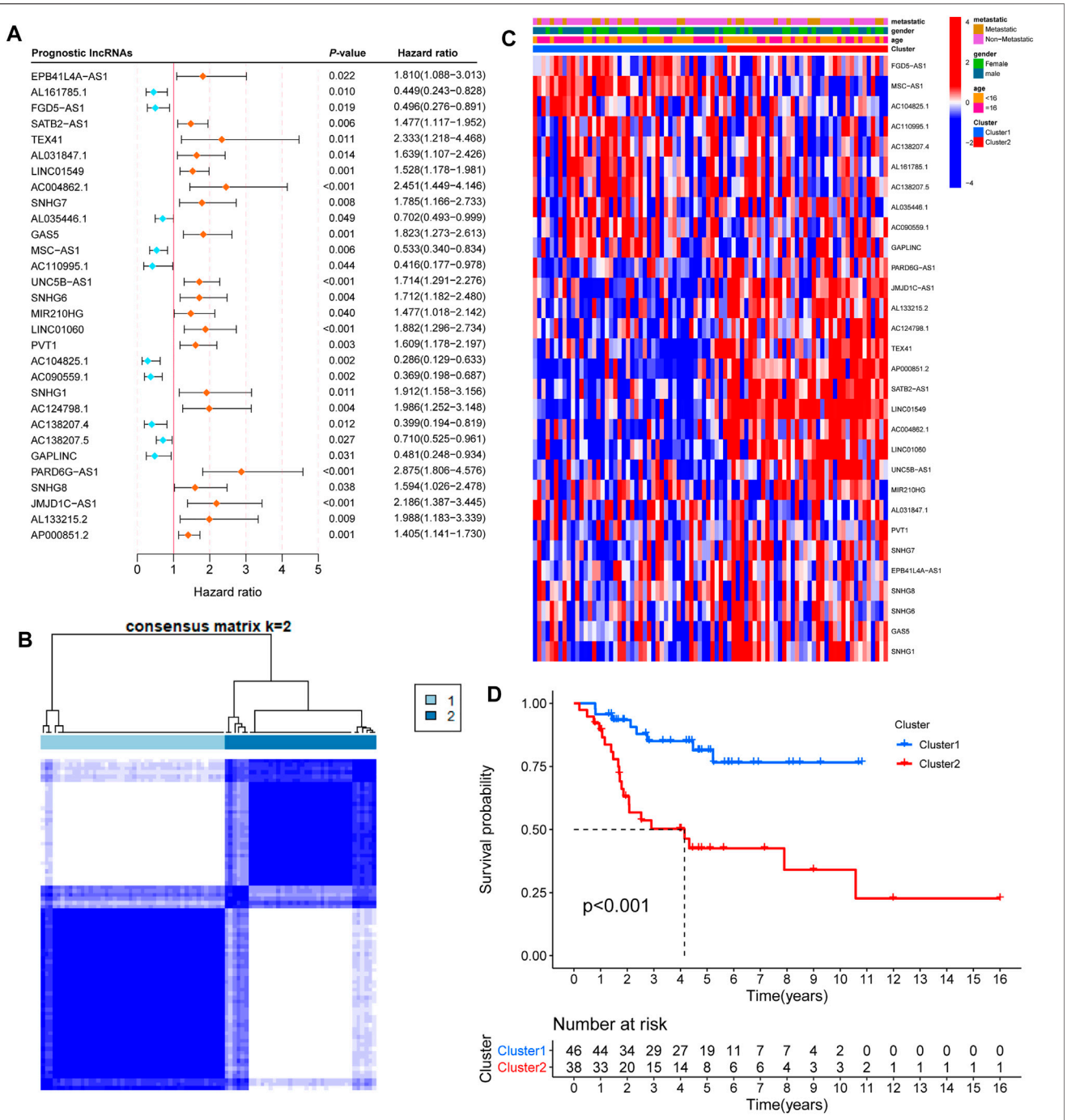

FIGURE 2 | Consensus clustering by prognosis-related lncRNAs. **(A)** Univariate Cox regression analysis showed that 30 iron metabolism-related lncRNAs significantly correlated with the overall survival of OS patients. Orange and bluish dots represent the point estimation of the hazard ratio. **(B)** The consensus score matrix of 84 samples when k = 2. **(C)** Heatmap with clinical information for 30 iron metabolism-related lncRNAs. **(D)** Kaplan–Meier curves of patients in two clusters.

showed that k = 2 seemed to be a more accurate and stable clustering. Meanwhile, Cluster 1 and Cluster 2 included 46 and 38 samples, respectively (**Figure 2B**). The results of k = 3–9 are shown in **Supplementary Figure S1**. Subsequently, we explored the difference between the two clusters. First, the heatmap of 30 prognosis-related lncRNAs showed differential expression in the two clusters (**Figure 2C**). Based on gender, age, and stage-specific characteristics, differential expression of 30 prognosis-related lncRNAs is shown in **Supplementary Figures S2A–C**. Additionally, the Kaplan–Meier survival curve analysis suggested that the overall survival of Cluster 2 patients was significantly shorter than that of Cluster 1 patients (**Figure 2D**).

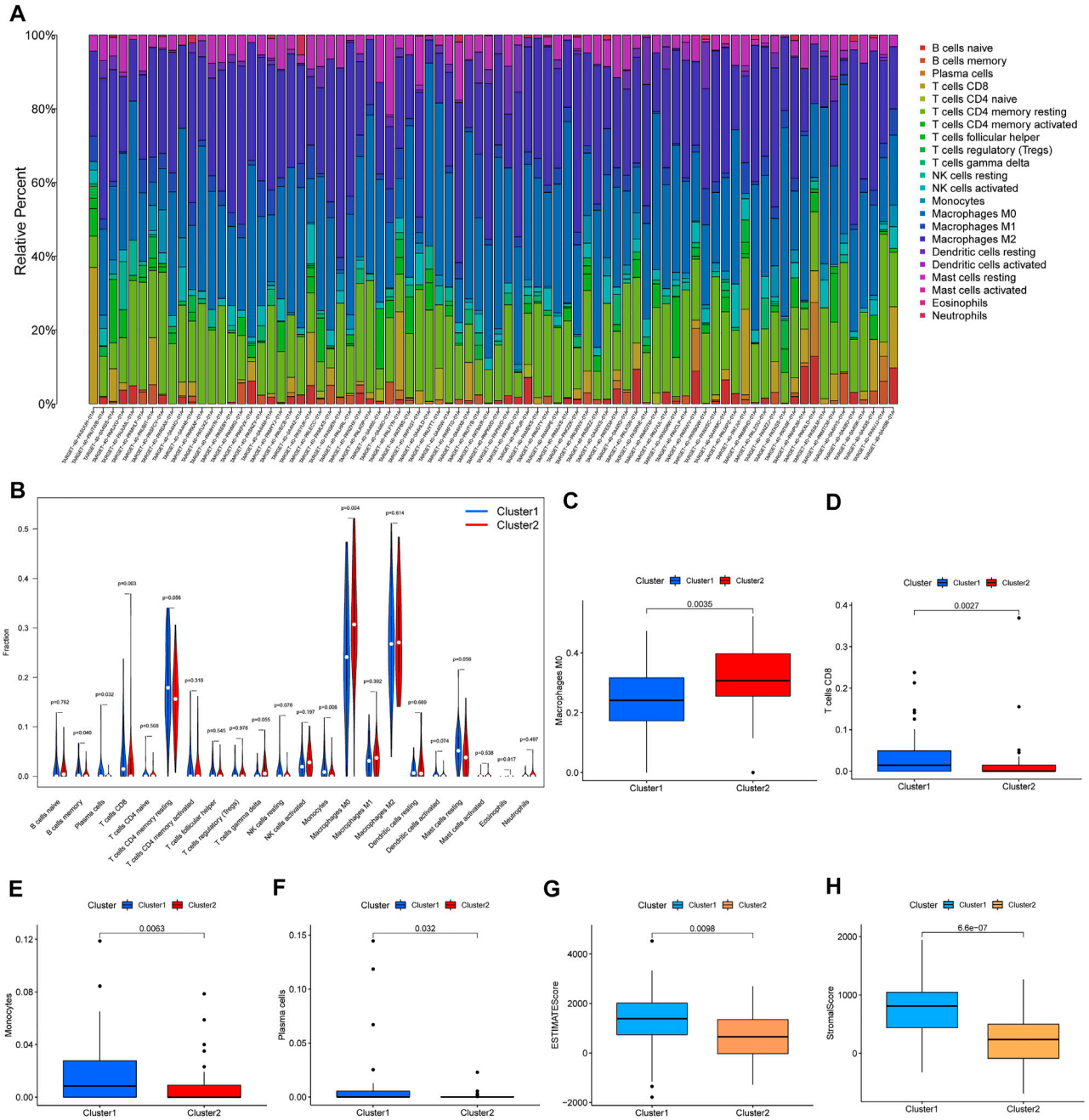

FIGURE 3 | Immune infiltration and the immune microenvironment in the two clusters. **(A)** The proportions of 22 types of immune cells in 84 samples. **(B)** The significant analysis for the same type of immune cell proportions in the two clusters. **(C–F)** The results for proportions of macrophages, CD8 T cells, monocytes, and plasma cells. **(G,H)** ESTIMATE score and stromal score in two clusters.

Immune Infiltration and the Immune Microenvironment in Two Prognosis-Related lncRNA Clusters

Furthermore, we analyzed the difference in immune infiltration and the immune microenvironment in the two prognosis-related lncRNA clusters. The percentage of 22 immune cells is shown in **Figure 3A**. We found that M0 macrophages presented the largest proportion and eosinophils accounted for a small scale. A violin plot was used to further explore the difference in 22 immune cell types in the two clusters (**Figure 3B**). The results of immune infiltration showed that Cluster 1 was observably enriched with B-cell memory, plasma cells, CD8 T cells, and monocytes (**Figures 3D–F**). Only M0 macrophages were enriched in Cluster 2 (**Figure 3C**). In addition, enrichment of M2 macrophages was not significant between Cluster 1 and

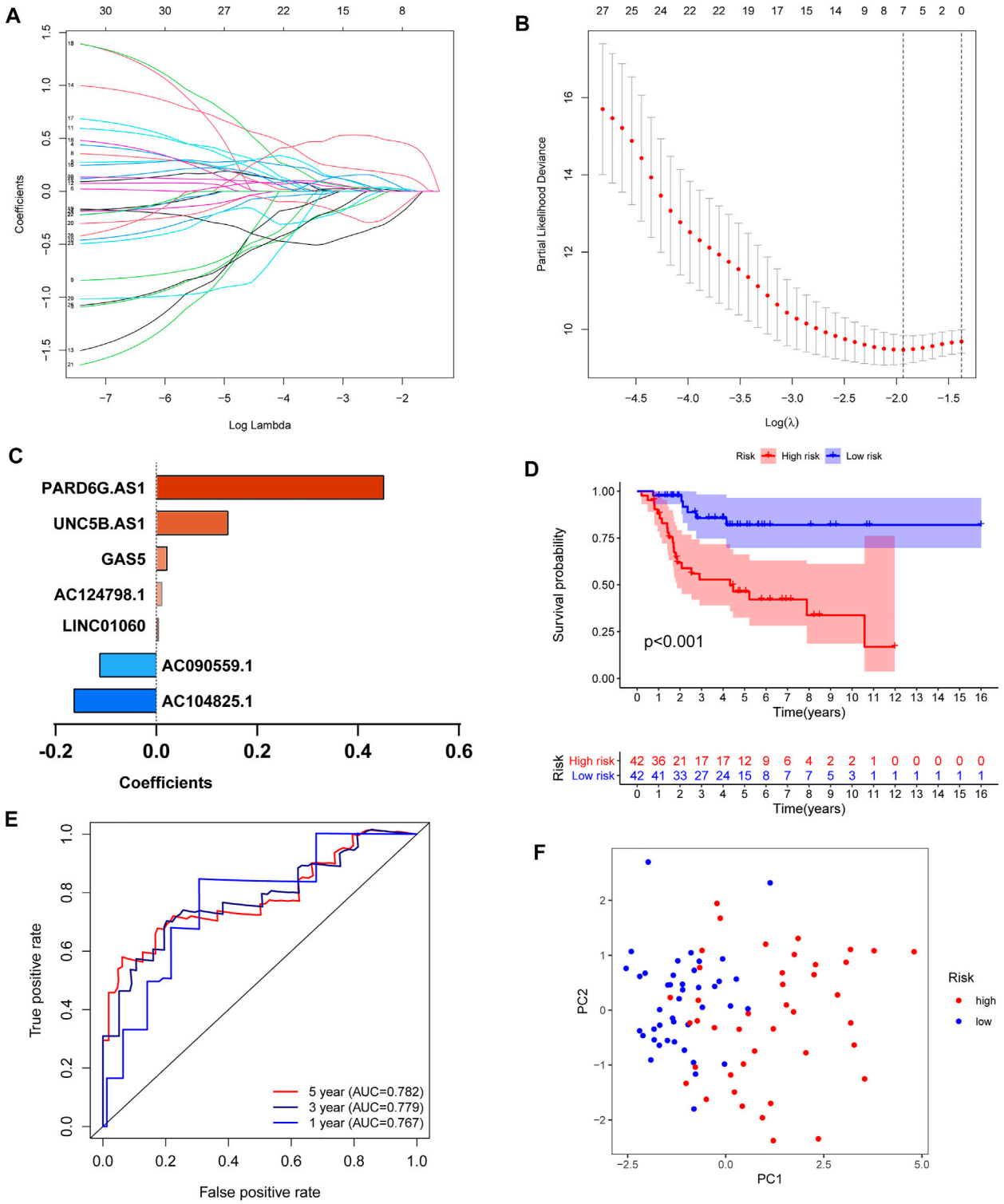

FIGURE 4 | Construction of an iron metabolism-related lncRNA signature. **(A,B)** LASSO Cox regression analysis showed that seven iron metabolism-related lncRNAs were good candidates for constructing the prognostic signature (λ = 0.0125, obtained seven nonzero coefficients). **(C)** Coefficients of the seven iron metabolism-related lncRNAs. **(D)** Kaplan–Meier curves of patients in the high- and low-risk groups. **(E)** ROC curve to evaluate the 1/3/5-year prediction efficiency of the iron metabolism-related lncRNA signature. **(F)** Principal component analysis (PCA) based on the identified iron metabolism-related lncRNA signature.

Cluster 2 (**Supplementary Figure S2D**). The difference in the immune microenvironment was estimated by the analysis of the stromal score, immune score, and ESTIMATE score. The results of the stromal score and ESTIMATE score showed that there was a significantly higher score in Cluster 1 than in Cluster 2 (**Figures 3G,H**), and the immune score did not present a significant result. Taken together, these results confirmed that Cluster 1 and Cluster 2 had different immune phenotypes.

Construction of an Iron Metabolism-Related lncRNA Signature

To further develop the prognostic signature, we performed LASSO Cox regression analysis for 30 prognosis-related lncRNAs. The analysis showed that seven of the thirty iron metabolism-related lncRNAs were good candidates for constructing the prognostic signature. When lambda was minimum (0.1445), the number of nonzero coefficients was seven in the model at this time (**Figures 4A,B**). Meanwhile, the coefficients of five lncRNAs (PARD6G.AS1, GAS5, UNC5B.AS1, LINC01060, and AC124798.1) were positive, while AC090559.1 and AC104825.1 were negative (**Figure 4C**). Based on the iron metabolism-related lncRNA signature, OS patients were divided into high-risk (n = 42) and low-risk (n = 42) groups. Then, the Kaplan–Meier survival curve analysis, receiver-operating characteristic (ROC) analysis, and principal component analysis (PCA) were used to examine the prognostic value of iron metabolism-related lncRNA signatures. The Kaplan–Meier survival curve analysis suggested that the overall survival of OS patients with high-risk scores was significantly shorter than that of patients with low-risk scores (**Figure 4D**). ROC analysis presented a good prediction efficiency of the iron metabolism-related lncRNA signature (1-year AUC = 0.767, 3-year AUC = 0.779, and 5-year AUC = 0.782; **Figure 4E**). Finally, PCA revealed two relatively different distribution patterns between high- and low-risk groups (**Figure 4F**).

Independent Prognostic Value and the Predictive Prognostic Ability of the Risk Score Model

Based on the iron metabolism-related lncRNA signature, we visualized the risk score distribution and survival status of every sample (**Figures 5A,B**). We also generated a heatmap of the seven iron metabolism-related lncRNAs (**Figure 5C**). Moreover, the respective Kaplan–Meier survival curves of seven iron metabolism-related lncRNAs showed that they were significantly correlated with the overall survival of patients (**Supplementary Figures S3A–G**). Then, we applied multivariate Cox analyses to evaluate the prognostic value of the risk score model. The results suggested that tumor metastasis and the risk score were significantly correlated with the overall survival of patients (**Figure 5D**). Compared with the iron metabolism-related lncRNA signature, ROC analysis of clinicopathological factors did not have an advantage in predicting prognosis (**Supplementary Figure S3H**). Additionally, we constructed a nomogram and calibration curve to accurately estimate the 1-, 3-, and 5-year survival probabilities based on the risk score and other clinicopathological factors, including age, gender, and the prognosis stage (**Figures 5E,F**). Overall, the above data verified that the risk score model had good performance in predicting the overall survival of OS patients.

Different Immune-Related Functions Between the High- and Low-Risk Groups

Based on the iron metabolism-related lncRNA signature, we subsequently carried out GSEA to examine the potential biological processes involved. Interestingly, the GSEA results showed that the most significant GO terms and KEGG pathways were mainly enriched in low-risk groups, and there were no significant terms or pathways enriched in the high-risk groups (**Figures 6A,B**). Then, we applied single-sample gene set enrichment analysis (ssGSEA) to compare scores of immune cells and immune-related pathways between high- and low-risk groups. The ssGSEA results confirmed that the scores of immune cells and immune-related pathways in low-risk groups were significantly higher than those in high-risk groups (**Figures 6C,D**). Based on the immune phenotypes, the GSEA score and Kaplan–Meier survival curve analysis, we speculated that the high-risk groups and Cluster 2 presented an immune-excluded phenotype. In addition, low-risk groups and Cluster 1 showed an immune-inflamed phenotype and presented a better survival (Chen & Mellman, 2017).

Immunotherapeutic Response Based on the Risk Score Model

Except for the above immune cell and immune-related pathway scores, we also calculated the correlation between immune infiltration and the risk score. The results confirmed that monocytes and CD8T cells were negatively related to the risk score, but M0 macrophages were positively associated with the risk score (**Figures 6E–G**). Then, we used the tumor immune dysfunction and exclusion (TIDE) algorithm to evaluate the immunotherapy response between the high- and low-risk groups. Consistently, we found that TIDE, microsatellite instability (MSI), and dysfunction were significantly higher in low-risk groups (**Figures 6H–J**). These results indicated that high-risk groups had a good response to immunotherapy.

DISCUSSION

Recently, increasing evidence has indicated that iron metabolism is a critical factor that promotes the carcinogenesis of OS (Lv et al., 2020). Meanwhile, many reports revealed that improving the process of iron metabolism, such as iron deprivation, might be an effective strategy for OS treatment (Li et al., 2016; Ni et al., 2020). In our study, we identified 30 iron metabolism-related lncRNAs that were related to OS prognosis. Meanwhile, the

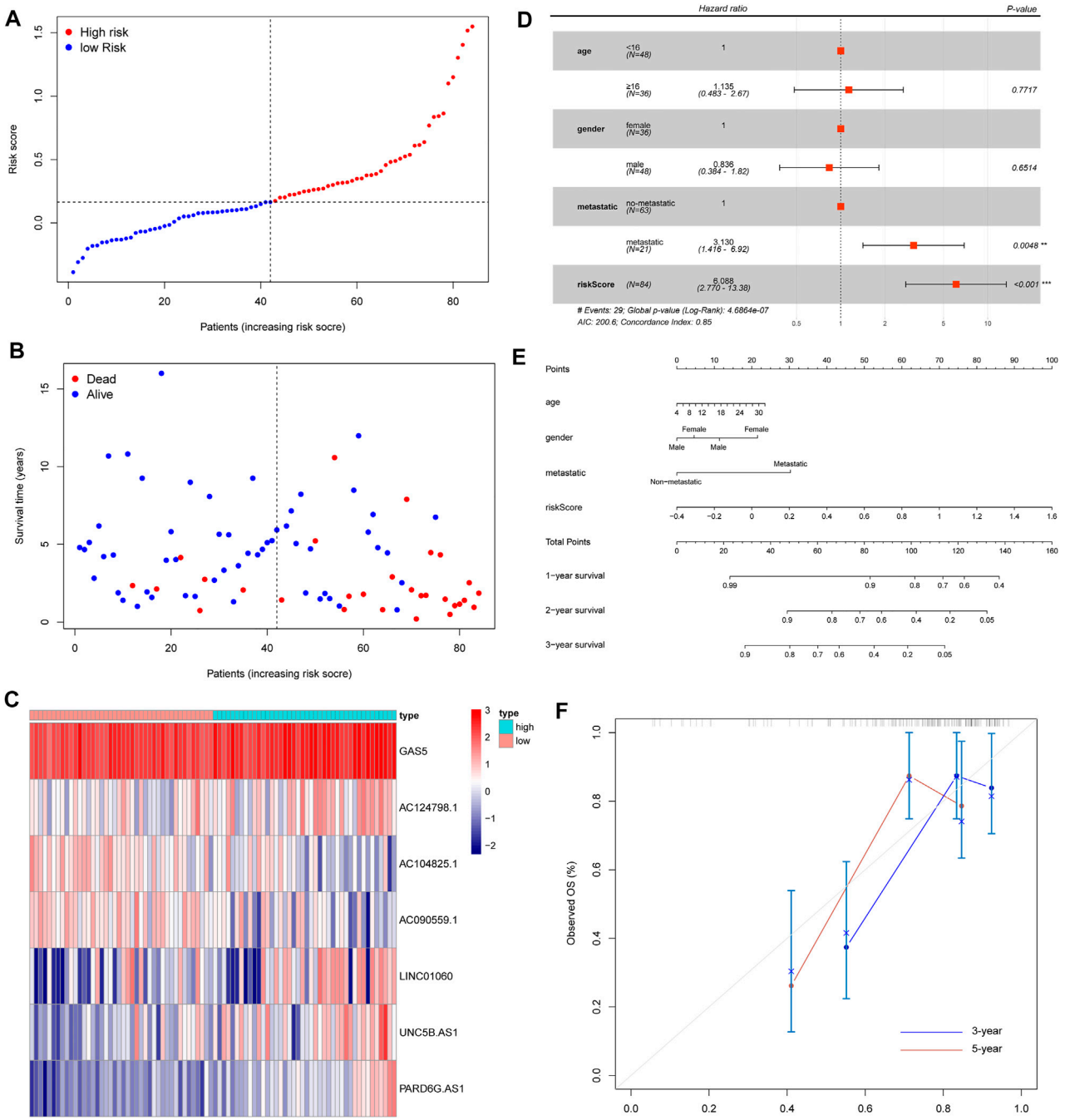

FIGURE 5 | Evaluation of an iron metabolism-related lncRNA signature. **(A)** Risk score distribution. **(B)** Survival time of OS patients. **(C)** Heatmap of seven iron metabolism-related lncRNAs. **(D)** Multivariate Cox analyses to evaluate whether the risk score and clinical features were independent prognostic indicators for the overall survival of OS patients. **(E)** Nomogram for predicting 1/3/5-year survival rates of OS patients. **(F)** Calibration curve of the nomogram for 3/5-year survival rates.

results of consensus clustering of 30 prognosis-related lncRNAs showed the differences in immune infiltration and the immune microenvironment in the two clusters. Through univariate Cox regression and LASSO Cox regression analysis, we constructed an iron metabolism-related lncRNA signature including seven iron metabolism-related lncRNAs. The signature was verified to have good performance in predicting the overall survival, immune-related functions, and immunotherapy response of OS patients between the high- and low-risk groups.

As important epigenetic regulators, lncRNAs play a crucial role in the processes of iron metabolism (Wu et al., 2020). Moreover, accumulating evidence confirmed that lncRNAs are involved in the regulation of ferroptosis and may serve as effective targets for cancer treatment (Jiang et al., 2021; Xie & Guo, 2021).

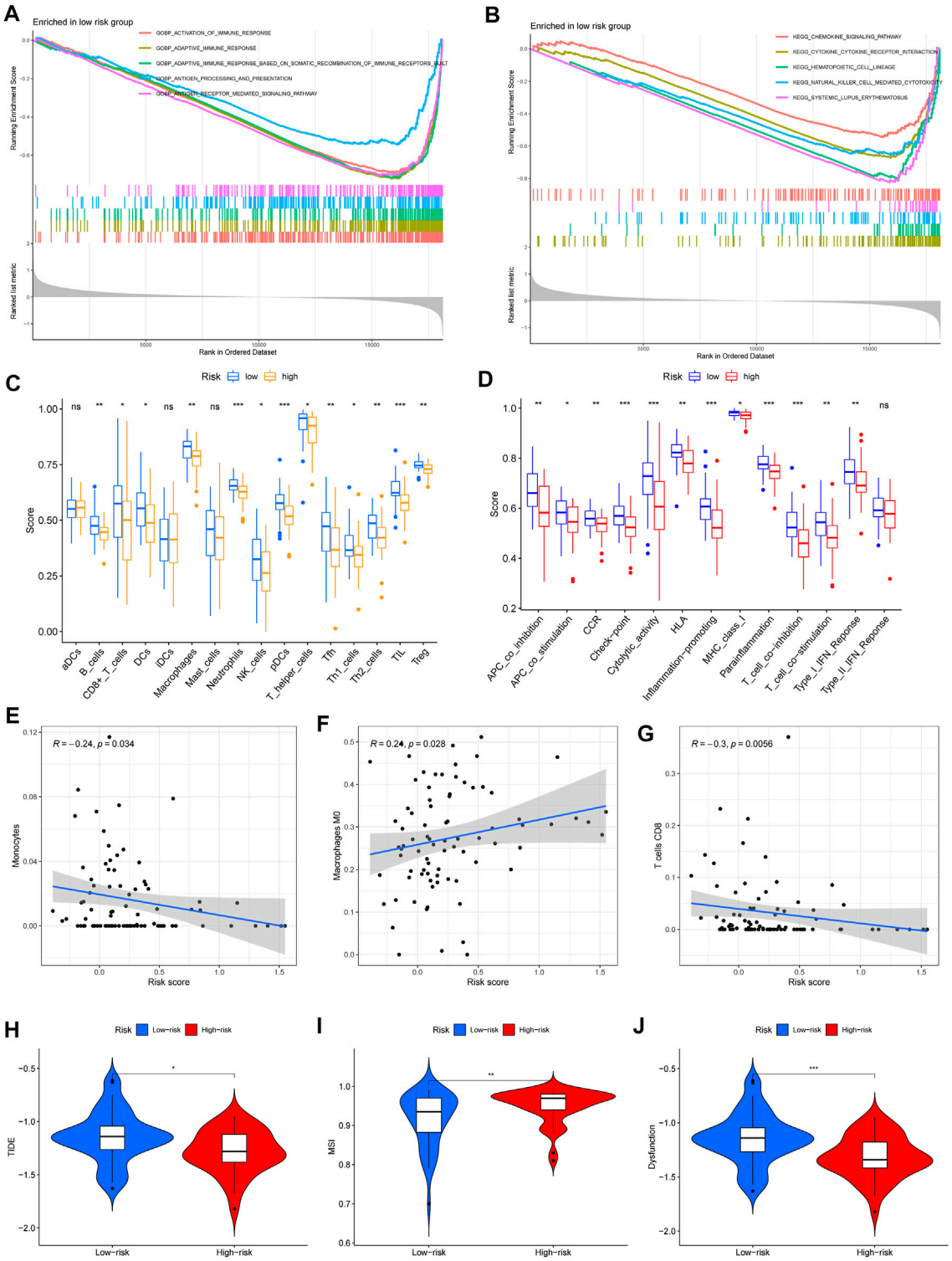

FIGURE 6 | Immune-related functions and immunotherapy response between the high- and low-risk groups. **(A,B)** Significantly enriched GO terms and KEGG pathways in low-risk groups. **(C,D)** Scores of immune cells and immune-related pathways in low- and high-risk groups. **(E–G)** The significant correlation between immune infiltration and risk scores, including monocytes, M0 macrophages, and CD8 T cells. **(H–J)** Analysis of TIDE, microsatellite instability (MSI), and dysfunction (*$p < 0.05$; **$p < 0.01$; and ***$p < 0.001$).

In this study, we developed an iron metabolism-related lncRNA signature including seven iron metabolism-related lncRNAs. In particular, lncRNA GAS5, UNC5B-AS1, PARD6G-AS1, and LINC01060 have been widely reported in cancer and other diseases. For example, it was proven that lncRNA GAS5 was associated with OS progression by regulating OS cell proliferation, migration, and invasion (Ye et al., 2017; Yao et al., 2020; Wang et al., 2021). Moreover, a report showed that lncRNA GAS5 was associated with ovarian cancer progression by regulating histone H3 at lysine 27 (H3K27me3) (Wang et al., 2020). However, except for the reports that lncRNA GAS5 correlated with OS progression, there was no evidence that other iron metabolism-related lncRNAs were involved in OS progression *in vitro* and *in vivo*. Therefore, OS treatment will be necessary to explore the molecular biological functions of the seven iron metabolism-related lncRNAs in the processes of iron metabolism and ferroptosis.

Iron metabolism is closely related to the immune system, including regulating immune cell proliferation, differentiation, and interfering with antimicrobial immune effectors (Ganz & Nemeth, 2015; Cronin et al., 2019; Haschka et al., 2021). Furthermore, imbalances in iron metabolism, including iron overload and iron deficiency, have an important effect on immune function (Porto & De Sousa, 2007; Cassat & Skaar, 2013; Nairz & Weiss, 2020). In our study, we found that many kinds of immune infiltration were enriched in Cluster 1. Meanwhile, the stromal score and ESTIMATE score were significantly higher in Cluster 1 than in Cluster 2. Taken together, we divided 84 samples into two clusters based on 30 iron metabolism-related lncRNAs and evaluated the different immune infiltrations and microenvironments. Therefore, focusing on the regulation of iron metabolism-related lncRNAs will be a novel strategy to change iron metabolism and improve immune functions.

To date, the tumor microenvironment is regarded as having a critical role in cancer development and treatment, and has become one of the most important factors affecting immunotherapy (Smyth et al., 2016; Kaymak et al., 2021). Meanwhile, strategies focusing on immunotherapy have been an increasingly attractive treatment option for OS patients (Dyson et al., 2019; Chen et al., 2021). In our study, the GSEA results confirmed that significant GO terms and KEGG pathways were mainly enriched in low-risk groups and were associated with immune pathways. Additionally, it was also found that the high-risk group presented an immune-excluded phenotype and the low-risk group showed an immune-inflamed phenotype. For the poorer prognosis of high-risk patients, we speculated that higher immunosuppression and lower immunoreactivity should have been the causes. Interestingly, we found that the high-risk groups well responded to immunotherapy through the TIDE algorithm. Therefore, this evidence seems to provide a theoretical basis for applying immunotherapy to OS patients in the future.

Although the iron metabolism-related lncRNA signature showed the ability to potentially predict prognosis, there are several limitations to our study. Except for RNA-sequence data and clinical information from the TARGET, there is a need to evaluate the value of the risk score model in the other testing dataset. Moreover, the risk score model showed a certain predictive ability for OS prognosis, and it is still necessary to verify this prediction in large cohorts.

In conclusion, we identified an iron metabolism-related lncRNA signature that had good performance in predicting survival outcomes and showed the immune landscape for OS patients. Furthermore, our study will provide valuable information to further develop immunotherapies.

DATA AVAILABILITY STATEMENT

The original contributions presented in the study are included in the article/**Supplementary Material**, further inquiries can be directed to the corresponding author.

AUTHOR CONTRIBUTIONS

ZP worked on designing this study. SH-B and YW-J were responsible for organizing the data, performing the data analysis, and drafting the manuscript. DC-H, YX-J, and LS-S participated in revising the language and checking the statistical results.

FUNDING

This study was supported by General Research Project of Military Logistics (No.:CWH17J007). Military Logistics Project (CLB18J027); Early diagnosis and prevention of anterior cruciate ligament injury caused by military training injury.

ACKNOWLEDGMENTS

We would like to thank Elsevier Language Editing Express for helping us to improve our manuscript language in English writing.

SUPPLEMENTARY MATERIAL

The Supplementary Material for this article can be found online at: https://www.frontiersin.org/articles/10.3389/fgene.2022.816460/full#supplementary-material

REFERENCES

Anwar, M. A., El-Baba, C., Elnaggar, M. H., Elkholy, Y. O., Mottawea, M., Johar, D., et al. (2020). Novel Therapeutic Strategies for Spinal Osteosarcomas. *Semin. Cancer Biol.* 64, 83–92. doi:10.1016/j.semcancer.2019.05.018

Bandos, A. I., Rockette, H. E., Song, T., and Gur, D. (2009). Area under the Free-Response ROC Curve (FROC) and a Related Summary index. *Biometrics* 65, 247–256. doi:10.1111/j.1541-0420.2008.01049.x

Brown, R. A. M., Richardson, K. L., Kabir, T. D., Trinder, D., Ganss, R., and Leedman, P. J. (2020). Altered Iron Metabolism and Impact in Cancer Biology, Metastasis, and Immunology. *Front. Oncol.* 10, 476. doi:10.3389/fonc.2020.00476

Cassat, J. E., and Skaar, E. P. (2013). Iron in Infection and Immunity. *Cell Host & Microbe* 13, 509–519. doi:10.1016/j.chom.2013.04.010

Chen, C., Xie, L., Ren, T., Huang, Y., Xu, J., and Guo, W. (2021). Immunotherapy for Osteosarcoma: Fundamental Mechanism, Rationale, and Recent Breakthroughs. *Cancer Lett.* 500, 1–10. doi:10.1016/j.canlet.2020.12.024

Chen, D. S., and Mellman, I. (2017). Elements of Cancer Immunity and the Cancer-Immune Set point. *Nature* 541, 321–330. doi:10.1038/nature21349

Cronin, S. J. F., Woolf, C. J., Weiss, G., and Penninger, J. M. (2019). The Role of Iron Regulation in Immunometabolism and Immune-Related Disease. *Front. Mol. Biosci.* 6, 116. doi:10.3389/fmolb.2019.00116

Dyson, K. A., Stover, B. D., Grippin, A., Mendez-Gomez, H. R., Lagmay, J., Mitchell, D. A., et al. (2019). Emerging Trends in Immunotherapy for Pediatric Sarcomas. *J. Hematol. Oncol.* 12, 78. doi:10.1186/s13045-019-0756-z

Forciniti, S., Greco, L., Grizzi, F., Malesci, A., and Laghi, L. (2020). Iron Metabolism in Cancer Progression. *Int. J. Mol. Sci.* 21, 2257. doi:10.3390/ijms21062257

Friedman, J., Hastie, T., and Tibshirani, R. (2010). Regularization Paths for Generalized Linear Models via Coordinate Descent. *J. Stat. Softw.* 33, 1–22. doi:10.18637/jss.v033.i01

Gai, C., Liu, C., Wu, X., Yu, M., Zheng, J., Zhang, W., et al. (2020). MT1DP Loaded by Folate-Modified Liposomes Sensitizes Erastin-Induced Ferroptosis via Regulating miR-365a-3p/NRF2 axis in Non-small Cell Lung Cancer Cells. *Cell Death Dis* 11, 751. doi:10.1038/s41419-020-02939-3

Ganz, T., and Nemeth, E. (2015). Iron Homeostasis in Host Defence and Inflammation. *Nat. Rev. Immunol.* 15, 500–510. doi:10.1038/nri3863

Gómez-Rubio, V. (2017). ggplot2 - Elegant Graphics for Data Analysis (2nd Edition). *J. Statal Softw.* 077. doi:10.18637/jss.v077.b02

Gordon, M., and Lumley, T. (2016). *Forestplot: Advanced Forest Plot Using 'grid' Graphics*.

Haschka, D., Hoffmann, A., and Weiss, G. (2021). Iron in Immune Cell Function and Host Defense. *Semin. Cel Developmental Biol.* 115, 27–36. doi:10.1016/j.semcdb.2020.12.005

Heagerty, P. J., Lumley, T., and Pepe, M. S. (2000). Time-dependent ROC Curves for Censored Survival Data and a Diagnostic Marker. *Biometrics* 56, 337–344. doi:10.1111/j.0006-341x.2000.00337.x

Jiang, N., Zhang, X., Gu, X., Li, X., and Shang, L. (2021). Progress in Understanding the Role of lncRNA in Programmed Cell Death. *Cell Death Discov.* 7, 30. doi:10.1038/s41420-021-00407-1

Kaymak, I., Williams, K. S., Cantor, J. R., and Jones, R. G. (2021). Immunometabolic Interplay in the Tumor Microenvironment. *Cancer Cell* 39, 28–37. doi:10.1016/j.ccell.2020.09.004

Kolde, R. (2015). *Pheatmap: Pretty Heatmaps*.

Kumar, M. M., and Goyal, R. (2017). LncRNA as a Therapeutic Target for Angiogenesis. *Ctmc* 17, 1750–1757. doi:10.2174/1568026617666161116144744

Lancia, C., Anninga, J. K., Sydes, M. R., Spitoni, C., Whelan, J., Hogendoorn, P. C. W., et al. (2019). A Novel Method to Address the Association between Received Dose Intensity and Survival Outcome: Benefits of Approaching Treatment Intensification at a More Individualised Level in a Trial of the European Osteosarcoma Intergroup. *Cancer Chemother. Pharmacol.* 83, 951–962. doi:10.1007/s00280-019-03797-3

Li, P., Zheng, X., Shou, K., Niu, Y., Jian, C., Zhao, Y., et al. (2016). The Iron Chelator Dp44mT Suppresses Osteosarcoma's Proliferation, Invasion and Migration: *In Vitro* and *In Vivo*. *Am. J. Transl Res.* 8, 5370–5385.

Liang, C., Zhang, X., Yang, M., and Dong, X. (2019). Recent Progress in Ferroptosis Inducers for Cancer Therapy. *Adv. Mater.* 31, e1904197. doi:10.1002/adma.201904197

Liberzon, A., Birger, C., Thorvaldsdóttir, H., Ghandi, M., Mesirov, J. P., and Tamayo, P. (2015). The Molecular Signatures Database Hallmark Gene Set Collection. *Cel Syst.* 1, 417–425. doi:10.1016/j.cels.2015.12.004

Lorent, M., Giral, M., and Foucher, Y. (2014). Net Time-dependent ROC Curves: a Solution for Evaluating the Accuracy of a Marker to Predict Disease-Related Mortality. *Statist. Med.* 33, 2379–2389. doi:10.1002/sim.6079

Luo, W., Wang, J., Xu, W., Ma, C., Wan, F., Huang, Y., et al. (2021). LncRNA RP11-89 Facilitates Tumorigenesis and Ferroptosis Resistance through PROM2-Activated Iron export by Sponging miR-129-5p in Bladder Cancer. *Cel Death Dis* 12, 1043. doi:10.1038/s41419-021-04296-1

Lv, H., Zhen, C., Liu, J., and Shang, P. (2020). β-Phenethyl Isothiocyanate Induces Cell Death in Human Osteosarcoma through Altering Iron Metabolism, Disturbing the Redox Balance, and Activating the MAPK Signaling Pathway. *Oxid Med. Cel Longev* 2020, 5021983. doi:10.1155/2020/5021983

Mercer, T. R., Dinger, M. E., and Mattick, J. S. (2009). Long Non-coding RNAs: Insights into Functions. *Nat. Rev. Genet.* 10, 155–159. doi:10.1038/nrg2521

Morales, M., and Xue, X. (2021). Targeting Iron Metabolism in Cancer Therapy. *Theranostics* 11, 8412–8429. doi:10.7150/thno.59092

Nairz, M., and Weiss, G. (2020). Iron in Infection and Immunity. *Mol. Aspects Med.* 75, 100864. doi:10.1016/j.mam.2020.100864

Newman, A. M., Steen, C. B., Liu, C. L., Gentles, A. J., Chaudhuri, A. A., Scherer, F., et al. (2019). Determining Cell Type Abundance and Expression from Bulk Tissues with Digital Cytometry. *Nat. Biotechnol.* 37, 773–782. doi:10.1038/s41587-019-0114-2

Ni, S., Kuang, Y., Yuan, Y., and Yu, B. (2020). Mitochondrion-mediated Iron Accumulation Promotes Carcinogenesis and Warburg Effect through Reactive Oxygen Species in Osteosarcoma. *Cancer Cel Int* 20, 399. doi:10.1186/s12935-020-01494-3

Pingping, B., Yuhong, Z., Weiqi, L., Chunxiao, W., Chunfang, W., Yuanjue, S., et al. (2019). Incidence and Mortality of Sarcomas in Shanghai, China, during 2002-2014. *Front. Oncol.* 9, 662. doi:10.3389/fonc.2019.00662

Porto, G., and De Sousa, M. (2007). Iron Overload and Immunity. *Wjg* 13, 4707–4715. doi:10.3748/wjg.v13.i35.4707

Smyth, M. J., Ngiow, S. F., Ribas, A., and Teng, M. W. L. (2016). Combination Cancer Immunotherapies Tailored to the Tumour Microenvironment. *Nat. Rev. Clin. Oncol.* 13, 143–158. doi:10.1038/nrclinonc.2015.209

Stockwell, B. R., Friedmann Angeli, J. P., Bayir, H., Bush, A. I., Conrad, M., Dixon, S. J., et al. (2017). Ferroptosis: A Regulated Cell Death Nexus Linking Metabolism, Redox Biology, and Disease. *Cell* 171, 273–285. doi:10.1016/j.cell.2017.09.021

Strauss, S. J., Ng, T., Mendoza-Naranjo, A., Whelan, J., and Sorensen, P. H. B. (2010). Understanding Micrometastatic Disease and Anoikis Resistance in ewing Family of Tumors and Osteosarcoma. *Oncologist* 15, 627–635. doi:10.1634/theoncologist.2010-0093

Torti, S. V., and Torti, F. M. (2013). Iron and Cancer: More Ore to Be Mined. *Nat. Rev. Cancer* 13, 342–355. doi:10.1038/nrc3495

Wang, H., Su, H., and Tan, Y. (2020). UNC5B-AS1 Promoted Ovarian Cancer Progression by Regulating the H3K27me on NDRG2 via EZH2. *Cell Biol Int* 44, 1028–1036. doi:10.1002/cbin.11300

Wang, Y., Ren, X., Yuan, Y., and Yuan, B.-S. (2021). Downregulated lncRNA GAS5 and Upregulated miR-21 Lead to Epithelial-Mesenchymal Transition and Lung Metastasis of Osteosarcomas. *Front. Cel Dev. Biol.* 9, 707693. doi:10.3389/fcell.2021.707693

Wilkerson, M. D., and Hayes, D. N. (2010). ConsensusClusterPlus: a Class Discovery Tool with Confidence Assessments and Item Tracking. *Bioinformatics* 26, 1572–1573. doi:10.1093/bioinformatics/btq170

Wu, Y., Zhang, S., Gong, X., Tam, S., Xiao, D., Liu, S., et al. (2020). The Epigenetic Regulators and Metabolic Changes in Ferroptosis-Associated Cancer Progression. *Mol. Cancer* 19, 39. doi:10.1186/s12943-020-01157-x

Xie, B., and Guo, Y. (2021). Molecular Mechanism of Cell Ferroptosis and Research Progress in Regulation of Ferroptosis by Noncoding RNAs in Tumor Cells. *Cel Death Discov.* 7, 101. doi:10.1038/s41420-021-00483-3

Xu, T., Ding, W., Ji, X., Ao, X., Liu, Y., Yu, W., et al. (2019). Molecular Mechanisms of Ferroptosis and its Role in Cancer Therapy. *J. Cel Mol Med* 23, 4900–4912. doi:10.1111/jcmm.14511

Yao, X., Li, X., Luo, Y., Xu, X., Liu, J., and Bu, J. (2020). LncRNA GAS5 Regulates Osteosarcoma Cell Proliferation, Migration, and Invasion by Regulating RHOB via Sponging miR-663a. *Cmar* 12, 8253–8261. doi:10.2147/cmar.s251881

Ye, K., Wang, S., Zhang, H., Han, H., Ma, B., and Nan, W. (2017). Long Noncoding RNA GAS5 Suppresses Cell Growth and Epithelial-Mesenchymal Transition in Osteosarcoma by Regulating the miR-221/ARHI Pathway. *J. Cel. Biochem.* 118, 4772–4781. doi:10.1002/jcb.26145

Yoshihara, K., Shahmoradgoli, M., Martínez, E., Vegesna, R., Kim, H., Torres-Garcia, W., et al. (2013). Inferring Tumour Purity and Stromal and Immune Cell Admixture from Expression Data. *Nat. Commun.* 4, 2612. doi:10.1038/ncomms3612

Conflict of Interest: The authors declare that the research was conducted in the absence of any commercial or financial relationships that could be construed as a potential conflict of interest.

Publisher's Note: All claims expressed in this article are solely those of the authors and do not necessarily represent those of their affiliated organizations, or those of the publisher, the editors, and the reviewers. Any product that may be evaluated in this article, or claim that may be made by its manufacturer, is not guaranteed or endorsed by the publisher.

frontiers | Frontiers in Genetics

ORIGINAL RESEARCH
published: 13 May 2022
doi: 10.3389/fgene.2022.867909

Comparative Proteome Profiling of Saliva Between Estrus and Non-Estrus Stages by Employing Label-Free Quantitation (LFQ) and Tandem Mass Tag (TMT)-LC-MS/MS Analysis: An Approach for Estrus Biomarker Identification in *Bubalus bubalis*

Laishram Kipjen Singh[1,2†], Mamta Pandey[2†], Rubina Kumari Baithalu[1,2], Abhijeet Fernandes[1], Syed Azmal Ali[3,4], Latika Jaiswal[2], Suryaprakash Pannu[1], Neeraj[1], Tushar K. Mohanty[1], A. Kumaresan[1], Tirtha K. Datta[5], Sudarshan Kumar[3] and Ashok K. Mohanty[3]*

[1]Animal Reproduction, Gynaecology and Obstetrics, ICAR-National Dairy Research Institute, Karnal, India, [2]Molecular Reproduction Lab, Animal Biotechnology Center, ICAR-National Dairy Research Institute, Karnal, India, [3]Proteomics and Cell Biology Lab, Animal Biotechnology Center, ICAR-National Dairy Research Institute, Karnal, India, [4]Division of Proteomics of Stem Cells and Cancer, German Cancer Research Center (DKFZ), Heidelberg, Germany, [5]Animal Biotechnology Centre, ICAR-National Dairy Research Institute, Karnal, India

Accurate determination of estrus is essentially required for efficient reproduction management of farm animals. Buffalo is a shy breeder and does not manifest overt signs of estrus that make estrus detection difficult resulting in a poor conception rate. Therefore, identifying estrus biomarkers in easily accessible biofluid such as saliva is of utmost interest. In the current study, we generated saliva proteome profiles during proestrus (PE), estrus (E), metestrus (ME), and diestrus (DE) stages of the buffalo estrous cycle using both label-free quantitation (LFQ) and labeled (TMT) quantitation and mass spectrometry analysis. A total of 520 proteins were identified as DEPs in LFQ; among these, 59 and four proteins were upregulated (FC ≥ 1.5) and downregulated (FC ≤ 0.5) during E vs. PE, ME, and DE comparisons, respectively. Similarly, TMT-LC-MS/MS analysis identified 369 DEPs; among these, 74 and 73 proteins were upregulated and downregulated during E vs. PE, ME, and DE stages, respectively. Functional annotations of GO terms showed enrichment of glycolysis, pyruvate metabolism, endopeptidase inhibitor activity, salivary secretion, innate immune response, calcium ion binding, oocyte meiosis, and estrogen signaling. Over-expression of SERPINB1, HSPA1A, VMO1, SDF4, LCN1, OBP, and ENO3 proteins during estrus was further confirmed by Western blotting. This is the first comprehensive report on differential proteome analysis of buffalo saliva between estrus and non-estrus stages. This study generated an important panel of candidate proteins that may be considered buffalo estrus biomarkers which can be applied in the development of a diagnostic kit for estrus detection in buffalo.

Keywords: biomarker, estrus, label-free quantitation, LC-MS/MS, tandem mass tag, saliva

OPEN ACCESS

Edited by:
Olanrewaju B. Morenikeji, University of Pittsburgh at Bradford, United States

Reviewed by:
Mihir Sarkar, Indian Council of Agricultural Research (ICAR), India
Cinzia Marchitelli, Research Centre for Animal Production and Aquaculture (CREA), Italy

****Correspondence:***
Rubina Kumari Baithalu
rbaithalu@gmail.com,
orcid.org/0000-0003-0681-7209

†These authors have contributed equally to this work and share first authorship

Specialty section:
This article was submitted to RNA, a section of the journal Frontiers in Genetics

Received: *01 February 2022*
Accepted: *05 April 2022*
Published: *13 May 2022*

Citation:
Singh LK, Pandey M, Baithalu RK, Fernandes A, Ali SA, Jaiswal L, Pannu S, Neeraj, Mohanty TK, Kumaresan A, Datta TK, Kumar S and Mohanty AK (2022) Comparative Proteome Profiling of Saliva Between Estrus and Non-Estrus Stages by Employing Label-Free Quantitation (LFQ) and Tandem Mass Tag (TMT)-LC-MS/MS Analysis: An Approach for Estrus Biomarker Identification in Bubalus bubalis. Front. Genet. 13:867909. doi: 10.3389/fgene.2022.867909

1 INTRODUCTION

Saliva is an important diagnostic body fluid since it contains explicit biomolecules such as metabolites, hormones, mRNA, miRNA, DNA, and proteins that may be a good source of biomarkers of health and disease (Levine, 1993). Saliva consists of secretion from serous and mucous acinar cells of salivary glands and a small portion originating from the blood (Edgar, 1992; Pedersen et al., 2002). Dietary and physiological variations bring changes in the salivary composition (Prout and Hopps., 1970; Mass et al., 2002). Furthermore, its stable nature, high biological half-life, and non-invasive approach make it preferable to other body fluids for biomarker discovery (Li et al., 2004; Archunan et al., 2014; Shashikumar et al., 2017). Proteomics using a mass spectrometer enables the identification of new biomarker proteins in a variety of bodily fluids, including saliva (Almeida et al., 2021). In recent past years, salivary proteomics has led to the discovery of biomarkers for several disease conditions such as oral squamous cell carcinoma (OSCC) (Jou et al., 2014; Wang et al., 2015), autoimmune disease (Castagnola et al., 2017), and genetic diseases such as Down's syndrome (Cabras et al., 2013) in humans. Unlike human saliva, the characterization of salivary proteins of farm animals has been little studied. A global proteome analysis of bovine saliva was carried out by Ang et al. (2011) using both non-targeted and targeted proteomics techniques to identify only extracellular proteins. They identified 402 proteins and 45 N-linked glycoproteins in bovine saliva with enrichment of low-abundance proteins.

Buffalo (*Bubalus bubalis*) is a premier livestock species that contributes immensely to milk and meat production (20th Livestock Census, 2019). Nevertheless, specific inherent reproductive problems such as delayed puberty, silent or poor expression of estrus signs, and seasonal anestrus compromise its reproductive efficiency and production potential. Accurate and efficient identification of estrus is essential for successful conception and efficient reproduction management of farm animals. However, estrus detection is difficult in buffaloes because of non-manifestation of overt signs of estrus and higher incidences (29%) of silent estrus, especially during the summer season (Singh et al., 2000; Roy and Prakash, 2009). This leads to difficulty in estrus detection, improper insemination time, and conception failure in buffaloes (Sharma et al., 2008; Das and Khan, 2010). In addition, various estrus detection tools, such as teaser bull parading, tail painting, KaMar heat mounting detector, behavioral monitoring using a closed circuit television, and activity monitor using a pedometer, were used in buffaloes that are not very efficient since their sensitivity and specificity vary widely (Selvam and Archunan 2017). Therefore, discovering estrus biomarkers in easily accessible body fluids such as saliva is of utmost importance for developing an easy, reliable, and accurate estrus detection method for buffaloes.

Saliva possesses biomarker potential to detect fertile periods in mammals. Saibaba et al. (2021) reported mass spectrometric analysis of salivary proteome profiles of women during the fertile phase of the menstruation cycle as characterized by mass spectrometry. They identified 16 unique and differentially expressed proteins during the ovulatory phase; among them, cystatin-S offers a biomarker potential. Similarly, Muthukumar et al. (2014a) reported proteome profiling of buffalo saliva during the estrous cycle by employing in-gel digestion followed by LC-MS/MS analysis. They identified 179 proteins collectively during proestrus (PE), estrus (E), and diestrus (DE) stages, and 37 proteins are found exclusively during estrus. Among estrus-specific proteins, β-enolase, toll-like receptor (TLR)-4, clusterin, lactoperoxidase, serotransferrin, TGM3, and UBA6 proteins are the most predominant. Our previous study reported global proteome profiling of buffalo saliva during the estrous cycle (Shashikumar et al., 2018) and identified 275, 371, 304, and 565 proteins with ≥2 peptides during PE, E, ME, and DE stages, respectively. Among these, 62 proteins are identified exclusively during the estrus stage, and heat shock 70-kDa protein 1A, 17-beta-hydroxysteroid dehydrogenase type 1, inhibin beta A chain, and testin proteins are found to be the most predominant during estrus. These two studies concluded that salivary secretion contains specific proteins, and their expression varies according to the estrous cycle stages. However, differential proteome analysis using labeled quantitation {tandem mass tag (TMT)} and label-free quantitation (LFQ) coupled to mass spectrometry for estrus biomarker discovery, which is lacking in buffaloes. Therefore, the aim of the present study was to identify candidate estrus biomarkers in saliva of buffaloes. We hypothesized that identifying differentially expressed proteins (DEPs) associated with estrus could lead to the identification of estrus biomarkers in buffaloes. Thus, for the first time, we identified differentially expressed estrus-associated proteins in buffalo saliva by employing both label-free quantitation (LFQ) and labeled quantitation (TMT) coupled to high-resolution mass spectrometry (LC-MS/MS) and their validation using Western blotting.

2 MATERIALS AND METHODS

2.1 Experimental Animals

The study was carried out at the Livestock Research Centre, ICAR-National Dairy Research Institute, Karnal, Haryana. Healthy pluriparous Murrah buffaloes (n = 15) of 2–4 parity maintained under iso-managerial conditions were included for the study. The nutrient requirement of the animals was provided as per National Research Council (NRC) standards. After completing the voluntary waiting period, all animals underwent gynecological examination using per-rectal examination and transrectal ultrasonography (Model UST-5820-5). For estrus induction, buffaloes with functional corpus luteum (CL) on the ovary are administered with $PGF_2\alpha$ (Vetmate; 500 μg I/M). Samples were collected from the next spontaneous estrous cycle, and stages of the estrous cycle were categorized as proestrus (PE; day 2 to 1 before the onset of estrus), estrus (E; day 0), metestrus (ME; day+3), and diestrus (DE; day +10). All the sampling was completed during the breeding season, that is, from November to February. All the experiments conducted in this study were approved by the Institute Animal Ethics Committee (42-IAEC-18-9).

2.2 Estrus Detection and Confirmation

Estrus in buffaloes was detected by physical observation of estrus signs. Teaser bull parading was carried out twice a day, that is, daily in the morning 5–6 AM and evening 5–6 PM for exhibition of estrus signs. The following estrus signs were observed: standing to be mounted, sniffing/licking the vulva, chin resting, flehmen's reaction, mounting on or by other buffaloes, restlessness, bellowing, and frequent micturition. The onset of estrus is marked by expression of a typical estrus sign, that is, standing to be mounted behavior (standing estrus). The onset of estrus was further confirmed by reproductive tract examination (uterine horn tonicity, cervical relaxation, tumefaction of vulva, hyperemia, or reddening of the vulvar mucous membrane), biochemical parameters (cervicovaginal mucus crystallization, fluidity, and spinnbarkeit value (Verma et al., 2014)), and progesterone hormone estimation in blood serum. Transrectal ultrasonography (USG) using a real-time B-mode scanner equipped with a 7.5 MHz rectal probe was used to confirm further presence of dominant follicle (DF; ≥ 10 mm) and absence of CL during the follicular phase (proestrus and estrus) and the onset of ovulation and presence of CL during the luteal phase. Progesterone hormone concentration was estimated in serum samples using an ELISA kit (Cayman Chemical, United States) to confirm the stages of the estrous cycle.

2.3 Sample Collection and Processing

Saliva samples were collected from the lower jaw of the mouth of the animal by the direct aspiration method using a 20-ml syringe without a needle in sterile polypropylene tubes (Thermo Fisher Scientific, NY). All the sampling was performed in the early morning (6–7 AM) before feeding, and samples after collection were immediately transported to the laboratory on ice. Samples were centrifuged at 12,000 rpm at 4°C for 30 min to eliminate any particulate matter or feed debris. Supernatant was collected in another 1.5-ml Eppendorf tube, and protease and phosphatase inhibitor (1 × MS-SAFE; Sigma-Aldrich, United States) was added to prevent protein degradation and stored at −80°C until further analysis. Saliva samples from animals wherein estrus and non-estrus stages confirmed through various methods were selected and processed further for proteomics analysis.

2.4 Quantification and SDS-PAGE Profiling of Saliva Proteins During Different Stages of the Estrous Cycle

Out of 15 buffaloes, seven animals showing all the cardinal signs of estrus confirmed by gynecological examination, USG, cervicovaginal mucus (CVM) parameters, and progesterone estimation were selected for further proteomics study. The protein concentration of neat saliva samples from PE (n = 7), E (n = 7), ME (n = 7), and DE (n = 7) stages were determined with a Bradford assay. Then, salivary proteins, that is, 25 μg from all stages of the estrous cycle, were taken, and initial protein profiling was carried using SDS-PAGE. Initially, proteins were resolved on a 4% stacking and 12% separating acrylamide–bis-acrylamide gel at 15 mA for 3 h using the mini-protean vertical electrophoresis system (Bio-Rad, United States). The gels were stained with Coomassie brilliant blue G (CBB) at room temperature for 1 h, de-stained for 2 h, and scanned using an Epson scanner (GE, Healthcare, United States). The initial protein profiles were identified by running the saliva proteins with a reference protein marker (RTU-BLUeye prestained protein ladder). Based on the intactness and uniformity of the bands, saliva samples from PE, E, ME, and DE stages of five animals were selected for further in-solution digestion and label-free quantification (LFQ) and labeled quantitation using TMT labels and LC-MS/MS analysis.

2.5 Label-Free Quantitation

2.5.1 Trypsin In-Solution Digestion of Proteins for LC-MS/MS Analysis

Neat saliva protein of 50 μg from PE, E, ME, and DE stages were taken from five animals, and all samples were processed separately for in-sol digestion. In brief, samples were dissolved in dissolution buffer (50 mM ammonium bicarbonate) and reduced with 50 mM dithiothreitol (Sigma-Aldrich, United States) at 50°C for 45 min. Further alkylation was carried out using 100 mM IAA at room temperature in the dark for 15 min. Trypsin digestion (Promega, Madison, WI) at 1:20 (enzyme: protein) of protein samples was carried out at 37°C for overnight, followed by quenching with 10% trifluoroacetic acid. Furthermore, tryptic-digested samples were vacuum-dried (SpeedVac concentrator, Thermo Fisher Scientific, United States) and desalted using Pierce® C18 Spin Columns (Thermo Fisher Scientific, United States). Desalted peptide samples were vacuum-dried using SpeedVac and reconstituted in 0.1% formic acid. Finally, all 20 samples from five animals of four stages were subjected to LC-MS/MS analysis.

2.6 Labeled Quantitation Using TMT Labels

Saliva proteins (75 μg) from each stages of the estrous cycle, that is, PE, E, ME, and DE from five animals were pooled. Proteins were dissolved in dissolution buffer (50 mM ammonium bicarbonate), followed by reduction (50 mM dithiothreitol) at 50°C for 45 min s. Alkylation of cysteine residues was carried out using 100 mM IAA at room temperature in the dark for 15 min s, followed by trypsin digestion at 1:20 (enzyme: protein) at 37°C for overnight. Peptides of PE, E, ME, and DE stages were labeled with 126, 127, 128, and 129 TMT labels, respectively, using TMT 6-plex (Thermo Fisher Scientific, Germany), according to the manufacturer's protocol. Peptides labeled with TMT tags were incubated for 3 h, quenched (5% hydroxylamine), vacuum-dried, and fractionated into eight fractions using a Pierce™ high pH reversed-phase peptide fractionation kit (Thermo Fisher Scientific, China), according to the manufacturer's protocol. Furthermore, the fractions were vacuum-dried and reconstituted in 0.1% formic acid and subjected to LC-MS/MS analysis.

2.7 ESI–LC-MS/MS Analysis

Peptide samples were analyzed using an EASY-nLC 1,000 mass spectrometer (Thermo Fisher Scientific, United States) coupled with Thermo Fisher Q Exactive equipped with nano-ESI. The

TABLE 1 | Behavioral signs of estrus in buffaloes.

Behavioral signs of estrus	% of animals showing estrus signs
Standing to be mounted	83.3
Cervicovaginal mucus discharge	89.9
Hyperemia of the vulval mucous membrane	89.9
Flehmen's response	81.1
Bellowing	77.7
Vulva tumefaction	72.2
Frequent micturition	65.1
Licking/sniffing of vulva	71.1
Chin resting	68.2

peptide mixture of 1 μg was resolved using a 25-cm PicoFrit column (360 μm outer diameter, 75 μm inner diameter, and 10 μm tip) filled with 1.8 μm of C18 resin (Dr. Maisch, Germany). The peptides were loaded with buffer A and eluted with a 0–40% gradient of buffer B (95% ACN and 0.1% formic acid) at a 300 nl/min flow rate for 100 min. MS data were acquired using a data-dependent top 10 method dynamically choosing the most abundant precursor ions from the survey scan.

2.8 Data Processing

The MS/MS data were searched and analyzed with Proteome Discoverer (v2.2) against the UniProt *Bos taurus* reference proteome database. In Proteome Discoverer, the Sequest search engine was used; the precursor and fragment mass tolerances were set at 10 ppm and 0.5 Da, respectively. The protease used to generate peptides, that is, enzyme specificity, was set at trypsin/P (cleavage at the C terminus of "K/R": unless followed by "P") along with a maximum missed cleavages value of two. The "ion score cutoff" was set to 20, thereby eliminating the lowest quality matches and minimum peptide length as six amino acid residues. Carbamidomethyl on cysteine was set at fixed modification and oxidation of methionine, and N-terminal acetylation was considered variable modifications for database search. The maximal number of modifications per peptide was set at 6. The minimum peptide length parameter was set to 6, and the "peptide" re-quantification function was enabled. Both peptide spectra match, and the protein false discovery rate (FDR) was set to 0.01. The decoy-reversed sequences database was included for the calculation of the FDR.

2.9 Bioinformative Analysis and Network Generation

Protein class analysis of the differentially expressed proteins based on molecular function, biological process, and cellular component was performed using Cytoscape ClueGo plug-in (v.3.7.2). A protein–protein interaction (PPI) network was constructed with the Search Tool for the Retrieval of Interacting Genes (STRING) database (v.11.5) and Cytoscape.

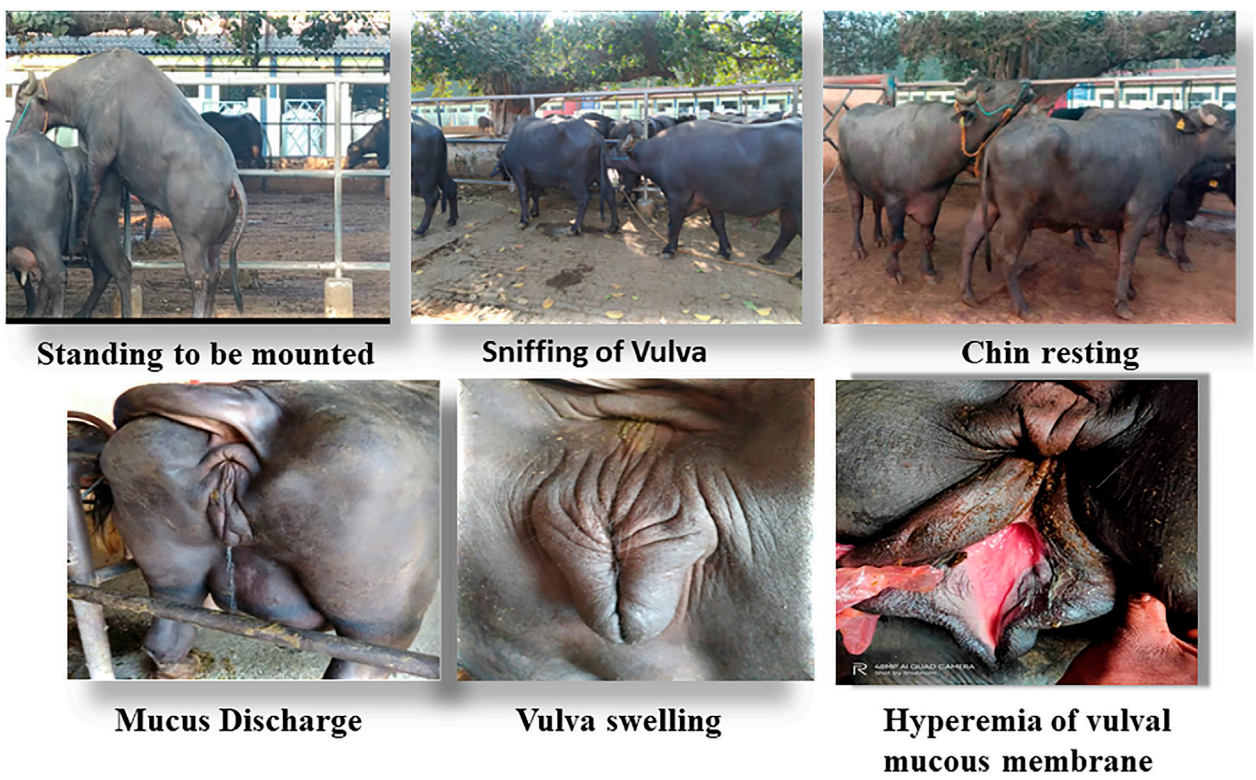

FIGURE 1 | Behavioral signs of estrus in buffaloes.

TABLE 2 | Intensity of expression of other estrus signs in buffaloes.

Estrus sign	Intensity of expression (%)		
	Mild	Moderate	Intense
Uterine horn tonicity	-	6	94
Vulva tumefaction	-	27.8	72.2
Hyperaemia/reddening of the vulval mucous membrane	-	10.1	89.9
Cervicovaginal mucus discharge	-	16.7	83.3

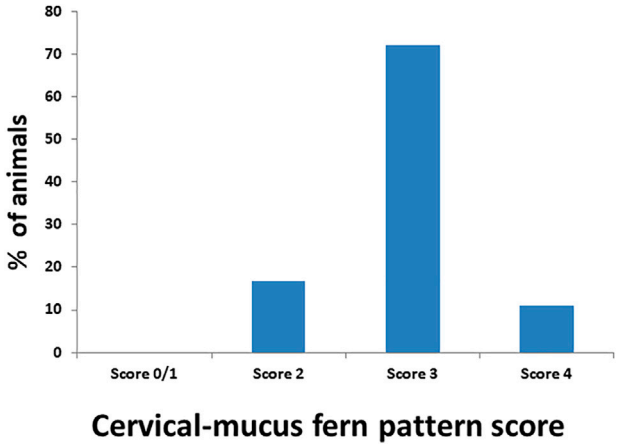

FIGURE 2 | Estimation of the crystallization/fern pattern score of cervicovaginal mucus during estrus in buffaloes.

A hypergeometric test ($p < 0.05$) was used in statistical analysis in the ClueGO tool. Furthermore, the online KEGG (Kyoto Encyclopedia of Genes and Genomes) pathway database was used for biological interpretation of higher-level systemic functions.

2.10 Western Blot Analysis

A quantity of 40 μg salivary proteins from four stages was loaded in a 12% SDS-PAGE gel and then transferred onto a polyvinylidene difluoride (PVDF) membrane using a semidry Western blot transfer system (Invitrogen, United States). The membrane was incubated with 5% BSA in TBST buffer (10 mM Tris, 150 mM NaCl, 0.05% Tween 20, and 5% BSA, pH 7.60) as blocking solution overnight at 4°C. After blocking, the membrane was incubated separately with seven primary antibodies: SERPINB1 (Aviva Systems Biology, San Diego, United States; 1:5,000), HSPA1A (Sigma-Aldrich, United States; 1:5,000), ENO3 (Sigma-Aldrich, MO, United States; 1:1,250), LCN1 (MyBiosource, CA, United States; 1:1,000), SDF4 (Aviva Systems Biology, San Diego, United States; 1:5,000), VMO1 (Thermo Fischer Scientific, United States; 1:5,000), and beta-actin (Sigma-Aldrich, MO, United States; 1:1,667) at room temperature for 1 h. Subsequently, the membranes were washed three times with TBST followed by incubation with horseradish peroxidase–conjugated secondary antibody (diluted 1:4,000, Sigma-Aldrich, United States) for 1 h at room temperature. The membranes were dried and developed using an X-ray film with Clarity Western ECL substrate (Bio-Rad, United States). The band intensity of the protein expression was normalized with beta-actin as an internal control, and values were analyzed using one way ANOVA with SPSS Inc (2007) after normalization.

3 RESULTS

3.1 Estrus Detection and Confirmation

Accurate and efficient identification of estrus is essential for successful conception and efficient breeding management of farm animals including cattle and buffaloes. Hence, the onset of estrus in buffaloes was determined by physical signs and confirmed by gynecological examination of reproductive tract, transrectal USG, biochemical parameters (CVM fern pattern, spinnbarkeit value, and other parameters), and progesterone hormone estimation in blood serum. Behavioral signs of estrus are listed in **Table 1**; **Figure 1**. Major estrus signs exhibited by female buffaloes were cervicovaginal mucus discharge (89.9%), standing to be mounted (83.3%), bellowing (77.7%), frequent micturition (65.1%), hyperemia of the vulval mucous membrane (89.9%), and vulva tumefaction (72.2%). Further male behavior toward estrus buffaloes such as flehmen's reaction (81.1%), sniffing the vulva (71.1%), and chin resting (68.2%) were also considered for estrus identification. Other estrus signs such as uterine horn tonicity, CVM crystallization, and spinnbarkeit value were considered for confirmation of estrus. Tonicity of uterine horns (94%) was mostly intense during the estrus stage (**Table 2**). The CVM crystallization/fern pattern was typical with scores 3 and 4 in 83.3% during estrus (**Figures 2**, **3**). The spinnbarkeit value of CVM was the highest (21.30 ± 1.56 cm) during estrus (**Figure 4**). Transrectal USG revealed the presence of dominant follicle (DF) during the follicular phase, and the size of DF was 12.1 ± 0.03 mm and 13.5 ± 0.04 mm during PE and E, respectively (**Figure 5**). The absence of preovulatory follicle confirmed ovulation during the ME stage and presence of CL during the DE stage (**Figure 5**). The serum progesterone level was found to be lowest during E (0.35 ± 0.04 ng/ml, $p < 0.05$) and PE (0.54 ± 0.08 ng/ml) than that in ME (1.56 ± 0.14 ng/ml) and DE (3.79 ± 0.09 ng/ml) stages (**Figure 6**).

3.2 Quantification and SDS-PAGE of Salivary Proteins

The salivary proteins were quantified, and the concentration was in the range of 500–1,000, 400–1,000, 400–900, and 466–800 μg/

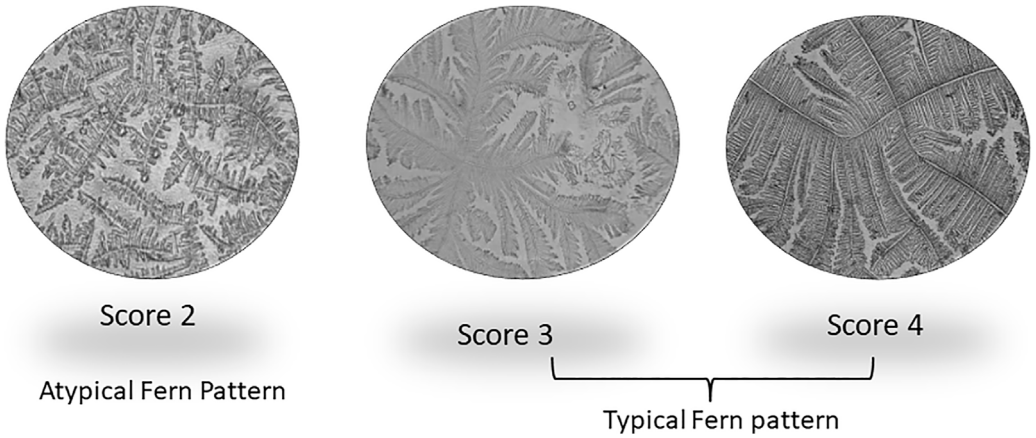

FIGURE 3 | Different crystallization/fern patterns of cervicovaginal mucus observed during estrus in buffaloes.

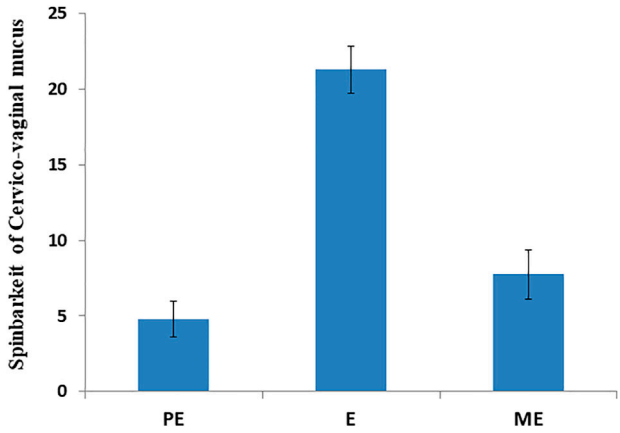

FIGURE 4 | Spinnbarkeit value of cervicovaginal mucus during proestrus (PE), estrus (E), and metestrus (ME) stages of the buffalo estrous cycle.

ml during PE, E, ME, and DE stage, respectively. Furthermore, salivary proteins were separated using SDS-PAGE. A total of seven major and several minor bands were exhibited in the CBB-stained gel invariably among four stages of the estrous cycle and their molecular mass ranged from 17 to 245 kDa (**Figure 7**).

3.3 LC-MS/MS Analysis and DEPs Comparisons

The LFQ-LC-MS/MS analysis identified 520 DEPs with 1% protein and peptide FDR cutoff. The detailed information related to accession, description, protein FDR confidence, peptide score, coverage %, peptides, PSM, unique peptides, protein groups, MW, calculated pI, Sequest score, gene name, and abundance of the identified proteins is shown in **Supplementary Table S1**. The number of upregulated and downregulated proteins was distinctly identified based on the fold-change criteria between E, PE, ME, and DE stages. The fold-change values were set between 0.5 and 1.5; the proteins expressed with values greater than 1.5 were upregulated, and the proteins expressed with values less than 0.5 were downregulated. The list of upregulated and downregulated proteins during E compared to other non-estrus stages (PE, ME, and DE) is listed in **Table 3**. By considering the fold-change range, a total of 59 proteins and four proteins were found to be upregulated and downregulated during E compared to PE, ME, and DE stages, respectively. Among the DEPs, few proteins with higher abundance at E than all other non-estrus stages and identified in all the biological replicate samples were gastric triacylglycerol lipase (LIPF; E/P: 33-fold, E/M: 38.8-fold, and E/D: 19-fold), peptidyl-prolyl cis-trans isomerase E (PPIE; E/P: 21-fold, E/M: 15-fold, and E/D: 25-fold), fatty acid–binding protein, (FABP3; E/P: 2.4-fold, E/M: 6.2-fold, and E/D: 10.8-fold), leukocyte elastase inhibitor (SERPINB1; E/P: 3-fold, E/M: 2.3-fold, and E/D: 3.4-fold), apolipoprotein A-I (APOA1; E/P: 1.9-fold, E/M: 9.7-fold, and E/D: 6.8-fold), heat shock 70-kDa protein 1A (HSPA1A; E/P: 1.5-fold, E/M: 2.3-fold, and E/D: 3.6-fold), and pyruvate kinase (PKLR; E/P: 5-fold, E/M: 2-fold, and E/D: 4.7-fold) were highly abundant proteins during E vs. PE, ME, and DE comparisons.

Similarly, TMT-LC-MS/MS analysis identified a total of 369 DEPs; among these 74 and 73 proteins were upregulated and downregulated during E compared to PE, ME, and DE stages, respectively. The detail information of identified proteins is listed in **Supplementary Table S2**. The list of upregulated and downregulated proteins during E than other non-estrus stages (PE, ME, and DE) is presented in **Tables 4**, **5**, respectively. Among the upregulated DEPs, odorant-binding protein (OBP; E/P: 2.5-fold, E/M: 2.5-fold, and E/D: 69-fold), lipocalin 1 (LCN1; E/P: 7.3-fold, E/M: 14.3-fold, and E/D: 11.3-fold), odorant-binding protein-like (MGC151921; E/P: 1.8-fold, E/M: 2.8-fold, and E/D: 24-fold), lipocln_cytosolic_FA-bd_dom domain-containing protein (LOC104969973; E/P: 11.3-fold, E/M: 14.6-fold, and E/D: 5.8-fold), heat shock protein beta-1 (HSPB1; E/P: 12.5-fold, E/M: 15.5-fold, and E/D: 7.3-fold), galectin (LGALS7B; E/P: 5.3-fold, E/M: 6.6-fold, and E/D: 4.6-fold), metalloproteinase inhibitor 2 (TIMP2; E/P: 11.2-fold, E/M: 11.9-fold, and E/D: 2.7-fold), 45-kDa calcium-binding protein (SDF4; E/P: 62.6-fold, E/M: 88.6-

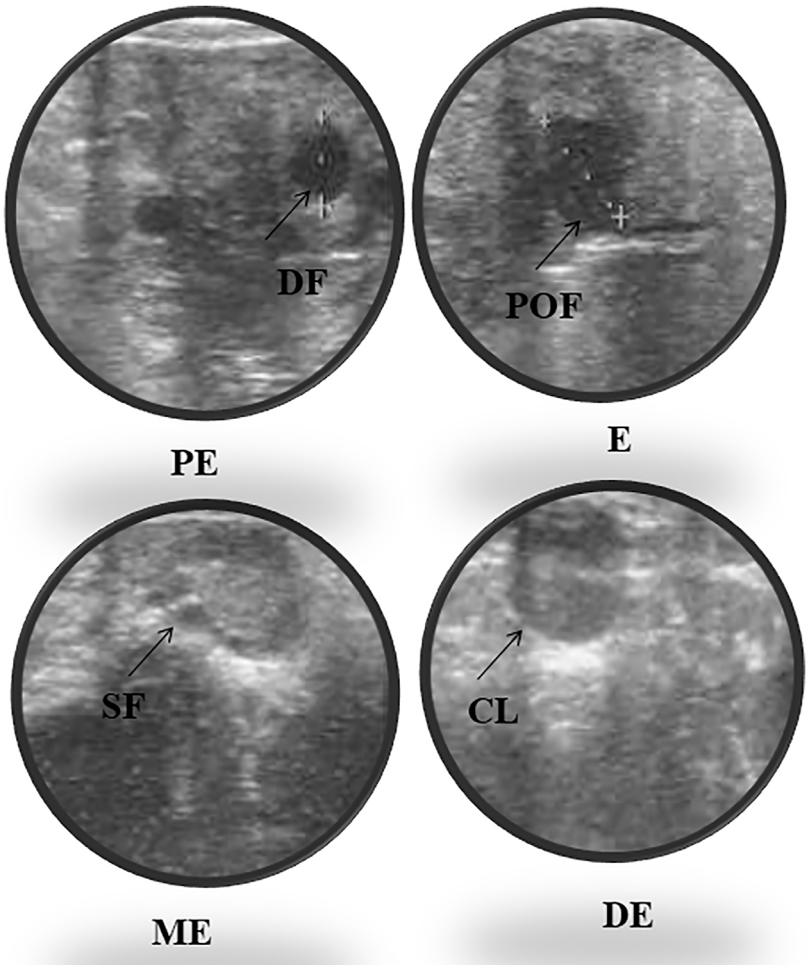

FIGURE 5 | Ultrasonography of ovarian follicles and corpus luteum (CL) during proestrus (PE), estrus (E), metestrus (ME), and diestrus (DE) stages of the buffalo estrous cycle (DF, dominant follicle; SF, small follicle; POF, preovulatory follicle; CL, corpus luteum).

fold, and E/D: 19.2-fold), peptidyl-prolyl isomerase (LOC526524; E/P: 13.6-fold, E/M: 17.3-fold, and E/D: 37.9-fold), and vitelline membrane outer layer 1 (VMO1; E/P: 62.6-fold, E/M: 88.6-fold, and E/D: 19.2-fold) were highly abundant proteins during E than other non-estrus stages, and few of these were also discovered in our previous investigation.

Hierarchical clustering (**Figure 8**) and principal component analysis (PCA) (**Figure 9**) of proteins identified during four stages depicts clear cut differences in the expression of proteins among four stages. A Venn diagram analysis revealed that 214 proteins were commonly identified by both techniques, that is, TMT and LFQ; however, 223 and 78 proteins were specifically identified using LFQ and TMT methods, respectively (**Figure 10**).

3.4 Validation of DEPs Using Western Blotting

A total of six DEPs were selected for validation using Western blot analysis based on their involvement in different signaling pathways and their over-expression during E compared to all other non-estrus stages: SERPINB1, HSPA1A, SDF4, VMO1, ENO3, and LCN1. Interestingly, Western blot analysis confirmed the significantly higher expression of these proteins during E than PE, ME, and DE stages. The intensity of the protein expression was normalized with beta-actin as an internal control (**Figure 11**).

3.5 Gene Ontology Annotation of DEPs

Gene Ontology annotation of DEPs was performed on the Cytoscape ClueGo plug-in tool and presented in **Figure 12**. Based on the molecular function (**Figure 12A**, **Supplementary Figure S1**), the DEPs were found to be mainly enriched in cell adhesion molecule binding, endopeptidase regulator activity, protein heterodimerization activity, cadherin binding, cytoskeletal protein binding, oxidoreductase activity, hydrolase activity, transferase activity, fatty acid-binding, cis–trans isomerase activity, lysozyme activity, calcium ion binding, ion binding, antioxidant activity, and protein folding chaperone. Based on biological process (**Figure 12B**, **Supplementary Figure S2**), the DEPs were enriched in response to external biotic stimulus,

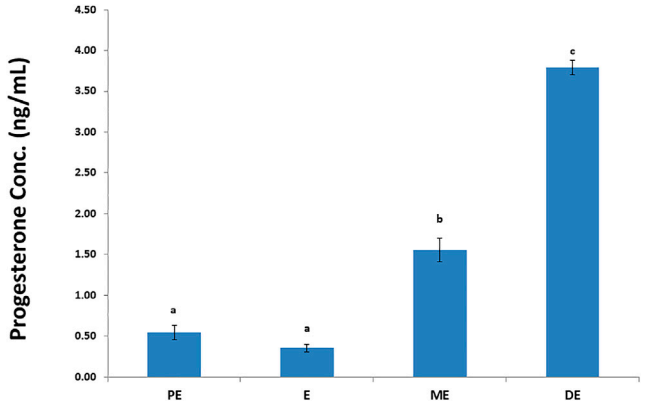

FIGURE 6 | Progesterone hormone concentration (ng/ml) during proestrus (PE), estrus (E), metestrus (ME), and diestrus (DE) stages of the buffalo estrous cycle.

metabolic process, regulation of endopeptidase activity, innate immune response, cytoskeleton organization, tissue homeostasis, generation of precursor metabolites and energy, ATP metabolic process, glycolytic process, chromatin assembly or disassembly, acute inflammatory response, cell redox homeostasis, and mucosal immune response. Based on the GO terms for cellular component (**Figure 12C**, **Supplementary Figure S3**), the DEPs belonged to endoplasmic reticulum lumen, plasma membrane, actin cytoskeleton, endoplasmic reticulum chaperone complex, myelin sheath, nucleosome, extracellular matrix, adherens junction, exosome, organelle, vesicle, and extracellular space.

3.6 Protein–Protein Interaction and Network Visualization

We performed protein–protein interaction (PPI) network analysis for DEPs using the STRING tool (v.11.5) with the *Bos taurus* database. The highly significant protein–protein interaction network ($p < 1.0E-16$) was created with 378 nodes, 810 edges, 4.29 average node degree, and 0.357 average local clustering coefficient (**Figure 13A**). A total of 31 clusters were found with the highest degree of connectivity among proteins. Furthermore, to explore the interactions between DEPs, we constructed protein networks using Cytoscape ClueGo plug-in tool (**Figure 13B**). A total 28 KEGG pathways were significantly enriched ($p < 0.05$), including glycolysis/gluconeogenesis, carbon metabolism, biosynthesis of amino acids, salivary secretion, fluid shear stress and atherosclerosis, glutathione metabolism, pentose phosphate pathway, innate immune response, antigen processing and presentation, oocyte meiosis, cell cycle, and estrogen signaling pathway (**Table 6**).

4 DISCUSSION

Due to the difficulty of detecting estrus in buffalo, the finding of an estrus biomarker in readily accessible bodily fluids such as

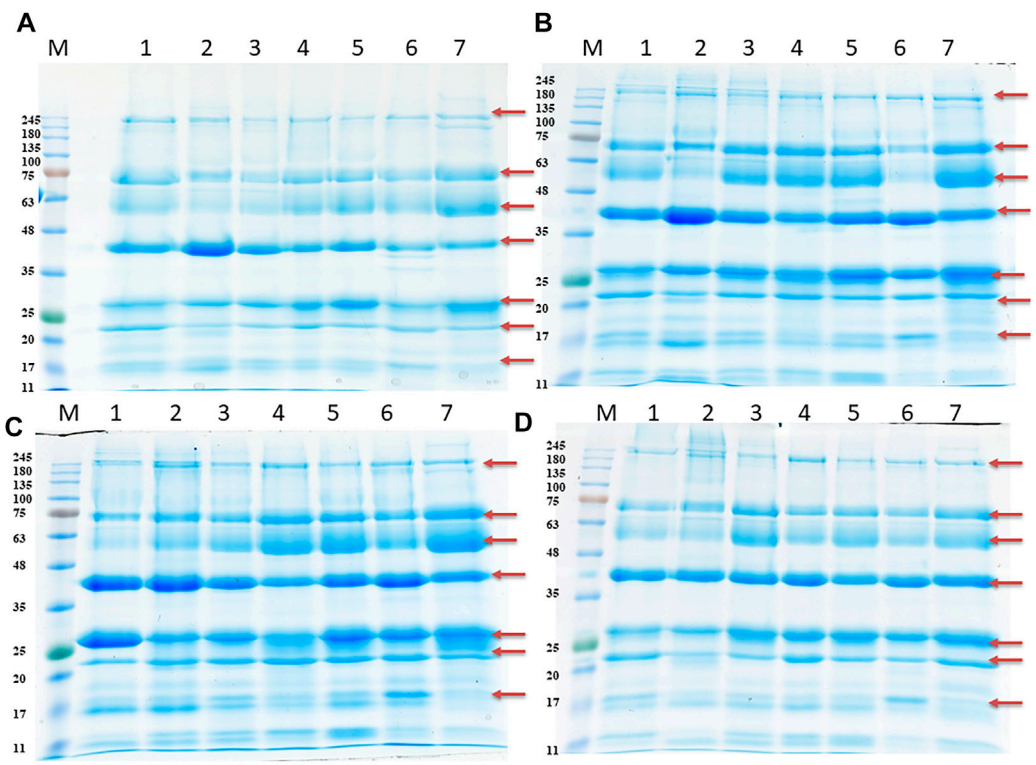

FIGURE 7 | SDS-PAGE of salivary proteins during proestrus (PE) **(A)**, estrus (E) **(B),** metestrus (ME) **(C),** and diestrus (DE) **(D)** stages of the buffalo estrous cycle. M, protein molecular markers; Lane 1-7 contains 25 µg protein from 7 individual buffaloes. Arrow indicates presence of 7 major bands.

TABLE 3 | List of differentially expressed proteins (DEPs) during estrus (E) vs. proestrus (PE), metestrus (ME), and diestrus (DE) stages using LFQ-LC-MS/MS analysis.

Accession	Gene symbol	Description	Peptide	Fold change	Fold change	Fold change
				E/PE	E/ME	E/DE
F1MES3	LIPF	Gastric triacylglycerol lipase	4	33.125	38.834	18.989
Q29458	LIPF	Gastric triacylglycerol lipase	7	32.65	39.416	19.173
A4FV72	PPIE	Peptidyl-prolyl cis–trans isomerase E	1	21.071	15.047	24.834
P00639	DNASE1	Deoxyribonuclease-1	2	7.005	4.783	10.895
F1N0N9	—	Uncharacterized protein	1	5.447	1.582	11.299
P0CG53	UBB	Polyubiquitin-B	1	2.301	10.493	3.44
P10790	FABP3	Fatty acid-binding protein, heart	1	2.445	6.187	10.788
P02690	PMP2	Myelin P2 protein	1	2.445	6.187	10.788
P15497	APOA1	Apolipoprotein A-I	6	1.942	9.793	6.824
G3MZU3	LOC783399	Uncharacterized protein	4	1.175	8.238	5.386
Q865V6	CAPG	Macrophage-capping protein	1	5.134	1.633	4.546
Q1JPG7	PKLR	Pyruvate kinase	1	5.05	2.016	4.72
G3N2P2	LOC613345	Uncharacterized protein	2	4.503	2.859	2.129
P19661	CATHL3	Cathelicidin-3	2	4.339	2.036	2.882
Q2KJF1	A1BG	Alpha-1B-glycoprotein	1	4.135	1.934	3.79
P02070	LOC100850059; HBB	Hemoglobin subunit beta	13	3.95	1.725	1.372
P02313	HMGN2	Non-histone chromosomal protein HMG-17	1	3.74	3.175	2.366
P19660	CATHL2	Cathelicidin-2	3	3.573	3.92	4.087
Q2KIT0	MGC137014	Protein HP-20 homolog	1	3.457	3.269	2.615
G1K1L8	SERPINB1	Leukocyte elastase inhibitor	7	3.116	2.307	3.904
Q1JPB0	SERPINB1	Leukocyte elastase inhibitor	10	3.01	2.349	3.419
P79125	BPIFA2B	Short palate, lung and nasal epithelium carcinoma–associated protein 2B	1	2.938	2.139	1.437
P54229	CATHL5	Cathelicidin-5	3	2.561	1.439	1.781
P56425	CAMP	Cathelicidin-7	2	2.351	2.847	1.202
Q0VCX4	CTNNB1	Catenin beta-1	1	2.348	5.891	2.679
Q3ZC09	ENO3	Beta-enolase	3	2.302	0.7	4.444
A5D984	PKM	Pyruvate kinase	11	2.293	1.513	1.65
Q0VCW4	SDS	L-Serine dehydratase/L-threonine deaminase	6	2.233	1.876	1.996
F1N0R8	SDS	L-Serine dehydratase/L-threonine deaminase	6	2.233	1.876	1.996
P00975	—	Serum basic protease inhibitor	1	2.154	1.683	1.943
Q148F1	CFL2	Cofilin-2	1	2.097	1.326	1.337
F1MLW2	BPIFB1	BPI fold-containing family B member 1	10	2.011	1.322	2.338
F1MKB7	GSTO1	Uncharacterized protein	2	1.859	1.86	4.825
A5PJE3	FGA	Fibrinogen alpha chain	1	1.821	5.715	5.472
P02672	FGA	Fibrinogen alpha chain	1	1.821	5.715	5.472
P54228	CATHL6	Cathelicidin-6	4	1.785	2.494	1.382
A6QR19	ENO2	ENO2 protein	2	1.779	1.309	1.637
P02754	PAEP	Beta-lactoglobulin	10	1.703	1.446	1.519
G5E5H7	PAEP	Uncharacterized protein	9	1.703	1.732	1.371
E1BI89	—	Uncharacterized protein	13	1.682	1.539	3.423
P02676	FGB	Fibrinogen beta chain	1	1.568	7.645	6.275
F1MBN5	FOLR1; FOLR3	Folate receptor alpha	3	1.526	2.006	0.975
P0CB32	HSPA1L	Heat shock 70-kDa protein 1-like	1	1.474	2.283	3.613
Q27975	HSPA1A	Heat shock 70-kDa protein 1A	1	1.474	2.283	3.613
Q27965	HSPA1A	Heat shock 70-kDa protein 1B	1	1.474	2.283	3.613
G3X701	LOC515966	Uncharacterized protein	2	1.44	1.708	2.409
P05307	P4HB	Protein disulfide-isomerase	1	1.393	1.54	1.98
Q0VCN9	FOLR2	Folate receptor 2 (Fetal)	1	1.384	2.006	2.372
G3MX65	WFDC2	Uncharacterized protein	2	1.322	2.324	3.6
G3X8G9	—	Uncharacterized protein	6	1.311	2.365	1.463
Q865S1	AP3D1	AP-3 complex subunit delta-1	1	1.285	7.378	5.363
Q2TBU0	HP	Haptoglobin	14	1.283	1.481	2.495
A6H6Z5	GALNT6	Polypeptide N-acetylgalactosaminyl transferase 6	3	1.271	1.388	1.416
E1BBX7	LCNL1	Uncharacterized protein	2	1.24	2.655	8.647
G5E5A7	—	Uncharacterized protein	34	1.142	1.536	1.602
G3MX66	VMO1	Uncharacterized protein	6	1.074	1.743	2.984
F1MK50	OBP2B	Uncharacterized protein	3	1.056	1.341	2.985
G3X799	OBP	Uncharacterized protein	9	0.944	1.437	1.674
Q8SPU5	BPIFA1	BPI fold-containing family A member 1	4	0.791	5.438	5.007
Downregulated protein						

(Continued on following page)

TABLE 3 | (*Continued*) List of differentially expressed proteins (DEPs) during estrus (E) vs. proestrus (PE), metestrus (ME), and diestrus (DE) stages using LFQ-LC-MS/MS analysis.

Accession	Gene symbol	Description	Peptide	Fold change E/PE	Fold change E/ME	Fold change E/DE
G3MZ19	LOC100295741; ZG16B	HRPE773-like	8	0.445	0.463	0.134
A6QLQ8	ENDOU	Poly(U)-specific endoribonuclease	2	0.453	0.364	0.433
A4IFU5	HIST3H2A	Histone H2A	3	0.43	0.443	0.539
G5E5V1		Uncharacterized protein	2	0.56	0.306	0.581

saliva is critical for the development of a simple, reliable estrus detection tool. Earlier investigation has confirmed the salivary proteins as a potential candidate to detect fertile periods in woman (Alagendran et al., 2013; Saibaba et al., 2021) and estrus (Muthukumar et al., 2014b; Shashikumar et al., 2018) in buffaloes. However, estrus biomarker discovery in buffalo saliva by differential proteome analysis using TMT and LFQ coupled to mass spectrometry is lacking. Comparative proteome profiling using LFQ-LC-MS/MS and TMT-LC-MS/MS analysis in buffalo saliva identified a total of 520 and 369 proteins as DEPs, respectively. These findings may be helpful for further understanding of buffalo estrus biology and development of an easy, reliable estrus detection method for buffalo.

4.1 Proteins Involved in Regulation of Endopeptidase Activity

Our study found the over-expression of leukocyte elastase inhibitor (SERPINB1) during estrus followed by proestrus and almost negligible expression during metestrus and diestrus stages of the estrous cycle. SERPINB1 and several other DEPs (A2M, A2ML1, C3, CST3, CST6, CSTB, LOC404103, LOC786263, LTF, OVOS2, PTI, S100A8, SERPINA3-8, SERPINB1, SERPINB6, SERPINB8, SERPINI2, SFN, SPINK5, THBS1, TIMP2, and WFDC2) in the present study were involved in the regulation of endopeptidase inhibitor activity. SERPINB1 and other protease inhibitors inactivate serine proteases and cysteine proteases and mediate important functions in fibrinolysis, coagulation, inflammation, cell mobility, cellular differentiation, apoptosis, and protein C pathways (Law et al., 2006), thus regulating the innate immune response, inflammation, and cellular homeostasis (Choi et al., 2019). The previous study demonstrated altered expression of three SERPINs, SERPINB2, SERPINE1, and SERPINE2 during follicular development in bovine ovarian follicles (Dow et al., 2002; Bedard et al., 2003). Expression of SERPINE2 gene in preovulatory follicles was markedly upregulated immediately after the LH surge and then decreased to the lowest level toward ovulation (Hasan et al., 2002; Cao et al., 2006). Similarly, over-expression of SERPINE2 in granulosa cells of mature follicles compared to that in small and medium follicles has also been observed (Cao et al., 2004). Previous studies also demonstrated over-expression of SERPINB6 in healthy follicles compared to that in the atretic ones, suggesting follicular development and atresia in bovine ovarian follicles are mediated through SERPINs (Hayashi et al., 2011). The increased abundance of SERPINB1 during the estrus stage may be a protective mechanism of follicular cells against several proteases and intrinsic for follicular development and final follicular maturation and steroid production by ovarian follicles.

4.2 Proteins Involved in Glycolysis and Pyruvate Metabolism

We observed increased expression of beta-enolase (ENO3) during E compared to PE, ME, and DE stages. ENO3 is a glycolytic enzyme and regulates the glycolysis process by catalyzing the reversible conversion of 2-phosphoglyceric acid to phosphoenolpyruvic acid (Giallongo et al., 1993). In addition, we observed 14 other DEPs (ALDOA, ALDOB, ALDOC, ENO1, ENO2, GAPDHS, GPI, LDHA, LDHB, LDHC, PGAM1, PGK1, PKLR, and TPI1) and five DEPs (LDHA, LDHB, LDHC, MDH1, and PKLR) were significantly involved in the glycolysis or gluconeogenesis metabolic pathway and pyruvate metabolism, respectively. It is speculated that these proteins associated with active synthesis of energy may support follicular development, steroidogenesis, final follicular maturation, and ovulation process. In a previous study, pyruvate metabolism has been essential for the completion of oogenesis, serving as a vital source of energy during the meiotic maturation of murine oocytes (Johnson et al., 2007). It has also been observed that the mature cumulus oocyte complex (COC) uses two times more glucose and pyruvate than the immature ones (Sutton et al., 2003), indicating high energy demand supported by upregulation of glycolysis by ovarian follicles during the process of final maturation of oocyte. The previous study has demonstrated that increased enolase expression is responsible for higher expression of the *FSH* gene in granulosa cells during the follicular phase (Hermann and Heckert, 2007). *FSH* has a significant role in reproduction by regulating granulosa cell differentiation, proliferation and ovarian steroidogenesis (Richards, 1994), and controlling follicular development and

TABLE 4 | List of upregulated proteins during estrus (E) vs. proestrus (PE), metestrus (ME), and diestrus (DE) stages using TMT-LC-MS/MS analysis.

Accession	Gene symbol	Description	Peptide	Fold change E/PE	Fold change E/ME	Fold change E/DE
F1MKI5	SDF4	45-kDa calcium-binding protein	2	71.71	100	19.73
Q3ZBZ1	SDF4	45-kDa calcium-binding protein	3	62.663	88.648	19.262
Q2NKS8	LOC526524	Peptidyl-prolyl isomerase	1	13.678	17.355	37.984
E1BKA1	LOC786350	Protein S100	1	14.447	19.419	1.34
G3MZ21	—	Uncharacterized protein	1	13.057	8.159	2.728
E1BEL8	HBE1	Globin B1	1	13.057	8.159	2.728
E1BEL7	HSPB1	Heat shock protein beta-1	6	12.524	15.547	7.289
Q58DP7	HSPB1	Heat shock 27-kDa protein 1	5	12.524	15.547	7.289
G3X7S2	HSPB1	Heat shock protein beta-1	5	12.524	15.547	7.289
Q5KR47	TPM3	Tropomyosin alpha-3 chain	1	11.813	13.017	1.782
A6QR15	LOC535277	LOC535277 protein	1	11.813	13.017	1.782
Q5KR48	TPM2	Tropomyosin beta chain	1	11.813	13.017	1.782
Q5KR47-2	TPM3	Isoform 2 of Tropomyosin alpha-3 chain	1	11.813	13.017	1.782
P81947	TUBA1B; TUBA1A	Tubulin alpha-1B chain	2	11.444	12.223	5.148
F1MNF8	LOC100141266	Tubulin alpha chain	1	11.444	12.223	5.148
G3X700	LOC104969973	Uncharacterized protein	7	11.348	14.639	5.809
Q862B8	TIMP2	Similar to metalloproteinase inhibitor	3	11.285	11.992	2.762
P07435	OBP	Odorant-binding protein	8	2.573	2.481	69.029
Q862Q0	PGAM1	Phosphoglycerate mutase	1	3.695	5.268	48.354
Q0IIA2	MGC151921	Odorant-binding protein-like	5	1.784	2.753	23.736
A5PJH7	LOC788112	LOC788112 protein	1	2.292	1.987	21.114
A8KC76	HSPA8	HSPA8 protein	1	4.673	4.937	18.413
Q865V6	CAPG	Macrophage-capping protein	1	3	3.531	14.154
Q3ZCL8	SH3BGRL3	SH3 domain-binding glutamic acid-rich-like protein 3	2	2.104	2.295	12.421
F1MS23	LCN1	Lipocalin 1	6	7.354	14.39	11.301
P02070	HBB	Hemoglobin subunit beta	9	9.977	6.41	2.243
F1MKC4	—	Uncharacterized protein	5	9.876	9.214	2.063
Q58DT9	ACTA2	Alpha 2 actin	9	9.561	8.913	2.069
G8JKX4	ACTA2	Actin, aortic smooth muscle	9	9.561	8.913	2.069
E1BLR9	CPD	Carboxypeptidase D	1	8.519	11.821	3.381
P60712	ACTB	Actin, cytoplasmic 1	17	8.154	7.925	2.061
F1MRD0	ACTB	Actin, cytoplasmic 1	14	8.154	7.925	2.061
P81265-2	PIGR	Isoform short of polymeric immunoglobulin receptor	15	7.975	8.284	5.803
G5E6M1	PIGR	Polymeric immunoglobulin receptor	14	7.975	8.284	5.803
G3N2H5	S100A12	Protein S100	1	7.311	3.613	2.133
A0A1C9EIX6	HSPB1	Heat shock protein family B member 1 variant 2	7	6.972	7.193	5.125
F1N650	ANXA1	Annexin	2	6.562	4.819	0.855
Q712W6	GAPDH	Glyceraldehyde 3-phosphate dehydrogenase	3	5.445	4.678	0.97
E1BDE6	LGALS7B	Galectin	6	5.339	6.629	4.633
G3N3D0	LGALS7	Galectin	6	5.339	6.629	4.633
G3MX66	VMO1	Vitelline membrane outer layer 1 homolog	5	5.3	5.5	4.1
P81265	PIGR	Polymeric immunoglobulin receptor	29	5.127	5.514	4.049
A6QNW3	PIGR	PIGR protein	29	5.127	5.514	4.049
G5E5C8	TALDO1	Transaldolase	3	4.986	4.795	1.281
A5D7E8	PDIA3	Protein disulfide-isomerase	2	4.969	3.617	1.212
E1B970	GOLGA3	Golgin A3	1	4.283	5.078	6.458
A6QQ07	BTD	Biotinidase	1	3.945	3.735	2.313
Q0P569	NUCB1	Nucleobindin-1	9	3.793	3.702	4.757
P68252	YWHAG	14-3-3 protein gamma	2	3.757	4.645	9.328
G3X894	LOC786263	Uncharacterized protein	5	3.71	5.005	0.897
Q629I2	RPVgp5	Fusion glycoprotein F0	1	3.705	4.751	3.904
P05307	P4HB	Protein disulfide-isomerase	3	3.338	3.649	9.38
Q3SZ62	PGAM1	Phosphoglycerate mutase 1	6	3.21	3.424	3.828
G3X799	OBP	Uncharacterized protein	9	3.041	2.813	2.032
F1N614	HSPA5	78-kDa glucose-regulated protein	2	3.018	3.507	2.316
Q2KJF1	A1BG	Alpha-1B-glycoprotein	2	2.625	2.919	2.931
Q3T145	MDH1	Malate dehydrogenase, cytoplasmic	2	2.547	2.689	1.172
F1N3A1	THBS1	Thrombospondin-1	10	2.524	2.7	0.95
F1MKE7	KRT6C	Uncharacterized protein	9	2.385	3.018	4.091
Q3T010	PEBP4	Phosphatidylethanolamine-binding protein 4	2	2.212	3.24	2.012
F2FB41	MUC5AC	Mucin-5AC	6	2.197	3.168	1.523
Q3SZH5	AGT	Angiotensinogen	4	1.98	1.909	2.112
F2Z4I6	HIST2H2AC	Histone H2A	5	1.928	2.208	2.153

(Continued on following page)

TABLE 4 | (*Continued*) List of upregulated proteins during estrus (E) vs. proestrus (PE), metestrus (ME), and diestrus (DE) stages using TMT-LC-MS/MS analysis.

Accession	Gene symbol	Description	Peptide	Fold change E/PE	Fold change E/ME	Fold change E/DE
A1A4R1	HIST2H2AC	Histone H2A type 2-C	5	1.928	2.208	2.153
F1MRN2	—	Histone H2A	3	1.928	2.208	2.153
F1MLQ1	LOC524236	Histone H2A	2	1.928	2.208	2.153
Q862L0	ACTG2	Similar to beta-actin	4	1.745	1.596	3.548
F1MB90	OVOS2	Uncharacterized protein	16	1.726	2.819	1.215
F6QEL0	—	Cystatin	2	1.427	1.338	3.907
Q5DPW9	CST6	Cystatin	2	1.427	1.338	3.907
F1MVR7	FAM25A	Uncharacterized protein	1	1.378	1.946	1.935
E1BI89	LOC101908058	Uncharacterized protein	4	1.355	1.541	2.142
K4JDT2	A2M	Alpha-2-macroglobulin variant 20	12	1.243	2.308	8.216
F1N4C3	BPIFA2B	Uncharacterized protein	3	0.428	0.285	1.713

fertility in females (Hermann and Heckert, 2007). Specific expression of ENO3 in buffalo saliva, particularly during estrus stage has also been observed by an earlier study (Muthukumar et al. (2014b). The increased expression of ENO3 during E compared to other stages of the estrous cycle suggests it has a defined role in follicular development, final follicular maturation, and steroid production by follicular granulosa cells that leads to the onset of estrus in buffaloes.

4.3 Proteins Involved in Estrogen Signaling

This study also found a higher abundance of the heat shock protein family A (HSPA1A/HSP70) during estrus than other stages of the estrous cycle. HSPA1A is a molecular chaperon and plays a role in the estrogen signaling pathway. The present study also found other molecular chaperons such as HSPA1L, HSPA2, and HSPA8 as DEPs. Chaperones are stress-response molecules and involved in housekeeping of the cells and facilitating the transport, folding, unfolding, assembly, and disassembly of multi-structured protein units and degradation of misfolded or aggregated proteins (Sorensen et al., 2003). HSPA1A plays a role in the assembly and trafficking of steroid hormone receptors, acts as a co-activator for the nuclear estrogen receptor-α activity, and regulates steroid hormone synthesis by ovarian follicles (Khanna et al., 1995; Liu and Stocco, 1997; Hurd et al., 2000). HSPA1A also mediates luteal regression in murine corpus luteum (Khanna et al., 1995). A previous study also identified a higher abundance of HSPA1A protein in cervical mucus during E than the DE stage of the buffalo estrous cycle (Muthukumar et al., 2014a). Our previous study also observed estrus-specific expression of HSPA1A in buffalo saliva (Shashikumar et al., 2018). Furthermore, our direct saliva transcript analysis also demonstrated a higher level of HSP70 transcript in saliva during estrus than the diestrus stage, suggesting it as a good indicator of estrus in buffaloes (Onteru et al., 2016). HSPA1A protects cells from the negative effect of stress by promoting the folding of proteins and correcting the misfolding of denatured proteins (Lindquist and Craig 1988). Steroid hormone, particularly estradiol plays a key role in inducing estrus signs in farm animals, and its level increased from 22.4–35 pg/ml (Roy and Prakash 2009; Mondal et al., 2010) just before the onset of estrus in buffaloes. An earlier study demonstrated estradiol treatment-induced stress or injury in rat brain vasculature and estradiol-induced heat shock protein expression occurred as a protective mechanism to prevent cellular damage (Lu et al., 2002; Raval et al., 2013). Suggestive increased abundance of HSPA1A protein during estrus could be a protective mechanism of granulosa cells against estrogen-induced stress and its possible role in follicular development and steroidogenesis process.

4.4 Calcium Ion Binding Activity

Increased expression of 45-kDa calcium-binding protein (SDF4) was observed during E compared to PE, ME and DE stages of the estrous cycle. SDF4 is a calcium-binding protein and regulates calcium-dependent activities in the lumen of the endoplasmic reticulum and is involved in calcium-ion regulated exocytosis. Calcium-binding proteins are mainly localized in the cytosol and various parts of the secretory pathway (Honore, 2009). They have diversified functions, including secretory process, chaperone activity, and signal transduction (Honore, 2009). Although its exact role in estrous physiology is unknown, its higher expression during estrus suggests its possible involvement in chaperon-mediated steroidogenesis and cellular protection against estradiol-induced stress.

4.5 Proteins Involved in Innate Immune Response

The present study also identified several DEPs (PIGR, S100A12, BPIFA2B, B2M, A2M, BPIFB1, BPIFA1, CATHL3, CATHL5, FGB, and FGA) involved in innate immune response. The whole estrous cycle is regulated by the differential level of steroid hormones; estradiol is predominant during follicular phase and progesterone during the luteal phase. These steroid hormones modulate the immune system depending on the estrous cycle stage. Binding with specific hormone receptors, steroid hormone induces genomic and non-genomic actions in immune cells (Gilliver, 2010; Kovacs et al., 2010; Bellavance and Rivest, 2014). In general, estradiol is immune-enhancing by stimulating functions of innate immune cells, Th1 responses, and antibody production from B cells. However, progesterone is immune-suppressing by

TABLE 5 | List of downregulated proteins during estrus (E) vs. proestrus (PE), metestrus (ME), and diestrus (DE) stages using TMT-LC-MS/MS analysis.

Accession	Gene symbol	Description	Peptide	Fold change E/PE	Fold change E/ME	Fold change E/DE
B9TUD2	CATHL7	Cathelicidin-7	1	0.01	0.01	0.01
G3N1R1	—	Uncharacterized protein	1	0.01	0.01	0.063
B9TUC3	CATHL2	Cathelicidin-2	1	0.01	0.01	0.01
Q148E6	CYP4B1	Cytochrome P450 family 4 subfamily B member 1	1	0.01	0.01	0.234
Q1RMN8	IGL@	Immunoglobulin light chain, lambda gene cluster	14	0.014	0.012	0.228
Q28133	BDA20	Allergen Bos d 2	2	0.019	0.095	0.045
A5D7Q2	LOC524810	Uncharacterized protein	9	0.021	0.023	0.112
K4JR84	A2M	Alpha-2-macroglobulin variant 17	2	0.021	0.038	0.393
E1BI82	LOC525947	Uncharacterized protein	1	0.022	0.028	0.275
G3X6K8	HP	Haptoglobin	3	0.028	0.057	0.069
Q3ZCL0	CRISP3	Cysteine-rich secretory protein 2	3	0.032	0.038	0.021
F6R3I5	CRISP3	Uncharacterized protein	4	0.032	0.038	0.021
P02702	FOLR1; FOLR3	Folate receptor alpha	1	0.039	0.049	0.586
E1B8Q6	LOC524080	Uncharacterized protein	1	0.044	0.045	0.01
F1MD73	—	Uncharacterized protein	7	0.045	0.054	0.133
P60986	PIP; LOC107131147	Prolactin-inducible protein homolog	10	0.047	0.062	0.056
F1MCV8	—	Uncharacterized protein	3	0.047	0.062	0.056
F1N6D1	LOC100847724	Uncharacterized protein	13	0.047	0.069	0.016
G3N269	FABP5	Fatty acid-binding protein, epidermal	3	0.053	0.071	0.136
F1MHQ2	BPIFA2A	Uncharacterized protein	21	0.056	0.047	0.048
Q6PVY3	MIF	Macrophage migration inhibitory factor	1	0.057	0.066	0.067
Q6H320	KLK1	Glandular kallikrein	6	0.058	0.071	0.148
A0JNP2	SCGB1D	Secretoglobin family 1D member	1	0.07	0.117	0.352
G3N2D7	LOC100297192	Uncharacterized protein	4	0.073	0.067	0.128
K4JR71	A2M	Alpha-2-macroglobulin variant 2	4	0.076	0.132	0.206
P17697	CLU	Clusterin	5	0.08	0.08	0.444
E1BL84	—	Uncharacterized protein	2	0.08	0.082	0.013
F1MSB7	PLS3	Plastin-3	9	0.082	0.091	0.036
Q862H7	S100A11	Protein S100	1	0.086	0.075	0.01
O62672	MUC19	Submaxillary mucin 1	9	0.087	0.084	0.428
F1MWN7	—	Uncharacterized protein	9	0.087	0.084	0.431
F1N0W1	FCHSD1	Uncharacterized protein	6	0.091	0.161	0.07
Q5E9B1	LDHB	L-Lactate dehydrogenase B chain	2	0.101	0.083	0.032
G1K1L8	—	Uncharacterized protein	9	0.106	0.117	0.104
A6QQF6	SBSN	Suprabasin	1	0.109	0.112	0.06
A2VE41	EFEMP1	EGF-containing fibulin-like extracellular matrix protein 1	14	0.12	0.099	0.161
E1BAU5	LOC512548; SLPI	Uncharacterized protein	1	0.124	0.171	0.479
A4IFI0	IGLL1	IGLL1 protein	9	0.132	0.115	0.289
F1MCF8	LOC100297192	Uncharacterized protein	11	0.132	0.115	0.289
A5PK49	IGL@	IGL@ protein	6	0.132	0.115	0.289
A6H7J7	LOC100297192	Uncharacterized protein	9	0.139	0.121	0.297
P02253	HIST1H1C	Histone H1.2	18	0.143	0.107	0.05
F2FB39	MUC19	Mucin-19	14	0.154	0.136	0.067
G3X6I0	—	Uncharacterized protein	10	0.172	0.213	0.246
P19858	LDHA	L-Lactate dehydrogenase A chain	21	0.172	0.134	0.032
G3MX67	—	Uncharacterized protein	2	0.176	0.157	0.213
F1MBA5	—	Uncharacterized protein	6	0.176	0.157	0.213
G3N0H7	—	Uncharacterized protein	4	0.176	0.157	0.213
A0A1Y0KDJ6	—	Beta-casein	9	0.177	0.181	0.495
F1MGF6	—	Uncharacterized protein	13	0.181	0.165	0.052
G9G9X6	LALBA	Alpha-lactalbumin protein variant D	14	0.188	0.254	0.352
Q3SYR8	IGJ; JCHAIN	Immunoglobulin J chain	10	0.19	0.166	0.191
B2BX69	AZGP1	Zn-alpha-2-glycoprotein	3	0.197	0.19	0.156
B2BX70	AZGP1	Zn-alpha-2-glycoprotein	2	0.197	0.19	0.156
A5D7V3	ESM1	ESM1 protein	2	0.213	0.297	0.145
G5E513	IGHM	Immunoglobulin heavy constant mu	5	0.219	0.455	0.126
P01035	CST3	Cystatin-C	6	0.221	0.184	0.302
G5E5Q6	TFF3	Trefoil factor 3	3	0.229	0.232	0.22
Q6LC78	LTF	Lactoferrin	8	0.23	0.432	0.369
G5E5T5	—	Uncharacterized protein	8	0.231	0.459	0.424
E1B8Q2	LOC104969118	Uncharacterized protein	5	0.241	0.216	0.775
Q8MII0	LTF	Lactotransferrin	8	0.244	0.388	0.394
F1MB32	A2ML1	Uncharacterized protein	3	0.244	0.318	0.087

(Continued on following page)

TABLE 5 | (*Continued*) List of downregulated proteins during estrus (E) vs. proestrus (PE), metestrus (ME), and diestrus (DE) stages using TMT-LC-MS/MS analysis.

Accession	Gene symbol	Description	Peptide	Fold change E/PE	Fold change E/ME	Fold change E/DE
Q6LBN7	LTF	Lactoferrin	18	0.254	0.424	0.295
Q3SZ57	AFP	Alpha-fetoprotein	1	0.258	0.427	0.063
Q19KS1	LTF	Lactoferrin	7	0.269	0.484	0.223
Q683R8	Cath	Cathelicidin	3	0.316	0.364	0.079
A6QQA8	QSOX1	Sulfhydryl oxidase	1	0.316	0.392	0.14
P00432	CAT	Catalase	1	0.33	0.385	0.023
P33046	CATHL4; LOC786887	Cathelicidin-4	1	0.377	0.335	0.058
F1MH40	—	Uncharacterized protein	1	0.417	0.43	0.413
X5F5B4	SERPINB4	Serpin B4-like protein	2	0.456	0.557	0.566
A6QPZ4	SERPINB4	SERPINB4 protein	2	0.456	0.557	0.566

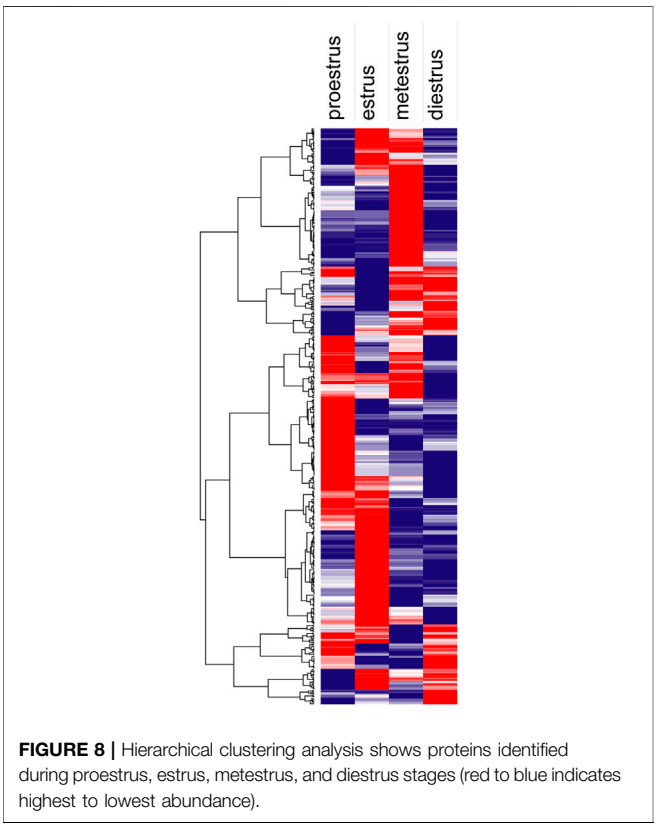

FIGURE 8 | Hierarchical clustering analysis shows proteins identified during proestrus, estrus, metestrus, and diestrus stages (red to blue indicates highest to lowest abundance).

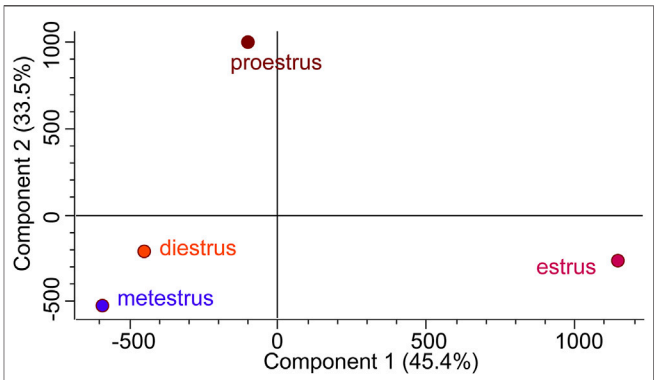

FIGURE 9 | Principal component analysis (PCA) attributes the more difference between estrus and other non-estrus stages (proestrus, metestrus, and diestrus).

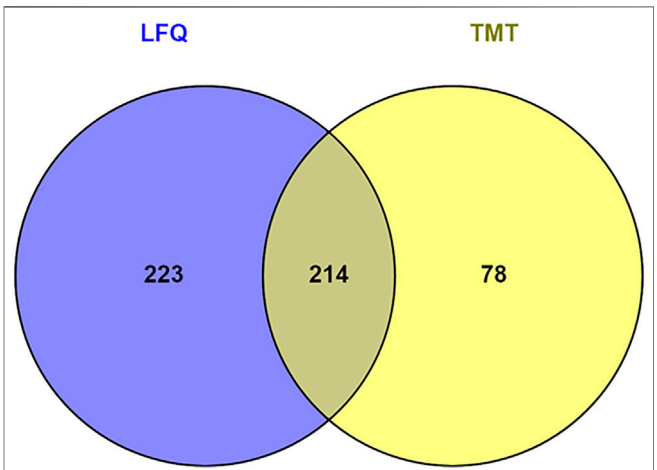

FIGURE 10 | Venn diagram represents number of proteins identified by tandem mass tag (TMT) and label-free quantitation (LFQ).

down-regulating functions of immune cells such as macrophages (Su et al., 2009), natural killer cells (Arruvito et al., 2008), or dendritic cells (Butts et al., 2007; Hughes et al., 2008). In addition, progesterone antagonizes the immune-enhancing function of estrogens on T-cell cycle progression (McMurray et al., 2001) and proliferation of T cells (Butts et al., 2007). Importance of antimicrobial peptides (S100A12, CATHL3, and CATHL5)(Diamond et al., 2009), BPI fold-containing family proteins (BPIFA2B, BPIFB1, and BPIFA1) (Li et al., 2020), polymeric immunoglobulin receptor (PIGR) (Wei and Wang, 2021), alpha-2-macroglobulin (A2M), and beta-2-macroglobulin (B2M) (Vandooren and Itoh, 2021) in mucosal immunity is well established. Mucosal immunity protects the internal genital tract against pathogens. During the estrus period, physical barriers between external genitalia and uterus breached, making pathogens to enter into the uterus. Hence, the estrogen-dominant estrus phase modulates the function of innate immune cells and

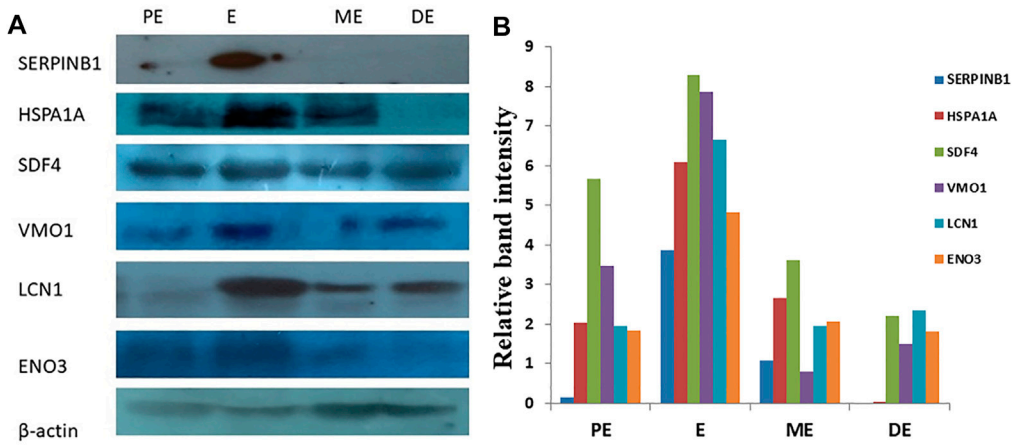

FIGURE 11 | Western blot analysis for validation of differentially expressed upregulated proteins. **(A)** Over-expression of SERPINB1, HSPA1A, SDF4, VMO1, LCN1, and ENO3, during estrus (E) compared to proestrus (PE), metestrus (ME), and diestrus (DE) stages of the buffalo estrous cycle. **(B)** Band intensity was normalized against beta-actin as an internal control.

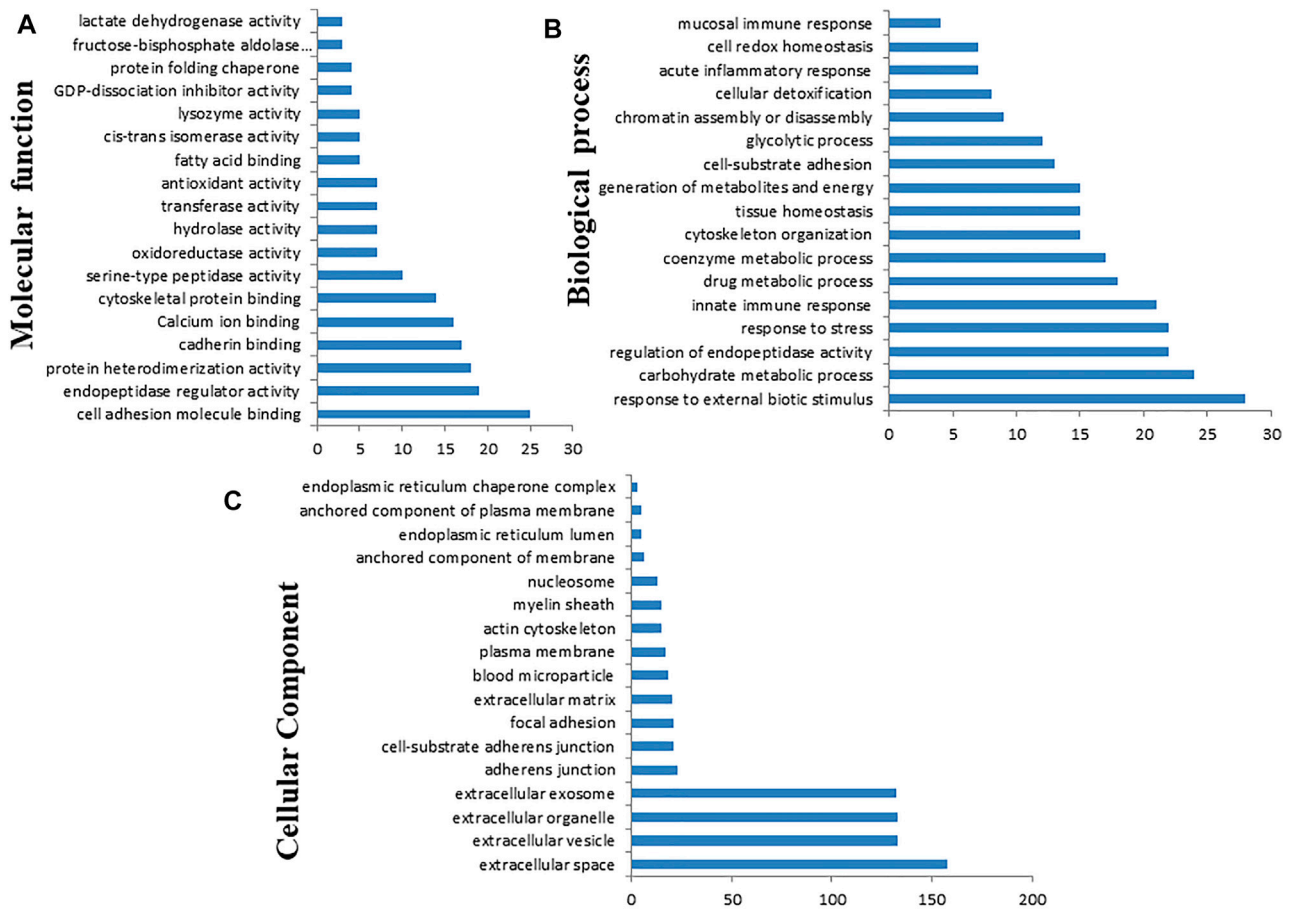

FIGURE 12 | Gene Ontology (GO) classification of the differentially expressed proteins based on molecular function **(A)**, biological process **(B)**, and cellular component **(C)** using Cytoscape software with ClueGO plug-in.

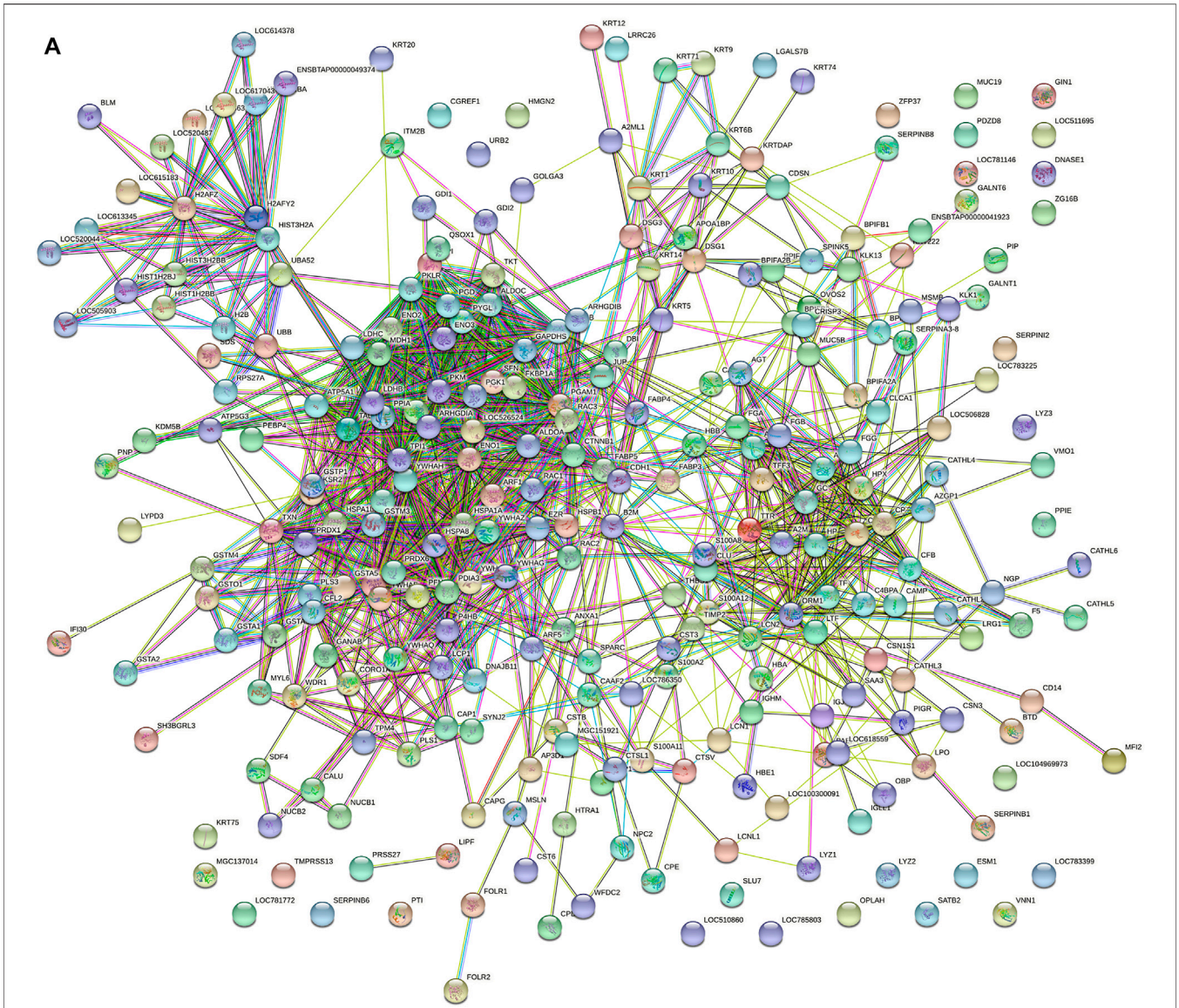

FIGURE 13 | (A) Protein–protein interaction (PPI) network constructed by the STRING tool using combined score of 0.9–0.4. A PPI network with high combined score was created (p < 1.0E-16) with 378 nodes, 810 edges, 4.29 average node degree, and 0.357 average local clustering coefficient. **(B)** Functional annotation of a protein–protein interacting hub using Cytoscape software with ClueGO plug-in.

secretes several antimicrobial peptides and proteins that protect the mucosa of the female reproductive tract against external pathogens.

4.6 Proteins Involved in Cytoskeleton Organization

The present study also depicted several DEPs involved in the cytoskeleton organization process (APOA1, ARF1, CAP1, CAPG, CFL1, CFL2, CORO1A, CSN1S1, EZR, FKBP1A, HSPA1A, KRT14, KRT20, KRT71, KRT9, LCP1, PFN1, PLS1, PLS3, RAC1, RAC2, and WDR1). It is during estrus that an oocyte that has been diplotene-restricted restarts meiosis before ovulation. Oocyte meiosis entails a number of intricate processes, including change of the mitotic cell cycle, chromosomal segregation, spindle reorganization, and accomplishment of oocyte asymmetry and polar body extrusion. These activities need reorganization of the cytoskeleton, coordination of cytoplasmic dynamics, and regulation of the cortex's tension forces (Brunet and Verlhac, 2011; Yi et al., 2011). These findings and our results support the role of cytoskeletal proteins in follicular and oocyte maturation during estrus.

4.7 Proteins With Miscellaneous Functions

Notably, we noticed an elevated expression of vitelline membrane outer layer protein 1 (VMO1) in comparisons between E and PE, ME, and DE. It is the first report of VMO1 protein in saliva during the estrous cycle. Its precise involvement in controlling

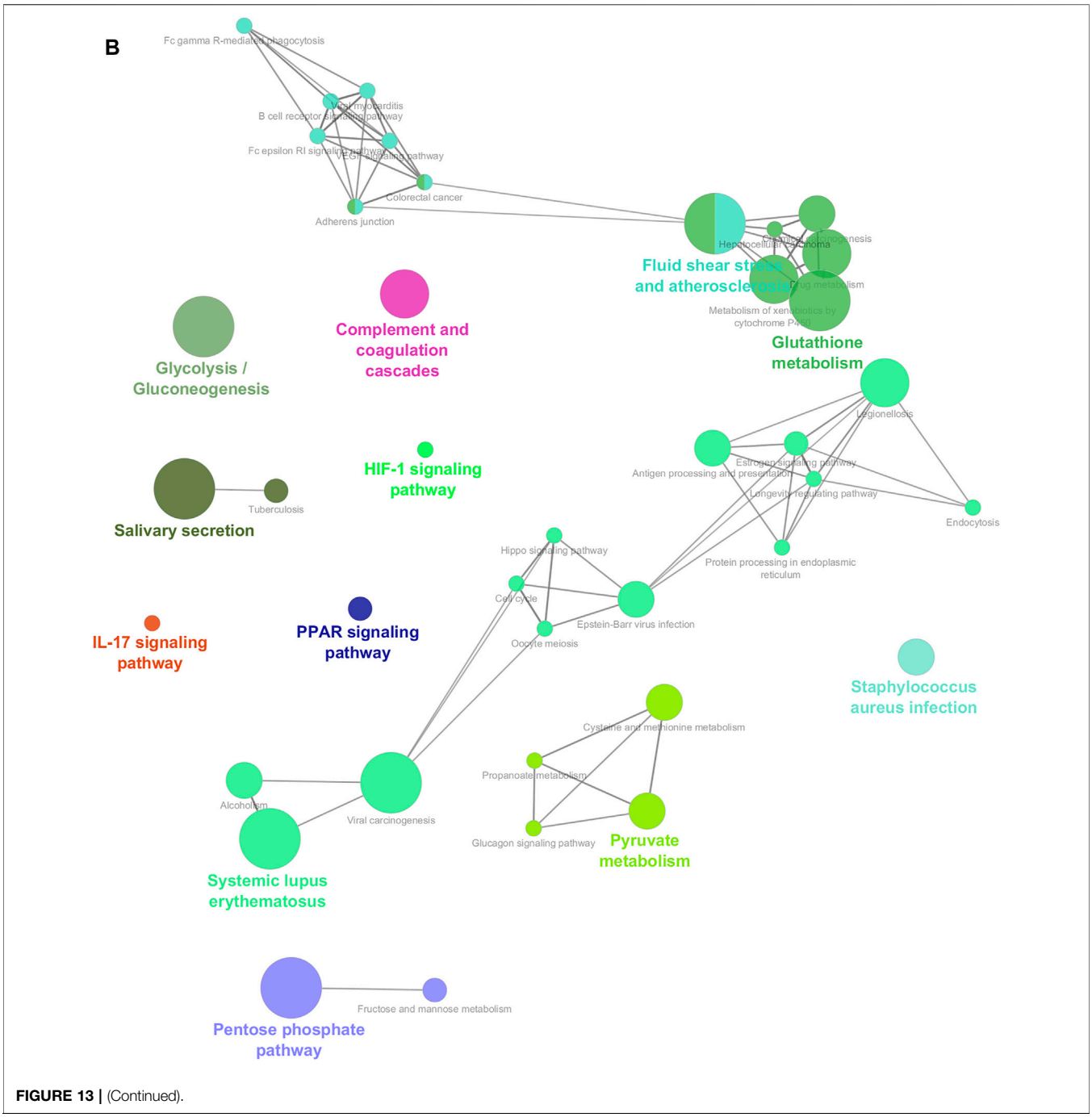

FIGURE 13 | (Continued).

folliculogenesis and estrous physiology is unknown. VMO1 protein was initially found in chicken as an important component of the egg's vitelline membrane's outer layer (Kido et al., 1992) and plays a critical function in oviductal recrudescence in laying hens (Lim and Song, 2015). It is anticipated to be a new estrogen-induced gene in laying hens and a possible diagnostic biomarker for ovarian cancer (Lim and Song, 2015). As a result, it is probable that the estradiol peak that occurs during estrus is the cause for the over-expression of VMO1 and its significant relationship with estrus physiology. Additional investigations in large animals using powerful genetic engineering technologies such as CRISPR-based knockout are required to characterize the mechanism of action (Singh et al., 2000). Another protein, nucleobindin-1 (NUCB1), was shown to be significantly increased during estrus compared to other non-estrus phases. Nucleobindins are multidomain Ca2+ and DNA-binding proteins that have a variety of roles in vertebrates. NUCB1 is converted from NUCB2 to biologically active NUCB1 by the action of prohormone convertase (Rajeswari et al., 2020). NUCB2 is claimed to operate as a local regulator in the mouse ovary, controlling steroidogenesis and energy balance through autocrine

TABLE 6 | Involvement of differentially expressed proteins (DEPs) in KEGG pathways.

S.No.	KEGG pathway	Number of genes	Associated gene	p-value
1	Glycolysis/gluconeogenesis	15	ALDOA, ALDOB, ALDOC, ENO1, ENO2, ENO3, GAPDHS, GPI, LDHA, LDHB, LDHC, PGAM1, PGK1, PKLR, and TPI1	0.00
2	PPAR signaling pathway	6	APOA1, DBI, FABP3, FABP4, FABP5, and UBC	0.00
3	Complement and coagulation cascades	9	A2M, C3, C4BPA, CFB, CLU, F5, FGA, FGB, and FGG	0.00
4	IL-17 signaling pathway	5	LCN2, LOC786350, MUC5AC, MUC5B, and S100A8	0.03
5	Salivary secretion	12	CAMP, CATHL2, CATHL3, CATHL4, CATHL5, CATHL6, CST3, LOC785803, LPO, LYZ2, LYZ3, and MUC5B	0.00
6	Pentose phosphate pathway	7	ALDOA, ALDOB, ALDOC, GPI, PGD, TALDO1, and TKT	0.00
7	Fructose and mannose metabolism	4	ALDOA, ALDOB, ALDOC, and TPI1	0.00
8	Cysteine and methionine metabolism	5	LDHA, LDHB, LDHC, MDH1, and SDS	0.00
9	Pyruvate metabolism	5	LDHA, LDHB, LDHC, MDH1, and PKLR	0.00
10	Propanoate metabolism	3	LDHA, LDHB, and LDHC	0.02
11	Glucagon signaling pathway	5	LDHA, LDHB, LDHC, PGAM1, and PYGL	0.03
12	VEGF signaling pathway	3	RAC1, RAC2, and RAC3	0.09
13	Adherens junction	5	CDH1, CTNNB1, RAC1, RAC2, and RAC3	0.01
14	B-cell receptor signaling pathway	4	LOC100300716, RAC1, RAC2, and RAC3	0.05
15	Fc epsilon RI signaling pathway	4	LOC100300716, RAC1, RAC2, and RAC3	0.04
16	Fc gamma R-mediated phagocytosis	5	CFL1, CFL2, LOC100300716, RAC1, and RAC2	0.02
17	Fluid shear stress and atherosclerosis	13	CTNNB1, CTSV, GSTA2, GSTA3, GSTA5, GSTM1, GSTM3, GSTO1, GSTP1, RAC1, RAC2, RAC3, and TXN	0.00
18	Glutathione metabolism	9	GSTA2, GSTA3, GSTA5, GSTM1, GSTM3, GSTO1, GSTP1, OPLAH, and PGD	0.00
19	Metabolism of xenobiotics by cytochrome P450	7	GSTA2, GSTA3, GSTA5, GSTM1, GSTM3, GSTO1, and GSTP1	0.00
20	Chemical carcinogenesis	7	GSTA2, GSTA3, GSTA5, GSTM1, GSTM3, GSTO1, and GSTP1	0.00
21	Fluid shear stress and atherosclerosis	13	CTNNB1, CTSV, GSTA2, GSTA3, GSTA5, GSTM1, GSTM3, GSTO1, GSTP1, RAC1, RAC2, RAC3, and TXN	0.00
22	Cell cycle	7	SFN, YWHAB, YWHAE, YWHAG, YWHAH, YWHAQ, and YWHAZ	0.01
23	Oocyte meiosis	6	YWHAB, YWHAE, YWHAG, YWHAH, YWHAQ, and YWHAZ	0.02
24	Protein processing in endoplasmic reticulum	8	GANAB, HSPA1A, HSPA1L, HSPA2, HSPA5, HSPA8, P4HB, and PDIA3	0.01
25	Endocytosis	11	ARF1, ARF3, ARF5, FOLR1, FOLR2, FOLR3, HSPA1A, HSPA1L, HSPA2, HSPA8, and UBB	0.01
26	Hippo signaling pathway	8	CDH1, CTNNB1, YWHAB, YWHAE, YWHAG, YWHAH, YWHAQ, and YWHAZ	0.01
27	Antigen processing and presentation	8	B2M, CTSV, HSPA1A, HSPA1L, HSPA2, HSPA8, IFI30, and PDIA3	0.00
28	Estrogen signaling pathway	4	HSPA1A, HSPA1L, HSPA2, and HSPA8	0.1

and paracrine signaling (Kim and Yang, 2012). Additionally, NUCB2 has been shown to bind predominantly to epithelial cells of uterine glands and neutrophils of the endometrium during the mouse estrous cycle, suggesting that its expression in the uterus may be regulated by estrogen secreted by the ovary but not by gonadotropin released by the pituitary gland (Kim et al., 2011). The precise involvement of NUCB1 in estrous physiology in farm animals is unknown and requires additional research. Additionally, the current research showed that two proteins, lipocalin 1 (LCN1) and odorant-binding protein-2B (OBP2B), were overexpressed during estrus compared to other non-estrus phases. Lipocalin one is a globular protein that interacts with and transports a variety of ligands including volatile pheromones/odorants, fatty acids, lipids, steroids, bilins, and retinol. Lipocalin has been extensively studied as a chemosignal in a variety of animals, including rats and pigs (Scaloni et al., 2001; Muthukumar et al., 2013; Cerna et al., 2017). It was more abundant in rodent urine during estrus than during diestrus (Muthukumar et al., 2013; Cerna et al., 2017). Additionally, it was isolated from bovine olfactory mucosa (Pevsner et al., 1986). Lipocalin is connected with chemical communication during estrus, that is, a unique volatile signal sent by urine from a female to male partner as a mating call (Brennan and Keverne, 2004). Lipocalin has also been identified as a significant progesterone-dependent protein released into the uterine lumen in mares (Crossett et al., 1996). Similarly, over-expression of odorant-binding protein during estrus compared to other stages of the estrous cycle was observed. Odorant-binding protein (OBP) plays a role in odor perception, olfactory stimulus, and chemical communication, especially in insects and mammals through body fluids (Pelosi and Maida, 1990). Cerna et al. (2017) also identified OBP as a pheromone-binding protein in the vaginal fluid of mice and observed its highest concentration before ovulation. OBP is an essential protein for the communication signal in rodents (Cavaggioni and Mucignat-Caretta, 2000; Rajkumar et al., 2009). A previous study also identified this protein in buffalo saliva ((Rajkumar et al., 2010; Muthukumar et al., 2018). Increased expression of LCN1 and OBP2B during estrus compared to other non-estrus phases implies that they play a critical role in mediating chemosignaling during estrus in buffalo.

CONCLUSION

This is the first comprehensive report on differential proteome analysis of buffalo saliva between the stages of estrus and non-estrus by employing both label-free and TMT-based labeled quantitation and mass spectrometry analysis. Numerous proteins involved in endopeptidase activity, glycolysis, pyruvate metabolism, calcium ion binding, estrogen signaling, and pheromone signaling were identified as differentially expressed between estrus and non-estrus phases. The extensive saliva proteome data set obtained in this work will provide insights into the cellular processes behind buffalo estrous biology. Taken together, this work identified a critical panel of potential proteins in saliva that may be used as a biomarker for buffalo estrus and paves the way for the development of a diagnostic kit for buffalo estrus detection.

DATA AVAILABILITY STATEMENT

The datasets presented in this study can be found in online repositories. The names of the repository/repositories and accession number(s) can be found in the article/ **Supplementary Material**.

ETHICS STATEMENT

The animal study was reviewed and approved by the Institute Animal Ethics Committee, NDRI, Karnal [42-IAEC-18-9].

AUTHOR CONTRIBUTIONS

RB, TKM, AKM and AK conceptualized the study and arranged the funds. LKS, SP, and Neeraj carried out the sampling. RB, AKM, and MP designed the experiments. MP and LKS performed all experiments. MP, AF, SP, Neeraj, and LKS performed Western blotting. RB and SA performed bioinformatics and statistical analysis. RB, MP, and LS wrote the manuscript, and all other authors reviewed the manuscript.

FUNDING

The study was supported by the Department of Biotechnology (DBT) under the research project entitled "Genomic and proteomics approaches to develop a specific diagnostic assay for detection of estrus/silent estrus in buffaloes" under Grant No. BT/PR23365/AAQ/1/688/2017.

ACKNOWLEDGMENTS

The authors thank the Director, ICAR-National Dairy Research Institute, Karnal, Haryana, for facilitating the work.

SUPPLEMENTARY MATERIAL

The Supplementary Material for this article can be found online at: https://www.frontiersin.org/articles/10.3389/fgene.2022.867909/full#supplementary-material

REFERENCES

20th Livestock Census (2019). 20th Livestock Census. Available at: https://dahd.nic.in/division/provisional-key-results-20th-livestock-census.

Alagendran, S., Saibaba, G., Muthukumar, S., Rajkumar, R., Guzman, R. G., and Archunan, G. (2013). Characterization of Salivary Protein during Ovulatory Phase of Menstrual Cycle through MALDI-TOF/MS. *Indian J. Dent. Res.* 24, 157–163. doi:10.4103/0970-9290.116669

Almeida, A. M., Ali, S. A., Ceciliani, F., Eckersall, P. D., Hernández-Castellano, L. E., Han, R., et al. (2021). Domestic Animal Proteomics in the 21st century: A Global Retrospective and Viewpoint Analysis. *J. Proteomics* 241, 104220. doi:10.1016/j.jprot.2021.104220

Ang, C.-S., Binos, S., Knight, M. I., Moate, P. J., Cocks, B. G., and McDonagh, M. B. (2011). Global Survey of the Bovine Salivary Proteome: Integrating Multidimensional Prefractionation, Targeted, and Glycocapture Strategies. *J. Proteome Res.* 10, 5059–5069. doi:10.1021/pr200516d

Archunan, G., Rajanarayanan, S., and Karthikeyan, K. (2014). *Cattle Pheromones. Neurobiology of Chemical Communication*. 1st edn. New York: CRC Press, 461–479.

Arruvito, L., Giulianelli, S., Flores, A. C., Paladino, N., Barboza, M., Lanari, C., et al. (2008). NK Cells Expressing a Progesterone Receptor Are Susceptible to Progesterone-Induced Apoptosis. *J. Immunol.* 180, 5746–5753. doi:10.4049/jimmunol.180.8.5746

Bédard, J., Brûlé, S., Price, C. A., Silversides, D. W., and Lussier, J. G. (2003). Serine Protease Inhibitor-E2 (SERPINE2) Is Differentially Expressed in Granulosa Cells of Dominant Follicle in Cattle. *Mol. Reprod. Dev.* 64, 152–165. doi:10.1002/mrd.10239

Bellavance, M.-A., and Rivest, S. (2014). The HPA Â€" Immune Axis and the Immunomodulatory Actions of Glucocorticoids in the Brain. *Front. Immunol.* 5, 136. doi:10.3389/fimmu.2014.00136

Brennan, P. A., and Keverne, E. B. (2004). Something in the Air? New Insights into Mammalian Pheromones. *Curr. Biol.* 14, R81–R89. doi:10.1016/j.cub.2003.12.052

Brunet, S., and Verlhac, M. H. (2011). Positioning to Get Out of Meiosis: The Asymmetry of Division. *Hum. Reprod. Update* 17, 68–75. doi:10.1093/humupd/dmq044

Butts, C. L., Shukair, S. A., Duncan, K. M., Bowers, E., Horn, C., Belyavskaya, E., et al. (2007). Progesterone Inhibits Mature Rat Dendritic Cells in a Receptor-Mediated Fashion. *Int. Immunol.* 19, 287–296. doi:10.1093/intimm/dxl145

Cabras, T., Pisano, E., Montaldo, C., Giuca, M. R., Iavarone, F., Zampino, G., et al. (2013). Significant Modifications of the Salivary Proteome Potentially Associated with Complications of Down Syndrome Revealed by Top-Down Proteomics. *Mol. Cell Proteomics* 12, 1844–1852. doi:10.1074/mcp.m112.026708

Cao, M., Nicola, E., Portela, V. M., and Price, C. A. (2006). Regulation of Serine Protease Inhibitor-E2 and Plasminogen Activator Expression and Secretion by Follicle Stimulating Hormone and Growth Factors in Non-luteinizing Bovine Granulosa Cells *In Vitro*. *Matrix Biol.* 25, 342–354. doi:10.1016/j.matbio.2006.05.005

Cao, M., Sahmi, M., Lussier, J. G., and Price, C. A. (2004). Plasminogen Activator and Serine Protease Inhibitor-E2 (Protease Nexin-1) Expression by Bovine Granulosa Cells *In Vitro*1. *Biol. Reprod.* 71, 887–893. doi:10.1095/biolreprod.104.029702

Castagnola, M., Scarano, E., Passali, G. C., Messana, I., Cabras, T., Iavarone, F., et al. (2017). Salivary Biomarkers and Proteomics: Future Diagnostic and Clinical Utilities. *Acta Otorhinolaryngol. Ital.* 37, 94–101. doi:10.14639/0392-100x-1598

Cavaggioni, A., and Mucignat-Caretta, C. (2000). Major Urinary Proteins, α2U-globulins and Aphrodisin. *Biochim. Biophys. Acta (Bba) - Protein Struct. Mol. Enzymol.* 1482, 218–228. doi:10.1016/s0167-4838(00)00149-7

Černá, M., Kuntová, B., Talacko, P., Stopková, R., and Stopka, P. (2017). Differential Regulation of Vaginal Lipocalins (OBP, MUP) during the Estrous Cycle of the House Mouse. *Sci. Rep.* 7, 11674–11710. doi:10.1038/s41598-017-12021-2

Choi, Y. J., Kim, S., Choi, Y., Nielsen, T. B., Yan, J., Lu, A., et al. (2019). SERPINB1-mediated Checkpoint of Inflammatory Caspase Activation. *Nat. Immunol.* 20, 276–287. doi:10.1038/s41590-018-0303-z

Crossett, B., Allen, W. R., and Stewart, F. (1996). A 19 kDa Protein Secreted by the Endometrium of the Mare Is a Novel Member of the Lipocalin Family. *Biochem. J.* 320, 137–143. doi:10.1042/bj3200137

Das, G. K., and Khan, F. A. (2010). Summer Anoestrus in buffalo--a Review. *Reprod. Domest. Anim.* 45, e483–94. doi:10.1111/j.1439-0531.2010.01598.x

Diamond, G., Beckloff, N., Weinberg, A., and Kisich, K. (2009). The Roles of Antimicrobial Peptides in Innate Host Defense. *Cpd* 15 (21), 2377–2392. doi:10.2174/138161209788682325

Dow, M. P. D., Bakke, L. J., Cassar, C. A., Peters, M. W., Pursley, J. R., and Smith, G. W. (2002). Gonadotropin Surge-Induced Up-Regulation of the Plasminogen Activators (Tissue Plasminogen Activator and Urokinase Plasminogen Activator) and the Urokinase Plasminogen Activator Receptor within Bovine Periovulatory Follicular and Luteal Tissue1. *Biol. Reprod.* 66, 1413–1421. doi:10.1095/biolreprod66.5.1413

Edgar, W. M. (1992). Saliva: its Secretion, Composition and Functions. *Br. Dent. J.* 172, 305–312. doi:10.1038/sj.bdj.4807861

Giallongo, A., Venturella, S., Oliva, D., Barbieri, G., Rubino, P., and Feo, S. (1993). Structural Features of the Human Gene for Muscle-specific Enolase. Differential Splicing in the 5'-untranslated Sequence Generates Two Forms of mRNA. *Eur. J. Biochem.* 214, 367–374. doi:10.1111/j.1432-1033.1993.tb17932.x

Gilliver, S. C. (2010). Sex Steroids as Inflammatory Regulators. *J. Steroid Biochem. Mol. Biol.* 120, 105–115. doi:10.1016/j.jsbmb.2009.12.015

Hasan, S., Hosseini, G., Princivalle, M., Dong, J.-C., Birsan, D., Cagide, C., et al. (2002). Coordinate Expression of Anticoagulant Heparan Sulfate Proteoglycans and Serine Protease Inhibitors in the Rat Ovary: A Potent System of Proteolysis Control1. *Biol. Reprod.* 66, 144–158. doi:10.1095/biolreprod66.1.144

Hayashi, K. G., Ushizawa, K., Hosoe, M., and Takahashi, T. (2011). Differential Gene Expression of Serine Protease Inhibitors in Bovine Ovarian Follicle: Possible Involvement in Follicular Growth and Atresia. *Reprod. Biol. Endocrinol.* 9, 72–79. doi:10.1186/1477-7827-9-72

Hermann, B. P., and Heckert, L. L. (2007). Transcriptional Regulation of the FSH Receptor: New Perspectives. *Mol. Cell Endocrinol.* 260-262, 100–108. doi:10.1016/j.mce.2006.09.005

Honoré, B. (2009). The Rapidly Expanding CREC Protein Family: Members, Localization, Function, and Role in Disease. *Bioessays* 31, 262–277. doi:10.1002/bies.200800186

Hughes, G. C., Thomas, S., Li, C., Kaja, M.-K., and Clark, E. A. (2008). Cutting Edge: Progesterone Regulates IFN-α Production by Plasmacytoid Dendritic Cells. *J. Immunol.* 180, 2029–2033. doi:10.4049/jimmunol.180.4.2029

Hurd, A. M., Schiff, R., Parra, I., Friedrichs, W. E., Osborne, C. K., Morimoto, R. I., et al. (2000). Heat Shock Protein 70 Can Modulate Estrogen Receptor Activity in Breast Cancer Cells. *Proc. Am. Assoc. Cancer Res.* 41, 73.

Johnson, M. T., Freeman, E. A., Gardner, D. K., and Hunt, P. A. (2007). Oxidative Metabolism of Pyruvate Is Required for Meiotic Maturation of Murine Oocytes *In Vivo*1. *Biol. Reprod.* 77, 2–8. doi:10.1095/biolreprod.106.059899

Jou, Y.-J., Hua, C.-H., Lin, C.-D., Lai, C.-H., Huang, S.-H., Tsai, M.-H., et al. (2014). S100A8 as Potential Salivary Biomarker of Oral Squamous Cell Carcinoma Using nanoLC-MS/MS. *Clinica Chim. Acta* 436, 121–129. doi:10.1016/j.cca.2014.05.009

Khanna, A., Aten, R. F., and Behrman, H. R. (1995). Heat Shock Protein-70 Induction Mediates Luteal Regression in the Rat. *Mol. Endocrinol.* 9, 1431–1440. doi:10.1210/mend.9.11.8584020

Kido, S., Morimoto, A., Kim, F., and Doi, Y. (1992). Isolation of a Novel Protein from the Outer Layer of the Vitelline Membrane. *Biochem. J.* 286, 17–22. doi:10.1042/bj2860017

Kim, J. H., Lee, K. R., Kim, H. K., No, S. H., Yoo, H. M., Moon, C. I., et al. (2011). 17beta-estradiol Regulates the Expression of nesfatin-1/Nucb2 in Mouse Uterus. *Dev. Reprod.* 15, 349–357. doi:10.12717/DR.2020.24.1.43

Kim, J., and Yang, H. (2012). Nesfatin-1 as a New Potent Regulator in Reproductive System. *Dev. Reprod.* 16, 253–264. doi:10.12717/dr.2012.16.4.253

Kovacs, P., Kovats, T., and Kaali, S. G. (2010). Results with Early Follicular Phase Recombinant Luteinizing Hormone Supplementation during Stimulation for *In Vitro* Fertilization. *Fertil. Sterility* 93, 475–479. doi:10.1016/j.fertnstert.2008.12.010

Kumar, G. (2015). "Comparative Proteome Analysis of Saliva in Pregnant and Non-pregnant Sahiwal Cows," (Karnal, Haryana, India: National Dairy Research Institute). M.Tech. Thesis.

Law, R. H., Zhang, Q., McGowan, S., Buckle, A. M., Silverman, G. A., Wong, W., et al. (2006). An Overview of the Serpin Superfamily. *Genome Biol.* 7, 216–311. doi:10.1186/gb-2006-7-5-216

Levine, M. J. (1993). Salivary Macromolecules. *Ann. NY Acad. Sci.* 694, 11–16. doi:10.1111/j.1749-6632.1993.tb18337.x

Li, J., Xu, P., Wang, L., Feng, M., Chen, D., Yu, X., et al. (2020). Molecular Biology of BPIFB1 and its Advances in Disease. *Ann. Transl. Med.* 8 (10), 651. doi:10.21037/atm-20-3462

Li, Y., St. John, M. A. R., Zhou, X., Kim, Y., Sinha, U., Jordan, R. C. K., et al. (2004). Salivary Transcriptome Diagnostics for Oral Cancer Detection. *Clin. Cancer Res.* 10, 8442–8450. doi:10.1158/1078-0432.ccr-04-1167

Lim, W., and Song, G. (2015). Differential Expression of Vitelline Membrane Outer Layer Protein 1: Hormonal Regulation of Expression in the Oviduct and in Ovarian Carcinomas from Laying Hens. *Mol. Cell Endocrinol.* 399, 250–258. doi:10.1016/j.mce.2014.10.015

Lindquist, S., and Craig, E. A. (1988). The Heat-Shock Proteins. *Annu. Rev. Genet.* 22 (1), 631–677. doi:10.1146/annurev.ge.22.120188.003215

Liu, Z., and Stocco, D. M. (1997). Heat Shock-Induced Inhibition of Acute Steroidogenesis in MA-10 Cells Is Associated with Inhibition of the Synthesis of the Steroidogenic Acute Regulatory Protein1. *Endocrinology* 138, 2722–2728. doi:10.1210/endo.138.7.5278

Lu, A., Ran, R.-q., Clark, J., Reilly, M., Nee, A., and Sharp, F. R. (2002). 17-β-Estradiol Induces Heat Shock Proteins in Brain Arteries and Potentiates Ischemic Heat Shock Protein Induction in Glia and Neurons. *J. Cereb. Blood Flow Metab.* 22, 183–195. doi:10.1097/00004647-200202000-00006

Mariani, M., Souto, M., Fanelli, M., and Ciocca, D. (2000). Constitutive Expression of Heat Shock Proteins HSP25 and HSP70 in the Rat Oviduct during Neonatal Development, the Oestrous Cycle and Early Pregnancy. *Reproduction* 120, 217–223. doi:10.1530/jrf.0.1200217

Mass, E., Gadoth, N., Harell, D., and Wolff, A. (2002). Can Salivary Composition and High Flow Rate Explain the Low Caries Rate in Children with Familial Dysautonomia? *Pediatr. Dent.* 24, 581–586.

McMurray, R. W., Suwannaroj, S., Ndebele, K., and Jenkins, J. K. (2001). Differential Effects of Sex Steroids on T and B Cells: Modulation of Cell Cycle Phase Distribution, Apoptosis and Bcl-2 Protein Levels. *Pathobiology* 69, 44–58. doi:10.1159/000048757

Mondal, S., Suresh, K. P., and Nandi, S. (2010). Endocrine Profile of Oestrous Cycle in Buffaloes: A Meta-Analysis. *Asian Aust. J. Anim.* 23, 169–174. doi:10.5713/ajas.2010.90193

Muthukumar, S., Rajesh, D., Saibaba, G., Alagesan, A., Rengarajan, R. L., and Archunan, G. (2013). Urinary Lipocalin Protein in a Female Rodent with Correlation to Phases in the Estrous Cycle: an Experimental Study Accompanied by In Silico Analysis. *PLoS One* 8, e71357. doi:10.1371/journal.pone.0071357

Muthukumar, S., Rajesh, D., Selvam, R. M., Saibaba, G., Suvaithenamudhan, S., Akbarsha, M. A., et al. (2018). Buffalo Nasal Odorant-Binding Protein (bunOBP) and its Structural Evaluation with Putative Pheromones. *Sci. Rep.* 8, 9323–9414. doi:10.1038/s41598-018-27550-7

Muthukumar, S., Rajkumar, R., Karthikeyan, K., Liao, C. C., Singh, D., Akbarsha, M. A., et al. (2014a). Buffalo Cervico-Vaginal Fluid Proteomics with Special Reference to Estrous Cycle: Heat Shock Protein (HSP)-70 Appears to Be an Estrus Indicator. *Biol. Reprod.* 90, 97–101. doi:10.1095/biolreprod.113.113852

Muthukumar, S., Rajkumar, R., Rajesh, D., Saibaba, G., Liao, C. C., Archunan, G., et al. (2014b). Exploration of Salivary Proteins in buffalo: an Approach to Find Marker Proteins for Estrus. *FASEB j.* 28, 4700–4709. doi:10.1096/fj.14-252288

Onteru, S. K., Baddela, V. S., Ravinder, R., Kaipa, O., Nayan, V., Singh, P., et al. (2016). Direct Saliva Transcript Analysis as a Novel Non-invasive Method for Oestrus Marker Detection in Buffaloes. *Biomarkers* 21, 99–101. doi:10.3109/1354750x.2015.1118549

Pedersen, A., Bardow, A., Jensen, S. B., and Nauntofte, B. (2002). Saliva and Gastrointestinal Functions of Taste, Mastication, Swallowing and Digestion. *Oral Dis.* 8, 117–129. doi:10.1034/j.1601-0825.2002.02851.x

Pelosi, P., and Maida, R. (1990). Odorant-binding Proteins in Vertebrates and Insects: Similarities and Possible Common Function. *Chem. Senses.* 15, 205–215. doi:10.1093/chemse/15.2.205

Pevsner, J., Sklar, P. B., and Snyder, S. H. (1986). Odorant-binding Protein: Localization to Nasal Glands and Secretions. *Proc. Natl. Acad. Sci. U.S.A.* 83, 4942–4946. doi:10.1073/pnas.83.13.4942

Prout, R. E. S., and Hopps, R. M. (1970). A Relationship between Human Oral Bacteria and the Menstrual Cycle. *J. Periodontol.* 41, 98–101. doi:10.1902/jop.1970.41.2.98

Rajeswari, J. J., Hatef, A., and Unniappan, S. (2020). Nesfatin-1-like Peptide Suppresses Hypothalamo-Pituitary-Gonadal mRNAs, Gonadal Steroidogenesis, and Oocyte Maturation in Fish. *Biol. Reprod.* 103, 802–816. doi:10.1093/biolre/ioaa106

Rajkumar, R., Ilayaraja, R., Mucignat, C., Cavaggioni, A., and Archunan, G. (2009). Identification of Alpha2u-Globulin and Bound Volatiles in the Indian Common House Rat (*Rattus rattus*). *Indian J. Biochem. Biophys.* 46, 319–324.

Rajkumar, R., Karthikeyan, K., Archunan, G., Huang, P. H., Chen, Y. W., Ng, W. V., et al. (2010). Using Mass Spectrometry to Detect buffalo Salivary Odorant-Binding Protein and its post-translational Modifications. *Rapid Commun. Mass. Spectrom.* 24, 3248–3254. doi:10.1002/rcm.4766

Raval, A. P., Borges-Garcia, R., Javier Moreno, W., Perez-Pinzon, M. A., and Bramlett, H. (2013). Periodic 17β-Estradiol Pretreatment Protects Rat Brain from Cerebral Ischemic Damage via Estrogen Receptor-β. *PLoS One* 8, e60716. doi:10.1371/journal.pone.0060716

Richards, J. S. (1994). Hormonal Control of Gene Expression in the Ovary. *Endocr. Rev.* 15, 725–751. doi:10.1210/edrv-15-6-725

Roy, K. S., and Prakash, B. S. (2009). Plasma Progesterone, Oestradiol-17β and Total Oestrogen Profiles in Relation to Oestrous Behaviour during Induced Ovulation in Murrah buffalo Heifers. *J. Anim. Physiol. Anim. Nutr.* 93, 486–495. doi:10.1111/j.1439-0396.2008.00830.x

Saibaba, G., Rajesh, D., Muthukumar, S., Sathiyanarayanan, G., Aarthy, A. P., and Archunan, G. (2021). Salivary Proteome Profile of Women during fertile Phase of Menstrual Cycle as Characterized by Mass Spectrometry. *Gynecol. Minim. Invasive Ther.* 10 (4), 226–234. doi:10.4103/GMIT.GMIT_78_20

Scaloni, A., Paolini, S., Brandazza, A., Fantacci, M., Bottiglieri, C., Marchese, S., et al. (2001). Purification, Cloning and Characterisation of Odorant- and Pheromone-Binding Proteins from Pig Nasal Epithelium. *Cmls, Cel. Mol. Life Sci.* 58, 823–834. doi:10.1007/pl00000903

Selvam, R. M., and Archunan, G. (2017). A Combinatorial Model for Effective Estrus Detection in Murrah buffalo. *Vet. World* 10 (2), 209–213. doi:10.14202/vetworld.2017.209-213

Sharma, H. C., Dhami, A. J., Sharma, S. K., Sarvaiya, N. P., and Kavani, F. S. (2008). Assessment of Estrus Detection and Insemination Efficiency of AI Workers in Buffaloes through Plasma Progesterone Profile under Field Conditions. *Indian J. Anim. Sci.* 27, 706–709.

Shashikumar, N. G., Baithalu, R. K., Bathla, S., Ali, S. A., Rawat, P., Kumaresan, A., et al. (2018). Global Proteomic Analysis of Water buffalo (Bubalus Bubalis) Saliva at Different Stages of Estrous Cycle Using High Throughput Mass Spectrometry. *Theriogenology* 110, 52–60. doi:10.1016/j.theriogenology.2017.12.046

Shashikumar, N. G. (2017). "Identification of Estrus Specific Proteins in buffalo Saliva," (Karnal, Haryana, India: National Dairy Research Institute). M.V.Sc.Thesis.

Singh, J., Nanda, A. S., and Adams, G. P. (2000). The Reproductive Pattern and Efficiency of Female Buffaloes. *Anim. Reprod. Sci.* 60-61, 593–604. doi:10.1016/s0378-4320(00)00109-3

Skalova, I., Fedorova, T., and Brandlova, K. (2013). Saliva Crystallization in Cattle: New Possibility for Early Pregnancy Diagnosis? *Agricultura Tropica Et Subtropica* 46, 102–104. doi:10.2478/ats-2013-0018

Sorensen, J. G., Kristensen, T. N., and Loeschcke, V. (2003). The Evolutionary and Ecological Role of Heat Shock Proteins. *Ecol. Lett.* 6, 1025–1037. doi:10.1046/j.1461-0248.2003.00528.x

SPSS Inc (2007). *SPSS for Windows, Version 16.0*. Chicago: SPSS Inc.

Su, L., Sun, Y., Ma, F., Lü, P., Huang, H., and Zhou, J. (2009). Progesterone Inhibits Toll-like Receptor 4-mediated Innate Immune Response in Macrophages by Suppressing NF-Kb Activation and Enhancing SOCS1 Expression. *Immunol. Lett.* 125, 151–155. doi:10.1016/j.imlet.2009.07.003

Sutton, M., Cetica, P., Beconi, M., Kind, K., Gilchrist, R., and Thompson, J. (2003). Influence of Oocyte-Secreted Factors and Culture Duration on the Metabolic Activity of Bovine Cumulus Cell Complexes. *Reprod* 126, 27–34. doi:10.1530/rep.0.1260027

Tsiligianni, T., Karagiannidis, A., Brikas, P., and Saratsis, P. (2001). Physical Properties of Bovine Cervical Mucus during normal and Induced (Progesterone And/or PGF2α) Estrus. *Theriogenology* 55, 629–640. doi:10.1016/s0093-691x(01)00431-9

Vandooren, J., and Itoh, Y. (2021). Alpha-2-macroglobulin in Inflammation, Immunity and Infections. *Front. Immunol.* 12, 803244. doi:10.3389/fimmu.2021.803244

Verma, K. K., Prasad, S., Kumaresan, A., Mohanty, T. K., Layek, S. S., Patbandha, T. K., et al. (2014). Characterization of Physico-Chemical Properties of Cervical Mucus in Relation to Parity and conception Rate in Murrah Buffaloes. *Vet. World* 7, 467–471. doi:10.14202/vetworld.2014.467-471

Wang, Z., Niu, W., Wang, Y., Teng, Z., Wen, J., Xia, G., et al. (2015). Follistatin288 Regulates Germ Cell Cyst Breakdown and Primordial Follicle Assembly in the Mouse Ovary. *PLoS One* 10, e0129643. doi:10.1371/journal.pone.0129643

Wei, H., and Wang, J.-Y. (2021). Role of Polymeric Immunoglobulin Receptor in IgA and IgM Transcytosis. *Ijms* 22, 2284. doi:10.3390/ijms22052284

Yi, K., Unruh, J. R., Deng, M., Slaughter, B. D., Rubinstein, B., and Li, R. (2011). Dynamic Maintenance of Asymmetric Meiotic Spindle Position through Arp2/3-Complex-Driven Cytoplasmic Streaming in Mouse Oocytes. *Nat. Cel Biol.* 13, 1252–1258. doi:10.1038/ncb2320

Conflict of Interest: The authors declare that the research was conducted in the absence of any commercial or financial relationships that could be construed as a potential conflict of interest.

Publisher's Note: All claims expressed in this article are solely those of the authors and do not necessarily represent those of their affiliated organizations, or those of the publisher, the editors, and the reviewers. Any product that may be evaluated in this article, or claim that may be made by its manufacturer, is not guaranteed or endorsed by the publisher.

frontiers | Frontiers in Genetics

ORIGINAL RESEARCH
published: 27 June 2022
doi: 10.3389/fgene.2022.894990

Risk Stratification and Validation of Eleven Autophagy-Related lncRNAs for Esophageal Squamous Cell Carcinoma

*Xu Zhao[1†], Yulun Wang[1†], Fanbiao Meng[1], Zhuang Liu[1] and Bo Xu[1,2]**

[1]*Department of Biochemistry and Molecular Biology, Key Laboratory of Breast Cancer Prevention and Therapy, Ministry of Education, Tianjin Medical University Cancer Institute and Hospital, National Clinical Research Center for Cancer, Key Laboratory of Cancer Prevention and Therapy, Tianjin's Clinical Research Center for Cancer, Tianjin Medical University, Tianjin, China,* [2]*Center for Intelligent Oncology, Chongqing Key Laboratory of Intelligent Oncology for Breast Cancer, Chongqing University Cancer Hospital, Chongqing University School of Medicine, Chongqing, China*

OPEN ACCESS

Edited by:
Nadeem Shabir,
Sher-e-Kashmir University of Agricultural Sciences and Technology, India

Reviewed by:
Lifeng Li,
First Affiliated Hospital of Zhengzhou University, China
Yi Cai,
Central South University, China

***Correspondence:**
Bo Xu
xubo@tmu.edu.cn

[†]*These authors have contributed equally to this work and share first authorship*

Specialty section:
This article was submitted to RNA, a section of the journal Frontiers in Genetics

Received: *12 March 2022*
Accepted: *03 June 2022*
Published: *27 June 2022*

Citation:
Zhao X, Wang Y, Meng F, Liu Z and Xu B (2022) Risk Stratification and Validation of Eleven Autophagy-Related lncRNAs for Esophageal Squamous Cell Carcinoma. Front. Genet. 13:894990. doi: 10.3389/fgene.2022.894990

Esophageal squamous cell carcinoma (ESCC), the most prevalent subtype of esophageal cancer, ranks sixth in cancer-related mortality, making it one of the deadliest cancers worldwide. The identification of potential risk factors for ESCC might help in implementing precision therapies. Autophagy-related lncRNAs are a group of non-coding RNAs that perform critical functions in the tumor immune microenvironment and therapeutic response. Therefore, we aimed to establish a risk model composed of autophagy-related lncRNAs that can serve as a potential biomarker for ESCC risk stratification. Using the RNA expression profile from 179 patients in the GSE53622 and GSE53624 datasets, we found 11 lncRNAs (AC004690.2, AC092159.3, AC093627.4, AL078604.2, BDNF-AS, HAND2-AS1, LINC00410, LINC00588, PSMD6-AS2, ZEB1-AS1, and LINC02586) that were co-expressed with autophagy genes and were independent prognostic factors in multivariate Cox regression analysis. The risk model was constructed using these autophagy-related lncRNAs, and the area under the receiver operating characteristic curve (AUC) of the risk model was 0.728. To confirm that the model is reliable, the data of 174 patients from The Cancer Genome Atlas (TCGA) esophageal cancer dataset were analyzed as the testing set. A nomogram for ESCC prognosis was developed using the risk model and clinic-pathological characteristics. Immune function annotation and tumor mutational burden of the two risk groups were analyzed and the high-risk group displayed higher sensitivity in chemotherapy and immunotherapy. Expression of differentially expressed lncRNAs were further validated in human normal esophageal cells and esophageal cancer cells. The constructed lncRNA risk model provides a useful tool for stratifying risk and predicting the prognosis of patients with ESCC, and might provide novel targets for ESCC treatment.

Keywords: esophageal squamous cell carcinoma, autophagy, prognosis, risk model, long noncoding RNA

INTRODUCTION

Esophageal cancer (EC) has an increasingly notable cancer burden, accounting for approximately 16% (Ferlay et al., 2015) cancer-related mortality worldwide (Smyth et al., 2017). According to GLOBOCAN estimates, over 604,100 new cases of EC and 544,076 EC-related deaths occurred in 2020 (Thrift, 2021). The two main histological subtypes of EC are esophageal squamous cell carcinoma (ESCC) and esophageal adenocarcinoma (EAC). In all EC cases, the proportion of ESCC was >90%. Although its incidence has declined over the past decades, the survival ratios for EC are among the lowest for cancers, mainly because of the late stage at diagnosis and high aggressiveness of the disease. The fatality rate of ESCC is even higher than that of EAC, with a 5-year overall survival rate of <15%. Hence, there is an urgent need to search for effective screening methods and risk stratification to improve patient prognoses.

In the transcriptome, less than 1–2% of RNAs encode proteins and undergo the translation process. Thus, most RNAs are non-coding (Beermann et al., 2016); among these, RNAs with more than 200 nucleotides are called long non-coding RNAs (lncRNAs) (Djebali et al., 2012; Dykes and Emanueli, 2017). Compared with protein-coding messenger RNAs, whose functions are extensively studied, the specific function of most lncRNAs remains unknown (Johnson et al., 2005). lncRNAs are reported to be crucial in many biological processes, including epigenetic modification, cell cycle regulation, and differentiation (Beermann et al., 2016). Although the mechanism by which lncRNAs regulate physiological activities is unclear, their significance, especially in tumor growth and metastasis, has been

TABLE 1 | Significant prognostic autophagy lncRNAs in ESCC patients.

LncRNA	KM	B	SE	HR	HR.95L	HR.95H	*p*-value
AC004690.2	0.003646	−0.21326	0.102314	0.807949	0.661141	0.987357	0.037131
AC009135.1	0.005497	0.165645	0.071065	1.180154	1.026711	1.356528	0.019758
AC010745.1	0.044803	0.153274	0.075702	1.165644	1.004913	1.352083	0.042898
AC011365.1	0.018151	0.276166	0.132672	1.318066	1.016264	1.709495	0.037382
AC011365.2	0.023922	0.302114	0.136334	1.352716	1.035522	1.767072	0.026692
AC012494.1	0.012603	0.762773	0.257307	2.144214	1.294935	3.550492	0.003032
AC017074.2	0.039703	−0.46976	0.159679	0.625153	0.457159	0.854881	0.003262
AC026412.3	0.007657	0.53665	0.250314	1.710268	1.04712	2.793393	0.03204
AC079349.1	0.049192	−0.33239	0.110128	0.717207	0.577968	0.88999	0.002542
AC079943.1	0.016194	0.566801	0.230095	1.762619	1.122798	2.76704	0.013765
AC090061.1	0.023284	0.457723	0.160335	1.580471	1.154275	2.164032	0.004306
AC092159.3	0.012035	0.276189	0.121963	1.318097	1.037845	1.674027	0.023541
AC093627.4	0.012721	−0.39403	0.140017	0.674332	0.512496	0.887272	0.00489
AC138123.2	0.007043	0.255316	0.121419	1.290869	1.017491	1.637699	0.035485
AC245297.3	0.015701	−0.2887	0.117788	0.749235	0.59478	0.9438	0.014245
AC254629.1	0.013056	0.93071	0.409419	2.53631	1.136853	5.658486	0.023011
AL078604.2	0.014692	−0.3034	0.1246	0.738301	0.578327	0.942526	0.014891
AL135960.1	0.011216	−0.37666	0.17255	0.686148	0.489264	0.962261	0.029042
AL137026.2	0.02769	0.287181	0.086905	1.332666	1.123952	1.580137	0.000951
AL139130.1	0.011762	−0.23579	0.089401	0.789948	0.66298	0.941232	0.008354
AL512631.2	0.035362	0.216095	0.101459	1.241221	1.01739	1.514296	0.033181
AL590068.1	0.025632	0.253603	0.109691	1.28866	1.039367	1.597747	0.020779
BDNF−AS	0.029138	0.909921	0.413291	2.484127	1.105044	5.584292	0.02769
C5orf66	0.027392	−0.87709	0.424911	0.415992	0.180884	0.956689	0.039002
CRNDE	0.007695	0.672485	0.314376	1.9591	1.057936	3.627887	0.032427
HAND2-AS1	0.017144	−0.74111	0.354538	0.476582	0.237878	0.954819	0.036585
LINC00395	0.027561	0.358055	0.12449	1.430545	1.120818	1.82586	0.004025
LINC00410	0.021815	−0.24107	0.118117	0.785785	0.623394	0.990479	0.041255
LINC00588	0.045615	−0.52531	0.233579	0.591374	0.374144	0.934729	0.024516
LINC01003	0.026687	−0.37946	0.190036	0.684232	0.47146	0.993029	0.04585
LINC02305	0.021849	−0.45951	0.167896	0.63159	0.454488	0.877705	0.006202
LINC02586	0.027443	−0.30574	0.155866	0.736575	0.54268	0.999746	0.04981
PSMD6-AS2	0.012729	−0.52696	0.20008	0.590394	0.398872	0.873879	0.008444
RARA-AS1	0.011405	−0.26451	0.128956	0.76758	0.596151	0.988306	0.040249
SNHG3	0.00561	0.585328	0.237023	1.795579	1.128365	2.857322	0.013531
SNHG5	0.043276	−0.70253	0.320349	0.495329	0.26437	0.928058	0.028306
TRBV11-2	0.036456	0.171816	0.086587	1.187459	1.002111	1.407088	0.04722
ZEB1-AS1	0.015706	0.619751	0.276488	1.858465	1.080955	3.195223	0.024993
ZIM2-AS1	0.005903	−0.42966	0.204767	0.650731	0.435616	0.972075	0.03588
ATG7	0.041523	0.488018	0.245711	1.629083	1.006453	2.636896	0.047017
DAPK2	0.049092	0.361962	0.143164	1.436145	1.084767	1.901341	0.011462
NAF1	0.027078	0.274767	0.098221	1.316224	1.085736	1.595642	0.005151
RGS19	0.003052	0.468488	0.165387	1.597577	1.155271	2.209225	0.004616

TABLE 2 | The 11 autophagy-related lncRNAs significant by multivariate Cox analysis.

LncRNA	Coefficients	HR
AC004690.2	−0.30132	0.739838
AC092159.3	0.405486	1.500032
AC093627.4	−0.60338	0.546961
AL078604.2	−0.38601	0.679762
BDNF-AS	1.393802	4.030144
HAND2-AS1	−1.24773	0.287157
LINC00410	0.279909	1.32301
LINC00588	−0.52222	0.593205
PSMD6-AS2	−0.83716	0.43294
ZEB1-AS1	0.906655	2.476026
LINC02586	−0.26822	0.764741

reported (Quinn and Chang, 2016; Li et al., 2018; Chi et al., 2019).

Autophagy has become a popular research topic since Yoshinori Ohsumi was awarded the Nobel Prize in Physiology or Medicine for his contribution in elucidating its mechanism in 2016. Thus, stimulation or inhibition of autophagy in cancer cells has also become a promising therapeutic strategy (Levy et al., 2017). Considering the complexity of various biological processes, the role of autophagy in tumors can be both positive and negative (Russo and Russo, 2018). Autophagy can be metaphorized as a double-edged sword (Pietrocola et al., 2016). In the specific cellular microenvironments of certain tumors (Galluzzi et al., 2015), autophagy can either promote or inhibit cancer development. Despite these paradoxical approaches, there are no reports on autophagy-related lncRNAs as prognostic biomarkers for patients with ESCC.

In this study, using transcriptional and clinical data from two databases, TCGA database and the Gene Expression Omnibus (GEO) datasets, GSE53622 and GSE53624, we first constructed an autophagy-associated lncRNA model and validated its prognostic value. Immune function, tumor mutation burden (TMB), and therapeutic response of the two risk groups were further explored. To determine the expression level of autophagy-related lncRNAs in cultured human cells, the selected lncRNAs were analyzed using quantitative real-time polymerase chain reaction (qRT-PCR).

METHODS

Esophageal Squamous Cell Carcinoma Clinical and Transcriptional Datasets

The clinical data and lncRNA expression profiles of 179 ESCC patients in the GSE53622 and GSE53624 datasets were obtained from the GEO database and re-annotated using the GPL18109 platform. Data from 174 patients with EC were obtained from TCGA (https://cancergenome.nih.gov/) and used for independent external validation.

Screening of Autophagy-Related Genes and Long Non-Coding RNAs Screening

After annotation and categorization using GENCOED (https://www.gencodegenes.org), all extracted mRNA and lncRNA expression profiles were compared against the HaDb website, an online database dedicated to collecting ARGs and proteins (http://autophagy.lu/clustering/index.html). After autophagy-related mRNAs were selected, correlations between autophagy-associated mRNAs and their co-expressed lncRNAs were analyzed using the Pearson method, and the screening criteria were $|R^2| > 0.3$ and $p < 0.001$. Autophagy-related lncRNAs were defined based on these criteria. Cytoscape was used to visualize the correlation network of autophagy genes and their associated lncRNAs. All mRNA sequencing data were standardized using the limma package (version 3.22.7).

Construction of a Prognostic Autophagy Long Non-Coding RNAs Model

Using univariate Cox regression analysis, 43 lncRNAs were identified from all selected autophagy-related lncRNAs. Further multivariate regression analysis revealed the statistically significant prognostic autophagy-associated lncRNAs, which were used in constructing the model. Based on the coefficients of these lncRNAs, the patient's risk value was calculated formula as follows:

$$\textit{Risk score} = \beta_1 X_1 + \beta_2 X_2 + \cdots + \beta_n X_n$$

The β value represents the regression coefficient of each lncRNA, and the X value represents its transcriptional expression. To increase the accuracy of this risk assessment formula, lncRNA expression levels were weighted using regression coefficients for the linear combination of allocating risk scores. The β value was obtained by the logarithmic transformation of the HR value. After evaluating the risk values of all patients, they were classified into high or low groups based on the median risk value.

Assessment and External Validation of the Prognostic Model

Kaplan-Meier (KM) survival curves of the high-and low-risk groups were plotted to compare the overall survival of the two groups. Based on the clinical data of the GSE53624 and GSE53622 training sets, the receiver operator characteristic curve (ROC) of clinical features such as age, sex, grade, and other characteristics were plotted, and the predictive ability of each feature was evaluated by the area under the curve (AUC). SPSS software was used for statistical analysis and statistical significance was set at $p < 0.05$. Using the same standards and methods, TCGA dataset was obtained as the testing set to further confirm the stability and reliability of the model.

Nomogram was generated including risk scores and other clinical characteristics with R package of "survival", "regplot" and "rms". Calibration curves of 1-year survival, 3-year survival and 5-year survival were delineated.

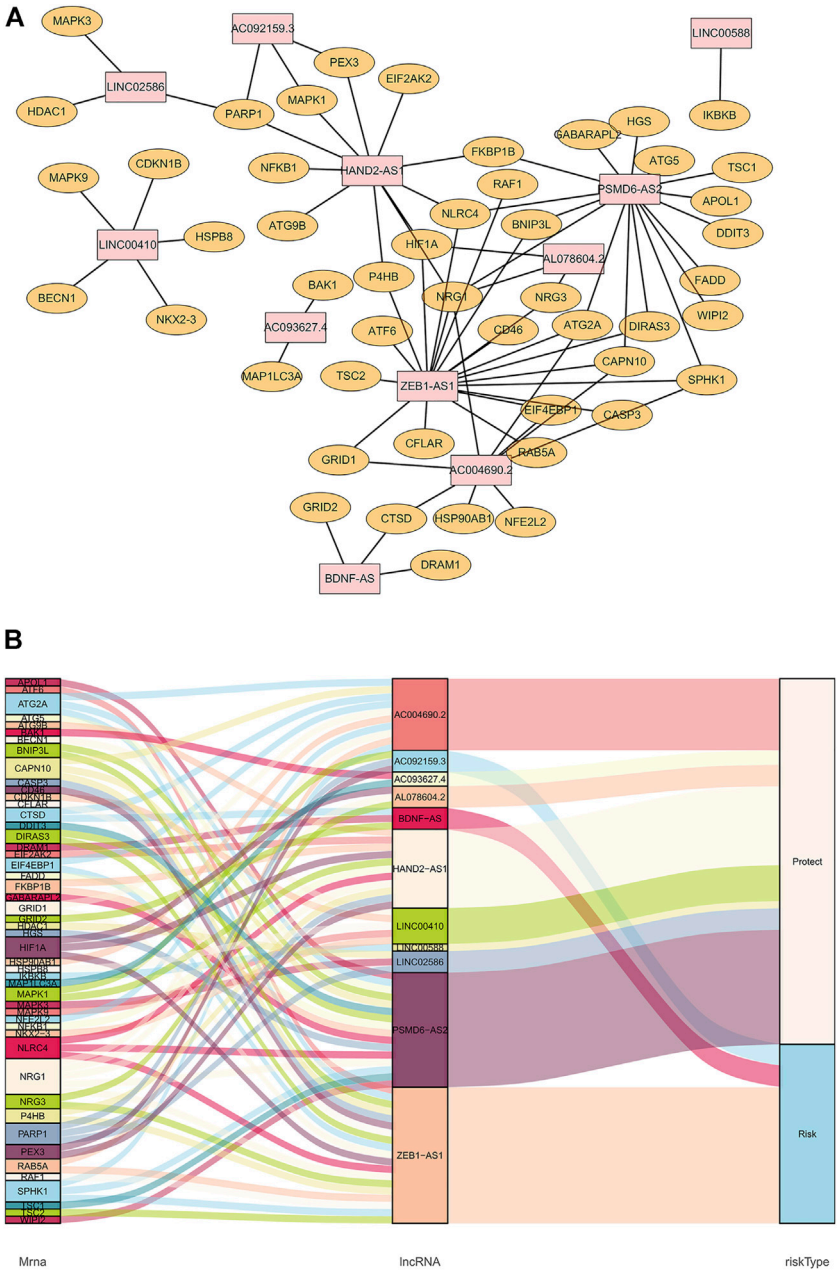

FIGURE 1 | Co-expression of autophagy-related genes and lncRNAs. **(A)**: Orange nodes are autophagy-related genes, and pink nodes are their related prognostic lncRNAs. The network was generated by Cytoscape 3.7.2. **(B)**: Sankey diagram of autophagy-related genes, lncRNAs, and their risk types in patients' prognosis.

Functional Analysis

Through Kyoto Encyclopedia of Genes and Genomes (KEGG) pathway analysis, we found that different signaling pathways were enriched in different groups. KEGG pathway analysis was implemented based on a gene-set enrichment analysis (GSEA) software, which was downloaded from the website, https://www.gsea-msigdb.org/gsea/index.jsp. A false discovery set of 1000 repeats, p-value < 0.05, and q-FDR < 0.25 were considered valid. The gene ontology (GO) database was used for gene and gene product classifications.

Immune Function Heatmap and Tumor Mutational Burden Analysis

Differential analysis of immune-associated genes in the high or low risk groups of patients were performed and visualized using the R package "ssGSEA". Simple nucleotide variation (SNV) profile of the TCGAdataset was downloaded to analyze the tumor mutational burden (TMB) in high or low risk group. Survival curves of different TMB and risk subgroups were analyzed.

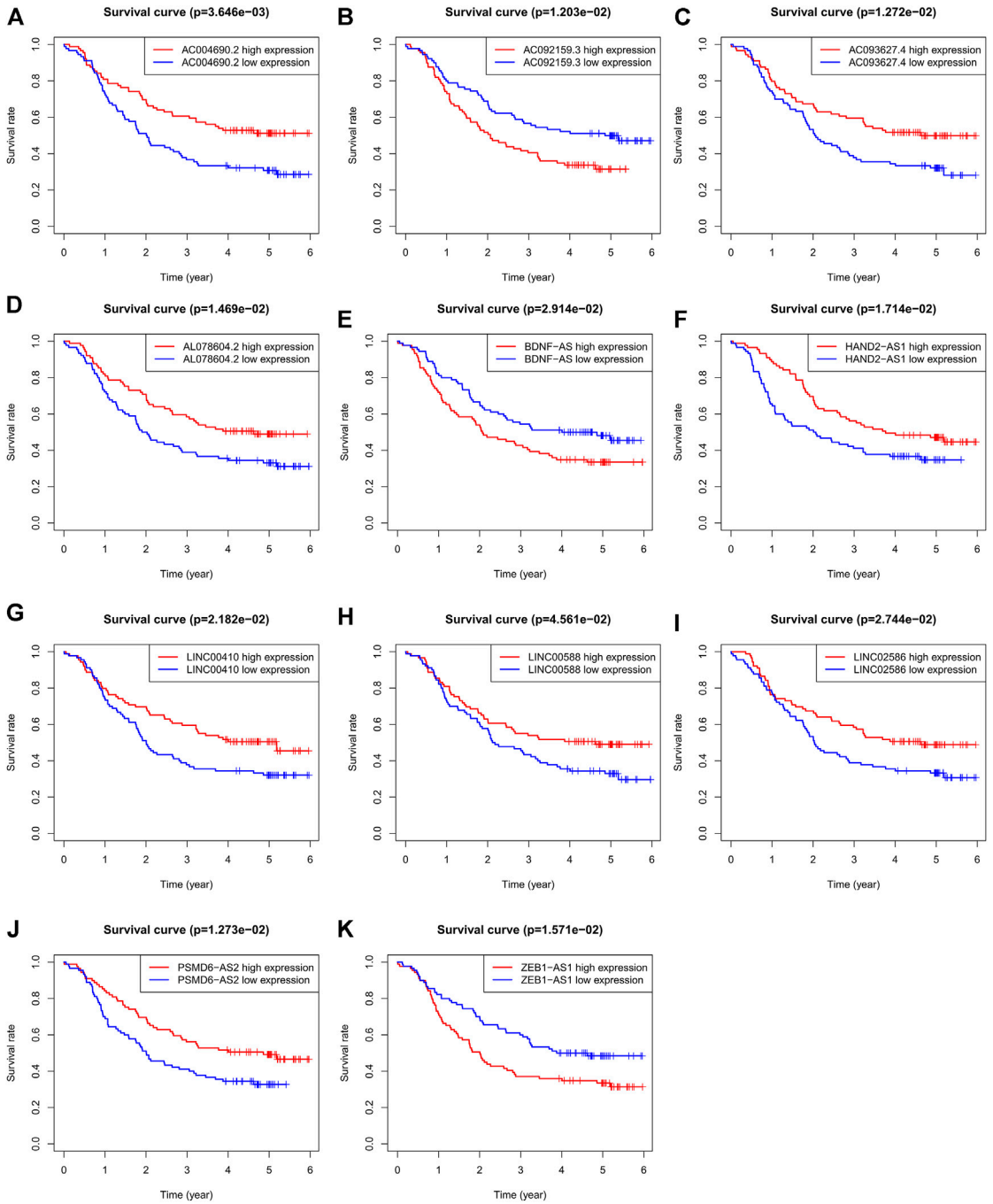

FIGURE 2 | KM analysis of the 11 autophagy-related lncRNAs in GSE63625 ESCC patients. **(A)**: OS curves of ESCC patients based on AC004690.2 expression. **(B)**: OS curves of ESCC patients based on AC092159.3 expression. **(C)**: OS curves of ESCC patients based on AC093627.4 expression. **(D)**: OS curves of ESCC patients based on AL078604.2 expression. **(E)**: OS curves of ESCC patients based on BDNF-AS expression. **(F)**: OS curves of ESCC patients based on HAND2-AS1 expression. **(G)**: OS curves of ESCC patients based on LINC00410 expression. **(H)**: OS curves of ESCC patients based on LINC00588 expression. **(I)**: OS curves of ESCC patients based on LINC02586 expression. **(J)**: OS curves of ESCC patients based on PSMD6-AS2 expression. **(K)**: OS curves of ESCC patients based on ZEB1-AS1 expression.

Therapeutic Response Analysis

The "pRRophetic" package was used to estimate the therapeutic sensitivity of patients in high or low risk group based on half maximal inhibitory concentration (IC50) of anticancer drugs in the Cancer Genome Project (CGP) database. Filtering criteria was $p < 0.05$.

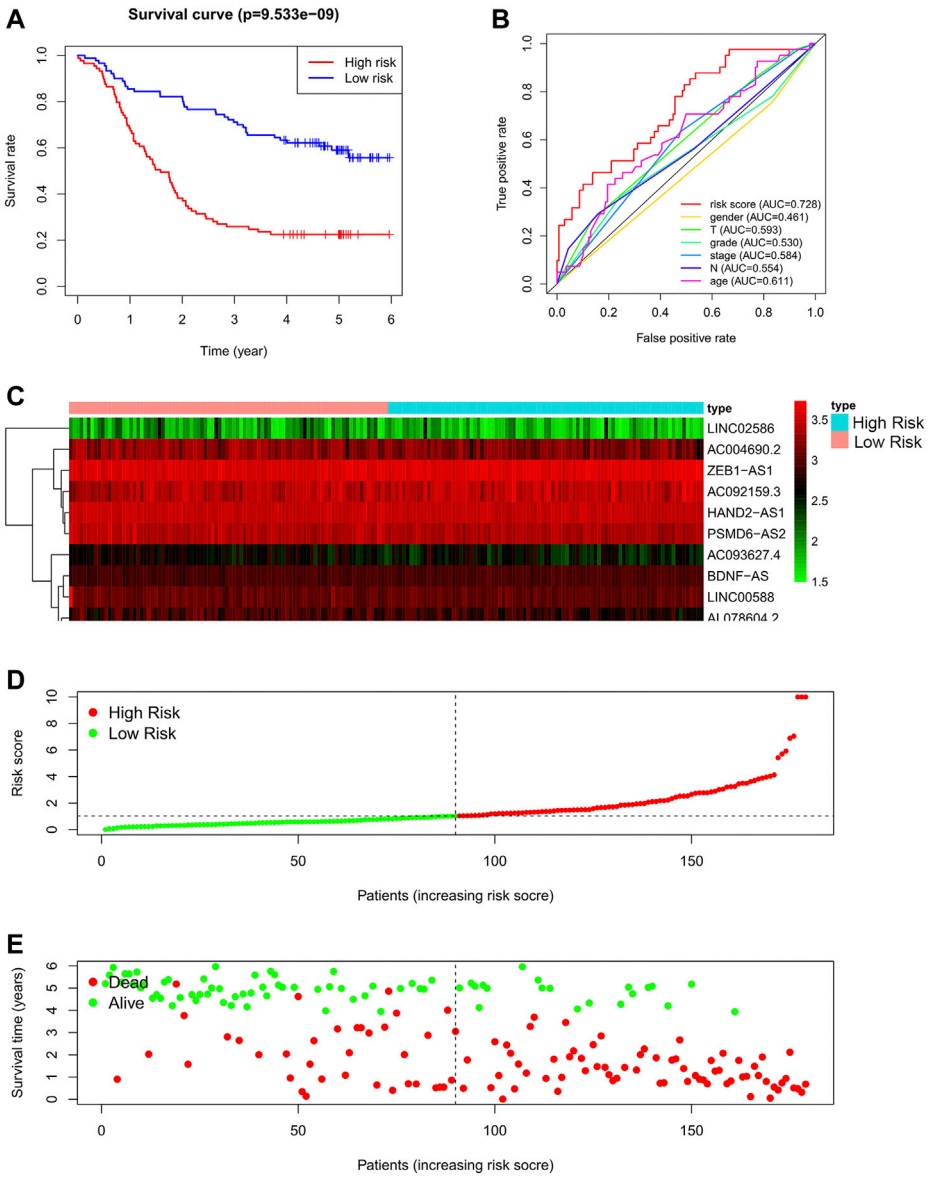

FIGURE 3 | Autophagy related lncRNA risk model in the GSE63625 training set. **(A)**: Survival curve of ESCC patients based on the risk value, **(B)**: ROC of the risk model compared with other clinical characteristics, **(C)**: Expression heatmap of the 11 lncRNAs in patients, **(D)**: Patients distribution based on the risk value, **(E)**: Survival status of all ESCC patients.

Cell Culture

Human normal esophageal cells (HEEpiC) and esophageal cancer cell lines KYSE30 and KYSE150 were cultured according to the manufacturer's instructions (Procell, Wuhan, China) in RPMI-1640 (Solarbio, Beijing, China) supplemented with 10% fetal bovine serum, at 37°C with 5% carbon dioxide.

Differential Validation Using Quantitative Real-Time Polymerase Chain Reaction

TRIZOL reagent (Invitrogen, Grand Island, NY, United States) was used to extract total RNA from cultured cells plated in a 6-well plate. The RNA concentration and quality were determined using a NanoDrop spectrophotometer (Thermo Fisher Scientific, MA, United States). The extracted total RNA was reverse-transcribed into cDNA. qRT-PCR was performed according to the manufacturer's instructions (Takara-Bio), using the following primer sequences: HAND2-AS1, 5′-CGGTCCCTAGCAACAAGGTT-3′ (F) and 5′-CTTTCTGCGCTTACACCTGG-3′ (R); ZEB1-AS1, 5′-TTGGGCGATTTTGAAGTGCG-3′ (F) and 5′-GTGGAGAGGACTGGTTTCGG-3′ (R). The relative lncRNA expression was calculated using the formula $2^{-\Delta\Delta Ct}$. The experiment was performed three times.

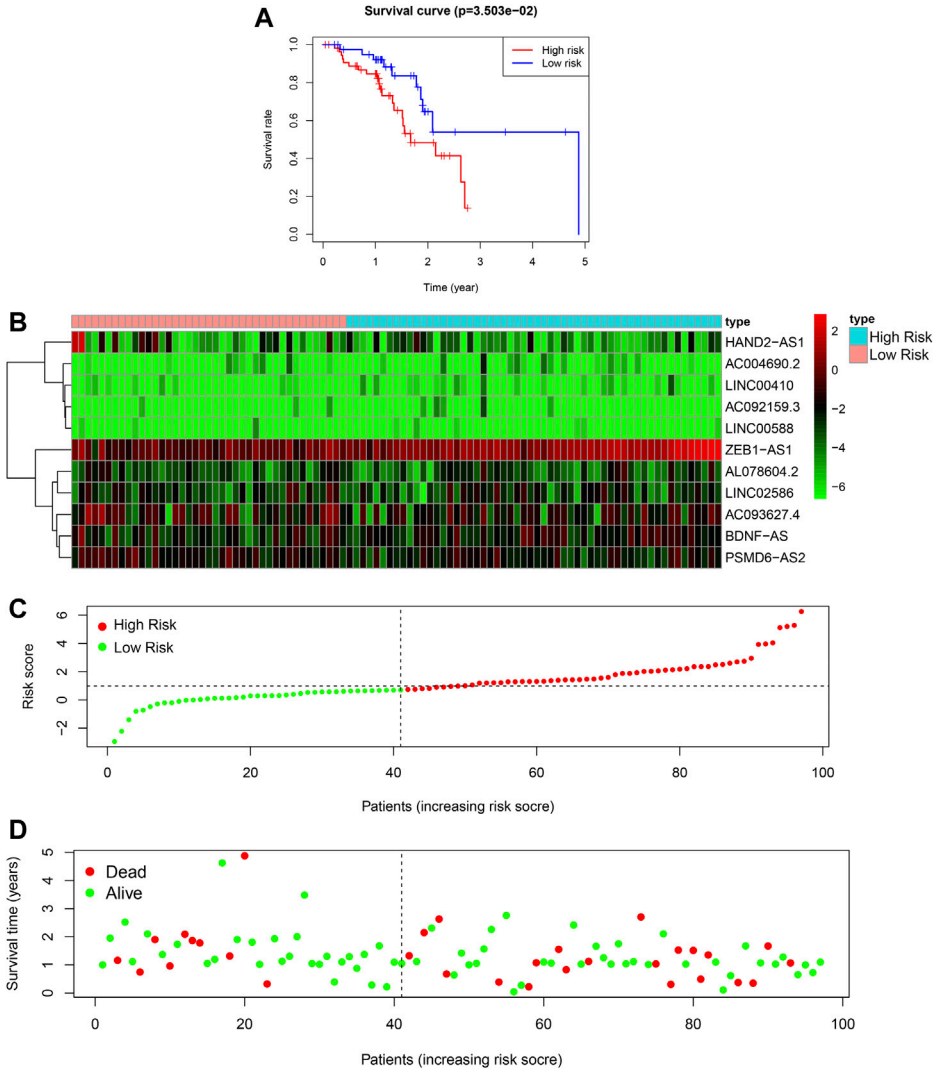

FIGURE 4 | Autophagy related lncRNA risk model in the TCGA testing set. **(A)**: Survival curve of ESCC patients based on the risk value, **(B)**: Expression heatmap of the 11 lncRNAs in patients, **(C)**: Patients distribution based on the risk value, **(D)**: Survival status of all ESCC patients.

Statistical Analysis

All calculations and visualization of bioinformatic data were performed using R language software (version x64 4.1.3, survival library), including generation of Kaplan-Meier survival curves, univariate and multivariate regression analyses, calculation of risk values, plotting risk heat maps and multi-catalog ROC curves, and evaluation of AUC values. GSEA (version 4.0.3) was used to visualize functional enrichment distinctions between the high-and low-risk groups of patients with ESCC. The statistical significance of each test was set at a separation value of $p < 0.05$.

RESULTS

Screening of Prognostic Long Non-Coding RNAs

Among the 179 patients with ESCC, 146 were male and 33 were female. The median patient age was 59 years. The histological distribution of these 179 patients was as follows: 10 patients were stage I, 77 were stage II, and 92 were stage III. The median overall survival was 2.81 years. Based on the combined clinical outcomes of these 179 patients, 43 prognostic-related lncRNAs were obtained after screening using univariate Cox regression (**Table 1**). Of these, 11 lncRNAs were identified as independent prognostic lncRNAs using multivariate Cox regression, including AC004690.2, AC092159.3, AC093627.4, AL078604.2, BDNF-AS, HAND2-AS1, LINC00410, LINC00588, PSMD6-AS2, ZEB1-AS1, and LINC02586 (**Table 2**).

Co-Expression Diagram of Autophagy-Related Long Non-Coding RNAs

The co-expression diagram of the 11 prognostic-related lncRNAs and ARGs is shown in **Figure 1A**. To describe the crosstalk between lncRNAs and ARGs as well as its role in patient survival outcomes, we

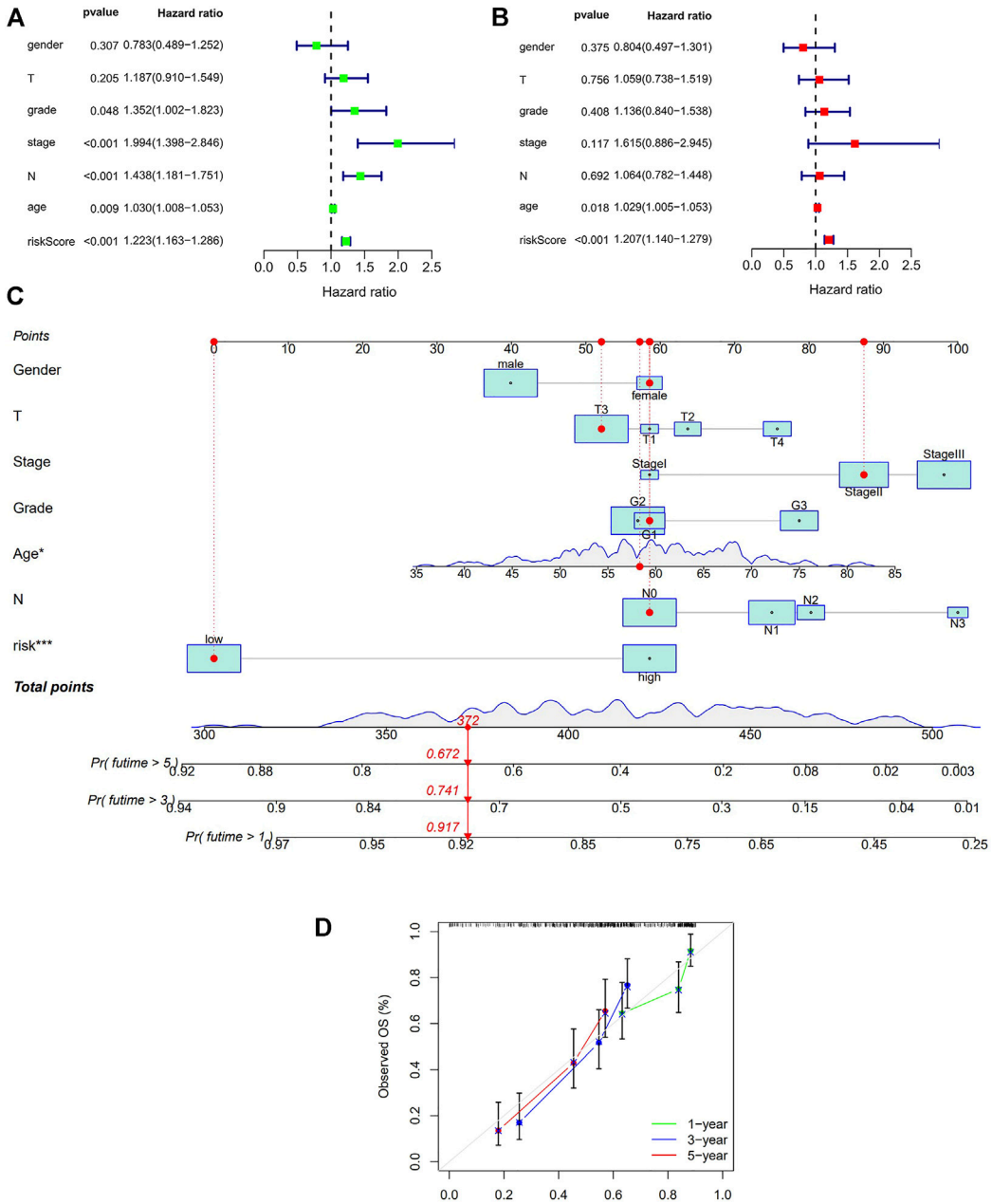

FIGURE 5 | Cox regression analysis and Nomogram in the training set. **(A)**: Univariate Cox regression of risk model and other clinical factors in the training set **(B)**: Multivariate Cox regression of risk model and other clinical factors in the training set **(C)**: Nomogram for both clinic-pathological factors and prognostic autohphagy-related lncRNAs. The value of each variable corresponds to a score on the point scale axis. A total point can be calculated by adding all scores according to each patient's situation and projected to the risk scale. **(D)**: Calibration curves for the nomogram. The x-axis represents the nomogram predicted OS and y-axis represents observed OS in reality. Perfect prediction would correspond to the 45-degree gray line.

constructed a Sankey diagram (**Figure 1B**). The results showed that patients with ESCC showing high AC092159.3, BDNF-AS, or ZEB1-AS1 expression levels were at a higher risk of poor prognosis. In contrast, patients with high AC004690.2, AC093627.4, AL078604.2, HAND2-AS1, LINC00410, LINC00588, LINC02586, or PSMD6-AS2 expression had a lower risk of longer overall survival.

To validate the ability of the 11 candidate lncRNAs to predict patient prognosis, KM analysis was performed using the survival data of patients with ESCC, as shown in **Figure 2**. Based on the Sankey analysis, patients with high AC092159.3, BDNF-AS, or ZEB1-AS1 expression showed significantly shorter survival with a lower median overall survival, whereas patients with high AC004690.2, AC093627.4, AL078604.2, HAND2-AS1, LINC00410, LINC00588, LINC02586, or PSMD6-AS2 expression had a lower risk and longer overall survival.

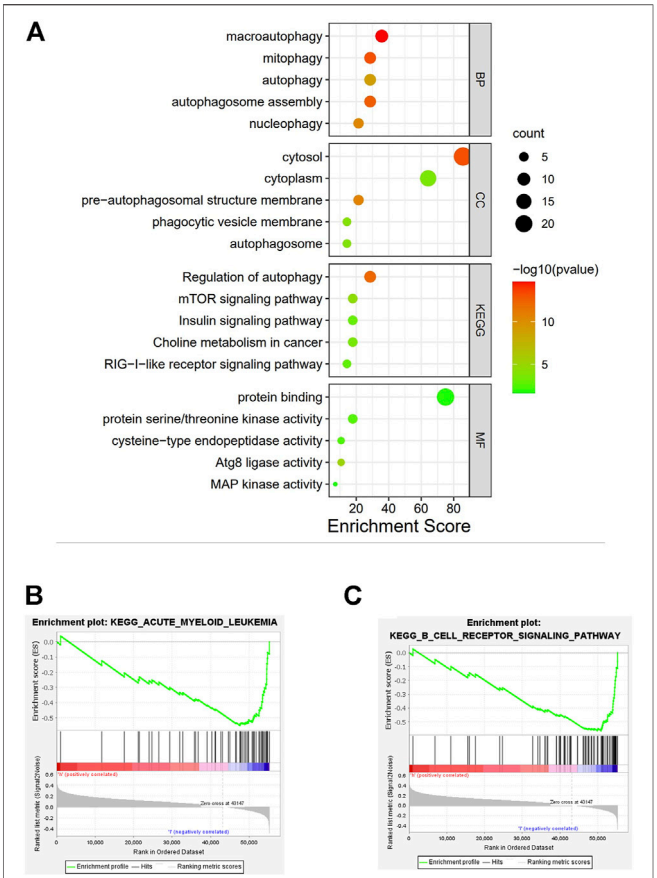

FIGURE 6 | (A): GO analysis of the risk model. **(B,C)**: KEGG pathway enrichment of the risk model.

Development of a Prognostic Autophagy Long Non-Coding RNAs Signature in Esophageal Squamous Cell Carcinoma

Based on the derivation equation, we comprehensively determined the risk value of every patient by multiplying the expression levels of the 11 lncRNAs with their correlation coefficients. Depending on the median value of the risk score, patients were categorized into high-or low-risk groups, and the prognosis of both groups was compared using Kaplan-Meier analysis (**Figure 3A**). We found that patients in the high-risk group had significantly worse outcomes, both in terms of survival and duration of survival, than those in the low-risk group. The 5-year survival rate of the high-risk group was approximately 20%, compared with 60% in the low-risk group ($p < 0.0001$).

To evaluate the performance of the risk model, we also drew a multi-index ROC curve (**Figure 3B**), with an AUC value of 0.728, which was higher than that of other clinical characteristics, indicating that the constructed risk model has the best value for predicting the outcome of patients with ESCC. Furthermore, the risk curve, in addition to the heat map of all patients, is shown in **Figures 3C–E**. As shown in **Figures 3B–D**, as the risk score of patients increases, the survival rate of patients decreases.

External Validation

To validate the model, we used data from patients in TCGA database as an external testing set. The risk analysis of the testing set, and KM survival curve are shown in **Figures 4A–C**. In the KM survival curve, the two groups were distinguished, and the *p*-value was less than 0.05. Our constructed risk model for autophagy and prognostic lncRNAs was thus validated as a significant prognostic indicator.

Independent Prognostic Analysis and Nomogram

Finally, we conducted univariate and multivariate prognostic analyses based on the risk values in both the training and testing sets. The results showed that in the univariate regression test (**Figures 5A,B**), the *p*-value was <0.001 and the HR value was 1.224, whereas in the multivariate regression, the *p*-value was <0.001 and the HR value was 1.191. Briefly, independent prognostic analysis, whether univariate or multivariate, confirmed that our established risk model can be an independent risk indicator to precisely evaluate the outcome of patients with ESCC. In order to obtain a more accurate evaluation tool for predicting each patient's prognosis, we combined the autophagy-related lncRNA risk model with other clinical characteristics and built a nomogram as shown in **Figures 5C–D**.

Gene Set Enrichment Analysis

Using GO annotation and KEGG pathway enrichment, the lncRNAs were found to be enriched in 19 pathways with 50 annotated terms; the top5 GO annotations are shown in **Figure 6A**. GO enrichment analysis showed that the selected lncRNAs were mainly involved in biological functions associated with various autophagy processes in cells, as well as autophagy-related signaling pathways. The other related pathways included mTOR signaling pathways, insulin signaling pathways, and choline metabolic signaling pathways (**Figure 6A**). To further investigate the underlying molecular interaction network of the screened features in esophageal squamous cell carcinoma, the gene sets were analyzed using GSEA. The filter criteria were *p*-value < 0.05 and q-FDR value <0.25 (**Figures 6B,C**). Different enrichments resulted in significantly different risk sets. As shown in **Figure 6B**, the B cell receptor signaling pathway and Acute myeloid leukemia pathway were significantly enriched in the low-risk set, which was connected with immune regulation, suggesting that activation of the B cell receptor signaling pathway can regulate immune function in the low-risk set, thus predicting a better prognosis and longer survival time. Unfortunately, in the high-risk set, we did not obtain distinct enrichment results, suggesting that the group with a low-risk score was associated with activated immune function. These data provide potential for further research on the personalized treatment of ESCC.

Immune Function Heatmap and Tumor Mutational Burden

It has been reported that autophagy plays certain role in mediating innate and adaptive immune responses. In the

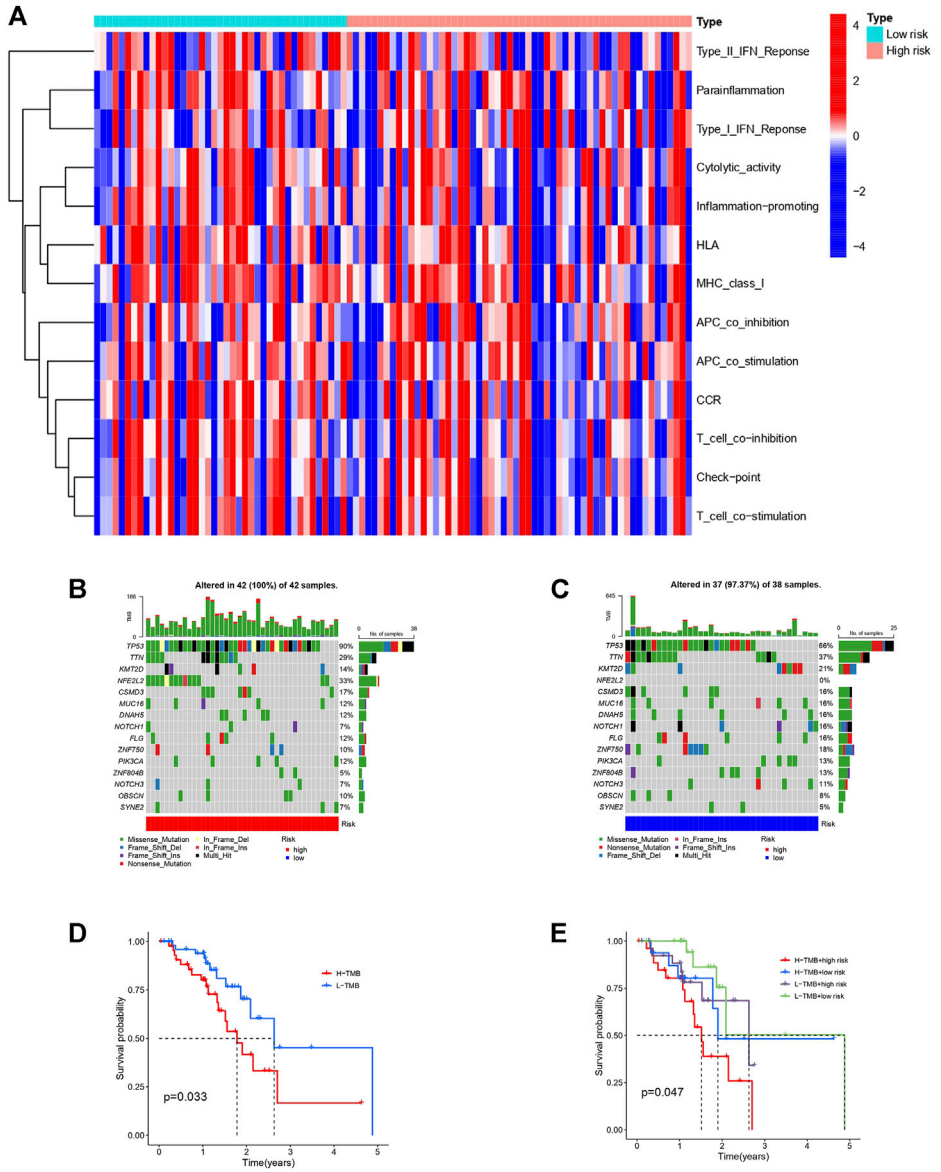

FIGURE 7 | Immune function heatmap and TMB in high and low risk groups of patients with ESCC. **(A)**: Heatmap of immune functions of the two risk groups. **(B)**: Waterfall plot of TMB in high-risk group. **(C)**: Waterfall plot of TMB in low-risk group. **(D)**: Survival curves of patients with ESCC divided into high or low-TMB groups. **(E)**: Survival curves of patients with different TMB based on high or low risk classification.

KEGG and GO analyses we noticed enrichments in cellular autophagy and immunity. Therefore, we compared the difference of immune functions of the high and low risk groups and the heatmap is shown in **Figure 7A**. Several attempts have been made to identify predictive biomarkers for immunotherapy response. One of the most intriguing and divisive is TMB. Hence, we explored the TMB of the high and low risk group as shown in **Figures 7B–C**. Generally, the frequency of mutation is higher in the high-risk group and we also found the majority mutation in the high-risk group was associated with mismatch-repair deficiency. Patients with high TMB had shorter OS and unfavorable prognosis. Survival analyses combining TMB and risk model of patients with ESCC is shown in **Figures 7D–E**.

Chemotherapy and Immunotherapy Sensitivity

Therapeutic response analysis showed patients with ESCC in the high-risk group showed lower IC50 in five commonly used chemotherapy drugs for cancer treatment (Cisplatin, Cytarabine, Docetaxel, Paclitaxel, and Vinblastine) (**Figure 8**), indicating that the high-risk patients are more sensitive to chemotherapy. We also found a lower IC50 of Lenalidomide in the high-risk group, suggesting that

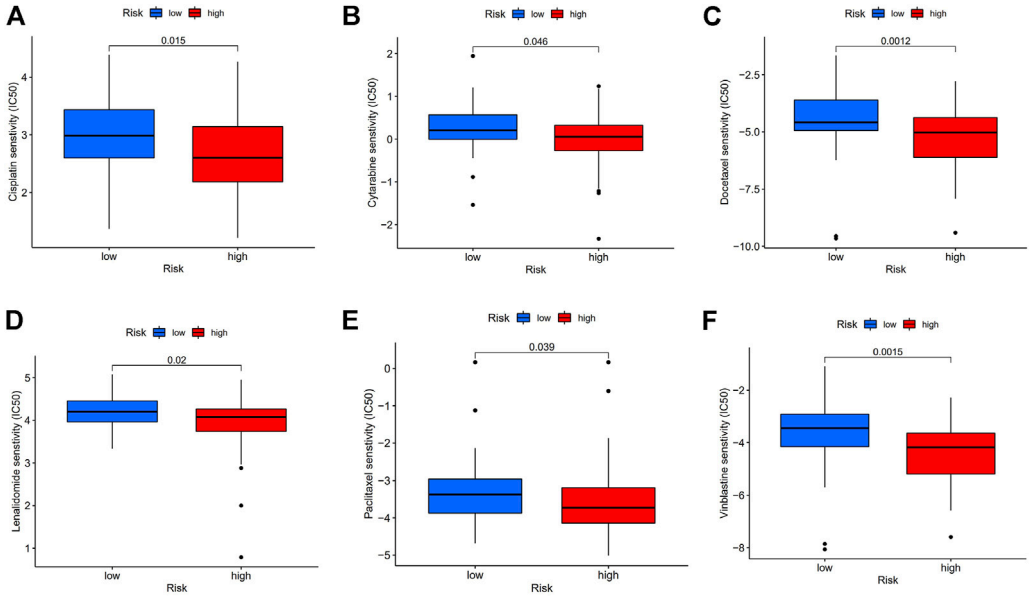

FIGURE 8 | Chemotherapy and immunotherapy response. **(A–F)**: Sensitivity to Cisplatin, Cytarabine, Docetaxel, Paclitaxel, Vinblastine, and Lenalidomide in high or low-risk group shown in box plot.

these patients are more likely to benefit from Lenalidomide immunotherapy.

Expression of Signature Long Non-Coding RNAs in Esophageal Squamous Cell Carcinoma Cell Lines by Quantitative Real-Time Polymerase Chain Reaction

Differential expression of the 11 autophagy-realted lncRNAs in cancer versus normal tissue is shown in **Figure 9A**. 7 (BDNF-AS, HAND2-AS1, LINC00410, LINC00588, PSMD6-AS2, ZEB1-AS1, and LINC02586) of the 11 lncRNAs were differentially expressed in cancer and normal tissues. Here we selected four sequence-available lncRNAs (BDNF-AS, HAND2-AS1, LINC00588, and ZEB1-AS1) of the seven differentially expressed lncRNAs with qRT-PCR. As shown in **Figures 9B–E**, the expression levels of HAND2-AS1 and LINC00588 were significantly lower in KYSE30 and KYSE150 cells than that in HEEpiC, $p < 0.05$, whereas the expression levels of BNDF-AS and ZEB1-AS1 were higher in KYSE30 and KYSE150 compared to that in HEEpiC cells. The remaining three lncRNAs could not be quantified because of a lack of transcriptome information in NCBI.

DISCUSSION

In 2018, more than 572,000 patients were newly diagnosed with EC (Bray et al., 2018). Treatment of EC remains a challenge because of its recurrence and unfavorable prognosis. The overall 5-year survival rate of EC can be as low as 20% owing to the advanced stage at diagnosis (mainly stage III or IV) and its high invasiveness (Anderson et al., 2015). Although the regional distribution of the two main pathological subtypes has changed over the past 4 decades, ESCC still accounts for the majority of EC cases (Siegel et al., 2019). Therefore, understanding the epidemiological characteristics and risk factors of EC is crucial for public health and clinical decision making, including risk assessment, disease screening, and prevention. The current research on risk stratification mainly focuses on screening Barrett's esophagus and gastroesophageal reflux disease (GERD) symptom rating scales (Rubenstein et al., 2013; Dong et al., 2018; Rubenstein et al., 2020). A valid risk stratification tool for ESCC thus remains lacking.

Autophagy is a highly conserved pathway that plays a crucial role in both normal and cancerous cells. Multiple cancers exhibit disrupted autophagy regulation. Autophagy is responsible for alterations in cancer cell metabolic regulation and plays a critical role in promoting immune escape. Targeting the autophagy mechanisms remains a promising strategy for the treatment of an increasing number of cancers. Emerging evidence suggests that lncRNAs may also play a crucial role in tumorigenesis (Liu et al., 2022a; Liu et al., 2022b). Recently, Zhang et al. (2020) reported a co-expression pattern of lncRNA HOTAIR and MTHFR, which regulate the biological behavior of EC cells. According to Hu et al. (2021), lncRNA RP11-465B22.8 can be delivered to macrophages *via* exosomes to induce the M2 phenotype, thus enhancing the migration and invasion of EC cells. Their research indicates that lncRNAs are a novel target and based on their regulation of immunity in EC they can potentially provide new therapeutic strategies. In a study by Wu et al. (2022), 22 autophagy-related lncRNAs were included in the risk assessment of patients with EAC, but none of these lncRNAs were identical to those included our stratification model. This may be caused by differences in histological classification. Prognostic lncRNAs in other cancer types have also been reported in recent years, including breast cancer (Wang J. et al., 2019), colon cancer (Zhou et al., 2020), pancreatic cancer (Deng et al., 2020), and bladder cancer (Lai et al., 2020). Most of these models have

been constructed based on public databases, with other datasets used for validation. The AUC value varied from 0.6 to 0.9, and was statistically significant.

In a previous study (Shi et al. (2021), also reported a prognostic model in ESCC consisted of nine autophagy-related lncRNAs. It is noticed that the 11 lncRNA signatures in our model had no overlap with theirs. This may due to different statistical approach and filtering criteria. In their study, three of the nine lncRNAs for model construction were independent prognostic factors. In comparison, all 11 lncRNAs in our model were significant by multivariate Cox analyses and the model was externally validated using other databases in addition to differential expression validation by qRT-PCR. In this study, we used autophagy-associated lncRNAs as prognostic stratification biomarkers to screen for ESCC risk. Validation in an independent database showed that the AUC value (0.647) of our signature was higher than that of other clinical characteristics. Kaplan-Meier analysis showed that the two risk groups based on our risk stratification model showed different prognoses, with a $p < 0.001$. A nomogram for predicting patients' OS was built with the risk model and clinic-pathological features. Further TMB and therapeutic response analyses displayed significant distinctions between the two risk groups. Among the 11 lncRNAs screened for our risk model, seven (BDNF-AS, HAND2-AS1, LINC00410, LINC00588, PSMD6-AS2, ZEB1-AS1, and LINC02586) were found to be differentially expressed in adjacent normal tissues and cancer tissues. Of these, four (BDNF-AS, HAND2-AS1, LINC00588, and ZEB1-AS1) lncRNAs were further quantified in cultured human ESCC cells and normal epithelial cells; the results obtained were consistent with our data analysis. Unfortunately, the remaining three lncRNAs could not be quantified because of a lack of transcriptome information in NCBI.

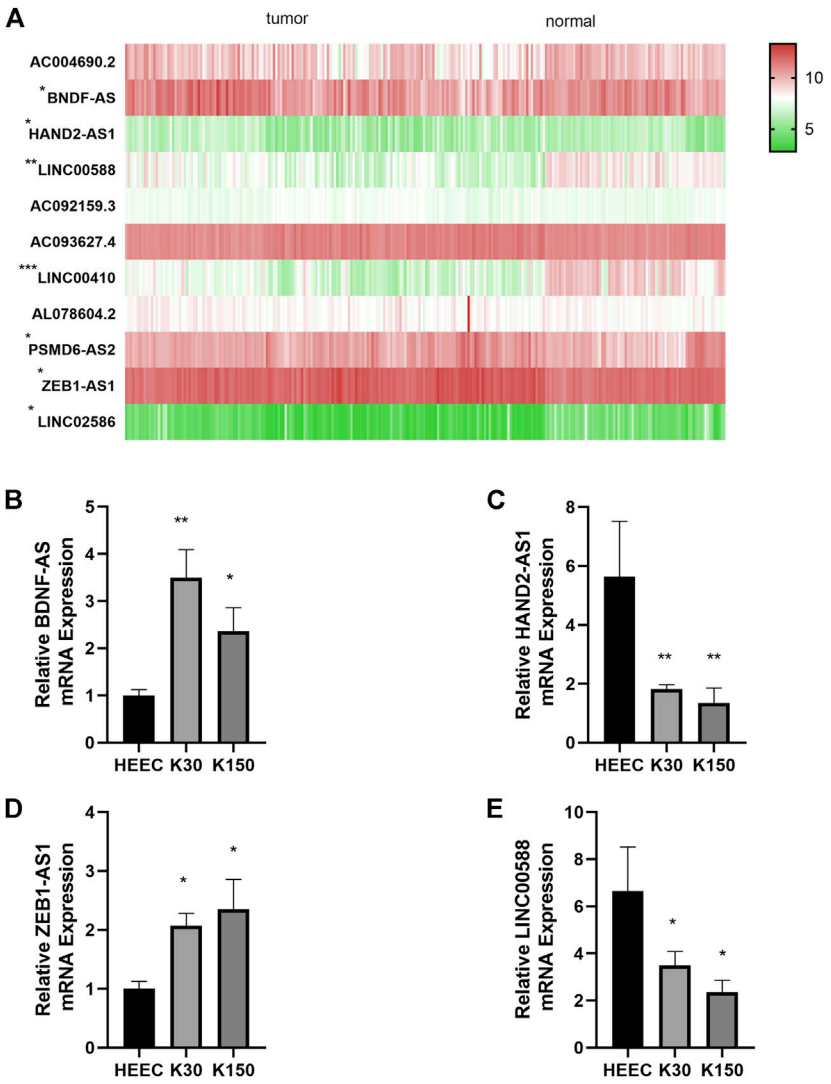

FIGURE 9 | Differential expression of autophagy-related lncRNAs. **(A)**: Differential expression of seven autophagy-related lncRNAs in cancer tissue vs. normal tissue **(B)**: Relative BDNF-AS1 expression in HEEC, K30, K150 cells. **(C)**: Relative HAND2-AS1 expression in HEEC, K30, K150 cells. **(D)**: Relative ZEB1-AS1 expression in HEEC, K30, K150 cells. **(E)**: Relative LINC00588 expression in HEEC, K30, K150 cells.

Among the autophagy-related lncRNAs in our risk model, differential expression of the following three lncRNAs, BDNF-AS1, HAND2-AS1, and ZEB1-AS1, in normal and cancer tissues is commonly found in several cancer types with critical roles in cancer progression. In colon cancer, low expression of BDNF-AS1 can upregulate glycogen synthase kinase-3+, thereby inhibiting the proliferation, invasion, and metastatic ability of colon cancer cells (Zhi and Lian, 2019). In esophageal cancer cell lines, BDNF-AS1 can co-regulate mir-214 and thus regulating the growth and invasion of esophageal cancer cells. Further, BDNF-AS1 has diverse effects on other cancer types, mostly inhibiting epithelial-mesenchymal transition (EMT) and tumor formation in tumor cells (Cao et al., 2010). The lncRNA HAND2-AS1 inhibits tumorigenesis and is expressed in various tumor tissues at lower levels than in adjacent normal tissues (Wang Y. et al., 2019). Abnormal HAND2-AS1 expression is associated with tumor progression and prognosis. Reduced HAND2-AS1 is reported to inhibit cancer growth and correlates with clinical features such as lymph node involvement, histological differentiation (Yang et al., 2017), tumor size, and staging. ZEB1-AS1 is localized on chromosome 10p11.22 with two exons and one intron in between (Gao et al., 2019), and is derived from the ZEB1 promoter (Jiao et al., 2020). Its subcellular localization is in the nucleus. ZEB1-AS1was identified early for its prominent role in promoting cancer cell proliferation (Chen and Shen, 2020). Further, ZEB1-AS1 expression is found to be significantly higher in hepatocellular tumor tissues than in normal tumor-adjacent tissues, and is abnormally elevated in metastatic HCC tissues. High ZEB1-AS1 expression has also been detected in various hepatocellular carcinoma cell lines.

The limitation of our research is that the enrolled patients' data were mainly obtained from public databases. A larger number of patients with follow-up data are needed to further validate the performance of the model. Moreover, the AUC of our model could potentially be improved by integrating multi-omics data if available. However, the biological functions and underlying mechanisms of most lncRNAs remain elusive.

To our knowledge, this study presents the first autophagy-associated lncRNA signature for risk assessment in ESCC. This autophagy-related lncRNA model provides an effective means for predicting the prognosis of patients with ESCC; moreover, some of these lncRNAs might also serve as novel targets for ESCC treatment.

DATA AVAILABILITY STATEMENT

The original contributions presented in the study are included in the article/supplementary material, further inquiries can be directed to the corresponding author.

AUTHOR CONTRIBUTIONS

BX: supervision, conceptualization. XZ: data curation, writing—original draft preparation, validation, formal analysis, YW: writing—review and editing, visualization, ZL: data curation, software, FM: methodology, data curation.

FUNDING

This work was supported by the Beijing Tianjin Hebei basic research cooperation project [19JCZDJC64500 (Z)].

ACKNOWLEDGMENTS

We gratefully acknowledge the TCGA Research Network and GSE53625 database for the availability of data in this study. Yujian Kang offered valuable suggestions in statistical analysis. We hereby express our gratitude.

REFERENCES

Anderson, L. A., Tavilla, A., Brenner, H., Luttmann, S., Navarro, C., Gavin, A. T., et al. (2015). Survival for Oesophageal, Stomach and Small Intestine Cancers in Europe 1999-2007: Results from EUROCARE-5. *Eur. J. Cancer* 51 (15), 2144–2157. doi:10.1016/j.ejca.2015.07.026

Beermann, J., Piccoli, M.-T., Viereck, J., and Thum, T. (2016). Non-coding RNAs in Development and Disease: Background, Mechanisms, and Therapeutic Approaches. *Physiol. Rev.* 96 (4), 1297–1325. doi:10.1152/physrev.00041.2015

Bray, F., Ferlay, J., Soerjomataram, I., Siegel, R. L., Torre, L. A., and Jemal, A. (2018). Global Cancer Statistics 2018: GLOBOCAN Estimates of Incidence and Mortality Worldwide for 36 Cancers in 185 Countries. *CA A Cancer J. Clin.* 68 (6), 394–424. doi:10.3322/caac.21492

Cao, L., Liu, X., Lin, E.-J. D., Wang, C., Choi, E. Y., Riban, V., et al. (2010). Environmental and Genetic Activation of a Brain-Adipocyte BDNF/leptin axis Causes Cancer Remission and Inhibition. *Cell* 142 (1), 52–64. doi:10.1016/j.cell.2010.05.029

Chen, S., and Shen, X. (2020). Long Noncoding RNAs: Functions and Mechanisms in Colon Cancer. *Mol. Cancer* 19 (1), 167. doi:10.1186/s12943-020-01287-2

Chi, Y., Wang, D., Wang, J., Yu, W., and Yang, J. (2019). Long Non-coding RNA in the Pathogenesis of Cancers. *Cells* 8 (9), 1015. doi:10.3390/cells8091015

Deng, Z., Li, X., Shi, Y., Lu, Y., Yao, W., and Wang, J. (2020). A Novel Autophagy-Related lncRNAs Signature for Prognostic Prediction and Clinical Value in Patients with Pancreatic Cancer. *Front. Cell Dev. Biol.* 8, 606817. doi:10.3389/fcell.2020.606817

Djebali, S., Davis, C. A., Merkel, A., Dobin, A., Lassmann, T., Mortazavi, A., et al. (2012). Landscape of Transcription in Human Cells. *Nature* 489 (7414), 101–108. doi:10.1038/nature11233

Dong, J., Buas, M. F., Gharahkhani, P., Kendall, B. J., Onstad, L., Zhao, S., et al. (2018). Determining Risk of Barrett's Esophagus and Esophageal Adenocarcinoma Based on Epidemiologic Factors and Genetic Variants. *Gastroenterology* 154 (5), 1273–1281. e1273. doi:10.1053/j.gastro.2017.12.003

Dykes, I. M., and Emanueli, C. (2017). Transcriptional and Post-transcriptional Gene Regulation by Long Non-coding RNA. *Genomics, Proteomics Bioinforma.* 15 (3), 177–186. doi:10.1016/j.gpb.2016.12.005

Ferlay, J., Soerjomataram, I., Dikshit, R., Eser, S., Mathers, C., Rebelo, M., et al. (2015). Cancer Incidence and Mortality Worldwide: Sources, Methods and Major Patterns in GLOBOCAN 2012. *Int. J. Cancer* 136 (5), E359–E386. doi:10.1002/ijc.29210

Galluzzi, L., Pietrocola, F., Bravo-San Pedro, J. M., Amaravadi, R. K., Baehrecke, E. H., Cecconi, F., et al. (2015). Autophagy in Malignant Transformation and Cancer Progression. *Embo J.* 34 (7), 856–880. doi:10.15252/embj.201490784

Gao, R., Zhang, N., Yang, J., Zhu, Y., Zhang, Z., Wang, J., et al. (2019). Long Non-coding RNA ZEB1-AS1 Regulates miR-200b/FSCN1 Signaling and Enhances Migration and Invasion Induced by TGF-B1 in Bladder Cancer Cells. *J. Exp. Clin. Cancer Res.* 38 (1), 111. doi:10.1186/s13046-019-1102-6

Hu, R., Bi, R., Jiang, L., Xiao, H., Xie, X., Liu, H., et al. (2021). LncRNA RP11-465B22.8 Triggers Esophageal Cancer Progression by Targeting miR-765/KLK4 axis. *Cell Death Discov.* 7 (1), 262. doi:10.1038/s41420-021-00631-9

Jiao, M., Ning, S., Chen, J., Chen, L., Jiao, M., Cui, Z., et al. (2020). Long Non-coding RNA ZEB1-AS1 Predicts a Poor Prognosis and Promotes Cancer Progression through the miR-200a/ZEB1 Signaling Pathway in Intrahepatic Cholangiocarcinoma. *Int. J. Oncol.* 56 (6), 1455–1467. doi:10.3892/ijo.2020.5023

Johnson, J. M., Edwards, S., Shoemaker, D., and Schadt, E. E. (2005). Dark Matter in the Genome: Evidence of Widespread Transcription Detected by Microarray Tiling Experiments. *Trends Genet.* 21 (2), 93–102. doi:10.1016/j.tig.2004.12.009

Lai, C., Wu, Z., Shi, J., Li, K., Zhu, J., Chen, Z., et al. (2020). Autophagy-related Long Noncoding RNAs Can Predict Prognosis in Patients with Bladder Cancer. *Aging* 12 (21), 21582–21596. doi:10.18632/aging.103947

Levy, J. M. M., Towers, C. G., and Thorburn, A. (2017). Targeting Autophagy in Cancer. *Nat. Rev. Cancer* 17 (9), 528–542. doi:10.1038/nrc.2017.53

Li, J., Li, Z., Leng, K., Xu, Y., Ji, D., Huang, L., et al. (2018). ZEB1-AS1: A Crucial Cancer-related Long Non-coding RNA. *Cell Prolif.* 51 (1), e12423. doi:10.1111/cpr.12423

Liu, Z., Guo, C., Dang, Q., Wang, L., Liu, L., Weng, S., et al. (2022a). Integrative Analysis from Multi-Center Studies Identities a Consensus Machine Learning-Derived lncRNA Signature for Stage II/III Colorectal Cancer. *EBioMedicine* 75, 103750. doi:10.1016/j.ebiom.2021.103750

Liu, Z., Liu, L., Weng, S., Guo, C., Dang, Q., Xu, H., et al. (2022b). Machine Learning-Based Integration Develops an Immune-Derived lncRNA Signature for Improving Outcomes in Colorectal Cancer. *Nat. Commun.* 13 (1), 816. doi:10.1038/s41467-022-28421-6

Pietrocola, F., Pol, J., Vacchelli, E., Rao, S., Enot, D. P., Baracco, E. E., et al. (2016). Caloric Restriction Mimetics Enhance Anticancer Immunosurveillance. *Cancer Cell* 30 (1), 147–160. doi:10.1016/j.ccell.2016.05.016

Quinn, J. J., and Chang, H. Y. (2016). Unique Features of Long Non-coding RNA Biogenesis and Function. *Nat. Rev. Genet.* 17 (1), 47–62. doi:10.1038/nrg.2015.10

Rubenstein, J. H., McConnell, D., Waljee, A. K., Metko, V., Nofz, K., Khodadost, M., et al. (2020). Validation and Comparison of Tools for Selecting Individuals to Screen for Barrett's Esophagus and Early Neoplasia. *Gastroenterology* 158 (8), 2082–2092. doi:10.1053/j.gastro.2020.02.037

Rubenstein, J. H., Morgenstern, H., Appelman, H., Scheiman, J., Schoenfeld, P., McMahon, L. F., Jr., et al. (2013). Prediction of Barrett's Esophagus Among Men. *Am. J. Gastroenterol.* 108 (3), 353–362. doi:10.1038/ajg.2012.446

Russo, M., and Russo, G. L. (2018). Autophagy Inducers in Cancer. *Biochem. Pharmacol.* 153, 51–61. doi:10.1016/j.bcp.2018.02.007

Shi, X., Liu, X., Pan, S., Ke, Y., Li, Y., Guo, W., et al. (2021). A Novel Autophagy-Related Long Non-coding RNA Signature to Predict Prognosis and Therapeutic Response in Esophageal Squamous Cell Carcinoma. *Int. J. Gen. Med.* 14, 8325–8339. doi:10.2147/ijgm.S333697

Siegel, R. L., Miller, K. D., and Jemal, A. (2019). Cancer Statistics, 2019. *CA A Cancer J. Clin.* 69 (1), 7–34. doi:10.3322/caac.21551

Smyth, E. C., Lagergren, J., Fitzgerald, R. C., Lordick, F., Shah, M. A., Lagergren, P., et al. (2017). Oesophageal Cancer. *Nat. Rev. Dis. Prim.* 3, 17048. doi:10.1038/nrdp.2017.48

Thrift, A. P. (2021). Global Burden and Epidemiology of Barrett Oesophagus and Oesophageal Cancer. *Nat. Rev. Gastroenterol. Hepatol.* 18 (6), 432–443. doi:10.1038/s41575-021-00419-3

Wang, J., Xie, S., Yang, J., Xiong, H., Jia, Y., Zhou, Y., et al. (2019). The Long Noncoding RNA H19 Promotes Tamoxifen Resistance in Breast Cancer via Autophagy. *J. Hematol. Oncol.* 12 (1), 81. doi:10.1186/s13045-019-0747-0

Wang, Y., Zhu, P., Luo, J., Wang, J., Liu, Z., Wu, W., et al. (2019). LncRNA HAND2-AS1 Promotes Liver Cancer Stem Cell Self-renewal via BMP Signaling. *Embo J.* 38 (17), e101110. doi:10.15252/embj.2018101110

Wu, L., Zheng, Y., Ruan, X., Wu, D., Xu, P., Liu, J., et al. (2022). Long-chain Noncoding Ribonucleic Acids Affect the Survival and Prognosis of Patients with Esophageal Adenocarcinoma through the Autophagy Pathway: Construction of a Prognostic Model. *Anticancer Drugs* 33 (1), e590–e603. doi:10.1097/cad.0000000000001189

Yang, Y., Chen, L., Gu, J., Zhang, H., Yuan, J., Lian, Q., et al. (2017). Recurrently Deregulated lncRNAs in Hepatocellular Carcinoma. *Nat. Commun.* 8, 14421. doi:10.1038/ncomms14421

Zhang, S., Zheng, F., Zhang, L., Huang, Z., Huang, X., Pan, Z., et al. (2020). LncRNA HOTAIR-Mediated MTHFR Methylation Inhibits 5-fluorouracil Sensitivity in Esophageal Cancer Cells. *J. Exp. Clin. Cancer Res.* 39 (1), 131. doi:10.1186/s13046-020-01610-1

Zhi, H., and Lian, J. (2019). LncRNA BDNF-AS Suppresses Colorectal Cancer Cell Proliferation and Migration by Epigenetically Repressing GSK-3β Expression. *Cell Biochem. Funct.* 37 (5), 340–347. doi:10.1002/cbf.3403

Zhou, W., Zhang, S., Li, H.-B., Cai, Z., Tang, S., Chen, L.-X., et al. (2020). Development of Prognostic Indicator Based on Autophagy-Related lncRNA Analysis in Colon Adenocarcinoma. *BioMed Res. Int.* 2020, 9807918. doi:10.1155/2020/9807918

Conflict of Interest: The authors declare that the research was conducted in the absence of any commercial or financial relationships that could be construed as a potential conflict of interest.

Publisher's Note: All claims expressed in this article are solely those of the authors and do not necessarily represent those of their affiliated organizations, or those of the publisher, the editors and the reviewers. Any product that may be evaluated in this article, or claim that may be made by its manufacturer, is not guaranteed or endorsed by the publisher.

NOMENCLATURE

Abbreviations

ESCC esophageal squama cell carcinoma

LncRNA long non-coding RNAs

AUC the area under the receiver operating

ARG autophagy related gene

TMB tumor mutation burden

CGP the cancer genome project

EC esophageal cancer

EAC esophageal adenocarcinoma

GEO gene expression omnibus

TCGA cancer genome atlas

HADb human autophagy database

The KM curves the kaplan meier survival curves

ROC the receiver operator characteristic curve

KEGG kyoto encyclopedia of genes and genomes

GO gene ontology

GSEA gene set enrichment analysis

HEEpiC human normal esophageal cells

K30 KYSE30

K150 KYSE150

frontiers | Frontiers in Genetics

REVIEW
published: 15 July 2022
doi: 10.3389/fgene.2022.927541

CircRNA ITCH: Insight Into Its Role and Clinical Application Prospect in Tumor and Non-Tumor Diseases

Tong Liu[†], *Tao Huang*[†], *Mei Shang and Gang Han* *

Department of Gastrointestinal Nutrition and Hernia Surgery, The Second Hospital of Jilin University, Changchun, China

CircRNA E3 ubiquitin protein ligase (ITCH) (circRNA ITCH, circ-ITCH), a stable closed-loop RNA derived from the 20q11.22 region of chromosome 20, is a new circRNA discovered in the cytoplasm in recent decades. Studies have shown that it does not encode proteins, but regulates proteins expression at different levels. It is down-regulated in tumor diseases and is involved in a number of biological activities, including inhibiting cell proliferation, migration, invasion, and promoting apoptosis. It can also alter disease progression in non-tumor disease by affecting the cell cycle, inflammatory response, and critical proteins. Circ-ITCH also holds a lot of promise in terms of tumor and non-tumor clinical diagnosis, prognosis, and targeted therapy. As a result, in order to aid clinical research in the hunt for a new strategy for diagnosing and treating human diseases, this study describes the mechanism of circ-ITCH as well as its clinical implications.

Keywords: circ-ITCH, malignant tumor, non-tumor diseases, mechanism, biomarkers

OPEN ACCESS

Edited by:
Olanrewaju B. Morenikeji, University of Pittsburgh at Bradford, United States

Reviewed by:
Annie Angers, Université de Montréal, Canada
Mabel Akinyemi, Fairleigh Dickinson University, United States
Olamide Crown, Jackson State University, United States
Mahesh Kathania, University of Texas Southwestern Medical Center, United States

***Correspondence:**
Gang Han
hangang@jlu.edu.cn

[†]*These authors have contributed equally to this work*

Specialty section:
This article was submitted to RNA, a section of the journal Frontiers in Genetics

Received: *24 April 2022*
Accepted: *21 June 2022*
Published: *15 July 2022*

Citation:
Liu T, Huang T, Shang M and Han G (2022) CircRNA ITCH: Insight Into Its Role and Clinical Application Prospect in Tumor and Non-Tumor Diseases. Front. Genet. 13:927541. doi: 10.3389/fgene.2022.927541

1 INTRODUCTION

In brief, diseases were categorized into two groups: tumors and non-tumor disorders. Malignant tumors, for example, are a type of incurable polygenic disease that has claimed the lives of millions of individuals worldwide. According to GLOBOCAN 2020, there were 19.3 million new malignant tumor cases and 9.9 million deaths globally in 2020 (Sung et al., 2021). Although surgical resection and advanced therapeutic interventions have improved the 5-year survival rate in patients with early-stage GC, the prognosis for late-stage GC patients remains poor due to uncontrolled tumor cell growth and migration (Lasithiotakis et al., 2014). Non-tumor disorders, such as degenerative, metabolic, congenital, and inflammatory pathologies, make up the great bulk of all pathologies, aside from tumors. As a result, finding effective diagnostic biomarkers and treatment targets is crucial for disease fundamental research.

Benefiting from high-throughput sequencing, researchers can take a nuanced and complete picture of the transcriptome and genome of a species. RNA sequencing (RNA-seq) technology has become one of the important means of transcriptomic studies of high-throughput sequencing, which can discover all RNAs that a particular cell can transcribe in a certain functional state, mainly including mRNAs and non-coding RNAs, while avoiding detection using standard molecular techniques. CircRNAs, which were previously thought to be misspliced products, have lately been shown to have a range of biological regulatory activities owing to the development of RNA-seq (Memczak et al., 2013). Most circular RNAs (circRNAs) are mainly composed of one or more exons encoding known proteins. The 3' and 5' terminals of circRNAs are covalently bonded to form a closed-loop structure, unlike typical linear RNAs. It has no free terminal and is unaffected by RNA exonuclease, resulting in a more stable and difficult-to-degrade copy. CircRNAs is primarily

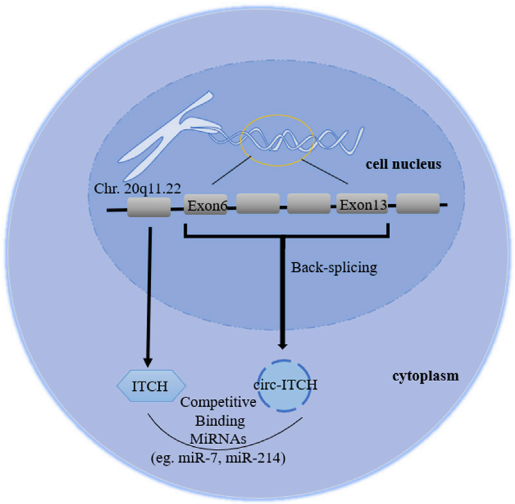

FIGURE 1 | Biogenesis diagram of circ-ITCH. The ID number of circ-ITCH is hsa_circ_0001141, whose gene is located in chr 20q11.22, derived from exon 6–13 of ITCH coding gene, formed by back-splicing, and its mature sequence is 873bp.

involved in the following four processes: 1) sponging microRNAs (miRNAs) or long noncoding RNAs (lncRNAs) as a competing endogenous RNA (ceRNA); 2) binding RNA binding proteins (RBPs); 3) interfering with gene transcription and splicing regulation; and 4) translating protein/polypeptide (Kristensen et al., 2019). Maass et al. (2017) identified 71 differentially expressed circRNAs in 20 human clinical samples including tissues, blood, proving that circRNAs can express stably *in vitro* and are associated with multiple diseases, which has good potential for biomarker development.

As a member of the E3 ubiquitin protein ligase (ITCH) HECT family, ITCH can ubiquitinate phosphorylated disheveled-2 (Dvl2), promoting its degradation (Bernassola et al., 2008). Phosphorylated Dvl2 is the upstream target of activating β-catenin in the canonical Wnt pathway, therefore ITCH can block the canonical Wnt pathway, regulating cell cycle (Li et al., 2015). In addition, ITCH can regulate immune responses, epidermal keratinocyte differentiation and receptor trafficking/signaling (Melino et al., 2008). Previous studies have shown that in ITCH$^{-/-}$ mice, some signal proteins (such as Jun family members and Notch) are abnormally accumulated, seriously affecting the autoimmune phenotype (Parravicini et al., 2008). Jun and Notch are also transcription factors that control the maintenance of epidermal stem cells and the regulation of keratinocytes. The degradation of these proteins mediated by ITCH may play a regulatory role in skin biology (Candi et al., 2005), indicating that it has certain potential in radiotherapy protection. Moreover, Sundvall et al. (2008) emphasized the role of pruritus in regulating the endocytosis and protein stability of erbb-4, a receptor belonging to the epidermal growth factor receptor (EGFR)/ErbB family. Therefore, ITCH involves a variety of physiological and pathological regulation through different mechanisms, including regulating Wnt, Jun, Notch, MAPK signaling, immune cells differentiation and EGFR family. CircRNA E3 ubiquitin protein ligase (circRNA ITCH, hereinafter referred to as circ-ITCH), a stable closed-loop RNA with no protein coding ability and derived from the 20q11.22 region of chromosome 20, is a new circRNA discovered in recent decades (Bernassola et al., 2008; Memczak et al., 2013). The initial study reported that circ-ITCH came from exon 6–13 of E3 ubiquitin protein ligase (ITCH) encoding gene (Li et al., 2015), but then it became exon 7–14 in related studies without any explanation (Han et al., 2020), which is a point that needs to be clarified in subsequent experiments. Combining the database (Circular RNA Interactome and circBase) and related literature search, we considered it derived from exons 6–13 (**Figure 1**), while 7–14 was a writing error in correlative papers. Recently, studies have revealed that circ-ITCH is down-regulated in multiple tumor tissues, and regulates cell proliferation, migration, invasion and apoptosis of malignant tumor, indicating it might be an important tumor suppressor (Li Y. et al., 2020; Ghafouri-Fard et al., 2021; Su et al., 2022). Additionally, the down-regulation can also be seen in the peripheral blood and exosomes of patients. Its low expression has some diagnostic relevance and is linked to negative clinical outcomes (such as tumor sizes, lymph node metastasis and distant metastasis). Furthermore, circ-ITCH plays an essential function in non-tumor illnesses. Understanding its function and mechanism could help clinical researchers discover novel strategies to diagnose and treat a variety of diseases earlier.

2 REGULATION MECHANISM AND ROLE OF CIRC-ITCH IN TUMOR DISEASES

MiRNA, as a part of the ceRNA network, causes polyadenylation by binding with target sites in the 3'-UTR of mRNA, lowering mRNA stability and interfering with translation to adversely control gene expression (Nawaz et al., 2016). CircRNAs may have biological impacts on tumors by sponging target miRNAs and limiting their function, according to previous studies (Li Y. et al., 2020; Ghafouri-Fard et al., 2021; Su et al., 2022). There is no exception for circ-ITCH. MiRNAs sponge locations of circ-ITCH downstream in malignant tumors now being researched, including miR-7, miR-10, miR-17, miR-20, miR-22, miR-93, miR-106, miR-145, miR-199, miR-214, miR-216, miR-224, miR-421, miR-524, and miR-615 (Huang et al., 2015; Li et al., 2015; Luo et al., 2018b; Hu et al., 2018; Wang et al., 2018; Yang et al., 2018; Lin et al., 2020; Liu et al., 2020; Wang et al., 2021). The specific regulation mechanism of circ-ITCH in a range of malignant tumors is also variable due to sponging distinct miRNAs (**Table 1**).

2.1 Regulating Canonical Wnt Signaling Pathway

The Wnt/β-catenin signaling pathway is highly conserved and important for cell motility, invasion, polarity formation, organogenesis, and cell stemness maintenance (Wei et al.,

TABLE 1 | Anti-tumor mechanism of circ-ITCH in a variety of malignant tumors.

Tumor types	ceRNA	Effect	Ref
OC	miR-106a, miR-145 and lncRNA HULC	proliferation↓; migration↓; invasion↓; apoptosis↑; glycolysis↓	Lin et al., 2020; Hu et al., 2018; Yan et al., 2020
ESCC	miR-7, miR-17 and miR-214	proliferation↓	Li et al. (2015)
CRC	miR-7, miR-20a and miR-214	proliferation↓	Huang et al. (2015)
BCa	miR-17, miR-224	apoptosis↑; proliferation↓; invasion↓; migration↓	Yang et al. (2018)
PTC	miR-22-3p	apoptosis↑; proliferation↓; invasion↓	Wang et al. (2018)
EOC	miR-10a-α	apoptosis↑; proliferation↓	Luo et al. (2018b)
GC	miR-199a-5p, miR-17	proliferation↓; migration↓; invasion↓; EMT↓	Peng et al., 2020; Wang et al., 2021
MM	miR-615-3p	apoptosis↑; proliferation↓; BTZ chemosensitivity↑	Liu et al. (2020)
TNBC	miR-17, miR-214	proliferation↓; migration↓; invasion↓	Wang et al. (2019a)
HCC	miR-7, miR-214, miR-421 and miR-224-5p, miR-184	apoptosis↑; proliferation↓; migration↓; invasion↓	Yang et al., 2020; Wu et al., 2020; Zhao et al., 2021; Guo et al., 2022
LC	miR-7, miR-214	proliferation↓	Wan et al. (2016)
Glioma	miR-106a-5p	proliferation↓; migration↓; invasion↓; apoptosis↑	Chen et al. (2021)
PCa	miR-17-5p, miR-197	proliferation↓; migration↓; invasion↓; apoptosis↑	Wang et al., 2019b; Yuan et al., 2019
Melanoma	miR-660	proliferation↓; migration↓	Zhang et al. (2022)
OS	miR-22, miR-524	proliferation↓; migration↓; invasion↓; apoptosis↑	Ren et al., 2019; Li et al. (2020a)
ccRCC	miR-106b-5p	proliferation↓; migration↓; invasion↓	Gao et al. (2021)
OSCC	miR-421	apoptosis↑; proliferation↓	Hao et al. (2020)
CC	miR-93-5p	proliferation↓; migration↓; invasion↓	Li et al. (2020b)
NPC	miR-214	proliferation↓; migration↓; invasion↓	Wang et al. (2022)

2012). The Wnt/β-catenin signaling pathway has two pathways: the canonical pathway and the non-canonical pathway, with the conventional pathway being the more common (Wei et al., 2012; Muralidhar et al., 2019). Canonical signal pathways consist of the Wnt protein, Wnt receptor [frizzled family protein (FZD) and low density lipoprotein receptor associated protein-5/6 (LRP-5/6)], Dvl2, β-catenin protein and et al. (Muralidhar et al., 2019) Wnt protein interacts with the FZD receptor on the cell membrane surface in an autocrine or paracrine manner, then recruits LRP-5/6 to create a complex that activates intracellular Dvl2 protein via a phosphorylation cascade. Through its PDZ domain (one of Dvl2's domains), phosphorylated Dvl2 favorably regulates β-catenin protein, facilitating its entry into the nucleus as a transcriptional regulator and activating the expression of downstream target genes including cyclinD1 and c-Myc (Muralidhar et al., 2019).

Through targeting certain miRNAs, Circ-ITCH inhibits the function of matching miRNAs, particularly miRNAs that inhibit linear ITCH. Specifically, researchers showed that reporter gene assays in the presence of circ-ITCH demonstrated that the inhibitory effects of different miRNAs (including miR-7, miR-17, miR-20a, miR-22-3p, and miR-214) were dampened by the co-expression of circ-ITCH, consistent with the "sponge" hypothesis (Huang et al., 2015; Li et al., 2015; Wang et al., 2018). Among these miRNAs, the miR-7 and miR-214 are most important because they can share the binding sites with the 3′-UTR of circ-ITCH and its parental gene ITCH (Verduci et al., 2021). It is worth mentioning that, as one of the most conservative and oldest miRNAs, miR-7 plays different roles in different cancers and participates in many signal pathways involving differentiation, proliferation regulation, apoptosis and migration. In most tumors, its expression is down-regulated because its main activity is to inhibit tumor by inhibiting cell proliferation and survival. However, in lung cancer and oral cancer, its expression is up-regulated as a carcinogen, which is consistent with the research on circ-ITCH (Kora´c et al., 2021). Since circ-ITCH and ITCH share the 3'-UTR of miR-7, they will produce competitive inhibition. When circ-ITCH is up-regulated, the remaining ITCH content *in vivo* will be up-regulated (Verduci et al., 2021). ITCH can identify and ubiquitinate a range of proteins, the most important of which is phosphorylated Dvl2 (Wei et al., 2012). It is well known that Dvl family proteins are mostly made up of Dvl1-3, with Dvl2 serving as a key scaffold in the canonical Wnt pathway, connecting upstream Wnt protein with downstream β-catenin protein (Wei et al., 2012). As a result, below is the whole regulator mechanism: via sponging miR-7, miR-17, miR-20a, miR-22-3p, and miR-214, circ-ITCH increases ITCH levels. While phosphorylated Dvl2 labeled by ITCH ubiquitin promoted its degradation and inhibited the canonical Wnt pathway. A summary of recent studies has found that in esophageal squamous cell carcinoma (ESCC), colorectal cancer (CRC), lung cancer (LC), three negative breast cancer (TNBC), prostate cancer (PCa), hepatocellular carcinoma (HCC) and gastric cancer (GC), circ-ITCH could up-regulate the expression of linear ITCH via sponging miR-7, miR-17 and miR-20a, thereby inhibiting the canonical Wnt pathway and further suppressing the activation of c-Myc and cyclinD1 (Wan et al., 2016; Wang S. et al., 2019; Li S. et al., 2020; Peng and Wang, 2020; Yang et al., 2020). As widely reported, c-Myc is an oncogene. Its aberrant activation frequently results in unrestricted cell proliferation and immortalization, promoting cell malignancy and tumorigenesis (Glöckner et al., 2002). CyclinD1 (also known as G1/S-specific cyclin D1), on the other hand, regulates the cell cycle and promotes cell proliferation, and is up-regulated in a number of malignancies

(Glöckner et al., 2002). In addition, Wang et al. (2018) also confirmed that circ-ITCH can sponge miR-22-3p and increase the expression of CBL in papillary thyroid cancer (PTC), inhibiting cell proliferation and invasion, increasing apoptosis, and repressing PTC progression. CBL is also a member of the E3 ubiquitin ligase family, which can ubiquitinate as well as label β-catenin to promote its destruction and so block the Wnt pathway (Shashar et al., 2016). In most tumors, the glucose transporter 1 (GLUT1) gene is overexpressed. By mediating glucose via the plasma membrane and increasing glucose absorption, it plays a vital function in the early stages of intracellular glucose metabolism and promotes tumor growth (Koch et al., 2015). ITCH can down-regulate the expression of GLUT1 in melanoma, reducing glucose uptake and tumor cell growth, according to Lin et al. (2021), but whether this regulation also involves the Wnt pathway needs to be confirmed in further experiments.

2.2 Regulating PI3K/Akt Signaling Pathways and MEK/Erk Cascade

In the progression of many malignancies, activation of the PI3K/Akt pathway and MEK/Erk cascade have been confirmed. Following activation, PI3K activates the Akt protein, which subsequently enters the nucleus and regulates cell proliferation, invasion, migration, metabolic reprogramming, autophagy, and aging, potentially causing malignant tumors (Hermida et al., 2017). The MEK/Erk cascade interacts closely with the PI3K/Akt cascade and is involved in tumor development. After activating signaling pathways, many phosphorylated Erk substrates have been shown to contribute to cell proliferation and invasion (Burotto et al., 2014). Phosphatase and tensin homolog deleted on chromosome ten (PTEN) is a miR-7, miR-22, and miR-224 target that inhibits the PI3K/Akt cascade (Sadri Nahand et al., 2021). P21 is the downstream target of the PI3K/Akt cascade. To promote cell proliferation, activated Akt can phosphorylate p21, blocking its cell cycle arrest function (Cheng et al., 2019). Circ-ITCH sponges these miRNAs to up-regulate PTEN expression in bladder cancer (BCa) and OS, blocking the PI3K/Akt cascade, and up-regulating p21 protein to prevent tumor cell proliferation, migration, invasion and promote apoptosis (Yang et al., 2018; Ren et al., 2019). A recent vitro experimental investigation found that circ-ITCH might further up-regulate PTEN in nasopharyngeal cancer (NPC) via sponging miR-214 (Wang et al., 2022), indicating that it can prevent NPC progression by blocking the PI3K/Akt pathway. Ras p21 protein activator 1 (RASA1) is a regulator of Ras-GDP and GTP, which promotes apoptosis and inhibits angiogenesis, cell proliferation by inhibiting Ras/Raf/MEK/Erk signals cascade (Zhang et al., 2020). RASA1 has been shown to be low expressed in a number of tumors, and miR-14 has been identified to mute it (Zhang et al., 2020). Additionally, Hu et al. (2018) found that in ovarian cancer (OC), circ-ITCH up-regulated RASA1 by sponging miR-145, blocking the PI3K/Akt pathway and MEK/Erk cascade, therefore decreasing tumor cell malignancy. Yan et al. (2020) found a negative connection between circ-ITCH expression and lncRNA HULC expression in OC. Previous research has demonstrated that through down-regulating the miR-125a-3p level, lncRNA HULC can activate the PI3K/Akt/mTOR pathway, promoting the proliferation, migration, and invasion of OC cells (Chu et al., 2019). Therefore, circ-ITCH might compete with lncRNA HULC for miR-125a-3p binding, blocking the PI3K/Akt/mTOR pathway and so acting as an anti-tumor agent. However, the hypothesis needs to be confirmed by further experiments. Published reports by two independent groups of researchers in 2019 and 2021 suggested that circ-ITCH expression decreased in patients' OS sample tissue, and that circ-ITCH hindered the proliferation, migration, and invasion of OS cells via sponging miR-22 and miR-524 (Ren et al., 2019; Zhou W. et al., 2021). But interestingly, in 2020, Li et al. (Li H. et al., 2020) discovered that the expression of circ-ITCH was up-regulated in U2OS and SJSA-1 cell lines, and enhanced the expression of epidermal growth factor receptor (EGFR) by reducing the level of tumor suppressor miR-7 in OS. Then, when EGFR is overexpressed, it activates the PI3K/Akt and MEK/Erk pathways, promoting OS development. This finding contradicts the findings of two previous investigations. However, there is a flaw in the experiment: it did not verify the degree of circ-ITCH expression in the OS tissue sample. It's possible that this is due to the heterogeneity of OS cell lines or the complexity of studying the regulatory network. Consequently, in the research of circ-ITCH in OS, more parameters should be explored.

2.3 Regulating Cell Cycle-Related Proteins

Programed cell death receptor 4 (PDCD4) is described as a tumor suppressor, which is often down-regulated in tumors, promoting tumor cell apoptosis and inhibiting its proliferation, invasion and metastasis (Yang et al., 2021). MiR-106b-5p and miR-421 are common upstream targeting miRNAs of PDCD4 and can inhibit its expression (Wang Y. et al., 2019; Yang et al., 2021). Circ-ITCH specifically targets miR-106b-5p and miR-421 in clear cell renal cell carcinoma (ccRCC) and oral squamous cell carcinoma (OSCC) to up-regulate PDCD4 expression and prevent tumor progression, respectively (Hao et al., 2020; Gao et al., 2021). RAS association domain family member 6 (RASSF6) inhibits cell growth and promotes apoptosis in a variety of tumors by interrupting the cell cycle (van der Weyden and Adams, 2007). In OS, circ-ITCH sponges miR-524 to up-regulate RASSF6, inducing OS cell death and limiting its proliferation, according to Zhou et al. (Zhou W. et al., 2021). SAM and SH3 domain containing protein 1 (SASH1) is a tumor-suppressive protein that can regulate cell apoptosis and proliferation (Burgess et al., 2020). Circ-ITCH can suppress glioma growth and invasion by up-regulating SASH1 by targeting miR-106a-5p (Chen et al., 2021). Cytoplasmic polyadenylation element binding protein 3 (CPEB3), a RNA binding protein, plays a tumor-suppressive role though regulating the expression of malignant transformation-related genes through post-transcriptional control (Pichon et al., 2012). In HCC, circ-ITCH binds to miR-421 to prevent CPEB3 down-regulation and tumor growth (Zhao et al., 2021). MafF belonging to the Maf family, a basic leucine zipper (bZIP) transcription factor, has been found to have anti-tumor properties in HCC (Tsuchiya and Oura, 2018). By modulating the miR-224-5p/MAFF axis, Circ-ITCH can also decrease cell

growth and increase apoptosis (Wu et al., 2020). Li et al. (2020b) found that circ-ITCH sponges miR-93-5p to up-regulate forkhead box K2 (FoxK2) and block tumor growth in cervical cancer (CC). Simultaneously, FoxK2 expression was dramatically reduced in CC tissues, and miR-93-5p mimic transfection further decreased FoxK2 expression in CC cell lines. FoxK2 deletion improved the capacity of cells transfected with miR-93-5p mimic to invade. Homeobox B13 (HOXB13), according to earlier research, inhibits the cell cycle by promoting the ubiquitination and degradation of cyclinD1 in a variety of malignancies (Hamid et al., 2014). Circ-ITCH restrains PCa cell proliferation, invasion, and migration via sponging miR-17-5p and boosting HOXB13 up-regulation, as well as promoting apoptosis (Wang X. et al., 2019). Furthermore, via targeting miR-197, circ-ITCH can attenuate PCa cell proliferation and increase apoptosis, however the underlying mechanism is uncertain (Yuan et al., 2019). In melanoma, circ-ITCH suppresses cell proliferation and metastasis through sponging miR-660, a previously reported tumor-promoting miRNA, further up-regulating transcription factor cellular promoter 2 (TFCP2) (Zhang et al., 2022). TFCP2, as a cell cycle regulating molecule, mainly plays a tumor suppressor role in melanoma. Its role is mainly to positively regulate the DAPK transcription by binding to the promoter of the death associated protein kinase (DAPK) gene, a tumor suppressor that is silenced in many cancers (Kotarba et al., 2018). Besides, TFCP2 can positively regulate the transcription of $p21^{CIP1}$, a well-known cell cycle inhibitor protein (Goto et al., 2016; Kotarba et al., 2018). In addition, previous studies have shown that Klotho can inhibit the IGF-1/insulin pathway and regulate the expression of Bax/Bcl-2, thereby inhibiting cell proliferation and promoting apoptosis in A549 cells (Chen et al., 2010). While recently Wang et al. (Wang et al., 2021) found that circ-ITCH boosted Klotho expression though acting as a miR-199a-5p sponge, thus, suggesting that the function of circ-ITCH in GC may involve cell cycle-related regulatory proteins. In short, recent studies have discovered that circ-ITCH regulates the expression level of a number of cell cycle-related proteins, as a ceRNA, to induce tumor cell apoptosis and limit tumor cell growth, thereby acting as an anti-tumor agent.

2.4 Regulating Epithelial Mesenchymal Transition Process

Epithelial mesenchymal transition (EMT) is a process that occurs in almost all forms of tumors and is linked to tumor incidence, invasion, metastasis, recurrence, and medication resistance (Iwatsuki et al., 2010). E-cadherin and vimentin are two crucial proteins that are frequently used as EMT indicators (Iwatsuki et al., 2010). E-cadherin, which is encoded by CDH1, is involved in EMT and is linked to tumor invasion and diffusion (Ye et al., 2012). Vimentin, in particular, promotes EMT, whereas E-cadherin opposes it. Lin et al. (2020) discovered that circ-ITCH inhibits EMT in OC by increasing CDH1 expression via sponging miR-106a. Guo et al. (2022) revealed that the tumor suppressor role of circ-ITCH in HCC is associated with regulating EMT progression through KEGG enrichment analysis, and its regulation function is associated with sponging miR-184. It is well known that Klotho-mediated regulation of cellular EMT is a way to regulate tumor progression (Chen et al., 2019). Therefore, by modulating the miR-199a-5p/Klotho axis, circ-ITCH can block EMT and delay tumor growth in GC (Wang et al., 2021). In addition, earlier research has demonstrated that the Wnt pathway is important for regulating EMT (Kumari et al., 2021). As a result, circ-ITCH's modulation of the Wnt pathway might have an impact on the downstream EMT process, but more research is needed to confirm this.

In summary, circ-ITCH modulates downstream targets including the Wnt pathway, the PI3K/Akt cascade, the MEK/Erk cascade, cell cycle-related proteins, and EMT process via sponging different miRNAs, performing an anti-tumor effect in a range of malignant tumors (**Figure 2**).

3 REGULATION MECHANISM AND ROLE OF CIRC-ITCH IN NON-TUMOR DISEASES

3.1 Bone Diseases

Osteoporosis is a systemic bone disease that causes decreased bone density and quality, disturbed bone microarchitecture, and increased bone fragility, all of which increase the risk of fracture (Compston et al., 2019). Zhong et al. (2021) demonstrated that compared to normal tissues circ-ITCH expression was down-regulated in osteoporosis samples, implying that it may play a protective role in bone degenerative diseases. Specifically, circ-ITCH up-regulated the expression of YAP1 by sponging miR-214. YAP1 is a prominent downstream effector of the Hippo pathway, and its up-regulation can stimulate the differentiation of mesenchymal stem cells into osteoblasts, according to previous research (Lorthongpanich et al., 2019). Moreover, YAP1 stimulates osteogenesis though interacting with β-catenin in osteoblasts (Pan et al., 2018). Taken together, the study found that circ-ITCH might enhance osteogenic differentiation in osteoporosis and ameliorate osteoporosis symptoms in mice (Zhong et al., 2021). Similarly, circ-ITCH expression is up-regulated during periodontal ligament stem cell (PDLSC) osteogenic differentiation and may trigger osteogenic differentiation though regulating MAPK pathway (Gu et al., 2017).

Intervertebral disc degeneration (IDD) is a type of degeneration that can cause a variety of minor or self-limiting symptoms. Spinal discomfort is currently thought to be mostly caused by IDD. Degradation of the extracellular matrix (ECM) and apoptosis of the nucleus pulposus (NP) cells are other key markers of IDD development (Wang et al., 2020). Recently, Zhang et al. (2021) discovered that circ-ITCH might sponge miR-17-5p/SOX4 signaling to positively regulate the activation of Wnt/β-catenin pathway in IDD, causing ECM degradation and NP cell apoptosis. However, this finding contradicts prior findings, particularly in tumor research, in that it activates Wnt/β-catenin pathway. After Wnt/β-catenin activation, Zhang et al. were unable to further illustrate the regulatory mechanism. Combined with earlier research (Zimmerman et al., 2013), we speculate that activating Wnt/β-catenin

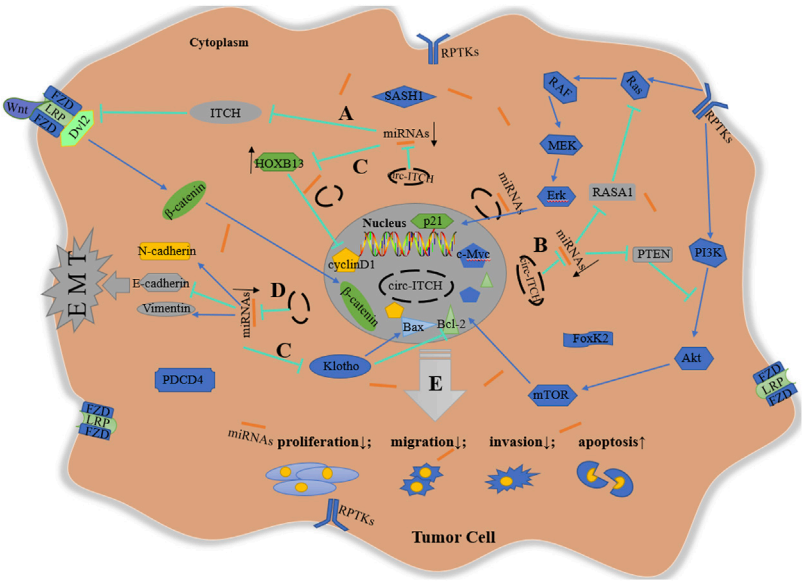

FIGURE 2 | Schematic diagram of anti-tumor mechanism of circ-ITCH. **(A)** *via* sponging miR-7, miR-17, miR-20a, miR-22-3p, and miR-214, circ-ITCH increases ITCH levels to inhibit Wnt signaling pathway in ESCC, CRC, LC, TNBC, PCa, HCC and GC; **(B)** *via* sponging miR-7, miR-14, miR-22, miR-145 and miR-224, circ-ITCH activate the inhibitory proteins (RASA1 and PTEN) of Erk and PI3K cascade to suppress the activation of these signaling pathway in BCa, OS, NPC and OC; **(C)** *via* sponging miR-17-5p, miR-421, miR-524, miR-660, miR-106a-5p, miR-224-5p, miR-93-5p and miR-199a-5p, circ-ITCH regulates cell cycle-related proteins to inhibit cell proliferation and promote cell apoptosis in PCa, OS, OSCC, HCC, ccRCC, CC, glioma, melanoma and GC; **(D)** *Via* sponging miR-184 and miR-199a-5p, circ-ITCH suppresses EMT process in HCC and GC; **(E)** In addition, circ-ITCH can directly regulate some proteins without specific target miRNAs. In a word, circ-ITCH plays an anti-tumor role by negatively regulating cell proliferation, invasion, migration, and positively regulating cell apoptosis.

promotes apoptosis by up-regulating the expression level of pro-apoptotic proteins BIM and Bax while down-regulating the expression level of anti-apoptotic proteins Mcl-1 and Bcl-xl.

3.2 Cardiac Diseases

CircRNAs have been linked to the development of a number of cardiac diseases, including atherosclerosis, myocardial damage, heart failure, and drug-induced cardiotoxicity, according to research (Min et al., 2021). The current emphasis of circ-ITCH research in cardiac diseases is ischaemia-reperfusion (I/R) injury and doxorubicin-induced cardiotoxicity (DOXIC). In I/R damage, a substantial amount of H2O2 can be created, aggravating oxidative stress injury (Wu et al., 2018). H2O2 caused apoptosis in H9c2 rat cardiac cells and reduced viability, ATP levels, and circ-ITCH expression in a recent study (Zhang and Wang, 2020). Furthermore, H2O2 treatment boosted the expression of Wnt3a, Wnt5a, and β-catenin (Zhang and Wang, 2020). Conversely, in H2O2 pretreatment H9c2 cells, overexpression of circ-ITCH reduced apoptosis and Wnt/β-catenin expression, suggesting that its cardioprotective effect is linked to the inactivation of Wnt/β-catenin signaling pathway in I/R injury (Zhang and Wang, 2020). Specifically, circ-ITCH reduced cardiomyocyte apoptosis in I/R injury by sponging miR-17-5p and then inactivating the Wnt/β-catenin signaling pathway (Zhang and Wang, 2020). Doxorubicin is an effective chemotherapeutic agent, but doxorubicin-treated patients are prone to cardiac toxicity and subsequently develop congestive heart failure (Yeh and Bickford, 2009). The two primary pathogenic processes leading to the pathogenesis of doxycycline have been identified in DOXIC as oxidative stress and DNA damage (Zhang et al., 2012). Recently, Han et al. (2020) discovered that overexpressed circ-ITCH reduces doxorubicin-induced oxidative stress and DNA damage in cells and mitochondria. They also discovered that via sponging miR-330-5p in DOXIC, circ-ITCH upregulated sirtuin 6 (SIRT6), Survivin, and sarcoplasmic/endoplasmic reticulum Ca2+-ATPase 2a (SERCA2a) (Han et al., 2020). SIRT6 has been found to reduce oxidative stress by activating Nrf2 and SOD2 proteins, two important endogenous anti-oxidant defense molecules (Rezazadeh et al., 2019; Tian et al., 2019). In addition, SIRT6 could also ameliorate DNA damage via activating PARP1, a key DNA repair enzyme (Tian et al., 2019). Reportedly, Survivin could inhibit doxorubicin-induced myocardial apoptosis and fibrosis (Lee et al., 2014). Additionally, SERCA2a could catalyze the hydrolysis of ATP and enhance cardiac contractility by binding to calcium translocating from the cytosol to the lumen of the sarcoplasmic reticulum (Reilly et al., 2001). Thus, circ-ITCH can alleviate DOXIC and has good potential as a therapeutic target in DOXIC.

3.3 Diabetic Microangiopathy

Diabetic patients' long-term glucose management is suboptimal, which can lead to diabetic microvascular problems such as diabetic neuropathy, diabetic retinopathy (DR) and diabetic nephropathy (DN). One of the most prevalent microvascular consequences of diabetes, diabetic retinopathy (DR), is a chronic,

progressive diabetes mellitus-induced leakage and occlusion of retinal micro-vessels, resulting in a series of fundus lesions. DR is a persistent microvascular inflammation and proliferative neovascularization of the retina (Semeraro et al., 2015). And there is an interaction between the two pathological process (Capitão and Soares, 2016). TNF-α has been shown to be an inflammatory factor that plays a major role in high-glucose environments, where it is linked to vascular inflammation, endothelial dysfunction, oxidative stress, and disruption of the blood-retinal barrier, and contributes to the progression of DR synergistically (Capitão and Soares, 2016). The major enzymes responsible for degrading the ECM, matrix metalloproteinase (MMPs), have been linked to inflammatory disorders and diabetes (Kowluru and Mishra, 2017). Among these MMPs, MMP-2 and MMP-9 were both significantly up-regulated in retinal cells under high glucose conditions (Giebel et al., 2005). By suppressing TNF-α, MMP-2 and MMP-9, Zhou et al. (Zhou L. et al., 2021) revealed that overexpression of circ-ITCH might prevent neovascularization and inflammation, hence delaying DR progression. DN refers to the microvascular consequences of diabetes mellitus, with microalbuminuria at its core, and renal impairment in a subgroup of patients. Long-term chronic inflammation has been linked to the advancement of DN in studies (Wada and Makino, 2013). Previous research has shown that overexpression of SIRT6 could stimulate M2 macrophage transformation, inhibit high glucose-induced mitochondrial dysfunction and cell apoptosis by activating AMPK, all of which help to reduce inflammation in DN (Fan et al., 2019; Ji et al., 2019). A recent study in diabetic mice produced with streptozotocin found that circ-ITCH reduced kidney inflammation and fibrosis through modulating the mir-33a-5p/SIRT6 axis (Liu et al., 2021). The role and mechanism of circ-ITCH in uncomplicated diabetes is also worth exploring, according to current research development.

3.4 Hirschsprung Disease

Hirschsprung's disease (HSCR) is caused by a lack of proliferation and migration of intestinal nerve cells (ENCC), which leads to the absence of peristalsis and colon defecation (Heanue and Pachnis, 2007). It then causes the proximal colon to expand and hypertrophy, eventually resulting in the formation of a megacolon. Rearranged during transfection (RET) has recently been identified as a major regulator of ENCC formation, and inactivating mutations in this gene could result in HSCR (Ohgami et al., 2021). Accumulating evidence indicates that circRNAs are dysregulated and play critical roles in the development of HSCR. Xia et al. (2022) revealed that circ-ITCH expression was dramatically reduced in HSCR tissues, and its overexpression greatly promoted the ability of proliferation and migration of 293T, SH-SY5Y cell lines. Mechanistically, circ-ITCH overexpression activated RET by sponging miR-146b-5p, thereby relieving HSCR progression (Xia et al., 2022).

All in all, in non-tumor diseases such as IDD, osteoporosis, I/R injury, DOXIC, DR, DN, HSCR, and others, circ-ITCH plays a more complex regulatory role. It can, for example, regulate distinct target proteins to cause different states of the same signal pathway. These findings imply that the expression level of circ-ITCH and its regulatory mechanism are disease-specific. The role and mechanism of circ-ITCH in non-tumor illnesses and PDLSC osteogenic development are shown in **Table 2**.

4 CLINICAL APPLICATION AND PERSPECTIVE

With the increasing popularity of RT-PCR, diagnosing a growing range of diseases has gotten easier. RT-PCR can also be used to determine the degree of circ-ITCH expression. It also shows that it is practical and convenient because it expresses consistently in sample tissues, peripheral blood, and exosomes from patients. As a result, RT-PCR can be employed in practice to detect the level of circ-ITCH expression in patients' sample tissues, peripheral blood, or exocrine, allowing for early diagnosis. The clinical significance of circ-ITCH in human diseases is shown in **Table 3**.

4.1 In Tumor Diseases

4.1.1 Diagnostic Biomarkers

Although surgery, chemoradiotherapy, targeted therapy, and the therapeutic outcome of tumor patients have all improved over time, overall survival and quality of life remain a serious problem for patients. Hence, it is critical to diagnose and treat patients as soon as possible. In recent years, scientists have experimented with many approaches to improve the detection and surveillance of early malignant tumors, including radiation, immunology, and biomarkers. Diagnostic biomarkers have received a lot of attention among them. Many circRNAs, notably circ-ITCH, have shown tremendous promise as diagnostic biomarkers in various investigations (Tang et al., 2019).

Many studies have anticipated and proven the clinical application potential of circ-ITCH as a diagnostic biomarker due to its down-regulation in a variety of malignancies (Huang et al., 2019). In GC, circ-ITCH in tissue and serum-derived exosomes were explored separately for their diagnostic value. Among them, the AUC for detecting circ-ITCH in tissues was 0.7055 (sensitivity: 52.71%, specificity: 74.55%); the AUC in serum-derived exosomes was 0.6538 (sensitivity: 42.42%, specificity: 90.91%) (Wang et al., 2021). In multiple myeloma (MM), the AUC was 0.809 (sensitivity: 59.8%, specificity: 80.0%) (Zhou et al., 2020). In PCa, circ-ITCH showed higher diagnostic value (AUC = 0.812 (95% CI: 0.780–0.845)), and its low expression was linked to a higher probability of lymph node metastases (p = 0.047) and an advanced T stage (p = 0.002) (Huang et al., 2019). Furthermore, the expression of circ-ITCH has been linked to tumor size, tumor grade, TNM stage and clinical stage. Specifically, in OC, the expression of circ-ITCH was linked to tumor size (p = 0.0009) and clinical stage (p = 0.0021) (Lin et al., 2020); in TNBC, it was linked to tumor size (p = 0.016), lymphatic metastasis (p = 0.008) and clinical stage (p = 0.002) (Wang S. et al., 2019); in OSCC, it was correlated with clinical stage (p = 0.027) and lymphatic metastasis (p = 0.035) (Hao et al., 2020); in EOC, it was associated with tumor size (p = 0.005) and International Federation of Gynecology and Obstetrics (FIGO) stage (p < 0.001) (Luo et al., 2018a); in GC, it was correlated with

TABLE 2 | Role and mechanism of circ-ITCH in non-tumor diseases and physiology.

Disease/ Physiology	miRNA	Target Proteins/Signaling Pathway	Effect	Ref
Osteoporosis	miR-214	YAP1	Promoting osteogenic differentiation	Zhong et al. (2021)
IDD	miR-17-5p	SOX4; Wnt/β-catenin (activating)	Promoting ECM degradation and NP cell apoptosis	Zhang et al. (2021)
Myocardial I/R injury	miR-17-5p	Wnt/β-catenin (inactivating)	Enhancing cardiomyocyte viability and ATP concentration; Inhibiting cardiomyocyte apoptosis	Zhang et al. (2020)
DOXIC	miR-330-5p	SIRT6, Survivin, SERCA2a	Alleviating cell/mitochondrial oxidative stress and DNA damage	Han et al. (2020)
DR	--	MMP-2, MMP-9, TNF-α	Preventing neovascularization and inflammation to delay DR progression	Zhou et al. (2021a)
DN	miR-33a-5p	SIRT6	Ameliorating renal inflammation and fibrosis	Liu et al. (2021)
HSCR	miR-146b-5p	RET; MAPK	Promoting cell proliferation and migration to delay HSCR progression	Xia et al. (2022)
PDLSC	--	MAPK	Promoting osteogenic differentiation	Gu et al. (2017)

TABLE 3 | Clinicopathological features related to circ-ITCH in human diseases.

Tumor Types	TNM Stage			Clinical Stage (*p* value)	Tumor Grade (*p* value)	Overall survival (*p* value)	Disease-free Survival (*p* value)	AUC (*p* value)	Ref
	T (*p* value)	N (*p* value)	M (*p* value)						
OC	$p = 0.0009$			$p = 0.0021$		$p = 0.0257$			Lin et al. (2020)
BCa					$p = 0.034$				Yang et al. (2018)
TNBC	$p = 0.016$	$p = 0.008$		$p = 0.002$		$p = 0.01$			Wang et al. (2019a)
NSLC	$p < 0.001$	$p < 0.001$		$p = 0.003$		$p = 0.006$	$p = 0.001$		Li et al. (2019)
OSCC	$p = 0.035$			$p = 0.027$					Hao et al. (2020)
PCa	$p = 0.002$	$p = 0.047$				$p < 0.001$	$p < 0.001$	0.812	Huang et al. (2019)
EOC	$p = 0.005$			$p < 0.001$		$p = 0.003$			Luo et al. (2018a)
GC	$p = 0.0216$	$p = 0.034$			$p = 0.02$			0.7055 (tissues); 0.6538 (serum)	Ghasemi et al., 2019; Peng and Wang 2020; Wang et al. (2021)
HCC						$p < 0.001$			Guo et al. (2017)
MM						$p = 0.018$	$p = 0.017$	0.809	Zhou et al. (2020)
Hepatitis C virus infection	positively correlated with ALT, AST level ($p < 0.001$)							0.661	Sharkawi et al. (2022)

tumor grade ($p = 0.02$), T stage ($p = 0.0216$) and lymphatic metastasis ($p = 0.034$) (Ghasemi et al., 2019; Peng and Wang, 2020; Wang et al., 2021); in NPC, it was correlated with lymphatic metastasis ($p = 0.0021$), clinical stage ($p = 0.0028$) and bone metastasis ($p = 0.0285$) (Wang et al., 2022); in non-small cell lung cancer (NSCL), it was linked to tumor size ($p < 0.001$), lymphatic metastasis ($p < 0.001$) and clinical stage ($p = 0.003$) (Li et al., 2019); in MM, it was correlated with international staging system (ISS) stage ($p = 0.036$) (Zhou et al., 2020). Guo et al. (2017), on the other hand, discovered that the single nucleotide polymorphisms rs10485505 and rs4911154 of circ-ITCH were strongly related with an elevated risk of HCC, suggesting that it might be employed as a biomarker for HCC susceptibility. Similarly, single nucleotide polymorphisms of rs4911154 of circ-ITCH could aggravate the malignant transformation from thyroid nodule (TN) to thyroid cancer (Guo et al., 2021). Furthermore, circ-ITCH's collaboration with established diagnostic indicators like carcinoembryonic antigen (CEA) and carbohydrate antigen 19–9 (CA19-9) may also boost diagnostic power. All in all, these findings indicate that it has a wide range of diagnostic utility in a variety of tumors, even in cancer susceptibility prediction, since it's convenient and non-invasive.

4.1.2 Prognostic Biomarkers

With the rapid growth of incidence rate and mortality rate of malignant tumors, its overall prognosis will be the main determinant of global public health and life expectancy. Surgery is the most effective treatment for malignant tumors,

but recurrence and metastasis have a significant impact on the prognosis (Lasithiotakis et al., 2014). Recent studies have found that circ-ITCH is closely linked to clinicopathological characteristics and can be employed as a tumor prognostic biomarker, which will aid in tumor treatment. The expression of circ-ITCH is linked to the prognosis of a range of tumors, including HCC, EOC, PCa, BCa, OC, and so on, according to Kaplan-Meier survival analysis (Guo et al., 2017; Luo et al., 2018a; Yang et al., 2018; Wang S. et al., 2019; Wang X. et al., 2019; Huang et al., 2019; Lin et al., 2020). These findings imply that reduced circ-ITCH expression was associated with lower overall survival (OS) and disease-free survival (DFS). Specifically, decrease in circ-ITCH was associated with worse OS ($p = 0.018$) and DFS ($p = 0.017$) in MM patients (Zhou et al., 2020); in NSLC, its down-regulation was correlated with worse OS ($p = 0.006$) and DFS ($p = 0.001$) (Li et al., 2019); in PCa, its down-regulation was correlated with worse OS and DFS (both $p < 0.001$) (Huang et al., 2019); in EOC, its down-regulation was correlated with worse OS ($p = 0.003$) (Luo et al., 2018a). Furthermore, 1604 patients with various malignancies were included in a meta-analysis, which yielded the same results. Patients with reduced circ-ITCH expression had a lower OS (HR = 2.45, 95% CI: 2.07–2.90, $p \leq 0.01$, univariate analysis; HR = 2.69, 95% CI: 1.82–3.96, $p \leq 0.01$, multivariate analysis) (Sun et al., 2021). Taken together, these results suggest its promising value as a prognostic biomarker.

4.1.3 Therapeutic Target

Many molecules and signal pathways may be appropriate for targeted therapy as our understanding of tumor development improves. Circ-ITCH is a promising therapeutic target since it has an anti-tumor impact that is connected to a range of substances and pathways, as evidenced by recent studies. Up-regulation of circ-ITCH to inhibit proliferation, invasion and migration of HCC cells, for instance, is one of the mechanisms by which lidocaine treats HCC (Zhao et al., 2021). Besides that, it also has great potential in improving chemoresistance and side effects of chemotherapy. Circ-ITCH can decrease MM cell growth and improve MM cell chemosensitivity to bortezomib (BTZ) (Liu et al., 2020). Furthermore, circ-ITCH can also alleviate the symptom of DOXIC, suggesting that it can be used simultaneously with chemotherapeutic drugs to alleviate chemotherapeutic side effects (Han et al., 2020). At present, noncoding RNA (ncRNA) therapy focuses primarily on alternative and inhibitory therapies (Ning et al., 2019). Circ-ITCH's alternative therapy is projected to play a significant role in tumor therapy since it suppresses tumor cell proliferation, increases apoptosis, and slows tumor growth by targeting a range of pathway molecules.

4.2 In Non-Tumor Diseases

According to recent research, circ-ITCH also has an important role in non-tumor tissue. These findings, together with circ-ITCH's stable expression in patient tissues and peripheral blood, as well as well-defined regulatory mechanisms, point to its potential as a biomarker. In Hepatitis C virus infection, for instance, circ-ITCH expression was positively correlated with liver enzymes AST, ALT ($p < 0.001$) and child grade. With AUC = 0.661 (sensitivity: 65 percent, specificity: 70 percent), circ-ITCH has diagnostic significance in plasma of Hepatitis C virus infection (Sharkawi et al., 2022). However, no studies have looked at the possibility of circ-ITCH as predictive biomarkers in non-tumor diseases, and this is currently a blank area of research. Circ-ITCH has been reported to play well-defined regulatory roles in bone illnesses, cardiac diseases, diabetic microangiopathy, and Hirschsprung disease, indicating that they could be therapeutically targeted. Specifically, circ-ITCH replacement therapy appears to have promise as a treatment for DOXIC. Moreover, further experiments with circ-ITCH replacement drugs are also worth studying.

5 CONCLUSION

The focus of this review is on how circ-ITCH, a circular RNA, regulates gene expression in the post-transcriptional stage by acting as a sponge for miRNAs, blocking them from binding to their target mRNAs. The role of circ-ITCH in cell proliferation, apoptosis, invasion, migration, and EMT regulation, as well as related signaling pathways, is then explored. Circ-ITCH's potential as a diagnostic and predictive biomarker in tumor and non-tumor diseases is then confirmed. Furthermore, circ-ITCH has a lot of potential in disease treatment because of its well-defined regulatory mechanism, notably in terms of enhancing chemosensitivity and reducing chemotherapy adverse effects in malignant tumor. These discoveries not only illuminate the molecular basis of circ-ITCH, but also pave the path for future clinical applications.

Based on the current research, we put forward some promising future research directions. To begin, the up-regulated biomarker is more ideal for clinical detection, but the down-regulated index can still be employed as long as the critical value is evident. As a result, it is crucial to explore the critical value of circ-ITCH in both patients and healthy people. Then, researchers should increase the sample size and AUC detection as much as possible in order to achieve a more accurate association between circ-ITCH and other classic diagnostic markers (CEA, CA19-9) or prognostic indicators (OS, DFS) (Li et al., 2020c). Furthermore, given its critical role in regulating human diseases, more simulations of activators or carrier administration are needed to validate their *in vitro* and *in vivo* effects. While circ-ITCH is low expressed in a number of malignancies, it is unclear which tumor has greater specificity and accuracy about circ-ITCH, meriting additional investigation. At the same time, it is also worthwhile to explore the translational applications of circ-ITCH in chemotherapy because of its demonstrated potential in tumor chemotherapy, including chemo-sensitization and alleviation of side effects. Besides, due to the increase of ITCH concentration and regulating epidermal keratinocyte differentiation, the potential of circ-ITCH in decreasing radiotherapy injury also needs to be developed. Finally, it was recently shown that circRNAs are plentiful and stable in exosomes, that they can be produced under a variety of physiological and pathological conditions, and that they can be detected in circulation and urine (He et al., 2021), all of which require further exploration.

AUTHOR CONTRIBUTIONS

TL and TH wrote a draft of the review, MS was involved in literature search and supervision, GH was involved in original idea and critical revision of the manuscript.

FUNDING

This research was supported by the Jilin Science and Technology Department Medical Department project (20160101092JC).

REFERENCES

Bernassola, F., Karin, M., Ciechanover, A., and Melino, G. (2008). The HECT Family of E3 Ubiquitin Ligases: Multiple Players in Cancer Development. *Cancer Cell* 14 (1), 10–21. doi:10.1016/j.ccr.2008.06.001

Burgess, J., Bolderson, E., Adams, M., Duijf, P., Zhang, S., Gray, S., et al. (2020). SASH1 Is a Prognostic Indicator and Potential Therapeutic Target in Non-small Cell Lung Cancer. *Sci. Rep.* 10 (1), 18605. doi:10.1038/s41598-020-75625-1

Burotto, M., Chiou, V., Lee, J., and Kohn, E. (2014). The MAPK Pathway across Different Malignancies: a New Perspective. *Cancer* 120 (22), 3446–3456. doi:10.1002/cncr.28864

Candi, E., Schmidt, R., and Melino, G. (2005). The Cornified Envelope: a Model of Cell Death in the Skin. *Nat. Rev. Mol. Cell Biol.* 6 (4), 328–340. doi:10.1038/nrm1619

Capitão, M., and Soares, R. (2016). Angiogenesis and Inflammation Crosstalk in Diabetic Retinopathy. *J. Cell. Biochem.* 117 (11), 2443–2453. doi:10.1002/jcb.25575

Chen, B., Huang, S., Pisanic, II, T. R., Stark, A., Tao, Y., Cheng, B., et al. (2019). Rab8 GTPase Regulates Klotho-Mediated Inhibition of Cell Growth and Progression by Directly Modulating its Surface Expression in Human Non-small Cell Lung Cancer. *EBioMedicine* 49, 118–132. doi:10.1016/j.ebiom.2019.10.040

Chen, B., Wang, X., Zhao, W., and Wu, J. (2010). Klotho Inhibits Growth and Promotes Apoptosis in Human Lung Cancer Cell Line A549. *J. Exp. Clin. Cancer Res.* 29 (1), 99. doi:10.1186/1756-9966-29-99

Chen, W., Wu, M., Cui, S., Zheng, Y., Liu, Z., and Luo, L. (2021). CircRNA Circ-ITCH Inhibits the Proliferation and Invasion of Glioma Cells through Targeting the miR-106a-5p/SASH1 Axis. *Cell Transpl.* 30, 096368972098378. doi:10.1177/0963689720983785

Cheng, S., Qian, K., Wang, Y., Wang, G., Liu, X., Xiao, Y., et al. (2019). PPARγ Inhibition Regulates the Cell Cycle, Proliferation and Motility of Bladder Cancer Cells. *J. Cell Mol. Med.* 23 (5), 3724–3736. doi:10.1111/jcmm.14280

Chu, P., Xu, L., and Su, H. (2019). RETRACTED ARTICLE: HULC Functions as an Oncogene in Ovarian Carcinoma Cells by Negatively Modulating miR-125a-3p. *J. Physiol. Biochem.* 75 (2), 163–171. doi:10.1007/s13105-019-00669-5

Compston, J. E., McClung, M. R., and Leslie, W. D. (2019). Osteoporosis. *Lancet* 393 (10169), 364–376. doi:10.1016/s0140-6736(18)32112-3

Fan, Y., Yang, Q., Yang, Y., Gao, Z., Ma, Y., Zhang, L., et al. (2019). Sirt6 Suppresses High Glucose-Induced Mitochondrial Dysfunction and Apoptosis in Podocytes through AMPK Activation. *Int. J. Biol. Sci.* 15 (3), 701–713. doi:10.7150/ijbs.29323

Gao, P., Huang, Y., Hou, Y., Li, Q., and Wang, H. (2021). Circular RNA ITCH Is a Tumor Suppressor in Clear Cell Renal Cell Carcinoma Metastasis through miR-106b-5p/PDCD4 Axis. *J. Immunol. Res.* 2021, 1–10. doi:10.1155/2021/5524344

Ghafouri-Fard, S., Khoshbakht, T., Taheri, M., and Jamali, E. (2021). CircITCH: A Circular RNA with Eminent Roles in the Carcinogenesis. *Front. Oncol.* 11, 774979. doi:10.3389/fonc.2021.774979

Ghasemi, S., Emadi-Baygi, M., and Nikpour, P. (2019). Down-regulation of Circular RNAITCH and circHIPK3 in Gastric Cancer Tissues. *Turk J. Med. Sci.* 49 (2), 687–695. doi:10.3906/sag-1806-50

Giebel, S. J., Menicucci, G., McGuire, P. G., and Das, A. (2005). Matrix Metalloproteinases in Early Diabetic Retinopathy and Their Role in Alteration of the Blood-Retinal Barrier. *Lab. Invest.* 85 (5), 597–607. doi:10.1038/labinvest.3700251

Glöckner, S., Buurman, H., Kleeberger, W., Lehmann, U., and Kreipe, H. (2002). Marked Intratumoral Heterogeneity of C-Myc and cyclinD1 but Not of C-erbB2 Amplification in Breast Cancer. *Lab. Invest.* 82 (10), 1419–1426. doi:10.1097/01.lab.0000032371.16521.40

Goto, Y., Yajima, I., Kumasaka, M., Ohgami, N., Tanaka, A., Tsuzuki, T., et al. (2016). Transcription Factor LSF (TFCP2) Inhibits Melanoma Growth. *Oncotarget* 7 (3), 2379–2390. doi:10.18632/oncotarget.6230

Gu, X., Li, M., Jin, Y., Liu, D., and Wei, F. (2017). Identification and Integrated Analysis of Differentially Expressed lncRNAs and circRNAs Reveal the Potential ceRNA Networks during PDLSC Osteogenic Differentiation. *BMC Genet.* 18 (1), 100. doi:10.1186/s12863-017-0569-4

Guo, W., Zhang, J., Zhang, D., Cao, S., Li, G., Zhang, S., et al. (2017). Polymorphisms and Expression Pattern of Circular RNA Circ-ITCH Contributes to the Carcinogenesis of Hepatocellular Carcinoma. *Oncotarget* 8 (29), 48169–48177. doi:10.18632/oncotarget.18327

Guo, X., Wang, Z., Deng, X., Lu, Y., Huang, X., Lin, J., et al. (2022). Circular RNA CircITCH (Has-circ-0001141) Suppresses Hepatocellular Carcinoma (HCC) Progression by Sponging miR-184. *Cell Cycle*, 1–21. doi:10.1080/15384101.2022.2057633

Guo, Y., Zheng, H., Yin, J., and Wang, H. J. S. r. (2021). Rs4911154 of Circ-ITCH Aggravated Tumor Malignancy of Thyroid Nodules via the Circ-ITCH/miR-22-3p/CBL axis. *Sci. Rep.* 11 (1), 18491. doi:10.1038/s41598-021-97471-5

Hamid, S., Cicek, S., Karamil, S., Ozturk, M., Debelec-Butuner, B., Erbaykent-Tepedelen, B., et al. (2014). HOXB13 Contributes to G1/S and G2/M Checkpoint Controls in Prostate. *Mol. Cell. Endocrinol.* 383, 38–47. doi:10.1016/j.mce.2013.12.003

Han, D., Wang, Y., Wang, Y., Dai, X., Zhou, T., Chen, J., et al. (2020). The Tumor-Suppressive Human Circular RNA CircITCH Sponges miR-330-5p to Ameliorate Doxorubicin-Induced Cardiotoxicity through Upregulating SIRT6, Survivin, and SERCA2a. *Circ. Res.* 127 (4), e108–e125. doi:10.1161/circresaha.119.316061

Hao, C., Wangzhou, K., Liang, Z., Liu, C., Wang, L., Gong, L., et al. (2020). Circular RNA ITCH Suppresses Cell Proliferation but Induces Apoptosis in Oral Squamous Cell Carcinoma by Regulating miR-421/PDCD4 Axis. *Cmar* Vol. 12, 5651–5658. doi:10.2147/cmar.S258887

He, Y., Tao, W., He, T., Wang, B., Tang, X., Zhang, L., et al. (2021). A Urine Extracellular Vesicle circRNA Classifier for Detection of High-Grade Prostate Cancer in Patients with Prostate-specific Antigen 2-10 ng/mL at Initial Biopsy. *Mol. Cancer* 20 (1), 96. doi:10.1186/s12943-021-01388-6

Heanue, T. A., and Pachnis, V. (2007). Enteric Nervous System Development and Hirschsprung's Disease: Advances in Genetic and Stem Cell Studies. *Nat. Rev. Neurosci.* 8 (6), 466–479. doi:10.1038/nrn2137

Hermida, M., Dinesh Kumar, J., and Leslie, N. (2017). GSK3 and its Interactions with the PI3K/AKT/mTOR Signalling Network. *Adv. Biol. Regul.* 65, 5–15. doi:10.1016/j.jbior.2017.06.003

Hu, J., Wang, L., Chen, J., Gao, H., Zhao, W., Huang, Y., et al. (2018). The Circular RNA Circ-ITCH Suppresses Ovarian Carcinoma Progression through Targeting miR-145/RASA1 Signaling. *Biochem. biophysical Res. Commun.* 505 (1), 222–228. doi:10.1016/j.bbrc.2018.09.060

Huang, E., Chen, X., and Yuan, Y. (2019). Downregulated Circular RNA Itchy E3 Ubiquitin Protein Ligase Correlates with Advanced Pathologic T Stage, High Lymph Node Metastasis Risk and Poor Survivals in Prostate Cancer Patients. *Cbm* 26 (1), 41–50. doi:10.3233/cbm-182111

Huang, G., Zhu, H., Shi, Y., Wu, W., Cai, H., and Chen, X. (2015). Cir-ITCH Plays an Inhibitory Role in Colorectal Cancer by Regulating the Wnt/β-Catenin Pathway. *PloS one* 10 (6), e0131225. doi:10.1371/journal.pone.0131225

Huang, J., Wu, D., Shen, J., Wu, P., Ni, C., Chen, J., et al. (2012). Enrichment of Colorectal Cancer Stem Cells through Epithelial-Mesenchymal Transition via CDH1 Knockdown. *Mol. Med. Rep.* 6 (3), 507–512. doi:10.3892/mmr.2012.938

Iwatsuki, M., Mimori, K., Yokobori, T., Ishi, H., Beppu, T., Nakamori, S., et al. (2010). Epithelial-mesenchymal Transition in Cancer Development and its Clinical Significance. *Cancer Sci.* 101 (2), 293–299. doi:10.1111/j.1349-7006.2009.01419.x

Ji, L., Chen, Y., Wang, H., Zhang, W., He, L., Wu, J., et al. (2019). Overexpression of Sirt6 Promotes M2 macrophage Transformation, Alleviating Renal Injury in Diabetic Nephropathy. *Int. J. Oncol.* 55 (1), 103–115. doi:10.3892/ijo.2019.4800

Koch, A., Lang, S., Wild, P., Gantner, S., Mahli, A., Spanier, G., et al. (2015). Glucose Transporter Isoform 1 Expression Enhances Metastasis of Malignant Melanoma Cells. *Oncotarget* 6 (32), 32748–32760. doi:10.18632/oncotarget.4977

Korać, P., Antica, M., and Matulić, M. (2021). MiR-7 in Cancer Development. *Biomedicines* 9 (3), 325. doi:10.3390/biomedicines9030325

Kotarba, G., Krzywinska, E., Grabowska, A. I., Taracha, A., and Wilanowski, T. (2018). TFCP2/TFCP2L1/UBP1 Transcription Factors in Cancer. *Cancer Lett.* 420, 72–79. doi:10.1016/j.canlet.2018.01.078

Kowluru, R. A., and Mishra, M. (2017). Regulation of Matrix Metalloproteinase in the Pathogenesis of Diabetic Retinopathy. *Prog. Mol. Biol. Transl. Sci.* 148, 67–85. doi:10.1016/bs.pmbts.2017.02.004

Kristensen, L., Andersen, M., Stagsted, L., Ebbesen, K., Hansen, T., and Kjems, J. (2019). The Biogenesis, Biology and Characterization of Circular RNAs. *Nat. Rev. Genet.* 20 (11), 675–691. doi:10.1038/s41576-019-0158-7

Kumari, N., Reabroi, S., and North, B. (2021). Unraveling the Molecular Nexus between GPCRs, ERS, and EMT. *Mediat. Inflamm.* 2021, 1–23. doi:10.1155/2021/6655417

Lasithiotakis, K., Antoniou, S., Antoniou, G., Kaklamanos, I., and Zoras, O. (2014). Gastrectomy for stage IV gastric cancer. a systematic review and meta-analysis. *Anticancer Res.* 34 (5), 2079–2085.

Lee, P. J., Rudenko, D., Kuliszewski, M. A., Liao, C., Kabir, M. G., Connelly, K. A., et al. (2014). Survivin gene therapy attenuates left ventricular systolic dysfunction in doxorubicin cardiomyopathy by reducing apoptosis and fibrosis. *Cardiovasc Res.* 101 (3), 423–433. doi:10.1093/cvr/cvu001

Li, F., Zhang, L., Li, W., Deng, J., Zheng, J., An, M., et al. (2015). Circular RNA ITCH has inhibitory effect on ESCC by suppressing the Wnt/β-catenin pathway. *Oncotarget* 6 (8), 6001–6013. doi:10.18632/oncotarget.3469

Li, H., Lan, M., Liao, X., Tang, Z., and Yang, C. (2020a). Circular RNA cir-ITCH Promotes Osteosarcoma Migration and Invasion through cir-ITCH/miR-7/EGFR Pathway. *Technol. Cancer Res. Treat.* 19, 153303381989872. doi:10.1177/1533033819898728

Li, J., Guo, R., Liu, Q., Sun, J., and Wang, H. (2020b). Circular RNA Circ-ITCH Inhibits the Malignant Behaviors of Cervical Cancer by microRNA-93-5p/FOXK2 Axis. *Reprod. Sci.* 27 (3), 860–868. doi:10.1007/s43032-020-00140-7

Li, J., Song, Y., Wang, J., and Huang, J. (2020c). Plasma circular RNA panel acts as a novel diagnostic biomarker for colorectal cancer detection. *Am. J. Transl. Res.* 12 (11), 7395–7403.

Li, S., Yu, C., Zhang, Y., Liu, J., Jia, Y., Sun, F., et al. (2020d). Circular RNA cir-ITCH Is a Potential Therapeutic Target for the Treatment of Castration-Resistant Prostate Cancer. *BioMed Res. Int.* 2020, 1–9. doi:10.1155/2020/7586521

Li, Y., Ge, Y., Xu, L., and Jia, R. (2020e). Circular RNA ITCH: A novel tumor suppressor in multiple cancers. *Life Sci.* 254, 117176. doi:10.1016/j.lfs.2019.117176

Li, Z., Guo, X., and Gao, S. (2019). Circ-ITCH correlates with less advanced tumor features as well as prolonged survival, and it inhibits cells proliferation but promotes apoptosis in non-small cell lung cancer. *Transl. Cancer Res.* 8 (5), 1672–1679. doi:10.21037/tcr.2019.08.01

Lin, C., Xu, X., Yang, Q., Liang, L., and Qiao, S. (2020). Circular RNA ITCH suppresses proliferation, invasion, and glycolysis of ovarian cancer cells by up-regulating CDH1 via sponging miR-106a. *Cancer Cell Int.* 20, 336. doi:10.1186/s12935-020-01420-7

Lin, Q., Jiang, H., and Lin, D. (2021). Circular RNA ITCH downregulates GLUT1 and suppresses glucose uptake in melanoma to inhibit cancer cell proliferation. *J. Dermatological Treat.* 32 (2), 231–235. doi:10.1080/09546634.2019.1654069

Liu, J., Du, F., Chen, C., Li, D., Chen, Y., Xiao, X., et al. (2020). CircRNA ITCH increases bortezomib sensitivity through regulating the miR-615-3p/PRKCD axis in multiple myeloma. *Life Sci.* 262, 118506. doi:10.1016/j.lfs.2020.118506

Liu, J., Duan, P., Xu, C., Xu, D., Liu, Y., and Jiang, J. (2021). CircRNA circ-ITCH improves renal inflammation and fibrosis in streptozotocin-induced diabetic mice by regulating the miR-33a-5p/SIRT6 axis. *Inflamm. Res.* 70 (7), 835–846. doi:10.1007/s00011-021-01485-8

Lorthongpanich, C., Thumanu, K., Tangkiettrakul, K., Jiamvoraphong, N., Laowtammathron, C., Damkham, N., et al. (2019). YAP as a key regulator of adipo-osteogenic differentiation in human MSCs. *Stem Cell Res. Ther.* 10 (1), 402. doi:10.1186/s13287-019-1494-4

Luo, L., Gao, Y., and Sun, X. (2018a). Circ-ITCH correlates with small tumor size, decreased FIGO stage and prolonged overall survival, and it inhibits cells proliferation while promotes cells apoptosis in epithelial ovarian cancer. *Cbm* 23 (4), 505–513. doi:10.3233/cbm-181609

Luo, L., Gao, Y., and Sun, X. (2018b). Circular RNA ITCH suppresses proliferation and promotes apoptosis in human epithelial ovarian cancer cells by sponging miR-10a-α. *Eur. Rev. Med. Pharmacol. Sci.* 22 (23), 8119–8126. doi:10.26355/eurrev_201812_16503

Maass, P. G., Glažar, P., Memczak, S., Dittmar, G., Hollfinger, I., Schreyer, L., et al. (2017). A map of human circular RNAs in clinically relevant tissues. *J. Mol. Med.* 95 (11), 1179–1189. doi:10.1007/s00109-017-1582-9

Melino, G., Gallagher, E., Aqeilan, R. I., Knight, R., Peschiaroli, A., Rossi, M., et al. (2008). Itch: a HECT-type E3 ligase regulating immunity, skin and cancer. *Cell Death Differ.* 15 (7), 1103–1112. doi:10.1038/cdd.2008.60

Memczak, S., Jens, M., Elefsinioti, A., Torti, F., Krueger, J., Rybak, A., et al. (2013). Circular RNAs are a large class of animal RNAs with regulatory potency. *Nature* 495 (7441), 333–338. doi:10.1038/nature11928

Min, X., Liu, D. L., and Xiong, X. D. (2021). Circular RNAs as Competing Endogenous RNAs in Cardiovascular and Cerebrovascular Diseases: Molecular Mechanisms and Clinical Implications. *Front. Cardiovasc. Med.* 8, 682357. doi:10.3389/fcvm.2021.682357

Muralidhar, S., Filia, A., Nsengimana, J., Poźniak, J., O'Shea, S., Diaz, J., et al. (2019). Vitamin D-VDR Signaling Inhibits Wnt/β-Catenin-Mediated Melanoma Progression and Promotes Antitumor Immunity. *Cancer Res.* 79 (23), 5986–5998. doi:10.1158/0008-5472.Can-18-3927

Nawaz, Z., Patil, V., Paul, Y., Hegde, A., Arivazhagan, A., Santosh, V., et al. (2016). PI3 kinase pathway regulated miRNome in glioblastoma: identification of miR-326 as a tumour suppressor miRNA. *Mol. Cancer* 15 (1), 74. doi:10.1186/s12943-016-0557-8

Ning, B., Yu, D., and Yu, A. (2019). Advances and challenges in studying noncoding RNA regulation of drug metabolism and development of RNA therapeutics. *Biochem. Pharmacol.* 169, 113638. doi:10.1016/j.bcp.2019.113638

Ohgami, N., Iizuka, A., Hirai, H., Yajima, I., Iida, M., Shimada, A., et al. (2021). Loss-of-function mutation of c-Ret causes cerebellar hypoplasia in mice with Hirschsprung disease and Down's syndrome. *J. Biol. Chem.* 296, 100389. doi:10.1016/j.jbc.2021.100389

Pan, J. X., Xiong, L., Zhao, K., Zeng, P., Wang, B., Tang, F. L., et al. (2018). YAP promotes osteogenesis and suppresses adipogenic differentiation by regulating β-catenin signaling. *Bone Res.* 6, 18. doi:10.1038/s41413-018-0018-7

Parravicini, V., Field, A. C., Tomlinson, P. D., Albert Basson, M. A., and Zamoyska, R. (2008). Itch−/−αβ and γδ T cells independently contribute to autoimmunity in Itchy mice. *Blood* 111 (8), 4273–7282. doi:10.1182/blood-2007-10-115667

Peng, Y., and Wang, H. (2020). Cir-ITCH inhibits gastric cancer migration, invasion and proliferation by regulating the Wnt/β-catenin pathway. *Sci. Rep.* 10 (1), 17443. doi:10.1038/s41598-020-74452-8

Pichon, X., A. Wilson, L., Stoneley, M., Bastide, A., A King, H., Somers, J., et al. (2012). RNA binding protein/RNA element interactions and the control of translation. *Cpps* 13 (4), 294–304. doi:10.2174/138920312801619475

Reilly, A. M., Petrou, S., Pancha, R. G., and Williams, D. A. (2001). Restoration of calcium handling properties of adult cardiac myocytes from hypertrophied hearts. *Cell Calcium* 30 (1), 59–66. doi:10.1054/ceca.2001.0213

Ren, C., Liu, J., Zheng, B., Yan, P., Sun, Y., and Yue, B. (2019). RETRACTED ARTICLE: The circular RNA circ-ITCH acts as a tumour suppressor in osteosarcoma via regulating miR-22. *Artif. cells, nanomedicine, Biotechnol.* 47 (1), 3359–3367. doi:10.1080/21691401.2019.1649273

Rezazadeh, S., Yang, D., Tombline, G., Simon, M., Regan, S. P., Seluanov, A., et al. (2019). SIRT6 promotes transcription of a subset of NRF2 targets by mono-ADP-ribosylating BAF170. *Nucleic Acids Res.* 47 (15), 7914–7928. doi:10.1093/nar/gkz528

Sadri Nahand, J., Shojaie, L., Akhlagh, S., Ebrahimi, M., Mirzaei, H., Bannazadeh Baghi, H., et al. (2021). Cell death pathways and viruses: Role of microRNAs. *Mol. Ther. - Nucleic Acids* 24, 487–511. doi:10.1016/j.omtn.2021.03.011

Semeraro, F., Cancarini, A., dell'Omo, R., Rezzola, S., Romano, M. R., and Costagliola, C. (2015). Diabetic Retinopathy: Vascular and Inflammatory Disease. *J. Diabetes Res.* 2015, 1–16. doi:10.1155/2015/582060

Sharkawi, F. Z. E., El-Sherbiny, M., Ali, S. A., and Nassif, W. M. H. (2022). The potential value of plasma Circ-ITCH in Hepatocellular carcinoma patients with current Hepatitis C virus infection. *Gastroenterol. Hepatol.* [Not Available]. doi:10.1016/j.gastrohep.2022.03.006

Shashar, M., Siwak, J., Tapan, U., Lee, S., Meyer, R., Parrack, P., et al. (2016). c-Cbl mediates the degradation of tumorigenic nuclear β-catenin contributing to the heterogeneity in Wnt activity in colorectal tumors. *Oncotarget* 7 (44), 71136–71150. doi:10.18632/oncotarget.12107

Su, K., Yi, Q., Dai, X., and Liu, O. (2022). Circular RNA ITCH: An Emerging Multifunctional Regulator. *Biomolecules* 12 (3), 359. doi:10.3390/biom12030359

Sun, X., Huan, C., Sun, D., and Lv, G. (2021). Prognostic and Clinicopathological Significance of Circular RNA circ-ITCH Expression in Cancer Patients: A Meta-analysis. *BioMed Res. Int.* 2021, 1–13. doi:10.1155/2021/8828299

Sundvall, M., Korhonen, A., Paatero, I., Gaudio, E., Melino, G., Croce, C. M., et al. (2008). Isoform-specific monoubiquitination, endocytosis, and degradation of alternatively spliced ErbB4 isoforms. *Proc. Natl. Acad. Sci. U.S.A.* 105, 4162–4167. doi:10.1073/pnas.0708333105

Sung, H., Ferlay, J., Siegel, R. L., Laversanne, M., Soerjomataram, I., Jemal, A., et al. (2021). Global cancer statistics 2020: GLOBOCAN estimates of incidence and mortality worldwide for 36 cancers in 185 countries. *CA A Cancer J. Clin.* 71, 209–249. doi:10.3322/caac.21660

Tang, X., Zhu, J., Liu, Y., Chen, C., Liu, T., and Liu, J. (2019). Current Understanding of Circular RNAs in Gastric Cancer. *Cmar* Vol. 11, 10509–10521. doi:10.2147/cmar.S223204

Tian, X., Firsanov, D., Zhang, Z., Cheng, Y., Luo, L., Tombline, G., et al. (2019). SIRT6 Is Responsible for More Efficient DNA Double-Strand Break Repair in Long-Lived Species. *Cell* 177 (3), 622–638. e622. doi:10.1016/j.cell.2019.03.043

Tsuchiya, H., and Oura, S. (2018). Involvement of MAFB and MAFF in Retinoid-Mediated Suppression of Hepatocellular Carcinoma Invasion. *Ijms* 19 (5), 1450. doi:10.3390/ijms19051450

van der Weyden, L., and Adams, D. (2007). The Ras-association domain family (RASSF) members and their role in human tumourigenesis. *Biochimica Biophysica Acta (BBA) - Rev. Cancer* 1776 (1), 58–85. doi:10.1016/j.bbcan.2007.06.003

Verduci, L., Tarcitano, E., Strano, S., Yarden, Y., and Blandino, G. (2021). CircRNAs: role in human diseases and potential use as biomarkers. *Cell Death Dis.* 12 (5), 468. doi:10.1038/s41419-021-03743-3

Wada, J., and Makino, H. (2013). Inflammation and the pathogenesis of diabetic nephropathy. *Clin. Sci. (Lond)* 124 (3), 139–152. doi:10.1042/cs20120198

Wan, L., Zhang, L., Fan, K., Cheng, Z., Sun, Q., and Wang, J. (2016). Circular RNA-ITCH Suppresses Lung Cancer Proliferation via Inhibiting the Wnt/β-Catenin Pathway. *BioMed Res. Int.* 2016, 1–11. doi:10.1155/2016/1579490

Wang, L., Sang, J., Zhang, Y., Gao, L., Zhao, D., and Cao, H. (2022). Circular RNA ITCH attenuates the progression of nasopharyngeal carcinoma by inducing PTEN upregulation via miR-214. *J. Gene Med.* 24 (1), e3391. doi:10.1002/jgm.3391

Wang, M., Chen, B., Ru, Z., and Cong, L. (2018). CircRNA circ-ITCH suppresses papillary thyroid cancer progression through miR-22-3p/CBL/β-catenin pathway. *Biochem. biophysical Res. Commun.* 504 (1), 283–288. doi:10.1016/j.bbrc.2018.08.175

Wang, S., Liu, L., Li, X., Wang, Y., Xie, P., Li, Q., et al. (2019a). Circ-ITCH regulates triple-negative breast cancer progression through the Wnt/β-catenin pathway. *neo* 66 (2), 232–239. doi:10.4149/neo_2018_180710N460

Wang, X., Wang, R., Wu, Z., and Bai, P. (2019b). Circular RNA ITCH suppressed prostate cancer progression by increasing HOXB13 expression via spongy miR-17-5p. *Cancer Cell Int.* 19, 328. doi:10.1186/s12935-019-0994-8

Wang, Y., Liu, Z., and Shen, J. (2019c). MicroRNA-421-targeted PDCD4 regulates breast cancer cell proliferation. *Int. J. Mol. Med.* 43 (1), 267–275. doi:10.3892/ijmm.2018.3932

Wang, Y., Wang, H., Zheng, R., Wu, P., Sun, Z., Chen, J., et al. (2021). Circular RNA ITCH suppresses metastasis of gastric cancer via regulating miR-199a-5p/Klotho axis. *Cell Cycle* 20 (5-6), 522–536. doi:10.1080/15384101.2021.1878327

Wang, Z., Han, L., Sun, T., Ma, J., Sun, S., Ma, L., et al. (2020). Extracellular matrix derived from allogenic decellularized bone marrow mesenchymal stem cell sheets for the reconstruction of osteochondral defects in rabbits. *Acta Biomater.* 118, 54–68. doi:10.1016/j.actbio.2020.10.022

Wei, W., Li, M., Wang, J., Nie, F., and Li, L. (2012). The E3 ubiquitin ligase ITCH negatively regulates canonical Wnt signaling by targeting dishevelled protein. *Mol. Cell Biol.* 32 (19), 3903–3912. doi:10.1128/mcb.00251-12

Wu, M., Deng, X., Zhong, Y., Hu, L., Zhang, X., Liang, Y., et al. (2020). MafF Is Regulated via the circ-ITCH/miR-224-5p Axis and Acts as a Tumor Suppressor in Hepatocellular Carcinoma. *Oncol. Res.* 28 (3), 299–309. doi:10.3727/096504020x15796890809840

Wu, Z., Wang, H., Fang, S., and Xu, C. (2018). Roles of endoplasmic reticulum stress and autophagy on H2O2-induced oxidative stress injury in HepG2 cells. *Mol. Med. Rep.* 18 (5), 4163–4174. doi:10.3892/mmr.2018.9443

Xia, R. P., Zhao, F., Ma, T. D., Zou, C. J., Xu, G., and Zhou, C. G. (2022). Circ-ITCH overexpression promoted cell proliferation and migration in Hirschsprung disease through miR-146b-5p/RET axis. *Pediatr. Res.* doi:10.1038/s41390-021-01860-5

Yan, H., Xiang, H., Sun, B., Feng, F., and Chen, P. (2020). Circular RNA-ITCH Inhibits the Proliferation of Ovarian Carcinoma by Downregulating lncRNA HULC. *Reprod. Sci.* 27 (1), 375–379. doi:10.1007/s43032-019-00049-w

Yang, B., Zhao, J., Huo, T., Zhang, M., and Wu, X. (2020). Effects of CircRNA-ITCH on proliferation and apoptosis of hepatocellular carcinoma cells through inhibiting Wnt/β-catenin signaling pathway. *J. BUON* 25 (3), 1368–1374.

Yang, C., Dou, R., Wei, C., Liu, K., Shi, D., Zhang, C., et al. (2021). Tumor-derived exosomal microRNA-106b-5p activates EMT-cancer cell and M2-subtype TAM interaction to facilitate CRC metastasis. *Mol. Ther.* 29 (6), 2088–2107. doi:10.1016/j.ymthe.2021.02.006

Yang, C., Yuan, W., Yang, X., Li, P., Wang, J., Han, J., et al. (2018). Circular RNA circ-ITCH inhibits bladder cancer progression by sponging miR-17/miR-224 and regulating p21, PTEN expression. *Mol. Cancer* 17 (1), 19. doi:10.1186/s12943-018-0771-7

Yeh, E. T., and Bickford, C. L. (2009). Cardiovascular Complications of Cancer Therapy. *J. Am. Coll. Cardiol.* 53 (24), 2231–2247. doi:10.1016/j.jacc.2009.02.050

Yuan, Y., Chen, X., and Huang, E. (2019). Upregulation of Circular RNA Itchy E3 Ubiquitin Protein Ligase Inhibits Cell Proliferation and Promotes Cell Apoptosis Through Targeting MiR-197 in Prostate Cancer. *Technol. Cancer Res. Treat.* 18, 153303381988686. doi:10.1177/1533033819886867

Zhang, F., Lin, F., Xu, Z., and Huang, Z. (2021). Circular RNA ITCH promotes extracellular matrix degradation via activating Wnt/β-catenin signaling in intervertebral disc degeneration. *Aging* 13 (10), 14185–14197. doi:10.18632/aging.203036

Zhang, J., Cai, Y., Sheng, S., Zhao, C., and Jiang, B. (2022). circITCH suppresses cell proliferation and metastasis through miR -660/ TFCP2 pathway in melanoma. *Cancer Med.* 11 (12), 2405–2413. doi:10.1002/cam4.4627

Zhang, N., and Wang, X. (2020). Circular RNA ITCH mediates H 2 O 2 -induced myocardial cell apoptosis by targeting miR-17-5p via wnt/β-catenin signalling pathway. *Int. J. Exp. Path* 102 (1), 22–31. doi:10.1111/iep.12367

Zhang, S., Liu, X., Bawa-Khalfe, T., Lu, L. S., Lyu, Y. L., Liu, L. F., et al. (2012). Identification of the molecular basis of doxorubicin-induced cardiotoxicity. *Nat. Med.* 18 (11), 1639–1642. doi:10.1038/nm.2919

Zhang, Y., Li, Y., Wang, Q., Su, B., Xu, H., Sun, Y., et al. (2020). Role of RASA1 in cancer: A review and update (Review). *Oncol. Rep.* 44 (6), 2386–2396. doi:10.3892/or.2020.7807

Zhao, L., Ma, N., Liu, G., Mao, N., Chen, F., and Li, J. (2021). Lidocaine Inhibits Hepatocellular Carcinoma Development by Modulating circ_ITCH/miR-421/CPEB3. *Dig. Dis. Sci.*, 66, 4384–4397. doi:10.1007/s10620-020-06787-1

Zhong, D., Xu, G. Z., Wu, J. Z., Liu, H., Tang, J. Y., and Wang, C. G. (2021). Circ-ITCH sponges miR-214 to promote the osteogenic differentiation in osteoporosis via upregulating YAP1. *Cell Death Dis.* 12 (4), 340. doi:10.1038/s41419-021-03586-y

Zhou, H., Zhang, J., Chen, B., Liu, H., Liu, X., Sun, Z., et al. (2020). Potential of circular RNA itchy E3 ubiquitin protein ligase as a biomarker and treatment target for multiple myeloma. *Transl. Cancer Res. TCR* 9 (1), 335–345. doi:10.21037/tcr.2019.12.71

Zhou, L., Li, F. F., and Wang, S. M. (2021a). Circ-ITCH restrains the expression of MMP-2, MMP-9 and TNF-α in diabetic retinopathy by inhibiting miR-22. *Exp. Mol. Pathology* 118, 104594. doi:10.1016/j.yexmp.2020.104594

Zhou, W., Liu, Y., and Wu, X. (2021b). Down-regulation of circITCH promotes osteosarcoma development and resistance to doxorubicin via the miR-524/RASSF6 axis. *J. Gene Med.* 23, e3373. doi:10.1002/jgm.3373

Zimmerman, Z. F., Kulikauskas, R. M., Bomsztyk, K., Moon, R. T., and Chien, A. J. (2013). Activation of Wnt/β-Catenin Signaling Increases Apoptosis in Melanoma Cells Treated with Trail. *PLoS One* 8 (7), e69593. doi:10.1371/journal.pone.0069593

Conflict of Interest: The authors declare that the research was conducted in the absence of any commercial or financial relationships that could be construed as a potential conflict of interest.

Publisher's Note: All claims expressed in this article are solely those of the authors and do not necessarily represent those of their affiliated organizations, or those of the publisher, the editors and the reviewers. Any product that may be evaluated in this article, or claim that may be made by its manufacturer, is not guaranteed or endorsed by the publisher.

frontiers | Frontiers in Genetics

TYPE Original Research
PUBLISHED 17 August 2022
DOI 10.3389/fgene.2022.929477

OPEN ACCESS

EDITED BY
Naseer A. Kutchy,
Children's National Hospital,
United States

REVIEWED BY
Ruhi Kabakci,
Kırıkkale University, Turkey
Hasan Alkan,
Selçuk University, Turkey

*CORRESPONDENCE
Mustafa Hitit,
vetdrmustafahitit@gmail.com
Mehmet Osman Atli,
moatli@hotmail.com

SPECIALTY SECTION
This article was submitted to RNA,
a section of the journal
Frontiers in Genetics

RECEIVED 26 April 2022
ACCEPTED 18 July 2022
PUBLISHED 17 August 2022

CITATION
Hitit M, Kose M, Kaya MS, Kırbas M, Dursun S, Alak I and Atli MO (2022), Circulating miRNAs in maternal plasma as potential biomarkers of early pregnancy in sheep.
Front. Genet. 13:929477.
doi: 10.3389/fgene.2022.929477

Circulating miRNAs in maternal plasma as potential biomarkers of early pregnancy in sheep

Mustafa Hitit[1]*, Mehmet Kose[2], Mehmet Salih Kaya[3], Mesut Kırbas[4], Sukru Dursun[5], Ilyas Alak[6] and Mehmet Osman Atli[7]*

[1]Department of Genetics, Faculty of Veterinary Medicine, Kastamonu University, Kastamonu, Turkey, [2]Department of Obstetrics and Gynecology, Faculty of Veterinary Medicine, Dicle University, Diyarbakir, Turkey, [3]Department of Physiology, Faculty of Medicine, Ankara Yildirim Beyazit University, Ankara, Turkey, [4]Bahri Dagdas International Agricultural Research Institute, Konya, Turkey, [5]Department of Obstetrics and Gynecology, Faculty of Veterinary Medicine, Aksaray University, Aksaray, Turkey, [6]Department of Animal Sciences, Vocational School of Technical Sciences, Ankara Yıldırım Beyazıt University, Ankara, Turkey, [7]Department of Reproduction and Artificial Insemination, Faculty of Veterinary Medicine, Harran University, Sanliurfa, Turkey

MicroRNA (miRNA) plays an important role in the control of gene expression and is implied in many biological functions, including embryo implantation and development. The aim was to assess plasma miRNA profiles during the peri-implantation and ascertain potential candidate miRNA markers for early pregnancy diagnosis in ovine plasma. The plasma samples were obtained from a total of 24 ewes on days 12 (pre-implantation; P12, n = 4), 16 (implantation; P16, n = 4) and 22 (post-implantation; P22, n = 4) after mating, and on their corresponding days of 12 (Pre-C; C12, n = 4), 16 (Imp-C; C16, n = 4) and 22 (Post-C; C22, n = 4) of the estrous cycle. The miRNA profiles in plasma were assessed by microarray technology. We detected the presence of 60 ovine-specific miRNAs in plasma samples. Of these miRNAs, 22 demonstrated a differential expression pattern, especially between the estrous cycle and early pregnancy, and targeted 521 genes. Two miRNAs (oar-miR-218a and oar-miR-1185-3p) were confirmed using RT-qPCR in the ovine plasma samples. Protein-protein interaction (PPI) network of target genes established six functional modules, of which modules 1 and 3 were enriched in the common GO terms, such as inflammatory response, defense response, and regulation of immune response. In contrast, module 2 was enriched in the developmental process involved in reproduction, embryo development, embryonic morphogenesis, and regulation of the developmental process. The results indicate that miRNAs profiles of plasma seemed to be modulated during the peri-implantation stage of pregnancy in ewes. Circulating miRNAs could be promising candidates for diagnosis in early ovine pregnancy.

KEYWORDS

ovine, plasma, microRNA, circulating, early pregnancy, expression

Introduction

In order to have a successful pregnancy, the uterine environment and a viable embryo must work together during the peri-implantation stage of pregnancy (Kose et al., 2016c; Kaya et al., 2017). Many molecules controlled at the gene expression level are implicated in the regulation of implantation (Kose et al., 2016a; Alak et al., 2020), but their particular regulatory mechanisms remain still unclear. Previous studies indicated that changes in microRNA (miRNA) expression play a functional role in embryo implantation in many species (Song et al., 2015; Gebremedhn et al., 2018). Apart from roles in expressed tissues of interest, particularly in the endometrium (Kiyma et al., 2015; Yan et al., 2021), miRNAs also could be released into the extracellular environment by cells, facilitating cell-cell interactions and providing valuable information related to the specific conditions (Bidarimath et al., 2021; Shi et al., 2021).

miRNAs, non-coding RNA molecules with 21–24 nucleotides, post-transcriptionally modulate gene expression and thus are implied in biological processes (Bartel, 2004; Hitit et al., 2015; WB, 2016). An understanding of miRNAs expressions and their functions in the female reproductive tract has been recently developed. Accordingly, miRNAs are functional at different stages of the reproduction process in the female (oocyte growth, maturation, embryo development, implantation, and placentation) (Guzeloglu et al., 2013; Hitit et al., 2013; Kaczmarek et al., 2020). miRNA expression profiles were shown to be different during the peri-implantation period and even differed between implantation and non-implantation regions in mice (Chakrabarty et al., 2007; Liu et al., 2015). Moreover, gene expression profiles concerning embryo implantation in ovine endometrium revealed pregnancy-associated miRNAs, of which many were differentially expressed in the endometrium on day 13 of pregnancy (Kiyma et al., 2015). Also, we determined differentially expressed miRNA profiles in the endometrium during the early pregnancy on days 12, 16, and 22 (Kose et al., 2022).

Placenta or embryo-derived miRNA molecules pass into body fluids, such as plasma, serum, and milk, within the extracellular vesicle (Tan et al., 2020). Therefore, their resistance with the stable structure to adverse effects such as freezing–thawing and high temperature is encouraging for detecting early pregnancy and monitoring the maintenance of pregnancy (De Bem et al., 2017). More specifically, in livestock animals, plasma samples from cattle and goats provide unique miRNA profiles between pregnant and non-pregnant groups, which circulating miRNAs were shown to be potential markers of early pregnancy stages and endometrial receptivity in the field of reproductive biology (Ioannidis and Donadeu, 2016; Zang et al., 2021; Zhao et al., 2021). El-Shorafa and Sharif (2016) determined that healthy fertile women exhibit different expression profiles of some miRNAs in maternal plasma than women who experienced recurrent pregnancy loss of unknown cause (El-Shorafa and Sharif, 2016). Similarly, Kotlabova et al. (2011) reported that seven miRNAs of placental origin were identified in the maternal circulation throughout pregnancy.

Considering the literature indicated above, we hypothesized that early pregnancy causes a change in plasma miRNA profiles, and this may be a candidate marker for early pregnancy diagnosis in sheep. The current study, therefore, aimed to ascertain the circulating miRNA profile in the plasma during peri-implantation, which is one of the most crucial stages for the establishment and maintenance of pregnancy in the ewe, and identify candidate miRNA markers for early pregnancy diagnosis.

Materials and methods

Experimental design and sample collection

All experimental steps were confirmed by the Bahri Dagdas International Agricultural Research Institute Ethical Research Committee (Number: 29/01/2016-49-7). Twenty-four multiparous ewes (n = 24) were used; assigned into cyclic (C, n = 12) and pregnant (P, n = 12) groups, randomly. Animal diets for 3- to 5-year-olds were adjusted to satisfy the NRC (2007) nutritional requirements. All other supplementals were given *ad libitum* during the study.

Before the experiment, cycles of the ewes were synchronized with two cloprostenol (a synthetic analog of prostaglandin F2alpha; PGF2α, 125 mcg) injections 11 days apart. Immediately after the second injection, estrus was checked three times a day using teaser rams. Estrus of ewes was obtained through teaser ram at 8 h intervals for 5 days after the second injection, and the ewes that showed estrus were recorded. Then, these ewes were followed to accomplish their entire cycle and noted for new natural estrus using teaser rams. In this new estrus, the pregnant ewes mated (day 0) two times, 12 h alone, using fertility-proven rams. The estrus day in the cyclic group was accepted as day zero (day 0). Ewes were scheduled for slaughter on days of 12 (pre-implantation, n = 4; P12), 16 (implantation, n = 4; P16) or 22 (post-implantation, n = 4; P22) of gestation following mating, and on their corresponding days of 12 (n = 4, C12), 16 (n = 4, C16) or 22 (n = 4, C22) of the estrous cycle. To provide a similar effect of progesterone and to observe the only effect of pregnancy or embryo on plasma miRNA expression, cyclic ewes were exposed to a natural progesterone implant via intravaginal on day 13 of the cycle for days 16 and 22 groups, and progesterone implants were kept until the ewes were slaughtered. The presence of only one embryonic trophoblast was observed for 12, 16, and 22 days of

pregnancy in the uterine lumen (Spencer et al., 2004; Bazer et al., 2012).

Processing of blood sample and RNA isolation

We collected blood samples from ewes in tubes containing EDTA for plasma isolation just before the ewes were slaughtered. We centrifuged collected blood samples at 1,600×*g* for 13 min, and plasma was extracted and kept at − 80°C. Plasma was thawed at 20°C in the dry bath. Then, total cell-free RNA was extracted from 250 µl of plasma through miRCURY RNA Isolation Kit—Biofluids (Exiqon #300112 Vedbaek- Denmark) according to the manufacturer's protocol. Plasma samples underwent on-column DNase to get rid of DNA contamination using the manufacturer's protocols. Consequently, we eluted RNA samples using 40 µl RNase-free water. Tubes containing the miRNA were kept at −80°C until the miRNA array analysis.

miRNA microarray

The profile of miRNAs from ovine plasma samples was investigated using the Affymetrix Microarray system with the GeneChip miRNA 4.0 Array (Affymetrix, United States) that is arranged to retrieve mature miRNA sequences in miRBase (20.0) (http://mirbase.org/ftp.shtml). Mature miRNA sequences of one hundred fifty from sheep are demonstrated in miRBase (20.0). A total of one 1) microgram of RNA was labeled with a FlashTagTM Biotin HSR RNA Labeling Kit (Affymetrix, United States). Following RNA labeling, through a GeneChip Hybridization Control Kit (Affymetrix, United States), microarray chips were hybridized with agitation at 60 rpm for 15 h. Then, the chip arrays were washed and subsequently stained through a Fluidics Station 450 (Affymetrix, Santa Clara, California, United States) with AGCC Fluidics Control Software. Fluorescence was detected from the array chip with an Affymetrix® GeneChip Scanner 3000.

Raw data preparation and statistical analysis

The signal of probes was generated as cell intensity files (*CEL files) computed using Affymetrix GeneChip Command Console software and analyzed in Transcriptome Analysis Console software. The intensity data of each chip was processed through the robust multi-array average (RMA) and identified above background (DABG) normalization with a default analysis setting of Affymetrix. Probe set summarization was performed through Median Polish. Probe values were generated as log2 transformed. Comparison between the cyclic and the pregnant samples was accomplished through fold-change with an independent *t*-test. One-way ANOVA was used to reveal statistically significant genes at the significance level of $p \leq 0.05$. To demonstrate biologically relevant gene expression changes of each of cyclic and pregnant conditions, the standard approach was employed through a *p*-value ($p \leq 0.05$) as the primary criterion followed by fold change ($-1.5 \geq FC \geq 1.5$) as the secondary criterion to select differentially expressed genes. Upon first analysis, criteria were relaxed to ($-1.25 \geq FC \geq 1.25$; $p < 0.05$) to identify all the family members of miRNAs of interest in all the ovine plasma samples.

Target gene prediction of differentially expressed miRNAs

The target gene prediction of miRNAs in plasma samples was accomplished using the miRNAconsTarget online tool from sRNAtoolbox (http://bioinfo5.ugr.es/srnatoolbox), providing consensus target prediction. The given input data are developed on independent prediction from animal-based tools. TargetSpy, PITA (energy score < −15), and miRanda (pairing score >150 and an energy score < −15), making a total of three prediction algorithms. The common target genes predicted by all three tools were considered a potential miRNA target.

Protein-protein interaction network construction and module analysis

The functional network association among target genes was established using the database of STRING (version 11.5, http://string-db.org), and eventually visualized in Cytoscape (version 3.9.0). The PPI network of target genes was transferred and subsequently assessed in Cytoscape. The functional modules were determined and shown by Molecular Complex Detection (MCODE), a plugin in Cytoscape for identifying intensively connected nodes in a current network. The module was set as follows: k-score = 2, cut-off degree = 2, max depth size = 100, MCODE score >5, and node score cut-off = 0.2 (Lou et al., 2019). The nodes included in the main modules are demonstrated as densely connected genes that show significant biological functions. CytoHubb CytoScape plugin was used to reveal important nodes by integrating topological calculations such as Maximal clique centrality (MCC), Maximum neighborhood component (MNC), Degree, Edge percolated component (EPC), and (EcCentricity) EC (Chin et al., 2014). The overlapping genes were ranked using the aforementioned five algorithms.

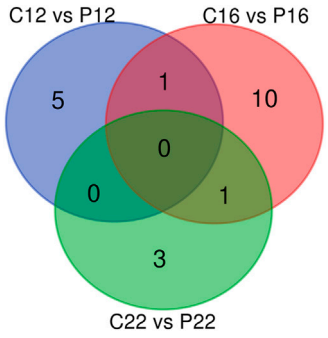

FIGURE 1
miRNA profiles in estrus cycle and pregnancy in ovine plasma. The Venn diagrams represent miRNA profiles between C12 and P12, C16 and P16, and C22 and P22.

Gene ontology and pathway enrichment analysis of target genes

The KEGG pathway and GO enrichment for the predicted target genes from the modules were analyzed using Cytoscape software with the ClueGO V2.5.7 plug-in (Bindea et al., 2009). The ClueGO plug-in generates functionally grouped GO annotation networks for many target genes. The GO categories were assigned to molecular function (MF), cellular component (CC), and biological process (BP). Two-sided hypergeometric tests set the *p*-value to 0.05, and multiple test corrections were performed using Bonferroni step-down adjustment. The threshold of the kappa score was adjusted to 0.7.

RT-qPCR

Forward primer, universal reverse primer, and Stem-Loop primer sequences of two miRNAs to be confirmed by RT-qPCR (Supplementary Material S1). For the confirmation with RT-qPCR, firstly, a reverse transcription reaction was prepared using the First-Strand cDNA (1 μg RNA to cDNA) Synthesis Kit for RT-qPCR (USB, Cat no: 75780). Reverse transcriptase reaction conditions were as follows: 32 min at 16°C, 60 min at 44°C, 10 min at 95°C, and 5 min at 4°C. Following cDNA synthesis by reverse transcriptase reaction, RT-qPCR analyses of the samples were performed using VeriQuest Fast SYBR Green RT-qPCR Master Mix (USB, Cat no: 75690). RT-qPCR reaction was used as follows: Polymerase for 8 min at 95°C, then 45 cycles of denaturation for 25 s at 94°C, annealing for 42 s at 58°C, and extension for 50 s at 70°C. Log transformation of the data was performed according to the previously mentioned 2−ΔCt method (Livak and Schmittgen, 2001). Statistical analysis of values normalized to reference genes was calculated by Relative Expression Software Tool (REST 2009) (Pfaffl et al., 2002).

Results

miRNA profiles of ovine plasma in estrous cycle and early pregnancy

Microarray results in plasma samples revealed a total of 183 miRNAs in all species between the estrous cycle and early pregnancy, while 60 were identified in ovine plasma samples (Supplementary Material S2). However, when respectively compared, there were 6, 12, and 4 statistically significant plasma-specific miRNAs between C12 vs. P12, C16 vs. P16, and C22 vs. P22, respectively. Among these, one was shared between C12 vs. P12, C16 vs. P16, C16 vs. P16 and C22 vs. P22, whereas 5, 10, and 3 miRNAs were unique to C12 vs. P12, C16 vs. P16, and C22 vs. P22, respectively (Figure 1).

Differentially expressed miRNAs between cyclic and pregnant ovine plasma

A total of 22 differentially expressed ovine plasma miRNAs were determined ($p < 0.05$, difference of miRNAs greater than 1.25-fold change) when cyclic ovine plasma samples compared to pregnant ovine plasma samples. While five miRNAs (oar-miR-23b, oar-let-7i, oar-miR-19b, oar-miR-21, oar-miR-487b-3p were upregulated between C12 and P12, one of them (oar-miR-329a-5p) was downregulated (Figure 2A). Between C16 and P16, 8 miRNAs (oar-miR-29a, oar-miR-299-3p, oar-miR-30d, oar-miR-379-5p, oar-miR-152, oar-miR-323b, oar-miR-329a-5p, and oar-miR-654-5p) were upregulated while 4 miRNAs (oar-let-7b, oar-miR-218a, oar-miR-487a-5p, and oar-miR-758-3p) were downregulated (Figure 2B). In C22 vs. P22, miRNAs (oar-miR-29b, oar-miR-1185-3p, oar-miR-487a-5p, and oar-miR-543-3p) were downregulated (Figure 2C). The list of the 22 significant miRNAs from cyclic and pregnant groups with their fold change is depicted in Table 1. Furthermore, the detailed information on the differentially expressed ovine plasma miRNAs is demonstrated in Supplementary Material S2.

Target prediction of selected microRNAs and PPI network construction

The target genes of the twenty-two miRNAs were predicted using the miRNAconsTarget online tool from sRNAtoolbox based on animal-based prediction with three algorithms

10.3389/fgene.2022.929477

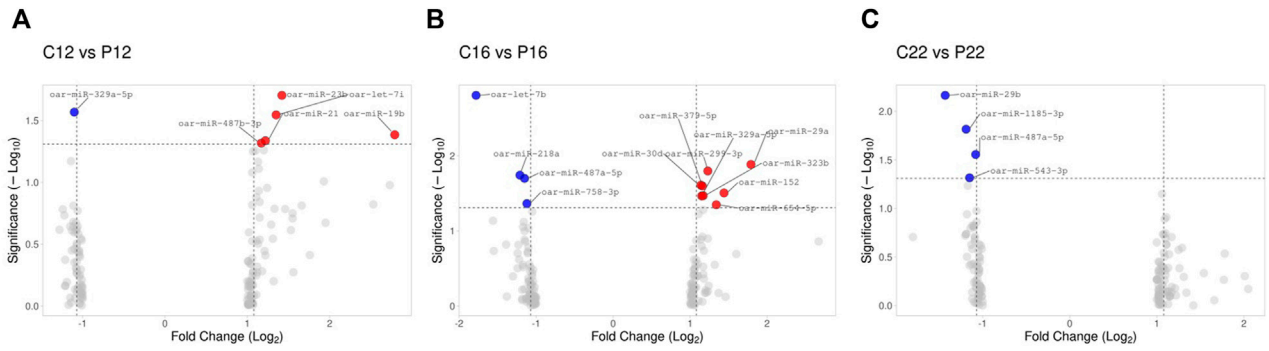

FIGURE 2
Illustration of volcano plot for differentially expressed miRNAs in estrus cycle and pregnancy in ovine plasma. The −log10 is set versus the log2 (fold change: cycle: pregnancy). **(A)** C12 vs. P12, **(B)** C16 vs. P16, and **(C)** C22 vs. P22. Color represents the fold change, red: up and blue: down.

TABLE 1 The list of the differentially expressed miRNAs between cyclic days (C12, C16, and C22) and pregnant days (P12, P16, and P22).

Groups	Transcript ID	Accession	Fold Change	ANOVA *p*-value
C12 vs. P12	oar-miR-23b, oar-miR-329a-5p, oar-let-7i, oar-miR-19b, oar-miR-21, oar-miR-487b-3p	MIMAT0030049, MIMAT0019265, MIMAT0030026, MIMAT0030041, MIMAT0014966, MIMAT0019295	1.42, −1.1, 1.35, 2.79, 1.22, 1.17	0.019804, 0.027071, 0.028503, 0.04126, 0.046065, 0.048208
C16 vs. P16	oar-let-7b, oar-miR-29a, oar-miR-299-3p, oar-miR-218a, oar-miR-487a-5p, oar-miR-30d, oar-miR-379-5p, oar-miR-152, oar-miR-323b, oar-miR-329a-5p, oar-miR-758-3p, oar-miR-654-5p	MIMAT0014963, MIMAT0014967, MIMAT0019252, MIMAT0030045, MIMAT0019304, MIMAT0030059, MIMAT0019247, MIMAT0030035, MIMAT0019314, MIMAT0019265, MIMAT0019262, MIMAT0019282	-1.78, 1.79, 1.23, -1.21, −1.15, 1.14, 1.16, 1.44, 1.17, 1.15, -1.12, 1.34	0.001568, 0.013043, 0.015942, 0.01812, 0.020003, 0.0246, 0.025283, 0.031226, 0.033997, 0.034248, 0.043262, 0.044898
C22 vs. P22	oar-miR-29b, oar-miR-1185-3p, oar-miR-487a-5p, oar-miR-543-3p	MIMAT0030054, MIMAT0019289, MIMAT0019304, MIMAT0019272	−1.43, −1.19, −1.08, −1.15	0.006853, 0.015291, 0.027848, 0.048368

(TargetSpy, PITA, and miRanda). Six differentially expressed miRNAs between C12 vs. P12 targeted 156 genes. Twelve miRNAs targeted 257 target genes between C16 and P16, whereas there were 108 in C22 and P22 by four differentially expressed miRNAs (Supplementary Material S3). Overlapping target genes from cyclic and pregnant were excluded, and then 326 were submitted to STRING online database. A PPI network including 328 nodes and 1,936 edges was directed employing the Cytoscape software (Supplementary Material S4).

qPCR for miRNA expression analysis

Among the miRNAs, oar-miR-1185-3p and oar-miR-218a were detected to be regulated in ovine plasma samples. The expression of oar-miR-1185-3p mRNA was similar between C12 and P12. It was found to be greater in P16 than in C16, while it did not change between C22 and P22 (Figure 3A). oar-miR-218a mRNA was found to be lower in pregnancy groups than in cyclic groups (C12 vs. P12, C16 vs. P16, and C22 vs. P22) identified (Figure 3B).

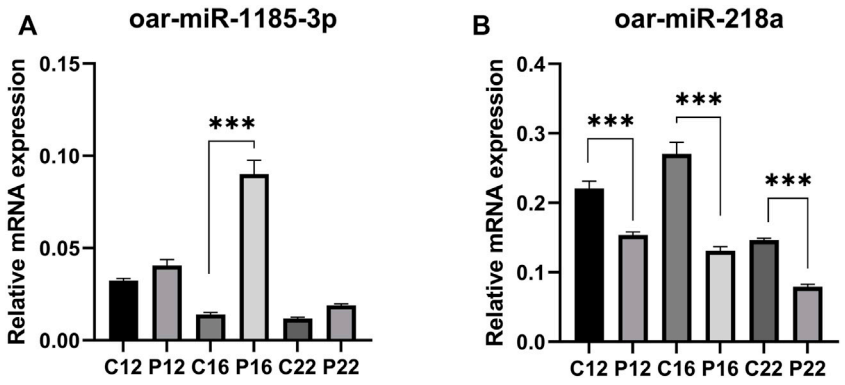

FIGURE 3
The relative abundance of selected miRNAs quantified by RT-qPCR were statistically significant. Expression of **(A)** oar-miR-218a and **(B)** oar-miR-1185-3p, between C12 vs P12, C16 vs P16, and C22 vs P22. Data are shown as relative abundance ± SEM, $p < 0.05$; (Estrous cyclic day 12: C12, Pregnant day 12: P12, Estrous cyclic day 16:C16, Pregnant day 16: P16, Estrous cyclic day 22:C22, Pregnant day 22: P22, indicates the group).

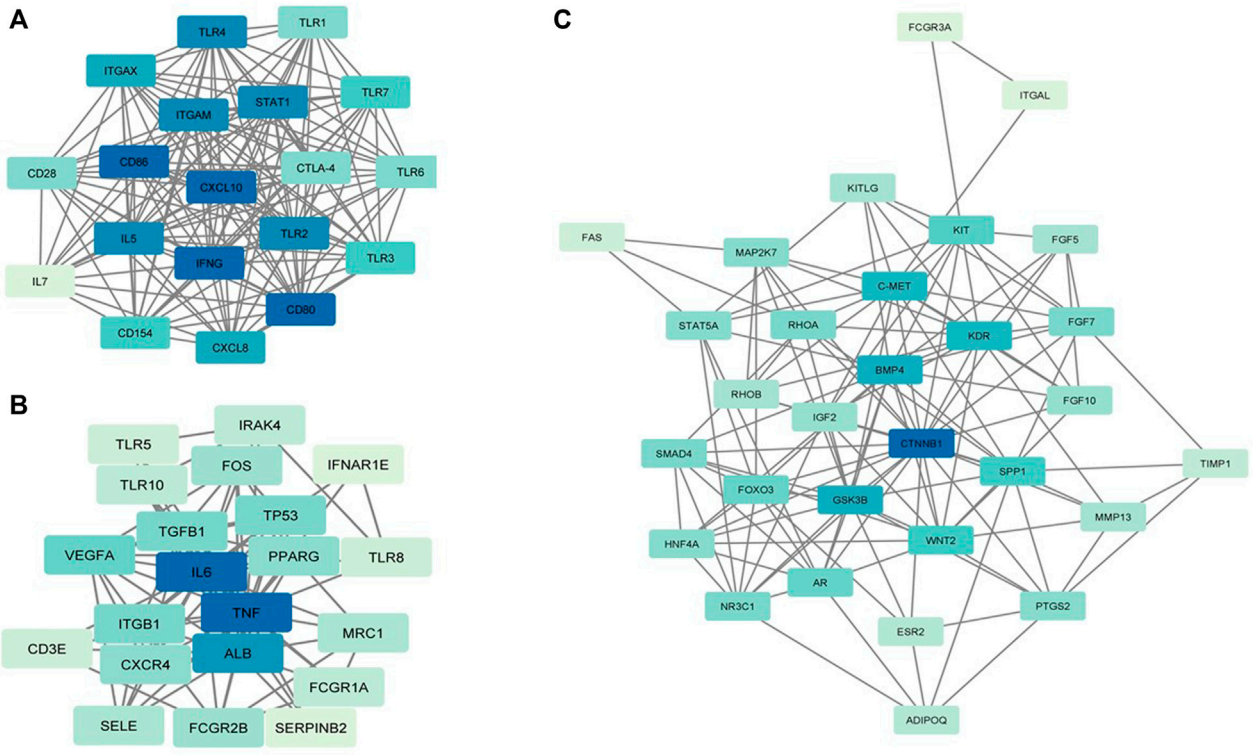

FIGURE 4
MCODE clustering of the top three clusters. **(A)** Module 1. **(B)** Module 2. **(C)** Module 3. In the modules, the nodes are colored in a continuous manner compliant with their |log2FC| values.

TABLE 2 Hub target genes of differentially expressed miRNAs from the modules. Overlapping hub protein symbols in the top 10, ranked methods were highlighted as bold. MCC: maximal clique centrality; MNC: maximum neighborhood component; Degree: node degree; EPC: edge percolated component; EC: EcCentricity.

	Node name	MCC	Node name	MNC	Node name	Degree	Node name	EPC	Node name	Ec Centricity
Module 1	CD80	1E+09	CD80	18	CD80	18	CD80	10.1	CD80	1
	CXCL10	1E+09	CXCL10	18	CXCL10	18	IFNG	10.0	IFNG	1
	CD86	1E+09	CD86	18	CD86	18	CXCL10	10.0	CXCL10	1
	IFNG	1E+09	IFNG	18	IFNG	18	CD86	9.9	CD86	1
	TLR2	1E+09	TLR2	17	TLR2	17	STAT1	9.8	STAT1	0.5
	TLR4	1E+09	TLR4	17	TLR4	17	TLR2	9.6	TLR2	0.5
	STAT1	1E+09	STAT1	17	STAT1	17	CXCL8	9.6	CXCL8	0.5
	TLR3	1E+09	ITGAM	17	ITGAM	17	TLR4	9.6	TLR4	0.5
	TLR1	1E+09	IL5	17	IL5	17	IL5	9.6	IL5	0.5
	TLR6	1E+09	CXCL8	16	CXCL8	16	ITGAX	9.5	ITGAX	0.5
Module 2	Node name	MCC	Node name	MNC	Node name	Degree	Node name	EPC	Node name	Ec Centricity
	CTNNB1	2,826	CTNNB1	22	CTNNB1	22	CTNNB1	10.73	CTNNB1	0.5
	GSK3B	2,298	GSK3B	15	GSK3B	15	GSK3B	9.52	C-MET	0.5
	AR	2,174	BMP4	15	BMP4	15	BMP4	9.49	GSK3B	0.33
	SMAD4	2,166	KDR	14	KDR	14	C-MET	9.2	BMP4	0.33
	HNF4A	2,160	C-MET	13	C-MET	14	KDR	9.06	KDR	0.33
	BMP4	1770	WNT2	12	WNT2	12	WNT2	8.77	WNT2	0.33
	FOXO3	1,464	SPP1	12	SPP1	12	SPP1	8.35	SPP1	0.33
	WNT2	834	AR	10	KIT	11	AR	8.06	AR	0.33
	NR3C1	734	FOXO3	10	AR	10	KIT	7.96	KIT	0.33
	KDR	516	KIT	10	FOXO3	10	FOXO3	7.88	FOXO3	0.33
Module 3	Node name	MCC	Node name	MNC	Node name	Degree	Node name	EPC	Node name	Ec Centricity
	TNF	11040	TNF	20	TNF	20	IL6	15.67	IL6	1
	IL6	11040	IL6	20	IL6	20	TNF	15.64	TNF	1
	ALB	11004	ALB	16	ALB	16	ALB	15.51	ALB	0.5
	VEGFA	10800	VEGFA	10	VEGFA	10	VEGFA	14.50	VEGFA	0.5
	TP53	10080	TP53	9	TP53	9	TGFB1	14.42	TGFB1	0.5
	TGFB1	10080	TGFB1	9	TGFB1	9	TP53	14.35	TP53	0.5
	ITGB1	5,784	ITGB1	9	ITGB1	9	ITGB1	14.18	ITGB1	0.5
	CXCR4	5,760	CXCR4	8	CXCR4	8	CXCR4	14.11	CXCR4	0.5
	PPARG	5,064	PPARG	8	PPARG	8	PPARG	13.78	PPARG	0.5
	FOS	5,040	FOS	7	FOS	7	FOS	13.35	FOS	0.5

Functional interaction network and module analysis of target genes

Six clusters were attained from the PPI network following module analysis through the MCODE plugin of Cytoscape, and we sorted out three modules among all as hub modules constructed from MCODE scores (Figures 4A–C). Module 1 consisted of 19 nodes and 151 edges and had the highest MCODE score (16.778) of all modules (Figure 4A). Module 2 has 30 nodes and 131edges (Figure 4B) Supplementary Material S5, whereas module 3 contained 21 nodes and 84 edges (Figure 4C). All five classifications of methods within the CytoHubba plugin were accepted, and the highest ranked genes of each method (top 10) were shown (Table 2). Module 1 was enriched in (GO: 0006468) protein phosphorylation, (GO:00069540) inflammatory response, (GO:0006952) defense response, (GO: 0042127) regulation of cell population proliferation, (GO: 0010033) response to organic substance, (GO:0009893) positive regulation of metabolic process, (GO:0002684) positive regulation of immune system process, (GO:2000026) regulation of multicellular organismal development, (GO: 0009966) regulation of signal transduction (Figure 5). Module 2 was involved in (GO:0009790) embryo development, (GO: 0003006) developmental process involved in reproduction, (GO:

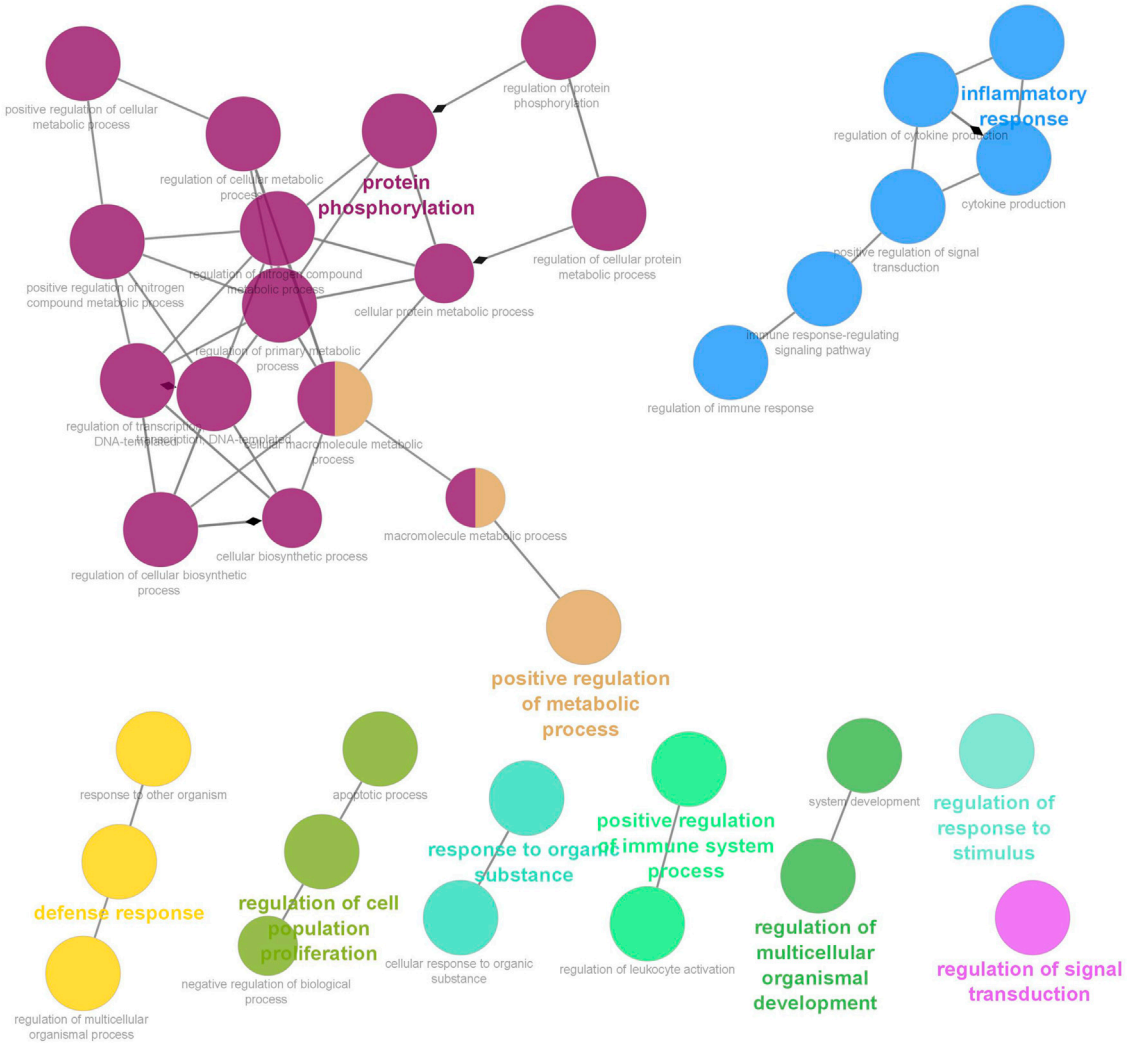

FIGURE 5
Functional interaction of network analysis of the target genes from module 1 between estrus cycle and pregnancy. GO terms are shown as nodes, the color depth of node shows distinct proportions of target genes. Nodes located in the same cluster are nominated as the same node color and size of nodes demonstrates the number of mapped genes in each GO term. Relationship between terms is shown by edges. Functionally associated groups partly overlap and are randomly colored.

0048598) embryonic morphogenesis, (GO:0050793) regulation of developmental process, (GO:0035295) tube development, (GO:0060429) epithelium development, (GO:0061138) morphogenesis of a branching epithelium, (GO:0009891) positive regulation of the biosynthetic process (Figure 6). Although module 3 had common GO terms with module 1, it contained (GO:0006952) defense response, (GO:0050776) regulation of immune response, (GO:0045087) innate immune response, (GO:0010033) response to organic substance, (GO:0006954) inflammatory response, (GO:0051240) positive regulation of the multicellular organismal process (Figure 7) (Supplementary Material S6).

Discussion

In this current study, we carried out profiling of plasma miRNA expression to determine potential miRNAs involved in the critical stages of peri-implantation. The circulating miRNA expression profile was evaluated on days 12, 16, and 22 during pregnancy after mating and on their corresponding days of 12, 16, and 22 of the estrous cycle. We already know that the estrous cycle in ewes is 17 days and declining progesterone levels start on day 16 after mating. Therefore, in the C16 and C22 groups, an external supply of progesterone was added. As a result, we were able to compare the plasma miRNA profiles of cyclic and

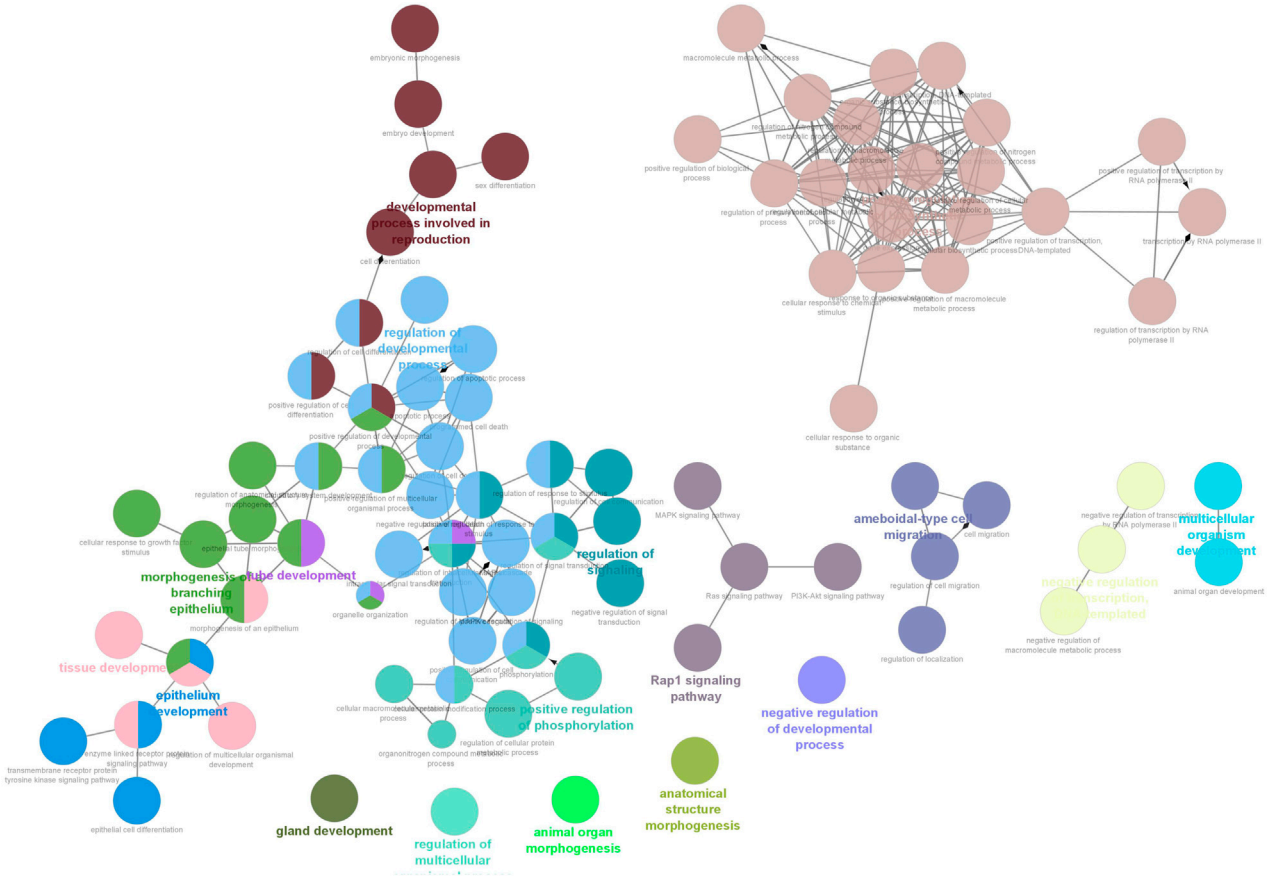

FIGURE 6
Functional interaction of network analysis of the target genes from module 2 between estrus cycle and pregnancy. GO terms are shown as nodes, the color depth of node shows distinct proportions of target genes. Nodes located in the same cluster are nominated as the same node color and size of nodes demonstrates the number of mapped genes in each GO term. Relationship between terms is shown by edges. Functionally associated groups partly overlap and are randomly colored.

pregnant sheep without being affected by the fluctuating levels of progesterone. We may therefore hypothesize that whatever changes we detected in the levels of miRNA expression in ovine plasma in pregnant ewes were a direct result of the conceptus given that progesterone levels were similar across the cyclic and pregnant groups.

Circulating plasma miRNAs have been detected in several studies that indicated a significant number of miRNAs to reveal the importance of transcriptomics in reproductive biology (Hitit and Kurar, 2017; Zong et al., 2021). As such, many miRNAs originating from villous trophoblasts circulate through maternal blood within or linked with extracellular vesicles (Miura et al., 2010; Cameron et al., 2011; Kotlabova et al., 2011). It has been identified that 374 human placenta-specific miRNAs, of which 10 with the highest global expression were also reflected in plasma (Smith et al., 2021). In another exploratory study, 208 plasma-specific miRNAs were identified in cattle; of these miRNAs, sixteen were statistically different between non-pregnant and pregnant plasma samples (Ioannidis and Donadeu, 2016). However, this is the first study elucidating the identification of circulating miRNA profiles in ovine plasma during the estrous cycle and pregnancy. In the current study, we discovered a total of 60 ovine circulating miRNAs between cyclic and pregnant plasma, indicating remarkable outcomes for sheep reproductive biology. Among these, 22 were differentially expressed in microarray results upon pregnancy groups were compared with cyclic (Table 1). The results may indicate that circulating plasma miRNAs may function as potential biomarkers in the regulation of pregnancy during the estrous cycle and early pregnancy (Ioannidis and Donadeu, 2017; Lim et al., 2021).

Our study is noteworthy that the target prediction of selected miRNAs uncovered a great many GO terms that ovine circulating miRNAs in plasma might regulate biological and molecular control of gene expression during

FIGURE 7
Functional interaction of network analysis of the target genes from module 3 between estrus cycle and pregnancy. GO terms are shown as nodes, the color depth of node shows distinct proportions of target genes. Nodes located in the same cluster are nominated as the same node color and size of nodes demonstrates the number of mapped genes in each GO term. Relationship between terms is shown by edges. Functionally associated groups partly overlap and are randomly colored.

early pregnancy. Accordingly, we particularly ascertained critical GO terms that may be involved in early pregnancy, such as (GO:0006468) protein phosphorylation, (GO: 00069540) inflammatory response, (GO:0006952) defense response, (GO:0042127) regulation of cell population proliferation, (GO:0009893 positive regulation of metabolic process, (GO:0010033) response to organic substance, (GO: 0002684) positive regulation of immune system process, (GO: 2000026) regulation of multicellular organismal development, (GO:0009966) regulation of signal transduction. This may illuminate that circulating miRNAs clarify molecular events during pregnancy recognition and embryo implantation because extracellular vesicles derived from the serum, trophectoderm, and uterine epithelia in pregnant ewes are implicated in intercellular communication, and microRNA-mediated pathways are involved in the key pathway in the pregnancy (Brooks et al., 2016; Ioannidis and Donadeu, 2017; Sun et al., 2021; Ono et al., 2022).

The potential of circulating miRNAs has been demonstrated, in many animals, to be identified in maternal circulation directly following initiation of implantation (Sun et al., 2021). Based upon this knowledge, for instance, elevated expression levels of circulating miRNAs (miR-23b) are shown to be expressed within either pregnant endometria (Krawczynski et al., 2015)

or serum (Reliszko et al., 2017) on a gestational day 16 of pregnant pigs. In sheep serum, expression of miR-23b, miR-30d, and miR-379 was found to be at greater levels in exosomes obtained from the umbilical vein on gestational day of 90 (Cleys et al., 2014). However, in line with the expression of miR-23b in pregnancy, our study detected higher expression levels of oar-miR-23b as early as day 12 of pregnancy compared to C12. In addition, our unpublished data showed that oar-miR-23b tended to be higher in P16 than C16 in the endometrium. We also showed that oar-miR-30d and oar-miR-379-5p were higher in P16 than in C16. Because the capability to detect miRNAs for endometrium has enabled us to reveal pregnancy-related markers (Kose et al., 2022), it is intriguing to monitor common miRNAs for conceptuses and maternal bloodstream. As such, broadly conserved miRNAs (Let-7b) have been detected at different stages of pregnancy in trophoblast (Liu et al., 2015) and serum (Ioannidis and Donadeu, 2017). We demonstrated that let-7i and let-7b were differentially expressed between C12 vs. P12 and C16 vs. P16. Likewise, as identified higher expression of miR-29a in cattle maternal blood on day 39 of pregnancy (Sánchez et al., 2021), conserved miR-29 family members, oar-miR-29a and oar-miR-29b, were found to be expressed in C16 vs. P16 and C22 vs. P22 in ovine plasma, respectively.

The gene targets of differentially expressed miRNA are underrepresented in common categories (inflammatory response (GO:0006954), defense response (GO:0006952), and regulation of immune response (GO:0050776)) relating to immune responses in functional interaction of network analysis of module 1 and 3, meaning that the pregnancy-stimulated changes require both activation and suppression of immune functions through circulating miRNAs (Bidarimath et al., 2014) Among them, CD80 and CD86, costimulatory molecules, involved in signaling in T cell activation (Gool et al., 1996) and upregulated during early pregnancy in the cattle endometrium (Kamat et al., 2016). We showed that CD80 and CD86 was modulated by oar-miR-329a-5p, oar-miR-23b, oar-miR-654-5p, oar-miR-29b, and oar-miR-29a. In similar lines to our results, the miR-29 family has been implied in the regulation of the immune system (Liston et al., 2012) and detected as a potential biomarker for adverse pregnancy outcomes (Deng et al., 2020; Sørensen et al., 2021). As determined in our study, miR-19b and miR-29a were potential candidates for pregnancy detection in cows (Ono et al., 2022). miR-19b was also detected in ovine extracellular vesicles of cyclic and pregnant uterine luminal fluid on day 14 (Burns et al., 2014). In our unpublished data, as in ovine plasma, we found that miR-19b and miR-29a were differentially expressed in C16 vs. P16 and C22 vs. P22 in the ovine endometrium. In module 3, we illuminated that differentially expressed miRNAs targeted a couple of hub genes, which are interleukins, in other words, proinflammatory cytokines (TNF and IL6). oar-miR-19b between C12 and P12 targeted TNF, which plays an indispensable role in very early pregnancy. On the other hand, miRNAs may directly regulate the expression of interferon tau (IFNT)-stimulated genes (ISGs) in peripheral blood cells as they are secreted into the uterine cavity and partially enter the blood circulation directly. As such, CXCL10, classical type I IFN-stimulated genes, was among the hub gene in module 1 and targeted by oar-let-7b and oar-let-7i. In addition, we detected that miRNAs targeted toll-like receptors (TLRs) that are part of the innate immune system because they have roles in the stimulation of the acquired immune system (Akira and Takeda, 2004; Atli et al., 2018). TLR2 and TLR4 in module 1 enriched in (GO:0045087) innate immune response, targeted by oar-miR-30d, oar-miR-758-3p, and oar-miR-654-5p.

Module 2 showed that targets (ADIPOQ, BMP4, CTNNB1, FGF10, HNF4A, IGF2, SMAD4, WNT2) were related to functional GOs that may be involved in early pregnancy because it was enriched in (GO:0009790) embryo development and (GO:0048598) embryonic morphogenesis. CTNNB1 was one of hub genes targeted by oar-miR-218a, oar-miR-543-3p, oar-miR-1185-3p, and oar-miR-19b. Wnt/β-catenin signaling pathway has an important function in early embryogenesis (Liu et al., 2016), that β-catenin-regulated adhesion is essential for successful preimplantation of embryo development in mice (Messerschmidt et al., 2016). In line with gene expression, the Wnt/β-catenin signaling pathway requires strict control of miRNA regulation in embryo development (Stepicheva et al., 2015; Caronia-Brown et al., 2016). As discussed above, the development process occurring during embryonic development requires branching morphogenesis of organs and tissues. Our study revealed that target genes were enriched in (GO:0061138) morphogenesis of a branching epithelium and (GO:0060429) epithelium development. Of these, BMP4 was one of the early developmental genes expressed in the epithelium (Warburton et al., 2005; Geng et al., 2011) and reported post-transcriptionally regulated by miRNAs (Spruce et al., 2010; Battista et al., 2013). Accordingly, we showed that WNT2 and BMP4, other hub genes, were targeted by the same miRNAs (oar-miR-30d, oar-miR-29a). These results were corroborative with those circulating miRNAs that may play a functional role in early pregnancy to modulate embryonic development.

Although the inconsistency in the expression of oar-miR-1185-3p between microarray and RT-PCR emerged, miRNA expression of oar-miR-218a is consistent with microarray results between C16 and P16. This is consistent with reports that oar-miR-218a has been recently reported to be an early pregnancy marker of extracellular vesicles in ovine serum (Sun et al., 2021). Also, serum and plasma identification of miR-218 expression was associated with pregnancy disorder (Lu et al., 2017; Akgör et al., 2020). The limitations of this study were that due to the lack of compatible miRNA expression probes with ewe, we were unable to confirm more miRNA markers using RT-PCR.

Conclusion

In our study, using microarray and qPCR profiling in ovine, we discovered for the first time changes in the levels of miRNAs in plasma during early pregnancy. Differently expressed miRNA profiles in the ovine plasma during the estrus cycle and early pregnancy indicate that miRNAs may function as promising candidates for diagnosis in early ovine pregnancy. More specifically, predicted target genes in modules showed different functional GO such as (GO:0003006) developmental process involved in reproduction, (GO:0009790) embryo development, and (GO:0002684) regulation of immune system process that circulating miRNAs may enable the identification of networks to reveal the molecular basis of early events during pregnancy in sheep.

Data availability statement

The datasets presented in this study can be found in online repositories. The names of the repository/repositories and accession number(s) can be found below: EMBL-EBI ArrayExpress, E-MTAB-11709.

Ethics statement

The animal study was reviewed and approved by the Bahri Dagdas International Agricultural Research Institute Ethical Research Committee (Number: 29/01/2016–49-7).

Author contributions

MH, MKo, and MA designed the study. MKo, MKi, MSK, SD, MA, and MH collected the data. MKo, MH, and MA analyzed the data. MKo, MKi, MSK, IA, MH, SD, and MA wrote the manuscript. All authors approved the final version of the manuscript and accepted the submission.

Funding

The study was financially funded by Scientific and Technological Research Council of Turkey (TUBITAK) projects (214O643) to MK. This study was partially submitted to the Proceedings of the 22nd Annual Conference of the European Society for Domestic Animal Reproduction (ESDAR), Cordoba, Spain, 27–29 September 2018.

Acknowledgments

The authors thank Dr. Aydin Guzeloglu (Department of Biomedical Sciences, College of Veterinary Medicine) for the support.

Conflict of interest

The authors declare that the research was conducted in the absence of any commercial or financial relationships that could be construed as a potential conflict of interest.

Publisher's note

Supplementary material

The Supplementary Material for this article can be found online at: https://www.frontiersin.org/articles/10.3389/fgene.2022.929477/full#supplementary-material

References

Akgör, U., Ayaz, L., and Çayan, F. (2020). Expression levels of maternal plasma microRNAs in preeclamptic pregnancies, *J. Obstet. Gynaecol.* 41, 910. doi:10.1080/01443615.2020.1820465

Akira, S., and Takeda, K. (2004). Toll-like receptor signalling. *Nat. Rev. Immunol.* 4, 499–511. doi:10.1038/NRI1391

Alak, I., Hitit, M., Kose, M., Kaya, M. S., Ucar, E. H., Atli, Z., et al. (2020). Relative abundance and localization of interferon-stimulated gene 15 mRNA transcript in intra- and extra-uterine tissues during the early stages of pregnancy in sheep. *Anim. Reprod. Sci.* 216, 106347. doi:10.1016/J.ANIREPROSCI.2020.106347

Atli, M. O., Kose, M., Hitit, M., Kaya, M. S., and Bozkaya, F. (2018). Expression patterns of Toll-like receptors in the ovine corpus luteum during the early pregnancy and prostaglandin F2α-induced luteolysis. *Theriogenology* 111, 25–33. doi:10.1016/J.THERIOGENOLOGY.2018.01.010

Bartel, D. P. (2004). MicroRNAs: genomics, biogenesis, mechanism, and function. *Cell* 116, 281–297. doi:10.1016/S0092-8674(04)00045-5

Battista, M., Musto, A., Navarra, A., Minopoli, G., Russo, T., and Parisi, S. (2013). miR-125b regulates the early steps of ESC differentiation through Dies1 in a TGF-independent manner. *Int. J. Mol. Sci.* 14, 13482–13496. doi:10.3390/ijms140713482

Bazer, F. W., Song, G., Kim, J., Dunlap, K. A., Satterfield, M. C., Johnson, G. A., et al. (2012). Uterine biology in pigs and sheep. *J. Anim. Sci. Biotechnol.* 313, 23–21. doi:10.1186/2049-1891-3-23

Bidarimath, M., Khalaj, K., Wessels, J. M., and Tayade, C. (2014). MicroRNAs, immune cells and pregnancy. *Cell. Mol. Immunol.* 11, 538–547. doi:10.1038/CMI.2014.45

Bidarimath, M., Lingegowda, H., Miller, J. E., Koti, M., and Tayade, C. (2021). Insights into extracellular vesicle/exosome and miRNA mediated Bi-directional

communication during porcine pregnancy. *Front. Vet. Sci.* 8, 654064. doi:10.3389/FVETS.2021.654064

Bindea, G., Mlecnik, B., Hackl, H., Charoentong, P., Tosolini, M., Kirilovsky, A., et al. (2009). ClueGO: A Cytoscape plug-in to decipher functionally grouped gene ontology and pathway annotation networks. *Bioinformatics* 25, 1091–1093. doi:10.1093/bioinformatics/btp101

Brooks, K., Burns, G. W., Moraes, J. G. N., and Spencer, T. E. (2016). Analysis of the uterine epithelial and conceptus transcriptome and luminal fluid proteome during the peri-implantation period of pregnancy in sheep. *Biol. Reprod.* 95, 88–17. doi:10.1095/BIOLREPROD.116.141945

Burns, G., Brooks, K., Wildung, M., Navakanitworakul, R., Christenson, L. K., and Spencer, T. E. (2014). Extracellular vesicles in luminal fluid of the ovine uterus. *PLoS One* 9, e90913. doi:10.1371/JOURNAL.PONE.0090913

Cameron, A., da Silveira, J. C., Bouma, G., and Bruemmer, J. E. (2011). Evaluation of exosomes containing miRNA as an indicator of pregnancy status in the mare. *J. Equine Vet. Sci.* 31, 314–315. doi:10.1016/J.JEVS.2011.03.148

Caronia-Brown, G., Anderegg, A., and Awatramani, R. (2016). Expression and functional analysis of the Wnt/beta-catenin induced mir-135a-2 locus in embryonic forebrain development. *Neural Dev.* 11, 9–15. doi:10.1186/s13064-016-0065-y

Chakrabarty, A., Tranguch, S., Daikoku, T., Jensen, K., Furneaux, H., and Dey, S. K. (2007). MicroRNA regulation of cyclooxygenase-2 during embryo implantation. *Proc. Natl. Acad. Sci. U. S. A.* 104, 15144–15149. doi:10.1073/PNAS.0705917104

Chin, C. H., Chen, S. H., Wu, H. H., Ho, C. W., Ko, M. T., and Lin, C. Y. (2014). cytoHubba: Identifying hub objects and sub-networks from complex interactome. *BMC Syst. Biol.* 8, S11. doi:10.1186/1752-0509-8-S4-S11

Cleys, E. R., Halleran, J. L., Mcwhorter, E., Hergenreder, J., Enriquez, V. A., da Silveira, J. C., et al. (2014). Identification of microRNAs in exosomes isolated from serum and umbilical cord blood, as well as placentomes of gestational day 90 pregnant sheep. *Mol. Reprod. Dev.* 81, 983–993. doi:10.1002/MRD.22420

De Bem, T. H. C., Da Silveira, J. C., Sampaio, R. V., Sangalli, J. R., Oliveira, M. L. F., Ferreira, R. M., et al. (2017). Low levels of exosomal-miRNAs in maternal blood are associated with early pregnancy loss in cloned cattle. *Sci. Rep.* 71 7, 14319–14411. doi:10.1038/s41598-017-14616-1

Deng, L., Huang, Y., Li, L., Chen, H., and Su, J. (2020). Serum miR-29a/b expression in gestational diabetes mellitus and itsinfluence on prognosis evaluation. *J. Int. Med. Res.* 48, 300060520954763. doi:10.1177/0300060520954763

El-Shorafa, H. M., and Sharif, F. A. (2016). Dysregulation of micro-RNA contributes to the risk of unexplained recurrent pregnancy loss. *Int. J. Reprod. Contracept. Obstet. Gynecol.* 2. doi:10.5455/2320-1770.ijrcog20130914

Gebremedhn, S., Salilew-Wondim, D., Hoelker, M., Held-Hoelker, E., Neuhoff, C., Tholen, E., et al. (2018). Exploring maternal serum microRNAs during early pregnancy in cattle. *Theriogenology* 121, 196–203. doi:10.1016/J.THERIOGENOLOGY.2018.08.020

Geng, Y., Dong, Y., Yu, M., Zhang, L., Yan, X., Sun, J., et al. (2011). Follistatin-like 1 (Fstl1) is a bone morphogenetic protein (BMP) 4 signaling antagonist in controlling mouse lung development. *Proc. Natl. Acad. Sci. U. S. A.* 108, 7058–7063. doi:10.1073/PNAS.1007293108

Gool, S. W., Vandenberghe, P., Boer, M. de, and Ceuppens, J. L. (1996). CD80, CD86 and CD40 provide accessory signals in a multiple-step T-cell activation model. *Immunol. Rev.* 153, 47–83. doi:10.1111/J.1600-065X.1996.TB00920.X

Guzeloglu, A., Atli, M., Kurar, E., Kayis, S., Semacan, A., Aslan, S., et al. (2013). Preliminary expression analysis of global microRNA and biogenesis pathway in equine endometrium during the estrous cycle and early pregnancy: OC 8.1. *Reprod. Domest. Anim.* 48.

Hitit, M., Atli, M., Kurar, E., Kose, M., Guzeloglu, A., Kaya, M., et al. (2013). Investigation of microRNA biogenesis at mRNA level in bovine corpus luteum and endometrium during the oestrous cycle: P93. *Reprod. Domest. Anim.* 48.

Hitit, M., Kurar, E., and Güzeloğlu, A. (2015). *MikroRNA biyogenezi. Atatürk üniversitesi vet. Bilim. Derg.* 10. doi:10.17094/avbd.35776

Hitit, M., and Kurar, E. (2017). Putative role of micro - RNA s i n female reproductive tract. *Open Access J. Vet. Sci. Res.* 2, 1–5. doi:10.23880/OAJVSR-16000131

Ioannidis, J., and Donadeu, F. X. (2017). Changes in circulating microRNA levels can be identified as early as day 8 of pregnancy in cattle. *PLoS One* 12, e0174892. doi:10.1371/JOURNAL.PONE.0174892

Ioannidis, J., and Donadeu, F. X. (2016). Circulating miRNA signatures of early pregnancy in cattle. *BMC Genomics* 17, 184. doi:10.1186/S12864-016-2529-1

Kaczmarek, M. M., Najmula, J., Guzewska, M. M., and Przygrodzka, E. (2020). MiRNAs in the peri-implantation period: contribution to embryo-maternal communication in pigs. *Int. J. Mol. Sci.* 21, E2229. doi:10.3390/ijms21062229

Kamat, M. M., Vasudevan, S., Maalouf, S. A., Townson, D. H., Pate, J. L., and Ott, T. L. (2016). Changes in myeloid lineage cells in the uterus and peripheral blood of dairy heifers during early pregnancy. *Biol. Reprod.* 95, 68–12. doi:10.1095/biolreprod.116.141069

Kaya, M. S., Kose, M., Guzeloglu, A., Kıyma, Z., and Atli, M. O. (2017). Early pregnancy-related changes in toll-like receptors expression in ovine trophoblasts and peripheral blood leukocytes. *Theriogenology* 93, 40–45. doi:10.1016/J.THERIOGENOLOGY.2017.01.031

Kiyma, Z., Hitit, M., Ozel, C., Sen, G., Kose, M., Guzeloglu, A., et al. (2015). Preliminary investigation of microRNAs in ovine endometrium: P70. *Reprod. Domest. Anim.* 50. doi:10.1111/rda.12581

Köse, M., Kaya, M. S., and Atli, M. O. (2016c). Effect of exogenous progesterone and gonadotropin-releasing hormone application on maintenance of pregnancy in early pregnant ewes after prostaglandin F2 alpha injection. *EurasianJVetSci.* 32, 26–29. doi:10.15312/EurasianJVetSci.2016115446

Kose, M., Kaya, M. S., Aydilek, N., Kucukaslan, I., Bayril, T., Bademkiran, S., et al. (2016a). Expression profile of interferon tau–stimulated genes in ovine peripheral blood leukocytes during embryonic death. *Theriogenology* 85, 1161–1166. doi:10.1016/J.THERIOGENOLOGY.2015.11.032

Kose, M., Hitit, M., Kaya, M. S., Kirbas, M., Dursun, S., Alak, I., et al. (2022). *Expression pattern of microRNAs in ovine endometrium during the peri-implantation. Theriogenology*. doi:10.1016/j.theriogenology.2022.07.015

Kotlabova, K., Doucha, J., and Hromadnikova, I. (2011). Placental-specific microRNA in maternal circulation--identification of appropriate pregnancy-associated microRNAs with diagnostic potential. *J. Reprod. Immunol.* 89, 185–191. doi:10.1016/J.JRI.2011.02.006

Krawczynski, K., Bauersachs, S., Reliszko, Z. P., Graf, A., and Kaczmarek, M. M. (2015). Expression of microRNAs and isomiRs in the porcine endometrium: Implications for gene regulation at the maternal-conceptus interface. *BMC Genomics* 16, 906–919. doi:10.1186/s12864-015-2172-2

Lim, H.-J., Kim, H. J., Lee, J. H., Lim, D. H., Son, J. K., Kim, E.-T., et al. (2021). Identification of plasma miRNA biomarkers for pregnancy detection in dairy cattle. *J. Anim. Reprod. Biotechnol.* 36, 35–44. doi:10.12750/JARB.36.1.35

Liston, A., Papadopoulou, A. S., Danso-Abeam, D., and Dooley, J. (2012). MicroRNA-29 in the adaptive immune system: Setting the threshold. *Cell. Mol. Life Sci.* 69, 3533–3541. doi:10.1007/S00018-012-1124-0

Liu, R., Wang, M., Su, L., Li, X., Zhao, S., and Yu, M. (2015). The expression pattern of micrornas and the associated pathways involved in the development of porcine placental folds that contribute to the expansion of the exchange surface area. *Biol. Reprod.* 93, 62. doi:10.1095/biolreprod.114.126540

Liu, Z., Guo, J., Wang, Y., Weng, Z., Huang, B., Yu, M. K., et al. (2016). CFTR- β -catenin interaction regulates mouse embryonic stem cell differentiation and embryonic development. *Cell Death Differ.* 241 24, 98–110. doi:10.1038/cdd.2016.118

Livak, K. J., and Schmittgen, T. D. (2001). Analysis of relative gene expression data using real-time quantitative PCR and the 2(-Delta Delta C(T)) Method. *Methods* 25, 402–408. doi:10.1006/meth.2001.1262

Lou, W., Liu, J., Ding, B., Chen, D., Xu, L., Ding, J., et al. (2019). Identification of potential miRNA-mRNA regulatory network contributing to pathogenesis of HBV-related HCC 11 medical and health sciences 1112 oncology and carcinogenesis 06 biological Sciences 0604 Genetics. *J. Transl. Med.* 17, 1–14. doi:10.1186/S12967-018-1761-7/FIGURES/10

Lu, Q., Yan, Q., Xu, F., Li, Y., Zhao, W., Wu, C., et al. (2017). MicroRNA-873 is a potential serum biomarker for the detection of ectopic pregnancy. *Cell. Physiol. biochem.* 41, 2513–2522. doi:10.1159/000475946

Messerschmidt, D., De Vries, W. N., Lorthongpanich, C., Balu, S., Solter, D., and Knowles, B. B. (2016). β-catenin-mediated adhesion is required for successful preimplantation mouse embryo development. *Development* 143, 1993–1999. doi:10.1242/DEV.133439

Miura, K., Miura, S., Yamasaki, K., Higashijima, A., Kinoshita, A., Yoshiura, K. I., et al. (2010). Identification of pregnancy-associated microRNAs in maternal plasma. *Clin. Chem.* 56, 1767–1771. doi:10.1373/CLINCHEM.2010.147660

Ono, K., Okamoto, S., Ninomiya, C., Toji, N., Kanazawa, T., Ishiguro-Oonuma, T., et al. (2022). Analysis of circulating microRNA during early gestation in Japanese black cattle. *Domest. Anim. Endocrinol.* 79, 106706. doi:10.1016/J.DOMANIEND.2021.106706

Pfaffl, M. W., Horgan, G. W., and Dempfle, L. (2002). Relative expression software tool (REST©) for group-wise comparison and statistical analysis of relative expression results in real-time PCR. *Nucleic Acids Res.* 30, e36. doi:10.1093/NAR/30.9.E36

Reliszko, Z. P., Gajewski, Z., and Kaczmarek, M. M. (2017). Signs of embryo-maternal communication: miRNAs in the maternal serum of pregnant pigs. *Reproduction* 154, 217–228. doi:10.1530/REP-17-0224

Sánchez, J. M., Gómez-Redondo, I., Browne, J. A., Planells, B., Gutiérrez-Adán, A., and Lonergan, P. (2021). MicroRNAs in amniotic fluid and maternal blood plasma associated with sex determination and early gonad differentiation in cattle. *Biol. Reprod.* 105, 345–358. doi:10.1093/BIOLRE/IOAB079

Shi, S., Tan, Q., Liang, J., Cao, D., Wang, S., Liang, J., et al. (2021). Placental trophoblast cell-derived exosomal microRNA-1290 promotes the interaction between endometrium and embryo by targeting LHX6, *Mol. Ther. - Nucleic Acids* 26, 760–772. doi:10.1016/J.OMTN.2021.09.009/ATTACHMENT/3DEC40E6-E6C4-4605-A186-3F0015C9DD55/MMC1

Smith, M. D., Pillman, K., Jankovic-Karasoulos, T., McAninch, D., Wan, Q., Bogias, K. J., et al. (2021). Large-scale transcriptome-wide profiling of microRNAs in human placenta and maternal plasma at early to mid gestation. *RNA Biol.* 18, 507–520. doi:10.1080/15476286.2021.1963105/SUPPL_FILE/KRNB_A_1963105_SM3313

Song, Y., An, X., Zhang, L., Fu, M., Peng, J., Han, P., et al. (2015). Identification and profiling of microRNAs in goat endometrium during embryo implantation. *PLoS One* 10, e0122202. doi:10.1371/JOURNAL.PONE.0122202

Sørensen, A. E., van Poppel, M. N. M., Desoye, G., Damm, P., Simmons, D., Jensen, D. M., et al. (2021). The predictive value of miR-16, -29a and -134 for early identification of gestational diabetes: a nested analysis of the dali cohort. *Cells* 10, 170. doi:10.3390/CELLS10010170

Spencer, T. E., Johnson, G. A., Bazer, F. W., and Burghardt, R. C. (2004). Implantation mechanisms: insights from the sheep. *Reproduction* 128, 657–668. doi:10.1530/REP.1.00398

Spruce, T., Pernaute, B., Di-Gregorio, A., Cobb, B. S., Merkenschlager, M., Manzanares, M., et al. (2010). An early developmental role for miRNAs in the maintenance of extraembryonic stem cells in the mouse embryo. *Dev. Cell* 19, 207–219. doi:10.1016/J.DEVCEL.2010.07.014

Stepicheva, N., Nigam, P. A., Siddam, A. D., Fu Peng, C., and Song, J. L. (2015). microRNAs regulate β-catenin of the Wnt signaling pathway in early sea urchin development. *Dev. Biol.* 402, 127–141. doi:10.1016/j.ydbio.2015.01.008

Sun, Y., Xu, M., Gao, R., Xie, S., Sun, X., He, J., et al. (2021). Identification of differentially expressed miRNAs in serum extracellular vesicles (EVs) of Kazakh sheep at early pregnancy. *Reprod. Domest. Anim.* 56, 713–724. doi:10.1111/RDA.13910

Tan, Q., Shi, S., Liang, J., Zhang, X., Cao, D., and Wang, Z. (2020). MicroRNAs in small extracellular vesicles indicate successful embryo implantation during early pregnancy. *Cells*. doi:10.3390/CELLS90306459

Warburton, D., Bellusci, S., De Langhe, S., Del Moral, P. M., Fleury, V., Mailleux, A., et al. (2005). Molecular mechanisms of early lung specification and branching morphogenesis. *Pediatr. Res.* 577 57, 26R-37R–37R. doi:10.1203/01.PDR.0000159570.01327.ED

Wb, N. (2016). Non-coding RNAs in uterine development, function and disease. *Adv. Exp. Med. Biol.* 886, 171–189. doi:10.1007/978-94-017-7417-8_9

Yan, C., Lv, H., Peng, Z., Yang, D., Shen, P., Yu, J., et al. (2021). Analysis of miRNA expression changes in bovine endometrial stromal cells treated with lipopolysaccharide. *Theriogenology* 167, 85–93. doi:10.1016/J.THERIOGENOLOGY.2021.03.012

Zang, X., Zhou, C., Wang, W., Gan, J., Li, Y., Liu, D., et al. (2021). Differential MicroRNA expression involved in endometrial receptivity of goats. *Biomolecules* 202111, 472. doi:10.3390/BIOM11030472

Zhao, L., Haili, Y., Rong, Z., Haoyu, T., Cheng, W., et al. (2021). Screening and identification of microRNAs from plasma-derived extracellular vesicles (EVs) of dazu black goat (Capra hircus) in early pregnant stages. *Gene* 790, 145706. doi:10.1016/J.GENE.2021.145706

Zong, L., Zheng, S., Meng, Y., Tang, W., Li, D., Wang, Z., et al. (2021). Integrated transcriptomic analysis of the miRNA–mRNA interaction network in thin endometrium. *Front. Genet.* 12, 183. doi:10.3389/fgene.2021.589408

frontiers | Frontiers in Genetics

TYPE Original Research
PUBLISHED 26 August 2022
DOI 10.3389/fgene.2022.973252

OPEN ACCESS

EDITED BY
Ye Wang,
Peking University, China

REVIEWED BY
Guanglin Li,
Shaanxi Normal University, China
Wenzheng Bao,
Xuzhou University of Technology, China

*CORRESPONDENCE
Olanrewaju B. Morenikeji,
obm3@pitt.edu

†These authors share senior authorship

SPECIALTY SECTION
This article was submitted to RNA, a section of the journal Frontiers in Genetics

RECEIVED 19 June 2022
ACCEPTED 28 July 2022
PUBLISHED 26 August 2022

CITATION
Morenikeji OB, Adegbaju MS, Okoh OS, Babalola AE, Grytsay A, Braimah OA, Akinyemi MO and Thomas BN (2022), Deciphering inhibitory mechanism of coronavirus replication through host miRNAs-RNA-dependent RNA polymerase interactome.
Front. Genet. 13:973252.
doi: 10.3389/fgene.2022.973252

Deciphering inhibitory mechanism of coronavirus replication through host miRNAs-RNA-dependent RNA polymerase interactome

Olanrewaju B. Morenikeji[1*†], Muyiwa S. Adegbaju[2], Olayinka S. Okoh[3], Asegunloluwa E. Babalola[4], Anastasia Grytsay[1], Olubumi A. Braimah[1], Mabel O. Akinyemi[5†] and Bolaji N. Thomas[6†]

[1]Division of Biological and Health Sciences, University of Pittsburgh at Bradford, Bradford, PA, United States, [2]Institute for Plant Biotechnology, Stellenbosch University, Stellenbosch, South Africa, [3]Department of Chemical Sciences, Anchor University, Lagos, Nigeria, [4]Department of Mathematical Sciences, Anchor University, Lagos, Nigeria, [5]Department of Biological Sciences, Fairleigh Dickinson University, Madison, NJ, United States, [6]Department of Biomedical Sciences, Rochester Institute of Technology, Rochester, NY, United States

Despite what we know so far, Covid-19, caused by SARS-CoV-2 virus, remains a pandemic that still require urgent healthcare intervention. The frequent mutations of the SARS-CoV-2 virus has rendered disease control with vaccines and antiviral drugs quite challenging, with newer variants surfacing constantly. There is therefore the need for newer, effective and efficacious drugs against coronaviruses. Considering the central role of RNA dependent, RNA polymerase (RdRp) as an enzyme necessary for the virus life cycle and its conservation among coronaviruses, we investigated potential host miRNAs that can be employed as broad-range antiviral drugs averse to coronaviruses, with particular emphasis on BCoV, MERS-CoV, SARS-CoV and SARS-CoV-2. miRNAs are small molecules capable of binding mRNA and regulate expression at transcriptional or translational levels. Our hypothesis is that host miRNAs have the potential of blocking coronavirus replication through miRNA-RdRp mRNA interaction. To investigate this, we retrieved the open reading frame (ORF1ab) nucleotide sequences and used them to interrogate miRNA databases for miRNAs that can bind them. We employed various bioinformatics tools to predict and identify the most effective host miRNAs. In all, we found 27 miRNAs that target RdRp mRNA sequence of multiple coronaviruses, of which three - hsa-miR-1283, hsa-miR-579-3p, and hsa-miR-664b-3p target BCoV, SARS-CoV and SARS-CoV-2. Additionally, hsa-miR-374a-5p has three bovine miRNA homologs viz bta-miR-374a, bta-miR-374b, and bta-miR-374c. Inhibiting the expression of RdRp enzyme *via* non-coding RNA is novel and of great therapeutic importance in the control of coronavirus replication, and could serve as a broad-spectrum antiviral, with hsa-miR-1283, hsa-miR-579-3p, and hsa-miR-664b-3p as highly promising.

KEYWORDS
miRNA, RNA-dependent RNA polymerase, prediction, markers, regulation, coronavirus

Introduction

The diseases caused by SARS-CoV-2, a member of the Coronaviridae family, have had profound impact on all human endeavors, leaving hardship, death and destruction in its trail (Aftab et al., 2020). The rate of transmission of SARS-CoV-2 from person to person is the major driver of the significant morbidity and mortality attendant to Covid-19 and its pandemic form (Gao et al., 2020; Walls et al., 2020). After a successful entry into the host, viral replication is another important step to its pathogenicity and transmission. A large portion of coronavirus genome encodes open reading frame (ORF) 1a/1b (Figure 1), which produces two precursor polyproteins (pp1a) and (pp1ab), dedicated to code for multiple enzymes among which is RNA dependent, RNA polymerase (RdRp). Each of these precursor polyproteins are subsequently cleaved into non-structural proteins (nsp). The pp1ab is cleaved into 16 nsps, of which nsp12 or RNA dependent, RNA polymerase (RdRp) is one, and pivotal for successful virus replication in the host (Gao et al., 2020). In addition, formation of protein complex between RdRp protein, nsp seven and nsp eight have been reported, as the latter duo serve as cofactor for RdRp (Kirchdoerfer and Ward, 2019; Gao et al., 2020). Except for retroviruses, most RNA viruses require the activity of RdRp protein for viral replication and may explain why its active site is the most conserved among these viruses (Aftab et al., 2020), thereby making it a prominent target for drug development.

Several vaccines have now been developed and approved for use to limit COVID-19 infection in humans. However, their safety and long-term efficacy against SARS-CoV-2 is not guaranteed (Saha et al., 2021). Other strategies recommended for treating disease include inhibition of RdRp activity using antiviral agents like the nucleoside analogues, Favipiravir, Galidesivir, and Remdesivir, and other plant-based compounds such as Tellimagrandin I, Saikosaponin B2,

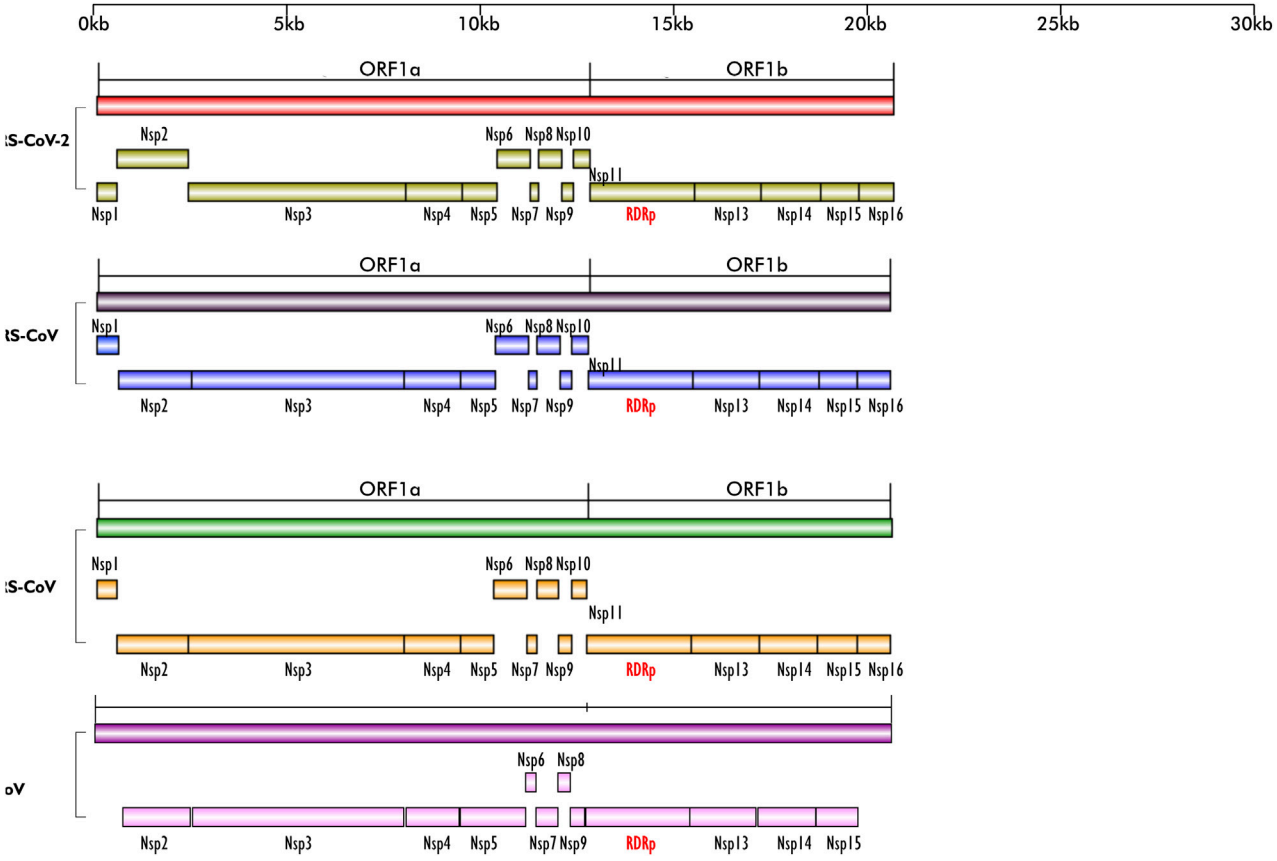

FIGURE 1
Schematics of the ORF1a and ORF1b regions of the genomes of SARS-CoV-2, MERS-CoV, SARS-CoV and BCoV; their encoded non-structural proteins (nsp) and RdRp layered on one another for easy comparison. The region is highly conserved in the four viruses; except for BCoV which does not have nsp1. All the nsps are present in the four viruses and they are arranged in the same sequence/order. Figures created with sketch pad.

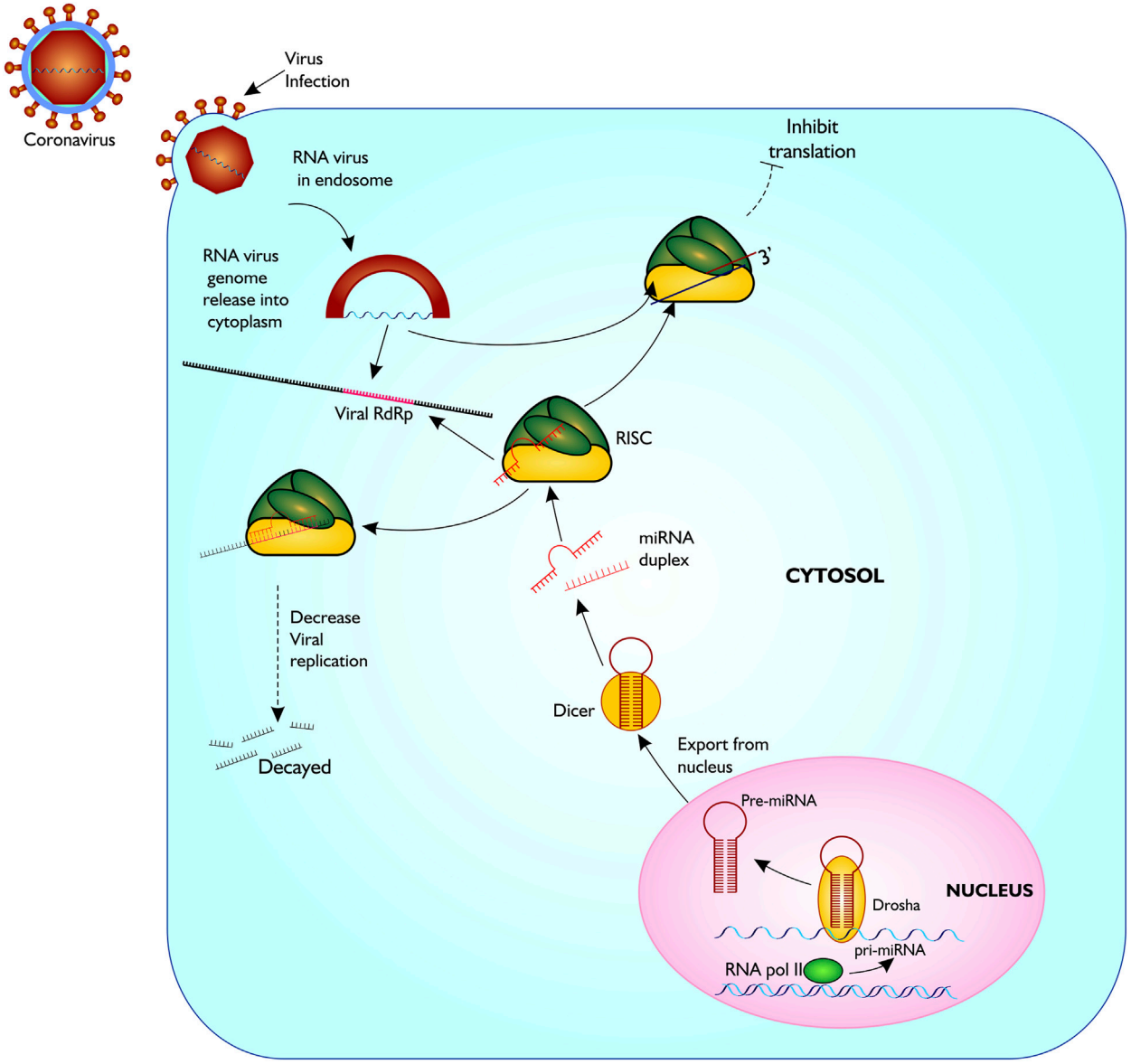

FIGURE 2
Proposed model of miRNA biogenesis and base pairing with coronavirus RdRp mRNA sequence. The figure gives a description of coronavirus infection on host cell, and release of host miRNA to base pair and degrade the virus or inhibit translation. Figure created with sketch pad.

Hesperidin and Epigallocatechin gallate (Saha et al., 2021). So far, these antiviral drugs have been reported to be ineffective against SARS-CoV-2, possibly due to single nucleotide polymorphism (SNP)-induced changes culminating in conformational, structural and functional amino acids changes and the high virus mutation rate. Therefore, alternate therapeutic options that are effective against the virus must be explored. Here, we propose an alternative option that utilizes blocking RdRp transcript *via* host microRNAs thereby inhibiting translation of the most important protein for viral replication, leading to reduced viral propagation and pathogenicity (Figure 2).

MicroRNAs are short non-coding RNAs, of about 23 nucleotides transcribe by RNA polymerase II from the genome of an organism (Trobaugh and Klimstra, 2017). They control several cellular operations at pre- and posttranscription by taking on target transcripts such as host mRNA and RNAs from the genome of pathogens, *via* sequence-specific interlink, influencing the function and/or stability of these targets (Morenikeji et al., 2020; Tucker et al., 2021). Several studies have shown the involvement of miRNAs in regulation of host immune responses. The use of machine learning and bioinformatic tools is pivotal in understanding pre- and post- translational regulation of

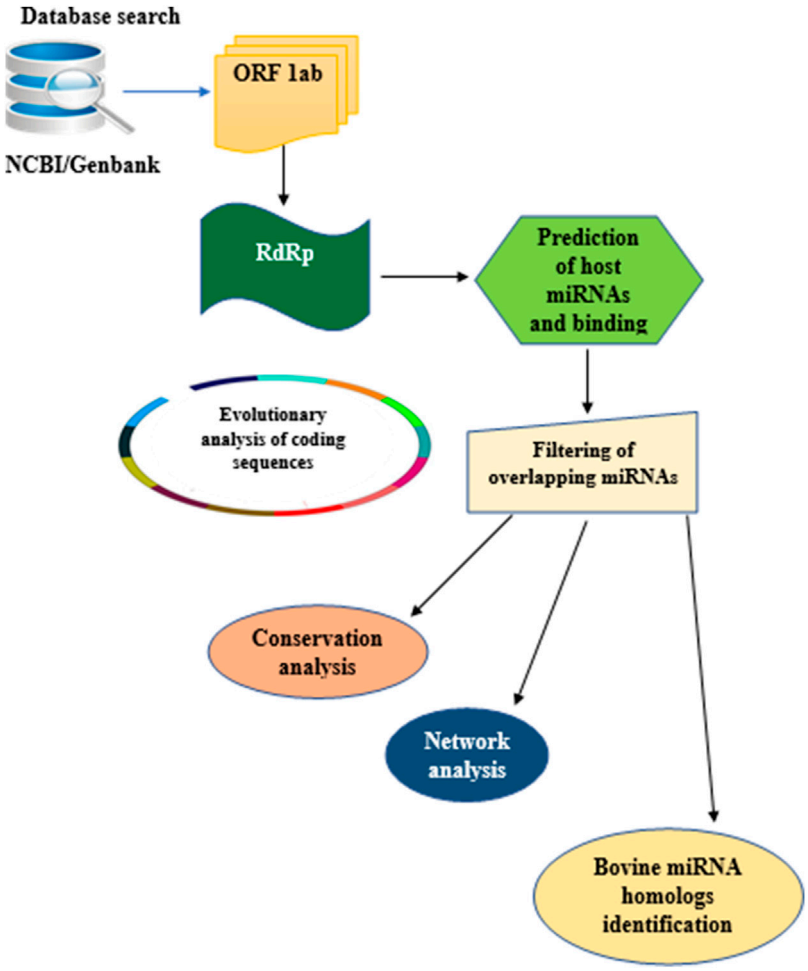

FIGURE 3
Flow chart of methodology used for the study. Step by Step pipeline for elucidating host miRNA–viral RdRp interaction.

genes and many biological processes (Bao et al., 2018). Morenikeji et al. (2020) demonstrated *via in silico* analysis that certain bovine miRNAs are involved in regulating specific immune response genes associated with Bovine coronavirus (BCoV) infection and were identified as drug targets and diagnostic biomarker for the virus. Additionally, miRNAs such as gga-miR-1603 and gga-miR-1794 were found in chicken binding the L gene region of Newcastle Disease virus, causing viral degradation and inhibiting replication *in vitro* (Chen et al., 2021). In humans, decrease in viral replication, translation and transmission from person to person due to binding of certain miRNAs to the genome of viruses such as Human immunodeficiency virus (HIV), Enterovirus 71 (E 71) and Human T cell leukemia virus, type I (HTLV-1) have also been reported (Nathans et al., 2009; Zheng et al., 2013; Bai and Nicot 2015). More evidence on the involvement of miRNA in altering viral replication and pathogenesis have continued to emerge (Ingle et al., 2015; Khongnomnan et al., 2015; Trobaugh and Klimstra, 2017), but none of these studies have examined the role of miRNA in inhibiting coronavirus replication through RdRp nucleotide sequence, showing the importance of our study.

Considering the significant role of RdRp in viral replication and survival, we elucidated host miRNAs that can bind mRNA of RdRp in four coronaviruses, resulting in its disintegration, thereby controlling the replication and pathogenesis of RNA viruses and opening a new door to therapeutic targets for coronaviruses.

Materials and methods

Sequence mining of RNA-dependent RNA polymerase region from the genome of various coronaviruses

In this study, the analytical pipeline employed, starting from sequence curation to interactome networks, is a slight modification of our previously described model (Figure 3),

(Morenikeji et al., 2020, 2021; Tucker et al., 2021). Since RdRp is one of the 16 non-structural proteins encoded by ORF1ab gene of coronaviruses, we carried out an extensive search for ORF1ab gene of 13 selected coronaviruses, whose genomes have either been fully or partially annotated. The corresponding nucleotide sequences and accession numbers were retrieved from NCBI GenBank (https://www.ncbi.nlm.nih.gov/genbank/). These viruses are: SARS-CoV (NC_004718.3), SARS-CoV-2 (NC_045512.2), tylonycteris bat coronavirus (NC_009019.1), MERS-CoV (NC_019843.3), duck coronavirus (NC_048214.1), Canada goose coronavirus (NC_046965.1), BCoV (NC_003045.1), betacoronavirus England 1 (NC_038294.1), alphacoronavirus (NC_046964.1), bat coronavirus (NC_034440.1), pipistrellus bat (NC_009020.1), rabbit coronavirus (NC_017083.1), rodent and coronavirus (NC_046954.1).

Evolutionary analysis of RNA-dependent RNA polymerase in 13 coronaviruses

To determine the evolutionary relationship and distance of the RdRp region from the 13 coronaviruses, we constructed a phylogenetic tree using https://ngphylogeny.fr/ with the following workflow. Preliminary multiple sequence alignment (MSA) was generated using MAFFT, followed by trimming of the MSA to focus on the informative regions using block mapping and gathering with entropy (BMGE) (Criscuolo and Gribaldo, 2010). The phylogenetic tree was inferred using PhyML (Guindon et al., 2010) and tree visualization carried out with interactive tree of life (iTol) (https://itol.embl.de). Using the MSA generated by BMGE, pairwise distance between the RdRp of the 13 coronaviruses was computed using MEGA X (Kumar et al., 2018).

Prediction and network of miRNA binding sites in the RNA-dependent RNA polymerase region of BCoV, MERS-CoV, SARS-CoV and SARS-CoV-2

To examine whether host cellular miRNA can target coronavirus RdRp, we selected four common coronaviruses in human and cattle for further analysis. Potential miRNA binding sites in the RdRp nucleotide sequences of BCoV, MERS-CoV, SAR-CoV and SARS-Cov-2 were predicted using mirDB software (http://mirdb.org). Each of the RdRp sequences from the four coronaviruses were used as the target sequence with human genome selected as the reference for miRNA prediction. After each prediction, miRNAs with a score of 60 and above were considered significant and selected for further analysis. The list of miRNAs from each coronavirus were intersected with Bioinformatic and Evolutionary Genomics (BEG) Venn diagram generator (http://bioinformatics.psb.ugent.be/webtools/Venn/). Based on the complementary base pairing of miRNAs and RdRp mRNA and the value of normalized binding free energy (ndG), possible miRNA-mRNA interactome network connections were determined using Cytoscape version 3.7.2, as previously described (Morenikeji et al., 2020; Tucker et al., 2021). To search for possible homologs of human miRNAs in the bovine genome, we searched the miRNA database (https://mirbase.org). The sequence of each of the top 25 miRNAs selected were used as query against the *Bos taurus* genome on mirDB (http://mirdb.org). Homologous bovine miRNAs were extracted and recorded for further analysis.

Results

Dataset of RNA-dependent RNA polymerase nucleotides from the genome of 13 coronaviruses

Our search for nucleotide sequences encoding RdRp in coronaviruses using the keyword "1 ab polyprotein" initially yielded about 59 organisms. After filtering for only coronaviruses, 13 viruses, whose genomes were either fully or partially annotated were subsequently selected for further analyses. The sequences encoding RdRp regions of tylonycteris bat coronavirus, MERS-CoV, duck coronavirus, SARS-CoV, Canada goose coronavirus, BCoV, betacoronavirus England 1, alphacoronavirus, bat coronavirus, SARS-CoV-2, pipistrellus bat, rabbit coronavirus and rodent coronavirus were identified to be within the ORF1ab gene (Table 1). Since RdRp protein is categorized to be one of the cleaved 16 non-structural proteins encoded by ORF1ab gene, its coding region which falls between nsp11 and nsp 13, is beyond the coding region of ORF1a gene, which partially overlaps with ORF1ab gene and encodes variants of nsp1 to nsp9 (Figure 1). Each of the 13 coronaviruses' RdRp nucleotide sequences were extracted and added to the pipeline (Figure 3) to determine their evolutionary relationship.

Evolutionary relatedness of RNA-dependent RNA polymerase coding sequences

To confirm that RdRp coding sequence is conserved among the coronaviruses, we examined their evolutionary relatedness through pairwise distance and phylogenetic analysis. The nucleotide sequence analysis of RdRp reveals minor variation across the 13 viruses though sharing common evolutionary origin (Figure 4). Two viruses, MERS-CoV and Betacoronavirus England 1, are not different from each other in this region, showing a pairwise distance of 0.00 (Table 2). Similarly, comparing the RdRp sequences of bat coronavirus with either MERS-CoV or Betacoronavirus England one indicated some

TABLE 1 List of coronavirus species; accession number of their ORF1ab gene, genome location and the location of RdRp coding sequence within ORF1ab genome location.

S/N	Virus	Accession number	Genome location of ORF1ab	Location of RdRp within ORF1ab
1	Tylonycteris bat CoV	NC_009019.1	267–21625	13553–16327
2	SARS-CoV	NC_004718.3	265..21485	13401–16163
3	MERS-CoV	NC_019843.3	279–21514	13410–16207
4	Duck coronavirus	NC_048214.1	347..20364	12211–15071
5	Bovine coronavirus	NC_003045.1	211..21494	13318–16100
6	Canada goose CoV	NC_046965.1	554..20085	11971–14786
7	Betacoronavirus England 1	NC_038294.1	278–21513	13400–16185
8	Alphacoronavirus Bat-CoV	NC_046964.1	281–20175	12136–14885
9	Bat CoV	NC_034440.1		13156–15970
10	Pipistrellus bat coronavirus	NC_009020.1	261–21808	13661–16332
11	Rabbit coronavirus	NC_017083.1	209–21663	13483–16270
12	Rodent coronavirus	NC_046954.1	211–21596	13386–16201
13	SARS-CoV-2	NC_045512.2	266–21555	13430–16221

level of closeness with a value of 0.18. A similar close relatedness was observed for SARS-CoV and SARS-CoV-2 having a pairwise distance of 0.29. Alphacoronavirus is the most distantly related from the rest of the viruses, showing consistent higher value for the pairwise distance, further supported by the phylogenetic tree analysis (Figure 4).

Open reading frame 1ab is conserved in BCoV, MERS-CoV, SARS-CoV and SARS-CoV-2

From the genome organization of BCoV, MERS-CoV, SARS-CoV and SARS-CoV-2 (Figure 1), ORF1ab in the viruses are very similar, indicating high level of conservation in this gene making it an excellent antiviral drug candidate. To ascertain the degree of conservation in BCoV, MERS-CoV, SARS-CoV and SARS-CoV-2, the well annotated ORF1ab genes of each of the viruses were overlayed on one another and compared. Comparing the gene across the viruses, we found that ORF1ab is highly conserved across the viruses as no conspicuous difference was noted in the arrangement of all the non-structural proteins and RdRp (Figure 1), emphasizing the choice of this region of RdRp as an excellent potential antiviral drug target.

Identification of miRNA binding to RNA-dependent RNA polymerase of BCoV, MERS-CoV, SARS-CoV and SARS-CoV-2

In this analysis, BCoV, MERS-CoV, SARS-CoV and SARS-CoV-2 miRNAs that bind to the RNA-dependent RNA polymerase (RdRp) of coronaviruses were examined. A total of one hundred and three (103) miRNAs were obtained for BCoV, seventy-eight (78) for MERS-CoV, fifty-seven (57) for SARS-CoV, and ninety-seven (97) for SARS-CoV-2. To ensure the binding of miRNAs to RdRp target, significant miRNAs were filtered based on the ranking scores as described above. The filtering generated a total of sixty-six (66) miRNAs for BCoV, forty-one (41) for MERS-CoV, twenty-nine (29) for SARS-CoV and fifty-three (53) for SARS-CoV-2 (Figure 5). The results of complementary binding of human miRNAs to the RdRp sequence for each of the four coronaviruses were intersected to identify broad-spectrum miRNAs, which can possibly inhibit viral replication. As shown, there was no miRNA that concomitantly bind to the RdRp region of all four viruses (Figure 6A). However, we uncovered three miRNAs; hsa-miR-1283, hsa-miR-664b-3p and hsa-miR-579-3p that could bind to this region in BCoV, SARS-CoV and SARS-CoV-2 (Table 3; Figure 6B). Similarly, miRNAs that could bind to the region in at least two coronaviruses were identified, ranging from as low as one (hsa-miR-8081) for MERS-CoV and SARS-CoV to as high as nine (hsa-miR-585-5p, hsa-miR-7159-5p, hsa-miR-1305, hsa-miR-15a-5p, hsa-miR-6507-5p, hsa-miR-16-5p, hsa-miR-3065-5p, hsa-miR-195-5p and hsa-miR-15b-5p) for BCoV and MERS-CoV (Table 3).

Interestingly, there was no miRNA concomitantly binding RdRp region in both MERS-CoV and SARS-CoV-2 (Figure 6A). The identity of the connections of miRNAs and RdRp between four coronaviruses (BCoV, MERS-CoV, SARS-CoV and SARS-CoV-2) are depicted through a network as shown (Figure 6B). This interactome reveals a possible molecular mechanism for regulating multiple coronavirus replication through miRNAs binding RdRp mRNA. Network of different nodes were created based on all identified miRNAs and potential binding sites on RdRp mRNA, while the network edges were determined through the value ndGs and correlation between each RNA.

FIGURE 4
Phylogenetic tree showing the evolutionary relationship of 13 coronaviruses. Tree was constructed using MEGA X.

From Table 3, it is shown that 27 human miRNAs targeted multiple viruses from BCoV, MERS-CoV, SARS-CoV and SARS-CoV-2. Of particular importance, among these 27 miRNAs are three miRNAs (hsa-miR-1283, hsa-miR-579-3p and hsa-miR-664b-3p) that are predicted to target BCoV, SARS-CoV and SARS-CoV-2. Additionally, we report five miRNAs targeting SARS-CoV and SARS-CoV-2, while another five targeted BCoV and SARS-CoV.

TABLE 2 Genetic pairwise distance of the 13 coronaviruses used in the study.

	Tylonycteris bat coronavirus	SARS-CoV	MERS CoV	Duck coronavirus	Canada goose coronavirus	B-CoV	Beta-Coronavirus england 1	Alpha-Coronavirus bat	Bat coronavirus	Pipistrellus bat coronavirus	Rabbit coronavirus	Rodent coronavirus	SARS-CoV-2
Tylonycteris bat coronavirus													
SARS-Cov	4.36												
MERS-CoV	1.8	4.25											
Duck coronavirus	4.85	5.27	4.83										
Canada goose coronavirus	4.89	5.17	4.81	2.34									
B-CoV	4.48	4.92	4.52	5.28	5.14								
Beta-coronavirus England 1	1.8	4.27	0	4.86	4.84	4.55							
Alpha-coronavirus bat	5.1	5.32	5.13	4.99	5.11	5.51	5.13						
Bat coronavirus	1.75	4.33	0.18	4.76	4.93	4.58	0.18	4.98					
Pipistrellus bat coronavirus	1.57	4.43	1.56	5.11	5.14	4.61	1.62	5.41	1.54				
Rabbit coronavirus	4.49	4.95	4.57	5.26	5.24	0.2	4.6	5.51	4.59	4.63			
Rodent coronavirus	4.57	4.83	4.58	5.26	5.21	0.57	4.61	5.44	4.56	4.71	0.54		
SARS-Cov-2	4.27	0.29	3.97	5.21	5.07	4.8	3.99	5.27	4.21	4.34	4.73	4.65	

The least distance is 0; which is between MERS-CoV and Beta coronavirus England one; while 5.51 is the highest pairwise genetic distance and this is between BCoV and Alpha coronavirus bat; and between Alpha-coronavirus bat and rabbit coronavirus.

10.3389/fgene.2022.973252

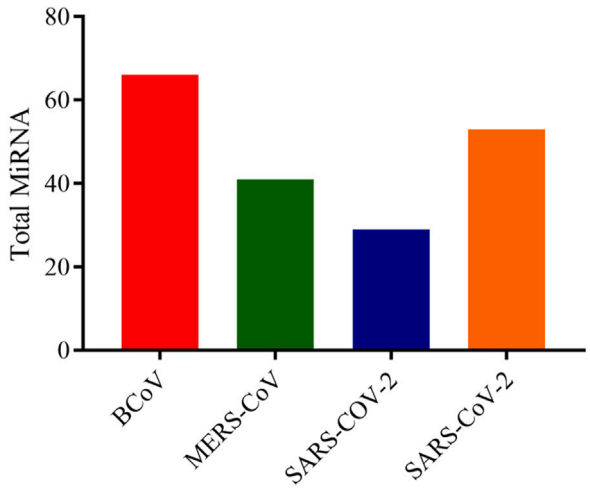

FIGURE 5
Bar chart showing the number of predicted human miRNA that can bind with the ORF1ab region of each of BCoV, MERS-CoV, SARS-CoV and SARS-CoV-2. Figure created with graphpad.

Human miRNA homologs found in bovine genome target RNA-dependent RNA polymerase mRNA sequences

Of the top 25 human miRNAs selected for further analysis, eight has bovine miRNA homologs as shown (Table 4). Interestingly, one of the human miRNAs, hsa-miR-374a-5p, had three bovine miRNA homologs including bta-miR-374a, bta-miR-374b, and bta-miR-374c. hsa-miR-3065-5p has two bovine homologs - bta-miR-338 and bta-miR-3065, while others have one homolog each. In all, we report 13 bovine homologs, and two of them, bta-miR-196a and bta-miR-338 are read in reverse direction while eleven are forward stranded.

Discussion

The genome arrangement of coronaviruses is similar and of particular importance is the open reading frame 1 ab (ORF1ab) gene, which encodes 1 ab polyprotein, a protein precursor that is further cleaved into sixteen non-structural proteins (nsps). One of the sixteen nsps is RdRp that plays a vital role in RNA virus replication (Aftab et al., 2020; Gao et al., 2020; Jiang et al., 2021). RdRp protein is a promising candidate for drug target for treating diseases caused by coronavirus because the active site is highly conserved and the protein lacks homologous counterparts in host cell (Jiang et al., 2021). Medical interventions in form of mRNA vaccines and antiviral drugs have been developed and approved to treat coronavirus disease such as Covid-19, but many of these drugs are still undergoing clinical trials. The concept behind antiviral drugs for treating Covid-19 and other diseases caused by RNA viruses is to identify compounds which can bind to active site of the RdRp enzymes and prevent its catalytic activity, which leads to viral replication (Markland et al., 2000; Yang et al., 2011; Elfiky 2016; Elfiky et al., 2017; Elfiky and Ismail 2019; Ezat et al., 2019; Wang et al., 2020). However,

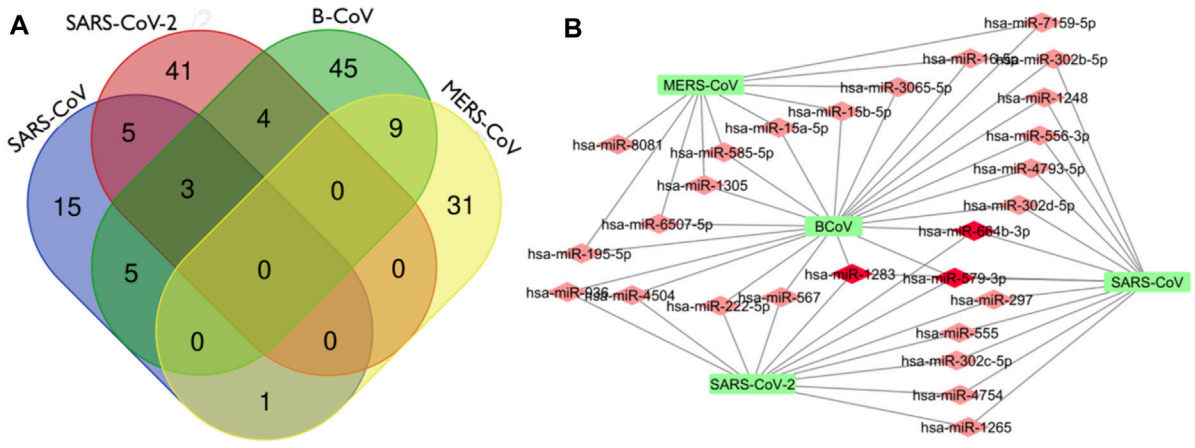

FIGURE 6
Venn Diagram (http://bioinformatics.psb.ugent.be/webtools/Venn/) showing the number of predicted human miRNA that can target multiple coronaviruses. The number in the intersection/overlapping regions represent the number of miRNAs that can concomitantly target the coronaviruses represented by the intersected shape **(A)**. Network connections among miRNAs and RdRp of SARS_CoV, B_CoV, MERS_CoV and SARS_CoV-2. **(B)** Generated using Cytoscape 3.7.2.

TABLE 3 Predicted miRNAs with regions of complementarity in multiple coronaviruses from BCoV, MERS-CoV, SARS-CoV and SARS-CoV-2.

RdRp from virus	Number of intercepts	miRNA
|B_Cov | SARS_Cov | SARS_Cov2 |	3	hsa-miR-1283 hsa-miR-579-3p hsa-miR-664b-3p
| SARS_Cov | SARS_Cov2 |	5	hsa-miR-4754 hsa-miR-555 hsa-miR-297 hsa-miR-1265 hsa-miR-302c-5p
|B_Cov | SARS_Cov |	5	hsa-miR-4793-5p hsa-miR-302b-5p hsa-miR-556-3p hsa-miR-1248 hsa-miR-302d-5p
| MERS_CoV | SARS_Cov |	1	hsa-miR-8081
B_Cov SARS_Cov2	4	hsa-miR-4504 hsa-miR-222-5p hsa-miR-567 hsa-miR-936
B_Cov MERS_CoV	9	hsa-miR-7159-5p hsa-miR-585-5p hsa-miR-1305 hsa-miR-195-5p hsa-miR-6507-5p hsa-miR-3065-5p hsa-miR-15a-5p hsa-miR-15b-5p hsa-miR-16-5p

Number of intercepts show the number of miRNAs, with complementary region.

TABLE 4 Predicted human miRNAs that have bovine miRNA homologs, their size and strands.

miRNA	Seed location	Bovine homolog	Size	Strand
hsa-miR-196a-1-3p	229, 1027, 1413, 1765, 1940	bta-miR-196a	3 to 20	-
hsa-miR-654-5p	1387	bta-miR-380-5p	1 to 22	+
hsa-miR-541-3p	1387	bta-miR-541	1 to 22	+
hsa-miR-374a-5p	1047, 1362, 1370	bta-miR-374a	1 to 22	+
		bta-miR-374b	2 to 22	+
		bta-miR-373c	1 to 21	+
hsa-miR-664b-3p	1628, 2626	bta-miR-664b	3 to 23	+
hsa-miR-545-5p	830, 2750	bta-miR-545-5p	1 to 21	+
hsa-miR-374b-5p	1047, 1362, 1370	bta-miR-374b	1 to 22	+
		bta-miR-374a	1 to 22	+
		bta-miR-374c	1 to 21	+
hsa-miR-3065-5p	227, 512, 1025	bta-miR-338	1 to 23	-
		bta-miR-3065	1 to 23	+

The seed location is with respect to the human miRNA, while the size and strand are the bovine miRNAs—strand miRNAs are read in reverse direction.

major concern on the efficacy of the antiviral drugs remains, necessitating exploring alternative options, including preventing RdRp protein translation. To our knowledge, the use of non-coding RNA such as miRNAs as an alternative route has not been explored as antiviral drug option. Since miRNA can bind directly to the genome of RNA virus or cause changes in the host transcriptome facilitated by the virus, it is noteworthy that finding host miRNA that can bind directly to the RdRp region of coronaviruses may provide insight on effective manipulation to control viral replication/load in the host and provide a remarkable alternative treatment.

To have an effective antiviral drug, it is important that a virus target be conserved. Therefore, we identify the conservation of miRNA binding site in the RdRp sequence of multiple coronaviruses through evolutionary analysis. First, 13 annotated RdRp nucleotide sequences were used to define the conservation of this region and construct a phylogenetic tree. Most of the viral species examined belong to the betacoronavirus subfamily, with our result showing high similarity between them, revealing this region as a potential drug target. Interestingly, the pairwise distance between MERS-CoV and Betacoronavirus England one show no difference in this region for both viruses, indicating that they are likely to have the same binding site for host miRNAs. A close similarity in the RdRp region of SARS-CoV and SARS-CoV-2 shows the virus evolved from a common origin, in agreement with previous findings (Aftab et al., 2020; Wu et al., 2020). The genetic conservation of RdRp gene across multiple viruses shows a strong positive selection for this region and justifies the fact that the enzyme coded by this region is important for almost all RNA virus replication, strengthening its choice for miRNA drug targeting. It is puzzling that the magnitude of the difference in pathogenicity, rate of transmission and virulence between SARS-CoV and SARS-CoV-2 is only caused by single nucleotide mutations (Ceraolo and Giorgi, 2020; Kruse, 2020; Lu et al., 2020; Nguyen et al., 2020; Wang et al., 2020). Thus, the slight difference in the pairwise distance as observed between the RdRp sequences of SARS-CoV and SARS-

CoV-2 may have remarkable implications on the number of miRNAs which can bind concomitantly with both viruses. Several regions of RNA viruses mutate at a faster rate as a mechanism to escape host immune system reaction. However, a slower mutation rate at the RdRp region means a miRNA could be broad spectrum antiviral drug for many viruses.

Remarkably, our study uncovered several miRNAs that bound to the RdRp sequence of coronaviruses including BcoV, MERS-CoV, SARS-CoV andSARS-CoV-2. The presence of human miRNA homologs in bovine genome is of great importance as this is indicative of the crucial functional role these miRNAs play has been preserved by evolutionary forces or selection. Additionally, some of the miRNAs have multiple binding sites within the RdRp region thereby increasing the binding probability and reducing off-target effects, strengthening their choice for possible antiviral molecule. This is contrary to the submission of Thorg et al. (2017), which stated that the common location of the miRNA binding site is the untranslated regions of the viral genome. Conversely, our results align with a similar study in chicken that identified multiple miRNA binding sites within the L gene of the NDV and infectious bursal disease virus (IBDV), reporting that the overexpression of ggam-miR-21 inhibits VP1 translation in chicken fibroblasts and suppresses overall viral replication (Chen et al., 2021).

We identified some miRNAs including hsa-miR-1283, hsa-miR-664b-3p, hsa-miR-579-3p, which targeted multiple regions in the RdRp sequence of BCoV, SARS-CoV, and SARS-CoV-2; these miRNAs have been previously linked with onco-protective roles, indicating their growth regulatory function. For example, hsa-miR-1283 has been connected with cardio-protection and inhibition of apoptosis (Liu et al., 2021), thereby blocking oncogenesis. In addition, this miRNA has also been implicated in hypertension (Chen et al., 2021). hsa-miR-579-3p, on the other hand has been reported to be associated with growth control and tumor suppression *via* control of melanoma progression (Fattore et al., 2016; Kalhori et al., 2019), while hsa-miR-664b-3p is reported to play a critical role in regulating cancer progression (Liu et al., 2020). From our study, an upregulation or administration of any of the three miRNAs might play a dual role of blocking viral replication/degradation and inhibition of cancer progression.

Conclusion

In summary, we utilized several computational approaches to examine genome plasticity and elucidate potential host miRNAs that could bind to the RdRp sequence region of coronaviruses. Although viral genome is known to be variable, we report high conservation of RdRp sequence in multiple coronaviruses, indicating evolutionary favorability, hence a candidate signature for genome targeting. In all, this study also provide an insight into possible alternative route for targeting and inhibiting viral replication *via* host non-coding RNA (miRNAs) to combat disease rather than common anti-coronavirus drug, based on inhibiting RdRp enzymatic activities. In particular, hsa-miR-1283, hsa-miR-664b-3p, hsa-miR-579-3p and hsa-miR-374a-5p with bovine homologs bta-miR-374a, bta-miR-374b, and bta-miR-374c are very promising. This study opens the door for developing non-coding RNAs as a broad-spectrum antiviral therapy and lays a foundation for further investigation to validate the effective binding of identified miRNAs to RdRp sequences of coronaviruses through *in vivo* or *in vitro* analysis.

Data availability statement

The original contributions presented in the study are included in the article/Supplementary Material, further inquiries can be directed to the corresponding author.

Author contributions

OM conceptualized and designed the experiments; MA, OO, AB, and OM carried out the experiments, analyzed the data and drafted the manuscript; MA, OO, AG, OB, MA, BT, and OM revised the manuscript, contributed to the discussion and scientific content. All authors read and approved the final version of the manuscript.

Acknowledgments

OBM and AG were supported by Pitt-Momentum Fund of the University of Pittsburgh. Ongoing support by the Division of Biological and Health Sciences, Pitt-Bradford, College of Health Sciences and Technology, Rochester Institute of Technology is acknowledged, APC charges for this article were fully paid by the University Library System, University of Pittsburgh.

Conflict of interest

The authors declare that the research was conducted in the absence of any commercial or financial relationships that could be construed as a potential conflict of interest.

Publisher's note

All claims expressed in this article are solely those of the authors and do not necessarily represent those

of their affiliated organizations, or those of the publisher, the editors and the reviewers. Any product that may be evaluated in this article, or claim that may be made by its manufacturer, is not guaranteed or endorsed by the publisher.

Supplementary material

The Supplementary Material for this article can be found online at: https://www.frontiersin.org/articles/10.3389/fgene.2022.973252/full#supplementary-material

References

Aftab, S. O., Ghouri, M. Z., Masood, M. U., Haider, Z., Khan, Z., Ahmad, A., et al. (2020). Analysis of SARS-CoV-2 RNA-dependent RNA polymerase as a potential therapeutic drug target using a computational approach. *J. Transl. Med.* 18 (1), 275. doi:10.1186/s12967-020-02439-0

Bai, X. T., and Nicot, C. (2015). miR-28-3p is a cellular restriction factor that inhibits human T cell leukemia virus, type 1 (HTLV-1) replication and virus infection. *J. Biol. Chem.* 290, 5381–5390. doi:10.1074/jbc.M114.626325

Bao, W., Yuan, C-A., Zhang, Y., Han, K., Nandi, A. K., Honig, B., et al. (2018). Mutli-features prediction of protein translational modification sites. *IEEE/ACM Trans. Comput. Biol. Bioinform.* 15, 1453–1460. doi:10.1109/TCBB.2017.2752703

Ceraolo, C., and Giorgi, F. M. (2020). Genomic variance of the 2019-nCoV coronavirus. *J. Med. Virol.* 92 (5), 522–528. doi:10.1002/jmv.25700

Chen, W., Liu, T., Liang, Q., Chen, X., Tao, W., Fang, M., et al. (2021). miR-1283 contributes to endoplasmic reticulum stress in the development of hypertension through the activating transcription factor-4 (ATF4)/C/EBP-Homologous protein (CHOP) signaling pathway. *Med. Sci. Monit.* 27, e930552–1. doi:10.12659/MSM.930552

Chen, Y., Zhu, S., Hu, J., Hu, Z., Liu, X., Wang, X., et al. (2021). gga-miR-1603 and gga-miR-1794 directly target viral L gene and function as a broad-spectrum antiviral factor against NDV replication. *Virulence* 12 (1), 45–56. doi:10.1080/21505594.2020.1864136

Criscuolo, A., and Gribaldo, S. (2010). BMGE (block mapping and gathering with entropy): a new software for selection of phylogenetic informative regions from multiple sequence alignments. *BMC Evol. Biol.* 10, 210. doi:10.1186/1471-2148-10-210

Elfiky, A. A., and Ismail, A. (2019). Molecular dynamics and docking reveal the potency of novel GTP derivatives against RNA-dependent RNA polymerase of genotype 4a HCV. *Life Sci.* 238, 116958. doi:10.1016/j.lfs.2019.116958

Elfiky, A. A., Mahdy, S. M., and Elshemey, W. M. (2017). Quantitative structure-activity relationship and molecular docking revealed a potency of anti-hepatitis C virus drugs against human corona viruses. *J. Med. Virol.* 89 (6), 1040–1047. doi:10.1002/jmv.24736

Elfiky, A. A. (2016). Zika viral polymerase inhibition using anti-HCV drugs both in market and under clinical trials. *J. Med. Virol.* 88 (12), 2044–2051. doi:10.1002/jmv.24678

Ezat, A. A., Elfiky, A. A., Elshemey, W. M., and Saleh, N. A. (2019). Novel inhibitors against wild-type and mutated HCV NS3 serine protease: An *in silico* study. *VirusDisease* 30 (2), 207–213. doi:10.1007/s13337-019-00516-7

Fattore, L., Mancini, R., Acunzo, M., Romano, G., Laganà, A., Pisanu, M. E., et al. (2016). miR-579-3p controls melanoma progression and resistance to target therapy. *Proc. Natl. Acad. Sci. U. S. A.* 113 (34), E5005–E5013. doi:10.1073/pnas.1607753113

Gao, Y., Yan, L., Huang, Y., Liu, F., Zhao, Y., Cao, L., et al. (2020). Structure of the RNA-dependent RNA polymerase from COVID-19 virus. *Science* 368 (6492), 779–782. doi:10.1126/science.abb7498

Guindon, S., Dufayard, J. F., Lefort, V., Anisimova, M., Hordijk, W., and Gascuel, O. (2010). New algorithms and methods to estimate maximum-likelihood phylogenies: Assessing the performance of PhyML 3.0. *Syst. Biol.* 59, 307–321. doi:10.1093/sysbio/syq010

Ingle, H., Kumar, S., Raut, A. A., Mishra, A., Kulkarni, D. D., Kameyama, Tet al., et al. (2015). The microRNA miR-485 targets host and influenza virus transcripts to regulate antiviral immunity and restrict viral replication. *Sci. Signal.* 8 (406), ra126. doi:10.1126/scisignal.aab3183

Jiang, Y., Yin, W., and Xu, H. E. (2021). RNA-dependent RNA polymerase: Structure, mechanism, and drug discovery for COVID-19. *Biochem. Biophys. Res. Commun.* 538, 47–53. doi:10.1016/j.bbrc.2020.08.116

Kalhori, M. R., Irani, S., Soleimani, M., Arefian, E., and Kouhkan, F. (2019). The effect of miR-579 on the PI3K/AKT pathway in human glioblastoma PTEN mutant cell lines. *J. Cell. Biochem.* 120 (10), 16760–16774. doi:10.1002/jcb.28935

Khongnomnan, K., Makkoch, J., Poomipak, W., Poovorawan, Y., and Payungporn, S. (2015). Human miR-3145 inhibits influenza a viruses replication by targeting and silencing viral PB1 gene. *Exp. Biol. Med.* 240 (12), 1630–1639. doi:10.1177/1535370215589051

Kirchdoerfer, R. N., and Ward, A. B. (2019). Structure of the SARS-CoV nsp12 polymerase bound to nsp7 and nsp8 co-factors. *Nat. Commun.* 10, 2342. doi:10.1038/s41467-019-10280-3

Kruse, R. L. (2020). Therapeutic strategies in an outbreak scenario to treat the novel coronavirus originating in Wuhan, China. *F1000Res.* 9, 72. doi:10.12688/f1000research.22211.2

Kumar, S., Stecher, G., Li, M., Knyaz, C., and Tamura, K. (2018). Mega X: Molecular evolutionary genetics analysis across computing platforms. *Mol. Biol. Evol.* 35, 1547–1549. doi:10.1093/molbev/msy096

Liu, C., Liu, H., Sun, Q., and Zhang, P. (2021). MicroRNA 1283 alleviates cardiomyocyte damage caused by hypoxia/reoxygenation via targeting GADD45A and inactivating the JNK and p38 MAPK signaling pathways. *Kardiol. Pol.* 79 (2), 147–155. doi:10.33963/KP.15696

Liu, T., Meng, W., Cao, H., Chi, W., Zhao, L., Cui, W., et al. (2020). lncRNA RASSF8-AS1 suppresses the progression of laryngeal squamous cell carcinoma via targeting the miR-664b-3p/TLE1 axis. *Oncol. Rep.* 44 (5), 2031–2044. doi:10.3892/or.2020.7771

Lu, R., Zhao, X., Li, J., Niu, P., Yang, B., Wu, H., et al. (2020). Genomic characterisation and epidemiology of 2019 novel coronavirus: Implications for virus origins and receptor binding. *Lancet* 395 (10224), 565–574. doi:10.1016/S0140-6736(20)30251-8

Markland, W., McQuaid, T. J., Jain, J., and Kwong, A. D. (2000). Broad-spectrum antiviral activity of the IMP dehydrogenase inhibitor VX-497: A comparison with ribavirin and demonstration of antiviral additivity with alpha interferon. *Antimicrob. Agents Chemother.* 44 (4), 859–866. doi:10.1128/AAC.44.4.859-866.2000

Morenikeji, O. B., Bernard, K., Strutton, E., Wallace, M., and Thomas, B. N. (2021). Evolutionarily conserved long non-coding RNA regulates gene expression in cytokine storm during COVID-19. *Front. Bioeng. Biotechnol.* 8. doi:10.3389/fbioe.2020.582953

Morenikeji, O. B., Wallace, M., Strutton, E., Bernard, K., and Thomas, B. N. (2020). Integrative network analysis of predicted miRNA-targets regulating expression of immune response genes in bovine coronavirus infection. *Front. Genet.* 11, 584392. doi:10.3389/fgene.2020.584392

Nathans, R., Chu, C. Y., Serquina, A. K., Lu, C. C., Cao, H., and Rana, T. M. (2009). Cellular microRNA and P bodies modulate host-HIV-1 interactions. *Mol. Cell* 34, 696–709. doi:10.1016/j.molcel.2009.06.003

Nguyen, T. M., Zhang, Y., and Pandolfi, P. P. (2020). Virus against virus: a potential treatment for 2019-nCov (SARS-CoV-2) and other RNA viruses. *Cell Res.* 30 (3), 189–190. doi:10.1038/s41422-020-0290-0

Saha, S., Nandi, R., Vishwakarma, P., Prakash, A., and Kumar, D. (2021). Discovering potential RNA dependent RNA polymerase inhibitors as prospective drugs against COVID-19: an *in silico* approach. *Front. Pharmacol.* 12, 634047. doi:10.3389/fphar.2021.634047

tenOever, B, R. (2013). RNA viruses and the host microRNA machinery. *Nat. Rev. Microbiol.* 11, 169–180. doi:10.1038/nrmicro2971

Trobaugh, D. W., and Klimstra, W. B. (2017). MicroRNA regulation of RNA virus replication and pathogenesis. *Trends Mol. Med.* 23 (1), 80–93. doi:10.1016/j.molmed.2016.11.003

Tucker, A. R., Salazar, N. A., Ayoola, A. O., Memili, E., Thomas, B. N., and Morenikeji, O. B. (2021). Regulatory network of miRNA, lncRNA, transcription factor and target immune response genes in bovine mastitis. *Sci. Rep.* 11 (1), 21899. doi:10.1038/s41598-021-01280-9

Walls, A. C., Park, Y. J., Tortorici, M. A., Wall, A., McGuire, A. T., and Veesler, D. (2020). Structure, function, and antigenicity of the SARS-CoV-2 spike glycoprotein. *Cell* 181 (2), 281–292. e6. doi:10.1016/j.cell.2020.02.058

Wang, M., Cao, R., Zhang, L., Yang, X., Liu, J., Xu, M., et al. (2020). Remdesivir and chloroquine effectively inhibit the recently emerged novel coronavirus (2019-nCoV) *in vitro*. *Cell Res.* 30 (3), 269–271. doi:10.1038/s41422-020-0282-0

Wang, Y. S., Ouyang, W., Pan, Q, X., Wang, X. L., Xia, X. X., Bi, Z. W., et al. (2013). Overexpression of microRNA gga-miR-21 in chicken fibroblasts suppresses replication of infectious bursal disease virus through inhibiting VP1 translation. *Antivir. Res.* 100 (1), 196–201. doi:10.1016/j.antiviral.2013.08.001

Wu, A., Peng, Y., Huang, B., Ding, X., Wang, X., Niu, P., et al. (2020). Genome composition and divergence of the novel coronavirus (2019-nCoV) originating in China. *Cell Host Microbe* 27 (3), 325–328. doi:10.1016/j.chom.2020.02.001

Yang, P. L., Gao, M., Lin, K., Liu, Q., and Villareal, V. A. (2011). Anti-HCV drugs in the pipeline. *Curr. Opin. Virol.* 1 (6), 607–616. doi:10.1016/j.coviro.2011.10.019

Zheng, Z., Ke, X., Wang, M., He, S., Li, Q., Zheng, C., et al. (2013). Human microRNA hsa-miR-296-5p suppresses enterovirus 71 replication by targeting the viral genome. *J. Virol.* 87, 5645–5656. doi:10.1128/JVI.02655-12

frontiers | Frontiers in Genetics

TYPE Original Research
PUBLISHED 29 August 2022
DOI 10.3389/fgene.2022.936937

OPEN ACCESS

EDITED BY
Olanrewaju B Morenikeji,
University of Pittsburgh at Bradford,
United States

REVIEWED BY
Muyiwa Adegbaju,
Federal University of Technology,
Nigeria
Mary Aigbiremo Oboh,
Medical Research Council The Gambia
Unit (MRC), Gambia

*CORRESPONDENCE
Minghua Zhang,
gzzhangminghua@163.com

†These authors have contributed equally to this work and share first authorship.

SPECIALTY SECTION
This article was submitted to RNA, a section of the journal Frontiers in Genetics

RECEIVED 05 May 2022
ACCEPTED 18 July 2022
PUBLISHED 29 August 2022

CITATION
Zhang M, Hu Y, Li H, Guo X, Zhong J and He S (2022), miR-22-3p as a potential biomarker for coronary artery disease based on integrated bioinformatics analysis.
Front. Genet. 13:936937.
doi: 10.3389/fgene.2022.936937

miR-22-3p as a potential biomarker for coronary artery disease based on integrated bioinformatics analysis

Minghua Zhang[1*†], Yan Hu[2†], Haoda Li[3], Xiaozi Guo[3], Junhui Zhong[3] and Sha He[3]

[1]Department of Cardiovascular Medicine, Key Laboratory of Biological Targeting Diagnosis, Therapy and Rehabilitation of Guangdong Higher Education Institutes, The Fifth Affiliated Hospital, Guangzhou Medical University, Guangzhou, China, [2]Nursing Department, Key Laboratory of Biological Targeting Diagnosis, Therapy and Rehabilitation of Guangdong Higher Education Institutes, The Fifth Affiliated Hospital, Guangzhou Medical University, Guangzhou, China, [3]Key Laboratory of Biological Targeting Diagnosis, Therapy and Rehabilitation of Guangdong Higher Education Institutes, The Fifth Affiliated Hospital, Guangzhou Medical University, Guangzhou, China

Background: Coronary artery disease (CAD) is a common cardiovascular disease that has attracted attention worldwide due to its high morbidity and mortality. Recent studies have shown that abnormal microRNA (miRNA) expression is effective in CAD diagnoses and processes. However, the potential relationship between miRNAs and CAD remains unclear.

Methods: Microarray datasets GSE105449 and GSE28858 were downloaded directly from the Gene Expression Omnibus (GEO) to identify miRNAs involved in CAD. Target gene prediction and enrichment analyses were performed using Gene Ontology (GO) and Kyoto Encyclopedia of Genes and Genomes (KEGG).

Results: There were nine differentially expressed miRNAs in CAD patients compared to the controls. A total of 352 genes were predicted and subjected to GO analysis, which showed that differentially expressed genes (DEGs) were mainly associated with axon guidance, neuron projection guidance, neuron-to-neuron synapses, and postsynaptic density. According to the KEGG pathway analysis, the most enriched pathways were those involved in transcriptional misregulation in cancer, growth hormone synthesis, secretion and action, endocrine resistance, axon guidance, and Cushing syndrome. Pathway analysis was mainly involved in the HIPPO and prion disease signaling pathways. Furthermore, a competing endogenous RNA (ceRNA) interaction network centered on miR-22-3p revealed eight related transcription factors in the cardiovascular system. The receiver operating characteristic (ROC) curve analysis suggested that miR-22-3p may be a better CAD predictor.

Conclusion: The results indicate that miR-22-3p may function in pathophysiological CAD processes. Our study potentiates miR-22-3p as a specific biomarker for diagnosing CAD.

KEYWORDS
microRNA, miR-22-3p, coronary artery disease, gene expression, blood

1 Introduction

Coronary artery disease (CAD) is a cardiovascular disease with a high global morbidity and mortality rate. Globally, it has caused serious social and economic burdens and has become a major health problem (Karakas et al., 2017). Although advancements in medical technology have continuously improved CAD treatment methods, including double-chain antiplatelet, enhanced low-density lipoprotein cholesterol reduction, and coronary stent implantation, there is still a lack of one or more biomarkers with high specificity and sensitivity for early diagnosis of CAD (Thomas and Lip, 2017). Therefore, it is of great significance to find biomarkers for early diagnosis of CAD through non-invasive and convenient methods. MicroRNAs (miRNAs) are a group of naturally occurring non-coding small RNAs, 21–25 nucleotides long, which regulate the expression of target genes by specifically inhibiting or degrading the translation of target mRNAs. It has been recently discovered that detecting non-invasive biomarker miRNAs (such as miR-15b-5p, miR-29c-3p, and miR-199a-3p) can provide a powerful means for predicting and diagnosing CAD (Su et al., 2020), helping clinicians provide the best prevention and treatment plans for CAD patients as soon as possible. Biomarker miRNA detection can greatly improve the overall prognosis of CAD patients.

Selective coronary angiography (CAG) is the current gold standard for diagnosing CAD. However, this surgical method is invasive, cumbersome, and expensive. It is mainly used in the late stages of the disease when multiple blood vessels are affected or arteries are seriously stenosed (Su et al., 2020). At present, the most widely used traditional biomarkers for diagnosing coronary heart disease, such as creatine kinase MB, B-type brain natriuretic peptide precursors, and high-sensitivity troponin T/I, are affected by age, genetic background, heart-related diseases, drugs, and lifestyle and cannot be used for early diagnosis of acute myocardial infarction nor can they predict the future complications of coronary heart disease (Raggi et al., 2018; Tanase et al., 2021).

In recent years, deep sequencing and microarrays have effectively detected complex networks in the atherosclerosis process. They can be used as biomarkers in CAD patient diagnosis and prognosis (Tan et al., 2017). The combination of microarray technology and bioinformatics analysis methods can comprehensively analyze the early-to-late module of gene expression changes in atherosclerosis development (Gu et al., 2021). Gene Expression Omnibus (GEO) is a public database containing numerous human gene profiles for multiple diseases. It is commonly used to screen for differentially expressed genes (DEGs) and construct regulatory networks of gene interactions (Meng et al., 2021). Bioinformatics analysis methods can provide effective biomarker candidates for clinical trials and clinical practice (Cheng et al., 2019). Lin et al. analyzed differentially expressed long non-coding RNAs (lncRNAs) (DELs) and differentially expressed coding genes in vascular smooth muscle cells (human aortic smooth muscle cells (HASMCs)) and found that hypoxia-inducible factor-1 alpha (HIF-1α) antisense RNA2 partially inhibited HASMC proliferation through the miR-30e-5p/ccnd2 axis (Lin et al., 2021). Another bioinformatics analysis study identified miRNA-376a-3p as a novel biomarker in CAD patients (Du et al., 2020).

In this study, we downloaded the original data of CAD and healthy control samples for microarray analysis from the GEO database. We used bioinformatics analysis methods to potentiate effective candidate biomarkers and key factors for early CAD screening and prognosis determination.

2 Materials and methods

2.1 Data acquisition

The GEO query package (Kok et al., 2015) of RStudio (version 3.6.5, http://r-project.org/) was used to download the coronary heart disease expression profile datasets GSE105449 (de Ronde et al., 2017) and GSE28858 (Sondermeijer et al., 2011) using *Homo sapiens* samples. The GSE105449 dataset was used as the test set. The platform was based on GPL22949, including 38 blood samples from patients with cardiovascular disease, 25 blood specimens from healthy individuals taking cardiovascular disease drugs (control 1), and 42 blood samples from healthy individuals not taking cardiovascular disease drugs (control 2). The GSE28858 dataset was a GPL8179-based validation set and included 12 blood samples from patients with cardiovascular disease and 12 blood samples from normal subjects (Table 1). We processed the raw data from the GSE105449 and GSE28858 datasets *via* the "affy" package (Gautier et al., 2004) and background-corrected and normalized the data. The gene expression matrices of the two datasets were obtained separately. The effect of inter-sample correction was demonstrated by plotting BOX and principal components analysis (PCA) with the "ggplot2" package (Wilkinson, 2011).

2.2 Boxplot analysis of the hsa-miR-22-3p gene

The hsa-miR-22-3p gene expression distribution values under different groups in the GSE105449 and GSE28858 datasets were visualized using a boxplot.

TABLE 1 Information of two datasets.

Dataset	Platforms	Organism	Source	CVD	Control
GSE105449	GPL22949	Homo sapiens	monocyte	38	25 (1) 42 (2)
GSE28858	GPL8179	Homo sapiens	platelets	12	12

CVD, Cardiovascular disease.
(1), Monocytes CTRL after medication
(2), Monocytes CTRL without medication

2.3 Receiver operating characteristic (ROC) analysis of the hsa-miR-22-3p gene

The GSE105449 and GSE28858 datasets were analyzed using the pROC package to construct a hsa-miR-22-3p molecular expression and prediction outcome model using the area under the ROC curve (AUC) to analyze prediction efficacy. The AUC value is the total area covered by the ROC curve. A larger AUC value indicated a better classifier.

2.4 DEG screening

We screened the GSE105449 dataset for DEGs by downloading the "limma" package (Ritchie et al., 2015), and heatmaps were drawn using the pheatmap package (Kolde, 2019) to show the differential distribution of sample DEGs. The DEG volcano maps were illustrated using the "ggplot2" package to present the differential expression of DEGs.

2.5 miRNA and mRNA network analysis and functional analysis

The miRWalk database (Dweep and Gretz, 2015) predicted nine DEGs, and the DEGs were demonstrated using Target Scan's gene list. DEG Gene Ontology (GO) and Kyoto Encyclopedia of Genes and Genomes (KEGG) pathway enrichment analyses were performed using the clusterProfiler package (Yu et al., 2012), and $p < 0.05$ was considered statistically significant. The DIANA TOOLS database showed pathway maps for pathways enriched in KEGGs (Vlachos et al., 2015).

2.6 DEGs and lncRNA network analysis

Possible lncRNAs for DEGs were predicted from the starBase v2.0 database (Ma et al., 2015), screening experimental grade >1. DEGs correlated with miRNAs, and lncRNAs were visualized using Cytoscape.

2.7 DEGs and transcription factor network analysis

We predicted the possible transcription factors of DEGs from the TransmiRv2.0 database (http://www.cuilab.cn/transmir) and visualized DEGs with transcription factors and the tissue association results using Cytoscape.

2.8 Statistical analysis

All data processing and analyses were performed using R software (version 4.0.2). For comparisons between two groups of continuous variables that conformed to a normal distribution, an independent Student's *t*-test was used to determine whether the variables were statistically different. For comparisons between non-normally distributed variables, a Mann–Whitney U-test (i.e., Wilcoxon rank-sum test) was used to analyze whether there was a statistical difference. Statistical significance between the two sets of categorical variables was compared and analyzed using a chi-square test or Fisher's exact probability test. The correlation coefficients between different genes were determined using Pearson's correlation analysis. All statistical *p*-values were two-sided, and statistical significance was set at $p < 0.05$.

3 Results

3.1 DEG screening

Supplementary Figure S1 shows the boxplots illustrating GSE105449 and GSE28858, and Figure S2 displays the PCA plots. Their findings showed that the samples of the two groups clustered more obviously after preprocessing, indicating that the samples were obtained from reliable sources. The GSE105449 dataset consisted of the case, control 1, and control 2 groups. The expression of miR-22-3p in the three groups of samples was detected and plotted with a box diagram (Figure 1A) and heat map (Figure 1B). In the case group, the disease groups were divided into high- and low-expression groups based on the median miR-22-3p value, and volcano plot analysis was performed to obtain nine DEGs: hsa-miR-365a-3p, hsa-miR-22-3p, hsa-miR-1274b_v16.0, hsa-miR-505-3p, hsa-miR-892b, hsa-miR-1305, hsa-miR-720, hsa-miR-129-1-3p, and hsa-miR-1288 (Figure 1C). The case group versus control 1 group and case group versus control 2 group DEGs were obtained using the "limma" package, and a Venn diagram displays the three-part genes (Figure 1D).

The GSE28858 dataset was used as the validation set and included the case and control groups. Hsa-miR-22-3p expression in the samples of both groups was extracted, as the boxplot (Figure 2A) and heatmap (Figure 2B) show. In the case group, the median hsa-miR-22-3p value was used to divide the high- and low-expression

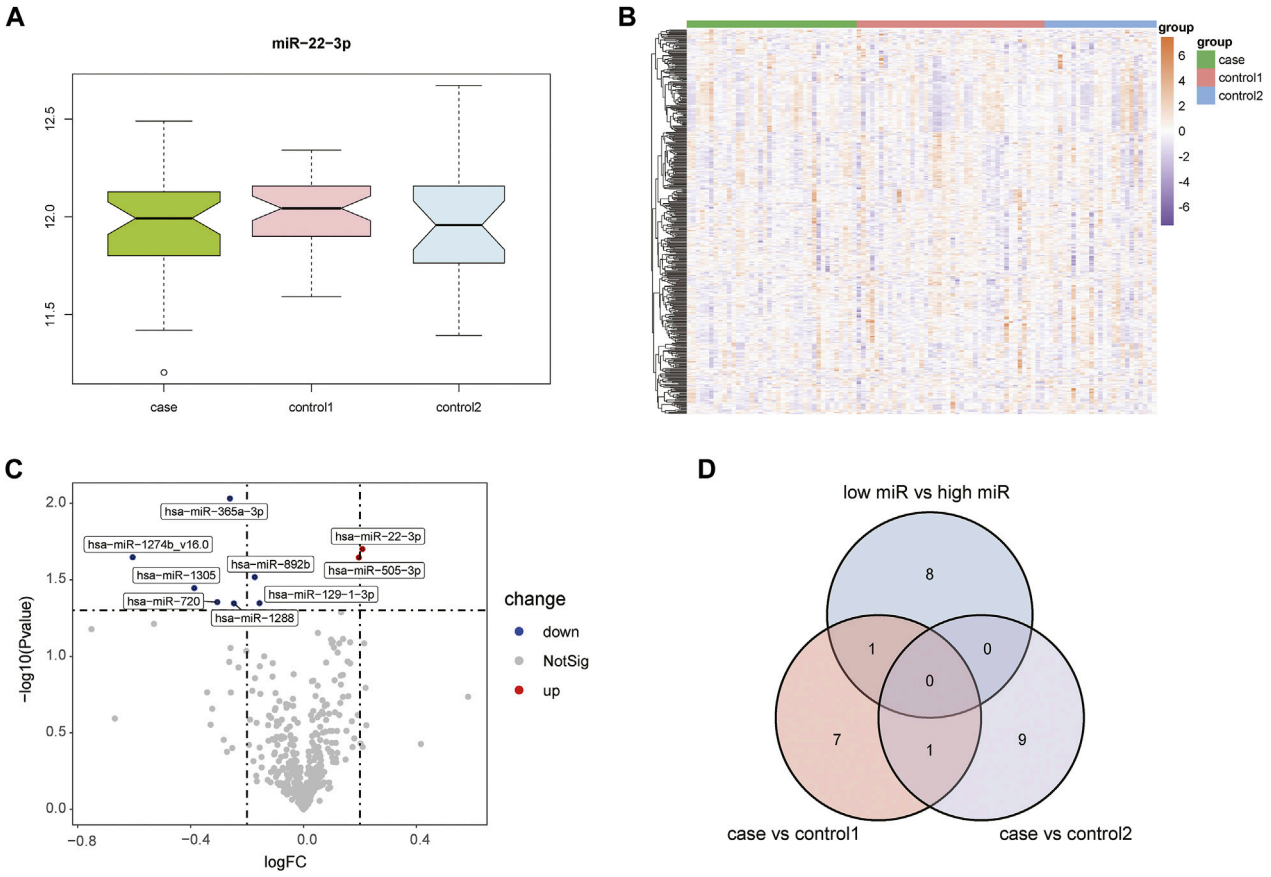

FIGURE 1
Acquisition of DEGs from the GSE105449 dataset. **(A)** Boxplot showing miR-22-3p expression. **(B)** Heatmap showing the mRNA expression profiles of case samples, control 1 and control 2. **(C)** Volcano map of DEGs. Red, green, and gray represent upregulated differential genes, downregulated differential genes, and no differential genes, respectively. **(D)** Venn diagram of overlapping DEGs from the intersection of two independent groups.

groups, and volcano plot analysis was performed to obtain 216 DEGs (Figure 2C). The Venn diagrams of the common differentially expressed miRNAs in both datasets detail this (Figure 2D).

3.2 Correlation analysis of DEGs

The miRWalk website was used for DEG target gene prediction, and three DEGs (hsa-miR-22-3p, hsa-miR-129-1-3p, and hsa-miR-365a-3p) were included, with a validation level of 352 target genes predicted for enrichment analysis. GO analysis showed that the DEGs were mainly associated with axon guidance, neuron projection guidance, neuron-to-neuron synapses, and postsynaptic density (Figures 3A–D). Supplementary Table S1 details the results. The KEGG analysis (Figures 3E,F) revealed that the pathways enriched by DEGs mainly included transcriptional misregulation in cancer, growth hormone synthesis, secretion and action, endocrine resistance, axon guidance, and Cushing syndrome. Pathview-enriched pathways mainly involved the HIPPO signaling and prion disease pathways (Figures 4A,B).

3.3 Analysis of the competing endogenous RNA interaction network

The ceRNA interaction network of mRNA–miRNA-long intergenic non-coding RNA (lincRNA) was constructed using miR-22-3p as the center. As Figure 5A shows, 37 possible lncRNAs for DEGs were predicted by Starbase V2.0, and 142 possible lncRNAs for DEGs were predicted by the miRWalk database. Potential transcription factors for DEGs were predicted using the TransmiR v2.0 database (Figure 5B) for various tissues, such as the heart, kidney, and liver. A total of eight associated transcription factors, CCCTC-binding factor (CTCF), JUN, JUND, NFATC1, NFE2L2, RAD21, RELA, and TAL1, were identified in the cardiovascular system.

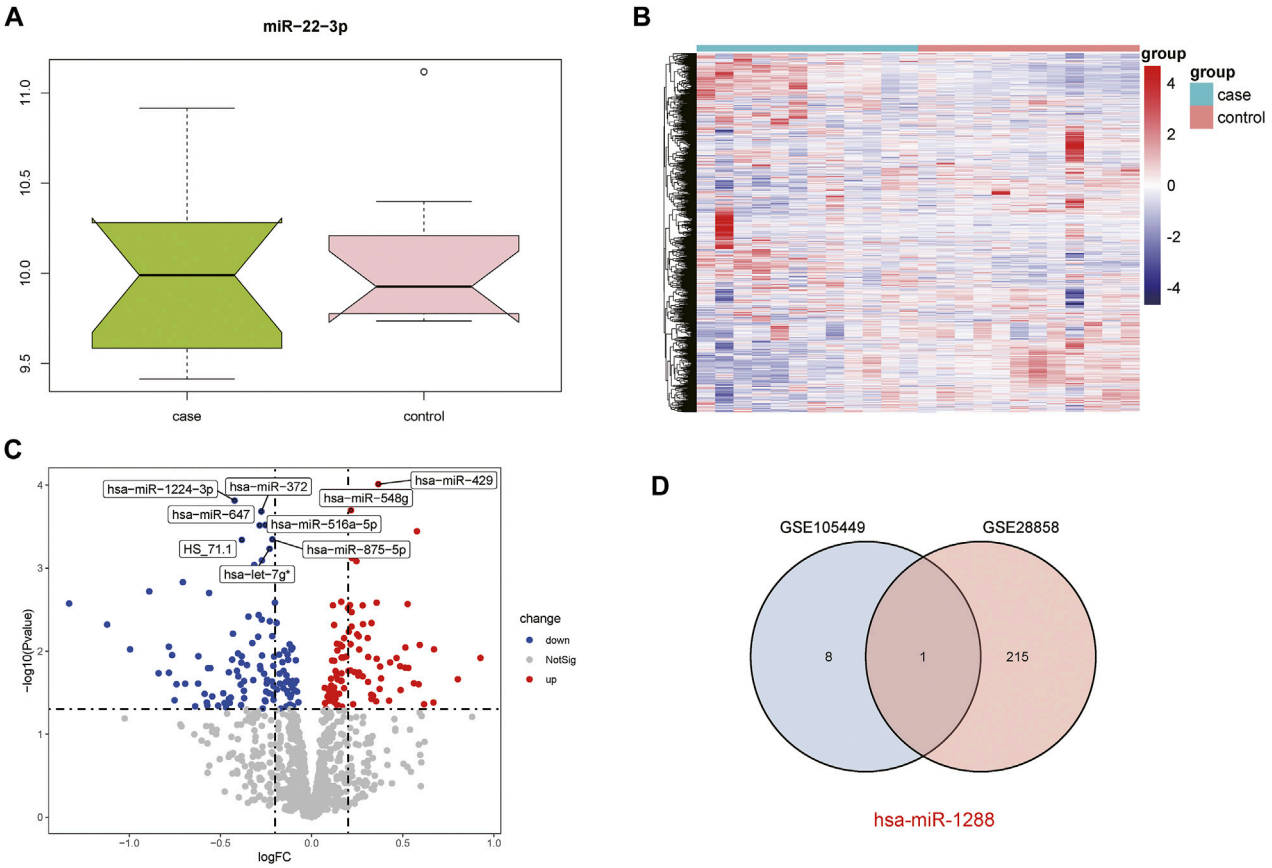

FIGURE 2
Acquisition of DEGs from the GSE28858 dataset. **(A)** Boxplot showing miR-22-3p expression. **(B)** Heatmap showing the mRNA expression profiles of case samples, control 1 and control 2. **(C)** DEG volcano map. Red, green, and gray represent upregulated differential genes, downregulated differential genes, and no differential genes, respectively. **(D)** Venn diagram of overlapping DEGs from the intersection of two independent datasets GSE105449 and GSE28858.

3.4 ROC curve analysis

ROC curves of the GSE105449 and GSE28858 datasets were constructed with miR-22-3p as the center. The area under the AUC curve of GSE105449 was 0.719 (Figure 6A), whereas the area under the AUC curve of the GSE28858 validation set was 0.642 (Figure 6B).

4 Discussion

Numerous studies have found that miRNAs play a large role in cell differentiation, biological development, and disease development. Evidence indicated that circulating miRNAs are crucial in CAD progression (Mayr et al., 2021). However, there is no consensus regarding which miRNAs are clinically relevant for cardiovascular disease expression. miR-22-3p was first discovered as a miRNA with antitumor properties (Pandey and Picard, 2009). Previous studies have reported that miR-22-3p is abundantly expressed in the heart (Hu et al., 2012), where it is vital in vascular remodeling (Zheng and Xu, 2014) and cardiac hypertrophy (Gurha et al., 2012a; Huang et al., 2013). Our previous research confirmed that miR-22-3p directly targeting the transcription factor specificity protein 1 (Sp1) suppresses vascular smooth muscle cell proliferation and migration and vascular neointima formation (Zhang et al., 2020). Zeng et al. (2021) reported that circular RNA circMAP3K5 acts as a miRNA-22-3p sponge and the circMAP3K5/miR-22-3p/TET2 axis may be a potential target for endothelial proliferation-related diseases, including revascularization and atherosclerosis. Recent studies have reported dysregulation of signal transducer and activator of transcription 1 (STAT1), miR-150, miR-223, miR-21, and miR-25 in the peripheral blood mononuclear cells (PBMCs) of patients with definite CAD (Nariman-Saleh-Fam et al., 2019; Saadatian et al., 2019). Another study suggested that miR-22-3p was downregulated in CAD patients and promoted CAD progression by targeting the inflammatory response-related factor monocyte chemoattractant protein-1 (MCP-1) (Chen et al., 2016). The present studies on miRNAs are controversial and inconsistent, and the mechanisms

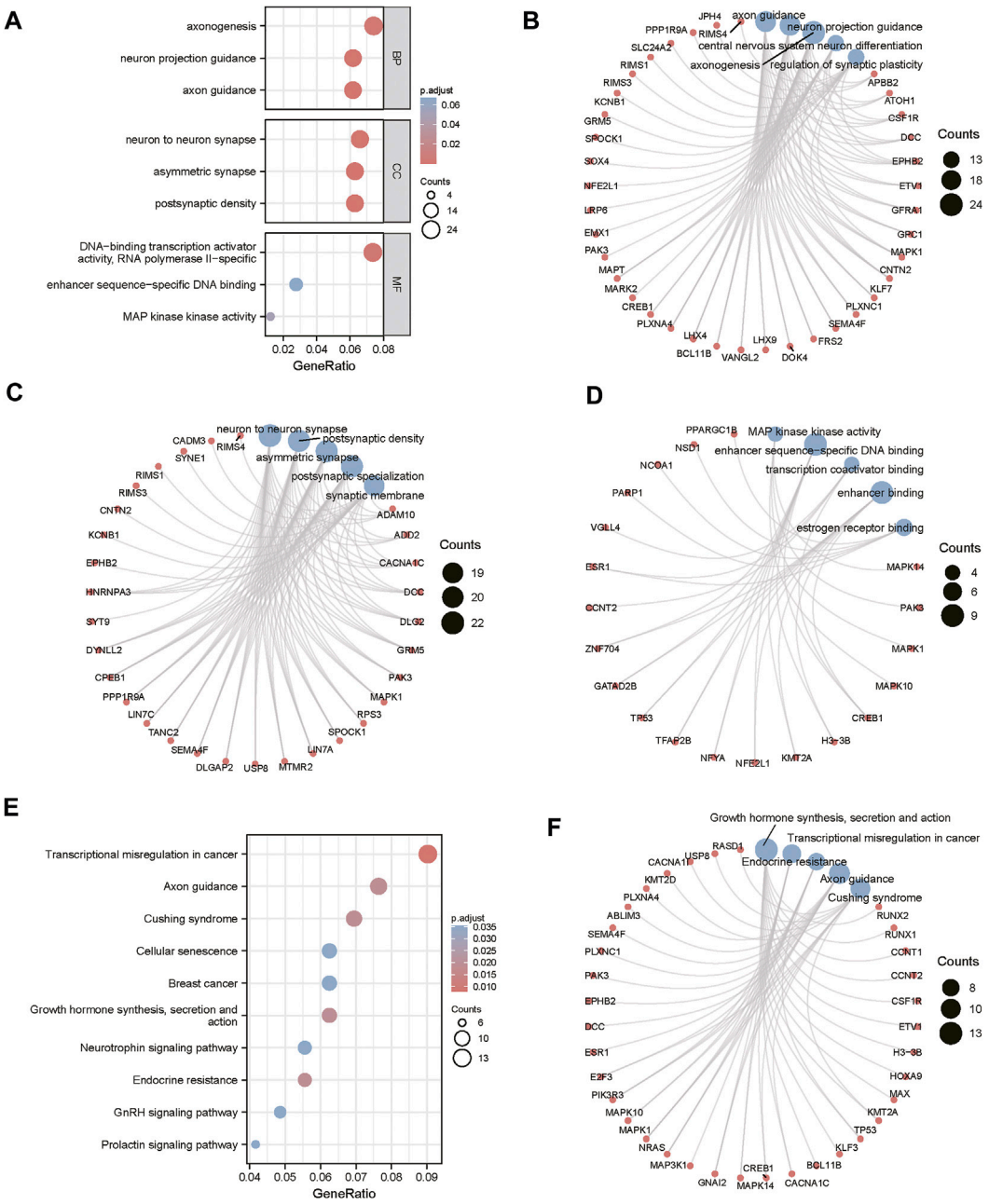

FIGURE 3
Functional correlation analysis of DEGs. **(A)** Functional enrichment analysis of the overall biology of GO. The X horizontal axis indicates the proportion of DEGs enriched in the GO terms, and the color of the dots shows the significant *p*-value: the redder the color, the smaller the corrected *p*-value; the bluer the color, the larger the corrected *p*-value. The size of the dots represents the number of enriched genes. **(B)** BP functional enrichment analysis; the color of the dots indicates the |logFC| of the genes. **(C)** CC functional enrichment analysis. **(D)** MF functional enrichment analysis. **(E)** KEGG pathway enrichment analysis. **(F)** Top five KEGG-enriched signaling pathways and related genes.

and potential significance of miRNAs regulating CAD-associated gene levels remain unclear (Zhelankin et al., 2021).

In this study, we identified potential miRNAs for the diagnosis and treatment of coronary heart disease based on two GEO datasets by analyzing differences in the expression of critical genes. However, the present study observed that PBMC miR-22-3p was increased in CAD patients compared to healthy control individuals (control 1 and control 2), suggesting that miR-22-3p upregulation might be crucial in the early stages of disease progression.

Three sets of DEGs (hsa-miR-22-3p, hsa-miR-129-1-3p, and hsa-miR-365a-3p) were subjected to functional enrichment analysis. The aforementioned three miRNAs have been studied in the context

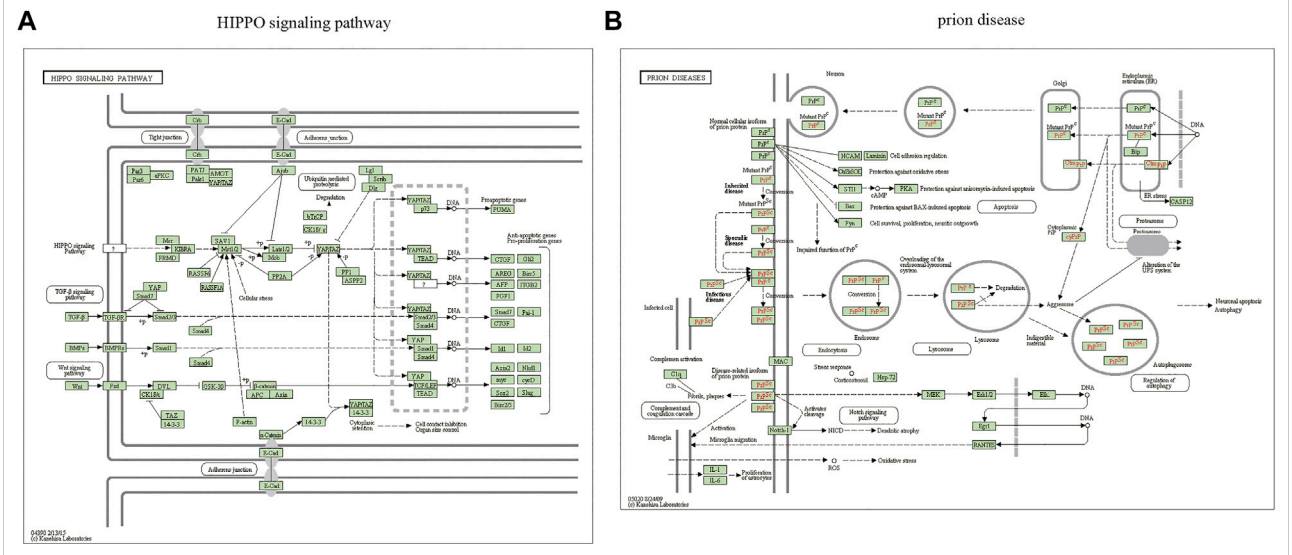

FIGURE 4
Pathview analysis of DEGs. **(A)** Pathview pathway map of the HIPPO signaling pathway. **(B)** Prion disease pathway map. Colors represent the location of DEGs in this pathway, and red represents upregulated genes.

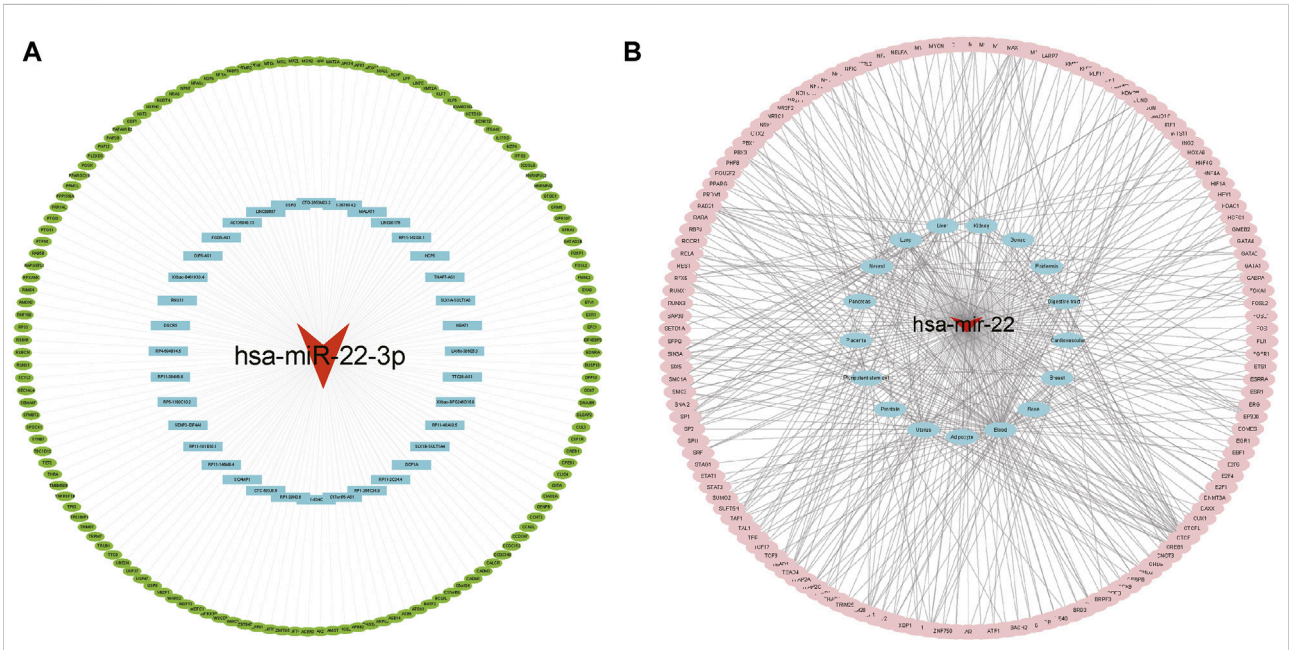

FIGURE 5
Interaction network analysis. **(A)** ceRNA network analysis. The red triangle represents miRNA, blue represents lncRNA, and green represents target genes. **(B)** Target gene-transcription factor analysis. Red represents miRNA genes, blue represents relevant disease tissue, and pink represents transcription factors.

of tumors, including breast cancer and intestinal tumors, and for their protective role in chemotherapeutic drugs against myocardial toxicity. Li et al. (2020) constructed miRNA expression profiles of rutin (RUT) interfering with anthracycline pirarubicin (THP)-induced cardiotoxicity in rats using microarray technology. They found that RUT reversed these results, suggesting that miR-129-1-3p might be a new therapeutic target for THP-induced cardiotoxicity and breast cancer. Circonol C1 promotes breast

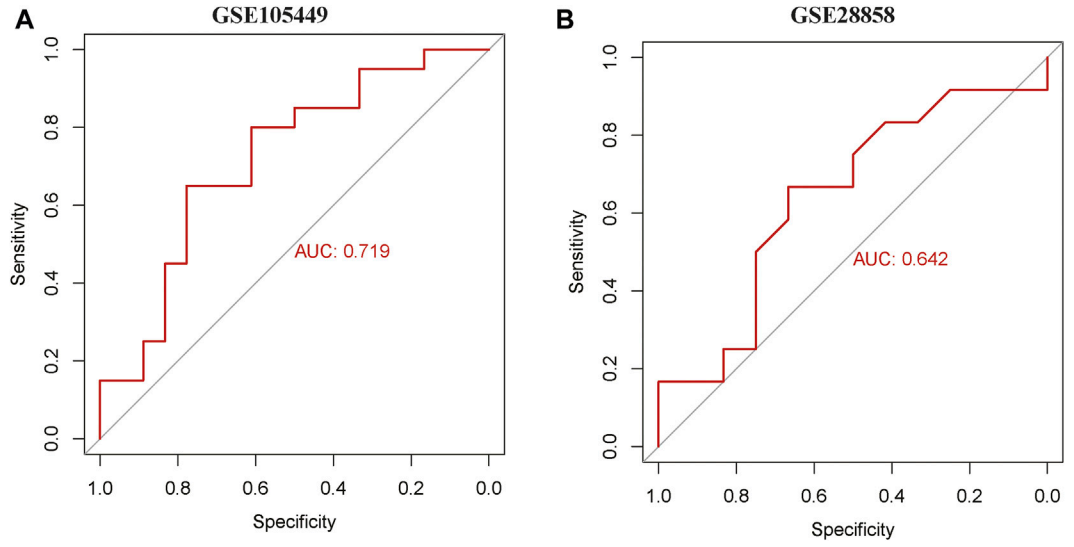

FIGURE 6
ROC curve analysis. **(A)** ROC curve of GSE105449. **(B)** ROC curve of GSE28858.

cancer progression by targeting the miR-365a-3p/STAT3 axis, while propofol inhibits Circonol C1 by reducing STAT3 expression (Liu et al., 2021). Previous studies have found that miR-129-1-3p, subjected to cyclic stretch, can activate Runx2 and vascular endothelial growth factors (VEGFs) to promote endothelial differentiation and angiogenesis in endothelial progenitor cells (EPCs), which could be a potential candidate for treating vascular injury (Li et al., 2019). miR-22 has been well-studied in various tumor metastases. It is an important epigenetic regulator that promotes epithelial–mesenchymal transition (EMT) and multifunctional metastasis in breast cancer (Kong et al., 2014). During the last decade, miR-22 has been shown to participate in angiogenesis, age-associated vascular diseases, and cardiac hypertrophy (Gurha et al., 2012a; Zheng and Xu, 2014; Takeda et al., 2016). miR-22 is significantly elevated in the aging rat heart, which partly accelerates cardiac fibroblast senescence (Jazbutyte et al., 2012). Targeted miR-22 knockdown promotes myocardial contractile function dysregulation (Gurha et al., 2012b). In an ischemia–reperfusion injury model, miR-22 was found to protect the heart by directly targeting the CREB binding protein (CBP), in part, through the CBP/AP-1 pathway to reduce apoptosis and inflammatory injury (Yang et al., 2014). Another observational study analyzed patients with CAD, including stable angina, unstable angina, non-ST-segment elevation myocardial infarction, or ST-segment elevation myocardial infarction, and found significantly reduced miR-22 expression levels in PBMCs using a real-time polymerase chain reaction (qRT-PCR) assay (Chen et al., 2016). However, the results of some studies are consistent with our results. These studies found that circulating miR-22-3p was significantly upregulated in CAD patients compared to healthy subjects (Coffey et al., 2015; Zhong et al., 2020). Therefore, in patients with coronary heart disease, the increase and decrease in miRNA levels is affected by the sample sources (such as heart tissue, plasma, platelets, and monocytes) and complications.

Enrichment analysis was performed on 352 predicted target genes. The DEG-enriched pathways mainly included transcriptional misregulation, growth hormone synthesis, secretion and action, endocrine resistance, axon guidance, and Cushing syndrome. The Pathview-enriched pathways were mainly related to the Hippo signaling and prion disease pathways. The Hippo signaling pathway is a cellular signaling pathway that is significant in animal development and is responsible for regulating cell proliferation and organ growth (Zhao et al., 2019). The core of the mammalian Hippo signaling pathway consists of large tumor suppressor kinase 1/2 (LATS1/LATS2), macrophage stimulating 1/2 (MST1/MST2), tumor suppressor protein MOB1, and transcriptional activator protein yes-associated protein (YAP) (White et al., 2019). The crystal structure of the human MOB1-NDR2 protein complex has been analyzed to show that MOB1 binding to LATS1/2 is essential for tissue growth and organ development, whereas MOB1 binding to MST1/2 is not vital (Moya et al., 2019). Significant discoveries have been made in the study of the Hippo pathway in the cardiovascular system (Ardestani et al., 2018; Wang et al., 2018). YAP/TAZ is crucial in the proliferation and differentiation of progenitor cells and contributes to homeostasis maintenance in adult cardiomyocytes (Mosqueira et al., 2014). The Hippo-YAP pathway alters the production or degradation of the extracellular matrix and growth and migration of vascular smooth muscle cells and endothelial cells, thereby promoting vascular remodeling (He et al., 2018). CAD-associated functional proteins negatively regulate Hippo signaling

in the endothelium, causing increased activity of YAP, a transcriptional effector of this pathway, leading to endothelial cell dysfunction that contributes to atherogenesis (Jones et al., 2018). YAP activation after myocardial infarction preserves cardiac function and reduces infarct size. Cardiac-specific YAP activation reduces myocardial injury, promotes myocardial regeneration and repair, improves cardiac function, and may improve survival (Lin et al., 2016). Functional enrichment analysis showed that miR-21-5p and miR-135b are associated with the Wnt and Hippo pathways, respectively, and may be associated with arrhythmogenic right ventricular cardiomyopathy (ARVC) (Byun et al., 2019). In conclusion, the Hippo signaling pathway is vital in cardiovascular processes, such as vascular smooth muscle cell remodeling, vascular endothelial growth, cardiac regenerative repair, and cardiomyopathy. However, its signaling interactions, pathophysiological mechanisms, and functional roles in the cardiovascular system remain to be investigated in depth.

We constructed an mRNA–miRNA–lincRNA ceRNA interaction network centered on miR-22-3p and used the starBase v2.0 and miRWalk databases to predict eight related transcription factors associated with cardiovascular disease, namely, CTCF, JUN, JUND, NFATC1, NFE2L2, RAD21, RELA, and TAL1. Several studies have been conducted on the aforementioned hub genes in various diseases. For instance, CTCF is a key chromatin architecture protein that binds to insulators, regulates enhancer–promoter interactions for transcriptional insulation, and acts as a transcriptional repressor to regulate gene expression (Shukla et al., 2011; Huang et al., 2021). More studies have shown that CTCF protein binding is influenced by DNA methylation levels in the cystathionine β-synthase (CBS) motif region and that CTCF haplotype dose expression can affect DNA methylation stability (Kemp et al., 2014). Nuclear factor E2-related factor 2 (NRF2) is encoded by the *NFE2L2* gene, and the NRF2/ARE signaling pathway is considered a potential therapeutic strategy for antioxidative stress-mediated diseases, such as diabetes, fibrosis, and cancer (Thiruvengadam et al., 2021). *NFE2L2* polymorphism is associated with acute type A aortic coarctation risk and severity in a Chinese Han population (Zhang et al., 2021). RAD21, RELA, and TAL1 are reportedly associated with tumors (Wu et al., 2019; Cao et al., 2021; Wang et al., 2021). However, few studies have investigated the relationship between hub genes and CAD. Therefore, this study is the first to potentiate eight CAD-associated hub genes (CTCF, JUN, JUND, NFATC1, NFE2L2, RAD21, RELA, and TAL1). However, this study had some limitations. First, the sample size for this study was relatively small, which could be a significant factor. Second, this project only completed bioinformatics analysis and did not provide experiments to further validate the aforementioned results. Subsequent studies will include cellular and animal experimental mechanism studies and clinical sample histological studies.

In conclusion, the present study suggests that miR-22-3p may be crucial in the onset and course of CAD. Our findings may provide potential targets for future CAD diagnoses and treatments.

Data availability statement

Publicly available datasets were analyzed in this study. These data can be found here: https://www.ncbi.nlm.nih.gov/geo/.

Author contributions

MZ and YH designed the experiments and performed the analysis. HL and XG contributed to data acquisition and manuscript drafting. JZ and SH contributed to software analysis, data curation, original draft preparation, and visualization. All authors read and approved the final article.

Funding

This study was supported by the Guangzhou Municipal Health Commission (Grant number: 20221A011108), the Bureau of Science and Technology of Guangzhou Municipality (Grant number: 202201011779), the Guangzhou Science and Technology Plan Project and Key Laboratory of Guangdong Higher Education Institutes (2021KSYS009).

Acknowledgments

We acknowledge TCGA and GEO databases for providing their platforms and contributors for uploading their meaningful datasets. We thank the associate editor and the reviewers for their useful feedback that improved this study.

Conflict of interest

The authors declare that the research was conducted in the absence of any commercial or financial relationships that could be construed as a potential conflict of interest.

Publisher's note

Supplementary material

The Supplementary Material for this article can be found online at: https://www.frontiersin.org/articles/10.3389/fgene.2022.936937/full#supplementary-material

SUPPLEMENTARY FIGURE S1
Boxplot plots before and after sample correction for two datasets. **(A)** and **(B)** represent the boxplot plots before and after sample correction with inter-batch differences removed for the GSE105449 dataset, respectively. **(C)** and **(D)** represent the boxplot plots before and after sample correction with inter-batch differences removed for the GSE28858 dataset, respectively.

SUPPLEMENTARY FIGURE S2
PCA plots before and after sample correction for the two datasets. **(A)** and **(B)** represent the PCA plots before and after sample correction with inter-batch differences removed for the GSE105449 dataset, respectively. **(C)** and **(D)** represent the PCA plots before and after samples correction with inter-batch differences removed for the GSE28858 dataset, respectively.

References

Ardestani, A., Lupse, B., and Maedler, K. (2018). Hippo signaling: Key emerging pathway in cellular and whole-body metabolism. *Trends Endocrinol. Metab.* 29 (7), 492–509. doi:10.1016/j.tem.2018.04.006

Byun, J., Del Re, D., Zhai, P., Ikeda, S., Shirakabe, A., Mizushima, W., et al. (2019). Yes-associated protein (YAP) mediates adaptive cardiac hypertrophy in response to pressure overload. *J. Biol. Chem.* 294 (10), 3603–3617. doi:10.1074/jbc.RA118.006123

Cao, H., Wang, D., Sun, P., Chen, L., Feng, Y., and Gao, R. (2021). RNA-seq reveals microRNA-302b as a suppressor of prostate cancer epithelial-mesenchymal transition by targeting RELA/NF-κB. *Am. J. Cancer Res.* 11 (11), 5715–5725.

Chen, B., Luo, L., Zhu, W., Wei, X., Li, S., Huang, Y., et al. (2016). miR-22 contributes to the pathogenesis of patients with coronary artery disease by targeting MCP-1: An observational study. *Medicine* 95 (33), e4418. doi:10.1097/MD.0000000000004418

Cheng, S., Xie, W., Miao, Y., Guo, J., Wang, J., Li, C., et al. (2019). Identification of key genes in invasive clinically non-functioning pituitary adenoma by integrating analysis of DNA methylation and mRNA expression profiles. *J. Transl. Med.* 17 (1), 407. doi:10.1186/s12967-019-02148-3

Coffey, S., Williams, M. J. A., Phillips, L. V., and Jones, G. T. (2015). Circulating microRNA profiling needs further refinement before clinical use in patients with aortic stenosis. *J. Am. Heart Assoc.* 4 (8), e002150. doi:10.1161/JAHA.115.002150

de Ronde, M. W. J., Kok, M. G. M., Moerland, P. D., Van den Bossche, J., Neele, A. E., Halliani, A., et al. (2017). High miR-124-3p expression identifies smoking individuals susceptible to atherosclerosis. *Atherosclerosis* 263, 377–384. doi:10.1016/j.atherosclerosis.2017.03.045

Du, L., Xu, Z., Wang, X., and Liu, F. (2020). Integrated bioinformatics analysis identifies microRNA-376a-3p as a new microRNA biomarker in patient with coronary artery disease. *Am. J. Transl. Res.* 12 (2), 633–648.

Dweep, H., and Gretz, N. (2015). miRWalk2.0: a comprehensive atlas of microRNA-target interactions. *Nat. Methods* 12 (8), 697. doi:10.1038/nmeth.3485

Gautier, L., Cope, L., Bolstad, B. M., and Irizarry, R. A. (2004). affy--analysis of Affymetrix GeneChip data at the probe level. *Bioinforma. Oxf. Engl.* 20 (3), 307–315. doi:10.1093/bioinformatics/btg405

Gu, Y., Ma, X., Li, J., Ma, Y., and Zhang, Y. (2021). Identification of candidate targets for the diagnosis and treatment of atherosclerosis by bioinformatics analysis. *Am. J. Transl. Res.* 13 (5), 4137–4151.

Gurha, P., Abreu-Goodger, C., Wang, T., Ramirez, M. O., Drumond, A. L., van Dongen, S., et al. (2012a). Targeted deletion of microRNA-22 promotes stress-induced cardiac dilation and contractile dysfunction. *Circulation* 125 (22), 2751–2761. doi:10.1161/CIRCULATIONAHA.111.044354

Gurha, P., Abreu-Goodger, C., Wang, T., Ramirez, M. O., Drumond, A. L., van Dongen, S., et al. (2012b). Targeted deletion of MicroRNA-22 promotes stress-induced cardiac dilation and contractile dysfunction. *Circulation* 125 (22), 2751–2761. doi:10.1161/circulationaha.111.044354

He, J., Bao, Q., Yan, M., Liang, J., Zhu, Y., Wang, C., et al. (2018). The role of Hippo/yes-associated protein signalling in vascular remodelling associated with cardiovascular disease. *Br. J. Pharmacol.* 175 (8), 1354–1361. doi:10.1111/bph.13806

Hu, Y., Matkovich, S. J., Hecker, P. A., Zhang, Y., Edwards, J. R., Dorn, G. W., et al. (2012). Epitranscriptional orchestration of genetic reprogramming is an emergent property of stress-regulated cardiac microRNAs. *Proc. Natl. Acad. Sci. U. S. A.* 109 (48), 19864–19869. doi:10.1073/pnas.1214996109

Huang, H., Zhu, Q., Jussila, A., Han, Y., Bintu, B., Kern, C., et al. (2021). CTCF mediates dosage- and sequence-context-dependent transcriptional insulation by forming local chromatin domains. *Nat. Genet.* 53 (7), 1064–1074. doi:10.1038/s41588-021-00863-6

Huang, Z. P., Chen, J., Seok, H. Y., Zhang, Z., Kataoka, M., Hu, X., et al. (2013). MicroRNA-22 regulates cardiac hypertrophy and remodeling in response to stress. *Circ. Res.* 112 (9), 1234–1243. doi:10.1161/CIRCRESAHA.112.300682

Jazbutyte, V., Fiedler, J., Kneitz, S., Galuppo, P., Just, A., Holzmann, A., et al. (2012). MicroRNA-22 increases senescence and activates cardiac fibroblasts in the aging heart. *Age* 35 (3), 747–762. doi:10.1007/s11357-012-9407-9

Jones, P. D., Kaiser, M. A., Ghaderi Najafabadi, M., Koplev, S., Zhao, Y., Douglas, G., et al. (2018). JCAD, a gene at the 10p11 coronary artery disease locus, regulates Hippo signaling in endothelial cells. *Arterioscler. Thromb. Vasc. Biol.* 38 (8), 1711–1722. doi:10.1161/ATVBAHA.118.310976

Karakas, M., Schulte, C., Appelbaum, S., Ojeda, F., Lackner, K., Münzel, T., et al. (2017). Circulating microRNAs strongly predict cardiovascular death in patients with coronary artery disease-results from the large AtheroGene study. *Eur. Heart J.* 38 (7), 516–523. doi:10.1093/eurheartj/ehw250

Kemp, C. J., Moore, J. M., Moser, R., Bernard, B., Teater, M., Smith, L. E., et al. (2014). CTCF haploinsufficiency destabilizes DNA methylation and predisposes to cancer. *Cell Rep.* 7 (4), 1020–1029. doi:10.1016/j.celrep.2014.04.004

Kok, M., Halliani, A., Moerland, P., Meijers, J., Creemers, E., and Pinto-Sietsma, S. (2015). Normalization panels for the reliable quantification of circulating microRNAs by RT-qPCR. *FASEB J. official Publ. Fed. Am. Soc. Exp. Biol.* 29 (9), 3853–3862. doi:10.1096/fj.15-271312

Kolde, R. (2019). *pheatmap: Pretty Heatmaps. R package. version 1.0.12.* Available at: https://CRAN.R-project.org/package=pheatmap.

Kong, L. M., Liao, C. G., Zhang, Y., Xu, J., Li, Y., Huang, W., et al. (2014). A regulatory loop involving miR-22, Sp1, and c-Myc modulates CD147 expression in breast cancer invasion and metastasis. *Cancer Res.* 74 (14), 3764–3778. doi:10.1158/0008-5472.CAN-13-3555

Li, N., Wang, W.-B., Bao, H., Shi, Q., Jiang, Z.-L., Qi, Y.-X., et al. (2019). MicroRNA-129-1-3p regulates cyclic stretch-induced endothelial progenitor cell differentiation by targeting Runx2. *J. Cell. Biochem.* 120 (4), 5256–5267. doi:10.1002/jcb.27800

Li, Q., Qin, M., Tan, Q., Li, T., Gu, Z., Huang, P., et al. (2020). MicroRNA-129-1-3p protects cardiomyocytes from pirarubicin-induced apoptosis by down-regulating the GRIN2D-mediated Ca2+ signalling pathway. *J. Cell. Mol. Med.* 24 (3), 2260–2271. doi:10.1111/jcmm.14908

Lin, J., Chen, W., Gong, M., Xu, X., Du, M., Wang, S., et al. (2021). Expression and functional analysis of lncRNAs involved in platelet-derived growth factor-BB-induced proliferation of human aortic smooth muscle cells. *Front. Cardiovasc. Med.* 8, 702718. doi:10.3389/fcvm.2021.702718

Lin, Z., Guo, H., Cao, Y., Zohrabian, S., Zhou, P., Ma, Q., et al. (2016). Acetylation of VGLL4 regulates hippo-YAP signaling and postnatal cardiac growth. *Dev. Cell* 39 (4), 466–479. doi:10.1016/j.devcel.2016.09.005

Liu, Y., Heng, J., Zhao, X., and Li, E. (2021). The inhibition of circular RNA circNOLC1 by propofol/STAT3 attenuates breast cancer stem cells function via miR-365a-3p/STAT3 signaling. *J. Transl. Med.* 19 (1), 467. doi:10.1186/s12967-021-03133-5

Ma, L., Li, A., Zou, D., Xu, X., Xia, L., Yu, J., et al. (2015). LncRNAWiki: Harnessing community knowledge in collaborative curation of human long non-coding RNAs. *Nucleic Acids Res.* 43, D187–D192. doi:10.1093/nar/gku1167

Mayr, B., Müller, E., Schäfer, C., Droese, S., Schönfelder, M., and Niebauer, J. (2021). Exercise-induced changes in miRNA expression in coronary artery disease. *Clin. Chem. Lab. Med.* 59, 1719–1727. doi:10.1515/cclm-2021-0164

Meng, Y., Zhang, C., Liang, L., Wei, L., Wang, H., Zhou, F., et al. (2021). Identification of potential key genes involved in the carotid atherosclerosis. *Clin. Interv. Aging* 16, 1071–1084. doi:10.2147/cia.s312941

Mosqueira, D., Pagliari, S., Uto, K., Ebara, M., Romanazzo, S., Escobedo-Lucea, C., et al. (2014). Hippo pathway effectors control cardiac progenitor cell fate by acting as dynamic sensors of substrate mechanics and nanostructure. *ACS Nano* 8 (3), 2033–2047. doi:10.1021/nn4058984

Moya, I. M., Castaldo, S. A., Van den Mooter, L., Soheily, S., Sansores-Garcia, L., Jacobs, J., et al. (2019). Peritumoral activation of the Hippo pathway effectors YAP and TAZ suppresses liver cancer in mice. *Sci. (New York, N.Y.)* 366 (6468), 1029–1034. doi:10.1126/science.aaw9886

Nariman-Saleh-Fam, Z., Vahed, S., Aghaee-Bakhtiari, S., Daraei, A., Saadatian, Z., Kafil, H., et al. (2019). Expression pattern of miR-21, miR-25 and PTEN in peripheral blood mononuclear cells of patients with significant or insignificant coronary stenosis. *Gene* 698, 170–178. doi:10.1016/j.gene.2019.02.074

Pandey, D., and Picard, D. (2009). miR-22 inhibits estrogen signaling by directly targeting the estrogen receptor alpha mRNA. *Mol. Cell. Biol.* 29 (13), 3783–3790. doi:10.1128/mcb.01875-08

Raggi, P., Genest, J., Giles, J. T., Rayner, K. J., Dwivedi, G., Beanlands, R. S., et al. (2018). Role of inflammation in the pathogenesis of atherosclerosis and therapeutic interventions. *Atherosclerosis* 276, 98–108. doi:10.1016/j.atherosclerosis.2018.07.014

Ritchie, M. E., Phipson, B., Wu, D., Hu, Y., Law, C. W., Shi, W., et al. (2015). Limma powers differential expression analyses for RNA-sequencing and microarray studies. *Nucleic Acids Res.* 43 (7), e47. doi:10.1093/nar/gkv007

Saadatian, Z., Nariman-Saleh-Fam, Z., Bastami, M., Mansoori, Y., Khaheshi, I., Parsa, S., et al. (2019). Dysregulated expression of STAT1, miR-150, and miR-223 in peripheral blood mononuclear cells of coronary artery disease patients with significant or insignificant stenosis. *J. Cell. Biochem.* 120 (12), 19810–19824. doi:10.1002/jcb.29286

Shukla, S., Kavak, E., Gregory, M., Imashimizu, M., Shutinoski, B., Kashlev, M., et al. (2011). CTCF-promoted RNA polymerase II pausing links DNA methylation to splicing. *Nature* 479 (7371), 74–79. doi:10.1038/nature10442

Sondermeijer, B. M., Bakker, A., Halliani, A., de Ronde, M. W., Marquart, A. A., Tijsen, A. J., et al. (2011). Platelets in patients with premature coronary artery disease exhibit upregulation of miRNA340* and miRNA624. *PLoS One* 6 (10), e25946. doi:10.1371/journal.pone.0025946

Su, M., Niu, Y., Dang, Q., Qu, J., Zhu, D., Tang, Z., et al. (2020). Circulating microRNA profiles based on direct S-Poly(T)Plus assay for detection of coronary heart disease. *J. Cell. Mol. Med.* 24 (11), 5984–5997. doi:10.1111/jcmm.15001

Takeda, E., Suzuki, Y., and Sato, Y. (2016). Age-associated downregulation of vasohibin-1 in vascular endothelial cells. *Aging Cell* 15 (5), 885–892. doi:10.1111/acel.12497

Tan, X., Zhang, X., Pan, L., Tian, X., and Dong, P. (2017). Identification of key pathways and genes in advanced coronary atherosclerosis using bioinformatics analysis. *Biomed. Res. Int.* 2017, 4323496. doi:10.1155/2017/4323496

Tanase, D. M., Gosav, E. M., Ouatu, A., Badescu, M. C., Dima, N., Ganceanu-Rusu, A. R., et al. (2021). Current knowledge of MicroRNAs (miRNAs) in acute coronary syndrome (ACS): ST-elevation myocardial infarction (STEMI). *Life (Basel, Switz.* 11 (10), 1057. doi:10.3390/life11101057

Thiruvengadam, M., Venkidasamy, B., Subramanian, U., Samynathan, R., Ali Shariati, M., Rebezov, M., et al. (2021). Bioactive compounds in oxidative stress-mediated diseases: Targeting the NRF2/ARE signaling pathway and epigenetic regulation. *Antioxidants (Basel, Switz.* 10 (12), 1859. doi:10.3390/antiox10121859

Thomas, M. R., and Lip, G. Y. H. (2017). Novel risk markers and risk assessments for cardiovascular disease. *Circ. Res.* 120 (1), 133–149. doi:10.1161/CIRCRESAHA.116.309955

Vlachos, I. S., Zagganas, K., Paraskevopoulou, M. D., Georgakilas, G., Karagkouni, D., Vergoulis, T., et al. (2015). DIANA-miRPath v3.0: Deciphering microRNA function with experimental support. *Nucleic Acids Res.* 43 (W1), W460–W466. doi:10.1093/nar/gkv403

Wang, J., Liu, S., Heallen, T., and Martin, J. F. (2018). The Hippo pathway in the heart: Pivotal roles in development, disease, and regeneration. *Nat. Rev. Cardiol.* 15 (11), 672–684. doi:10.1038/s41569-018-0063-3

Wang, J., Zhao, H., Yu, J., Xu, X., Jing, H., Li, N., et al. (2021). MiR-320b/RAD21 axis affects hepatocellular carcinoma radiosensitivity to ionizing radiation treatment through DNA damage repair signaling. *Cancer Sci.* 112 (2), 575–588. doi:10.1111/cas.14751

White, S., Murakami, S., and Yi, C. (2019). The complex entanglement of Hippo-Yap/Taz signaling in tumor immunity. *Oncogene* 38 (16), 2899–2909. doi:10.1038/s41388-018-0649-6

Wilkinson, L. (2011). ggplot2: Elegant graphics for data analysis by WICKHAM, H. *Biometrics* 67 (2), 678–679. doi:10.1111/j.1541-0420.2011.01616.x

Wu, Y., Hu, Y., Yu, X., Zhang, Y., Huang, X., Chen, S., et al. (2019). TAL1 mediates imatinib-induced CML cell apoptosis via the PTEN/PI3K/AKT pathway. *Biochem. Biophys. Res. Commun.* 519 (2), 234–239. doi:10.1016/j.bbrc.2019.08.164

Yang, J., Chen, L., Yang, J., Ding, J., Li, S., Wu, H., et al. (2014). MicroRNA-22 targeting CBP protects against myocardial ischemia-reperfusion injury through anti-apoptosis in rats. *Mol. Biol. Rep.* 41 (1), 555–561. doi:10.1007/s11033-013-2891-x

Yu, G., Wang, L.-G., Han, Y., and He, Q.-Y. (2012). clusterProfiler: an R package for comparing biological themes among gene clusters. *Omics a J. Integr. Biol.* 16 (5), 284–287. doi:10.1089/omi.2011.0118

Zeng, Z., Xia, L., Fan, S., Zheng, J., Qin, J., Fan, X., et al. (2021). Circular RNA CircMAP3K5 acts as a MicroRNA-22-3p sponge to promote resolution of intimal hyperplasia via TET2-mediated smooth muscle cell differentiation. *Circulation* 143 (4), 354–371. doi:10.1161/circulationaha.120.049715

Zhang, M., Li, Y., Xie, H., Chen, J., and Liu, S. (2020). Curcumin inhibits proliferation, migration and neointimal formation of vascular smooth muscle via activating miR-22. *Pharm. Biol.* 58 (1), 610–619. doi:10.1080/13880209.2020.1781904

Zhang, Y., Zheng, Q., Chen, R., Dai, X., Zhu, Y., and Ma, L. (2021). Association of NFE2L2 gene polymorphisms with risk and clinical characteristics of acute type A aortic dissection in han Chinese population. *Oxid. Med. Cell. Longev.* 2021, 5173190. doi:10.1155/2021/5173190

Zhao, W., Lu, Q., Nguyen, M., Su, Y., Ziemann, M., Wang, L., et al. (2019). Stimulation of β-adrenoceptors up-regulates cardiac expression of galectin-3 and BIM through the Hippo signalling pathway. *Br. J. Pharmacol.* 176 (14), 2465–2481. doi:10.1111/bph.14674

Zhelankin, A., Stonogina, D., Vasiliev, S., Babalyan, K., Sharova, E., Doludin, Y., et al. (2021). Circulating extracellular miRNA analysis in patients with stable CAD and acute coronary syndromes. *Biomolecules* 11 (7), 962. doi:10.3390/biom11070962

Zheng, Y., and Xu, Z. (2014). MicroRNA-22 induces endothelial progenitor cell senescence by targeting AKT3. *Cell. Physiol. biochem.* 34 (5), 1547–1555. doi:10.1159/000366358

Zhong, Z., Zhong, W., Zhang, Q., Zhang, Q., Yu, Z., and Wu, H. (2020). Circulating microRNA expression profiling and bioinformatics analysis of patients with coronary artery disease by RNA sequencing. *J. Clin. Lab. Anal.* 34 (1), e23020. doi:10.1002/jcla.23020

frontiers | Frontiers in Genetics

TYPE Mini Review
PUBLISHED 02 September 2022
DOI 10.3389/fgene.2022.910733

OPEN ACCESS

EDITED BY
Olanrewaju B. Morenikeji,
University of Pittsburgh at Bradford, United States

REVIEWED BY
Olamide Crown,
Jackson State University, United States
Manmeet Bhalla,
University at Buffalo, United States
Sayan Chakraborty,
University at Buffalo, United States

*CORRESPONDENCE
Asim K. Duttaroy,
a.k.duttaroy@medisin.uio.no
Sujay Paul,
spaul@tec.mx

SPECIALTY SECTION
This article was submitted to RNA, a section of the journal Frontiers in Genetics

RECEIVED 01 April 2022
ACCEPTED 10 August 2022
PUBLISHED 02 September 2022

CITATION
Ruiz-Manriquez LM, Carrasco-Morales O, Sanchez Z EA, Osorio-Perez SM, Estrada-Meza C, Pathak S, Banerjee A, Bandyopadhyay A, Duttaroy AK and Paul S (2022), MicroRNA-mediated regulation of key signaling pathways in hepatocellular carcinoma: A mechanistic insight. *Front. Genet.* 13:910733. doi: 10.3389/fgene.2022.910733

MicroRNA-mediated regulation of key signaling pathways in hepatocellular carcinoma: A mechanistic insight

Luis M. Ruiz-Manriquez[1], Oscar Carrasco-Morales[1], E. Adrian Sanchez Z[1], Sofía Madeline Osorio-Perez[1], Carolina Estrada-Meza[1], Surajit Pathak[2], Antara Banerjee[2], Anindya Bandyopadhyay[3,4], Asim K. Duttaroy[5]* and Sujay Paul[1]*

[1]Tecnologico de Monterrey, School of Engineering and Sciences, Queretaro, Mexico, [2]Department of Medical Biotechnology, Faculty of Allied Health Sciences, Chettinad Hospital and Research Institute (CHRI), Chettinad Academy of Research and Education (CARE), Chennai, India, [3]International Rice Research Institute, Manila, Philippines, [4]Reliance Industries Ltd., Navi Mumbai, India, [5]Department of Nutrition, Institute of Basic Medical Sciences, Faculty of Medicine, University of Oslo, Oslo, Norway

Hepatocellular carcinoma (HCC) is the most common type of primary liver cancer. The molecular pathogenesis of HCC varies due to the different etiologies and genotoxic insults. The development of HCC is characterized by complex interactions between several etiological factors that result in genetic and epigenetic changes in proto-onco and/or tumor suppressor genes. MicroRNAs (miRNAs) are short non-coding RNAs that also can act as oncomiRs or tumor suppressors regulating the expression of cancer-associated genes post-transcriptionally. Studies revealed that several microRNAs are directly or indirectly involved in cellular signaling, and dysregulation of those miRNAs in the body fluids or tissues potentially affects key signaling pathways resulting in carcinogenesis. Therefore, in this mini-review, we discussed recent progress in microRNA-mediated regulation of crucial signaling networks during HCC development, concentrating on the most relevant ones such as PI3K/Akt/mTOR, Hippo-YAP/TAZ, and Wnt/β-catenin, which might open new avenues in HCC management.

KEYWORDS

hepatocellular carcinoma, miRNA, gene regulation, signaling pathways, therapeutics

Introduction

Hepatocellular carcinoma (HCC) is the most frequent primary hepatic neoplasm with variable incidence throughout the geographical locations and represents the world's fourth most common cause of cancer-related mortality (Kim and Viatour, 2020; Llovet et al., 2021). By 2025, the global burden of HCC-associated mortality is expected to approach 1 million per year (Siegel et al., 2017; Llovet et al., 2021). In general, HCC has a negative prognosis, given the limited therapy options, including hepatic resection and liver transplantation (Siegel et al., 2017; Singh et al., 2020; Llovet et al., 2021).

The molecular pathogenesis of HCC depends on the etiologies and genotoxic insults involved (Fardi et al., 2018; Llovet et al., 2021). Typically, activating oncogenes or inhibiting tumor suppressor genes lead to aberrations in cell signaling pathways that control cancer hallmark characteristics such as increased cell proliferation, cell fate and differentiation alterations, and resistance to programmed cell death (Juliano, 2020). Although the knowledge about the pathophysiology of HCC has recently been improved, it has yet to be implemented in advanced clinical practice (Alqahtani et al., 2019).

MicroRNAs (miRNAs) are small single-stranded RNA molecules (20–24 nucleotides) that mediate post-transcriptional gene regulation either by translational repression or mRNA degradation (Vishnoi and Rani, 2017). According to MirBase (http://www.mirbase.org) database, a total of 2,654 mature miRNAs have been reported in the *Homo sapiens* so far. Studies have shown that miRNAs are key regulators of a variety of biological activities, including cell differentiation, apoptosis, proliferation, and tumorigenesis (Paul et al., 2021; Vázquez et al., 2021; Paul et al., 2022), and their dysregulation is associated with different cancers, including HCC (Vasuri et al., 2018; Ruiz-Manriquez et al., 2021). Moreover, miRNAs are highly stable and can be quantified in several biological fluids such as blood, saliva, and urine, representing an excellent cancer biomarker (Ruiz-Manriquez et al., 2022). Intriguingly, alteration in miRNA expression profile due to certain external and internal factors potentially affects numerous signaling pathways resulting in odd changes that might lead to carcinogenesis (Leichter et al., 2017; Juliano, 2020). Hence, this review presents the current research regarding the molecular crosstalk between miRNAs and critical signal transduction networks during HCC development, focusing on the most relevant ones such as PI3K/Akt/mTOR, Hippo-YAP/TAZ, and Wnt/β-catenin.

PI3K/Akt/mTOR pathway

The phosphatidylinositide 3-kinase (PI3K)/Akt pathway has been linked to cancer pathogenesis since its enzymatic activity was shown to be allied with viral oncoproteins (Fruman et al., 2017). It comprises several serine/threonine kinases that mediate numerous biological functions, including cell cycle progression, cell survival, migration, and protein synthesis (Alzahrani, 2019). PI3Ks are part of a family of lipid kinases that phosphorylate the 3′hydroxyl group of phosphoinositides and consist of several classes, among which the class IA PI3Ks are the most studied one and implicated in human cancers (Rahmani et al., 2020). Class IA PI3Ks are heterodimers activated downstream of receptor tyrosine kinases or RAS oncogene and contain a regulatory (p85) and a catalytic subunit (p110). Subsequently, activated PI3K triggers the production of Phosphatidylinositol-3,4,5-trisphosphate (PIP3), a crucial second messenger that in turn induces AKT (a protein kinase with pleckstrin homology domain). Afterward, AKT endorses proliferation, cellular metabolism, differentiation, angiogenesis, and apoptosis by eliciting downstream effector proteins such as the mammalian target of rapamycin (mTOR), which is key to maintaining the balance between cell proliferation and autophagy in response to cellular stress (Jiang et al., 2018; Rahmani et al., 2020).

To date, it has been well established that miRNA dysregulation is crucial in HCC development and progression. In this context, Sun et al. (2019) revealed that being a tumor suppressor, miR-1914 (poorly expressed in HCC cell lines) might hinder tumor growth and colony formation, leading to cell cycle arrest and increased apoptosis. Notably, the main target of miR-1914 is GPR39, a zinc-activated G protein-coupled receptor, which regulates HCC cell proliferation and differentiation, leading to PI3K/AKT/mTOR repression.

Likewise, Wu et al. (2020) reported that tumor sizes, tumor numbers, TNM stage, and histological grade are strongly linked with miR-660-5p expression. Furthermore, *in vitro* and *in vivo* experiments revealed that miR-660-5p could dramatically increase HCC cell proliferation, clone formation, migration, invasion, and tumorigenic potential, whereas its downregulation suppresses malignant growth. It has been proposed that epithelial cancer cells undergo an epithelial-mesenchymal transition (EMT), which is characterized by cell adhesion loss, E-cadherin suppression, acquisition of mesenchymal markers (such as N-cadherin, Vimentin, and Fibronectin), and enhanced cell motility and invasiveness (Roche, 2018). Interestingly, Wu et al. (2020) also found that miR-660-5p directly targets YWHAH, a 14-3-3 family protein that binds to phosphoserine-containing proteins to facilitate signal transduction and activates PI3K/AKT signaling pathway resulting in EMT promotion.

Yu et al. (2019) noticed that HCC tissues had considerably greater levels of miR-106b-5p than normal liver tissues. Moreover, induced miR-106b-5p could diminish the expression of FOG2, a novel inhibitor of PI3K/Akt signaling to promote the proliferation and invasion of HCC cells. In another analogous study, Yao et al. (2015) observed Metastasis-associated with Colon Cancer 1 (MACC1) gene as a novel prognostic HCC indicator that inhibited apoptosis of HCC cells by targeting the PI3K/AKT pathway. Intriguingly, Zhang Y. M. et al. (2020) established that miR-34a and miR-125a-5p refrained proliferation and metastasis while inducing apoptosis by suppressing the MACC1-mediated PI3K/AKT/mTOR pathway in HCC both *in vitro* and *in vivo*.

In various cancers, the oncogenic tripartite motif-containing 27 (TRIM27) protein enhances cell survival, proliferation, migration, and invasion (Zhang et al., 2018). In this context, Gao et al. (2019) demonstrated that miR-30b-3p might prevent HCC cells from proliferating, migrating, and invading by downregulating TRIM27 and subsequently inactivating the PI3K/Akt pathway. Contrastingly, Du et al. (2019) noticed a

significant overexpression of miR-3691-5p in HCC tissues and cell lines substantially linked to clinicopathological characteristics such as TNM stage and vascular invasion through activating PI3K/Akt signaling by targeting PTEN, and they considered this miRNA as an HCC oncomiR. Likewise, Wang et al. (2021) demonstrated that when miR-92a-3p is overexpressed, N-cadherin and Vimentin protein (two crucial markers in the transition of malignant cells from normal cells) expression levels increase, and HCC cell proliferation, migration, and invasion were stimulated, suggesting that miR-92a-3p plays a vital role in HCC cell EMT as an oncomiR. Remarkably, they also found that the PI3K/AKT/mTOR signaling pathway is activated by miR-92a-3p and induces EMT, promoting the HCC's malignant development.

As discussed, the PI3K pathway might represent an attractive candidate for tumor therapeutic targeting. In this sense, multiple kinases in the PI3K/AKT/mTOR pathway were chosen for inhibitory activity, and the development of kinase inhibitors with improved specificity and pharmacokinetics has recently facilitated research on the PI3K pathway inhibition clinical trials. Moreover, since numerous miRNAs modulate PI3K/Akt/mTOR pathway during carcinogenesis, they could also be a promising tool for HCC management.

Hippo-YAP/TAZ pathway

In a highly conserved manner, the Hippo-YAP/TAZ pathway modulates tissue homeostasis, organ size, cell regeneration, and growth (Samji et al., 2021), and its dysregulation has been allied with a variety of malignancies, including HCC (Xin Y. et al., 2020). A kinase cascade containing serine/threonine-protein kinase 4/3 (MST1/2), large tumor suppressor kinases (LATS) 1/2, the transcription coactivators yes-associated protein (YAP), and its paralog WW domain-containing transcription regulator protein 1 [WWTR1 or transcriptional coactivator with PDZ-binding motif (TAZ)] are critical components of this signaling pathway in mammalian cells. MST1/2 is activated by phosphorylation or trans-autophosphorylation; later, it binds to the Salvador family WW domain-containing protein 1 (SAV1) in a heterotetramer to mediate MST1/2 activation and localization to the plasma membrane. MOB 1 (monopolar spindle one-binder) aids in the recruitment of LATS1/2 to MST1/2, allowing MST1/2 to phosphorylate LATS, causing LATS autophosphorylation and activation. The linker phosphorylation sites of MST1/2 also use the striatin-interacting phosphatase and kinase complex to dephosphorylate and inactivate MST1/2, providing negative responses that limit MST activity. Upstream regulators KIBRA and Mer/NF2 soothed the Hippo kinase cascade by recruiting LATS to the plasma membrane, where Hippo/MST will activate it. Activated LATS1/2 then phosphorylate and inactivate YAP/TAZ, which leads to proteasomal decay. YAP and TAZ are not phosphorylated and hence stable when the Hippo kinase cascade is inactivated; therefore, they translocate into the nucleus and bind to transcription factors to modulate target gene expression (Liu et al., 2020). Unphosphorylated YAP penetrates the nucleus and activates oncogenes such as CYR61, AREG, AKD1, and CTGF (Zhang and Zhou, 2019).

Intriguingly, YAP and TAZ directly control miRNA biogenesis (Mori et al., 2014); while several miRNAs have been shown to target and modulate the Hippo-YAP/TAZ signaling pathway's main components. For example, Xin Y. et al. (2020) noticed that being a transcriptional target of the Hippo-YAP/TAZ pathway miR-135b silences MST1 expression as an oncomiR, and consequently, the MST1-YAP-miR-135b axis generates a positive feedback loop in HCC advancement. Moreover, the level of miR-135b was shown to be favorably connected with HCC stages and negatively associated with HCC patient survival. These findings provide a clue by which miR-135b promotes HCC tumorigenesis through Hippo signaling pathway modulation. Guan et al. (2019) revealed that the expression of MEIS2C/D (a critical transcription factor linked to the development of human cancer) is significantly upregulated in HCC and correlated with poor prognosis. Furthermore, employing both *in vitro* and *in vivo* approaches, they demonstrated that MEIS2D enhances hepatoma cell proliferation and metastasis *via* the Hippo-YAP/TAZ signaling pathway. Interestingly, MiR-1307-3p is a key component of the MEIS2D route because MEIS2D and its synergistic molecule, PBX1, co-activated its expression. They also discovered that LATS1 is a functional target of miR-1307-3p, whose inhibition reduces YAP phosphorylation. These data imply that MEIS2D promotes HCC development *via* the miR-1307-3p/LATS1/YAP circuit. Following the same line, Wu et al. (2019) reported that miR-29c-3p expression was considerably reduced in HCC cell lines and tissues. Since this miRNA regulates the methylation of LATS1 by targeting DNMT3B, and aberrant methylation of LATS1 inactivates the Hippo-YAP/TAZ signaling pathway, its poor expression induces tumor growth, multiple pathologic characteristics, and shorter overall survival. However, overexpression of miR-29c-3p has also been shown to suppress HCC cell proliferation, apoptosis, migration, and tumor growth *in vivo* by negatively regulating the DNA methyltransferases 3B (DNMT3B). These findings suggest that this miRNA potentially functions as a tumor suppressor in HCC by inhibiting DNMT3B and the LATS1-associated Hippo-YAP/TAZ signaling pathway, representing a novel potential therapeutic target for HCC.

Hypoxia is a key component of the microenvironment of solid tumors, and it promotes cancer growth. Zhang B. et al. (2020) noticed that hypoxia triggers the miR-512-3p expression in HCC, and its upregulation is linked with adverse clinicopathological features, including tumor size, vascular invasion, and advanced tumor-node-metastasis phases. Moreover, LATS2 was found to be a direct functional target

of miR-512-3p, and therefore, in HCC tissues, the level of miR-512-3p was negatively correlated with LATS2 expression and Hippo-YAP/TAZ signaling. Altogether, the results suggested that hypoxia-induced miR-512-3p expression inhibits the Hippo-YAP/TAZ pathway, which leads to HCC cell proliferation, migration, and invasion.

It is well established that miR-21 is strongly connected with the Hippo-YAP/TAZ signaling pathway (An et al., 2018). Recently, Hong et al. (2021) showed that miR-21-3p levels are substantially increased in HCC tissues compared to the adjacent healthy liver tissues, and the targets of this miRNA exhibited a significant association with the TGF-β transduction and Hippo-YAP/TAZ signaling pathway. Moreover, they demonstrated that one of the most significant targets of miR-21-3p, intranuclear SMAD7, promotes YAP1 translocation to the cytoplasm and hinders YAP1 transcription. Interestingly, YAP1 promotes SMAD7 to activate TbRI and inhibits the TGF-β/SMAD signal transduction; therefore, the counterbalance between SMAD7 and YAP1 significantly impacts the TGF-β signal transduction. This result highlighted the oncogenic role of miR-21-3p in HCC by promoting malignant phenotype progression *via* the Hippo-YAP/TAZ pathway.

Even though a number of studies have been conducted recently to identify miRNAs and their regulatory role in HCC *via* modulating Hippo-YAP/TAZ pathway, it is only the tip of the iceberg, and further research is needed to deeply understand the mechanism to develop novel therapeutics strategies against HCC.

Wnt/β-catenin pathway

The Wnt/β-catenin is a conserved signaling axis involved in a variety of physiological settings, including differentiation, proliferation, apoptosis, migration, invasion, and tissue homeostasis (He and Tang, 2020; Zhang and Wang, 2020). Over the past years, onco or tumor suppressor miRNAs have been demonstrated to regulate HCC cell proliferation, invasion, metastasis, and drug sensitivity through modulating the key regulatory factors in the canonical Wnt/β-catenin signaling pathway.

In this milieu, Huang et al. (2020) highlighted miR-1246 as a potential factor that promotes HCC tumor formation by suppressing the expression of its target RORα. Notably, they confirmed that artificial induction of miR-1246 expression or RORα knockdown substantially augments the metastatic capacity of HCC both *in vitro* and *in vivo* through the activation of the Wnt/β-catenin pathway and epithelial-mesenchymal transition (EMT) promotion. Likewise, Xin R. Q. et al. (2020) showed that USP22, a histone-modifying enzyme principally regulated by miR-329-3p (normally downregulated in HCC), is linked to distant metastasis, poor prognosis, and high recurrence rates in HCC since it critically modulates the proliferation, metastasis, DNA repair, and stemness of tumor cells *via* modulating Wnt/β-catenin pathway.

C-x-C motif chemokine ligand 12 (CXCL12) is a crucial cancer immunity and angiogenesis regulator that triggers HCC progression through Wnt/β-catenin pathway regulation. Lu et al. (2019) revealed that upregulated miR-342 (which is usually poorly expressed in HCC cells) could significantly suppress the proliferation of HCC cells and increase apoptosis by targeting CXCL12 expression and subsequent inhibition of Wnt/β-catenin signaling activity. Correspondingly, the SOX family of transcription factors has emerged as modulators of canonical Wnt/β-catenin signaling (Ashrafizadeh et al., 2020). Specifically, SOX6 (downregulated in cancerous tissue, including HCC) is an anti-tumor gene that prevents cancer cells from proliferating and becoming tumorigenic (Jiang et al., 2018). Recently, Cao et al. (2021) showed that miR-19a-3p and miR-376c-3p might stimulate the Wnt/β-catenin pathway in HCC cells by targeting the SOX6. Moreover, they observed that SOX6 might bind to β-catenin and prevent it from dissociating from the transcriptional complex, preventing it from being translocated to the nucleus. Overall, this finding suggested that both miR-19a-3p and miR-376c-3p are highly expressed in HCC cells and might play a role in HCC formation by targeting SOX6 and altering the Wnt/β-catenin signaling pathway.

The protein regulator of cytokinesis 1 (PRC1) has been shown to exert an oncogenic function by promoting tumor formation, transfer, stemness, and progression of early HCC through the Wnt/β-catenin signaling pathway modulation, and its overexpression has been linked to poor HCC patient survival (Chen et al., 2016; Wang et al., 2017). Remarkably, Tang et al. (2019) demonstrated that the upregulation of miR-194 in HCC diminishes the expression of PRC1 and β-catenin accompanied by increased E-cadherin expression leading to EMT inhibition and Wnt/β-catenin signaling pathway inactivation. While in another study, WW domain-binding protein 2 (WBP2) was reported to interrelate with various WW domain-containing proteins, including WW domain-containing transcription regulator protein 1 (TAZ) and WW domain-containing oxidoreductase (WWOX), and favorably linked with the Wnt/β-catenin signaling pathway to promote downstream gene transcription, resulting in HCC progression (Chen et al., 2017). In this regard, Gao et al. (2020) proved that upregulation of miR-485-5p in HCC cells suppresses WBP2 expression and prevents Wnt/β-catenin signaling, leading to the inhibition of proliferation, migration, and invasion, as well as most significantly, suppression of tumor development *in vivo*. The authors transfected HCC cells with miR-485-5p mimic to better understand the role of miR485-5p in HCC, and they discovered that E-cadherin expression was upregulated while MMP-9, c-myc, cyclin D, and MMP-7 expression was considerably reduced. E-cadherin, also known as CDH1, is an important cancer suppressor, and its poor expression is allied with EMT, which is known to accelerate cancer cell migration and invasion.

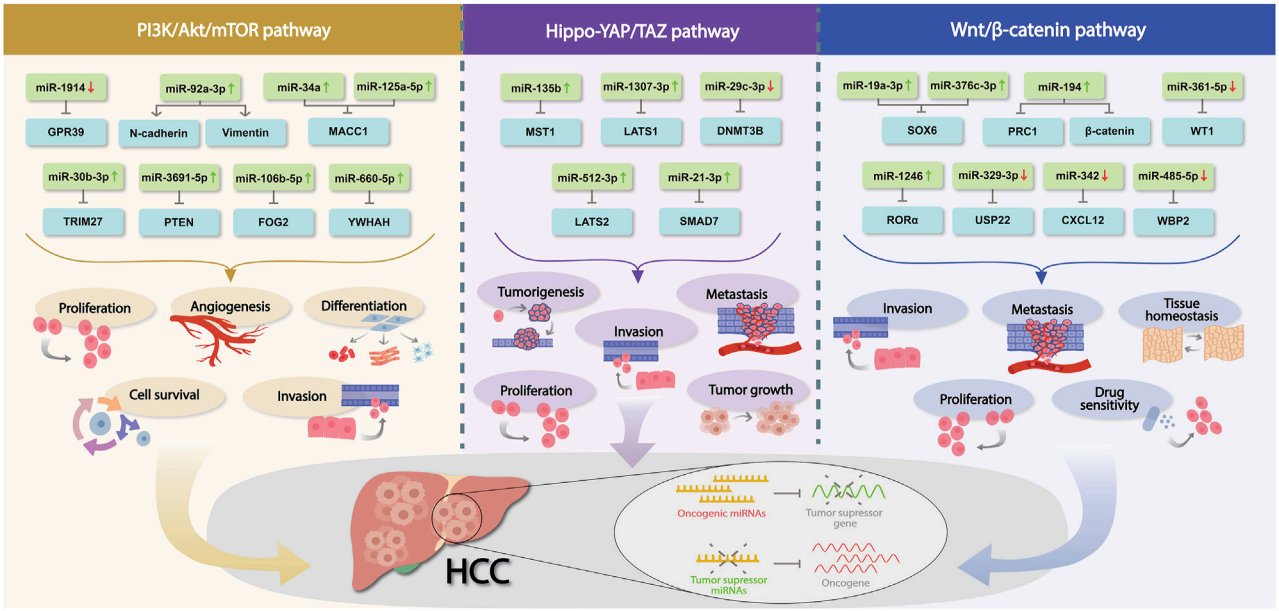

FIGURE 1
Dysregulated miRNAs in HCC involved in PI3K/Akt/mTOR, Hippo-YAP/TAZ and Wnt/β-catenin pathways. Association of a number of miRNAs in those crucial signaling pathways during HCC development, their corresponding mRNAs targets and the biological mechanism implicated are shown. Red and green arrows indicate the differential expression of each miRNA (↑ = upregulation, ↓ = downregulation).

Wilms' tumor 1 gene (WT1) is an essential nuclear factor for organ development and cell growth. Overexpression of WT1 has been shown to be oncogenic in several types of cancers (Qi et al., 2015). Notably, it was also stated that miR-361-5p directly targets WT1 and negatively regulates its expression in HCC; moreover, its downregulation is associated with lymph node metastasis and advanced TNM stage, resulting in a poor prognosis for HCC patients. Furthermore, the effect of miR-361-5p on EMT and the WNT/β-catenin pathway was explored, and it was revealed that the overexpression of miR-361-5p hinders the N-cadherin and Vimentin expressions and promotes E-cadherin expression, inhibiting cell metastasis *via* blocking EMT as well as inactivating WNT/β-catenin pathway (Cheng et al., 2019).

In the past few years, it has been noticed that the Wnt/β-catenin pathway is abnormally activated in several types of cancer, and hence Wnt-targeted therapy has received much attention, and recently Wnt signaling has been translated to preclinical research since effective small-molecule drugs have been developed to modulate the pathway. Nevertheless, an in-depth investigation regarding the microRNA-mediated modulation of this pathway in HCC is necessary to develop advanced disease management strategies.

Discussion

It is well established that miRNAs are significantly involved in hepatic tumorigenicity and progression, and investigators have observed that dysregulated miRNAs promote tumorigenesis post-transcriptionally by influencing oncogenes and tumor suppressors, impacting associated canonical pathways (Figure 1). In this background, due to its crucial involvement in tumor development, metastasis, angiogenesis, stemness, and chemoresistance, PTEN/PI3K/Akt was thoroughly investigated. Indisputably, the PTEN/PI3K/Akt -signaling pathway was found to be highly dysregulated in HCC, and different miRNAs control several associated dysregulated genes. However, further investigations about miRNAs and PTEN/PI3K/Akt signaling and their molecular interactions are necessary to improve the clinical management of patients with HCC. Likewise, the hepatocyte appears to be an important cell type that is influenced by the Hippo-YAP/TAZ signaling pathway in a variety of ways. However, the explicit molecular mechanisms by which Hippo-YAP/TAZ signaling regulates multiple aspects of hepatocyte physiology and pathology remain elusive. Although a number of studies have been performed to identify miRNAs and their contribution to the Hippo-YAP/TAZ regulatory pathway during HCC development, there is still a long way to go to thoroughly understand its underlying molecular mechanism. Similarly, oncogenic or tumor suppressor miRNAs have been shown to influence HCC cell proliferation, invasion, metastasis, and drug response by targeting regulatory factors in the canonical Wnt/β-catenin signaling pathway. Notably, feedback regulation of miRNAs *via* the canonical Wnt/β-catenin signaling pathway might have a role in HCC progression; however, specific upstream regulators of miRNAs

TABLE 1 Differentially expressed miRNA profile in crucial signaling pathways of HCC.

miRNA	Target gene	Effect on signaling pathway	Affected biological mechanism	Function	Reference
PI3K/Akt/mTOR					
miR-1914 ↓	GPR39	Repression	Tumor growth and apoptosis	Tumor suppressor	Sun et al. (2019)
miR-660-5p ↑	YWHAH	Activation	Cell proliferation, clone formation, migration, invasion	OncomiR	Roche (2018); Wu et al. (2020)
miR-106b-5p ↑	FOG2	Activation	Cell proliferation and cell invasion	OncomiR	Yu et al. (2019)
miR-30b-3p ↑	TRIM27	Repression	Proliferation, migration, and invasion	Tumor suppressor	Gao et al. (2019)
miR-3691-5p ↑	PTEN	Activation	Vascular invasion	OncomiR	Du et al. (2019)
miR-92a-3p ↑	N-cadherin and Vimentin protein	Activation	Cell proliferation, migration, and invasion	OncomiR	Wang et al. (2021)
Hippo-YAP/TAZ					
miR-135b ↑	MST1	Activation	Cell proliferation, migration, and invasion	OncomiR	Xin et al. (2020b)
miR-1307-3p ↑	LATS1	Activation	Cell proliferation, migration, and invasion	OncomiR	Guan et al. (2019)
miR-29c-3p ↓	DNMT3B	Repression	Cell proliferation, apoptosis, migration, and tumor growth	Tumor suppressor	Wu et al. (2019)
miR-512-3p ↑	LATS2	Repression	Cell proliferation, migration, and invasion	OncomiR	Zhang et al. (2020a)
miR-21-3p ↑	SMAD7	Activation	Malignant phenotype progression	OncomiR	Hong et al. (2021)
Wnt/β-catenin					
miR-1246 ↑	RORα	Activation	Tumor growth	OncomiR	Huang et al. (2020)
miR-329-3p ↓	USP22	Activation	Proliferation, migration, invasion, DNA repair, and stemness	Tumor suppressor	Xin et al. (2020a)
miR-342 ↓	CXCL12	Repression	Cell proliferation and apoptosis	Tumor suppressor	Lu et al. (2019)
miR-19a-3p ↑ and miR-376c-3p ↑	SOX6	Activation	Cell proliferation, migration, and invasion	OncomiR	Cao et al. (2021)
miR-194 ↑	PRC1 and β-catenin	Repression	Proliferation, migration, invasion, and stemness	OncomiR	Tang et al. (2019)
miR-485-5p ↓	WBP2	Repression	Proliferation, migration, and invasion	Tumor suppressor	Gao et al. (2020)
miR-361-5p ↓	WT1	Repression	Proliferation, migration, and invasion	Tumor suppressor	Cheng et al. (2019)

targeting this pathway must be thoroughly investigated before it reaches the clinics. Nevertheless, a greater understanding of the interaction between miRNAs and the canonical Wnt/β-catenin signaling pathway would disclose the underlying cause of HCC and aid in the development of innovative therapeutic approaches.

Additionally, significant risk factors for HCC include non-alcoholic fatty liver disease (NAFLD), chronic alcohol consumption, aflatoxin B1 exposure, hepatitis B (HBV) and C virus (HCV) infection (Fujiwara et al., 2018); and strong evidence has drawn attention to the notion that miRNAs could be critical determinants in setting these risk factors and, therefore, might play essential roles in the pathogenesis of HCC (Morishita et al., 2021). For example, some essential miRNAs are related to NAFLD pathogenesis since they perform pivotal regulatory functions of hepatic lipid metabolism (López-Sánchez et al., 2021). At the same time, the role of miRNAs in alcohol-related liver disease (ARLD) and the modulatory effects of alcohol consumption on miRNA expression have been reviewed in the past years since miRNAs can regulate the complex interplay between heavy alcohol consumption along with susceptibility to the disease (Torres et al., 2018). Moreover, in HCC pathogenesis, the alteration of miRNAs' expression in response to xenobiotic exposure (including aflatoxin B1 exposure Balasubramanian et al., 2020); as well as their regulatory role in early HBV and HCV infection, has also been explicitly studied (Lee et al., 2017; Sartorius et al., 2019).

In recent years, significant progress has been made demonstrating miRNA regulation in various cancer, including HCC, and since several signaling pathways are substantially associated with it (Table 1), we believe it is worth writing this review describing miRNA-mediated modulation of the most relevant signaling pathways in HCC development. Undoubtedly, the interaction between miRNAs and signaling pathways in hepatic pathophysiology is complex, but new relevant information is rapidly growing, which might help to develop advanced HCC therapy.

Author contributions

LR-M and SPau conceived, performed the literature search, and wrote the manuscript. OC-M, EZ, SO-P, and CE-M performed the literature search and contributed to writing the manuscript. SPat, AntB, AniB, and AD critically revised the manuscript. All authors have reviewed and approved the final manuscript.

Conflict of interest

Author AniB was employed by the company Reliance Industries Ltd.

The remaining authors declare that the research was conducted in the absence of any commercial or financial relationships that could be construed as a potential conflict of interest.

Publisher's note

All claims expressed in this article are solely those of the authors and do not necessarily represent those of their affiliated organizations, or those of the publisher, the editors and the reviewers. Any product that may be evaluated in this article, or claim that may be made by its manufacturer, is not guaranteed or endorsed by the publisher.

References

Alqahtani, A., Khan, Z., Alloghbi, A., Ahmed, T. S. S., Ashraf, M., and Hammouda, D. M. (2019). Hepatocellular carcinoma: Molecular mechanisms and targeted therapies. *Med. (B Aires)* 55. doi:10.3390/MEDICINA55090526

Alzahrani, A. S. (2019). PI3K/Akt/mTOR inhibitors in cancer: At the bench and bedside. *Semin. Cancer Biol.* 59. doi:10.1016/J.SEMCANCER.2019.07.009

An, Y., Zhang, Q., Li, X., Wang, Z., Li, Y., and Tang, X. (2018). Upregulated microRNA miR-21 promotes the progression of lung adenocarcinoma through inhibition of KIBRA and the Hippo signaling pathway. *Biomed. Pharmacother.* 108, 1845–1855. doi:10.1016/J.BIOPHA.2018.09.125

Ashrafizadeh, M., Taeb, S., Hushmandi, K., Orouei, S., Shahinozzaman, M., Zabolian, A., et al. (2020). Cancer and SOX proteins: New insight into their role in ovarian cancer progression/inhibition. *Pharmacol. Res.* 161. doi:10.1016/J.PHRS.2020.105159

Balasubramanian, S., Gunasekaran, K., Sasidharan, S., Jeyamanickavel Mathan, V., and Perumal, E. (2020). MicroRNAs and xenobiotic toxicity: An overview. *Toxicol. Rep.* 7, 583–595. doi:10.1016/J.TOXREP.2020.04.010

Cao, X., Zhang, J., Apaer, S., Yao, G., and Li, T. (2021). microRNA-19a-3p and microRNA-376c-3p promote hepatocellular carcinoma progression through SOX6-mediated wnt/β-catenin signaling pathway. *Int. J. General Med.* 14, 89. doi:10.2147/IJGM.S278538

Chen, J., Rajasekaran, M., Xia, H., Zhang, X., Kong, S. N., Sekar, K., et al. (2016). The microtubule-associated protein PRC1 promotes early recurrence of hepatocellular carcinoma in association with the Wnt/β-catenin signalling pathway. *Gut* 65, 1522–1534. doi:10.1136/GUTJNL-2015-310625

Chen, S., Wang, H., Huang, Y. F., Li, M. L., Cheng, J. H., Hu, P., et al. (2017). WW domain-binding protein 2: An adaptor protein closely linked to the development of breast cancer. *Mol. Cancer* 16. doi:10.1186/S12943-017-0693-9

Cheng, Y., Qiu, L., He, G. L., Cai, L., Peng, B. J., Cao, Y. L., et al. (2019). MicroRNA-361-5p suppresses the tumorigenesis of hepatocellular carcinoma through targeting WT1 and suppressing WNT/β-cadherin pathway. *Eur. Rev. Med. Pharmacol. Sci.* 23, 8823–8832. doi:10.26355/EURREV_201910_19277

Du, W., Zhang, X., and Wan, Z. (2019). miR-3691-5p promotes hepatocellular carcinoma cell migration and invasion through activating PI3K/Akt signaling by targeting PTEN. *Onco Targets Ther.* 12, 4897–4906. doi:10.2147/OTT.S208127

Fardi, M., Solali, S., and Farshdousti Hagh, M. (2018). Epigenetic mechanisms as a new approach in cancer treatment: An updated review. *Genes Dis.* 5, 304–311. doi:10.1016/J.GENDIS.2018.06.003

Fruman, D. A., Chiu, H., Hopkins, B. D., Bagrodia, S., Cantley, L. C., and Abraham, R. T. (2017). The PI3K pathway in human disease. *Cell* 170, 605. doi:10.1016/J.CELL.2017.07.029

Fujiwara, N., Friedman, S. L., Goossens, N., and Hoshida, Y. (2018). Risk factors and prevention of hepatocellular carcinoma in the era of precision medicine. *J. Hepatol.* 68, 526–549. doi:10.1016/J.JHEP.2017.09.016

Gao, D., Zhou, Z., and Huang, H. (2019). miR-30b-3p inhibits proliferation and invasion of hepatocellular carcinoma cells *via* suppressing PI3K/Akt pathway. *Front. Genet.* 10, 1274. doi:10.3389/FGENE.2019.01274/BIBTEX

Gao, J., Dai, C., Yu, X., Yin, X. B., and Zhou, F. (2020). microRNA-485-5p inhibits the progression of hepatocellular carcinoma through blocking the WBP2/Wnt signaling pathway. *Cell Signal* 66. doi:10.1016/J.CELLSIG.2019.109466

Guan, L., Li, T., Ai, N., Wang, W., He, B., Bai, Y., et al. (2019). MEIS2C and MEIS2D promote tumor progression *via* Wnt/β-catenin and hippo/YAP signaling in hepatocellular carcinoma. *J. Exp. Clin. Cancer Res.* 38, 1–14. doi:10.1186/S13046-019-1417-3/FIGURES/7

He, S., and Tang, S. (2020). WNT/β-catenin signaling in the development of liver cancers. *Biomed. Pharmacother.* 132, 110851. doi:10.1016/J.BIOPHA.2020.110851

Hong, Y., Ye, M., Wang, F., Fang, J., Wang, C., Luo, J., et al. (2021). MiR-21-3p promotes hepatocellular carcinoma progression *via* SMAD7/YAP1 regulation. *Front. Oncol.* 11, 303. doi:10.3389/FONC.2021.642030/BIBTEX

Huang, J. L., Fu, Y. P., Gan, W., Liu, G., Zhou, P. Y., Zhou, C., et al. (2020). Hepatic stellate cells promote the progression of hepatocellular carcinoma through microRNA-1246-RORα-Wnt/β-Catenin axis. *Cancer Lett.* 476, 140–151. doi:10.1016/J.CANLET.2020.02.012

Jiang, W., Yuan, Q., Jiang, Y., huang, L., Chen, C., Hu, G., et al. (2018). Identification of Sox6 as a regulator of pancreatic cancer development. *J. Cell. Mol. Med.* 22, 1864. doi:10.1111/JCMM.13470

Juliano, R. L. (2020). Addressing cancer signal transduction pathways with antisense and siRNA oligonucleotides. *Nar. Cancer* 2(3):zcaa025. doi:10.1093/NARCAN/ZCAA025

Kim, E., and Viatour, P. (2020). Hepatocellular carcinoma: Old friends and new tricks. *Exp. Mol. Med.* 52 (12). 1898-1907. doi:10.1038/s12276-020-00527-1

Lee, C. H., Kim, J. H., and Lee, S.-W. (2017). The role of MicroRNA in pathogenesis and as markers of HCV chronic infection. *Curr. Drug Targets* 18, 756–765. doi:10.2174/1389450117666160401125213

Leichter, A. L., Sullivan, M. J., Eccles, M. R., and Chatterjee, A. (2017). MicroRNA expression patterns and signalling pathways in the development and progression of childhood solid tumours. *Mol. Cancer* 16 (1), 1–17. doi:10.1186/S12943-017-0584-0

Liu, Y., Wang, X., and Yang, Y. (2020). Hepatic Hippo signaling inhibits development of hepatocellular carcinoma. *Clin. Mol. Hepatology* 26, 742. doi:10.3350/CMH.2020.0178

Llovet, J. M., Kelley, R. K., Villanueva, A., Singal, A. G., Pikarsky, E., Roayaie, S., et al. (2021). Hepatocellular carcinoma. *Nat. Rev. Dis. Prim.* 7 (1 7), 1–28. doi:10.1038/s41572-020-00240-3

López-Sánchez, G. N., Dóminguez-Pérez, M., Uribe, M., Chávez-Tapia, N. C., and Nuño-Lámbarri, N. (2021). Non-alcoholic fatty liver disease and microRNAs expression, how it affects the development and progression of the disease. *Ann. Hepatology* 21, 100212. doi:10.1016/J.AOHEP.2020.04.012

Lu, C., Jia, S., Zhao, S., and Shao, X. (2019). MiR-342 regulates cell proliferation and apoptosis in hepatocellular carcinoma through Wnt/β-catenin signaling pathway. *Cancer Biomark.* 25, 115–126. doi:10.3233/CBM-192399

Mori, M., Triboulet, R., Mohseni, M., Schlegelmilch, K., Shrestha, K., Camargo, F. D., et al. (2014). Hippo signaling regulates microprocessor and links cell-density-dependent miRNA biogenesis to cancer. *Cell* 156, 893–906. doi:10.1016/J.CELL.2013.12.043

Morishita, A., Oura, K., Tadokoro, T., Fujita, K., Tani, J., and Masaki, T. (2021). MicroRNAs in the pathogenesis of hepatocellular carcinoma: A review. *Cancers (Basel)* 13, 1–29. doi:10.3390/CANCERS13030514

Paul, S., Bravo Vázquez, L. A., Reyes-Pérez, P. R., Estrada-Meza, C., Aponte Alburquerque, R. A., Pathak, S., et al. (2022). The role of microRNAs in solving COVID-19 puzzle from infection to therapeutics: A mini-review. *Virus Res.* 308. doi:10.1016/J.VIRUSRES.2021.198631

Paul, S., Ruiz-Manriquez, L. M., Ledesma-Pacheco, S. J., Benavides-Aguilar, J. A., Torres-Copado, A., Morales-Rodríguez, J. I., et al. (2021). Roles of microRNAs in chronic pediatric diseases and their use as potential biomarkers: A review. *Archives Biochem. Biophysics* 699, 108763. doi:10.1016/J.ABB.2021.108763

Qi, X. W., Zhang, F., Wu, H., Liu, J. L., Zong, B. G., Xu, C., et al. (2015). Wilms' tumor 1 (WT1) expression and prognosis in solid cancer patients: A systematic review and meta-analysis. *Sci. Rep.* 5. doi:10.1038/SREP08924

Rahmani, F., Ziaeemehr, A., Shahidsales, S., Gharib, M., Khazaei, M., Ferns, G. A., et al. (2020). Role of regulatory miRNAs of the PI3K/AKT/mTOR signaling in the pathogenesis of hepatocellular carcinoma. *J. Cell. Physiology* 235, 4146–4152. doi:10.1002/JCP.29333

Roche, J. (2018). The epithelial-to-mesenchymal transition in cancer. *Cancers (Basel)* 10, 52. doi:10.3390/CANCERS10020052

Ruiz-Manriquez, L. M., Estrada-Meza, C., Benavides-Aguilar, J. A., Ledesma-Pacheco, S. J., Torres-Copado, A., Serrano-Cano, F. I., et al. (2021). Phytochemicals mediated modulation of microRNAs and long non-coding RNAs in cancer prevention and therapy. *Phytother. Res.* 36 (2), 705–729. doi:10.1002/PTR.7338

Ruiz-Manriquez, L. M., Ledesma Pacheco, S. J., Medina-Gomez, D., Uriostegui-Pena, A. G., Estrada-Meza, C., Bandyopadhyay, A., et al. (2022). A brief review on the regulatory roles of MicroRNAs in cystic diseases and their use as potential biomarkers. *Genes (Basel)* 13. doi:10.3390/GENES13020191

Samji, P., Rajendran, M. K., Warrier, V. P., Ganesh, A., and Devarajan, K. (2021). Regulation of hippo signaling pathway in cancer: A MicroRNA perspective. *Cell. Signal.* 78, 109858. doi:10.1016/J.CELLSIG.2020.109858

Sartorius, K., Makarova, J., Sartorius, B., An, P., Winkler, C., Chuturgoon, A., et al. (2019). The regulatory role of MicroRNA in hepatitis-B virus-associated hepatocellular carcinoma (HBV-HCC) pathogenesis. *Cells* 8, 1504. doi:10.3390/CELLS8121504

Siegel, R. L., Miller, K. D., and Jemal, A. (2017). Cancer statistics, 2017. *CA Cancer J. Clin.* 67, 7–30. doi:10.3322/CAAC.21387

Singh, G., Yoshida, E. M., Rathi, S., Marquez, V., Kim, P., Erb, S. R., et al. (2020). Biomarkers for hepatocellular cancer. *World J. Hepatology* 12, 558. doi:10.4254/WJH.V12.I9.558

Sun, L., Wang, L., Chen, T., Yao, B., Wang, Y., Li, Q., et al. (2019). microRNA-1914, which is regulated by lncRNA DUXAP10, inhibits cell proliferation by targeting the GPR39-mediated PI3K/AKT/mTOR pathway in HCC. *J. Cell. Mol. Med.* 23, 8292. doi:10.1111/JCMM.14705

Tang, H., Zhao, H., Yu, Z. Y., Feng, X., Fu, B. S., Qiu, C. H., et al. (2019). MicroRNA-194 inhibits cell invasion and migration in hepatocellular carcinoma through PRC1-mediated inhibition of Wnt/β-catenin signaling pathway. *Dig. Liver Dis.* 51, 1314–1322. doi:10.1016/J.DLD.2019.02.012

Torres, J. L., Novo-Veleiro, I., Manzanedo, L., Suárez, L. A., MacÍas, R., Laso, F. J., et al. (2018). Role of microRNAs in alcohol-induced liver disorders and non-alcoholic fatty liver disease. *World J. Gastroenterology* 24, 4104. doi:10.3748/WJG.V24.I36.4104

Vasuri, F., Visani, M., Acquaviva, G., Brand, T., Fiorentino, M., Pession, A., et al. (2018). Role of microRNAs in the main molecular pathways of hepatocellular carcinoma. *World J. Gastroenterology* 24, 2647. doi:10.3748/WJG.V24.I25.2647

Vázquez, B., Becerril, M., Hernández, M., Carmona, L., Padilla, A., Phylactou, A., et al. (2021). The emerging role of MicroRNAs in bone diseases and their therapeutic potential. *Molecules* 27, 211. *Page 211* 27. doi:10.3390/MOLECULES27010211

Vishnoi, A., and Rani, S. (2017). MiRNA biogenesis and regulation of diseases: An overview. *Methods Mol. Biol.* 1509, 1. doi:10.1007/978-1-4939-6524-3_1

Wang, L., Cui, M., Qu, F., Cheng, D., Yu, J., Tang, Z., et al. (2021). MiR-92a-3p promotes the malignant progression of hepatocellular carcinoma by mediating the PI3K/AKT/mTOR signaling pathway. *Curr. Pharm. Des.* 27, 3244–3250. doi:10.2174/1381612827666210612054156

Wang, Y., Shi, F., Xing, G. H., Xie, P., Zhao, N., Yin, Y. F., et al. (2017). Protein regulator of cytokinesis PRC1 confers chemoresistance and predicts an unfavorable postoperative survival of hepatocellular carcinoma patients. *J. Cancer* 8, 801–808. doi:10.7150/JCA.17640

Wu, H., Zhang, W., Wu, Z., Liu, Y., Shi, Y., Gong, J., et al. (2019). miR-29c-3p regulates DNMT3B and LATS1 methylation to inhibit tumor progression in hepatocellular carcinoma. *Cell Death Dis.* 10 (2), 48. doi:10.1038/s41419-018-1281-7

Wu, Y., Zhang, Y., Wang, F., Ni, Q., and Li, M. (2020). MiR-660-5p promotes the progression of hepatocellular carcinoma by interaction with YWHAH *via* PI3K/Akt signaling pathway. *Biochem. Biophysical Res. Commun.* 531, 480–489. doi:10.1016/J.BBRC.2020.07.034

Xin, R. Q., Li, W. B., Hu, Z. W., Wu, Z. X., and Sun, W. (2020a). MiR-329-3p inhibits hepatocellular carcinoma cell proliferation and migration through USP22-Wnt/β-Catenin pathway. *Eur. Rev. Med. Pharmacol. Sci.* 24, 9932–9939. doi:10.26355/EURREV_202010_23204

Xin, Y., Yang, X., Xiao, J., Zhao, W., Li, Y., Lu, L., et al. (2020b). MiR-135b promotes HCC tumorigenesis through a positive-feedback loop. *Biochem. Biophysical Res. Commun.* 530, 259–265. doi:10.1016/J.BBRC.2020.07.008

Yao, Y., Dou, C., Lu, Z., Zheng, X., and Liu, Q. (2015). MACC1 suppresses cell apoptosis in hepatocellular carcinoma by targeting the HGF/c-MET/AKT pathway. *Cell. Physiology Biochem.* 35, 983–996. doi:10.1159/000369754

Yu, L. X., Zhang, B. L., Yang, M. Y., Liu, H., Xiao, C. H., Zhang, S. G., et al. (2019). MicroRNA-106b-5p promotes hepatocellular carcinoma development *via* modulating FOG2. *Onco Targets Ther.* 12, 5639. doi:10.2147/OTT.S203382

Zhang, B., Huang, L., Tu, J., and Wu, T. (2020a). Hypoxia-induced placenta-specific microRNA (miR-512-3p) promotes hepatocellular carcinoma progression by targeting large tumor suppressor kinase 2. *Onco Targets Ther.* 13, 6073. doi:10.2147/OTT.S254612

Zhang, S., and Zhou, D. (2019). Role of the transcriptional coactivators YAP/TAZ in liver cancer. *Curr. Opin. Cell Biol.* 61, 64–71. doi:10.1016/J.CEB.2019.07.006

Zhang, Y., Feng, Y., Ji, D., Wang, Q., Qian, W., Wang, S., et al. (2018). TRIM27 functions as an oncogene by activating epithelial-mesenchymal transition and p-AKT in colorectal cancer. *Int. J. Oncol.* 53, 620. doi:10.3892/IJO.2018.4408

Zhang, Y. M., Wu, Q. M., Chang, L. Y., and Liu, J. C. (2020b). miR-34a and miR-125a-5p inhibit proliferation and metastasis but induce apoptosis in hepatocellular carcinoma cells *via* repressing the MACC1-mediated PI3K/AKT/mTOR pathway. *Neoplasma* 67, 1042–1053. doi:10.4149/NEO_2020_191019N1062

Zhang, Y., and Wang, X. (2020). Targeting the Wnt/β-catenin signaling pathway in cancer. *J. Hematol. Oncol.* 13 (1 13), 1–16. doi:10.1186/S13045-020-00990-3

frontiers | Frontiers in Genetics

TYPE Systematic Review
PUBLISHED 02 September 2022
DOI 10.3389/fgene.2022.927079

OPEN ACCESS

EDITED BY
Naseer A. Kutchy,
Children's National Hospital,
United States

REVIEWED BY
Muhammet Rasit Ugur,
IVF Michigan Fertility Centers,
United States
Mudasir Rashid,
Howard University Hospital,
United States

*CORRESPONDENCE
Bangshun He,
bhe@njmu.edu.cn
Junrong Zhu,
junrong_zhu@aliyun.com

†These authors have contributed equally to this work and share first authorship

SPECIALTY SECTION
This article was submitted to RNA, a section of the journal Frontiers in Genetics

RECEIVED 23 April 2022
ACCEPTED 02 August 2022
PUBLISHED 02 September 2022

CITATION
Lu F, Zhao X, Zhang Z, Xiong M, Wang Y, Sun Y, He B and Zhu J (2022), The diagnostic and prognostic value of the miR-17-92 cluster in hepatocellular carcinoma: A meta-analysis.
Front. Genet. 13:927079.
doi: 10.3389/fgene.2022.927079

The diagnostic and prognostic value of the miR-17-92 cluster in hepatocellular carcinoma: A meta-analysis

Fang Lu[1,2†], Xianghong Zhao[1,2†], Zhongqiu Zhang[1,2], Mengqiu Xiong[3], Ying Wang[1,2], Yalan Sun[1,2], Bangshun He[1,3*] and Junrong Zhu[1,2*]

[1]School of Basic Medicine and Clinical Pharmacy, China Pharmaceutical University, Nanjing, China, [2]Department of Pharmacy, Nanjing First Hospital, China Pharmaceutical University, Nanjing, China, [3]Department of Laboratory Medicine, Nanjing First Hospital, Nanjing Medical University, Nanjing, China

Previous studies demonstrated that microRNAs (miRNAs) could serve as biomarkers in various cancers. This meta-analysis aimed to determine the roles of a miR-17-92 cluster in hepatocellular carcinoma (HCC). Here, eligible included studies were searched through PubMed, Embase, and Wan Fang databases up to 1st February 2022. Relevant data were extracted from each eligible study to evaluate the relationship between miRNA-17-92 cluster miRNA expression and the diagnosis and prognosis of HCC. Finally, a total of 21 studies were pooled and included in the meta-analysis, of which four articles were used for diagnostic meta-analysis and eight articles were used for prognostic meta-analysis. The pooled sensitivity, specificity, and diagnostic odds ratios (DOR) of the miR17-92 cluster for diagnosis of HCC were 0.75 [95% confidence interval (CI): 0.64–0.83], 0.73 (95% CI: 0.65–0.79), and 7.87 (95% CI: 5.36–11.54), respectively. Also, the area under the curve (AUC) for the miR-17-92 cluster when diagnosing HCC was 0.79 (95% CI: 0.76–0.83). For prognostic analysis, hazard ratios (HRs) with 95% CIs were extracted from the included studies and pooled HRs were determined to assess the associations. Patients with increased expression of miR17-92 cluster miRNA were associated with poor overall survival (OS) and recurrence-free survival (RFS) (HR=1.86, 95% CI: 1.04–3.33; HR = 4.18, 95% CI: 3.02–5.77, respectively), but not progression-free survival (PFS) (HR = 0.43, 95% CI: 0.25–0.73), while no association of the miR-17-92 cluster high-expression was detected with disease-free survival (DFS) (HR: 0.95, 95% CI: 0.21–4.34). In short, current pieces of evidence suggested that the miR-17-92 cluster may serve as a novel diagnostic and prognostic biomarker for HCC. However, given the limited study number, larger-size, multi-center, and higher-quality studies are indispensable in the future.

KEYWORDS

miR-17-92 cluster, hepatocellular carcinoma, diagnostic value, prognostic value, meta-analysis

Introduction

Hepatocellular carcinoma (HCC) is one of the most malignant tumors, accounting for approximately 90% of primary liver cancers (Llovet et al., 2021). Worldwide, it ranks sixth in incidence and fourth in cancer death-related causes (Villanueva, 2019). As a country with a relatively high incidence of HCC, China accounts for more than 50% of the world's annual new cases (4,66,000) and deaths (approximately 4,22,000) each year (Chen et al., 2016; Gordan et al., 2020), which are mainly due to the highly complex heterogeneity and multiple etiologies of HCC, including cirrhosis, hepatitis B virus (HBV), hepatitis C virus (HCV) infection, and nonalcoholic steatohepatitis (NASH) (Estes et al., 2018; Zhang et al., 2022). Moreover, aflatoxin-contaminated foodstuffs, heavy alcohol intake, obesity, smoking, type 2 diabetes, and other related cofactors contribute to the pathogenesis of HCC (Llovet et al., 2016).

Currently, alpha-fetoprotein (AFP), a carcinoembryonic glycoprotein, is used alone or in combination with ultrasound and other imaging modalities as a tumor marker for HCC, whereas its utility is limited due to low sensitivity and specificity, as well as differences between different measurement methods, which were attributed to patient characteristics, study design, and AFP cutoff values (Gupta et al., 2003). The traditional treatments such as surgical resection, liver transplantation, local minimally invasive, precision radiotherapy, radical treatment, systemic treatment (targeted therapy and immunotherapy), optimal treatment, and palliative treatment were mainly selected for HCC patients. However, due to the high recurrence rate and high metastasis rate of HCC, the prognosis of HCC has always been unsatisfactory. The 5-year survival rate of patients with early HCC is as high as 75%, while the 1-year survival rate of patients diagnosed with generalized cancer is less than 10% (El-Serag et al., 2008; El-Serag, 2011). The HCC has a serious impact on human health and quality of life around the world. Despite reasonable and well-established treatment options, the prognosis of patients is also very poor because HCC is often diagnosed at a rapidly progressive and advanced stage. Hence, it is urgent to further understand the mechanism underlining the pathological progression of HCC and find new markers for early diagnosis and treatment prognosis.

MicroRNAs (miRNAs) are a type of short, single-stranded non-coding RNAs with 19–25 nucleotides regulating the gene expression mainly by targeting the 3′-UTR of mRNAs, posttranscriptional effects (O'Brien et al., 2018). Therefore, they are involved in regulating numerous biological events such as apoptosis, cell cycle, proliferation, and invasion, playing key roles in tumorigenesis and malignant development (Gebert and MacRae, 2019). Accumulating studies have demonstrated that abnormal expression of miRNAs could serve as the biomarker for early diagnosis and treatment of HCC. For example, combining serum miR497 and miR-1246 together for HCC diagnosis, the sensitivity and specificity reach 94.0% and 70.0%, respectively, which increased the accuracy of HCC diagnosis (Chen et al., 2021). Huang et al. (2021) found that the expression of miR-125b-2-3p was downregulated in HCC tissues compared with non-tumor tissues, and the lower expression of miR-125b-2-3p indicated poor progression and prognosis in HCC. El-Mezayen et al. (2021) found that miR-25 modulated an oncogenic function by regulating the Ubiquitin Ligase Fbxw7 in HCC.

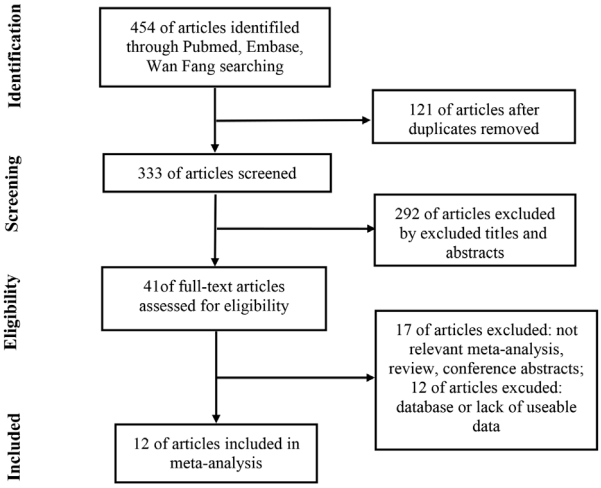

FIGURE 1
Flow chart of the article selection process.

The miR-17-92 is a typical highly conserved miRNA cluster, which is found in human chromosome 13 open-reading frame 25 (C13orf25) (Fang et al., 2017). The cluster encodes six mature miRNAs, namely, miR-17, miR-18a, miR-19a, miR-19b, miR-20a, and miR-92a (Ota et al., 2004; Concepcion et al., 2012; Zhang et al., 2018). Recently, multiple studies have shown that members of the miRNA-17-92 cluster are specifically expressed in types of cancer, suggesting that the miR-17-92 cluster may serve as a new biomarker for cancer diagnosis and treatment. For example, miR-92a is closely associated with colorectal cancer lymphoma metastasis, suggesting that miR-92a may be a potential marker of colorectal cancer (Zhou et al., 2013); in a meta-analysis on the diagnostic value of serum miRNA in gastric cancer, it was indicated that the area under the curve (AUC) for the combination of miR-19a and miR-92a was the highest at 0.850, with a sensitivity of 91.3% and a specificity of 61.0% (Liu et al., 2018). However, evidence for the diagnostic and prognostic role of miR-17-92 cluster expression in HCC was still lacking. Therefore, this study aims to explore the diagnostic and prognostic value of the miR-17-92 cluster in HCC by investigating expression levels of this miRNA in HCC patients. The findings of this study might provide a potential reference for clinicians

10.3389/fgene.2022.927079

TABLE 1 Main characteristics of the eligible studies for diagnostic meta-analysis.

First author	Year	Country	Sample source	Sample range	Patient case/control	microRNA	Test method	SEN (%)	SPE (%)	Tp	FP	FN	TN	Cut off	QUADAS-2
Yang Wen	2015	China	Plasma	I-IV	67/82	miR-20a	qRT-PCR	86.6	57.3	58	35	9	47	2.555×10^{-3}	5
Yang Wen	2015	China	Plasma	NR	67/82	miR-92a	qRT-PCR	76.1	68.3	51	26	16	56	5.573×10^{-3}	5
Lihua Li	2012	China	serum	NR	101/60	miR-18a	qRT-PCR	86.1	75	87	15	14	45	1.765	6
Tarek K. Motawi	2015	Egypt	serum	NR	112/42	miR-19a	qRT-PCR	60.7	89.2	68	5	44	37	<0.625	7
Tarek K. Motawi	2015	Egypt	serum	NR	112/125	miR-19a	qRT-PCR	92.9	75.5	68	31	44	94	<1.58	7
Fatma A. Fathy.Elmougy	2019	Egypt	serum	NR	40/40	miR-19a	qRT-PCR	70	77.5	28	12	9	31	≥0.65	5

NR, not report; qRT-PCR, quantitative reverse transcription-polymerase chain reaction; SEN, sensitivity; SPE, specificity; TP, true positive; FP, false positive; FN, false negative; TN, true negative; QUADAS-2, quality assessment of diagnostic accuracy studies 2.

Materials and methods

Literature search

A comprehensive literature search was conducted in PubMed, Embase, and Wan Fang, with an update on 1st February 2022 to obtain potentially eligible studies. The search was conducted with the keywords (hepatocellular carcinoma OR HCC) AND (miR-17 OR microRNA-17 OR miR-18a OR microRNA-18a OR miR-19a OR microRNA-19a OR miR-19b OR microRNA-19b OR miR-92a OR microRNA-92a OR miR-20a OR microRNA-20a) AND (survival OR prognosis OR outcomes OR diagnosis). The searches were limited to human studies and articles in English. Additionally, other relevant articles were also obtained by manually screening the reference lists.

Inclusion and exclusion criteria

Inclusion criteria for the studies were as follows: 1) the study's patients had been diagnosed with HCC (any stage or histology) and tumor samples are naïve or associated with HBV/HCV; 2) clinical study about the association of expression of the miR-17-92 cluster with HCC diagnostic or prognostic value; 3) studies investigating the expression in whole blood, plasma or serum or tissues or Formalin-Fixed and Paraffin-Embedded (FFPE) of the miR-17-92 cluster in HCC patients and healthy controls; 4) the sensitivity and specificity are reported to provide enough information to construct a 2 × 2 contingency table, which includes true positive, false positive, false negative, and true negative; 5) relevant available data of the hazard ratios (HRs) and their corresponding 95% confidence intervals (CIs) to evaluate its associations could be obtained; and 6) patient prognostic outcomes including overall survival (OS), recurrence-free survival (RFS), disease-free survival (DFS), and progression-free survival (PFS).

Studies were excluded according to these exclusion criteria as follows: 1) duplicate publications; 2) other types of articles, such as meeting minutes, abstracts, comments, meta-analysis, patents, case reports, and letters; 3) insufficient data, unable to calculate true and false positive and negative information and unable to calculate HRs and 95% CIs; and 4) diagnostic or prognostic data from the TCGA data set.

Data extraction and quality assessment

The studies of diagnostic value extracted the following data: first author's name, publication year, study country, sample size, sample type, sample stage, microRNA, test method, and cut-off value; data are extracted by designing a table that includes sensitivity, specificity, number of true positives,

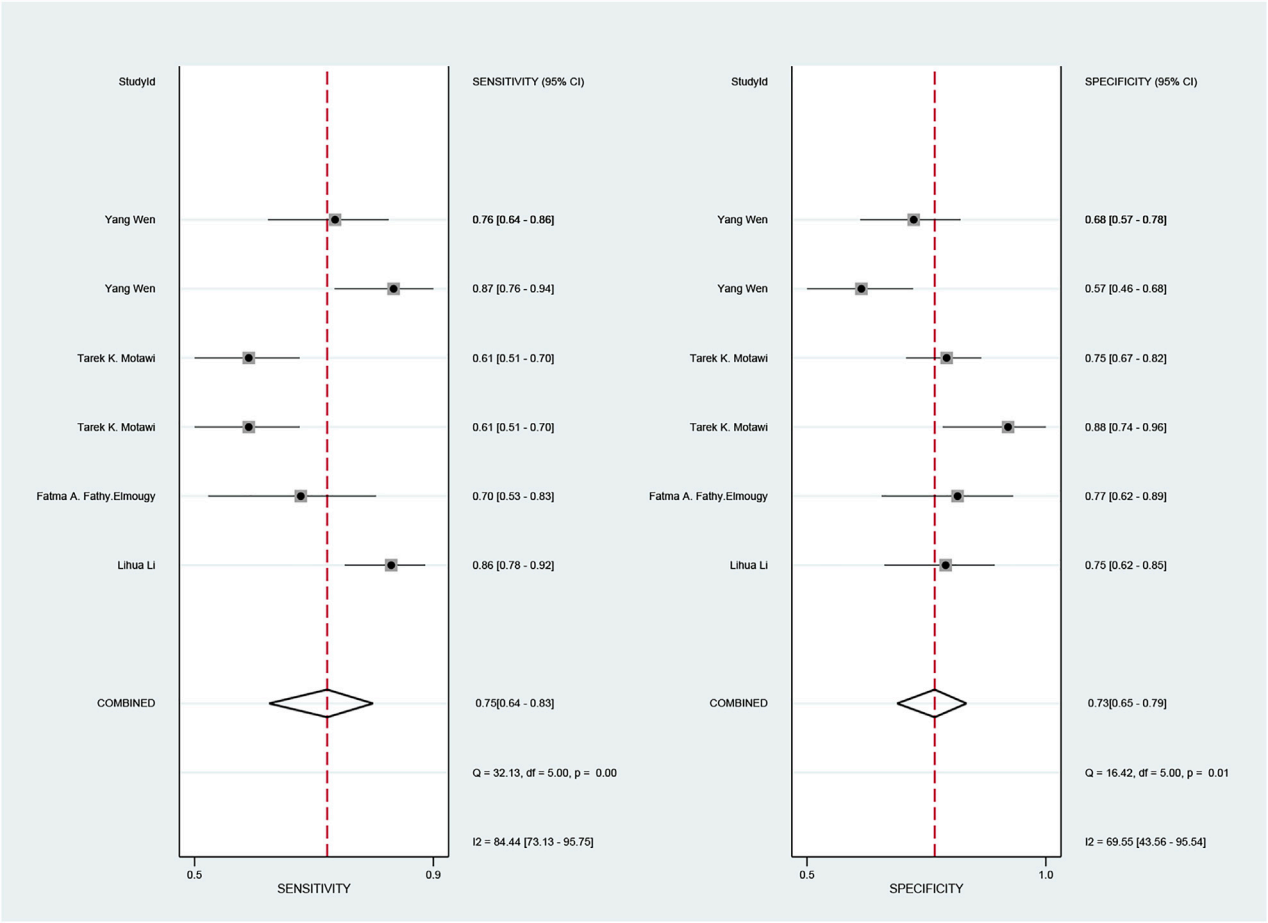

FIGURE 2
Forest plot of sensitivity and specificity for the miR-17–92 cluster in the diagnosis of hepatocellular carcinoma.

number of false positives, number of false negatives, and number of true negatives. The study of prognostic value extracted the following information: first author's name, publication year, study country, sample size, sample type, sample stage, microRNA, test method, cut-off value, outcome indicator, and HRs along with their corresponding 95% CIs.

Two researchers (Fang Lu and Xianghong Zhao) independently assessed whether each included study met the quality standards. Then, another researcher (Zhongqiu Zhang) reevaluated and made a unified conclusion if there was a discrepancy between the first two researchers. The quality assessment of each included diagnosis-related study was performed with the Quality Assessment of Diagnostic Accuracy Studies 2 (QUADAS 2) (Whiting et al., 2003), which is considered reliable for the quality assessment of test accuracy studies. The quality of involved prognosis-related studies was evaluated with the Newcastle–Ottawa Scale (NOS) (Lo et al., 2014), which is the tool most commonly used to assess the quality of non-randomized research (Roysri et al., 2014).

Statistical analysis

For diagnostic accuracy studies, the sensitivity, specificity, positive likelihood ratio (PLR), negative likelihood ratio (NLR), and corresponding 95% CIs from included studies were pooled to preliminarily assess the diagnostic value of the miR-17-92 cluster in HCC. Then, based on the original data, the summary receiver operating characteristic (SROC) curve was drawn, and the AUC was calculated to comprehensively determine the diagnostic accuracy of the miR-17-92 cluster. To assess the heterogeneity across studies, the Q-statistic and I^2 statistics were utilized. The I^2 value typically fluctuates within a range of 0 (unobserved heterogeneity) to 100% (maximum heterogeneity). P value < 0.05 or I^2 > 50% was recognized statistically significant (Raponi et al., 2009). If the studies were proved to be heterogeneous, the

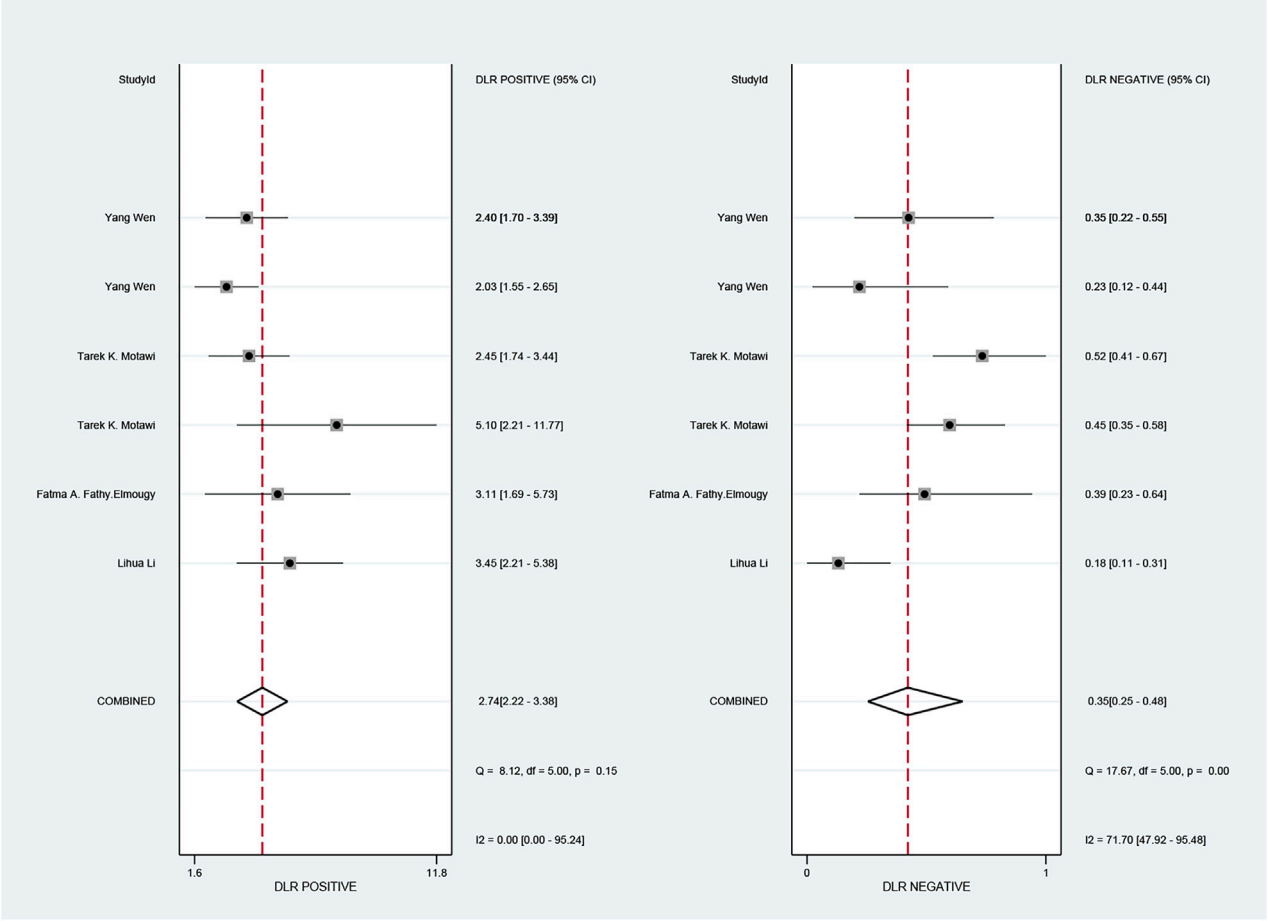

FIGURE 3
Forest plot of positive likelihood ratios (PLRs) and negative likelihood ratios (NLRs) for the miR-17–92 cluster in the diagnosis of hepatocellular carcinoma.

random-effects model would be utilized for further analysis. Subsequently, subgroups were analyzed to find potential sources of heterogeneity. Finally, the publication bias of all the included diagnostic accuracy studies was assessed by Deek's funnel plots Deeks et al. (2005) (significant at $P < 0.05$).

For the prognostic meta-analysis, the HRs and 95% CIs extracted from the eligible studies were combined to elucidate the relationship between the expression of miR-17-92 of cluster members and the survival results of HCC. I^2 statistics were applied to perform the heterogeneity of the pooled results (Higgins et al., 2003). The heterogeneity of the combined HRs would be considered acceptable if I^2 was <50%. In addition, the publication bias of all the included prognostic studies was evaluated by funnel plots and by Begg's and Egger's tests. $P < 0.05$ suggests the existence of publication bias in studies (Begg and Berlin, 1989). All abovementioned statistical calculations were carried out with STATA Statistical Software Version 12.0 (Stata Corp, College Station, TX, SA) and Excel software 2019.

Results

Summary of included study characteristics

The detailed article retrieval process is shown in Figure 1. Initially, a total of 454 articles were retrieved by the keywords, of which 121 duplicate articles were removed by checking article titles. After screen titles and abstracts of 292 articles were further removed, a total of 41 articles were all downloaded to obtain valid information individually. After reading the full text, 17 articles were removed due to irrelevant meta-analyses, reviews, and conference abstracts. Meanwhile, 12 articles were excluded due to the database or lack of useable diagnostic or prognostic data. Finally, 12 articles that met all the inclusion criteria were included in the current study. All enrolled eligible articles were published from 2012 to 2020, accumulating 1039 HCC patients and 349 case-control subjects.

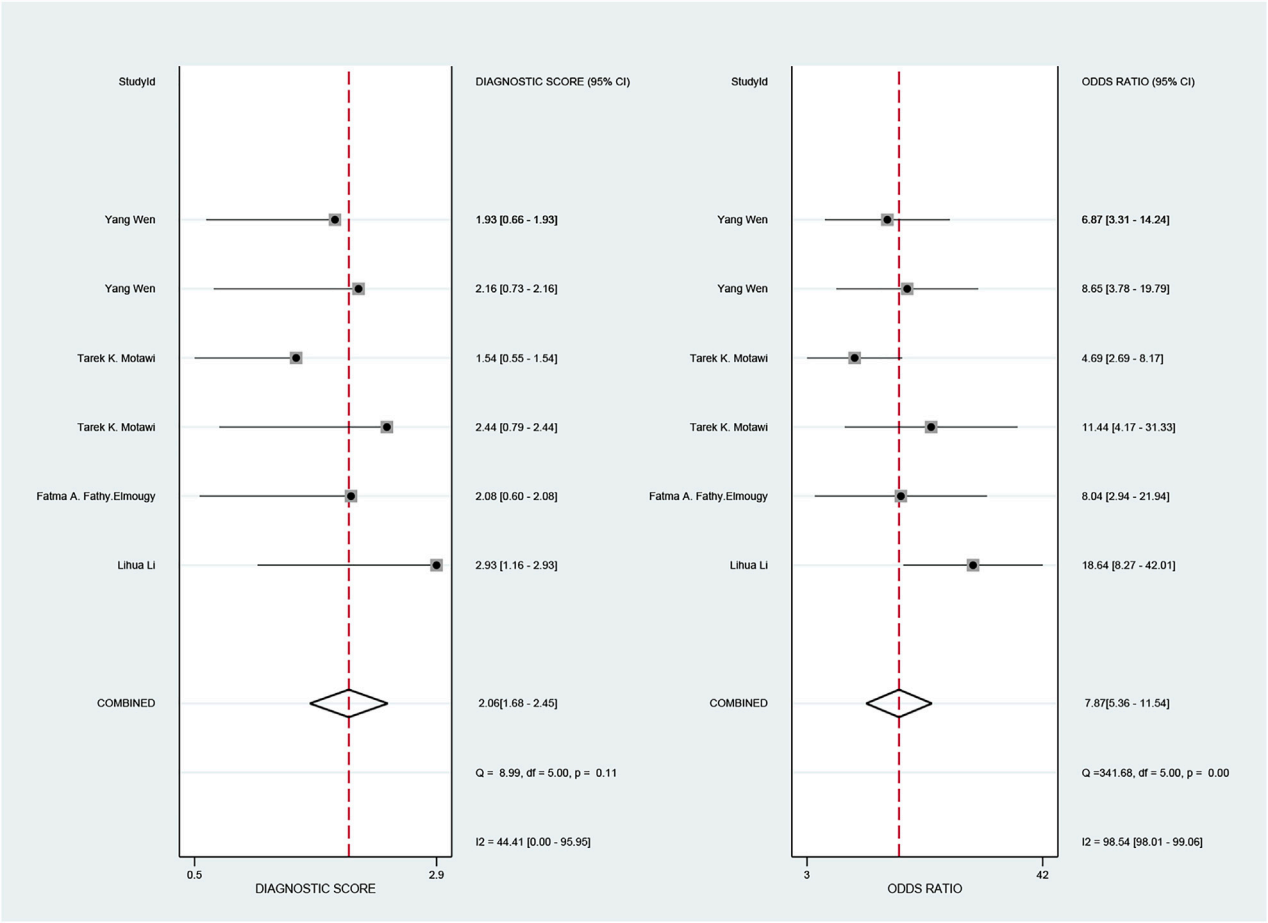

FIGURE 4
Forest plot of the diagnostic odds ratio (DOR) for the miR-17–92 cluster in the diagnosis of hepatocellular carcinoma.

The results of the diagnostic meta-analysis of hepatocellular carcinoma

Six studies (Li et al., 2012; Motawi et al., 2015; Wen et al., 2015; FathyElmougy et al., 2019) reported the role of the miR-17-92 cluster as a biomarker in HCC diagnosis, including 320 HCC patients and 349 control subjects. The characteristics and methods related to the diagnostic accuracy of the included studies are shown in Table 1. Of which, two ethnic groups were analyzed, three studies from Asians and the remaining three from Africans. All studies were performed with serum or plasma. Moreover, all included studies used real-time quantitative real-time polymerase chain reaction (qRT-PCR) to detect miR-17-92 miRNA expression.

The pooled sensitivity and specificity of the diagnostic value were 0.75 (95% CI: 0.64–0.83) and 0.73 (95% CI: 0.65–0.79), respectively, as shown in Figure 2. Meanwhile, the PLR and NLR were 2.74 (95% CI: 2.22–3.38) and 0.35 (95% CI: 0.25–0.48), respectively, which means that the probability of miR-17-92 positive in HCC patients was 2.74 times higher than that in controls, while HCC patients had miR-17-92 which was 0.35 times more likely to be negative than that of non-patients, shown in Figure 3. In addition, the pooled Diagnostic Odds Ratio (DOR) was 7.87 (95% CI: 5.36–11.54), as shown in Figure 4, and the area under the SROC (AUC) was 0.79 (95% CI: 0.76–0.83), suggesting that the miR-17-92 cluster has an acceptable diagnostic value, shown in Figure 5.

Fagan's nomogram was applied for assessing the clinical utility of the index test. We used likelihood ratios to simulate three clinical scenarios by implementing different pretest probabilities, with 25%, 50%, and 75% representing relatively low, moderate, and relatively high clinical suspicion, respectively. We used these likelihood ratios to evaluate post-test probabilities and plot the Fagan nomogram, as shown in Figure 6. When the pretest probability was 25%, the posttest probability positive (PPP) and the posttest probability negative (PPN) was 48% and 10%, respectively. When the pre-test probability is 50%, the PPP and PPN are 73% and 26%, respectively; when the pre-

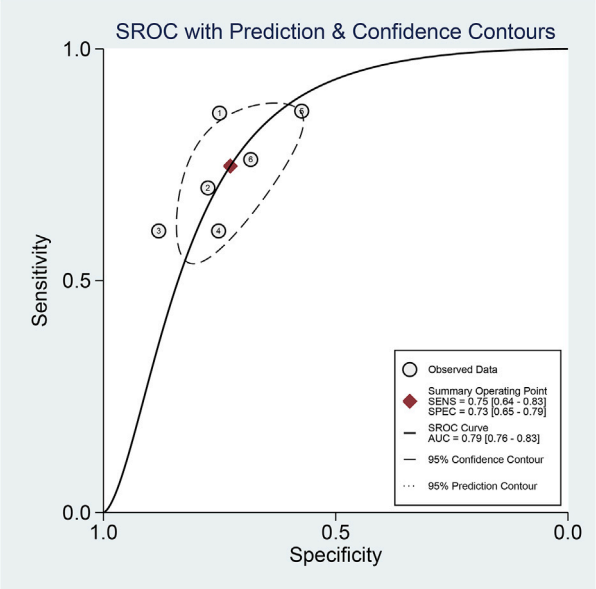

FIGURE 5
Summary receiver operating characteristic curve (SROC) for the miR-17–92 cluster in the diagnosis of hepatocellular carcinoma.

test probability is 75%, the PPP and PPN are 89% and 51%, respectively. Taken together, the miR-17-92 cluster had relatively acceptable accuracy for the identification of HCC patients. Deek's funnel plot showed that *P*-value across the studies was 0.36, indicating that there is almost no publication bias in diagnostic meta-analysis, as shown in Figure 7.

The ROC curve was a nontypical "shoulder–arm" appearance, so there was no significant threshold effect in the current meta-analysis, as shown in Figure 5. Moreover, the Spearman correlation coefficient between the log of sensitivity and the log of specificity was −0.95 (p = 0.90), also showing no significant threshold effect existing. According to the results of diagnostic accuracy analysis, significant heterogeneity was found across studies of sensitivity (I^2 = 84.44%, p = 0.00) and specificity (I^2 = 69.55%, p = 0.01), which suggested the significant heterogeneity caused by the non-threshold effect has existed among these studies. Hence, a meta-regression was used to distinguish the potential origins of heterogeneity between studies by exploring research characteristics, such as country, patients, sample type, and sample stage, and the results showed that heterogeneity was mainly derived from patients (P < 0.01) and sample type (P < 0.05), as shown in Figure 8.

The subgroup analysis results based on sample type, sample size, country, and tumor stage are summarized in Table 2. Stratified analysis by sample type showed that the sensitivity, specificity, and AUC of miR-17-92 cluster miRNA expression in serum were 0.70 (95% CI: 0.58–0.83), 0.77(0.72–0.82), and 0.79, respectively. However, since only two studies were included in the miR-17-92 cluster miRNA expression in plasma, no relevant data were calculated. The stratified analysis by sample size showed that according to the difference in sample size, the expression of miR-17-92 cluster miRNAs had no significant difference in AUC values for HCC detection (sample size < 100: AUC = 0.80; sample size > 100: AUC = 0.838). However, the miR-17-92 cluster miRNAs had higher sensitivity in the sample size < 100 group [sample size < 100: SEN = 0.79 (0.72–0.85); sample size > 100: SEN =0.69 (0.63–0.74)]. In addition, differences in sensitivity, specificity, and AUC were investigated by ethnicity. The results indicated that the sensitivity and AUC of miR-17-92 cluster miRNAs for HCC detection in the Chinese group were higher than those in the Egyptian group due to higher sensitivity and higher AUC [SEN=0.83 (0.78-0.88); AUC = 0.83]. Finally, the results of subgroup analysis of the tumor stage showed that the miR-17-92 cluster miRNAs had higher AUC and sensitivity in patients in the I–IV stage [SEN = 0.86 (0.78–0.92); AUC = 0.88].

The results of prognostic meta-analysis of hepatocellular carcinoma

In the 15 studies (Fan et al., 2013; Zheng et al., 2013; Hung et al., 2015; Su et al., 2015; Yang et al., 2015; Wang et al., 2018; Liu et al., 2020a; Yang et al., 2020) enrolled for ascertaining the relationship between the miR-17-92 cluster and the prognosis of HCC patients, a total of 719 participants were identified for OS/DFS/RFS/PFS in this meta-analysis. The characteristics and methods of the included studies related to prognosis are shown in Table 3. Eligible included studies in the prognostic analysis were all from one country. In addition, seven of the included studies were based on the *in situ* hybridization (ISH) detection method, and the remaining studies were based on the qRT-PCR detection method.

To assess the association between miR-17-92 cluster expression and OS, DFS, RFS, and PFS in HCC, the forest plot and meta-analysis of individual HR estimates are shown in Figure 9. The miR-17-92 cluster miRNA expression levels and the outcome of OS in HCC patients were examined in nine studies. In nine studies evaluating OS, the pooled HR and its 95% CI were calculated using a random-effects model with a result of 1.86 (95% CI: 1.04–3.33) because of a statistically significant heterogeneity (I^2 = 80.0 %, p = 0.000). Unexpectedly, there was also a significant heterogeneity between the two studies involving DFS (I^2 = 87.8%, p = 0.742), and the pooled result was HR = 0.95 (95% CI: 0.21–4.34). In addition, in enrolled studies appraising the RFS and PFS, the pooled HR and its 95% CI were 4.18 (3.02–5.77) and 0.43 (0.25–0.73), respectively, but no apparent

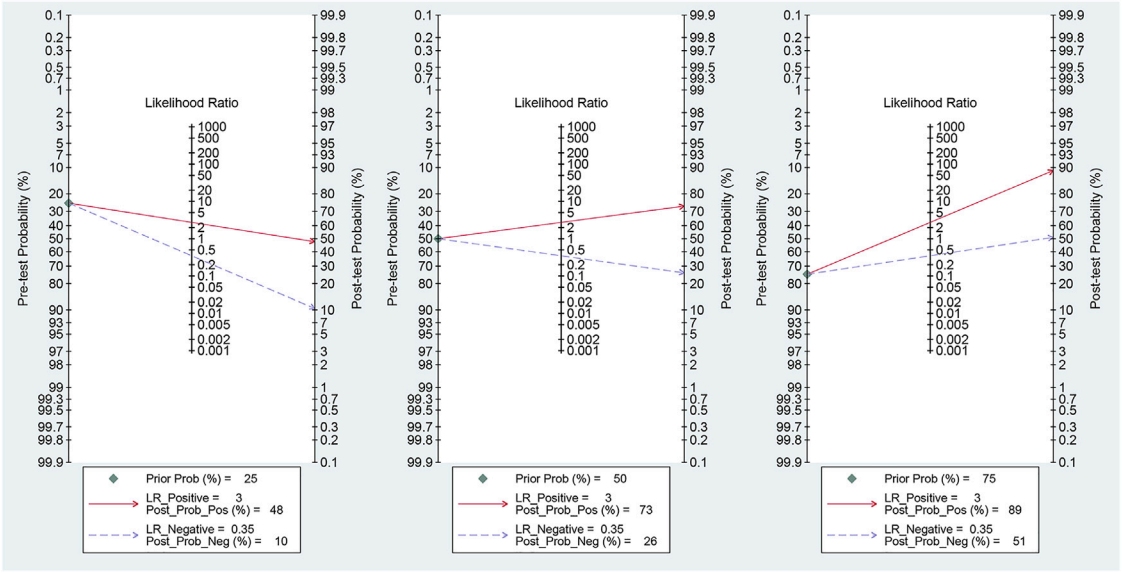

FIGURE 6
Fagan plots for the miR-17–92 cluster with 25, 50, and 75% pre-test probability of diagnosing hepatocellular carcinoma.

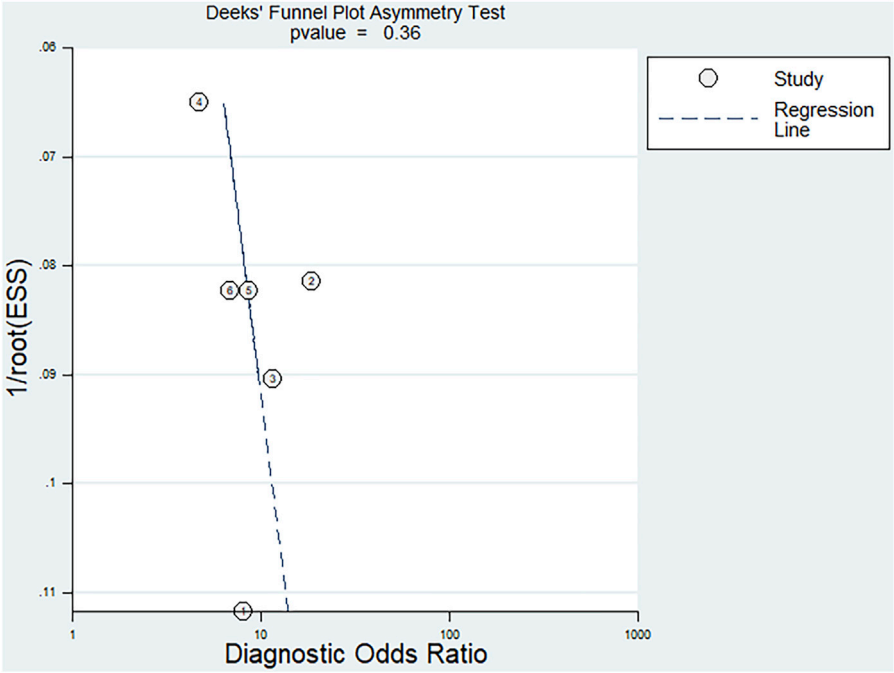

FIGURE 7
Deek's funnel plot asymmetry test for assessing publication bias.

heterogeneity was observed (I^2 = 0.0%, p = 0.742; I^2 = 0.0%, and p = 0.799, respectively). These results demonstrated that high expression of the miR-17-92 cluster miRNA is an unfavorable factor associated with OS and PFS, but a favorable factor for RFS. In fact, no correlation between the miR-17-92 cluster and DFS was detected.

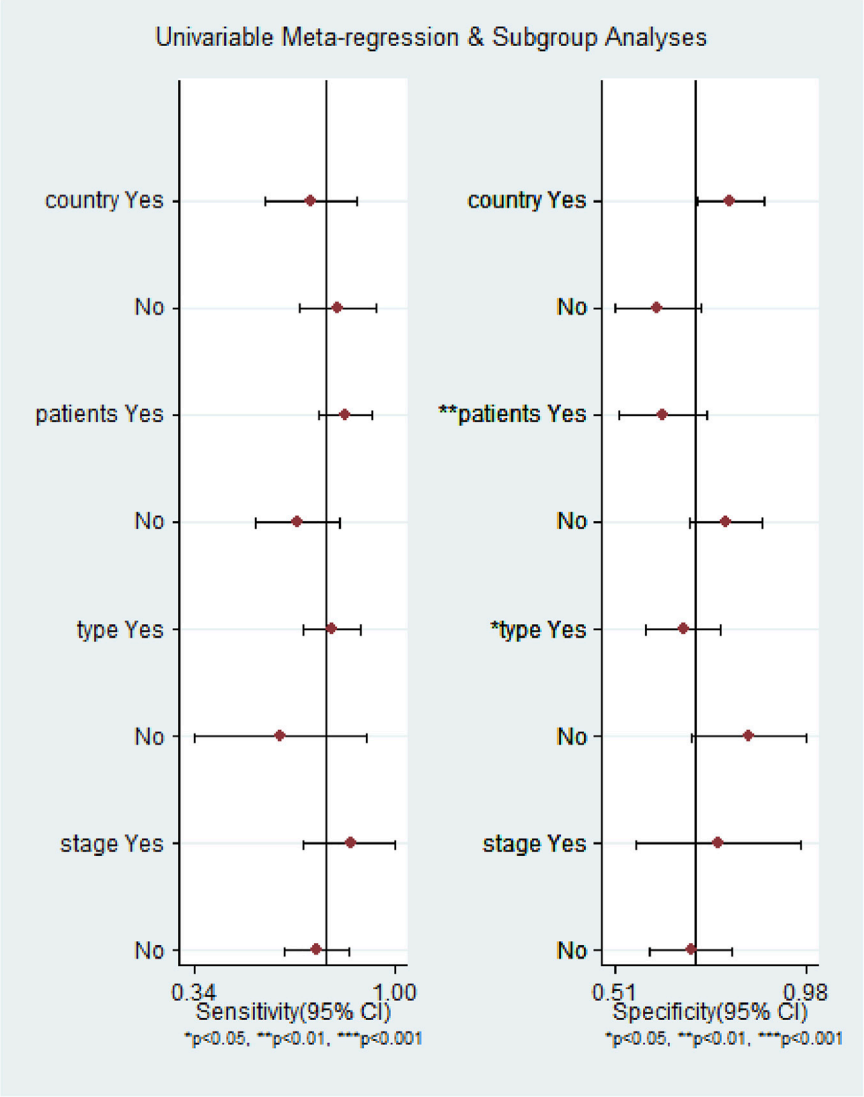

FIGURE 8
Meta-regression analysis to detect the source of heterogeneity for the miR-17–92 cluster in the diagnosis of hepatocellular carcinoma.

The results of the heterogeneity test are shown in Table 4. Subgroup analyses were performed to find the sources that there was significant heterogeneity across studies for the pooled analysis of the miR-17-92 cluster and OS in the HCC patients. Subgroup analysis of sample types found that high expression of miR-17-92 cluster miRNAs in blood and FFPE samples was significantly associated with poor OS (HR = 2.39, 95 CI%: 1.34–4.27, I^2 = 0.00%, $P_{\text{Heteqrogennity}}$ = 0.727; HR = 3.39, 95 CI%: 1.74–6.61, I^2 = 50.9%, $P_{\text{Heteqrogennity}}$ = 0.153). However, the miR-17-92 cluster miRNA expression was not associated with OS in fresh tissue samples (HR = 1.24, 95 CI%: 0.44–3.57, I^2 = 87.4%, $P_{\text{Heteqrogennity}}$ = 0.000). Similarly, in the subgroup analysis of tumor stage, when the cases were stage I–IV, the high expression of miR-17-92 cluster miRNA was also unfavorable for prognosis of HCC patients, and the pooled HR and its 95% CI was 1.96 (1.02–3.78). Furthermore, no significant associations were found between high or low expression of the miR-17-92 cluster and OS in subgroups of sample size (sample size ≤100 and sample size >100) and test method (ISH or qRT-PCR).

The funnel plot was symmetrical, and Begg's test (p = 0.166) and Egger's test (p = 0.059) also indicated that there was no significant publication bias in these studies, as shown in Figure 10. Additionally, sensitivity analysis of OS, DFS, RFS, and PFS was performed, and every single

TABLE 2 Subgroup analysis of the diagnostic value of the miR-17-92 cluster in HCC.

Subgroup		Pooled results						
		AUC	SEN (95% CI)	I^2 (%)	*p*	SPE (95% CI)	I^2 (%)	*p*
Sample type	Serum	0.831	0.69 (0.64–0.73)	86.9	0.000	0.78 (0.72–0.82)	18.8	0.2961
	Plasma	/	/	/	/	/	/	/
Sample size	<100	0.80	0.79 (0.72–0.85)	57.2%	0.9167	0.66 (0.59–0.72)	62.8	0.0681
	>100	0.838	0.69 (0.63–0.74)	91.3	0.0000	0.78 (0.72–0.83)	45.9	0.1575
Country	China	0.839	0.83 (0.78–0.88)	41.3	0.1821	0.66 (0.59–0.72)	61.6	0.0767
	Egypt	0.727	0.62 (0.56–0.68)	0.0	0.5279	0.78 (0.72–0.84)	41.5	0.1811
Tumor stage	I–IV	0.881	0.86 (0.78–0.92)	0	1	0.75 (0.62–0.85)	0	1
	NR	0.786	0.69 (0.64–0.73)	79.8	0.0005	0.71 (0.67–0.76)	75.3	0.0027

AUC, the area under the curve; SEN, sensitivity; SPE, specificity; NR, not reported.

TABLE 3 Main characteristics of the eligible studies for prognostic meta-analysis.

First author	Year	Country	Patient	Sample type	Sample stage	microRNA	Test method	Cut-off	Outcome	HR (95%CI)	NOS score
Beng Yang	2020	China	42	Blood	I–IV	miR-92a	ISH	NR	DFS	2.13 (1.53–8.53)	6
Chung-Lin Hung	2015	China	81	Fresh tissues	II–IV	miR-19b	qRT-PCR	NR	DFS	0.453 (0.245–0.845)	6
Jianjian Zheng	2013	China	96	Blood	I–IV	miR-17-5p	qRT-PCR	Median	OS	2.192 (1.024–4.691)	8
Beng Yang	2020	China	42	Blood	I–IV	miR-92a	ISH	NR	OS	2.7 (1.44–8.49)	6
Chung-Lin Hung	2015	China	81	Fresh tissues	II–IV	miR-19b	qRT-PCR	NR	OS	0.318 (0.12–0.846)	6
Dong-Li Liu	2020	China	104	Fresh tissues	I–IV	miR-17-5P	ISH	Mean	OS	0.7 (0.27–1.84)	7
Dong-Li Liu	2020	China	104	Fresh tissues	I–IV	miR-20a	ISH	Mean	OS	0.78 (0.19–1.05)	7
Ming-Qi Fan	2013	China	100	FFPE	I–III	miR-20a	qRT-PCR	NR	OS	4.937 (2.221–9.503)	6
Wei Yang	2015	China	106	Fresh tissues	I–IV	miR-92a	qRT-PCR	Median	OS	2.283 (1.104–4.717)	8
Xiaodong Wang	2018	China	123	Fresh tissues	I–IV	miR-18a	qRT-PCR	Mean	OS	6.29 (3.12–12.68)	7
Xiaoping Su	2015	China	90	FFPE	II–IV	miR-92a	ISH	NR	OS	2.49 (1.37–4.51)	6
Dong-Li Liu	2020	China	104	Fresh tissues	I–IV	miR-17-5P	ISH	Mean	PFS	0.4 (0.19–0.85)	7
Dong-Li Liu	2020	China	104	Fresh tissues	I–IV	miR-20a	ISH	Mean	PFS	0.46 (0.21–0.99)	7
Ming-Qi Fan	2013	China	100	FFPE	I–III	miR-20a	qRT-PCR	NR	RFS	4.281 (3.316–6.741)	6
Wei Yang	2015	China	106	Fresh tissues	I–IV	miR-92a	qRT-PCR	Median	RFS	3.706 (1.079–5.155)	8

NR, not reported; FFPE, formalin-fixed and paraffin-embedded; ISH, *In Situ* Hybridization; qRT-PCR, quantitative reverse transcription-polymerase chain reaction; OS, overall survival; DFS, disease-free survival; PFS, progression-free survival; RFS, recurrence or relapse-free survival; HR, hazard ratio; CI, confidence interval; NOS, Newcastle–Ottawa scale.

study here was trimmed at a time to assess the specific effect of the single study on the pooled HRs, and the results suggested that pooled results were relatively stable, as shown in Figure 11.

Discussion

In this meta-analysis, a total of 12 articles were included to determine the value of miR-17-92 cluster miRNAs in HCC

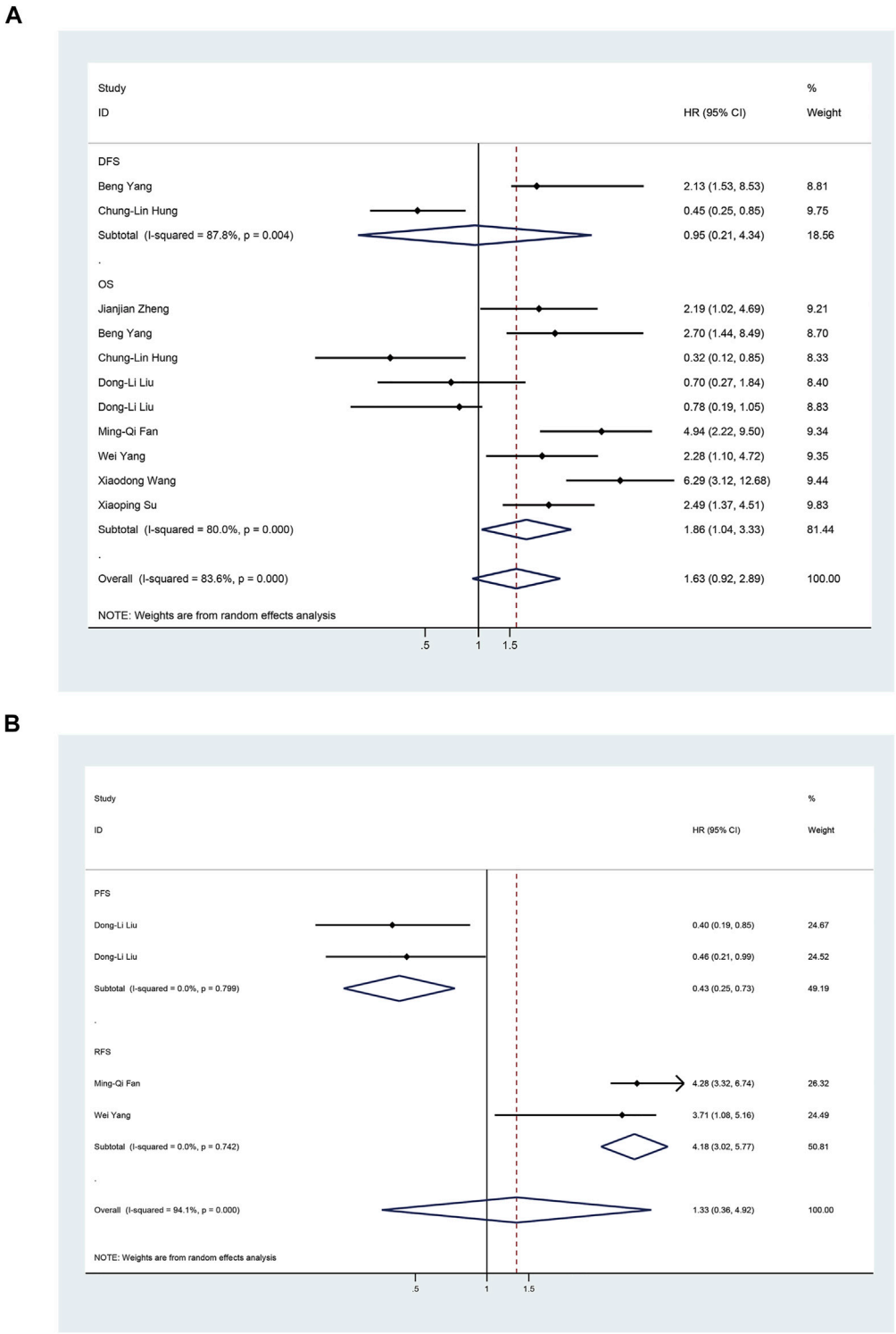

FIGURE 9
Forest plot of studies evaluating the hazard ratio of high miR-17–92 cluster expression in association with survival outcomes in hepatocellular carcinoma patients. **(A)** Studies are based on overall survival (OS) and disease-free survival (DFS); **(B)** Studies are based on Recurrence-Free Survival (RFS) and Progression-Free-Survival (PFS).

TABLE 4 Results of quantitative analysis.

Subgroup	HR	95% CI	I^2 (%)	P_H
OS				
Overall	1.86	1.04–3.33	80.0	0.000
Sample type				
blood	2.39	1.34–4.27	0	0.727
FFPE	3.39	1.74–6.61	50.9	0.153
Fresh Tissues	1.24	0.44–3.53	87.4	0.000
Test method				
ISH	1.44	0.71–2.92	66.7	0.029
qRT-PCR	2.27	0.93–5.56	85.3	0.000
Sample size				
≤100	1.96	0.90–4.25	80.2	0.000
>100	1.73	0.62–4.82	84.7	0.000

HR, hazard ratio; OS, overall survival; DFS, disease-free survival; FFPE, formalin-fixed and paraffin-embedded; P_H, p heterogeneity.

diagnosis and prognosis. The pooled results showed that the expression of the miR-17-92 cluster could be used as a new diagnosis and prognosis biomarker for HCC.

In the present study, a total of six diagnosis-related studies were included to determine the association of abnormal miRNA expression levels of the miR-17-92 cluster with the diagnosis of HCC patients. In conclusion, the miR-17-92 cluster discriminated HCC from controls with an AUC value of 0.79 (0.76–0.83). For different diagnostic tests, the AUC value that can be calculated closer to one indicates a better test (Jones and Athanasiou, 2005). The results of the overall and subgroup analyses indicated that the miR-17-92 cluster had an acceptable moderate diagnostic value in HCC.

In fact, published studies have evidenced that the miR-17-92 cluster miRNAs have relatively high diagnostic value in HCC patients. For example, based on 11 GEO and TCGA databases, a meta-analysis showed (Chi et al., 2018) that the AUC of the sROC reached 0.88 (0.85–0.91), suggesting a certain distinguishing value of the miR-18a-5p in HCC, which was consistent to some extent with the results of the current study. In addition, previous studies have also demonstrated that the miR-17-92 cluster miRNAs can be used as a biomarker for HCC screening when used in combination with other miRNAs. For instance, Wen et al. (2015) reported that an

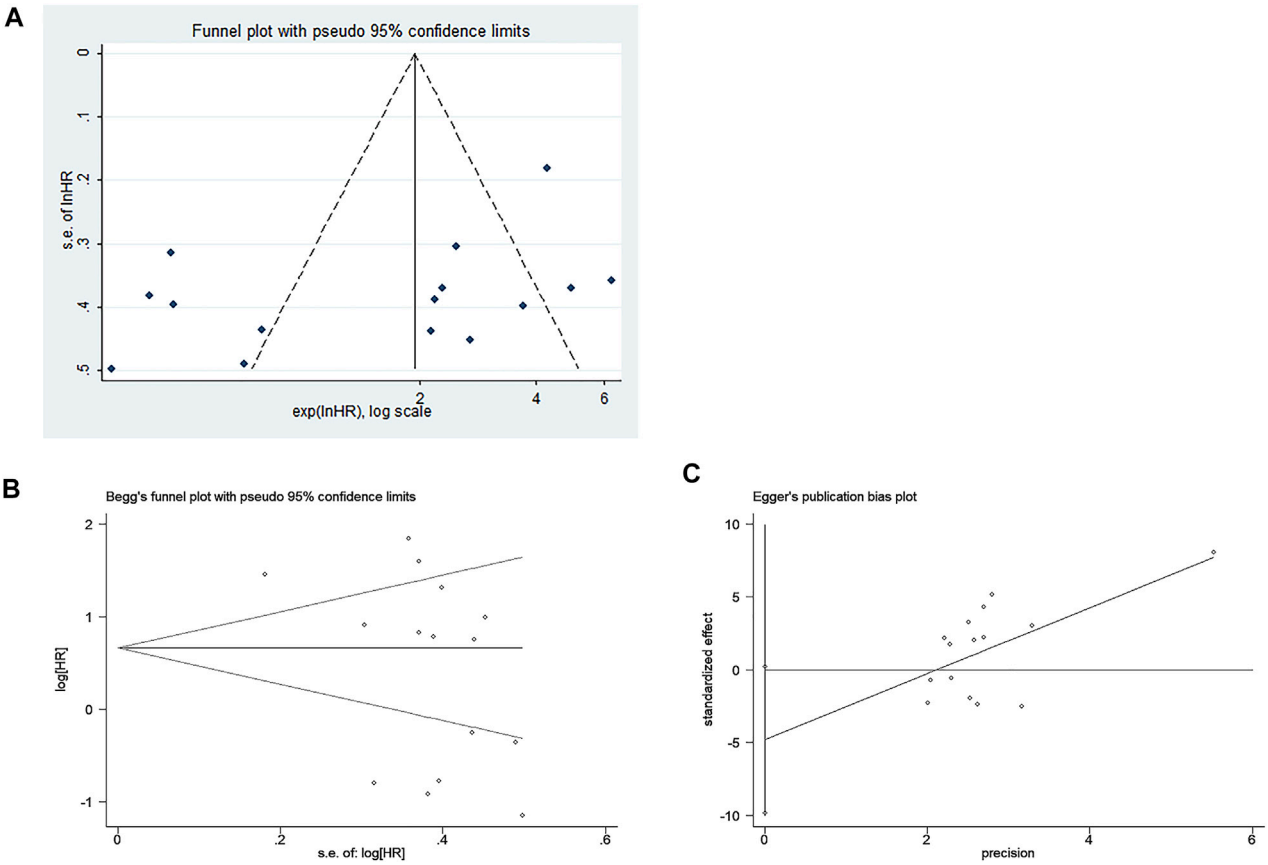

FIGURE 10
Publication bias of included studies for the prognostic meta-analysis. **(A)** Funnel plot; **(B)** Begg's test; **(C)** Egger's test.

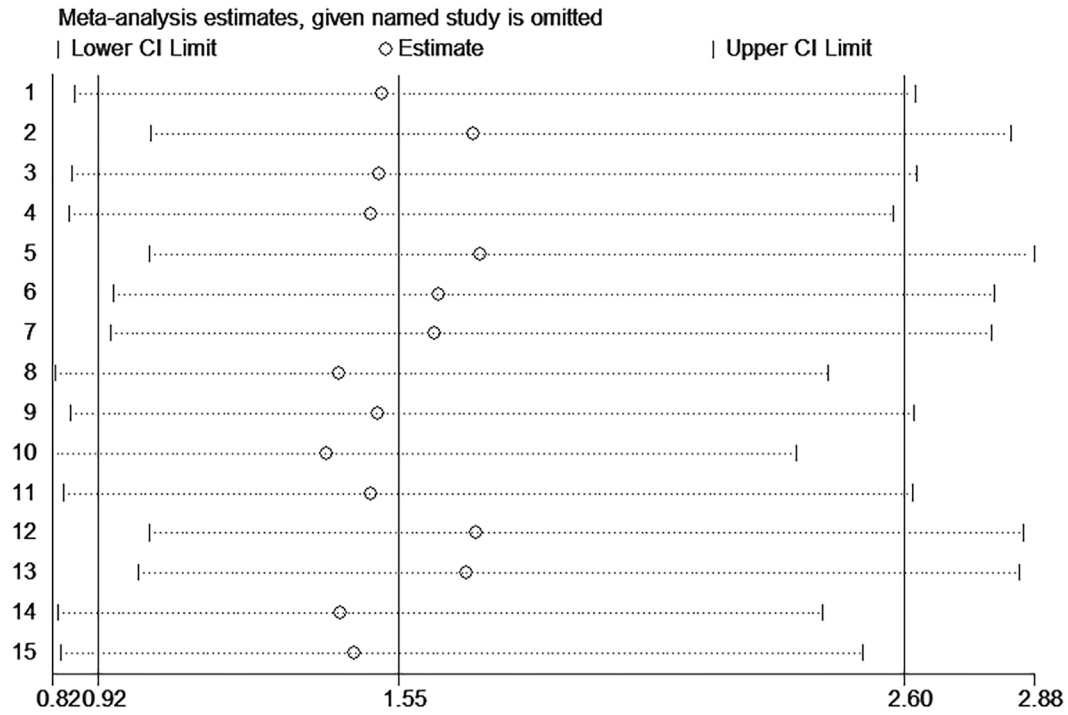

FIGURE 11
Sensitivity analysis of the miR-17–92 cluster for the prognosis of hepatocellular carcinoma patients.

eight-miRNA panel (miR-20a-5p, miR-25-3P, miR-30a-5p, miR-92a-3p, miR-132-3p, miR-185-5P, miR-320a, and miR-324-3P) had a diagnostic sensitivity and specificity of 86.6% and 64.6% for the HCC patients from the controls, respectively. In HCC following orthotopic liver transplantation (OLT), it had been reported that, compared with the miR-19a, the six-miRNA signature (miR-19a, miR-24, miR-126, miR-147, miR-223, and miR-886-5P) could improve the sensitivity and specificity from 71.9% and 71.4% to 86.7% and 82.3%, respectively (Han et al., 2012). Moreover, Sorop et al. (2020) reported that, together with serum AFP, plasma exosomal miR-21-5p and miR-92a-3p could be performed significantly better than AFP alone, whose AUC value for HCC diagnosis can increase from 0.72 to 0.85.

In recent years, accumulating evidence described the molecular mechanism of abnormal expression of miR-17-92 cluster miRNAs through several complex pathways in HCC. In the tumor microenvironment, exosomal miR-92a-5p from macrophages could inhibit AR translation and increase the invasive ability of hepatoma cells by altering the PHLPP/p-AKT/β-catenin signaling pathway (Liu et al., 2020b) Zhang et al. (2021) reported that overexpression of miR-20a could directly target EZH1, which was significantly upregulated in HCC and may be involved in H3K27 methylation, causing cell proliferation and gene transcriptional repression, ultimately leading to tumorigenesis. For the TGF-β signaling pathway, miR-17 bound to the three untranslated regions (3-UTR) of Smad3 mRNA and inhibited its protein expression at the posttranscriptional level (Lu et al., 2019).

In this study, the ROC plane showed an atypical shoulder-arm appearance with a Spearman correlation coefficient of −0.95 ($p = 0.90$), and there was no threshold effect on the heterogeneity. Therefore, our inclusion of diagnostic-related primary analysis results was relatively precise. Furthermore, it was meta-regression analysis that discovered such factors as different sample sizes of HCC patients and different sample types were probably important sources of heterogeneity. The reason might be that sample sources and sample size could affect the detection results of miRNA levels.

Studies have shown that a cluster of miRNAs may be a better predictor of survival than a single miRNA (Sapre et al., 2014). The role of miR-17-92 cluster miRNAs in various tumors has been demonstrated by statistical analysis (Zhang et al., 2017), which can serve as therapeutic prognostic biomarkers for various cancers. Indeed, the miR-17-92 cluster has been shown to play critical regulatory roles in the occurrence, metastasis, and prognosis of several cancer types. For example, miR-18a-5p inhibits tumor growth by targeting matrix metalloproteinase-3, and high levels of miR-18a are associated with better OS in cisplatin-resistant ovarian cancer patients (QuiÃ±ones-DÃaz et al., 2020). Zhang et al. (2020) reported that inhibition of SERTAD3-dependent miR-92a alleviated the growth, invasion, and migration of prostate cancer cells by regulating the

expression of the key genes of the p53 pathway, including p38, p53, and p21. In addition, the ectopic expression of miR-19a-3p contributes to HCC metastasis and chemoresistance by modulating PTEN expression and the PTEN-dependent pathways (Jiang et al., 2018). In short, the miR-17-92 cluster, as a potential diagnostic and prognostic biomarker for tumor diseases, has played a significant role in understanding the mechanisms and clinical treatment of different cancers.

For prognostic-related meta-analysis, there was a significant correlation between high expression of the miR-17-92 cluster and poor OS and poor RFS in HCC patients. However, the correlation of increasing expression of miR-17-92 cluster miRNAs with DFS in HCC was not detected. Additionally, the current meta-analysis detected a favorable correlation between high expression of the miR-17-92 cluster miRNA and PFS in HCC. A possible problem was that due to the relatively small number of included studies related to RFS/PFS/DFS, these results remain inconclusive and further research is needed to confirm them.

Since significant heterogeneity was presented in this prognostic meta-analysis, it was necessary to elucidate the factors influencing heterogeneity. The detection and quantification method, patient-related sample size (sample size ≤100 and sample size >100), and sample type were considered key factors that may affect the magnitude of heterogeneity. Subgroup analysis showed that when samples were taken from blood and FFPE, high expression of the miR-17-92 cluster was associated with poorer OS in HCC; when the cases were stage I–IV, high expression of miR-17-92 cluster miRNA was significantly associated with poor OS in HCC patients. Therefore, when the samples were collected from blood or FFPE, the abnormal expression of miR-17-92 cluster miRNAs could indicate the OS of HCC patients. In short, there was a clear correlation between the miR-17-92 cluster and the prognosis of HCC patients, which can serve as a new prognostic biomarker for HCC.

Ultimately, certain limitations were presented in our meta-analysis: 1) none of the studies ultimately included in this study had both diagnostic and prognostic values; 2) the number of studies available for meta-analysis was still small, and the kind of ethnicity was monotonous; 3) among the included studies, the cut-off values were different or not reported; 4) the abnormal expression miR-17-92 cluster was previously reported for other human tumors, such as gastric and colorectal cancer. This phenomenon suggested that the high expression of miR-17-92 miRNA may be indirectly associated with HCC itself. Therefore, it will improve test performance when miR-17-92 cluster miRNAs are used in combination with other biomarkers; 5) chemosensitivity of patients with HCC may also be a factor affecting the prognosis, which is related to the abnormal expression of miR-17-92 miRNAs in the patient's tissues or blood; and 6) studies that provided survival curves artificially provided relevant HRs and CIs through relevant software, which may cause a certain degree of bias in our analysis results. Larger sample size and deeper data analysis are required to validate our findings.

To the best of our knowledge, this study was the first meta-analysis to assess the potential roles of the miR-17-92 cluster for HCC. The miR-17-92 cluster is a promising biomarker for diagnosis and prognosis of HCC. The current results echo those of previously published studies reporting that targeted overexpression of the miR-17-92 cluster enhanced hepatocarcinoma-induced liver tumorigenesis (Zhu et al., 2015). Although the reasons for the inconsistent results of the included studies have not been systematically addressed, further studies are clearly needed to demonstrate that mature miRNAs of members of the miR-17-92 cluster may differ as prognostic biomarkers in HCC patients. Finally, this study did not assess the prognostic value of a combination of the miR-17-92 cluster and other miRNA markers. Therefore, larger-size, multi-center, and higher-quality studies with a unified criterion for determining the expression of miR-17-92 cluster miRNAs are required.

Data availability statement

The original contributions presented in the study are included in the article/Supplementary Material; further inquiries can be directed to the corresponding authors.

Author contributions

FL, XZ, and ZZ designed the study, screened the literature, performed the quality assessment, extracted and analyzed the data, and drafted the manuscript. MX, YW, and YS extracted, analyzed, and interpreted the data and revised the manuscript. BH and JZ designed, supervised the study, and revised the manuscript. All authors read and approved the final version of the manuscript.

Funding

This study was supported by the National Nature Science Foundation of China (No. 82073288).

Acknowledgments

We wish to thank the participants in this study.

Conflict of interest

The authors declare that the research was conducted in the absence of any commercial or financial relationships that could be construed as a potential conflict of interest.

Publisher's note

References

Begg, C. B., and Berlin, J. A. (1989). Publication bias and dissemination of clinical research. *J. Natl. Cancer Inst.* 81 (2), 107–115. doi:10.1093/jnci/81.2.107

Chen, S., Fu, Z., Wen, S., Yang, X., Yu, C., Zhou, W., et al. (2021). Expression and diagnostic value of miR-497 and miR-1246 in hepatocellular carcinoma. *Front. Genet.* 12, 666306. doi:10.3389/fgene.2021.666306

Chen, W., Zheng, R., Baade, P. D., Zhang, S., Zeng, H., Bray, F., et al. (2016). Cancer statistics in China, 2015. *Ca. Cancer J. Clin.* 66 (2), 115–132. doi:10.3322/caac.21338

Chi, X., Cai, K., Lan, A., Chen, G., Ma, J., Mo, W., et al. (2018). Upregulated miR-18a-5p and its regulatory roles in hepatocellular carcinoma: A study based on bioinformatics analysis with miRNA-seq and miRNA-microarray data. *Int. J. Biol. Sci.* 11 (9), 8802–8819.

Concepcion, C. P., Bonetti, C., and Ventura, A. (2012). The microRNA-17-92 family of microRNA clusters in development and disease. *Cancer J.* 18 (3), 262–267. doi:10.1097/PPO.0b013e318258b60a

Deeks, J. J., Macaskill, P., and Irwig, L. (2005). The performance of tests of publication bias and other sample size effects in systematic reviews of diagnostic test accuracy was assessed. *J. Clin. Epidemiol.* 58 (9), 882–893. doi:10.1016/j.jclinepi.2005.01.016

El-Mezayen, H., Yamamura, K., Yusa, T., Nakao, Y., Uemura, N., Kitamura, F., et al. (2021). MicroRNA-25 exerts an oncogenic function by regulating the Ubiquitin Ligase Fbxw7 in hepatocellular carcinoma. *Ann. Surg. Oncol.* 28 (12), 7973–7982. doi:10.1245/s10434-021-09778-2

El-Serag, H. B. (2011). Hepatocellular carcinoma. *N. Engl. J. Med.* 365 (12), 1118–1127. doi:10.1056/NEJMra1001683

El-Serag, H. B., Marrero, J. A., Rudolph, L., and Reddy, K. R. (2008). Diagnosis and treatment of hepatocellular carcinoma. *Gastroenterology* 134 (6), 1752–1763. doi:10.1053/j.gastro.2008.02.090

Estes, C., Razavi, H., Loomba, R., Younossi, Z., and Sanyal, A. J. (2018). Modeling the epidemic of nonalcoholic fatty liver disease demonstrates an exponential increase in burden of disease. *Hepatology* 67 (1), 123–133. doi:10.1002/hep.29466

Fan, M. Q., Huang, C. B., Gu, Y., Xiao, Y., Sheng, J. X., and Zhong, L. (2013). Decrease expression of microRNA-20a promotes cancer cell proliferation and predicts poor survival of hepatocellular carcinoma. *J. Exp. Clin. Cancer Res.* 32 (1), 21. doi:10.1186/1756-9966-32-21

Fang, L. L., Wang, X. H., Sun, B. F., Zhang, X. D., Zhu, X. H., Yu, Z. J., et al. (2017). Expression, regulation and mechanism of action of the miR-17-92 cluster in tumor cells (Review). *Int. J. Mol. Med.* 40 (6), 1624–1630. doi:10.3892/ijmm.2017.3164

FathyElmougy, F. A., Mohamed, R. A., Hassan, M. M., Elsheikh, S. M., Marzban, R. N., Ahmed, F. e. M., et al. (2019). Study of serum microRNA19a and microRNA223 as potential biomarkers for early diagnosis of hepatitis C virus-related hepatocellular carcinoma. *Gene Rep.* 15, 100398. doi:10.1016/j.genrep.2019.100398

Gebert, L. F. R., and MacRae, I. J. (2019). Regulation of microRNA function in animals. *Nat. Rev. Mol. Cell Biol.* 20 (1), 21–37. doi:10.1038/s41580-018-0045-7

Gordan, J. D., Kennedy, E. B., Abou-Alfa, G. K., Beg, M. S., Brower, S. T., Gade, T. P., et al. (2020). Systemic therapy for advanced hepatocellular carcinoma: ASCO guideline. *J. Clin. Oncol.* 38 (36), 4317–4345. doi:10.1200/jco.20.02672

Gupta, S., Bent, S., and Kohlwes, J. (2003). Test characteristics of alpha-fetoprotein for detecting hepatocellular carcinoma in patients with hepatitis C. A systematic review and critical analysis. *Ann. Intern. Med.* 139 (1), 46–50. doi:10.7326/0003-4819-139-1-200307010-00012

Han, Z. B., Zhong, L., Teng, M. J., Fan, J. W., Tang, H. M., Wu, J. Y., et al. (2012). Identification of recurrence-related microRNAs in hepatocellular carcinoma following liver transplantation. *Mol. Oncol.* 6 (4), 445–457. doi:10.1016/j.molonc.2012.04.001

Higgins, J. P., Thompson, S. G., Deeks, J. J., and Altman, D. G. (2003). Measuring inconsistency in meta-analyses. *Bmj* 327 (7414), 557–560. doi:10.1136/bmj.327.7414.557

Huang, H. Q., Chen, G., Xiong, D. D., Lai, Z. F., Liu, L. M., Fang, Y. Y., et al. (2021). Down-regulation of microRNA-125b-2-3p is a risk factor for a poor prognosis in hepatocellular carcinoma. *Bioengineered* 12 (1), 1627–1641. doi:10.1080/21655979.2021.1921549

Hung, C. L., Yen, C. S., Tsai, H. W., Su, Y. C., and Yen, C. J. (2015). Upregulation of MicroRNA-19b predicts good prognosis in patients with hepatocellular carcinoma presenting with vascular invasion or multifocal disease. *BMC Cancer* 15, 665. doi:10.1186/s12885-015-1671-5

Jiang, X. M., Yu, X. N., Liu, T. T., Zhu, H. R., Shi, X., Bilegsaikhan, E., et al. (2018). microRNA-19a-3p promotes tumor metastasis and chemoresistance through the PTEN/Akt pathway in hepatocellular carcinoma. *Biomed. Pharmacother.* 105, 1147–1154. doi:10.1016/j.biopha.2018.06.097

Jones, C. M., and Athanasiou, T. (2005). Summary receiver operating characteristic curve analysis techniques in the evaluation of diagnostic tests. *Ann. Thorac. Surg.* 79 (1), 16–20. doi:10.1016/j.athoracsur.2004.09.040

Li, L., Guo, Z., Wang, J., Mao, Y., and Gao, Q. (2012). Serum miR-18a: A potential marker for Hepatitis B virus-related hepatocellular carcinoma screening. *Dig. Dis. Sci.* 57 (11), 2910–2916. doi:10.1007/s10620-012-2317-y

Liu, D. L., Lu, L. L., Dong, L. L., Liu, Y., Bian, X. Y., Lian, B. F., et al. (2020). miR-17-5p and miR-20a-5p suppress postoperative metastasis of hepatocellular carcinoma via blocking HGF/ERBB3-NF-κB positive feedback loop. *Theranostics* 10 (8), 3668–3683. doi:10.7150/thno.41365

Liu, G., Ouyang, X., Sun, Y., Xiao, Y., You, B., Gao, Y., et al. (2020). *The miR-92a-2-5p in exosomes from macrophages increases liver cancer cells invasion via altering the AR/PHLPP/p-AKT/Î²-catenin signaling*. *Cell Death Differ.* 27 (12), 3258–3272. doi:10.1038/s41418-020-0575-3

Liu, H. N., Wu, H., Tseng, Y. J., Chen, Y. J., Zhang, D. Y., Zhu, L., et al. (2018). Serum microRNA signatures and metabolomics have high diagnostic value in gastric cancer. *BMC Cancer* 18 (1), 415. doi:10.1186/s12885-018-4343-4

Llovet, J. M., Kelley, R. K., Villanueva, A., Singal, A. G., Pikarsky, E., Roayaie, S., et al. (2021). Hepatocellular carcinoma. *Nat. Rev. Dis. Prim.* 7 (1), 6. doi:10.1038/s41572-020-00240-3

Llovet, J. M., Zucman-Rossi, J., Pikarsky, E., Sangro, B., Schwartz, M., Sherman, M., et al. (2016). Hepatocellular carcinoma. *Nat. Rev. Dis. Prim.* 2, 16018. doi:10.1038/nrdp.2016.18

Lo, C. K., Mertz, D., and Loeb, M. (2014). Newcastle-ottawa Scale: Comparing reviewers' to authors' assessments. *BMC Med. Res. Methodol.* 14, 45. doi:10.1186/1471-2288-14-45

Lu, Z., Li, X., Xu, Y., Chen, M., Chen, W., Chen, T., et al. (2019). microRNA-17 functions as an oncogene by downregulating Smad3 expression in hepatocellular carcinoma. *Cell Death Dis.* 10 (10), 723. doi:10.1038/s41419-019-1960-z

Motawi, T. K., Shaker, O. G., El-Maraghy, S. A., and Senousy, M. A. (2015). Serum MicroRNAs as potential biomarkers for early diagnosis of hepatitis C virus-related hepatocellular carcinoma in Egyptian patients. *PLoS One* 10 (9), e0137706. doi:10.1371/journal.pone.0137706

O'Brien, J., Hayder, H., Zayed, Y., and Peng, C. (2018). Overview of MicroRNA biogenesis, mechanisms of actions, and circulation. *Front. Endocrinol.* 9, 402. doi:10.3389/fendo.2018.00402

Ota, A., Tagawa, H., Karnan, S., Tsuzuki, S., Karpas, A., Kira, S., et al. (2004). Identification and characterization of a novel gene, C13orf25, as a target for 13q31-q32 amplification in malignant lymphoma. *Cancer Res.* 64 (9), 3087–3095. doi:10.1158/0008-5472.can-03-3773

QuiÃ±ones-DÃaz, B. I., Reyes-Gonzalez, J. M., Sanchez-Guzman, V., Conde-Del Moral, I., Valiyeva, F., Santiago-Sanchez, G. S., et al. (2020). MicroRNA-18a-5p suppresses tumor growth via targeting matrix metalloproteinase-3 in cisplatin-resistant ovarian cancer. *Front. Oncol.* 10, 602670. doi:10.3389/fonc.2020.602670

Raponi, M., Dossey, L., Jatkoe, T., Wu, X., Chen, G., Fan, H., et al. (2009). MicroRNA classifiers for predicting prognosis of squamous cell lung cancer. *Cancer Res.* 69 (14), 5776–5783. doi:10.1158/0008-5472.Can-09-0587

Roysri, K., Chotipanich, C., Laopaiboon, V., and Khiewyoo, J. (2014). Quality assessment of research articles in nuclear medicine using STARD and QUADAS-2 tools. *Asia Ocean. J. Nucl. Med. Biol.* 2 (2), 120–126.

Sapre, N., Hong, M. K. H., Macintyre, G., Lewis, H., Kowalczyk, A., Costello, A. J., et al. (2014). Curated microRNAs in urine and blood fail to validate as predictive

biomarkers for high-risk prostate cancer. *PLoS One* 9 (4), e91729. doi:10.1371/journal.pone.0091729

Sorop, A., Iacob, R., Iacob, S., Constantinescu, D., Chitoiu, L., Fertig, T. E., et al. (2020). Plasma small extracellular vesicles derived miR-21-5p and miR-92a-3p as potential biomarkers for hepatocellular carcinoma screening. *Front. Genet.* 11, 712. doi:10.3389/fgene.2020.00712

Su, X., Wang, H., Ge, W., Yang, M., Hou, J., Chen, T., et al. (2015). An *in vivo* method to identify microRNA targets not predicted by computation algorithms: p21 targeting by miR-92a in cancer. *Cancer Res.* 75 (14), 2875–2885. doi:10.1158/0008-5472.Can-14-2218

Villanueva, A. (2019). Hepatocellular carcinoma. *N. Engl. J. Med.* 380 (15), 1450–1462. doi:10.1056/NEJMra1713263

Wang, X., Lu, J., Cao, J., Ma, B., Gao, C., and Qi, F. (2018). MicroRNA-18a promotes hepatocellular carcinoma proliferation, migration, and invasion by targeting Bcl2L10. *Onco. Targets. Ther.* 11, 7919–7934. doi:10.2147/ott.S180971

Wen, Y., Han, J., Chen, J., Dong, J., Xia, Y., Liu, J., et al. (2015). Plasma miRNAs as early biomarkers for detecting hepatocellular carcinoma. *Int. J. Cancer* 137 (7), 1679–1690. doi:10.1002/ijc.29544

Whiting, P., Rutjes, A. W. S., Reitsma, J. B., Bossuyt, P. M. M., and Kleijnen, J. (2003). The development of QUADAS: A tool for the quality assessment of studies of diagnostic accuracy included in systematic reviews. *BMC Med. Res. Methodol.* 3, 25. doi:10.1186/1471-2288-3-25

Yang, B., Feng, X., Liu, H., Tong, R., Wu, J., Li, C., et al. (2020). High-metastatic cancer cells derived exosomal miR92a-3p promotes epithelial-mesenchymal transition and metastasis of low-metastatic cancer cells by regulating PTEN/Akt pathway in hepatocellular carcinoma. *Oncogene* 39 (42), 6529–6543. doi:10.1038/s41388-020-01450-5

Yang, W., Dou, C., Wang, Y., Jia, Y., Li, C., Zheng, X., et al. (2015). MicroRNA-92a contributes to tumor growth of human hepatocellular carcinoma by targeting FBXW7. *Oncol. Rep.* 34 (5), 2576–2584. doi:10.3892/or.2015.4210

Zhang, C. H., Cheng, Y., Zhang, S., Fan, J., and Gao, Q. (2022). Changing epidemiology of hepatocellular carcinoma in Asia. *Liver Int.* 42, 2029–2041. doi:10.1111/liv.15251

Zhang, K., Zhang, L., Zhang, M., Zhang, Y., Fan, D., Jiang, J., et al. (2017). Prognostic value of high-expression of miR-17-92 cluster in various tumors: Evidence from a meta-analysis. *Sci. Rep.* 7 (1), 8375. doi:10.1038/s41598-017-08349-4

Zhang, Q., Deng, X., Tang, X., You, Y., Mei, M., Liu, D., et al. (2021). MicroRNA-20a suppresses tumor proliferation and metastasis in hepatocellular carcinoma by directly targeting EZH1. *Front. Oncol.* 11, 737986. doi:10.3389/fonc.2021.737986

Zhang, S., Yu, J., Sun, B. F., Hou, G. Z., Yu, Z. J., and Luo, H. (2020). MicroRNA-92a targets SERTAD3 and regulates the growth, invasion, and migration of prostate cancer cells via the P53 pathway. *Onco. Targets. Ther.* 13, 5495–5514. doi:10.2147/ott.S249168

Zhang, X., Li, Y., Qi, P., and Ma, Z. (2018). Biology of MiR-17-92 cluster and its progress in lung cancer. *Int. J. Med. Sci.* 15 (13), 1443–1448. doi:10.7150/ijms.27341

Zheng, J., Dong, P., Gao, S., Wang, N., and Yu, F. (2013). High expression of serum miR-17-5p associated with poor prognosis in patients with hepatocellular carcinoma. *Hepatogastroenterology.* 60 (123), 549–552. doi:10.5754/hge12754

Zhou, T., Zhang, G., Liu, Z., Xia, S., and Tian, H. (2013). Overexpression of miR-92a correlates with tumor metastasis and poor prognosis in patients with colorectal cancer. *Int. J. Colorectal Dis.* 28 (1), 19–24. doi:10.1007/s00384-012-1528-1

Zhu, H., Han, C., and Wu, T. (2015). MiR-17-92 cluster promotes hepatocarcinogenesis. *Carcinogenesis* 36 (10), 1213–1222. doi:10.1093/carcin/bgv112

frontiers | Frontiers in Genetics

TYPE Review
PUBLISHED 04 October 2022
DOI 10.3389/fgene.2022.968919

OPEN ACCESS

EDITED BY
Olanrewaju B. Morenikeji,
University of Pittsburgh at Bradford,
United States

REVIEWED BY
Saurav Saha,
North Eastern Hill University, India
Hui Li,
Guangxi University, China

*CORRESPONDENCE
Bin Shen,
shenbin_1971@163.com

†These authors have contributed equally to this work and share first authorship

SPECIALTY SECTION
This article was submitted to RNA, a section of the journal Frontiers in Genetics

RECEIVED 14 June 2022
ACCEPTED 31 August 2022
PUBLISHED 04 October 2022

CITATION
Li S, Si H, Xu J, Liu Y and Shen B (2022), The therapeutic effect and mechanism of melatonin on osteoarthritis: From the perspective of non-coding RNAs. *Front. Genet.* 13:968919. doi: 10.3389/fgene.2022.968919

The therapeutic effect and mechanism of melatonin on osteoarthritis: From the perspective of non-coding RNAs

Shuai Li†, Haibo Si†, Jiawen Xu, Yuan Liu and Bin Shen*

Department of Orthopedics, Orthopedic Research Institute, West China Hospital, Sichuan University, Chengdu, Sichuan, China

Osteoarthritis (OA) is a slowly progressing and irreversible joint disease. The existing non-surgical treatment can only delay its progress, making the early treatment of OA a research hotspot in recent years. Melatonin, a neurohormone mainly secreted by the pineal gland, has a variety of regulatory functions in different organs, and numerous studies have confirmed its therapeutic effect on OA. Non-coding RNAs (ncRNAs) constitute the majority of the human transcribed genome. Various ncRNAs show significant differentially expressed between healthy people and OA patients. ncRNAs play diverse roles in many cellular processes and have been implicated in many pathological conditions, especially OA. Interestingly, the latest research found a close interaction between ncRNAs and melatonin in regulating the pathogenesis of OA. This review discusses the current understanding of the melatonin-mediated modulation of ncRNAs in the early stage of OA. We also delineate the potential link between rhythm genes and ncRNAs in chondrocytes. This review will serve as a solid foundation to formulate ideas for future mechanistic studies on the therapeutic potential of melatonin and ncRNAs in OA and better explore the emerging functions of the ncRNAs.

KEYWORDS

osteoarthritis, melatonin, microRNA, circular RNA, long non-coding RNA, circadian clocks, epigenetics

Introduction

Osteoarthritis (OA), a slowly progressing disease with irreversible structural changes, can develop and show the clinical manifestation of chronic pain. Active early treatment can delay the progress of the OA (Hunter and Bierma-Zeinstra, 2019). OA can not only cause local joint symptoms, reducing the quality of life of patients but also coexists with heart disease, diabetes, and mental health problems, which will significantly increase the incidence of adverse events such as hip fractures, bringing a considerable burden to patients, families, and society (Wang et al., 2021a). OA is the leading cause of disability in the elderly (Hunter and Bierma-Zeinstra, 2019). More than 500 million people worldwide suffer from OA, accounting for 7% of the global population (Hunter et al., 2020). This number may be exacerbated by the aging population and the growing trend of obesity

(Hunter et al., 2020). Before progressing to the terminal stage of OA that can only be effectively solved by joint replacement, the mainstream drug treatment of OA is to inhibit inflammation and reduce pain. New treatment methods are constantly being explored, but significant progress has not been made compared with the treatment of many other musculoskeletal and chronic non-communicable diseases.

Melatonin (N-acetyl-5-methoxytryptamine) is an endogenous indole hormone mainly secreted by the mammalian pineal gland. Its production and secretion duration directly depends on the length of the night. In other words, its secretion has a circadian rhythm (Cipolla-Neto and Amaral, 2018). With the aging of the body, the secretion of melatonin also gradually decreases (Hardeland, 2012). Coincidentally, the incidence rate of OA is also increasing (Neogi and Zhang, 2013; Quicke et al., 2022). Melatonin can regulate a variety of rhythm genes. Previous studies mainly focused on melatonin regulation in the nervous system, such as regulating circadian rhythm and promoting sleep. However, in recent years, the functions of melatonin have been gradually explored, such as participating in anti-tumor, anti-oxidation, regulating circadian rhythm, regulating immunity, regulating inflammatory response, promoting wound healing, and tissue regeneration (Hardeland, 2019). The disorder of circadian rhythm will hinder the normal production of melatonin, leading to a high level of inflammatory factors in body fluid, and making the body stay in a state of chronic inflammation, suggesting the relationship between melatonin and chronic inflammatory diseases (Zhang et al., 2019b).

Non-coding RNAs (ncRNAs) can't encode proteins, but they have properties that affect normal gene expression and disease progression, making them new targets for exploring how drugs work (Matsui and Corey, 2017). As a research hotspot in recent years, numerous ncRNAs and their role in OA have been found with the development of gene sequencing technology. MicroRNA (miRNAs), circular RNAs (circRNAs), and long non-coding RNAs (lncRNAs) are ncRNAs that play a major regulatory role in OA (Wu et al., 2019). Numerous studies have also proved the therapeutic strategy of introducing exogenous ncRNAs into the joint to regulate OA in the past few years (Liang et al., 2020). Meanwhile, innumerable substances with therapeutic effects on OA, including melatonin, have achieved their therapeutic effect by regulating ncRNAs (Qiu et al., 2020).

The role of melatonin in the skeletal muscle system

The regulatory effect of melatonin on bone and cartilage has been found in the musculoskeletal system, especially in degenerative diseases. A previous study found that In patients with intervertebral disc degeneration (IVDD), melatonin can promote proliferation, induce autophagy and inhibit apoptosis of annulus fibrosus cells (Hai et al., 2019). Moreover, melatonin regulates the expression of autophagy-related proteins by inhibiting the function of miR-106a-5p (Hai et al., 2019). In addition, melatonin can also affect bone metabolism by regulating the function of osteoblasts and osteoclasts, and its role in osteoporosis (Zhang et al., 2016; Han et al., 2021), fracture healing (Histing et al., 2012), and other diseases have also been confirmed.

Melatonin has been found to protect chondrocytes by inhibiting inflammation, promoting matrix synthesis, and promoting cartilage differentiation of bone marrow mesenchymal stem cells (BMSCs) (Wu et al., 2018) and other ways (Jorge et al., 2021). The previous study (Han et al., 2021a) found that melatonin plays a protective role on synovial cells by alleviating the effect of D-galactose (D-gal) on synovial cells by upregulating silent information regulator 1 (SIRT1), finally promoting hyaluronic acid synthesis and interrupting cell aging. The imbalance of endogenous hormones, including melatonin, leads to the expression of inflammation-related cytokines and matrix degradation-related proteases in articular cartilage, causing cartilage erosion, synovitis, and osteophyte formation (Hossain et al., 2019). Compared with other drugs, melatonin has a wide range of advantages and almost no side effects (Lu et al., 2021b).

The interaction of melatonin with ncRNAS

The relationship between melatonin and ncRNAs has been verified in inflammation, oxidative stress, cancer, aging, energy consumption, obesity, type 2 diabetes, neuropsychiatric disorders, and neurogenesis (Hardeland, 2014; Mori et al., 2016). When melatonin regulates its target genes, the level of specific ncRNAs also changes accordingly, suggesting that melatonin can exert its potential by regulating ncRNAs. A previous study (Han et al., 2020) found that melatonin induced the increase of miR-149 and inhibited the expression of pro-inflammatory cytokine tumor necrosis factor-α (TNF-α) and extracellular matrix (ECM) components such as type I collagen and fibronectin in the mouse model of hindlimb ischemia, to produce anti-inflammatory and anti-fibrosis protective effect on ischemic tissue. Meanwhile, this protective effect can be blocked by inhibiting miR-149. Che et al. (2020) suggested that melatonin could regulate the lncRNAs-miRNAs axis (Che et al., 2020). That is, melatonin administration significantly ameliorated cardiac dysfunction and reduced collagen production by inhibiting transforming growth factor-β (TGF-β1) /SMAD signaling and nucleotide-binding domain and leucine-rich repeat containing PYD-3 (NLRP3) inflammasome activation in the diabetes mice model (Che et al., 2020).

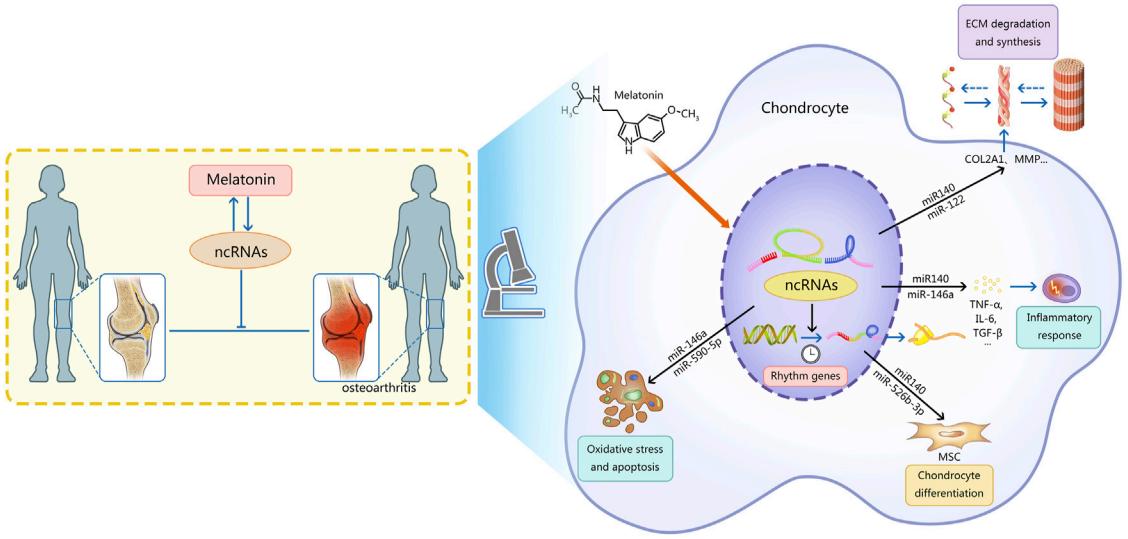

FIGURE 1
This figure describes the mechanism of interaction between ncRNAs and melatonin in osteoarthritis. Note: Melatonin can regulate OA by regulating the level of ncRNAs, which is mainly reflected in five aspects: 1) regulating the degradation and synthesis of the chondrocyte matrix; 2) regulating the oxidative stress and apoptosis of chondrocytes; 3) regulating the differentiation of chondrocytes; 4) regulating rhythm genes; 5) regulating inflammatory mediators.Ultimately the progression of osteoarthritis is delayed. Meanwhile, ncRNAs can regulate the synthesis and function of melatonin. AANAT, arylalkylamine N-acetyltransferase; ncRNAs, non-coding RNAs; MSC, mesenchymal stem cells; MMP, matrix metalloproteinase; ADAMTS, a disintegrin metalloproteinase with thrombospondin motifs; ECM, extracellular matrix; TNF-α, tumor necrosis factor-α; IL-6, interleukin 6; TGF-β, transforming growth factor-β.

The researchers found that some miRNAs were highly enriched in the pineal gland, and a few miRNAs were enriched differently between day and night which is similar to the rhythm of pineal gland secretion of melatonin (Clokie et al., 2012). Some specific ncRNAs can further regulate the circadian rhythm by regulating the expression of enzymes related to the synthesis and secretion of melatonin. A previous study found that miR-483 directly targets the mRNA of arylalkylamine N-acetyltransferase (AANAT), the main rate-limiting enzyme for melatonin formation, and inhibited melatonin synthesis (Clokie et al., 2012). Similarly, Zheng et al. (2022) found that circRNA-WNK2 was highly expressed at night and could competitively bind to miR-328a-3p and reduce the expression of miR-328a-3p, thereby enhancing the expression of AANAT inhibited by miR-328a-3p, and ultimately stimulated melatonin secretion (Zheng et al., 2022). Meanwhile, the expression of ncRNAs in the pineal gland is regulated by signals from the suprachiasmatic nucleus. Some ncRNAs can also regulate the expression of related receptors on melatonin target cells. As in a genetic mouse model of atherosclerosis, a high-fat diet induces miR-29 expression and targets and inhibits MT1's expression by binding to MT1 mRNA 30-UTR of melatonin, showing the protective effect of reducing the molecular and cellular damage function of cardiac ischemia-reperfusion (Zhu et al., 2014). Other ncRNAs, such as piR015520, can also regulate the expression of melatonin-related genes (Esposito et al., 2011). Zheng et al. (2021) constructed a competing endogenous RNAs (ceRNAs) network composed of circRNAs, miRNAs, and mRNAs by analyzing and screening circRNAs and miRNAs differentially expressed in the pineal gland of rats, which may play an essential regulatory role in the circadian rhythm and melatonin secretion of the pineal gland (Zheng et al., 2021).

The role of melatonin in osteoarthritis

Recently, the therapeutic effects of melatonin and ncRNAs in OA have been gradually discovered. Exogenous melatonin can stimulate the growth of chondrocytes and regulate the expression of cartilage-related genes. At the same time, chondrocytes can synthesize a small amount of melatonin (Fu et al., 2019). Endogenous and exogenous melatonin can regulate cartilage growth and maturation through MT1 and MT2 receptors (Fu et al., 2019). Melatonin can regulate OA by adjusting the level of ncRNAs, which is mainly reflected in five aspects (Figure 1): 1) regulating the degradation and synthesis of the chondrocyte matrix; 2) regulating the oxidative stress and apoptosis of chondrocytes; 3) regulating the differentiation of chondrocytes; 4) regulating rhythm genes; 5) regulating

inflammatory mediators. In addition, melatonin can also alleviate the adverse effects of other drugs on OA.

Regulation of extracellular matrix degradation and synthesis

It is widely believed that the dysregulation of cartilage matrix synthesis and degradation is the cause of OA (Guo et al., 2017). The main components of the cartilage matrix are collagen and proteoglycans. Collagen type II is the most abundant component in the cartilage matrix (Xie et al., 2021). The latest research proposes the concept of the pericellular matrix (PCM) and regards the changes that occur in PCM as initiating or progressive factors for OA (Guilak et al., 2018). *In vitro* experiments, melatonin was found to increase the expression of chondrogenesis marker genes such as COL2A1, SOX9, and aggrecan, which are major components of the ECM of cartilage (Pei et al., 2009).

The enzymes related to cartilage ECM are enhanced during OA, mainly including matrix metalloproteinase (MMP) that degrades type II collagen and a disintegrin metalloproteinase with thrombospondin motifs (ADAMTS). ADAMTS is a family of 19 secreted metalloproteinases involved in various developmental and homeostatic processes (Kelwick et al., 2015). And several members of the ADAMTS family have been shown to degrade the cartilage proteoglycans (Verma and Dalal, 2011). Melatonin is a multifaceted regulator of MMP gene expression and activity (Swarnakar et al., 2011). In addition, melatonin can inhibit ADAMTS activity by regulating miRNAs and has an inhibitory effect on cartilage ECM degradation (Zhang et al., 2019c).

Regulation of oxidative stress and apoptosis

Reactive oxygen species (ROS) is the leading cause of chondrocyte damage and OA development (Blanco et al., 2011). Oxidative stress caused by ROS can oxidize and subsequently disrupt cartilage homeostasis, promoting catabolism by inducing cell death and damaging many components of the joint (Lu et al., 2021a). In addition, oxidative stress also destroys the cartilage matrix by inhibiting ECM synthesis and upregulating potential ECM-degrading related enzymes (Lu et al., 2021a). Mitochondria are the primary source of intracellular reactive oxygen species, and mitochondrial dysfunction plays a vital role in chondrocyte autophagy (Hosseinzadeh et al., 2016). Melatonin and its derivatives are a broad range of free radical scavengers and antioxidants due to their potential to scavenge ROS and reactive nitrogen species (RNS) and promote glutathione and antioxidant enzymes expression and activity (Reiter et al., 2010). In addition, melatonin can regulate chondrocyte apoptosis by regulating TNF-α, interleukin 6 (IL-6), SIRT, TGF-β, and other signaling pathways (Reiter et al., 2010). Exosomes secreted by adipose tissue-derived stem cells (ADSCs) can significantly reduce H_2O_2-induced apoptosis of articular chondrocytes and promote chondrogenesis by upregulating miR-145 and miR-221 (Zhao et al., 2020). Melatonin indirectly regulates the downstream signal miR-210 by scavenging reactive oxygen species, suggesting the role of melatonin and miRNAs in oxidative stress-related diseases (He et al., 2020). Melatonin was found to inhibit H_2O_2-induced oxidative stress and exert a protective effect on chondrocytes by maintaining mitochondrial redox homeostasis and regulating autophagy (Chen et al., 2021c). Changes in the expression of miR-223 affect the metabolic status of cells and alter the conditions of apoptosis and proliferation of cells, whereas melatonin reduces the expression of miR-223 in wild-type (WT) aged mice (Sayed et al., 2021).

Regulation of chondrocyte differentiation

As a pleiotropic regulator, melatonin has been shown to regulate many biological behaviors of stem cells in numerous studies. BMSCs have inherent chondrogenic differentiation potential and are an ideal choice for cartilage regeneration. Previous studies speculated that BMP/SMAD signaling pathway is involved in the melatonin-induced chondrogenic differentiation of human mesenchymal stem cells (hMSCs) (Zheng et al., 2015). The treatment of early OA often happens in an inflammatory microenvironment, and it may be more practical to promote the chondrogenic differentiation of BMSCs in an inflammatory environment. Melatonin was found to alleviate chondrogenesis of human bone marrow mesenchymal stem cells (hBMSCs) inhibited by IL-1β treatment by restoring chondrocyte size and cartilage matrix accumulation, maintaining metabolic balance, and reducing apoptosis (Gao et al., 2018). Further studies revealed that melatonin rescued chondrogenic differentiation inhibited by IL-1β mainly through inhibiting the activation of the NF-κB (nuclear factor kappa-B) signaling pathway, one of the most critical pathways involved in inflammation and apoptosis.

Regulation of rhythm genes

The regulatory effect of the central nervous system on OA has been discovered in recent years (Morris et al., 2019). Clinical studies have shown that the clinical manifestations of OA patients, such as pain or stiffness, are rhythmic changes (Bellamy et al., 2002). As mentioned above, chondrocytes can be regulated by both exogenous melatonin and endogenous melatonin produced by themselves. Chondrocytes may synchronize the rhythm gene expression of chondrocytes with the central biological clock by producing melatonin and upregulating the expression of melatonin receptors (Fu et al., 2019). Chondrocyte rhythm genes are important regulatory targets of melatonin, and the normal expression of rhythm genes is necessary for cartilage homeostasis.

The local inflammatory environment may disrupt the normal rhythm of chondrocytes by affecting the expression of rhythm genes (Haas and Straub, 2012). Knockout of specific essential rhythm genes worsens experimental OA in rats (Hashiramoto et al., 2010). For example, the expression of the rhythm gene *bmal1* was found to be decreased in the cartilage of OA patients and the cartilage of aged mice. In addition, the inhibition of targeting *bmal1* in mouse chondrocytes can make the circadian rhythm disappear and further downregulate the expression of matrix-related genes Sox 9, ACAN, and Col2a1, as well as upregulation of phosphorylated SMAD 2/3 (p-SMAD 2/3) levels, leading to progressive degeneration of articular cartilage (Dudek et al., 2016).

Rhythm genes are thought to be the bridge between melatonin and OA. The disturbances in circadian rhythms are closely related to inflammatory joint diseases. Appropriate melatonin concentrations can correct abnormal chondrocyte phenotype by restoring abnormal rhythm gene expression in OA (Reiter et al., 2010). Previous studies have found that melatonin regulates rhythmic genes through a post-translational mechanism. Melatonin may inhibit the destruction of rhythm gene transcription factors by directly inhibiting the proteasome or limiting the destruction of rhythm proteins involved in the negative feedback of gene transcription (Vriend and Reiter, 2015). Melatonin is involved in rhythm gene expression in chondrocytes in at least two ways: 1) direct inhibition of pro-inflammatory cytokine release, indirect regulation of the expression of *per1, per2, and cry2* (Jahanban-Esfahlan et al., 2018); For example, IL-1β severely disrupted circadian gene expression rhythm in cartilage (Guo et al., 2015) , and melatonin may inhibit inflammatory mediators including IL-1β and further regulate the expression of commandment genes regulated by inflammatory mediators. 2) blockade of NF-κB signalings, such as *clock* and *bmal1* (Jahanban-Esfahlan et al., 2018). Abnormal changes in cartilage specimens accompany the low-level expression of rhythm genes. In contrast, a specific dose of melatonin restored the expression of rhythm-controlling genes and corrected the abnormal chondrocyte phenotype. However, long-term use of melatonin promoted the cleavage of Receptor Activator of Nuclear Factor-κ B Ligand (RANKL) protein in the synovium, resulting in severe subchondral bone erosion, and these changes were by regulating rhythm genes (Hong et al., 2017). There are also interactions between rhythm genes and ncRNAs. Nuclear receptor subfamily 1 group D member 1 (NR1D1/Rev-erbα), a protein encoded by rhythm genes, is present in adipocytes, macrophages, and muscle cells, controlling circadian rhythms and lipid and glucose metabolism. MiR-882 negatively regulates Rev-erbα expression by binding to Rev-erbα 3′-UTR to inhibit the translation of Rev-erbα, while melatonin may indirectly regulate Rev-erbα by reducing the expression of miR-882 (Tian et al., 2021). Na et al. (2009) predicted the relationship between miRNAs and rhythm genes. miR-181d and miR-191 could target and inhibit the expression of *clock* and *bmal1* genes, respectively, thereby regulating biological rhythms (Na et al., 2009).

Regulation of inflammatory mediators and inflammatory responses

The regulatory effect of melatonin on inflammation is related to the state of cells (Vriend and Reiter, 2015). The adverse effects of inflammatory mediators on chondrocytes are multifaceted. The inflammatory response induced by local inflammatory mediators in the joints can lead to ROS production, inducing apoptosis, promoting collagen degradation, and inhibiting chondrocyte differentiation, finally affecting the self-repair of chondrocytes. Numerous studies have proved the anti-inflammatory effect of melatonin. The anti-inflammatory effect of melatonin is partly achieved through ncRNAs in chondrocytes (Liu et al., 2022) Previous study found that melatonin treatment enhanced mesenchymal stem cells (MSC) viability and increased the levels of anti-inflammatory miRNAs (e.g., miR-34a, miR-124, and miR-135b) in exosomes (Liu et al., 2014; Heo et al., 2020). Melatonin was found to reverse inflammatory mediator-induced inhibition of chondrogenic differentiation and modulate ROS and MMP levels. Melatonin significantly reduces the expression of miR-21, miR-146a, and miR-223, which are positively correlated with pro-inflammatory and pro-apoptotic molecules in WT mice (Sayed et al., 2021). Multiple studies have demonstrated that melatonin and ncRNAs modulate inflammatory responses in OA chondrocytes by regulating TNF-α/IL-6 levels.

Prevent moderate adverse effects of other drugs in osteoarthritis

Intra-articular injection of glucocorticoids is a common clinical treatment for relieving symptoms of OA. However, long-term use of glucocorticoids may induce cartilage degeneration and inhibit cartilage growth and ECM synthesis. It was found that melatonin may play a preventive effect on dexamethasone-induced chondrocyte injury through the SIRT1-related signaling pathway (Yang et al., 2017). Researchers have constructed an injectable hydrogel/microparticle system composed of melatonin and methylprednisolone and verified its ability to promote cartilage formation *in vitro* and *in vivo* (Naghizadeh et al., 2021).

The role of ncRNAs in osteoarthritis and its interaction with melatonin

The regulatory effect of melatonin on OA has been described above. The regulatory effect of melatonin on OA is partly achieved by acting on ncRNAs. At the same time, some

TABLE 1 Summary of differentially expressed miRNAs concerning the regulatory effect of melatonin on OA discussed in this review.

miRNAs	OA influence	MT influence	Target gene	Main influence of miRNAs	Model	References
miR-140	↓	↑	ADAMTS 5	↓ ECM degradation	hBMSCs	Karlsen et al. (2016)
			MMP 13	↓ ECM degradation	Human osteoarthritic chondrocytes	Liang et al. (2020)
			Notch	↑ Chondrocyte differentiation	Cartilage progenitor cells	Si et al. (2019)
			IL1B, IL6, SDC4	↓ Inflammatory mediators and response	hBMSCs	Karlsen et al. (2016)
miR-146a	↑	↓	NRF2	↑ Oxidative stress and apoptosis	Human osteoarthritic chondrocytes	Zhou et al. (2022)
			Tgif1, Camk2d&Ppp3r2	↓ ECM synthesis	Mouse chondrocytes	Zhang et al.(2017)
			TRAF6	↑ Oxidative stress and apoptosis	Human osteoarthritic chondrocytes	Shao et al. (2020)
	↓		Notch	↓ Inflammatory mediators and response	Mouse chondrocytes	Guan et al. (2018)
miR-526b-3p	↓	↑	Smad7	↑ Chondrocyte differentiation	hBMSCs	Wu et al. (2019)
miR-590-5p	↑	↑	Smad7	↑ Chondrocyte differentiation	hBMSCs	Wu et al. (2018)
			FGF18	↑ Oxidative stress and apoptosis	Human osteoarthritic chondrocytes	Jiang et al. (2021b)
miR-122		uncertain	SIRT1	↑ ECM degradation	SW1353	Bai et al. (2020)

Note: Table 1 show the differentially expressed miRNAs concerning the regulatory effect of melatonin on OA discussed in this review. The up and down arrow represent upregulation and downregulation respectively. "OA influence" means changes of miRNA in OA. "MT influence" means the effect of MT on miRNA. This table is based on the findings from various studies cites appropriately in the text. miRNAs, microRNAs; OA, osteoarthritis; MT, melatonin; ADAMTS5, a disintegrin metalloproteinase with thrombospondin motifs 5; ECM, extracellular matrix; hBMSCs, human bone marrow mesenchymal stem cells; MMP 13, matrix metalloproteinase 13; NRF2, nuclear factor-erythroid 2-related factor 2; SIRT1, silent information regulator 1.

ncRNAs are not regulated by melatonin, but they can function on a similar pathway to melatonin. These types of ncRNAs are highlighted below. The related ncRNAs and their expression and regulatory mechanisms for OA are shown in Tables 1, 2, 3.

MiR-140

MiR-140 is expressed specifically in articular cartilage and plays an important role in cartilage protection. A previous study found that various miRNAs were differentially expressed in Melatonin-treated chondrocytes, so they chose miR-140 as the target for further study and found that melatonin could prevent OA-induced cartilage destruction by promoting the expression of miR-140 and regulating the expression of matrix-degrading enzymes at the post-transcriptional level (Zhang et al., 2019c). Meanwhile, inhibition of miR 140 could counteract the anti-inflammatory effect of melatonin in chondrocytes. IL-1β stimulation inhibited the expression of miR-140 (Zhang et al., 2019c). MiR-140 is widely involved in the regulation of chondrocyte function and can directly downregulate enzymes related to chondrocyte matrix degradation like ADAMTS-5 (Karlsen et al., 2016) and MMP-13 (Liang et al., 2016) at the mRNA level. Furthermore, the expression of miR-140 was increased in chondrogenic hBMSCs (Miyaki et al., 2009). MiR-140 is a strong inducer of the Chondrogenic differentiation of BMSCs (Mahboudi et al., 2018). In fact, miR-140 may activate the cartilage progenitor cells (CPCs) by inhibiting the Notch signaling pathway and promoting the potential of OA cartilage damage repair (Si et al., 2019). TGFBR1, the BMP pathway receptor, is a direct target of miR-140, and up-regulation of miR-140 can inhibit the expression of TGFBR1 and its downstream SMAD1, suggesting that miR-140 can regulate chondrocyte homeostasis through the TGF-β/BMP pathway (Tardif et al., 2013; Zhang et al., 2019c). In addition, miR-140 can inhibit the NF-κB pathway by directly degrading IL1B, IL6, and SDC4 mRNA and binding and inhibiting several distinct points of attack of NF-κB downstream signaling IKBA (Karlsen et al., 2016).

MiR-146a

It is found that miR-146a knockout aggravates joint degeneration in a mouse model of OA characterized by cartilage degeneration, synovitis, and osteophyte (Guan et al.,

TABLE 2 Summary of differentially expressed lncRNAs concerning the regulatory effect of melatonin on OA discussed in this review.

lncRNAs	OA influence	MT influence	Target gene	Main influence on OA	Model	References
lncRNA MALAT1	↑	↓	miR-150-5p/AKT	↓ ECM degradation ↓ Oxidative stress and apoptosis	Human osteoarthritic chondrocytes	Zhang et al. (2018)
			miR-146a-PI3K/Akt/mTO	↓ Oxidative stress and apoptosis	Human osteoarthritic chondrocytes	Li et al. (2017)
			JNK	↓ ECM degradation	Rat chondrocytes	Gao et al. (2018)
				↓ Oxidative stress and apoptosis	Rat chondrocytes	Gao et al. (2019)
			miR-145/ADAMTS5	↑ ECM degradation	Human osteoarthritic chondrocytes	Liu et al. (2014)
lncRNA MEG3	↓	Uncertain	miR-93/TGFBR2	↓ ECM degradation	Rat chondrocytes	Chen et al. (2021a)
			mir-16/smad7	↑ Oxidative stress and apoptosis	Rat chondrocytes	Xu et al. (2022)
			miR-9-5p/KLF4	↓ Oxidative stress and apoptosis	CHON-001 and ATDC5	Huang et al. (2021)
			P2X3	↓ Inflammatory mediators and response	SW1353	Li et al. (2020)
			TRIB2	↑ Chondrocyte differentiation	SMSCs	You et al. (2019)
lncRNA H19	↓	↑	miR-483–5p/dusp 5	↓ ECM degradation ↑ ECM synthesis	Rat chondrocytes	Wang et al. (2021a)
			miR-106b-5p/TIMP2	↓ ECM degradation	Rat chondrocytes	Tan et al. (2020)
			miR-106a-5p	↑ Oxidative stress and apoptosis	Human articular chondrocytes	Zhang et al. (2016)

Note: Table 2 show the differentially expressed lncRNAs concerning the regulatory effect of melatonin on OA discussed in this review. The up and down arrow represent upregulation and downregulation respectively. "OA influence" means changes of lncRNAs in OA. "MT influence" means the effect of MT on lnRNA. This table is based on the findings from various studies cites appropriately in the text. lncRNAs, long non-coding RNAs; OA, osteoarthritis; MT, melatonin; ECM, extracellular matrix; ADAMTS5, a disintegrin metalloproteinase with thrombospondin motifs 5; SMSCs, synovial mesenchymal stem cells.

TABLE 3 Summary of differentially expressed circRNAs concerning the regulatory effect of melatonin on OA discussed in this review.

circRNAs	OA influence	MT influence	Target gene	Main influence on OA	Model	References
circRNA 3503	↑	↓	miR-181c-3p	↓ ECM degradation	Human articular chondrocytes	Tao et al. (2021)
			hsa-let-7b-3p	↑ECM synthesis	Human articular chondrocytes	Tao et al. (2021)
circRNA 0045714	↑	Uncertain	miR-218-5p/HRAS	↓ ECM degradation ↓ Inflammatory mediators and response ↑ Oxidative stress and apoptosis	Human articular chondrocytes	Jiang et al. (2021b)
			miR-193b/IGF1R	↑ ECM synthesis ↓ Oxidative stress and apoptosis	Human articular chondrocytes	Li et al. (2020)
			miR-331-3p/PIK3R3	↑ ECM synthesis ↓ Inflammatory mediators and response ↓ Oxidative stress and apoptosis	Human articular chondrocytes	Ding et al. (2021)

Note: Table 3 show the differentially expressed circRNAs concerning the regulatory effect of melatonin on OA discussed in this review. The up and down arrow represent upregulation and downregulation respectively. "OA influence" means changes of circRNAs in OA. "MT influence" means the effect of MT on circRNAs. This table is based on the findings from various studies cites appropriately in the text. circRNAs, circular RNAs; OA, osteoarthritis; MT, melatonin; ECM, extracellular matrix; IGF1R, insulin-like growth factor 1 receptor.

2018). Advanced research showed that miR-146a suppressed inflammatory responses in joints by inhibiting Notch signaling. However, miR-146a was significantly upregulated in articular cartilage tissue and serum of OA patients (Skrzypa et al., 2019) and negative regulation in the maintenance of cartilage homeostasis, such as inhibiting cartilage ECM synthesis and promoting chondrocyte apoptosis (Zhang et al., 2017; Shao et al., 2020). Numerous studies have proved the antioxidant

effect of melatonin. Zhou et al. (2022) found a novel antioxidative pathway of melatonin in OA chondrocytes: melatonin can upregulate nuclear factor-erythroid 2-related factor 2 (NRF2) protein level by releasing the binding of miR-146a to key antioxidant transcription factor: NRF2 mRNA in early OA cartilage, further enhanced the activity of heme oxygenase 1 (HO-1), an antioxidant enzyme in chondrocytes by the NRF2/HO-1 axis, playing an antioxidant role in chondrocytes (Zhou et al., 2022). However, the regulation mechanism of melatonin on chondrocyte homeostasis through miR-146a still needs to be further studied.

MiR-526b-3p and miR-590-5p

It was found that melatonin can upregulate miR-526b-3p and miR-590-5p, which can target and inhibit SMAD7, thereby enhancing the phosphorylation of SMAD1 and finally activating the BMP/SMAD pathway to promote the chondrogenic differentiation of hBMSCs (Wu et al., 2018). Melatonin concentration-dependent and reversible by BMP/SMAD pathway inhibitors. The promoting effect of melatonin on cartilage differentiation is concentration-dependent and can be reversed by BMP/SMAD pathway inhibitors. Various ncRNAs can regulate cartilage differentiation through the BMP/SMAD pathway, but their interaction with melatonin has not yet been demonstrated (Lin et al., 2009). In addition, miR-590-5p was found to promote OA progression by targeting fibroblast growth factor18 (FGF18) (Jiang et al., 2021b).

MiR-122

Melatonin exerted cytoprotective and anti-inflammatory effects in hydrogen peroxide (H_2O_2)-stimulated human chondrocyte cell line (CHON-001) and rabbit OA model through the SIRT1 pathway (Lim et al., 2012). It was found that overexpression of miR-122 increased the expression of ECM catabolic factors, such as disintegrins, MMPs, and ADAMTS, and inhibited anabolic genes such as collagen II and aggrecan glycan expression. Inhibition of miR-122 expression had the opposite effect. Furthermore, it was identified as a direct target of miR-122, suggesting the potential of the miR-122/SIRT1 axis in regulating the degradation of ECM in OA (Bai et al., 2020). In addition, rhythm genes are also involved in the regulation of the SIRT1 pathway (Yang et al., 2016). Transfection of siRNA targeting SIRT1 resulted in not only a reduction in protein expression of *bmal1* but also a modest increase in *per2* and Rev-Erbα, the key rhythm gene involved in cartilage homeostasis mediated by SIRT1 concomitantly. All miR-122, melatonin and the rhythm gene *bmal1* can protect cartilage through the SIRT1 pathway, suggesting that the three may interact to maintain cartilage homeostasis.

LncRNA metastasis-associated lung adenocarcinoma transcript 1

Highly sequence-conserved across species and widely studies show that lncRNA metastasis-associated lung adenocarcinoma transcript 1 (MALAT1) has been documented to play a critical role in multiple diseases (Kim et al., 2018; Chen et al., 2021b). Lnc-MALAT1 was upregulated in OA chondrocytes and positively correlated with the severity of OA, and further experiments found that lnc-MALAT1 could target and inhibit miR-150-5p, thereby regulating the proliferation, apoptosis, and ECM degradation of human OA chondrocyte model through the miR-150-5p/AKT3 axis (Zhang et al., 2019d). Similarly, lnc-MALAT1 inhibits miR-146a by targeting and producing similar effects through the miR-146a-PI3K/Akt/mTOR axis (Li et al., 2020). Besides miRNAs, lnc-MALAT1 can also inhibit chondrocyte apoptosis and reduce cartilage ECM degradation by inhibiting the JNK signaling pathway (Gao et al., 2019). Liu et al. (2019) found that IL-1β-stimulated intracellular lnc-MALAT1 in human chondrocytes could target miR-145 and inhibit its function, thereby enhancing ADAMTS5 expression and ultimately leading to enhanced degradation of the chondrocyte ECM (Liu et al., 2019). Lnc-MALAT1 is also an important signaling molecule for regulating drugs on OA (Zhang et al., 2020). Meanwhile, melatonin significantly downregulates lncRNA-MALAT levels in cardiomyocytes (Che et al., 2020). Further research is needed to verify the interaction between melatonin and lncRNA-MALAT in chondrocytes.

LncRNA maternally expressed 3

Numerous experiments have demonstrated the regulatory role of maternally expressed 3 (MEG3) in OA. And this regulation is mainly achieved by functioning as the ceRNAs of miRNAs. It was found that MEG3 was significantly downregulated in chondrocytes treated with IL-1β. Further research found that MEG3 regulates the miR-93/TGFBR2 axis by targeting miR-93, thereby activating the TGF-β signaling pathway, Regulating IL-1β-induced chondrocyte ECM degradation. A previous study (Chen et al., 2021a) found that MEG3 was significantly downregulated in IL-1β-treated chondrocytes. Further studies found that MEG3 regulates the miR-93/TGFBR2 axis by targeting miR-93, activating the TGF-β signaling pathway, and regulating IL-1β-induced chondrocyte ECM degradation. A previous study found that MEG3 exerted anti-proliferative and pro-apoptotic effects on OA chondrocytes by regulating miR-16 and SMAD7 (Xu and Xu, 2017). However, some studies have reached the opposite result. It is found that MEG3 induces KLF4 expression by inhibiting miR-9-5p, thereby promoting chondrocyte proliferation and migration and inhibiting apoptosis and inflammation. The different regulatory effects of MEG3 on chondrocytes may be caused

by differences in experimental subjects (Huang et al., 2021). In addition, LncRNA MEG3 can also exert an anti-OA effect by regulating other genes (Li et al., 2018; You et al., 2019). At the same time, the regulatory effect of melatonin on LncRNA MEG3 has been verified in a variety of diseases, such as atherosclerosis (Zhang et al., 2018), stroke (Chen et al., 2020), and febrile convulsion (Wang et al., 2021b). Melatonin also showed negative regulation of LncRNA MEG production. However, in an experimental diabetic retinopathy cell model, melatonin delays diabetic retinopathy (DR) progression by upregulating MEG3 and inhibiting model cell activation and pro-inflammatory cytokine production via the MEG3/miR-204/SIRT1 axis (Tu et al., 2021). Unfortunately, there is still nothing we know about the interaction of melatonin with lncRNA MEG3 in the regulation of OA.

LncRNA H19

LncRNA H19 is highly expressed in the peripheral blood of OA patients, is closely related to the occurrence and development of OA, and has a diagnostic value for OA (Zhou et al., 2020). It was found that lncRNA-H19 promoted ECM synthesis and inhibited the expression of degradation-related enzymes through the lncRNA H19/miR-483–5p/Dusp 5 axis, and then activated the Erk and p38 pathways in the cartilage degradation induced by intermittent cyclic mechanical stress (ICMS) (Wang et al., 2020). A previous study found that the level of H19 was significantly downregulated in cartilage samples from OA patients and found that lncRNA H19 may promote chondrocyte proliferation and migration by targeting the miR-106b-5p/TIMP2 axis and inhibit ECM degradation in OA cell experiments (Tan et al., 2020). Zhang et al (2019a) found that lncRNA-H19 could regulate the proliferation and apoptosis of OA chondrocytes treated with IL-1β by targeting miR-106a-5p (Zhang et al., 2019a). In addition, the regulatory effect of melatonin on H19 has also been verified in a variety of diseases, such as melatonin promotes the osteogenic differentiation of BMSCs and inhibits adipogenic differentiation by up-regulation of the H19/miR-541-3p/APN axis (Han et al., 2021). Melatonin promotes the expression of lncRNA H19 in delayed brain injury (DBI) after subarachnoid hemorrhage (SAH) (Xu et al., 2022). However, research on melatonin's regulatory effects on H19 in OA is still lacking.

CircRNA 3503

It was found that circRNA 3503 was significantly upregulated in melatonin-treated chondrocytes. Meanwhile, the expression of circRNA 3503 was inhibited by TNF-α or IL-1β (Tao et al., 2021). As sleep-related ncRNAs, circRNA3503 maintains cartilage homeostasis by inhibiting apoptosis and upregulating the expression of genes (aggrecan, Col-II, and SOX9) related to ECM synthesis. However, the researchers found that circRNA3503 was not the direct cause of the protective effect on chondrocytes. Through further experiments, it was speculated and verified that circRNA3503 could promote the expression of PPARGC1A (PGC-1α) by acting as a molecular sponge of miR-181c-3p, thereby releasing the effect of IL-1β on the expression of genes related to CASPASE-3 activation and ECM degradation. Indirect regulation of chondrocyte homeostasis by inhibiting and promoting the expression of ECM synthesis-related gene SOX9 by acting as a molecular sponge for let-7b-3p (Tao et al., 2021).

CircRNA 0045714

The expression of circ 0045714 in knee cartilage tissues and cells of OA patients was lower than that of normal controls, and circ 0045714 could regulate chondrocyte homeostasis by regulating various miRNAs. It is found that the up-regulation of circ 0045714 inhibited TNF-α-induced chondrocyte growth inhibition, inflammation, and ECM degradation by inhibiting the miR-218-5p/HRAS axis (Jiang et al., 2021a). While melatonin could inhibit collagenase-induced OA (Hong et al., 2014), it suggested that melatonin may interact with circ 0045714 when regulating TNF-α. Li et al. (2017)found that circ 0045714 could regulate the synthesis of ECM by inhibiting the transcriptional activity of miR-193b and promoting the expression of miR-193b target gene insulin-like growth factor 1 receptor (IGF1R) (Li et al., 2017). Ding et al. (2021).up found that circ 0045714 plays a protective role in IL-1β-induced chondrocyte injury by targeting and inhibiting miR-331-3p and then upregulating PIK3R3, which is manifested in alleviating chondrocyte apoptosis, inflammatory response and ECM degradation (Ding et al., 2021).

Prospect of combined application of melatonin and ncRNAS in osteoarthritis treatment

The regulatory roles of ncRNAs on osteoarthritis

The therapeutic effects of ncRNAs on OA are complex and diverse. One ncRNA can regulate OA from multiple pathways by acting on one or more target genes (Della Bella et al., 2020). Meanwhile, there are also interactions between different ncRNAs. For example, lncRNAs can act on multiple miRNAs simultaneously, and there are also complex interactions between circRNAs and lncRNAs (Sen et al., 2014; Noh et al., 2018). This further expands the regulatory role of ncRNAs on OA. One ncRNA can regulate OA by acting on multiple target genes, but this regulatory effect is not necessarily consistent. Under the

premise of excluding experimental error, there are two possible reasons for this situation: one is that ncRNAs play different regulatory roles in chondrocytes in different physiological or pathological states, the other reason is that ncRNAs can both positively and negatively regulate the OA process, for example, one ncRNA inhibits autophagy in chondrocytes while promoting ECM synthesis. Therefore, determining whether one ncRNA can really protect OA requires further experimental verification, which is also conducive to screening the most suitable ncRNAs for OA treatment.

The therapeutic effects of melatonin on osteoarthritis

A large number of animal experiments have demonstrated the modulating effect of intra-articular melatonin on OA (Zhang et al., 2019c), and serum melatonin concentrations also appear to play a modulating effect on arthritic disease (Hong et al., 2014). Although previous experiments found that intraperitoneal melatonin aggravated the inflammatory response in rats with collagen-induced arthritis (Bang et al., 2012), pinealectomy reduces the level of local focal inflammation in rats (Vriend and Reiter, 2015). The dual effect of serum melatonin concentration and local inflammation of the joint needs further research on whether increasing serum melatonin can produce a therapeutic effect similar to local injection of melatonin in OA and whether increasing serum melatonin concentrations enhances or diminishes the therapeutic effect of topical melatonin injections. These issues need further research and verification, especially considering that the regulatory effect of melatonin on chronic inflammatory pain, which is one of the most common clinical manifestations of OA patients, has been verified in human trials (Vidor et al., 2013).

Melatonin has been a research hotspot for the past two decades, and its therapeutic potential in various diseases has been found. Recent studies have been focusing on the regenerative potential of melatonin (Majidinia et al., 2018). Melatonin, a pleiotropic hormone with few side effects and easy access, has multiple regulatory effects on cartilage and has potential therapeutic effects on OA-related clinical manifestations and complications such as pain, insomnia, and depression, suggesting that melatonin is one of the best candidates for OA treatment. However, there are also limitations. The antiarthritic effect of melatonin is determined by several factors, including dose, duration of therapy, combined exercise, and duration of the initial intervention (Hong et al., 2017), which means that the dose and duration of melatonin application should be based on the patient's condition. Precise regulation and regulation of ncRNAs provide a feasible research idea for alleviating the adverse effects of melatonin.

Combined application of melatonin and ncRNAs in osteoarthritis treatment

Research on the interaction of melatonin and ncRNAs have been carried out in the treatment of other diseases with the corresponding results (Alamdari et al., 2021). However, the application of melatonin in clinical practice can only be established since the corresponding ncRNAs and their signaling pathways are fully exploited. Unfortunately, the existing research is not comprehensive. Studies on the relationship between melatonin and ncRNAs in the treatment and pathogenesis of OA mainly focus on miRNAs, causing studies on other ncRNAs, especially lncRNAs, are still lacking. Although we can infer that lncRNAs also interacts with melatonin in OA from the evidence that lncRNAs and melatonin can regulate the same miRNAs and the interaction between lncRNAs and melatonin in other diseases, further experiments are needed to verify this our hypothesis. The complex relationship between melatonin and ncRNAs has created a new perspective for a better understanding of OA pathogenesis contributing to find new treatment strategies based on endogenous compounds. By modulating certain local ncRNAs levels, we can effectively improve the limitations of melatonin in the treatment of OA and enhanced the power of melatonin achieve better therapeutic efficacy.

Conclusion

The ncRNAs and melatonin interactome are now considered significant regulators for most aspects of the mechanism and treatment of OA. This review summarizes the interplay between melatonin and several types of regulatory ncRNAs, including miRNAs, lncRNAs, and circRNAs in OA. miRNAs play a regulatory role by directly targeting and inhibiting genes involved in multiple parts of the pathogenesis of OA, while lncRNAs and circRNAs can play an indirect regulatory role through miRNAs in addition to acting on target genes. The interaction between ncRNAs and the one-to-many, many-to-one relationship between ncRNAs and target genes constitute a complex network of OA regulation, and we found that not only does ncRNAs are one important way for melatonin to regulate OA, but also combing ncRNAs or their regulators with melatonin may be a new approach for the treatment of OA in the future. To the best of our knowledge, this is the first review to explore the therapeutic effect of melatonin on OA from the perspective of ncRNAs, however, further researches are required to screen the most suitable ncRNAs for OA treatment and reduce the side effect of long-term melatonin supplementation.

Author contributions

Conception and design: SL, HS, and BS. Writing- Original draft preparation: SL and HS. Manuscript writing: SL, HS, JX, and YL. Revising drafting critically for important intellectual content: HS and BS. Final approval of manuscript: All authors. SL and HS have contributed equally to this work and share first authorship.

Funding

This work was supported by the National Natural Science Foundation of China (grant number 81974347 and 81802210).

Conflict of interest

The authors declare that the research was conducted in the absence of any commercial or financial relationships that could be construed as a potential conflict of interest.

Publisher's note

All claims expressed in this article are solely those of the authors and do not necessarily represent those of their affiliated organizations, or those of the publisher, the editors and the reviewers. Any product that may be evaluated in this article, or claim that may be made by its manufacturer, is not guaranteed or endorsed by the publisher.

References

Alamdari, A. F., Rahnemayan, S., Rajabi, H., Vahed, N., Kashani, H. R. K., Rezabakhsh, A., et al. (2021). Melatonin as a promising modulator of aging related neurodegenerative disorders: Role of microRNAs. *Pharmacol. Res.* 173, 105839. doi:10.1016/j.phrs.2021.105839

Bai, Y., Chen, K., Zhan, J., and Wu, M. (2020). miR-122/SIRT1 axis regulates chondrocyte extracellular matrix degradation in osteoarthritis. *Biosci. Rep.* 40, BSR20191908. doi:10.1042/BSR20191908

Bang, J., Chang, H. W., Jung, H. R., Cho, C. H., Hur, J. A., Lee, S. I., et al. (2012). Melatonin attenuates clock gene cryptochrome1, which may aggravate mouse anti-type II collagen antibody-induced arthritis. *Rheumatol. Int.* 32, 379–385. doi:10.1007/s00296-010-1641-9

Bellamy, N., Sothern, R. B., Campbell, J., and Buchanan, W. W. (2002). Rhythmic variations in pain, stiffness, and manual dexterity in hand osteoarthritis. *Ann. Rheum. Dis.* 61, 1075–1080. doi:10.1136/ard.61.12.1075

Blanco, F. J., Rego, I., and Ruiz-Romero, C. (2011). The role of mitochondria in osteoarthritis. *Nat. Rev. Rheumatol.* 7, 161–169. doi:10.1038/nrrheum.2010.213

Che, H., Wang, Y., Li, H., Li, Y., Sahil, A., Lv, J., et al. (2020). Melatonin alleviates cardiac fibrosis via inhibiting lncRNA MALAT1/miR-141-mediated NLRP3 inflammasome and TGF-β1/Smads signaling in diabetic cardiomyopathy. *FASEB J.* 34, 5282–5298. doi:10.1096/fj.201902692R

Chen, K., Zhu, H., Zheng, M. Q., and Dong, Q. R. (2021a). LncRNA MEG3 inhibits the degradation of the extracellular matrix of chondrocytes in osteoarthritis via targeting miR-93/TGFBR2 Axis. *Cartilage* 13, 1274S–1284S. doi:10.1177/1947603519855759

Chen, Y., He, L., Pang, M., Ke, Z., Zheng, X., Feng, F., et al. (2020). Melatonin promotes neuroprotection of H2O2-induced neural stem cells via lncRNA MEG3/miRNA-27a-3p/MAP2K4 axis. *Neuroscience* 446, 69–79. doi:10.1016/j.neuroscience.2020.06.026

Chen, Y., Li, S., Zhang, Y., Wang, M., Li, X., Liu, S., et al. (2021b). The lncRNA Malat1 regulates microvascular function after myocardial infarction in mice via miR-26b-5p/Mfn1 axis-mediated mitochondrial dynamics. *Redox Biol.* 41, 101910. doi:10.1016/j.redox.2021.101910

Chen, Z., Zhao, C., Liu, P., Huang, H., Zhang, S., and Wang, X. (2021c). Anti-apoptosis and autophagy effects of melatonin protect rat chondrocytes against oxidative stress via regulation of AMPK/Foxo3 pathways. *Cartilage* 13, 1041s–1053s. doi:10.1177/19476035211038748

Cipolla-Neto, J., and Amaral, F. G. D. (2018). Melatonin as a hormone: New physiological and clinical insights. *Endocr. Rev.* 39, 990–1028. doi:10.1210/er.2018-00084

Clokie, S. J., Lau, P., Kim, H. H., Coon, S. L., and Klein, D. C. (2012). MicroRNAs in the pineal gland: miR-483 regulates melatonin synthesis by targeting arylalkylamine N-acetyltransferase. *J. Biol. Chem.* 287, 25312–25324. doi:10.1074/jbc.M112.356733

Della Bella, E., Menzel, U., Basoli, V., Tourbier, C., Alini, M., and Stoddart, M. J. (2020). Differential regulation of circRNA, miRNA, and piRNA during early osteogenic and chondrogenic differentiation of human mesenchymal stromal cells. *Cells* 9, E398. doi:10.3390/cells9020398

Ding, R., Zhou, J., Xu, J., Lu, H., Zhang, T., Xiang, X., et al. (2021). Circ_0045714/miR-331-3p interaction affects IL-1β-evoked human articular chondrocyte injury through regulating PIK3R3 in a ceRNA regulatory cascade. *J. Orthop. Surg. Res.* 16, 595. doi:10.1186/s13018-021-02738-2

Dudek, M., Gossan, N., Yang, N., Im, H. J., Ruckshanthi, J. P., Yoshitane, H., et al. (2016). The chondrocyte clock gene Bmal1 controls cartilage homeostasis and integrity. *J. Clin. Invest.* 126, 365–376. doi:10.1172/JCI82755

Esposito, T., Magliocca, S., Formicola, D., and Gianfrancesco, F. (2011). piR_015520 belongs to Piwi-associated RNAs regulates expression of the human melatonin receptor 1A gene. *PLoS One* 6, e22727. doi:10.1371/journal.pone.0022727

Fu, S., Kuwahara, M., Uchida, Y., Koudo, S., Hayashi, D., Shimomura, Y., et al. (2019). Circadian production of melatonin in cartilage modifies rhythmic gene expression. *J. Endocrinol.* 241, 161–173. doi:10.1530/JOE-19-0022

Gao, B., Gao, W., Wu, Z., Zhou, T., Qiu, X., Wang, X., et al. (2018). Melatonin rescued interleukin 1β-impaired chondrogenesis of human mesenchymal stem cells. *Stem Cell Res. Ther.* 9, 162. doi:10.1186/s13287-018-0892-3

Gao, G. C., Cheng, X. G., Wei, Q. Q., Chen, W. C., and Huang, W. Z. (2019). Long noncoding RNA MALAT-1 inhibits apoptosis and matrix metabolism disorder in interleukin-1β-induced inflammation in articular chondrocytes via the JNK signaling pathway. *J. Cell. Biochem.* 120, 17167–17179. doi:10.1002/jcb.28977

Guan, Y. J., Li, J., Yang, X., Du, S., Ding, J., Gao, Y., et al. (2018). Evidence that miR-146a attenuates aging- and trauma-induced osteoarthritis by inhibiting Notch1, IL-6, and IL-1 mediated catabolism. *Aging Cell* 17, e12752. doi:10.1111/acel.12752

Guilak, F., Nims, R. J., Dicks, A., Wu, C. L., and Meulenbelt, I. (2018). Osteoarthritis as a disease of the cartilage pericellular matrix. *Matrix Biol.* 71-72, 40–50. doi:10.1016/j.matbio.2018.05.008

Guo, B., Yang, N., Borysiewicz, E., Dudek, M., Williams, J. L., Li, J., et al. (2015). Catabolic cytokines disrupt the circadian clock and the expression of clock-controlled genes in cartilage via an NFκB-dependent pathway. *Osteoarthr. Cartil.* 23, 1981–1988. doi:10.1016/j.joca.2015.02.020

Guo, J. Y., Li, F., Wen, Y. B., Cui, H. X., Guo, M. L., Zhang, L., et al. (2017). Melatonin inhibits Sirt1-dependent NAMPT and NFAT5 signaling in chondrocytes to attenuate osteoarthritis. *Oncotarget* 8, 55967–55983. doi:10.18632/oncotarget.18356

Haas, S., and Straub, R. H. (2012). Disruption of rhythms of molecular clocks in primary synovial fibroblasts of patients with osteoarthritis and rheumatoid arthritis, role of IL-1β/TNF. *Arthritis Res. Ther.* 14, R122. doi:10.1186/ar3852

Hai, B., Ma, Y., Pan, X., Yong, L., Liang, C., He, G., et al. (2019). Melatonin benefits to the growth of human annulus fibrosus cells through inhibiting miR-106a-5p/ATG7 signaling pathway. *Clin. Interv. Aging* 14, 621–630. doi:10.2147/CIA.S193765

Han, H., Tian, T., Huang, G., Li, D., and Yang, S. (2021). The lncRNA H19/miR-541-3p/Wnt/β-catenin axis plays a vital role in melatonin-mediated osteogenic differentiation of bone marrow mesenchymal stem cells. *Aging (Albany NY)* 13, 18257–18273. doi:10.18632/aging.203267

Han, N., Wang, Z., and Li, X. (2021a). Melatonin alleviates d-galactose-decreased hyaluronic acid production in synovial membrane cells via Sirt1 signalling. *Cell biochem. Funct.* 39, 488–495. doi:10.1002/cbf.3613

Han, Y. S., Lee, J. H., and Lee, S. H. (2020). Melatonin suppresses ischemia-induced fibrosis by regulating miR-149. *Biochem. Biophys. Res. Commun.* 525, 354–359. doi:10.1016/j.bbrc.2020.02.090

Hardeland, R. (2019). Aging, melatonin, and the pro- and anti-inflammatory networks. *Int. J. Mol. Sci.* 20, E1223. doi:10.3390/ijms20051223

Hardeland, R. (2012). Melatonin in aging and disease -multiple consequences of reduced secretion, options and limits of treatment. *Aging Dis.* 3, 194–225.

Hardeland, R. (2014). Melatonin, noncoding RNAs, messenger RNA stability and epigenetics--evidence, hints, gaps and perspectives. *Int. J. Mol. Sci.* 15, 18221–18252. doi:10.3390/ijms151018221

Hashiramoto, A., Yamane, T., Tsumiyama, K., Yoshida, K., Komai, K., Yamada, H., et al. (2010). Mammalian clock gene Cryptochrome regulates arthritis via proinflammatory cytokine TNF-alpha. *J. Immunol.* 184, 1560–1565. doi:10.4049/jimmunol.0903284

He, M., Zhou, C., Lu, Y., Mao, L., Xi, Y., Mei, X., et al. (2020). Melatonin antagonizes nickel-induced aerobic glycolysis by blocking ROS-mediated HIF-1α/miR210/ISCU Axis Activation. *Oxid. Med. Cell. Longev.* 2020, 5406284. doi:10.1155/2020/5406284

Heo, J. S., Lim, J. Y., Yoon, D. W., Pyo, S., and Kim, J. (2020). Exosome and melatonin additively attenuates inflammation by transferring miR-34a, miR-124, and miR-135b. *Biomed. Res. Int.* 2020, 1621394. doi:10.1155/2020/1621394

Histing, T., Anton, C., Scheuer, C., Garcia, P., Holstein, J. H., Klein, M., et al. (2012). Melatonin impairs fracture healing by suppressing RANKL-mediated bone remodeling. *J. Surg. Res.* 173, 83–90. doi:10.1016/j.jss.2010.08.036

Hong, Y., Kim, H., Lee, S., Jin, Y., Choi, J., Lee, S. R., et al. (2017). Role of melatonin combined with exercise as a switch-like regulator for circadian behavior in advanced osteoarthritic knee. *Oncotarget* 8, 97633–97647. doi:10.18632/oncotarget.19276

Hong, Y., Kim, H., Lee, Y., Lee, S., Kim, K., Jin, Y., et al. (2014). Salutary effects of melatonin combined with treadmill exercise on cartilage damage. *J. Pineal Res.* 57, 53–66. doi:10.1111/jpi.12143

Hossain, F. M., Hong, Y., Jin, Y., Choi, J., and Hong, Y. (2019). Physiological and pathological role of circadian hormones in osteoarthritis: Dose-dependent or time-dependent? *J. Clin. Med.* 8, E1415. doi:10.3390/jcm8091415

Hosseinzadeh, A., Kamrava, S. K., Joghataei, M. T., Darabi, R., Shakeri-Zadeh, A., Shahriari, M., et al. (2016). Apoptosis signaling pathways in osteoarthritis and possible protective role of melatonin. *J. Pineal Res.* 61, 411–425. doi:10.1111/jpi.12362

Huang, Y., Chen, D., Yan, Z., Zhan, J., Xue, X., Pan, X., et al. (2021). LncRNA MEG3 protects chondrocytes from IL-1β-induced inflammation *via* regulating miR-9-5p/KLF4 Axis. *Front. Physiol.* 12, 617654. doi:10.3389/fphys.2021.617654

Hunter, D. J., and Bierma-Zeinstra, S. (2019). Osteoarthritis. *Lancet* 393, 1745–1759. doi:10.1016/S0140-6736(19)30417-9

Hunter, D. J., March, L., and Chew, M. (2020). Osteoarthritis in 2020 and beyond: A lancet commission. *Lancet* 396, 1711–1712. doi:10.1016/S0140-6736(20)32230-3

Jahanban-Esfahlan, R., Mehrzadi, S., Reiter, R. J., Seidi, K., Majidinia, M., Baghi, H. B., et al. (2018). Melatonin in regulation of inflammatory pathways in rheumatoid arthritis and osteoarthritis: Involvement of circadian clock genes. *Br. J. Pharmacol.* 175, 3230–3238. doi:10.1111/bph.13898

Jiang, H., Dai, J., Zhang, C., Sun, H., and Tang, X. (2021a). Circ_0045714 alleviates TNF-α-induced chondrocyte injury and extracellular matrix degradation through miR-218-5p/HRAS axis. *J. Bioenerg. Biomembr.* 53, 97–107. doi:10.1007/s10863-020-09868-y

Jiang, P., Dou, X., Li, S., Jia, Q., Ling, P., Liu, H., et al. (2021b). miR-590-5p affects chondrocyte proliferation, apoptosis, and inflammation by targeting FGF18 in osteoarthritis. *Am. J. Transl. Res.* 13, 8728–8741.

Jorge, A., Fu, X., Cook, C., Lu, N., Zhang, Y., Choi, H. K., et al. (2021). *Kidney transplantation and cardiovascular events among patients with end-stage renal disease due to lupus nephritis*.

Karlsen, T. A., De Souza, G. A., Ødegaard, B., Engebretsen, L., and Brinchmann, J. E. (2016). microRNA-140 inhibits inflammation and stimulates chondrogenesis in a model of interleukin 1β-induced osteoarthritis. *Mol. Ther. Nucleic Acids* 5, e373. doi:10.1038/mtna.2016.64

Kelwick, R., Desanlis, I., Wheeler, G. N., and Edwards, D. R. (2015). The ADAMTS (A disintegrin and metalloproteinase with thrombospondin motifs) family. *Genome Biol.* 16, 113. doi:10.1186/s13059-015-0676-3

Kim, J., Piao, H. L., Kim, B. J., Yao, F., Han, Z., Wang, Y., et al. (2018). Long noncoding RNA MALAT1 suppresses breast cancer metastasis. *Nat. Genet.* 50, 1705–1715. doi:10.1038/s41588-018-0252-3

Li, B. F., Zhang, Y., Xiao, J., Wang, F., Li, M., Guo, X. Z., et al. (2017). Hsa_circ_0045714 regulates chondrocyte proliferation, apoptosis and extracellular matrix synthesis by promoting the expression of miR-193b target gene IGF1R. *Hum. Cell* 30, 311–318. doi:10.1007/s13577-017-0177-7

Li, H., Xie, S., Li, H., Zhang, R., and Zhang, H. (2020). LncRNA MALAT1 mediates proliferation of LPS treated-articular chondrocytes by targeting the miR-146a-PI3K/Akt/mTOR axis. *Life Sci.* 254, 116801. doi:10.1016/j.lfs.2019.116801

Li, X., Tang, C., Wang, J., Guo, P., Wang, C., Wang, Y., et al. (2018). Methylene blue relieves the development of osteoarthritis by upregulating lncRNA MEG3. *Exp. Ther. Med.* 15, 3856–3864. doi:10.3892/etm.2018.5918

Liang, Y., Duan, L., Xiong, J., Zhu, W., Liu, Q., Wang, D., et al. (2016). E2 regulates MMP-13 via targeting miR-140 in IL-1β-induced extracellular matrix degradation in human chondrocytes. *Arthritis Res. Ther.* 18, 105. doi:10.1186/s13075-016-0997-y

Liang, Y., Xu, X., Li, X., Xiong, J., Li, B., Duan, L., et al. (2020). Chondrocyte-Targeted MicroRNA delivery by engineered exosomes toward a cell-free osteoarthritis therapy. *ACS Appl. Mat. Interfaces* 12, 36938–36947. doi:10.1021/acsami.0c10458

Lim, H. D., Kim, Y. S., Ko, S. H., Yoon, I. J., Cho, S. G., Chun, Y. H., et al. (2012). Cytoprotective and anti-inflammatory effects of melatonin in hydrogen peroxide-stimulated CHON-001 human chondrocyte cell line and rabbit model of osteoarthritis via the SIRT1 pathway. *J. Pineal Res.* 53, 225–237. doi:10.1111/j.1600-079X.2012.00991.x

Lin, E. A., Kong, L., Bai, X. H., Luan, Y., and Liu, C. J. (2009). miR-199a, a bone morphogenic protein 2-responsive MicroRNA, regulates chondrogenesis via direct targeting to Smad1. *J. Biol. Chem.* 284, 11326–11335. doi:10.1074/jbc.M807709200

Liu, C., Ren, S., Zhao, S., and Wang, Y. (2019). LncRNA MALAT1/MiR-145 adjusts IL-1β-induced chondrocytes viability and cartilage matrix degradation by regulating ADAMTS5 in human osteoarthritis. *Yonsei Med. J.* 60, 1081–1092. doi:10.3349/ymj.2019.60.11.1081

Liu, S. C., Tsai, C. H., Wang, Y. H., Su, C. M., Wu, H. C., Fong, Y. C., et al. (2022). Melatonin abolished proinflammatory factor expression and antagonized osteoarthritis progression *in vivo*. *Cell Death Dis.* 13, 215. doi:10.1038/s41419-022-04656-5

Liu, X., Xu, Y., Chen, S., Tan, Z., Xiong, K., Li, Y., et al. (2014). Rescue of proinflammatory cytokine-inhibited chondrogenesis by the antiarthritic effect of melatonin in synovium mesenchymal stem cells via suppression of reactive oxygen species and matrix metalloproteinases. *Free Radic. Biol. Med.* 68, 234–246. doi:10.1016/j.freeradbiomed.2013.12.012

Lu, K. H., Lu, P. W., Lu, E. W., Tang, C. H., Su, S. C., Lin, C. W., et al. (2021a). The potential remedy of melatonin on osteoarthritis. *J. Pineal Res.* 71, e12762. doi:10.1111/jpi.12762

Lu, X., Yu, S., Chen, G., Zheng, W., Peng, J., Huang, X., et al. (2021b). Insight into the roles of melatonin in bone tissue and bone-related diseases (Review). *Int. J. Mol. Med.* 47, 82. doi:10.3892/ijmm.2021.4915

Mahboudi, H., Soleimani, M., Hanaee-Ahvaz, H., Ghanbarian, H., Bandehpour, M., Enderami, S. E., et al. (2018). New approach for differentiation of bone marrow mesenchymal stem cells toward chondrocyte cells with overexpression of MicroRNA-140. *Asaio J.* 64, 662–672. doi:10.1097/MAT.0000000000000688

Majidinia, M., Reiter, R. J., Shakouri, S. K., Mohebbi, I., Rastegar, M., Kaviani, M., et al. (2018). The multiple functions of melatonin in regenerative medicine. *Ageing Res. Rev.* 45, 33–52. doi:10.1016/j.arr.2018.04.003

Matsui, M., and Corey, D. R. (2017). Non-coding RNAs as drug targets. *Nat. Rev. Drug Discov.* 16, 167–179. doi:10.1038/nrd.2016.117

Miyaki, S., Nakasa, T., Otsuki, S., Grogan, S. P., Higashiyama, R., Inoue, A., et al. (2009). MicroRNA-140 is expressed in differentiated human articular chondrocytes and modulates interleukin-1 responses. *Arthritis Rheum.* 60, 2723–2730. doi:10.1002/art.24745

Mori, F., Ferraiuolo, M., Santoro, R., Sacconi, A., Goeman, F., Pallocca, M., et al. (2016). Multitargeting activity of miR-24 inhibits long-term melatonin anticancer effects. *Oncotarget* 7, 20532–20548. doi:10.18632/oncotarget.7978

Morris, J. L., Letson, H. L., Gillman, R., Hazratwala, K., Wilkinson, M., Mcewen, P., et al. (2019). The CNS theory of osteoarthritis: Opportunities beyond the joint. *Semin. Arthritis Rheum.* 49, 331–336. doi:10.1016/j.semarthrit.2019.03.008

Na, Y. J., Sung, J. H., Lee, S. C., Lee, Y. J., Choi, Y. J., Park, W. Y., et al. (2009). Comprehensive analysis of microRNA-mRNA co-expression in circadian rhythm. *Exp. Mol. Med.* 41, 638–647. doi:10.3858/emm.2009.41.9.070

Naghizadeh, Z., Karkhaneh, A., Nokhbatolfoghahaei, H., Farzad-Mohajeri, S., Rezai-Rad, M., Dehghan, M. M., et al. (2021). Cartilage regeneration with dual-drug-releasing injectable hydrogel/microparticle system: *In vitro* and *in vivo* study. *J. Cell. Physiol.* 236, 2194–2204. doi:10.1002/jcp.30006

Neogi, T., and Zhang, Y. (2013). Epidemiology of osteoarthritis. *Rheum. Dis. Clin. North Am.* 39, 1–19. doi:10.1016/j.rdc.2012.10.004

Noh, J. H., Kim, K. M., Mcclusky, W. G., Abdelmohsen, K., and Gorospe, M. (2018). Cytoplasmic functions of long noncoding RNAs. *Wiley Interdiscip. Rev. RNA* 9, e1471. doi:10.1002/wrna.1471

Pei, M., He, F., Wei, L., and Rawson, A. (2009). Melatonin enhances cartilage matrix synthesis by porcine articular chondrocytes. *J. Pineal Res.* 46, 181–187. doi:10.1111/j.1600-079X.2008.00646.x

Qiu, B., Xu, X., Yi, P., and Hao, Y. (2020). Curcumin reinforces MSC-derived exosomes in attenuating osteoarthritis via modulating the miR-124/NF-kB and miR-143/ROCK1/TLR9 signalling pathways. *J. Cell. Mol. Med.* 24, 10855–10865. doi:10.1111/jcmm.15714

Quicke, J. G., Conaghan, P. G., Corp, N., and Peat, G. (2022). Osteoarthritis year in review 2021: Epidemiology & therapy. *Osteoarthr. Cartil.* 30, 196–206. doi:10.1016/j.joca.2021.10.003

Reiter, R. J., Tan, D. X., and Fuentes-Broto, L. (2010). Melatonin: A multitasking molecule. *Prog. Brain Res.* 181, 127–151. doi:10.1016/S0079-6123(08)81008-4

Sayed, R. K., Fernández-Ortiz, M., Fernández-Martínez, J., Aranda Martínez, P., Guerra-Librero, A., Rodríguez-Santana, C., et al. (2021). The impact of melatonin and NLRP3 inflammasome on the expression of microRNAs in aged muscle.*Antioxidants (Basel)*, 10, 524, doi:10.3390/antiox10040524

Sen, R., Ghosal, S., Das, S., Balti, S., and Chakrabarti, J. (2014). Competing endogenous RNA: The key to posttranscriptional regulation. *ScientificWorldJournal.* 2014, 896206. doi:10.1155/2014/896206

Shao, J., Ding, Z., Peng, J., Zhou, R., Li, L., Qian, Q., et al. (2020). MiR-146a-5p promotes IL-1β-induced chondrocyte apoptosis through the TRAF6-mediated NF-kB pathway. *Inflamm. Res.* 69, 619–630. doi:10.1007/s00011-020-01346-w

Si, H., Liang, M., Cheng, J., and Shen, B. (2019). [Effects of cartilage progenitor cells and microRNA-140 on repair of osteoarthritic cartilage injury]. *Zhongguo Xiu Fu Chong Jian Wai Ke Za Zhi* 33, 650–658. doi:10.7507/1002-1892.201806060

Skrzypa, M., Szala, D., Gablo, N., Czech, J., Pajak, J., Kopanska, M., et al. (2019). miRNA-146a-5p is upregulated in serum and cartilage samples of patients with osteoarthritis. *Pol. Przegl. Chir.* 91, 1–5. doi:10.5604/01.3001.0013.0135

Swarnakar, S., Paul, S., Singh, L. P., and Reiter, R. J. (2011). Matrix metalloproteinases in health and disease: Regulation by melatonin. *J. Pineal Res.* 50, 8–20. doi:10.1111/j.1600-079X.2010.00812.x

Tan, F., Wang, D., and Yuan, Z. (2020). The fibroblast-like synoviocyte derived exosomal long non-coding RNA H19 alleviates osteoarthritis progression through the miR-106b-5p/TIMP2 Axis. *Inflammation* 43, 1498–1509. doi:10.1007/s10753-020-01227-8

Tao, S. C., Huang, J. Y., Gao, Y., Li, Z. X., Wei, Z. Y., Dawes, H., et al. (2021). Small extracellular vesicles in combination with sleep-related circRNA3503: A targeted therapeutic agent with injectable thermosensitive hydrogel to prevent osteoarthritis. *Bioact. Mat.* 6, 4455–4469. doi:10.1016/j.bioactmat.2021.04.031

Tardif, G., Pelletier, J. P., Fahmi, H., Hum, D., Zhang, Y., Kapoor, M., et al. (2013). NFAT3 and TGF-β/SMAD3 regulate the expression of miR-140 in osteoarthritis. *Arthritis Res. Ther.* 15, R197. doi:10.1186/ar4387

Tian, Y., Gong, Z., Zhao, R., and Zhu, Y. (2021). Melatonin inhibits RANKL-induced osteoclastogenesis through the miR-882/Rev-erbα axis in Raw264.7 cells. *Int. J. Mol. Med.* 47, 633–642. doi:10.3892/ijmm.2020.4820

Tu, Y., Song, E., Wang, Z., Ji, N., Zhu, L., Wang, K., et al. (2021). Melatonin attenuates oxidative stress and inflammation of Muller cells in diabetic retinopathy via activating the Sirt1 pathway. *Biomed. Pharmacother.* 137, 111274. doi:10.1016/j.biopha.2021.111274

Verma, P., and Dalal, K. (2011). ADAMTS-4 and ADAMTS-5: Key enzymes in osteoarthritis. *J. Cell. Biochem.* 112, 3507–3514. doi:10.1002/jcb.23298

Vidor, L. P., Torres, I. L., Custodio De Souza, I. C., Fregni, F., and Caumo, W. (2013). Analgesic and sedative effects of melatonin in temporomandibular disorders: A double-blind, randomized, parallel-group, placebo-controlled study. *J. Pain Symptom Manage.* 46, 422–432. doi:10.1016/j.jpainsymman.2012.08.019

Vriend, J., and Reiter, R. J. (2015). Melatonin feedback on clock genes: A theory involving the proteasome. *J. Pineal Res.* 58, 1–11. doi:10.1111/jpi.12189

Wang, C. L., Zuo, B., Li, D., Zhu, J. F., Xiao, F., Zhang, X. L., et al. (2020). The long noncoding RNA H19 attenuates force-driven cartilage degeneration via miR-483-5p/Dusp5. *Biochem. Biophys. Res. Commun.* 529, 210–217. doi:10.1016/j.bbrc.2020.05.180

Wang, Y. F., Zhang, Y., Lin, Z., Zhang, H., Wang, T. Y., Cao, Y., et al. (2021b). Identification of 38 novel loci for systemic lupus erythematosus and genetic heterogeneity between ancestral groups. *Nat. Commun.* 12, 772. doi:10.1038/s41467-021-21049-y

Wang, Y., Nguyen, U. D. T., Lane, N. E., Lu, N., Wei, J., Lei, G., et al. (2021a). Knee osteoarthritis, potential mediators, and risk of all-cause mortality: Data from the osteoarthritis initiative. *Arthritis Care Res. Hob.* 73, 566–573. doi:10.1002/acr.24151

Wu, Y., Lu, X., Shen, B., and Zeng, Y. (2019). The therapeutic potential and role of miRNA, lncRNA, and circRNA in osteoarthritis. *Curr. Gene Ther.* 19, 255–263. doi:10.2174/1566523219666190716092203

Wu, Z., Qiu, X., Gao, B., Lian, C., Peng, Y., Liang, A., et al. (2018). Melatonin-mediated miR-526b-3p and miR-590-5p upregulation promotes chondrogenic differentiation of human mesenchymal stem cells. *J. Pineal Res.* 65, e12483. doi:10.1111/jpi.12483

Xie, W. Q., Chen, S. F., Tao, X. H., Zhang, L. Y., Hu, P. W., Pan, W. L., et al. (2021). Melatonin: Effects on cartilage homeostasis and therapeutic prospects in cartilage-related diseases. *Aging Dis.* 12, 297–307. doi:10.14336/AD.2020.0519

Xu, J., and Xu, Y. (2017). The lncRNA MEG3 downregulation leads to osteoarthritis progression via miR-16/SMAD7 axis. *Cell Biosci.* 7, 69. doi:10.1186/s13578-017-0195-x

Xu, Z., Zhang, F., Xu, H., Yang, F., Zhou, G., Tong, M., et al. (2022). Melatonin affects hypoxia-inducible factor 1α and ameliorates delayed brain injury following subarachnoid hemorrhage via H19/miR-675/HIF1A/TLR4. *Bioengineered* 13, 4235–4247. doi:10.1080/21655979.2022.2027175

Yang, W., Kang, X., Liu, J., Li, H., Ma, Z., Jin, X., et al. (2016). Clock gene Bmal1 modulates human cartilage gene expression by crosstalk with Sirt1. *Endocrinology* 157, 3096–3107. doi:10.1210/en.2015-2042

Yang, W., Kang, X., Qin, N., Li, F., Jin, X., Ma, Z., et al. (2017). Melatonin protects chondrocytes from impairment induced by glucocorticoids via NAD(+)-dependent SIRT1. *Steroids* 126, 24–29. doi:10.1016/j.steroids.2017.08.005

You, D., Yang, C., Huang, J., Gong, H., Yan, M., and Ni, J. (2019). Long non-coding RNA MEG3 inhibits chondrogenic differentiation of synovium-derived mesenchymal stem cells by epigenetically inhibiting TRIB2 via methyltransferase EZH2. *Cell. Signal.* 63, 109379. doi:10.1016/j.cellsig.2019.109379

Zhang, G., Zhang, H., You, W., Tang, X., Li, X., and Gong, Z. (2020). Therapeutic effect of Resveratrol in the treatment of osteoarthritis via the MALAT1/miR-9/NF-κB signaling pathway. *Exp. Ther. Med.* 19, 2343–2352. doi:10.3892/etm.2020.8471

Zhang, W. L., Meng, H. Z., Yang, R. F., Yang, M. W., Sun, G. H., Liu, J. H., et al. (2016). Melatonin suppresses autophagy in type 2 diabetic osteoporosis. *Oncotarget* 7, 52179–52194. doi:10.18632/oncotarget.10538

Zhang, X., Liu, X., Ni, X., Feng, P., and Wang, Y. U. (2019a). Long non-coding RNA H19 modulates proliferation and apoptosis in osteoarthritis via regulating miR-106a-5p. *J. Biosci.* 44, 128. doi:10.1007/s12038-019-9943-x

Zhang, X., Wang, C., Zhao, J., Xu, J., Geng, Y., Dai, L., et al. (2017). miR-146a facilitates osteoarthritis by regulating cartilage homeostasis via targeting Camk2d and Ppp3r2. *Cell Death Dis.* 8, e2734. doi:10.1038/cddis.2017.146

Zhang, Y., He, F., Chen, Z., Su, Q., Yan, M., Zhang, Q., et al. (2019b). Melatonin modulates IL-1β-induced extracellular matrix remodeling in human nucleus pulposus cells and attenuates rat intervertebral disc degeneration and inflammation. *Aging NY)* 11, 10499–10512. doi:10.18632/aging.102472

Zhang, Y., Lin, J., Zhou, X., Chen, X., Chen, A. C., Pi, B., et al. (2019c). Melatonin prevents osteoarthritis-induced cartilage degradation via targeting MicroRNA-140. *Oxid. Med. Cell. Longev.* 2019, 9705929. doi:10.1155/2019/9705929

Zhang, Y., Liu, X., Bai, X., Lin, Y., Li, Z., Fu, J., et al. (2018). Melatonin prevents endothelial cell pyroptosis via regulation of long noncoding RNA MEG3/miR-223/NLRP3 axis. *J. Pineal Res.* 64, e12449. doi:10.1111/jpi.12449

Zhang, Y., Wang, F., Chen, G., He, R., and Yang, L. (2019d). LncRNA MALAT1 promotes osteoarthritis by modulating miR-150-5p/AKT3 axis. *Cell Biosci.* 9, 54. doi:10.1186/s13578-019-0302-2

Zhao, C., Chen, J. Y., Peng, W. M., Yuan, B., Bi, Q., and Xu, Y. J. (2020). Exosomes from adipose-derived stem cells promote chondrogenesis and suppress inflammation by upregulating miR-145 and miR-221. *Mol. Med. Rep.* 21, 1881–1889. doi:10.3892/mmr.2020.10982

Zheng, H. F., Forgetta, V., Hsu, Y. H., Estrada, K., Rosello-Diez, A., Leo, P. J., et al. (2015). Whole-genome sequencing identifies EN1 as a determinant of bone density and fracture. *Nature* 526, 112–117. doi:10.1038/nature14878

Zheng, Y., Jiang, H., Wang, H. Q., Guo, H. X., Han, D. X., Huang, Y. J., et al. (2021). Identifying daily changes in circRNAs and circRNA-associated-ceRNA networks in the rat pineal gland. *Int. J. Med. Sci.* 18, 1225–1239. doi:10.7150/ijms.51743

Zheng, Y., Wang, H. Q., Guo, H. X., Xie, H. L., Zhang, W. D., Han, D. X., et al. (2022). CircRNA-WNK2 acts as a ceRNA for miR-328a-3p to promote AANAT expression in the male rat pineal gland. *Endocrinology* 163, bqab255. doi:10.1210/endocr/bqab255

Zhou, L., Wan, Y., Cheng, Q., Shi, B., Zhang, L., and Chen, S. (2020). The expression and diagnostic value of LncRNA H19 in the blood of patients with osteoarthritis. *Iran. J. Public Health* 49, 1494–1501. doi:10.18502/ijph.v49i8.3893

Zhou, X., Zhang, Y., Hou, M., Liu, H., Yang, H., Chen, X., et al. (2022). Melatonin prevents cartilage degradation in early-stage osteoarthritis through activation of miR-146a/NRF2/HO-1 Axis. *J. Bone Min. Res.* 37, 1056–1072. doi:10.1002/jbmr.4527

Zhu, H. Q., Li, Q., Dong, L. Y., Zhou, Q., Wang, H., and Wang, Y. (2014). MicroRNA-29b promotes high-fat diet-stimulated endothelial permeability and apoptosis in apoE knock-out mice by down-regulating MT1 expression. *Int. J. Cardiol.* 176, 764–770. doi:10.1016/j.ijcard.2014.07.095

Glossary

AANAT arylalkylamine N-acetyltransferase

ADAMTS a disintegrin metalloproteinase with thrombospondin motifs

ADSCs adipose tissue-derived stem cells

BMSCs bone marrow mesenchymal stem cells

ceRNAs competing endogenous RNAs

CHON-001 human chondrocyte cell line

circRNAs circular RNAs

CPCs cartilage progenitor cells

DBI delayed brain injury

D-gal D-galactose

DR diabetic retinopathy

ECM extracellular matrix

FGF18 fibroblast growth factor18

hBMSCs human bone marrow mesenchymal stem cells

hMSCs human mesenchymal stem cells

HO-1 heme oxygenase 1

ICMS intermittent cyclic mechanical stress

IGF1R insulin-like growth factor 1 receptor

IL-6 interleukin 6

IVDD intervertebral disc degeneration

lncRNAs long non-coding RNAs

MALAT1 metastasis-associated lung adenocarcinoma transcript 1

MEG3 maternally expressed gene3

miRNAs microRNAs

MMP matrix metalloproteinase

MSC mesenchymal stem cells

ncRNAs non-coding RNAs

NF-κB nuclear factor kappa-B

NLRP3 nucleotide-binding domain and leucine-rich repeat containing PYD-3

NR1D1 nuclear receptor subfamily 1 group D member 1

NRF2 nuclear factor-erythroid 2-related factor 2

OA osteoarthritis

PCM pericellular matrix

PGC-1α PPARGC1A

p-SMAD 2/3 phosphorylated SMAD 2/3

RANKL Receptor Activator of Nuclear Factor-κ B Ligand

RNS reactive nitrogen species

ROS Reactive oxygen species

SAH subarachnoid hemorrhage

SIRT1 silent information regulator 1

TGF-β1 transforming growth factor-β

TNF-α tumor necrosis factor-α

WT wild-type

frontiers | Frontiers in Genetics

TYPE Review
PUBLISHED 11 October 2022
DOI 10.3389/fgene.2022.1013637

OPEN ACCESS

EDITED BY
Nadeem Shabir,
Sher-e-Kashmir University of Agricultural Sciences and Technology, India

REVIEWED BY
Suman Dutta,
University of California, Los Angeles, United States
Debalina Bhattacharya,
University Of Calcutta, India
Faizah Alotaibi,
King Saud bin Abdulaziz University for Health Sciences, Saudi Arabia

*CORRESPONDENCE
Juan Jin,
lang_018@163.com
Qiang He,
qianghe1973@126.com

†These authors have contributed equally to this work and share first authorship

SPECIALTY SECTION
This article was submitted to RNA, a section of the journal Frontiers in Genetics

RECEIVED 07 August 2022
ACCEPTED 27 September 2022
PUBLISHED 11 October 2022

CITATION
Luo C, Liu H, Shao L, Tang J, He Q and Jin J (2022), The role of small extracellular vesicle non-coding RNAs in kidney diseases.
Front. Genet. 13:1013637.
doi: 10.3389/fgene.2022.1013637

The role of small extracellular vesicle non-coding RNAs in kidney diseases

Chuxuan Luo[1,2†], Haojie Liu[1,3†], Lina Shao[1], Jiyu Tang[1,3], Qiang He[4*] and Juan Jin[1*]

[1]Urology & Nephrology Center, Department of Nephrology, Zhejiang Provincial People's Hospital (Affiliated People's Hospital, Hangzhou Medical College), Hangzhou, China, [2]Division of Health Sciences, Hangzhou Normal University, Hangzhou, China, [3]The 2nd Clinical Medical College, Zhejiang Chinese Medical University, Hangzhou, China, [4]Department of Nephrology, The First Affiliated Hospital of Zhejiang Chinese Medical University (Zhejiang Provincial Hospital of Traditional Chinese Medicine), Hangzhou, China

Kidney diseases have become an increasingly common public health concern worldwide. The discovery of specific biomarkers is of substantial clinical significance in kidney disease diagnosis, therapy and prognosis. The small extracellular vesicle (sEV) can be secreted by several cell types, like renal tubular epithelial cells, podocytes, collecting duct cells and leap cells, and functions as a communication medium between cells by delivering signaling molecules, including proteins, lipids and nucleic acids. There has been growing evidence that kidney diseases are associated with aberrant expression of sEV-derived non-coding RNAs (sEV-ncRNAs). As a result, sEV-ncRNAs may provide valuable information about kidney diseases. In this paper, a systematic review is presented of what has been done in recent years regarding sEV-ncRNAs in kidney disease diagnosis, treatment and prognosis.

KEYWORDS

biomarkers, diagnosis, kidney disease, non-coding RNAs, prognosis, small extracellular vesicles, therapeutics

1 Introduction

Kidney diseases are a category of complicated disorders with diverse and uncertain etiologies. The diagnosis of kidney disease is commonly delayed, and patients often miss the best opportunity for treatment owing to its insidious onset and lack of a specific clinical manifestation in early stage. Patients with chronic kidney disease (CKD) are inextricably faced with dialysis and kidney transplant surgery as they progress to end-stage renal disease (ESRD). It has been estimated that there were approximately 4.9-7 million patients with ESRD requiring renal replacement therapy worldwide (Lv and Zhang, 2019). The reported annual treatment costs for dialysis patients accounted for 10% of total healthcare expenditure in China, which imposed significant financial burden on individuals, families, healthcare systems and society (Zhang and Wang, 2009).

As of now, percutaneous renal biopsy (PRB) is the only method used to definitively diagnose kidney diseases. Bleeding risks caused by PRB range in severity from transient

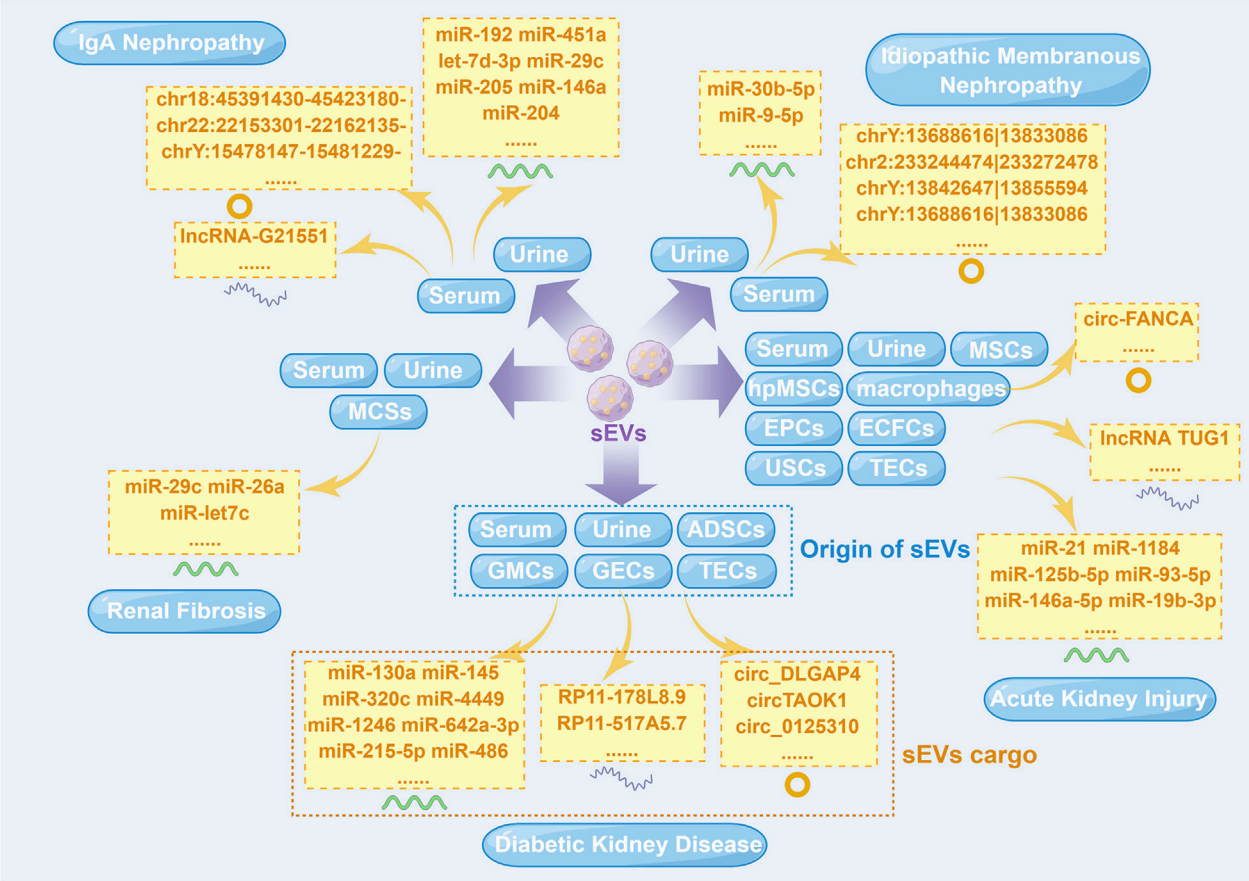

FIGURE 1
Small extracellular vesicle non-coding RNAs isolated from different cells in five major kidney diseases. ADSCs, adipose-derived stem cells; ECFCs, endothelial colony-forming cells; EPCs, endothelial progenitor cells; GECs, glomerular endothelial cells; GMCs, glomerular mesangial cells; hpMSCs, human placental mesenchymal stem cells; lncRNA, long non-coding RNA; miR, microRNA; MSCs, mesenchymal stem cells; sEVs, small extracellular vesicles; TECs, tubular epithelial cells; USCs, urine-derived stem cells. This figure was created by Figdraw (www.figdraw.com) (ID: YWWOI4c8de).

gross hematuria to fatal (Bakdash et al., 2019). Due to these reasons, this examination is not performed in most cases. In addition to blood analyses (serum creatinine, blood urea nitrogen and creatinine clearance), urinalyses (urine density, proteinuria, hematuria, cylindruria and 24-h urine protein) are the currently widely used diagnostic markers in the clinical practice. Nevertheless, further examination is still needed to help clarify the pathological diagnoses of kidney diseases. As such, it is of paramount importance to develop novel non-invasive diagnostic methods for discriminating pathological types.

The exosome is a nano-sized extracellular vesicle of spherical shape, which was first discovered during the maturation of sheep reticulocytes in 1983 (Pan and Johnstone, 1983) and named by Johnstone et al. (1987) in 1987. A mature exosome forms by inward budding of endosomal membrane and then is released into the extracellular environment along with the plasma membrane (Amini et al., 2021). Recently, it has been revealed that exosomes with high purity were difficult to isolate. Accordingly, the International Society for Extracellular Vesicle recommended referring to vesicle with a diameter less than 200 nm as small extracellular vesicle (sEV) (Théry et al., 2018). Nearly all kidney inherent cells release sEVs, including renal tubular epithelial cells, podocytes, collecting duct cells and leap cells (Miranda et al., 2010). Moreover, they can be found in multiple body fluids, such as blood, urine, saliva, cerebrospinal fluid and milk (van Niel et al., 2018). There have been various molecular components found in sEVs, such as proteins, lipids and nucleic acids, which are protected from external environment by the lipid bilayer membrane structures of sEVs (Kim et al., 2017; Jeppesen et al., 2019). These molecules vary greatly with the pathophysiological conditions of parent cells (Pegtel and Gould, 2019). Accumulating evidence has revealed that sEVs were rich in non-coding RNAs (ncRNAs), like microRNAs (miRNAs), long non-coding RNAs (lncRNAs)

TABLE 1 The role of small extracellular vesicle non-coding RNAs in diabetic kidney disease.

Origin of sEVs	sEVs cargo	Pathway	ncRNA expression	Mechanism	References
urine samples GMCs	miR-145	N/A	high	represent a novel candidate diagnostic biomarker for diabetic kidney disease	Barutta et al. (2013)
urine samples	miR-320c	TGF-β signaling pathway	high	represent a novel candidate diagnostic biomarker for diabetic kidney disease	Delić et al. (2016)
ADSCs	miR-215-5p	ZEB2	high	protect against high glucose-induced metastasis	Jin et al. (2020)
ADSCs	miR-486	Smad1/mTOR signaling pathway	high	lead to the increase of autophagy and the reduction of podocyte apoptosis	Jin et al. (2019)
serum samples	miR-1246	MAPK signaling pathway	high	represent a novel candidate diagnostic biomarker for diabetic kidney disease	Kim et al. (2019)
	miR-642a-3p				
	let-7c-5p				
	miR-1255b-5p				
	let-7i-3p				
	miR-5010-5p				
	miR-150-3p				
	miR-4449				
urine samples	miR-21-5p	N/A	high		
	miR-30b-5p		low	represent a novel candidate diagnostic biomarker for diabetic kidney disease	Zang et al. (2019)
TECs	miR-6724-5p	N/A	high	represent a novel candidate diagnostic biomarker for diabetic kidney disease	Zhou et al. (2021)
	miR-6716-3p				
	miR-2355-3p				
	miR-135b-3p				
	miR-3180				
	miR-5008-3p		low		
	miR-6785-5p				
	miR-3654				
	miR-335-3p				
	RP11-178L8.9		high		
	CTD-2530H12.2				
	RP11-503N18.4				
	RP11-20B24.7				
	RP11-256I23.1				
	RP11-517A5.7		low		
	RN7SL870P				
	CTD-2298J14.2				
	ANKRD10-IT1				
	AP000442.1		low		
	circRNA_164				
	circRNA_225				
	circRNA_57				
GMCs	circ_DLGAP4	miR-143/ERBB3/NF-κB/MMP2 axis	high	promote proliferation and fibrosis of GMCs	Bai et al. (2020)
GECs	circTAOK1	miR-520h/Smad3 axis	high	promote proliferation, fibrosis, and EMT of GMCs	Li et al. (2022a)
GMCs	circ_0125,310	miR-422a/IGF1R/p38 axis	high	promote proliferation and fibrosis of GMCs	Zhu et al. (2022)

ADSCs, adipose-derived stem cells; circRNA, circular RNA; EMT, epithelial-mesenchymal transition; ERBB3, Erb-b2, receptor tyrosine kinase 3; GECs, glomerular endothelial cells; GMCs, glomerular mesangial cells; IGF1R, insulin-like growth factor 1 receptor; MAPK, mitogen-activated protein kinase; miR, microRNA; MMP2, matrix metalloproteinase 2; mTOR, mechanistic target of rapamycin; N/A, not available; ncRNA, non-coding RNA; NF-κB, nuclear factor-κB; sEVs, small extracellular vesicles; Smad1, SMAD, family member 1; Smad3, SMAD, family member 3; TECs, tubular epithelial cells; TGF-β, transforming growth factor-β; ZEB2, zinc finger E-box-binding homeobox 2.

and circular RNAs (circRNAs), which are involved in various disease pathophysiology (Liu et al., 2019; Ren and Wang, 2021).

In the last few years, a number of previous studies have demonstrated a close relationship between sEV-derived ncRNAs (sEV-ncRNAs) and kidney diseases, providing innovative insights for their diagnosis and treatment (Ichii and Horino, 2018). Different sEV-ncRNAs have different mechanisms in kidney diseases (Figure 1). This review is primarily concerned with providing an overview of sEV-ncRNAs and their potential use in five major kidney disease, including diabetic kidney disease (DKD), acute kidney injury (AKI), IgA nephropathy (IgAN), idiopathic membranous nephropathy (IMN) and renal fibrosis.

2 Roles of sEV-ncRNAs in DKD

There are several microvascular complications associated with diabetes, but the most prevalent and serious is DKD, which has become a major cause of ESRD (Alicic et al., 2017). Although PRB remains the gold standard diagnostic criteria for DKD at the present time, there is a certain amount of controversy regarding its indications in clinical practice. Accordingly, the diagnosis of DKD is made on clinical presentation in the majority of the cases. But the clinical diagnosis of DKD is challenging in clinical use and a misdiagnosis rate has been reported to be as high as 49.2% in a recent meta-analysis (Fiorentino et al., 2017). For this reason, the need for early detection and intervention of DKD becomes an imperative issue. Increasing number of studies revealed that sEV-ncRNAs contributed to the progression of DKD, even serving as biomarkers for diagnostics and therapeutic purposes (Table 1).

2.1 Roles of sEV-miRNAs in DKD

The latest research suggested the diagnostic value of aberrant expression of sEV-derived miRNAs (sEV-miRNAs) in DKD. According to Barutta et al. (2013), the expression of urinary sEV-derived miR-130a as well as miR-145 was markedly elevated in type 1 diabetic mellitus (T1DM) patients with microalbuminuria than health donors and those without microalbuminuria. Researchers further verified their results by cell-based and animal experiments. miR-145 expression was more than nine-fold higher in diabetic mice's glomerulus and two-fold higher in their urine sEVs as compared to healthy mice. Similarly, high glucose conditions increase the expression of miR-145 in glomerular mesangial cells (GMCs). These results suggested the diagnostic value of miR-145 applied in DKD early diagnosis. Another study from Delić et al. (2016) has revealed that fourteen upregulated urinary sEV-miRNAs (miR-320c, miR-6068, miR-1234-5p, miR-6133, miR-4270, miR-4739, miR-371b-5p, miR-638, miR-572, miR-1227-5p, miR-6126, miR-1915-5p, miR-4778-5p and miR-2861) and two downregulated urinary sEV-miRNAs (miR-30d-5p and miR-30e-5p) were significantly differentially expressed in DKD patients as compared to health donors and type 2 diabetes mellitus (T2DM) patients. Among these miRNAs, miR-320c, the most strongly upregulated miRNA in urine sEVs from DKD patients, may be involved in the development of DKD through transforming growth factor-β (TGF-β) signaling pathway. Considering the above study results, miR-320c appeared to represent an intriguing candidate marker for the diagnosis of DKD, which needed to be further investigated. As well, Kim et al. (2019) analyzed sEV-miRNAs derived from serum samples of healthy donors as well as diabetics with and without nephropathy. They observed a significant upregulation of seven sEV-miRNAs (miR-1246, miR-642a-3p, let-7c-5p, miR-1255b-5p, let-7i-3p, miR-5010-5p and miR-150-3p) in DKD patients compared to health donors and a dramatic upregulation of miR-4449 in DKD patients in comparison with patients who do not have DKD. It was determined that the above-mentioned miRNAs play a role in mitogen-activated protein kinase (MAPK) signaling, integrin function in angiogenesis, and activator protein 1 (AP-1) transcription factor regulation. The authors thus concluded that these miRNAs are expected to be targets for DKD diagnosis. Beyond these, Zang et al. (2019) found that urinary sEV-derived miR-21-5p was upregulated and miR-30b-5p was downregulated in DKD individuals compared to controls, pointing out possible functions of these miRNAs as diagnostic biomarkers for DKD.

Furthermore, miRNA-containing sEVs may be effective in the therapy of DKD. In our laboratory, sEVs from adipose-derived stem cells (ADSCs) were demonstrated to be a mediator of miR-215-5p uptake by podocytes, thus preventing glucose-induced metastasis, possibly by inhibiting of zinc finger E-box-binding homeobox 2 (ZEB2) transcription (Jin et al., 2020). Another study from our research group found that sEVs derived from ADSCs improved the DKD patients' symptoms through inhibiting SMAD family member 1 (Smad1)/mechanistic target of rapamycin (mTOR) signaling pathway by enhancing miR-486 expression in podocytes (Jin et al., 2019). These finding illustrated that sEV derived from ADSCs was a potential therapeutic strategy for DKD.

2.2 Roles of sEV-lncRNAs in DKD

At present, the study toward the role of sEV-derived lncRNAs (sEV-lncRNAs) in early diagnosis of DKD has only just begun to make headway. According to Zhou et al. (2021), lncRNAs were expressed differently in sEVs from human renal tubular epithelial cells (TECs) that were treated or not with high glucose. There were a total of 169 lncRNAs differentially expressed in sEVs, of which 93 were upregulated and 76 were downregulated. Among these, the top five upregulated lncRNAs

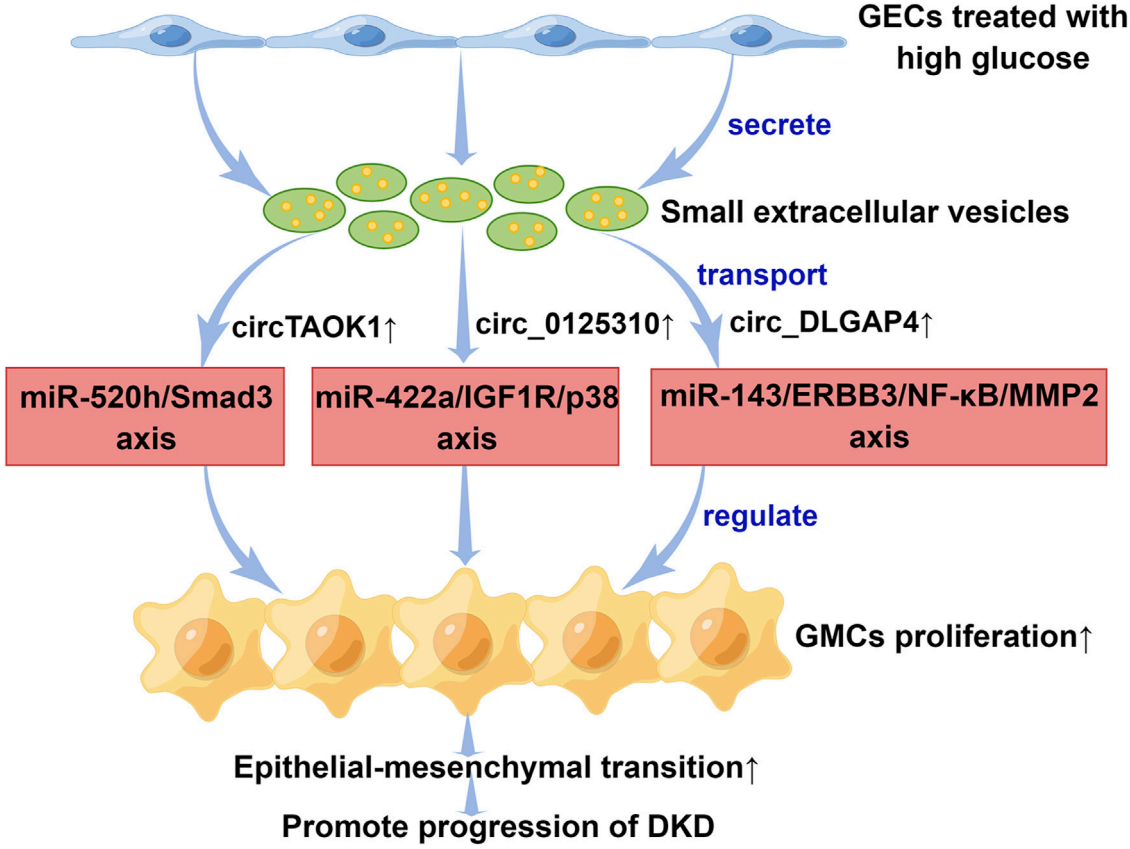

FIGURE 2
The mechanisms of small extracellular vesicle circular RNAs in the progression of diabetic kidney disease. Small extracellular vesicles secreted by GECs promoted epithelial interstitial transition process in diabetic kidney disease through transporting different circular RNAs. DKD, diabetic kidney disease; ERBB3, Erb-b2 receptor tyrosine kinase 3; GECs, glomerular endothelial cells; GMCs, glomerular mesangial cells; IGF1R, insulin-like growth factor 1 receptor; miR, microRNA; MMP2, matrix metalloproteinase 2; NF-κB, nuclear factor-κB; Smad3, SMAD family member 3. This figure was created by Figdraw (www.figdraw.com) (ID: PWOUSd94f7).

were RP11-178L8.9, CTD-2530H12.2, RP11-503N18.4, RP11-20B24.7 and RP11-256I23.1, while the top five downregulated lncRNAs were RP11-517A5.7, RN7SL870P, CTD-2298J14.2, ANKRD10-IT1 and AP000442.1, respectively. Afterward, investigators further performed Kyoto Encyclopedia of Genes and Genomes (KEGG) enrichment analyses to investigate potential functions of sEV-lncRNAs with differential expression. It was found that lncRNAs were involved in such pathways as T2DM. Preliminary results from this study demonstrated that the aforementioned sEV-lncRNAs might contribute to the progression of DKD, and may also be served as biomarkers in this disease.

2.3 Roles of sEV-circRNAs in DKD

circRNAs are a special class of ncRNAs and one of the current research hotspots of scholars in various countries. There has been an increase in the number of studies that focus on sEV-derived circRNAs (sEV-circRNAs) in DKD pathophysiology over the past few years (Figure 2). Interestingly, the study of Li et al. (2022) indicated that when high glucose is applied to glomerular endothelial cells (GECs), the expression of circTAOK1 (also known as circ_0003928) is upregulated. Mechanically, circTAOK1 was identified to accelerate GMCs proliferation and epithelial interstitial transition (EMT) *via* targeting the miR-520h/SMAD family member 3 (Smad3) axis. In addition, high expression of circ_0125310 have been found in sEVs from high glucose-induced GMCs in a study by Zhu et al. (2022). They revealed that circ_0125310 could promote GMCs proliferation and fibrosis in DKD through sponging miR-422a and activating the insulin-like growth factor 1 receptor (IGF1R)/p38 pathway. Bai et al. (2020) demonstrated that circ_DLGAP4 was significantly upregulated in sEVs from high glucose-treated GMCs, which led to an increase in the

TABLE 2 The role of small extracellular vesicle non-coding RNAs in acute kidney injury.

Origin of sEVs	sEVs cargo	Pathway	ncRNA expression	Mechanism	References
MSCs	miR-125b-5p	p53	high	promote tubular repair	Cao et al. (2021)
serum samples	miR-181a-5p and miR-23b-3p	N/A	high	represent a novel candidate diagnostic biomarker for acute kidney injury	Da-Silva et al. (2022)
serum samples	miR-500a-3p	MLKL	high	suppress cell injury and inflammation	Jiang et al. (2019)
USCs	miR-146a-5p	IRAK1	high	protect TECs from H/R injury	Li et al. (2020)
TECs	miR-19b-3p	NF-κB/SOCS-1	high	promote M1 macrophage activation	Lv et al. (2020)
ECFCs	miR-486-5p	PTEN/Akt signaling pathway	high	reduce ischemic kidney injury	Viñas et al. (2016)
TECs	miR-20a-5p	N/A	high	inhibit mitochondrial injury and apoptosis of TECs	Yu et al. (2020)
urine samples	miR-21	N/A	high	have good accuracy in the diagnosis of diabetic kidney disease	Yun et al. (2021)
MSCs	miR-1184	FOXO4, p27 Kip1 and CDK2	high	induce G1 phase arrest in TECs	Zhang et al. (2021a)
hPMSCs	miR-93-5p	N/A	high	protect from progression of I/R	Zhang et al. (2022a)
EPCs	miR-21-5p	RUNX1	high	improve renal function and renal tissue pathological damage, attenuate serum inflammatory response, as well as reduce apoptosis and oxidative stress response in renal tissues, and regulate endothelial glycocalyx damage marker proteins syndecan-1 and heparanase-1	Zhang et al. (2021b)
macrophages	miR-155	NF-κB/SOCS-1	high	mediate the communication between activated macrophages and injured tubules	Zhang et al. (2022b)
USCs	lncRNA TUG1	SRSF1	high	regulate ASCL4-mediated ferroptosis	Sun et al. (2022)
TECs	circ-FANCA	miR-93-5p/ OXSR1 axis	high	alleviate LPS-induced HK2 cell injury	Li et al. (2021)

ASCL4, acyl-CoA, synthetase long-chain family member 4; CDK2, cyclin dependent kinase 2; ECFCs, endothelial colony-forming cells; EPCs, endothelial progenitor cells; FOXO4, forkhead box O4; hPMSCs, human placental MSCs; H/R, hypoxia-reoxygenation; I/R, ischemia-reperfusion; IRAK1, interleukin-1, receptor-associated kinase 1; lncRNA, long non-coding RNA; LPS, lipopolysaccharide; miR, microRNA; MLKL, mixed lineage kinase domain-like; MSCs, mesenchymal stem cells; N/A, not available; ncRNA, non-coding RNA; NF-κB, nuclear factor-κB; OXSR1, oxidative stress responsive 1; PTEN, phosphatase and tensin homolog; RUNX1, runt-related transcription factor 1; sEVs, small extracellular vesicle; SOCS-1, suppressor of cytokine signaling 1; SRSF1, serine/arginine splicing factor 1; TECs, tubular epithelial cells; USCs, urine-derived stem cells.

progression of DKD by modulating miR-143/Erb-b2 receptor tyrosine kinase 3 (ERBB3)/nuclear factor-κB (NF-κB)/matrix metalloproteinase 2 (MMP2). Hopefully, these results will help scientists gain a better understanding of DKD pathogenesis.

3 Roles of sEV-ncRNAs in AKI

Clinically, AKI is the result of a brief duration of prerenal, renal, or postrenal injury, which is closely associated with poor prognosis of hospitalized patients (Liangos et al., 2006). It is currently diagnosed primarily by serum creatinine and urinary output, according to the Kidney Disease Improving Global Outcomes clinical practice guideline (Khwaja, 2012). However, several investigators have argued that the diagnosis of AKI made by measuring serum creatinine levels was problematic since serum creatinine levels tend to rise after renal function declines and do not indicate injury (Slocum et al., 2012). Consequently, the search for sensitive, reliable and early biomarkers represent urgent topics to be explored in the future. sEV-ncRNAs have been reported to participate in the development of AKI and could be served as specific biomarkers for AKI (Table 2).

3.1 Roles of sEV-miRNAs in AKI

sEV-miRNA can be isolated from most body fluids and is one of the research hot spots in the field of AKI diagnosis, with a promising future in liquid biopsy. As one of the most studied miRNAs, urinary sEV-derived miR-21 levels were increasingly recognized as diagnostic predictors of AKI. The analysis of urinary sEV-miRNA expression in 25 scrub typhus patients with and without AKI was performed by Yun et al. (2021), and revealed significantly higher expression levels of miR-21 in the AKI patients compared to controls. In a receiver operating characteristic (ROC) curve analysis, urinary sEV-derived miR-21 was demonstrated to have good discriminative power for the diagnosis of scrub typhus-associated AKI, with an area under the curve (AUC) of 0.908, suggesting good diagnostic potential. Moreover, the expressions of serum sEV-derived miR-181a-5p and miR-23b-3p were found to be increased in

lipopolysaccharide (LPS)-induced AKI mouse models (Da-Silva et al., 2022). It has been shown by bioinformatics analysis that both miRNAs target transcription factors that regulate genes expressing proinflammatory cytokines. These findings yield great promise for a future of precision medicine as sEV-miRNAs might be used clinically to identify patients with AKI early.

For now, numerous important advances regarding the therapeutic potential of sEV-miRNAs in AKI have been reported. As an example of this, Cao et al. (2021) confirmed that sEV-miR-125b-5p from mesenchymal stem cells (MSCs) could stimulate tubular repair by suppressing p53 in AKI. Similarly, our laboratory discovered that sEV-miR-1184 from MSCs can mitigate cisplatin-associated AKI (Zhang et al., 2021). Additionally, sEVs from three-dimensional (3D) cultures of human placental MSCs (hPMSCs) have been reported to be effective for the treatment of AKI (Zhang et al., 2022). A significant change in miR-93-5p was found in sEVs obtained from hPMSCs cultured in 3D. Hence, it is easily conceivable that sEVs from 3D culture of hPMSCs might exert therapeutic effects through miR-93-5p modulation, but its specific molecular mechanism remains unknown currently. Moreover, Zhang et al. (2021) discovered that miR-21-5p-containing sEVs derived from endothelial progenitor cells (EPCs) were able to alleviate sepsis-induced AKI by silencing runt-related transcription factor 1 (RUNX1). Urine-derived stem cells (USCs) have also been shown to perform a protective effect on ischemic/reperfusion injury (IRI)-induced AKI *via* sEV-derived miR-146a-5p targeting interleukin-1 receptor-associated kinase 1 (IRAK1) in a recent study (Li et al., 2020). Apart from these, miR-486-5p-enriched sEVs from endothelial colony-forming cells (ECFCs) (Viñas et al., 2016), miR-500a-3p-enriched sEVs from serum samples (Jiang et al., 2019), as well as miR-20a-5p-enriched sEVs from TECs (Yu et al., 2020) have all been considered the promising therapies for AKI.

In addition, several sEV-miRNA association studies have offered new insights into the pathogenesis of AKI. Lv et al. (2020) have originally found that sEV-miR-19b-3p derived from TECs facilitated M2 macrophage activation *via* targeting the NF-κB/suppressor of cytokine signaling 1 (SOCS-1) in LPS-induced AKI. Another study in China discovered that sEV-derived miR-155 promoted the progression of AKI by mediating communication between activated macrophages and damaged tubules. The results of all of these studies have contributed to our understanding of AKI's pathophysiology (Zhang et al., 2022).

3.2 Roles of sEV-lncRNAs in AKI

Recently, there is preliminary evidence of a positive therapeutic effect of sEV-lncRNAs in patients with AKI. The latest discovery from Sun et al. (2022) has revealed that IRI-induced AKI was attenuated by lncRNA TUG1 derived from USCs that inhibited acyl-CoA synthetase long-chain family member 4 (ASCL4)-mediated ferroptosis through interaction with serine/arginine splicing factor 1 (SRSF1). Hence, lncRNA TUG1 might represent an ideal target for developing a AKI therapeutic.

3.3 Roles of sEV-circRNAs in AKI

sEV-circRNAs have been found associated with the pathogenesis of AKI. It is known that those suffering from septic shock are more likely to experience AKI in the intensive care unit. LPS-induced sepsis is the leading cause of AKI in critically ill patients (Netti et al., 2019). It was discovered that sepsis-induced AKI was characterized by a high expression of circ-FANCA, which was generated by precursor mRNA FANCA (Kölling et al., 2018). As yet, it remains unclear how circ-FANCA contributes to the pathogenesis of sepsis-induced AKI. In recent years, investigators found that sEV-derived circ-FANCA was able to directly interact with miR-93-5p and regulate oxidative stress responsive 1 (OXSR1) expression, thus modulating LPS-induced TECs injury (Li et al., 2021). The results provided a potential therapeutic target for septic AKI.

4 Roles of sEV-ncRNAs in IgAN

IgAN currently represents the most prevalent form of primary glomerulonephritis worldwide with IgA deposition within the glomerular mesangium (Lai et al., 2016). IgAN may occur in any age group but typically between age 16 and 35, which has been reported to be one of the leading causes of ESRD in young adults (Huang and Xu, 2021). Although histological confirmation is still necessary for the diagnosis of IgAN, this approach has a limited indication for clinical application till now. Regrettably, no specified laboratory markers for identifying IgAN are available up to now. In the following, we have summarized the latest advances in the emerging role of sEV-ncRNAs in kidney diseases (Table 3).

4.1 Roles of sEV-miRNAs in IgAN

sEV-miRNAs have shown diagnostic potential in early diagnosis of IgAN in various studies. Min et al. (2018) found that the urinary sEVs of IgAN patients expressed significantly lower levels of miR-29c and miR-205 than did those of healthy controls, while miR-146a was significantly higher. In a study by Pawluczyk et al. (2021), the miR-204 expression was significantly decreased in urine sEVs from the patients with IgAN compared to healthy controls. Li et al. (2022) discovered that there existed significant differences in the expression of miR-451a and let-7d-3p in urine sEVs between IgAN patients and healthy individuals. To assess the diagnostic performance of these miRNAs,

TABLE 3 The role of small extracellular vesicle non-coding RNAs in IgA nephropathy.

Origin of sEVs	sEVs cargo	Pathway	ncRNA expression	Mechanism	References
serum samples	miR-192	N/A	low	accelerate decline in renal function	Fan et al. (2019)
urine samples	miR-451a	N/A	high	regulation of mRNA stability, extracellular exosome and transferase activity	Li et al. (2022b)
urine samples	miR-29c	N/A	low		
	miR-205				Min et al. (2018)
	miR-146a		high		
urine samples	miR-204	N/A	low	N/A	Pawluczyk et al. (2021)
serum samples	lncRNA-G21551	N/A	low	N/A	Guo et al. (2020)
urine samples	chr18:45391430-45423180-	PI3K/Akt signaling pathway	high	regulate primary miRNA processing, the ability of angiotensin receptor binding, and stress fibre function	Luan et al. (2021)
	chr22:22153301-22162135-				
	chr1:243708812-243736350-				
	chr19:42740758-42744294-				
	chr17:11984673-12016677+				
	chr18:11862394-11876687+				
	chr17:8409636-8413,267-				
urine samples	chrY:15478147-15481229-	N/A	high	alter the expression of the coding gene UTY protein	Luan et al. (2022)

LncRNA, long non-coding RNA; mRNA, messenger RNA; miR/miRNA, microRNA; N/A, not available; ncRNA, non-coding RNA; PI3K, phosphoinositide-3-kinase-protein kinase B; sEVs, small extracellular vesicles.

researchers further carried out ROC curve analysis and concluded that miR-451a and let-7d-3p can be served as biomarkers for early diagnosis of IgAN. These results revealed that specific sEV-miRNAs may be used as non-invasive biomarkers for the detection of IgAN. Despite these very promising results, validation in large sample cohorts is still pending.

sEV-miRNAs are related not only to the early diagnosis but also to the prognosis of IgAN. A study comprising 50 IgAN patients and 25 healthy control individuals indicated that the higher the expression level of serum miR-192 was, the less likely the patient is to have renal function decline within 2 years (Fan et al., 2019). This observation illustrated that miR-192 possessed great potential to become a prognostic biomarker in IgAN.

4.2 Roles of sEV-lncRNAs in IgAN

There have been relatively few studies on the potential role of sEV-lncRNAs in IgAN diagnosis. A recent study found that among IgAN patients, serum sEV-derived lncRNA-G21551, with the closest protein coding gene, was markedly downregulated, suggesting its promising diagnostic value (Guo et al., 2020).

4.3 Roles of sEV-circRNAs in IgAN

The study regarding sEV-circRNAs involvement in the diagnosis of IgAN is only just emerging from its infancy. Luan et al. (2021) have showed a total of seven urinary sEV-circRNAs (circRNAchr18:45391430-45423180-, circRNAchr22:22153301-22162135-, circRNAchr1:243708812-243736350-, circRNAchr19:42740758-42744294-, circRNAchr17:11984673-12016677+, circRNAchr18:11862394-11876687+ and circRNAchr17:8409636-8413,267-) were significantly upregulated in IgAN patients. Gene ontology (GO) analysis demonstrated that the above-mentioned sEV-circRNAs may be involved in primary miRNA processing, the ability of angiotensin receptor binding, and stress fiber function. According to KEGG analysis, these sEV-circRNAs are likely closely related to the phosphoinositide-3-kinase-protein kinase B (PI3K)/Akt signaling

TABLE 4 The role of small extracellular vesicle non-coding RNAs in idiopathic membranous nephropathy.

Origin of sEVs	sEVs cargo	Pathway	ncRNA expression	Mechanism	References
urine samples	miR-30b-5p	MAPK signaling pathway	low	N/A	Guo et al. (2022)
	miR-9-5p				
serum samples	chrY:13688616|13833086	platelet activation signaling pathway	high	N/A	Ma et al. (2019)
	chr2:233244474|233272478				
urine samples	chrY:13842647|13855594	P13K/Akt signaling pathway	high		
	chrY:13688616|13833086		low		

MAPK, mitogen-activated protein kinase; miR, microRNA; N/A, not available; ncRNA, non-coding RNA; PI3K, phosphoinositide-3-kinase-protein kinase B; sEVs, small extracellular vesicles.

pathway. Another study from the same research group found that the expression of urinary sEV-circRNA chrY:15478147-15481229-derived from sex chromosomes was remarkably upregulated in male patients with IgAN (Luan et al., 2022). Thus, the authors concluded that these sEV-circRNAs holds promise as novel biomarkers in the early diagnosis of IgAN.

5 Roles of sEV-ncRNAs in IMN

Idiopathic membranous nephropathy (IMN) is one of the principal causes of primary nephrotic syndrome in adults, which is characterized by the accumulation of immune complexes between podocytes and the basement membranes of the glomerulus. Nowadays, the diagnosis of IMN is made based on pathologic confirmation. A specific biomarker for accurate diagnosis of IMN is still lacking. Herein, we have provided a brief summary of latest research on sEV-ncRNAs in IMN (Table 4).

5.1 Roles of sEV-miRNAs in IMN

Presently, only a few scholars are exploring the diagnostic value of sEV-miRNAs in IMN. Guo et al. (2022) investigated the expression profile of urinary sEV-miRNA in IMN patients and found that miR-30b-5p and miR-9-5p were markedly downregulated in patients with IMN as compared to healthy controls. In their study, the potential diagnostic value for IMN of miR-30b-5p and miR-9-5p was also demonstrated by the authors through ROC curve analysis.

5.2 Roles of sEV-circRNAs in IMN

Only a few studies exist assessing the diagnostic potential of sEV-circRNAs on IMN. In the study by Ma et al. (2019), the comparison of serum sEV-circRNAs between IMN patients and healthy controls found 89 differentially expressed sEV-circRNAs, 49 of which were upregulated and 40 of which were downregulated. In detail, chrY:13688616|13833086 was the most prominent upregulated circRNA, while chr2:233244474|233272478 was the most prominent downregulated circRNA. In addition to serum sEV-circRNAs, the authors found 60 urinary sEV-circRNAs with significantly differentially expression, of which 54 expressions were upregulated and 6 expressions were downregulated. Among these, chrY:13842647|13855594 was the most prominent upregulated circRNA, while chrY:13688616|13833086 was the most prominent downregulated circRNA. As discussed above, sEV-circRNAs may be useful diagnostic biomarkers for kidney disease.

6 Roles of sEV-miRNAs in Renal fibrosis

Renal fibrosis is an unavoidable progressive component of virtually all forms of chronic kidney diseases, culminating in renal failure. sEV-miRNAs were considered to correlate with renal fibrosis (Abbasian et al., 2018) (Table 5).

Renal fibrosis is primarily caused by EMT. miR-29c was found to participate in the process mentioned above, and therefore, it was proposed to support an early diagnosis of renal fibrosis. For instance, Lv et al. (2013) found that urine sEV-derived miR-29a and miR-29c levels were significantly lower in moderate-to-severe renal fibrosis patients than mild ones. Both the aforementioned miRNAs were of predictive value in the assessment of degree of renal fibrosis, with an AUC of 0.883 and 0.738. In addition, further analysis revealed that miR-29c is significantly correlated with fibrosis severity. Similar to these earlier findings, another study demonstrated that a considerable decrease in urine miR-29c was measured in patients with renal fibrosis when compared with controls (Chun-Yan et al., 2018). Moreover, AUC of miR-29c in diagnosis of renal fibrosis was 0.862. These findings gave credence to the notion that miR-29c had the potential to be introduced as a new diagnostic marker in the future.

TABLE 5 The role of small extracellular vesicle non-coding RNAs in renal fibrosis.

Origin of sEVs	sEVs cargo	Pathway	ncRNA expression	Mechanism	References
urine samples	miR-29c	N/A	low	have good accuracy in the diagnosis of renal fibrosis	Chun-Yan et al. (2018)
urine samples	miR-29c	N/A	low	have good accuracy in the diagnosis of renal fibrosis	Lv et al. (2013)
MSCs	miR-let7c	TGF-βR1	high	attenuate renal fibrosis	Wang et al. (2016)
serum samples	miR-26a	CTGF	high	attenuate UUO-induced renal fibrosis	Zhang et al. (2019)

CTGF, connective tissue growth factor; miR, microRNA; MSCs, mesenchymal stem cells; N/A, not available; ncRNA, non-coding RNA; sEVs, small extracellular vesicles; TGF-βR1, transforming growth factor-β type 1 receptor; UUO, unilateral ureteral obstruction.

The significant role that sEVs play in kidney diseases has prompted researchers to explore them as promising therapeutics. The mouse unilateral ureteral obstruction (UUO) model has been extensively utilized in studies of renal fibrosis, since it offers obvious advantages of rapid renal fibrosis development by induction (Wu et al., 2017). Zhang et al. (2019) demonstrated in the mouse UUO model that serum miR-26a combated renal fibrosis by inhibiting connective tissue growth factor (CTGF). Moreover, Wang et al. (2016) observed that miR-let7c was transported to damaged kidney cells *via* sEVs from MSCs, thus slowing renal fibrosis progression.

7 Discussion

CKD is one of the most frequent chronic disease worldwide, which is characterized by its high prevalence and low awareness (Zhang et al., 2012; Al Rahbi and Al Salmi, 2020). Once CKD progresses to ESRD, patients tend to have a dismal prognosis. As such, developing an *in vitro* testing technique at the same time possessing high sensitivity and high specificity are fundamentally important to achieving early detection, intervention, as well as good prognosis for the patients with kidney diseases. A convincing number of studies have confirmed that sEV-ncRNAs participate in the regulation of numerous cellular functions and play an essential role in the development of kidney disorders during the recent years. Also, using serum and urine samples to diagnose kidney diseases has the advantage of easy access, as well as being non-invasive, and reproducible, which are beneficial for achieving ambulatory monitoring of disease progression. As a result, liquid biopsies based on sEVs have begun to show its great benefits and application prospects in diagnosing kidney disorders.

The present review provide a thorough summary of the role of sEV-ncRNAs (including miRNAs, lncRNAs and circRNAs) in kidney disorders. Currently, the study addressing the relationship between sEV-ncRNAs and kidney disorders focuses mainly on the following four aspects. Firstly, a significant difference exists between healthy people and patients with kidney disease regarding the composition and contents of sEV-ncRNAs (Bai et al., 2020; Ling et al., 2019). Thus, we speculate that sEV-ncRNAs contribute to the initiation and development of kidney diseases, although the precise mechanism remains to be determined. Secondly, sEV-ncRNAs have shown an exceptional value for diagnosing kidney diseases (Li et al., 2022; Guo et al., 2022). At present, the global research efforts primarily focus on exploring the possibility of using sEV-ncRNAs as diagnostic tools for kidney diseases. However, it still requires considerably more work to make sEV-ncRNA a rountine diagnostic method in clinical practice. Thirdly, the therapeutic potential of sEV-ncRNAs in treating kidney diseases is relatively understudied (Jin et al., 2019). More work is required to determine how can they be used in the field of kidney disease therapy in the future. Fourthly, although there is a growing number of studies demonstrating the potential for sEV-ncRNAs to serve as prognostic biomarkers in patients with kidney disorders, the total amount of relevant research remains limited (Fan et al., 2019).

Despite tremendous advances in our understanding of the role of sEV-ncRNAs in kidney diseases in recent decades, the research in this regard is still in its nascent stage with many areas that can be improved upon. Firstly, since sEV-ncRNAs have been studied primarily in the above commonly prevalent kidney diseases, there is a need to examine their role in other kidney diseases before a consensus about their role in the progression of kidney diseases can be reached. Secondly, there was at least one methodological flaw in most of the studies reviewed, primarily that their sample sizes were too small, which may influence the reliability of the outcomes. Thus, it will be necessary to confirm these preliminary results with large-scale and well-designed studies. Thirdly, there has been an increase in research exploring how sEV-miRNAs contribute to kidney diseases over the past few years. Contrary to this, studies examining sEV-lncRNAs or sEV-circRNAs in kidney disorders are relatively rare, which offers a possible entry point for future research. Last but not least, in spite of promising early evidence, sEV-ncRNAs still suffer from several major difficulties in terms of clinical application. On the one hand, owing to the limited quantities of genetic material in the

sEVs, how to make the best use of sEV-ncRNAs become an urgent problem that needs to be solved. On the other hand, it is still unclear how molecules are synthesized and packaged into sEVs, so further, more elaborate research is needed.

8 Conclusion

In summary, sEV-ncRNAs play fundamental roles in the early detection, treatment and prognosis of kidney disease. With the gradual maturity of experimental techniques, sEV-ncRNAs have become one of the most potential candidate diagnostic and prognostic biomarkers and therapeutic targets of kidney diseases. This review merely scratches the tip of the iceberg referring to sEV-ncRNAs in kidney diseases. Several have yet to be explored, while others deserve further investigation. Intensive investigation of sEV-ncRNAs could lend insights into the biological functions and regulatory mechanisms of sEVs, and hopefully reveal new interactive molecules and signaling pathways, providing new insight into the diagnostic and therapeutic approaches to kidney disease.

Author contributions

CL and HL contributed to writing the manuscript. CL contributed to designing the figures. LS and JT contributed to supervising the manuscript. QH and JJ contributed to reviewing the final manuscript.

Funding

This research was supported by the Huadong Medicine Joint Funds of the Zhejiang Provincial Natural Science Foundation of China (Grant No. LHDMZ22H050001), the Zhejiang Province Chinese Medicine Modernization Program (Grant No. 2020ZX001), the Key Project of Scientific Research Foundation of Chinese Medicine (Grant No. 2022ZZ002), the "Pioneer" and "Leading Goose" R&D Program of Zhejiang (Grant No. 2022C03118) and the Key project of Basic Scientific Research Operating Funds of Hangzhou Medical College (Grant No. KYZD202002).

Conflict of interest

The authors declare that the research was conducted in the absence of any commercial or financial relationships that could be construed as a potential conflict of interest.

Publisher's note

All claims expressed in this article are solely those of the authors and do not necessarily represent those of their affiliated organizations, or those of the publisher, the editors and the reviewers. Any product that may be evaluated in this article, or claim that may be made by its manufacturer, is not guaranteed or endorsed by the publisher.

References

Abbasian, N., Herbert, K. E., Pawluczyk, I., Burton, J. O., and Bevington, A. (2018). Vesicles bearing gifts: The functional importance of micro-RNA transfer in extracellular vesicles in chronic kidney disease. *Am. J. Physiol. Ren. Physiol.* 315, F1430–F1443. doi:10.1152/ajprenal.00318.2018

Al Rahbi, F., and Al Salmi, I. (2020). Awareness, knowledge, and perception of chronic kidney disease patients at renal medicine outpatients' clinic. *Saudi J. Kidney Dis. Transpl.* 31, 1351–1360. doi:10.4103/1319-2442.308344

Alicic, R. Z., Rooney, M. T., and Tuttle, K. R. (2017). Diabetic kidney disease: Challenges, progress, and possibilities. *Clin. J. Am. Soc. Nephrol.* 12, 2032–2045. doi:10.2215/CJN.11491116

Amini, H., Rezabakhsh, A., Heidarzadeh, M., Hassanpour, M., Hashemzadeh, S., Ghaderi, S., et al. (2021). An examination of the putative role of melatonin in exosome biogenesis. *Front. Cell Dev. Biol.* 9, 686551. doi:10.3389/fcell.2021.686551

Bai, S., Xiong, X., Tang, B., Ji, T., Li, X., Qu, X., et al. (2020). Exosomal circ_DLGAP4 promotes diabetic kidney disease progression by sponging miR-143 and targeting ERBB3/NF-κB/MMP-2 axis. *Cell Death Dis.* 11, 1008. doi:10.1038/s41419-020-03169-3

Bakdash, K., Schramm, K. M., Annam, A., Brown, M., Kondo, K., and Lindquist, J. D. (2019). Complications of percutaneous renal biopsy. *Semin. Interv. Radiol.* 36, 97–103. doi:10.1055/s-0039-1688422

Barutta, F., Tricarico, M., Corbelli, A., Annaratone, L., Pinach, S., Grimaldi, S., et al. (2013). Urinary exosomal microRNAs in incipient diabetic nephropathy. *PLoS One* 8, e73798. doi:10.1371/journal.pone.0073798

Cao, J. Y., Wang, B., Tang, T. T., Wen, Y., Li, Z. L., Feng, S. T., et al. (2021). Exosomal miR-125b-5p deriving from mesenchymal stem cells promotes tubular repair by suppression of p53 in ischemic acute kidney injury. *Theranostics* 11, 5248–5266. doi:10.7150/thno.54550

Chun-Yan, L., Zi-Yi, Z., Tian-Lin, Y., Yi-Li, W., Bao, L., Jiao, L., et al. (2018). Liquid biopsy biomarkers of renal interstitial fibrosis based on urinary exosome. *Exp. Mol. Pathol.* 105, 223–228. doi:10.1016/j.yexmp.2018.08.004

Da-Silva, C., Anauate, A. C., Guirao, T. P., Novaes, A., Maquigussa, E., and Boim, M. A. (2022). Analysis of exosome-derived microRNAs as early biomarkers of lipopolysaccharide-induced acute kidney injury in rats. *Front. Physiol.* 13, 944864. doi:10.3389/fphys.2022.944864

Delić, D., Eisele, C., Schmid, R., Baum, P., Wiech, F., Gerl, M., et al. (2016). Urinary exosomal miRNA signature in type II diabetic nephropathy patients. *PLoS One* 11, e0150154. doi:10.1371/journal.pone.0150154

Fan, Q., Lu, R., Zhu, M., Yan, Y., Guo, X., Qian, Y., et al. (2019). Serum miR-192 is related to tubulointerstitial lesion and short-term disease progression in IgA nephropathy. *Nephron* 142, 195–207. doi:10.1159/000497488

Fiorentino, M., Bolignano, D., Tesar, V., Pisano, A., Biesen, W. V., Tripepi, G., et al. (2017). Renal biopsy in patients with diabetes: A pooled meta-analysis of 48 studies. *Nephrol. Dial. Transpl.* 32, 97–110. doi:10.1093/ndt/gfw070

Guo, N., Zhou, Q., Huang, X., Yu, J., Han, Q., Nong, B., et al. (2020). Identification of differentially expressed circulating exosomal lncRNAs in IgA nephropathy patients. *BMC Immunol.* 21, 16. doi:10.1186/s12865-020-00344-1

Guo, S., Hao, H., Li, S., Zhang, L., and Li, R. (2022). Differential expression of urinary exosomal miRNA in idiopathic membranous nephropathy and evaluation of its diagnostic value. *Tohoku J. Exp. Med.* 256, 327–336. doi:10.1620/tjem.2022.J002

Huang, X., and Xu, G. (2021). An update on targeted treatment of IgA nephropathy: An autoimmune perspective. *Front. Pharmacol.* 12, 715253. doi:10.3389/fphar.2021.715253

Ichii, O., and Horino, T. (2018). MicroRNAs associated with the development of kidney diseases in humans and animals. *J. Toxicol. Pathol.* 31, 23–34. doi:10.1293/tox.2017-0051

Jeppesen, D. K., Fenix, A. M., Franklin, J. L., Higginbotham, J. N., Zhang, Q., Zimmerman, L. J., et al. (2019). Reassessment of exosome composition. *Cell* 177, 428–445. e18. doi:10.1016/j.cell.2019.02.029

Jiang, L., Liu, X. Q., Ma, Q., Yang, Q., Gao, L., Li, H. D., et al. (2019). hsa-miR-500a-3P alleviates kidney injury by targeting MLKL-mediated necroptosis in renal epithelial cells. *Faseb. J.* 33, 3523–3535. doi:10.1096/fj.201801711R

Jin, J., Shi, Y., Gong, J., Zhao, L., Li, Y., He, Q., et al. (2019). Exosome secreted from adipose-derived stem cells attenuates diabetic nephropathy by promoting autophagy flux and inhibiting apoptosis in podocyte. *Stem Cell Res. Ther.* 10, 95. doi:10.1186/s13287-019-1177-1

Jin, J., Wang, Y., Zhao, L., Zou, W., Tan, M., and He, Q. (2020). Exosomal miRNA-215-5p derived from adipose-derived stem cells attenuates epithelial-mesenchymal transition of podocytes by inhibiting ZEB2. *Biomed. Res. Int.* 2020, 2685305. doi:10.1155/2020/2685305

Johnstone, R. M., Adam, M., Hammond, J. R., Orr, L., and Turbide, C. (1987). Vesicle formation during reticulocyte maturation. Association of plasma membrane activities with released vesicles (exosomes). *J. Biol. Chem.* 262, 9412–9420. doi:10.1016/s0021-9258(18)48095-7

Khwaja, A. (2012). KDIGO clinical practice guidelines for acute kidney injury. *Nephron. Clin. Pract.* 120, c179–c184. doi:10.1159/000339789

Kim, H., Bae, Y. U., Jeon, J. S., Noh, H., Park, H. K., Byun, D. W., et al. (2019). The circulating exosomal microRNAs related to albuminuria in patients with diabetic nephropathy. *J. Transl. Med.* 17, 236. doi:10.1186/s12967-019-1983-3

Kim, K. M., Abdelmohsen, K., Mustapic, M., Kapogiannis, D., and Gorospe, M. (2017). *RNA in extracellular vesicles.* Wiley, 8. doi:10.1002/wrna.1413*Interdiscip. Rev. RNA.*

Kölling, M., Seeger, H., Haddad, G., Kistler, A., Nowak, A., Faulhaber-Walter, R., et al. (2018). The circular RNA ciRs-126 predicts survival in critically ill patients with acute kidney injury. *Kidney Int. Rep.* 3, 1144–1152. doi:10.1016/j.ekir.2018.05.012

Lai, K. N., Tang, S. C., Schena, F. P., Novak, J., Tomino, Y., Fogo, A. B., et al. (2016). IgA nephropathy. *Nat. Rev. Dis. Prim.* 2, 16001. doi:10.1038/nrdp.2016.1

Li, B., Sun, G., Yu, H., Meng, J., and Wei, F. (2022a). Exosomal circTAOK1 contributes to diabetic kidney disease progression through regulating SMAD3 expression by sponging miR-520h. *Int. Urol. Nephrol.* 54, 2343–2354. doi:10.1007/s11255-022-03139-y

Li, H., Zhang, X., Wang, P., Zhou, X., Liang, H., and Li, C. (2021). Knockdown of circ-FANCA alleviates LPS-induced HK2 cell injury via targeting miR-93-5p/OXSR1 axis in septic acute kidney injury. *Diabetol. Metab. Syndr.* 13, 7. doi:10.1186/s13098-021-00625-8

Li, S., Hao, H., Li, R., and Guo, S. (2022b). Urinary exosomal MicroRNAs as new noninvasive biomarkers of IgA nephropathy. *Tohoku J. Exp. Med.* 256, 215–223. doi:10.1620/tjem.256.215

Li, X., Liao, J., Su, X., Li, W., Bi, Z., Wang, J., et al. (2020). Human urine-derived stem cells protect against renal ischemia/reperfusion injury in a rat model via exosomal miR-146a-5p which targets IRAK1. *Theranostics* 10, 9561–9578. doi:10.7150/thno.42153

Liangos, O., Wald, R., O'Bell, J. W., Price, L., Pereira, B. J., and Jaber, B. L. (2006). Epidemiology and outcomes of acute renal failure in hospitalized patients: A national survey. *Clin. J. Am. Soc. Nephrol.* 1, 43–51. doi:10.2215/CJN.00220605

Liu, Z., Wang, Y., Shu, S., Cai, J., Tang, C., and Dong, Z. (2019). Non-coding RNAs in kidney injury and repair. *Am. J. Physiol. Cell Physiol.* 317, C177–C188. doi:10.1152/ajpcell.00048.2019

Luan, R., Tian, G., Ci, X., Zheng, Q., Wu, L., and Lu, X. (2021). Differential expression analysis of urinary exosomal circular RNAs in patients with IgA nephropathy. *Nephrology* 26, 432–441. doi:10.1111/nep.13855

Luan, R., Tian, G., Zhang, H., Shi, X., Li, J., Zhang, R., et al. (2022). Urinary exosomal circular RNAs of sex chromosome origin are associated with gender-related risk differences of clinicopathological features in patients with IgA nephropathy. *J. Nephrol.* 35, 1069–1078. doi:10.1007/s40620-021-01118-7

Lv, J. C., and Zhang, L. X. (2019). Prevalence and disease burden of chronic kidney disease. *Adv. Exp. Med. Biol.* 1165, 3–15. doi:10.1007/978-981-13-8871-2_1

Lv, L. L., Cao, Y. H., Ni, H. F., Xu, M., Liu, D., Liu, H., et al. (2013). MicroRNA-29c in urinary exosome/microvesicle as a biomarker of renal fibrosis. *Am. J. Physiol. Ren. Physiol.* 305, F1220–F1227. doi:10.1152/ajprenal.00148.2013

Lv, L. L., Feng, Y., Wu, M., Wang, B., Li, Z. L., Zhong, X., et al. (2020). Exosomal miRNA-19b-3p of tubular epithelial cells promotes M1 macrophage activation in kidney injury. *Cell Death Differ.* 27, 210–226. doi:10.1038/s41418-019-0349-y

Ma, H., Xu, Y., Zhang, R., Guo, B., Zhang, S., and Zhang, X. (2019). Differential expression study of circular RNAs in exosomes from serum and urine in patients with idiopathic membranous nephropathy. *Arch. Med. Sci.* 15, 738–753. doi:10.5114/aoms.2019.84690

Min, Q. H., Chen, X. M., Zou, Y. Q., Zhang, J., Li, J., Wang, Y., et al. (2018). Differential expression of urinary exosomal microRNAs in IgA nephropathy. *J. Clin. Lab. Anal.* 32, e22226. doi:10.1002/jcla.22226

Miranda, K. C., Bond, D. T., McKee, M., Skog, J., Păunescu, T. G., Da Silva, N., et al. (2010). Nucleic acids within urinary exosomes/microvesicles are potential biomarkers for renal disease. *Kidney Int.* 78, 191–199. doi:10.1038/ki.2010.106

Netti, G. S., Sangregorio, F., Spadaccino, F., Staffieri, F., Crovace, A., Infante, B., et al. (2019). LPS removal reduces CD80-mediated albuminuria in critically ill patients with Gram-negative sepsis. *Am. J. Physiol. Ren. Physiol.* 316, F723–F731. doi:10.1152/ajprenal.00491.2018

Pan, B. T., and Johnstone, R. M. (1983). Fate of the transferrin receptor during maturation of sheep reticulocytes *in vitro*: Selective externalization of the receptor. *Cell* 33, 967–978. doi:10.1016/0092-8674(83)90040-5

Pawluczyk, I., Nicholson, M., Barbour, S., Er, L., Selvaskandan, H., Bhachu, J. S., et al. (2021). A pilot study to predict risk of IgA nephropathy progression based on miR-204 expression. *Kidney Int. Rep.* 6, 2179–2188. doi:10.1016/j.ekir.2021.05.018

Pegtel, D. M., and Gould, S. J. (2019). Exosomes. *Annu. Rev. Biochem.* 88, 487–514. doi:10.1146/annurev-biochem-013118-111902

Ren, H., and Wang, Q. (2021). Non-coding RNA and diabetic kidney disease. *DNA Cell Biol.* 40, 553–567. doi:10.1089/dna.2020.5973

Slocum, J. L., Heung, M., and Pennathur, S. (2012). Marking renal injury: Can we move beyond serum creatinine? *Transl. Res.* 159, 277–289. doi:10.1016/j.trsl.2012.01.014

Sun, Z., Wu, J., Bi, Q., and Wang, W. (2022). Exosomal lncRNA TUG1 derived from human urine-derived stem cells attenuates renal ischemia/reperfusion injury by interacting with SRSF1 to regulate ASCL4-mediated ferroptosis. *Stem Cell Res. Ther.* 13, 297. doi:10.1186/s13287-022-02986-x

Théry, C., Witwer, K. W., Aikawa, E., Alcaraz, M. J., Anderson, J. D., Andriantsitohaina, R., et al. (2018). Minimal information for studies of extracellular vesicles 2018 (MISEV2018): A position statement of the international society for extracellular vesicles and update of the MISEV2014 guidelines. *J. Extracell. Vesicles* 7, 1535750. doi:10.1080/20013078.2018.1535750

van Niel, G., D'Angelo, G., and Raposo, G. (2018). Shedding light on the cell biology of extracellular vesicles. *Nat. Rev. Mol. Cell Biol.* 19, 213–228. doi:10.1038/nrm.2017.125

Viñas, J. L., Burger, D., Zimpelmann, J., Haneef, R., Knoll, W., Campbell, P., et al. (2016). Transfer of microRNA-486-5p from human endothelial colony forming cell-derived exosomes reduces ischemic kidney injury. *Kidney Int.* 90, 1238–1250. doi:10.1016/j.kint.2016.07.015

Wang, B., Yao, K., Huuskes, B. M., Shen, H. H., Zhuang, J., Godson, C., et al. (2016). Mesenchymal stem cells deliver exogenous MicroRNA-let7c via exosomes to attenuate renal fibrosis. *Mol. Ther.* 24, 1290–1301. doi:10.1038/mt.2016.90

Wu, Y. L., Xie, J., An, S. W., Oliver, N., Barrezueta, N. X., Lin, M. H., et al. (2017). Inhibition of TRPC6 channels ameliorates renal fibrosis and contributes to renal protection by soluble klotho. *Kidney Int.* 91, 830–841. doi:10.1016/j.kint.2016.09.039

Yu, W., Zeng, H., Chen, J., Fu, S., Huang, Q., Xu, Y., et al. (2020). miR-20a-5p is enriched in hypoxia-derived tubular exosomes and protects against acute tubular injury. *Clin. Sci.* 134, 2223–2234. doi:10.1042/CS20200288

Yun, C. Y., Lim, J. H., Oh, J. H., Cho, A. Y., Lee, K. Y., and Sun, I. O. (2021). Urinary exosomal microRNA-21 as a marker for scrub typhus-associated acute kidney injury. *Genet. Test. Mol. Biomarkers* 25, 140–144. doi:10.1089/gtmb.2020.0238

Zang, J., Maxwell, A. P., Simpson, D. A., and McKay, G. J. (2019). Differential expression of urinary exosomal MicroRNAs miR-21-5p and miR-30b-5p in individuals with diabetic kidney disease. *Sci. Rep.* 9, 10900. doi:10.1038/s41598-019-47504-x

Zhang, A., Wang, H., Wang, B., Yuan, Y., Klein, J. D., and Wang, X. H. (2019). Exogenous miR-26a suppresses muscle wasting and renal fibrosis in obstructive kidney disease. *Faseb. J.* 33, 13590–13601. doi:10.1096/fj.201900884R

Zhang, J., He, W., Zheng, D., He, Q., Tan, M., and Jin, J. (2021a). Exosomal-miR-1184 derived from mesenchymal stem cells alleviates cisplatin-associated acute kidney injury. *Mol. Med. Rep.* 24, 795. doi:10.3892/mmr.2021.12435

Zhang, L., Wang, F., Wang, L., Wang, W., Liu, B., Liu, J., et al. (2012). Prevalence of chronic kidney disease in China: A cross-sectional survey. *Lancet* 379, 815–822. doi:10.1016/S0140-6736(12)60033-6

Zhang, L., and Wang, H. (2009). Chronic kidney disease epidemic: Cost and health care implications in China. *Semin. Nephrol.* 29, 483–486. doi:10.1016/j.semnephrol.2009.06.012

Zhang, X., Wang, N., Huang, Y., Li, Y., Li, G., Lin, Y., et al. (2022a). Extracellular vesicles from three dimensional culture of human placental mesenchymal stem cells ameliorated renal ischemia/reperfusion injury. *Int. J. Artif. Organs* 45, 181–192. doi:10.1177/0391398820986809

Zhang, Y., Huang, H., Liu, W., Liu, S., Wang, X. Y., Diao, Z. L., et al. (2021b). Endothelial progenitor cells-derived exosomal microRNA-21-5p alleviates sepsis-induced acute kidney injury by inhibiting RUNX1 expression. *Cell Death Dis.* 12, 335. doi:10.1038/s41419-021-03578-y

Zhang, Z., Chen, H., Zhou, L., Li, C., Lu, G., and Wang, L. (2022b). Macrophage-derived exosomal miRNA-155 promotes tubular injury in ischemia-induced acute kidney injury. *Int. J. Mol. Med.* 50, 116. doi:10.3892/ijmm.2022.5172

Zhou, S., Fang, J., Hu, M., Pan, S., Liu, D., Xing, G., et al. (2021). Determining the influence of high glucose on exosomal lncRNAs, mRNAs, circRNAs and miRNAs derived from human renal tubular epithelial cells. *Aging* 13, 8467–8480. doi:10.18632/aging.202656

Zhu, Y., Zha, F., Tang, B., Ji, T. T., Li, X. Y., Feng, L., et al. (2022). Exosomal hsa_circ_0125310 promotes cell proliferation and fibrosis in diabetic nephropathy via sponging miR-422a and targeting the IGF1R/p38 axis. *J. Cell. Mol. Med.* 26, 151–162. doi:10.1111/jcmm.17065

Glossary

ADSCs adipose-derived stem cells
AKI acute kidney injury
AP-1 activator protein 1
ASCL4 acyl-CoA synthetase long-chain family member 4
AUC area under the curve
circRNAs circular RNAs
CKD chronic kidney disease
CTGF connective tissue growth factor
DKD diabetic kidney disease
EMT epithelial interstitial transition
EPCs endothelial progenitor cells
ERBB3 Erb-b2 receptor tyrosine kinase 3
ESRD end-stage renal disease
GECs glomerular endothelial cells
GMCs glomerular mesangial cells
GO gene ontology
hPMSCs human placental MSCs
IgAN IgA nephropathy
IGF1R insulin-like growth factor 1 receptor
IMN idiopathic membranous nephropathy
IRAK1 interleukin-1 receptor-associated kinase 1
IRI ischemic/reperfusion injury
KEGG Kyoto Encyclopedia of Genes and Genomes
lncRNAs long non-coding RNAs
LPS lipopolysaccharide
MAPK mitogen-activated protein kinase
miRNAs microRNAs
MMP2 matrix metalloproteinase 2
MSCs mesenchymal stem cells
mTOR mechanistic target of rapamycin
ncRNAs non-coding RNAs
NF-κB nuclear factor-κB
OXSR1 oxidative stress responsive 1
PI3K phosphoinositide-3-kinase-protein kinase B
PRB percutaneous renal biopsy
ROC receiver operating characteristic
RUNX1 runt-related transcription factor 1
sEV-circRNAs small extracellular vesicle-derived circular RNAs
sEV-lncRNAs small extracellular vesicle-derived long non-coding RNAs
sEV-miRNAs small extracellular vesicle-derived microRNAs
sEV-ncRNAs small extracellular vesicle-derived non-coding RNAs
sEVs small extracellular vesicles
Smad1 SMAD family member 1
Smad3 SMAD family member 3
SOCS-1 suppressor of cytokine signaling 1
SRSF1 serine/arginine splicing factor 1
T1DM type 1 diabetic mellitus
T2DM type 2 diabetes mellitus
TECs tubular epithelial cells
TGF-β transforming growth factor-β
USCs urine-derived stem cells
UUOunilateral ureteral obstructionZEB2 unilateral ureteral obstructionZEB2zinc finger E-box-binding homeobox 2

frontiers | Frontiers in Genetics

TYPE Original Research
PUBLISHED 15 November 2022
DOI 10.3389/fgene.2022.929787

OPEN ACCESS

EDITED BY
Naseer A. Kutchy,
Children's National Hospital,
United States

REVIEWED BY
Muhammet Rasit Ugur,
IVF Michigan Fertility Centers,
United States
Annadurai Thangaraj,
Anna University, India
Mudasir Rashid,
Howard University Hospital,
United States

*CORRESPONDENCE
Dil Afroze,
afrozedil@gmail.com

†These authors have contributed equally to this work

SPECIALTY SECTION
This article was submitted to RNA, a section of the journal Frontiers in Genetics

RECEIVED 27 April 2022
ACCEPTED 26 August 2022
PUBLISHED 15 November 2022

CITATION
Yousuf T, Dar SB, Bangri SA, Choh NA, Rasool Z, Shah A, Rather RA, Rah B, Bhat GR, Ali S and Afroze D (2022), Diagnostic implication of a circulating serum-based three-microRNA signature in hepatocellular carcinoma. *Front. Genet.* 13:929787. doi: 10.3389/fgene.2022.929787

Diagnostic implication of a circulating serum-based three-microRNA signature in hepatocellular carcinoma

Tahira Yousuf[1,2], Sadaf Bashir Dar[1], Sadaf Ali Bangri[3†], Naseer A. Choh[4†], Zubaida Rasool[5†], Altaf Shah[6†], Rafiq Ahmed Rather[1], Bilal Rah[1], Gh Rasool Bhat[1], Shazia Ali[1] and Dil Afroze[1,2]*

[1]Advance Centre for Human Genetics, Sher-I-Kashmir Institute of Medical Sciences (SKIMS), Srinagar, Jammu and Kashmir, India, [2]Department of Immunology and Molecular Medicine, SKIMS, Srinagar, Jammu and Kashmir, India, [3]Department of Surgical Gastroenterology, SKIMS, Srinagar, Jammu and Kashmir, India, [4]Department of Radio-Diagnosis, SKIMS, Srinagar, Jammu and Kashmir, India, [5]Department of Pathology, SKIMS, Srinagar, Jammu and Kashmir, India, [6]Department of Gastroenterology, SKIMS, Srinagar, Jammu and Kashmir, India

Owing to the diagnostic dilemma, the prognosis of hepatocellular carcinoma (HCC) remains impoverished, contributing to the globally high mortality rate. Currently, HCC diagnosis depends on the combination of imaging modalities and the measurement of serum alpha-fetoprotein (AFP) levels. Nevertheless, these conventional modalities exhibit poor performance in detecting HCC at early stages. Thus, there is a pressing need to identify novel circulating biomarkers to promote diagnostic accuracy and surveillance. Circulating miRNAs are emerging as promising diagnostic tools in screening various cancers, including HCC. However, because of heterogenous and, at times, contradictory reports, the universality of miRNAs in clinical settings remains elusive. Consequently, we proposed to explore the diagnostic potential of ten miRNAs selected on a candidate-based approach in HCC diagnosis. The expression of ten candidate miRNAs (Let-7a, miR-15a, miR-26a, miR-124, miR-126, miR-155, miR-219, miR-221, miR-222, and miR-340) was investigated in serum and tissue of 66 subjects, including 33 HCC patients and 33 healthy controls (HC), by rt-PCR. Receiver operating characteristic curve (ROC) analysis was used to determine the diagnostic accuracy of the prospective serum miRNA panel. To anticipate the potential biological roles of a three-miRNA signature, the target genes were evaluated using the Kyoto Encyclopedia of Genes and Genomes (KEGG) signaling pathway. The serum and tissue expression of miRNAs (Let-7a, miR-26a, miR-124, miR-155, miR-221, miR-222, and miR-340) were differentially expressed in HCC patients ($p < 0.05$). The ROC analysis revealed promising diagnostic performance of Let-7a (AUC = 0.801), miR-221 (AUC = 0.786), and miR-2 (AUC = 0.758) in discriminating HCC from HC. Furthermore, in a logistic regression equation, we identified a three-miRNA panel (Let-7a, miR-221, and miR-222; AUC = 0.932) with improved diagnostic efficiency in differentiating HCC from HC. Remarkably, the combination of AFP and a three-miRNA panel offered a higher accuracy of HCC diagnosis (AUC = 0.961) than AFP alone. The functional enrichment

analysis demonstrated that target genes may contribute to pathways associated with HCC and cell-cycle regulation, indicating possible crosstalk of miRNAs with HCC development. To conclude, the combined classifier of a three-miRNA panel and AFP could be indispensable circulating biomarkers for HCC diagnosis. Furthermore, targeting predicted genes may provide new therapeutic clues for the treatment of aggressive HCC.

KEYWORDS

circulating miRNA, biomarker, diagnosis, therapeutics, hepatocellular carcinoma

Introduction

Globally, hepatocellular carcinoma (HCC) is the third primary cause of cancer-allied mortality and accounts for 90% of primary liver cancers (Yang et al., 2019) (Fattovich et al., 2004; Jemal et al., 2011). Often, HCC is diagnosed at an advanced stage, and due to rapid tumor progression, most HCC patients die early. More than 80% of patients with underlying cirrhosis develop HCC, and, amongst these, only 10% are potentially resectable at the time of detection (Yang and Roberts, 2010; Llovet et al., 2021). The remainders are unresectable because of location, size, or severity of underlying liver disease (Zhang et al., 2014a). Consequently, to improve prognosis, an earlier HCC diagnosis is vital (Bargellini et al., 2014). These imaging techniques are routinely combined with the use of serum tumor markers, such as α-fetoprotein (AFP), which is the most commonly used biomarker to detect HCC. Although several western countries have discontinued using AFP due to its poor sensitivity and precision, this protein is still widely used in many Asian countries, including India (Patel et al., 2012). Although the precise molecular mechanisms involved in the development and progression of HCC remain elusive, various risk factors for HCC development are well defined. HBV infection and aflatoxin B exposure are the major risk factors for HCC in high-incidence countries such as Asia and Africa, whereas HCV virus infection, alcohol consumption, and metabolic syndromes are crucial risk factors in low-incidence countries such as Europe, North and South America, and the Middle East. In addition, increased body mass index (BMI) and diabetes, which can lead to non-alcoholic steatohepatitis (NASH), are both substantial risk factors for HCC (Noureddin and Rinella, 2015). This is particularly alarming in view of the rising obesity epidemic in children and adults over the last 25 years (Bhasin Lal et al., 2015). Despite this, around 70–80% of HCC cases emerge from a background of liver cirrhosis, with a median period of 10 years to HCC development (Parkin et al., 2005; Patel et al., 2012). Overall, the poor prognosis and high mortality of HCC are attributable to the underlying cirrhosis, adverse early diagnosis, and paucity of effective late-stage therapy choices (Aleman et al., 2013). This establishes an urgent need to find sensitive markers, especially those correlated with early diagnosis and also for monitoring postoperative recurrence in order to stipulate adequate treatment for HCC. MicroRNAs (miRNAs) are a vital component of the short non-coding RNA family that governs endogenous RNA interference in almost 30% of protein-coding genes by pairing with the 3′ untranslated region (UTR) of mRNA targets, resulting in post-transcriptional and/or post-translational repression (Friedman et al., 2009). miRNAs are known to regulate a broad range of key biological functions, including differentiation, development, proliferation, apoptosis, migration, and invasion in normal cells (Giovannetti et al., 2012). Lately, formidable evidence suggests that miRNAs enact as oncogenes or tumor suppressors, thereby facilitating neoplastic transformation in innumerable cancers, including HCC (Kim, 2005; Acunzo et al., 2015). Additionally, studies have shown the presence of a stable cell-free form of miRNAs in body fluids such as plasma/serum. As a consequence of their inherent stability, miRNAs are considered useful diagnostic biomarkers for noninvasive testing of various types of cancers (Vaz et al., 2015). Numerous studies have recently reported the potential clinical utility of circulating miRNAs in the diagnosis and prognosis of HCC (Arrese et al., 2015). As a result, further research on dysregulated miRNA expression could lead to the identification of novel miRNA biomarkers for HCC. Based on a comprehensive literature review, a panel of ten candidate miRNAs (Let-7a, miR-340, miR-221, miR-222, miR-219, miR-155, miR-126, miR-124, miR-26a, and miR-15a) reported in diverse cancers including HCC were selected for further extensive investigation (Ladeiro et al., 2008; Lawrie et al., 2008; Melo and Esteller, 2011; Cheng et al., 2011; Borel et al., 2012; Anwar and Lehmann, 2015; Arrese et al., 2015; Li et al., 2015; Vasuri and Wang, 2015; Zhuang and Meng, 2015; Dong et al., 2016; He et al., 2018; Wu et al., 2018; Chirshev et al., 2019; Ravegnini et al., 2019; Zhou et al., 2019; Zhu et al., 2020; Liu et al., 2021; Zhang et al., 2021). Prominently, tissue specificity is an essential property of specific biomarkers to perceive cancer progression. Thus, we performed validation in HCC tissues compared to adjacent peritumor sections to confirm the liver-originating serum miRNAs in HCC diagnosis.

Materials and methods

Patients and specimen collection

Following stringent inclusion and exclusion criteria, a total of 66 subjects (33 HCC patients and 33 healthy controls) were recruited between January 2018 to December 2020 from the department of Surgical Gastroenterology, Medical Gastroenterology and Radio-diagnosis, Sher-I-Kashmir Institute of Medical Sciences (SKIMS). The details of all participants were collected through a comprehensive questionnaire along with signed informed consent in accordance with approved guidelines of the SKIMS institutional ethics committee (IEC/SKIMS Protocol # RP: 96/2018). The HCC cases enlisted in the study were histopathologically confirmed by liver biopsy or by the radiological findings encompassing abdominal ultrasound (USG), computed tomography (CT) abdomen, magnetic resonance imaging (MRI), or by virtue of elevated serum AFP levels (AFP≥200 μg/ml). Healthy volunteers with no known significant health issues were included as a control group in this research. Additionally, information on clinical features such as BCLC & TNM staging was collected from medical records.

3 ml peripheral blood samples were collected by venous puncture in non-EDTA vacutainers and centrifuged at 4500 x rpm for 10 min at room temperature (RT) to separate the serum fraction for miRNA extraction. Without disturbing the pellet, sera were transferred to fresh collection tubes and stored at −80°C for further analysis. The hemolyzed samples were excluded from the study. Fresh frozen HCC and paired peritumor specimens were collected from HCC patients undergoing surgical resection.

RNA isolation

The isolation of miRNA from tissue and plasma was done using miRNAeasy Mini Kit (# 1038703, QIAGEN, Germany) and miRNAeasy® Serum/Plasma Kit (# 1071073, QIAGEN, Germany), respectively, by following the manufacturer's protocol. The concentration and purification of extracted miRNA from tissue and serum/plasma were measured by micro-volume UV-Vis spectrophotometer (Thermo Scientific NanoDrop 2000) at 260 nm wavelength using A_{260}/A_{280} ratio. cDNA was synthesized using a universal cDNA kit (# QIAGEN, 21816, Germany). The concentration for each RNA template was adjusted to 5 ng/μL by using nuclease-free water.

Real-time PCR amplification for the expression of miRNA in tissue and plasma

MiRCURY LNA™ SYBR Green PCR kit (#339346, QIAGEN, United States), commercially designed primers, cDNA, and nuclease-free water were used for amplification of the product. The desired master mix was prepared from the abovementioned reagents in a tube, and the obtained mixture was mixed well by vortexing and spun down. The mixture was dispensed in tubes, and cDNA was diluted (1: 60) in nuclease-free water and added to these tubes separately. The tubes were placed in a thermocycler (Rotor-Gene Q MDx, QIAGEN, working on Q-Rex software, Germany) by following reaction conditions as 95°C for 2-min, followed by 40 cycles of denaturation at 95°C for 10-min, annealing at 56°C for 1-min, and melting curve at 60–95°C. U6 was used as an internal reference gene. The ΔΔCt model was used for the relative quantification of RT-PCR data of miRNA.

Target genes for miRNA signature prediction

From three different miRNA target gene prediction websites, namely, miRTarBase (http://mirtarbase.mbc.nctu.edu.tw/), TargetScan (http://www.targetscan.org), and miRDB (http://www.mirdb.org/), the database for miRNA prediction was downloaded. The Perl language was used to find miRNA signature targeted genes, which are covered by at least 2 databases. The relationship between miRNAs and target genes was plotted using a Venn diagram and map network.

Functional enrichment analysis of target genes

The enrichment analysis for predicted genes of potential miRNAs was performed by Gene Ontology (GO) annotation and Kyoto Encyclopedia of Genes and Genomes (KEGG) by using the DAVID database (http://david.abcc.ncifcrf.gov/).

Statistical analysis

A statistically relevant sample size was calculated by open EPI Statistical Software. All the data are presented as the mean ± SD and/or mean ± SE. The statistical analysis, i.e., "*t*-test", Spearman correlation (r), univariate logistic regression analysis, stepwise logistic regression analysis and receiver operator curve (AUC), and Kruskal–Wallis test were performed using SPSS version 17.0 (IBM, Chicago, IL, United States), and all figures were generated using GraphPad Prism 5.01 (GraphPad Software, La Jolla, CA, United States). $p < 0.05$ were considered statistically significant.

TABLE 1 Clinico-pathological parameters of study subjects: demographics of the two participating groups. Values are expressed as mean ± SD or depicted as the number of cases (%). Data were analyzed using a non-parametric pair *t*-test (GraphPad Prism 5.0). The statistically significant *p*-value was denoted as < 0.05.

Clinical parameters	Healthy controls (n = 33)	Hepatocellular carcinoma (n = 33)	p-value
Age (Years)	51.68 ± 15.09	56.58 ± 12.29	0.19
Gender (M/F)	23/10	22/11	0.26
S. Bil (mg/dl)	0.95 ± 0.68	1.8293939 ± 1.71	0.01
ALT (U/L)	14.96 ± 8.71	76.263636 ± 72.41	0.001
AST (U/L)	12.36 ± 4.77	141.32 ± 141.35	0.001
ALP (U/L)	94.44 ± 33.64	271.84 ± 231.85	0.001
S. Protein (g/dl)	6.81 ± 1.84	7.12 ± 1.90	0.53
S. Albumin (g/dl)	2.71 ± 0.97	3.096 ± 1.02	0.14
PT (sec)	15.89 ± 3.08	16.8 ± 4.06	0.34
INR (Ratio)	1.23 ± 0.25	1.28 ± 0.31	0.55
Platelet count (*10^9 per litre)	272.49 ± 93.55	130.15 ± 90.47	0.001
AFP (IU/L)	9.67 ± 4.61	562.77 ± 980.17	0.003
HBsAg positive	0	09 (27%)	—
HCV positive	0	08 (24%)	—
Non-B, Non-C	0	16 (48%)	—
BCLC staging (0-D)	0	02 (6%)	—
0	0	06 (18%)	—
A	0	12 (36%)	—
B	0	11 (33%)	—
C	0	02 (6%)	—
D	—	—	—
TNM staging (I–IV)	0	04 (12%)	—
I	0	09 (27%)	—
II	0	08 (24%)	—
III	0	12 (36%)	—
IV	—	—	—
Tumor size	0	20 (60%)	—
> 5	0	13 (39%)	—
< 5	—	—	—

Abbreviations: SD; standard deviation, S.Bil; serum bilirubin, ALT; alanine amino transferase, AST; aspartate transaminase, ALP; alkaline phosphatase, PT; prothrombin time, INR; international normalized ratio, AFP; alpha-fetoprotein, HbsAg; hepatitis-B surface antigen, HCV; hepatitis C virus, BCLC; Barcelona clinic liver cancer, TNM; tumor, node, and metastasis.

Results

Clinico-pathological characteristics of the study population

The age and gender distribution were indistinguishable in both participating study groups, whereas the liver function parameters of serum bilirubin, ALT, AST, ALP, and AFP were significantly deranged among the participants of the HCC group compared to those of the HC group.

Furthermore, HCC patients had a considerable reduction in platelet counts compared to that in HC patients. However, there were no variations in the serum protein and albumin levels and rates of PT and INR concentration across the two groups. According to CT imaging, 20 of the 33 HCC participants in the study had tumors larger than 5 cm (60%), while 13 had tumors smaller than 5 cm (39%). BCLC 0/A, B/C, and D scores were recorded in 8 (24%), 18 (54%), and 2 (6%) patients, respectively, indicating all patients were in the intermediate to late stages of the disease. In terms of TNM staging, four cases were registered in TNM-I, nine cases in TNM-II, eight cases in TNM-III, and 12 cases in TNM-IV. The demographic features of the study groups, as summarized in Table 1, certify that the subjects recruited in the study are properly classified and accurately represent the allocated group.

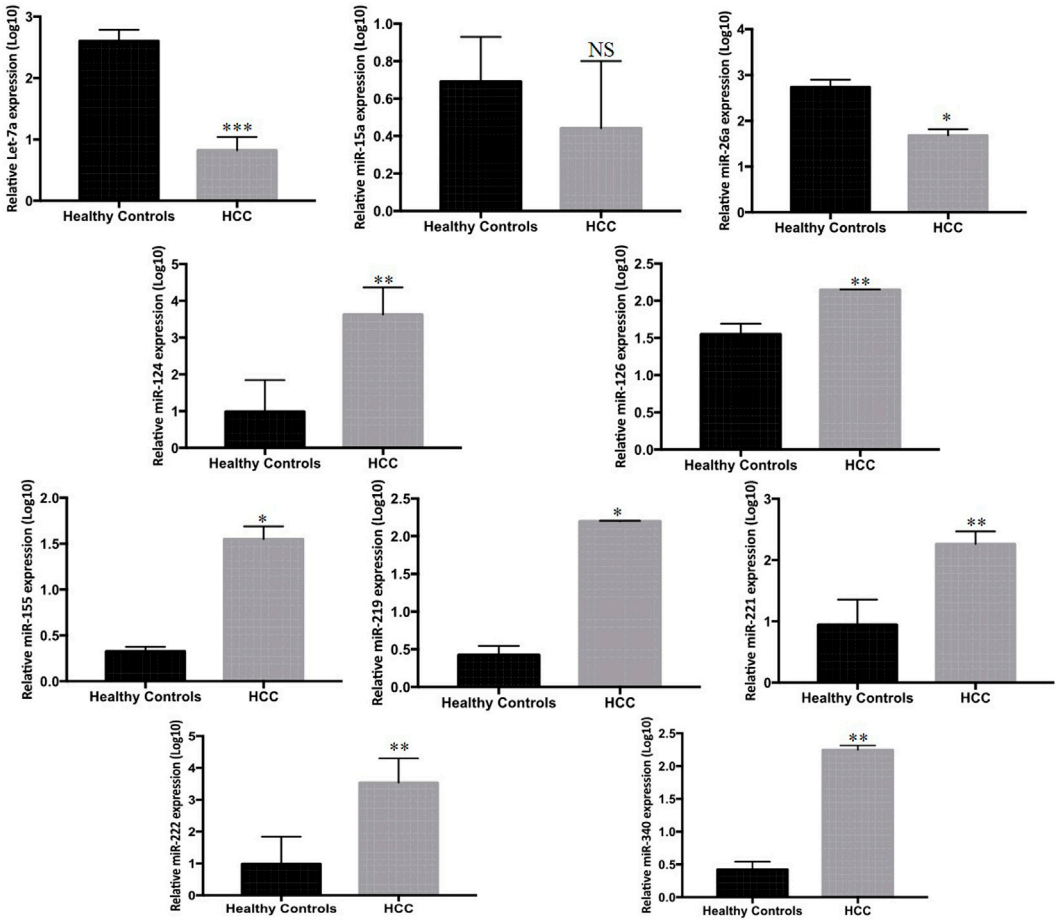

FIGURE 1
Differential expression of ten candidate miRNAs in sera of HCC patients (n = 33) and HC (n = 33) measured by Rt-qPCR. The statistical analysis was performed using Mann–Whitney test (GraphPad Prism 5.0). The statistically significant p-value was denoted as < 0.05.

Screening and validation of candidate miRNAs differentially expressed in HCC

Serum expression profiles for the panel of ten miRNAs, entailing (Let-7a, miR-15a, miR-26a, miR-124, miR-126, miR-155, miR-219, miR-221, miR-222, and miR-340) between 33 HCC and 33 HC subjects were observed by real-time qPCR. Our results indicate downregulation of serum miR-221 ($p < 0.001$), miR-340 ($p < 0.003$), miR-126 ($p < 0.001$), miR-219 ($p < 0.01$), and miR-155 ($p < 0.04$) between HCC and control group. Furthermore, Let-7a ($p < 0.0001$), miR-26a ($p < 0.04$), miR-124 ($p < 0.007$), and miR-222 ($p < 0.005$) were downregulated in serum of HCC patients compared to that in HC patients. Furthermore, the expression of miR-15a was non-significant when compared among the groups (Figure 1).

To further verify the tissue expression profile of the listed miRNAs, the expression levels were measured in 33 tumor and paired peritumor tissues of HCC patients by qPCR. Among the 33 matched samples, miR-221 ($p < 0.0001$), miR-124 ($p < 0.003$), miR-340 ($p < 0.03$), miR-222 ($p < 0.005$), and miR-155 ($p < 0.0001$) exhibited significantly higher expression, while Let-7a ($p < 0.0007$) and miR-26a ($p < 0.0006$) showed marked lower expression in the tumor tissues of HCC patients compared to the peritumor counterparts. Nevertheless, no significant differential expression was found in miR-126, miR-15a, and miR-219 among the groups (Figure 2).

Clinical significance and diagnostic accuracy of candidate miRNAs in HCC diagnosis

To validate the discriminatory potential of significantly deranged miRNAs, the area under the curve (AUC) was determined using ROC analysis. Among nine differentially expressed serum miRNAs in HCC patients, Let-7a showed the best diagnostic efficacy with the highest AUC value (AUC = 0.801, 95% CI of 0.684–0.919, and at a cut off <0.9121, sensitivity

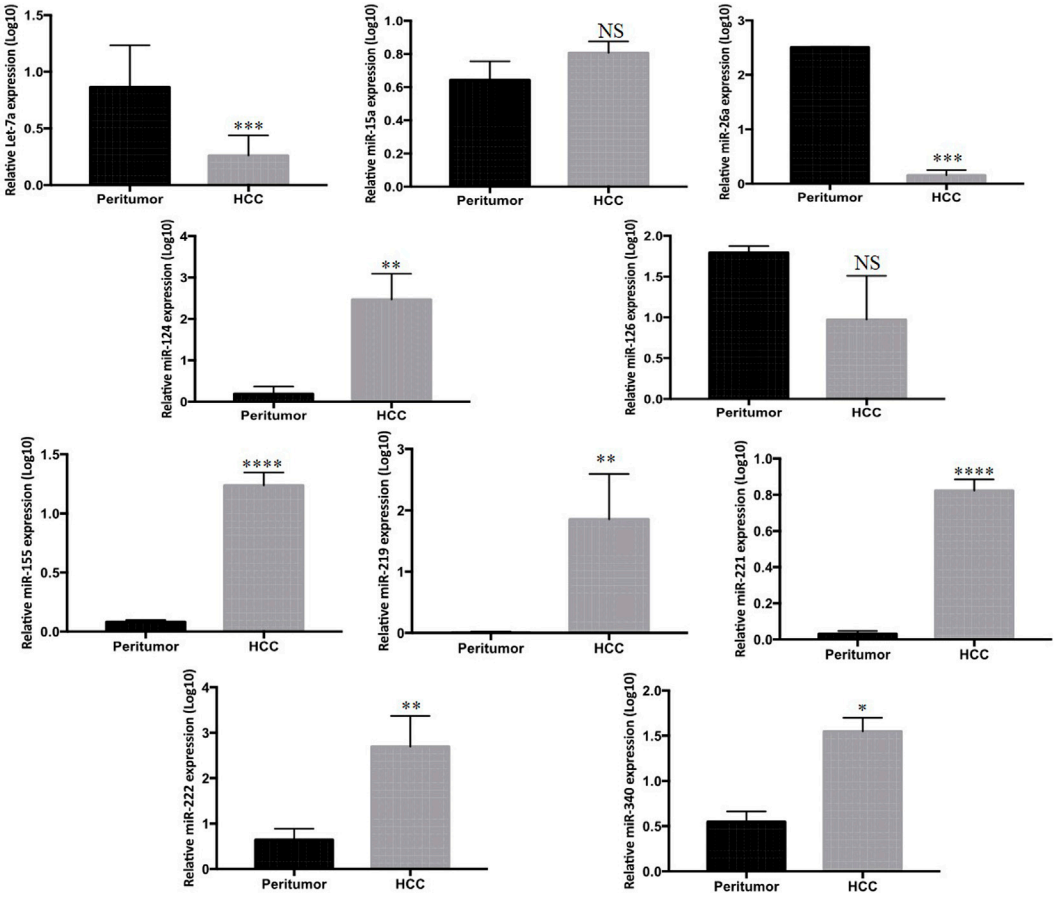

FIGURE 2
Mean $\log_{10}$ expression of ten candidate miRNAs in tumor of HCC patients (n = 33) compared to paired peritumor tissue (n = 33) determined by Rt-qPCR. The statistical analysis was performed using Mann–Whitney test (GraphPad Prism 5.0). The statistically significant p-value was denoted as < 0.05. NS; non-significant.

of 83.33%, and a specificity of 68.97%; $p < 0.0001$), followed by miR-221 (AUC 0.786, 95% CI = 0.666–0.906, cut off <1.626; 228, sensitivity 77.14%, specificity 80.77%, $p < 0.0001$), and miR-222 (AUC 0.758, 95% 229 CI = 0.583–0.932, cut off >0.6096; sensitivity 86.96%, specificity 68.75%, p < 230 0.0067). Furthermore, miR-26a (with AUC 0.531), miR-124 (AUC 0.668), miR-340 (AUC 0.548), miR-126 (AUC 0.527), and miR-155 (AUC 0.583) were unable to distinguish HCC patients from HC, as shown in Figure 3.

Establishment of the predictive three-miRNA panel and to evaluate its efficacy for diagnosis

Based on the univariate logistic regression model, the levels of Let-7a ($p < 0.001$), miR-221 ($p < 0.0001$), and miR-222 ($p < 0.004$) depicted considerable variation among HCC patients and healthy controls and, thus, were accordingly included in the further verification, as shown in Table 2.

Altogether, the three chosen miRNAs were found to be significant predictors for HCC, as shown in Table 3. To assess the predicted likelihood of being diagnosed with HCC, the logit model [logit (p) = 0.997 + 3.641 × (Let-7a) -2.985 × (miR-221) + 5.438× (miR-222)] was used to construct the ROC curve. Our analysis affirmed that the AUC of the three-miRNA panel was 0.932 ($p < 0.0001$), with a sensitivity and specificity of 93.75% and 84.62%, respectively, as shown in Figure 4.

Compounding accuracy of three-miRNA signature and AFP for the diagnosis of HCC

A step-wise logistic regression model was utilized to analyze the performance of the three-miRNA panel in combination with

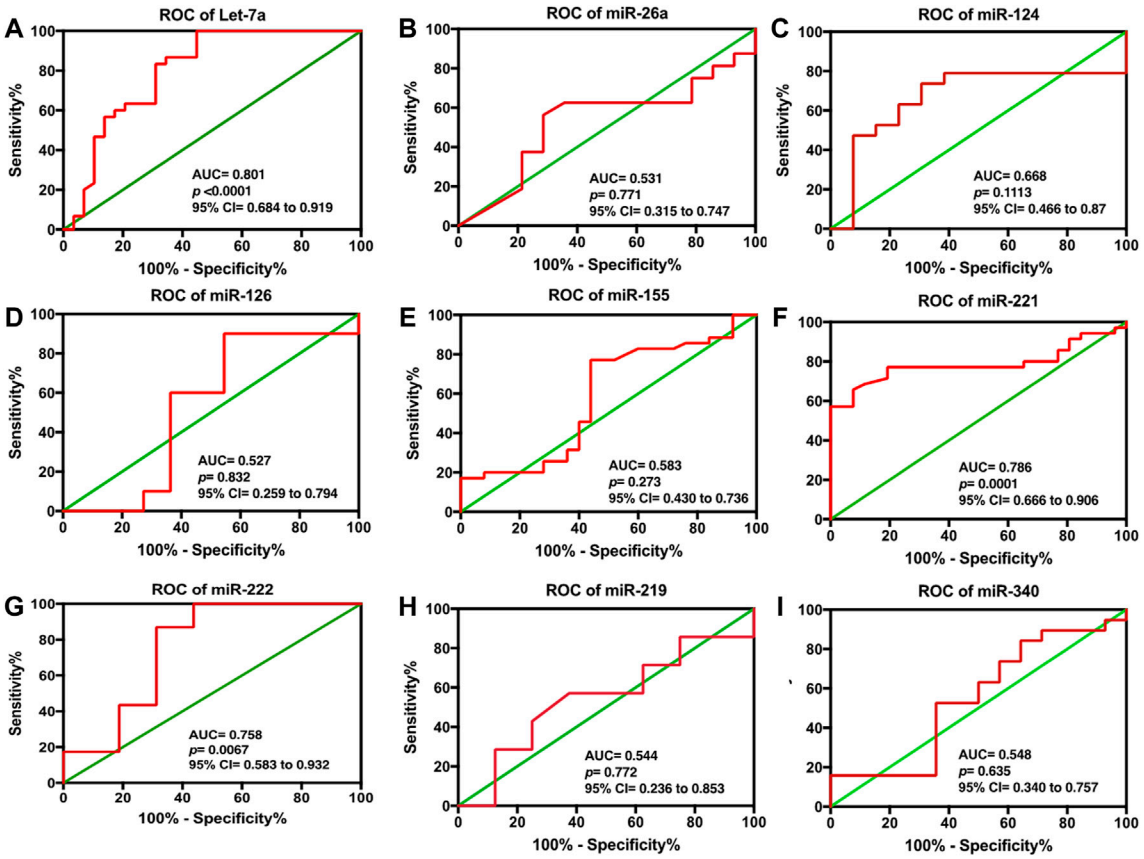

FIGURE 3
ROC analysis for serum **(A)** Let-7a, **(B)** miR-26a, **(C)** miR-124, **(D)** miR-126, **(E)** miR-155, **(F)** miR-221, **(G)** miR-222, **(H)** miR-219, and **(I)** miR-340 in HCC patients. The statistical analysis was done using GraphPad Prism 5.0.

TABLE 2 Establishment of the predictive three-miRNA panel and to evaluate its efficacy for diagnosis: univariate logistic regression analysis of candidate miRNAs. The statistical analysis was done using GraphPad Prism 5.0.

miRNAs	Estimate	Std. Error	*p*-value
hsa-Let-7a-5p	2.426	0.997	<0.001
hsa-miR-221-3p	-3.175	1.105	<0.0001
hsa-miR-222-5p	5.098	1.968	<0.004

AFP in discriminating HCC from HC. ROC analysis revealed that the combination of miRNAs (Let-7a, miR-221, and miR-222) had a significant superiority (AUC = 0.961; 95% CI = 0.882), than each miRNA separately; *viz* let-7a (AUC = 0.801, 95% CI = 0.684–0.919), miR-221 (AUC = 0.786, 95% CI = 0.666–0.906), and miR-222 (AUC = 0.758, 95% CI = 0.583–0.932) and AFP alone (AUC = 0.766; 95% CI = 0.632–0.901) in discriminating patients with HCC from those with HC. Additionally, our data suggest that the diagnostic efficacy of Let-7a and miR-221 alone

TABLE 3 Stepwise logistic regression analysis of candidate miRNAs. The statistical analysis was done using GraphPad Prism 5.0.

miRNAs	Estimate	Std. Error	*p*-value	Optimal cut-off	Diagnostic performance
Intercept	0.997	0.245	<0.0001	<7.895	AUC = 0.932 CI = 0.845–1.02 Sensitivity = 93.75% Specificity = 84.62%
Let-7a	3.641	1.420	0.004		
miR-221	−2.985	1.088	0.0005		
miR-222	5.438	2.721	0.0132		

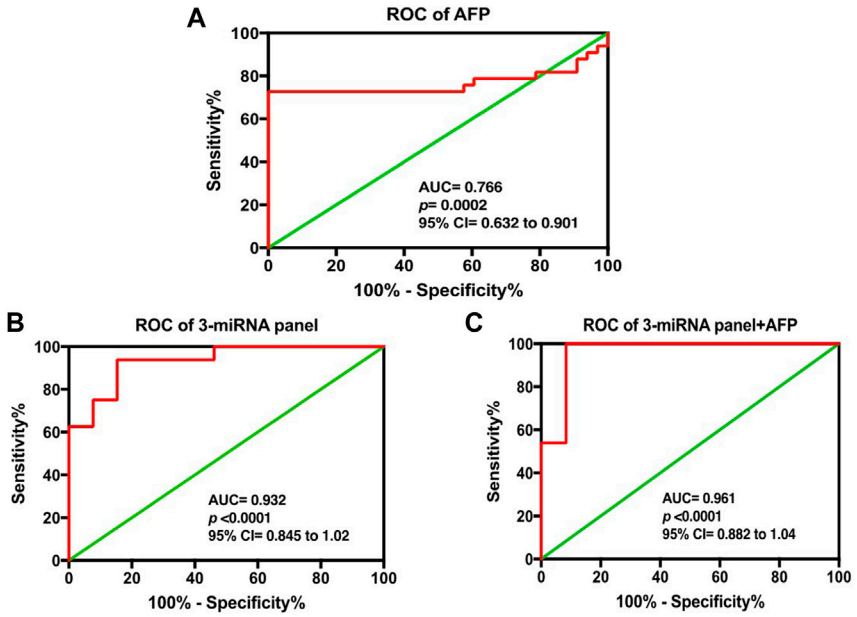

FIGURE 4
ROC analysis based on logit model for serum **(A)** AFP alone, **(B)** three-miRNA panel alone, and **(C)** combination of three-miRNA with AFP in discriminating HCC from. HC. The statistical analysis was done using GraphPad Prism 5.0.

TABLE 4 Stepwise logistic regression analysis of candidate miRNAs in combination with AFP. The statistical analysis was done using GraphPad Prism 5.0.

miRNAs	Estimate	Std error	*p*-value	Optimal cut-off	Diagnostic performance
Intercept	−1.372	2.90	0.0071	—	—
hsa-Let-7a-5p	0.523	0.253	0.0506	—	—
hsa-miR-221-3p	0.890	0.482	0.0700	>6.38	AUC = 0.961
hsa-miR-222-	−0.849	0.320	0.0004	—	CI = 0.882
5p	—	—	—	—	Sensitivity = 100%
AFP	0.107	0.038	0.0301	—	—
				—	Specificity = 91.67%

was superior to that of AFP, while miR-222 had a diagnostic efficiency equal to that of AFP, as shown in Table 4.

Expression of three-miRNA panel signature in viral etiology (HBV/HCV)-related HCC

In a further detailed analysis, we investigated serum Let-7a, miR-221, and miR-222 expression profiles in patients with hepatitis B- and hepatitis C-associated HCC. Using the non-parametric Kruskal–Wallis test, we examined that the expressions of three studied miRNAs were significantly different in the sera and tissue of hepatitis B infected, hepatitis C infected, and non-viral groups compared to the healthy controls and peritumor samples ($p < 0.05$), respectively. No significant difference was found in miRNA levels among hepatitis B infected, hepatitis C infected, and non-viral groups (Figures 5 and 6).

The correlation of serum Let-7a, miR-221, and miR-222 expression and clinical indicators of patients with HCC

Next, to investigate whether an altered expression profile of serum Let-7a, miR-221, and miR-222 is indicative of HCC diagnosis, the clinical correlation was measured. No

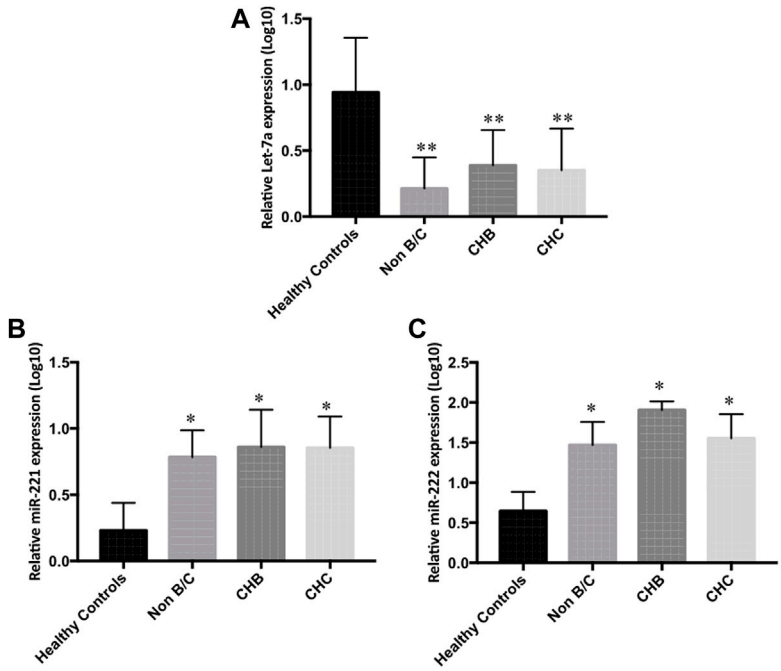

FIGURE 5
Differential serum expression levels of **(A)** Let-7a, **(B)** miR-221, and **(C)** miR-222 in non-B/C (non-hepatitis B and non-hepatitis C), CHB (chronic hepatitis B), and CHC (chronic hepatitis C) groups of patients compared to peritumor tissue were measured by rt-qPCR. The statistical analysis was done using Mann–Whitney test (GraphPad Prism 5.0). The statistically significant *p*-value was denoted as < 0.05. NS; non-significant.

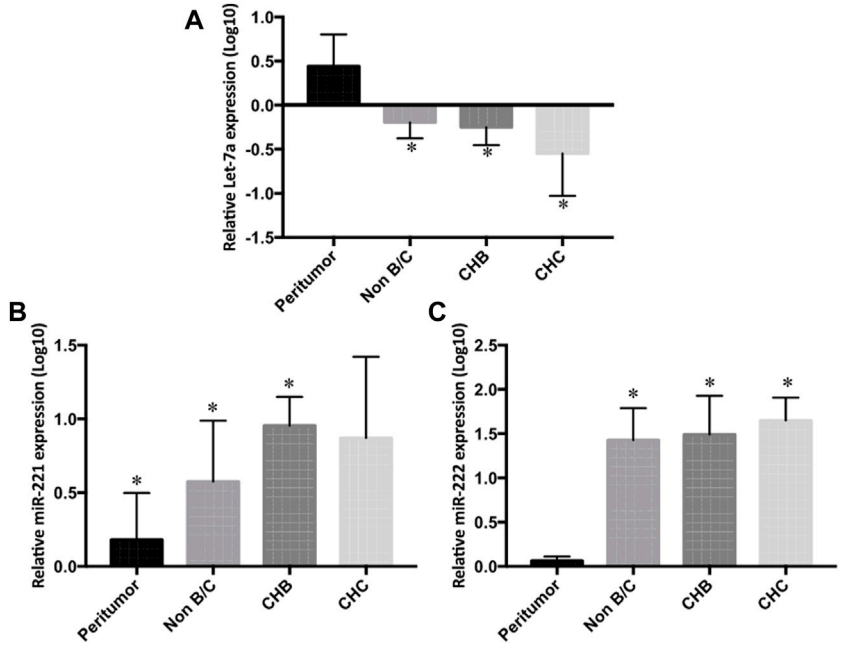

FIGURE 6
Differential tissue expression of **(A)** Let-7a, **(B)** miR-221, and **(C)** miR-222 in non-B/C (non-hepatitis B and non-hepatitis C), CHB (chronic hepatitis B), and CHC (chronic hepatitis C) groups compared to peritumor tissue were measured by rt-qPCR. The statistical analysis was done using Mann–Whitney test (GraphPad Prism 5.0). The statistically significant *p*-value was denoted as < 0.05. NS; non-significant.

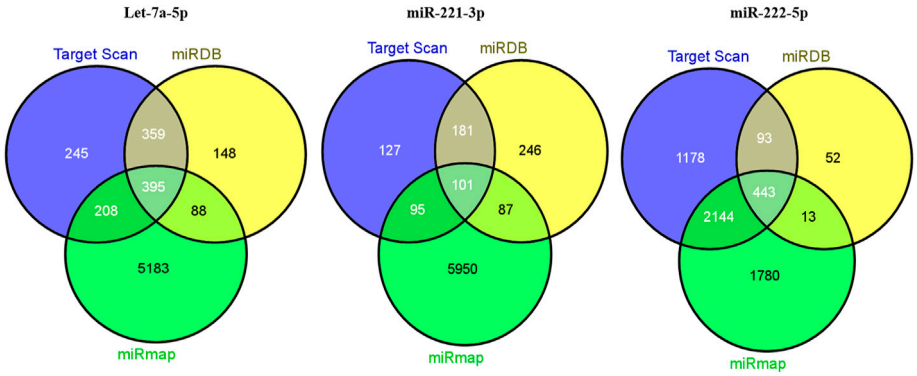

FIGURE 7
Venn diagram for target genes prediction for miRNA signature.

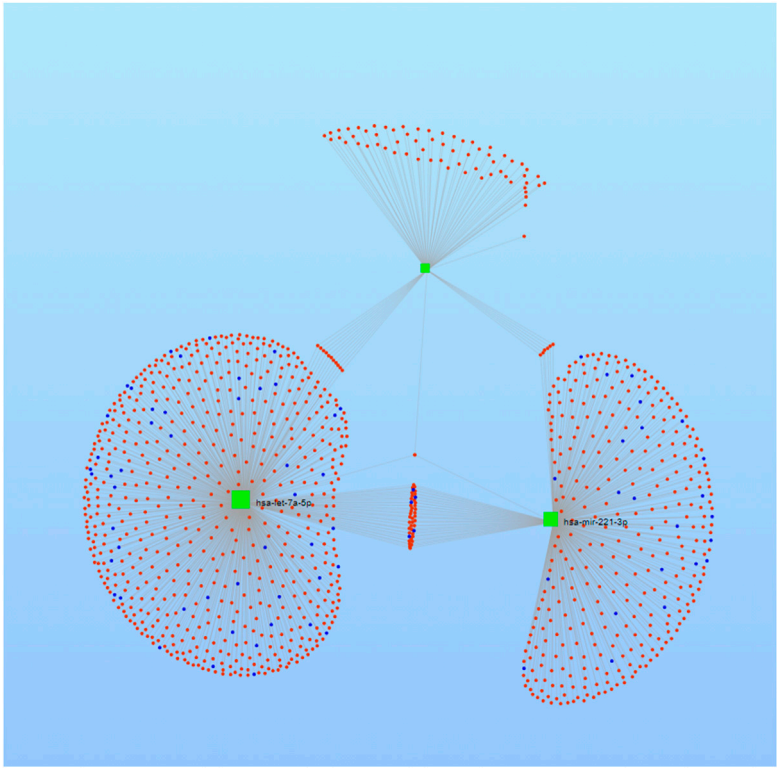

FIGURE 8
Network map of miRNA target genes.

significant association was found between age, gender, S.Bil, S.ALT, S.AST, S.ALP, S.protein, S.albumin, PT, INR, S.AFP, and BCLC/TNM staging and the expression of Let-7a, miR-221, and miR-222.

Prediction of target genes for the three miRNAs

The target genes regulated by the three miRNAs were predicted by three databases. To further enhance the reliability of the bioinformatic analysis, the overlapping target

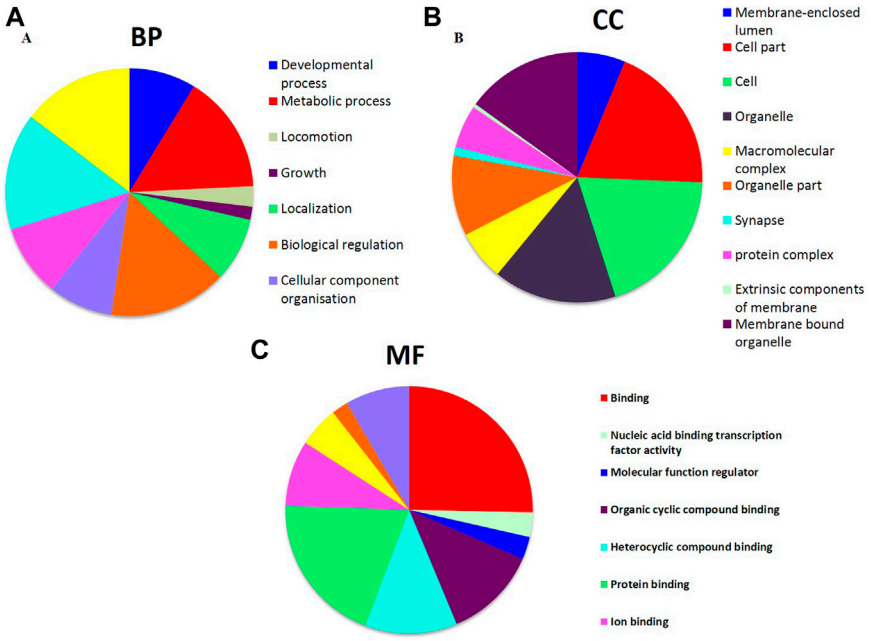

FIGURE 9
GO annotation for the predicted target genes of potential differentially expressed miRNAs. **(A)** Top ten enriched biological process (BP) for target genes of miRNAs. **(B)** Top ten enriched cellular component (CC) for target genes of miRNAs. **(C)** Top ten enriched molecular function (MF) for target genes of miRNAs.

genes were identified. The results indicated that 395, 101, and 443 overlapping genes were identified for Let-7a, miR-221, and miR-222, respectively, by the three databases mentioned previously, which were shown using a Venn diagram (Figure 7).

A total of 1207, 990, and 5874 for hsa-Let-7a-5p, 504, 615, and 6233 for hsa-miR-221-3p, and 3858, 601, and 4380 for hsa-miR-222-5p target genes were predicted using three databases *viz.* TargetScan, miRDB, and mirMap, respectively. To clarify whether the target genes of these miRNAs are likely to participate in the progression of HCC, the intersection of target mRNAs for downregulated miRNAs (hsa-Let-7a-5p) and upregulated mRNAs and target mRNAs for upregulated miRNAs (hsa-miR-221-3p and hsa-miR-222-5p) and downregulated mRNAs were taken. The results were performed on a total of 1,034 genes, including 780 upregulated genes and 254 downregulated genes, respectively. The network between the three miRNAs and their 1034 target genes is shown in Figure 8.

Functional enrichment analysis of target genes associated with HCC

In order to perceive the structured features and biological interpretation of the 1034 predicted target genes, the Gene Ontology (GO) annotation was conducted using the AVID database. The results for the three listed categories of GO, comprising cellular component (CC), biological process (BP), and molecular function (MF), were demonstrated in a pie chart. Among the top ten particulars of target genes, BP analysis mostly includes metabolic process, biological regulation, and organic substance metabolic process. Furthermore, CC analysis mainly contained cell, cell part, and organelle, while MF analysis mainly contained binding, protein binding, and organic cyclic compound binding (Figure 9). The results of KEGG pathways enrichment analysis about the target genes associated with HCC were mainly enriched in the microRNAs in cancer, oncogene induction senescence, pancreatic adenocarcinoma pathway, Fas ligand pathway, stress induction of heat shock proteins regulation, and hepatitis C and HCC pathway (Figure 10 and Supplementary Figures S1 and S2).

Discussion

HCC is the fifth most prevalent malignancy and the second dominant cause of cancer-related mortality worldwide, with a 5-year survival rate of barely 5%, making it the third most lethal malignancy (Huang et al., 2021). The dismal prognosis of HCC is mostly owing to the late diagnosis of this disease. Hence, early detection of HCC can facilitate effective treatment and minimize disease mortality. Currently, serum levels of liver enzymes such as ALT, AST, glutamyl transpeptidase (GGT), and AFP are being utilized as biomarkers to assess liver damage and therapy response (Gowda et al., 2009). Even so, ALT, AST, and

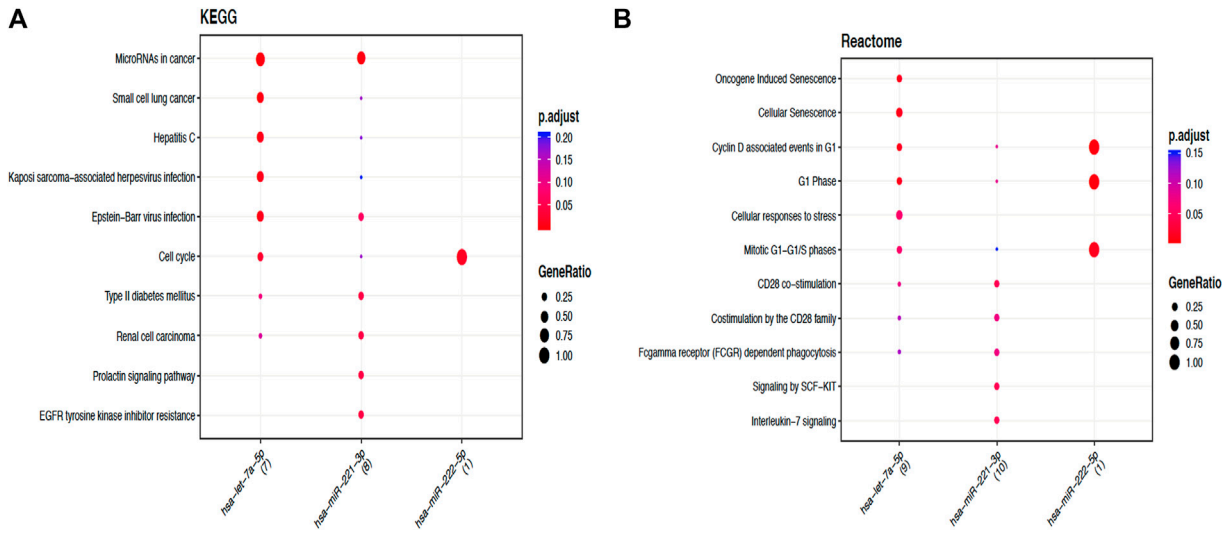

FIGURE 10
Functional enrichment analysis of target genes associated with HCC. **(A)**. Dotplot of the KEGG signal pathway showing the counts of genes. Functional enrichment analysis of target genes associated with HCC. **(B)** Reactome of the KEGG signal pathway showing the "pathway–gene" network.

alkaline phosphatase levels might also be raised as a result of muscle and bone injury (Giannini et al., 2005). In addition to this, numerous novel serum indicators, such as DCP and AFP-L3, have been found to have higher diagnostic efficacy for HCC, yet these have to be widely verified in routine clinical practice (Zhou et al., 2021). This raises concerns about the specificity of existing diagnostic markers utilized in clinics, necessitating a deeper knowledge of the present liver-specific biomarkers. Furthermore, since HCC is frequently identified at an advanced stage, resulting in severe liver damage and restricted treatment choices, new sensitive biomarkers should be sought to overcome early detection.

Recently, miRNAs have emerged as novel non-invasive biomarkers for the diagnosis and prognosis of various human cancers, including HCC. Importantly, a number of studies have documented the tissue- or organ-specific expression of microRNAs, suggesting the high specificity of microRNAs as biomarkers. Since the first report on the use of microRNA as potential diagnostic biomarkers by Lawrie et al. in 2008 on large B-cell lymphoma, the notion has been pursued in a number of studies involving various other cancer types, including the potential use of circulating miRNAs as biomarkers for HCC (Yang et al., 2019). An extensive and considerable number of studies have reported dysregulation of microRNAs during the initiation and progression of HCC. These studies were largely based on comparisons between malignant, benign, and pre-cancerous lesions compared with a healthy liver or adjacent peritumoral tissues. The approach of direct measurement of tissue microRNAs is challenging as invasive biopsy or surgery is required for collecting tissue samples. Conversely, circulating microRNAs provide an alternative non-invasive approach to be used as tumor biomarkers. Notably, the level of liver microRNAs has been found to correlate with serum microRNA levels in many studies (Shao et al., 2019; Mohamed et al., 2020). One of the major advantages of mature microRNAs as biomarkers is their stability in body fluids such as serum, plasma, urine, saliva, and cerebrospinal fluid over a wide range of temperatures (Ting et al., 2020). Mature microRNAs are complexed with AGO2 or other argonaute proteins, thereby augmenting their stability (Yang et al., 2018). Liver microRNAs may be secreted into the circulation passively through apoptosis and necrosis as ribonucleoprotein complexes or may be transported within viral particles such as HBV surface antigen (HBsAg) or enclosed within exosomes/microvesicles (Shimizu et al., 2010; Yang et al., 2018; Singal et al., 2020). Therefore, the capability to measure microRNA levels secreted in the serum might stipulate a way to estimate microRNA activity in the liver.

In recent years, several miRNAs have been proposed to exhibit high diagnostic accuracy in discriminating patients with HCC from healthy controls. Studies have shown serum miR-143 and miR-215 as promising biomarkers for hepatocellular carcinoma (Zhang et al., 2014b). Xie et al. found that miR-101 could significantly differentiate HBV-HCC from HBV-associated liver cirrhosis (Moeini et al., 2012). Another study reported serum miR-150 as a biomarker for the diagnosis and prognosis of HCC patients (Joyce and Pollard, 2009). Li et al. classified miR-18a as a potential biomarker for screening hepatitis B virus-related HCC

(Hatziapostolou et al., 2011). (El-Ahwany et al., 2019) So far, the conclusions on the use of serum miRNAs as non-invasive biomarkers have been contradictory, and efforts to develop a less-invasive approach using serum miRNA combination have met limited success. Thus, in the present study, we hypothesized that inclusion of additional markers, such as miRNAs, might further increase the value of the HCC diagnosis investigations.

Consequently, based on the comprehensive literature review, a panel of ten miRNAs (Let-7a, miR-221, miR-26a, miR-124, miR-222, miR-340, miR-126, miR-15a, miR-219, and miR-155) that were reported in diverse cancers together with HCC was chosen for the study.

In order to examine the regulation of differentially expressed miRNAs in hepatocellular carcinoma, regulation of the panel of ten miRNAs (Let-7a, miR-221, miR-222, miR-26a, miR-124, miR-340, miR-126, miR-15a, miR-219, and miR-155) selected on the basis of literature and *In Silico* analysis was carried out in HCC patients. Our results indicated that miR-221, miR-340, miR-126, miR-219, and miR-155 were upregulated, whereas Let-7a, miR-26a, miR-124, and miR-222 were downregulated in HCC patients compared to HC. However, the expression of miR-15a was non-significant when compared among the groups (Figure 1).

Correspondingly, while investigating the tissue levels, we found the high expression of miR-221, miR-124, miR-340, miR-222, and miR-155 and low expression of Let-7a and miR-26a in the tumor tissue of HCC patients compared to their peritumor counterparts. Nevertheless, the expression of miR-126, miR-15a, and hsa-miR-219 was found to be non-significant (Figure 2).

Furthermore, our data indicated that among the nine differentially expressed miRNAs, Let- 7a showed the best diagnostic efficacy, followed by miR-221 and miR-222, whereas miR-26a, miR-124, miR-340, miR-126, and miR-155 were unable to distinguish HCC patients from HC patients (Figure 3).

Subsequently, a step-wise logistic regression model was utilized to analyze the performance of the three-miRNA panel in combination with AFP in discriminating HCC from HC. We found that the combination of Let-7a, miR-221, and miR-222 had a significant superiority over each miRNA separately and AFP alone in distinguishing HCC patients from HC. Additionally, our data also suggested that the diagnostic efficacy of Let-7a and miR-221 alone were superior to that of AFP, while miR-222 had a diagnostic efficiency equal to that of AFP (Figure 4).

Subsequently, with the aim to understand the interactome of predicted target genes for Let-7a, miR-221, and miR-222, a total of 1,034 intersecting genes predicted by three bioinformatic tools were used to construct the miRNA-mRNA interaction network (Figure 8). Among the top ten particulars of target genes, BP analysis mostly includes metabolic process, biological regulation, and organic substance metabolic process. Furthermore, CC analysis mainly contained cell, cell part, and organelle, while MF analysis mainly contained binding, protein binding, and organic cyclic compound binding (Figure 9). KEGG pathway enrichment analysis revealed that the genes were mainly enriched in the microRNAs in cancer, oncogene induction senescence, pancreatic adenocarcinoma pathway, and hepatitis C and HCC pathway, indicating possible crosstalk of miRNAs in cancer with HCC (Figure 10 and Supplementary Figures S1 and S2).

Conclusion

In conclusion, we identified three miRNAs; Let-7a, significantly expressed at a lower level, and miR-221 and miR-222, significantly expressed at higher levels, in HCC patients compared to HC volunteers. Based on the ROC analysis, we propose that these three miRNAs can be feasible noninvasive HCC biomarkers. Notably, the panel of the three miRNAs (Let-7a, miR-221, and miR-222) showed the best diagnostic performance than a single miRNA. In a profound analysis, we found that plasma Let-7a, miR-221, and miR-222 expression profiles were common to patients with hepatitis B- and hepatitis C-associated HCC irrespective of the underlying etiology. It is, thus, worthwhile to validate the use of the three-miRNA panel reported in our study for second-line testing in a larger cohort of patients and elucidate the underlying mechanism of the deregulation of circulatory miRNAs. Furthermore, the possible function is inferred by predicting the model for target genes, which improves our understanding of HCC carcinogenesis and progression. To our knowledge, this is the first clinical study that delineated the role of a three-miRNA-panel (comprising Let-7a, miR-221, and miR-222) in the non-invasive diagnosis and plausible therapeutic management of HCC patients. Given the critical role of Let-7a, miR-221, and miR-222 in HCC development, this three-miRNA-panel may improve risk prediction and furnish new insights into the pathological mechanism of HCC development. Together with AFP, this three-miRNA-panel reposes better efficacy in discriminating HCC patients from healthy controls (HCs) than the existing miRNA-based biomarkers. This study may also help in the identification of novel targets for the therapeutic intervention of HCC and may provide a rationale for improving existing cancer therapies, prominently driven by the fact that both hepatitis B virus (HBV) and hepatitis C virus (HCV) infections result in chronic hepatitis paramounting to the HCC development. Furthermore, the expression of miRNAs in response to HBV and HCV infection varies dramatically between the two viruses. Henceforth, the early detection and rapid development of new therapeutic antivirals for HCC necessitate the discovery of novel miRNA biomarkers common to the array of all etiologies.

Data availability statement

The original contributions presented in the study are included in the article/Supplementary Material; further inquiries can be directed to the corresponding author.

Ethics statement

The studies involving human participants were reviewed and approved by IEC/Sher-I-Kashmir Institute of Medical Sciences Protocol # RP:96/2018. Written informed consent to participate in this study was provided by the participants' legal guardian/ next of kin.

Author contributions

TY carried out the experiments and drafted the manuscript. SD planned the experiments and was involved in writing the manuscript. SA, NC, ZR, and AS were involved in patient enrollment and collection of clinical samples. RR critically evaluated the manuscript. TY, SD, and RR performed the statistical analysis. DA was involved in conceiving the project, planning the experiments and overall analysis of the manuscript, and arranging intramural grants for the study. All the authors finally approved the manuscript.

Funding

The study was funded by the intramural grants approved by Sher-I-Kashmir Institute of Medical Sciences.

Conflict of interest

The authors declare that the research was conducted in the absence of any commercial or financial relationships that could be construed as a potential conflict of interest.

Publisher's note

Supplementary material

The Supplementary Material for this article can be found online at: https://www.frontiersin.org/articles/10.3389/fgene.2022.929787/full#supplementary-material

References

Acunzo, M., Romano, G., Wernicke, D., and Croce, C. M. (2015). MicroRNA and cancer--a brief overview. *Adv. Biol. Regul.* 57, 1–9.

Aleman, S., Rahbin, N., Weiland, O., Davidsdottir, L., Hedenstierna, M., Rose, N., et al. (2013). A risk for hepatocellular carcinoma persists long-term after sustained virologic response in patients with hepatitis C-associated liver cirrhosis. *Clin. Infect. Dis.* 57, 230–236.

Anwar, S. L., and Lehmann, U. (2015). MicroRNAs: Emerging novel clinical biomarkers for hepatocellular carcinomas. *J. Clin. Med.* 4, 1631–1650. doi:10.3390/jcm4081631

Arrese, M., Eguchi, A., and Feldstein, A. E. (2015). Circulating microRNAs: Emerging biomarkers of liver disease. *Semin. Liver Dis.* 35, 43–54. doi:10.1055/s-0034-1397348

Bargellini, I., Battaglia, V., Bozzi, E., and Luca, D. (2014). Radiological diagnosis of hepatocellular carcinoma. *J. Hepatocell. Carcinoma* 1, 137–148. doi:10.2147/JHC.S44379

Bhasin Lal, S., Venkatesh, V., Kumar, A., and Aneja, A. (2021). Liver abscess in children-experience from a single tertiary care center of North India: Etiology, clinical profile and predictors of complications. *J. Pediatr. Infect. Dis.* doi:10.1097/INF.0000000000003053

Borel, F., Konstantinova, P., and Jansen, P. L. (2012). Diagnostic and therapeutic potential of miRNA signatures in patients with hepatocellular carcinoma. *J. Hepatol.* 56, 1371–1383. doi:10.1016/j.jhep.2011.11.026

Cheng, S. Q., Wang, H., Li, N., Chen, Y. F., and Gao, C. F. (2011). Serum microRNAs as biomarkers for hepatocellular carcinoma in Chinese patients with chronic Hepatitis B virus infection. *PLoS One* 6, e28486. doi:10.1371/journal.pone.0028486

Chirshev, E., Oberg, K. C., Ioffe, Y. J., and Unternaehrer, J. J. (2019). Let-7 as biomarker, prognostic indicator, and therapy for precision medicine in cancer. *Clin. Transl. Med.* 8, 24.

Dong, Y., Fu, C., Guan, H., Zhang, Z., Zhou, T., and Li, B. (2016). Prognostic significance of miR-126 in various cancers: A meta-analysis. *Onco Targets Ther.* 9, 2547–2555.

El-Ahwany, E. G. E., Mourad, L., Zoheiry, M. M. K., and Abu-Taleb, H. (2019). MicroRNA-122a as a non-invasive biomarker for HCV genotype 4-related hepatocellular carcinoma in Egyptian patients. *Arch. Med. Sci.* doi:10.5114/aoms.2019.86621

Fattovich, G., Stroffolini, T., Zagni, I., and Donato, F. (2004). Hepatocellular carcinoma in cirrhosis: Incidence and risk factors. *Gastroenterology* 127, S35–S50. doi:10.1053/j.gastro.2004.09.014

Friedman, R. C., Farh, K. K., Burge, C. B., and Bartel, D. P. (2009). Most mammalian mRNAs are conserved targets of microRNAs. *Genome Res.* 19, 92–105. doi:10.1101/gr.082701.108

Giannini, D. M., Bray, F., Ferlay, J., and Pisani, P. (2005). Global cancer statistics. *CA Cancer J. Clin.* 55, 74–108.

Giovannetti, E., Erozenci, A., Smit, J., Danesi, R., and Peters, G. J. (2012). Molecular mechanisms underlying the role of microRNAs (miRNAs) in anticancer drug resistance and implications for clinical practice. *Crit. Rev. Oncol. Hematol.* 81, 103–122. doi:10.1016/j.critrevonc.2011.03.010

Gowda, S., Desai, P. B., Hull, V. V., and Math, A. A. K. (2009). A review on laboratory liver function tests. *Pan. Afr. Med. J.* 22 (3), 17.

Hatziapostolou, M., Polytarchou, C., Aggelidou, E., Drakaki, A., Poultsides, G. A., Jaeger, S. A., et al. (2011). An HNF4α-miRNA inflammatory feedback circuit regulates hepatocellular oncogenesis. *Cell.* 147, 1233–1247.

He, R. Q., Yang, X., Liang, L., Chen, G., and Ma, J. (2018). MicroRNA-124-3p expression and its prospective functional pathways in hepatocellular carcinoma: A quantitative polymerase chain reaction, gene expression omnibus and bioinformatics study. *Oncol. Lett.* 15, 5517–5532.

Huang, G. L., Guo, H. Q., Guo, C. C., Li, H., Ye, S., Ling, S., et al. (2010). Circulating miR-221 directly amplified from plasma is a potential diagnostic and

prognostic marker of colorectal cancer and is correlated with p53 expression. *J. Gastroenterol. Hepatol.* 25, 1674–1680.

Huang, Z., Xu, Y., Wan, M., Zeng, X., and Wu, J. (2021). miR-340: A multifunctional role in human malignant diseases. *Int. J. Biol. Sci.* 17, 236–246.

Jemal, A., Bray, F., Center, M. M., Ferlay, J., Ward, E., and Forman, D. (2011). Global cancer statistics. *Ca. Cancer J. Clin.* 61, 69–90. doi:10.3322/caac.20107

Joyce, J. A., and Pollard, J. W. (2009). Microenvironmental regulation of metastasis. *Nat. Rev. Cancer* 9, 239–252. doi:10.1038/nrc2618

Kim, V. N. (2005). MicroRNA biogenesis: Coordinated cropping and dicing. *Nat. Rev. Mol. Cell. Biol.* 6, 376–385. doi:10.1038/nrm1644

Ladeiro, Y., Couchy, G., Balabaud, C., Bioulac-Sage, P., Pelletier, L., Rebouissou, S., et al. (2008). MicroRNA profiling in hepatocellular tumors is associated with clinical features and oncogene/tumor suppressor gene mutations. *Hepatology* 47, 1955–1963. doi:10.1002/hep.22256

Lawrie, C. H., Gal, S., Dunlop, H. M., Pushkaran, B., Liggins, A. P., Pulford, K., et al. (2008). Detection of elevated levels of tumour-associated microRNAs in serum of patients with diffuse large B-cell lymphoma. *Br. J. Haematol.* 141, 672–675.

Li, H., Li, X. Y., Liu, L. H., Sun, W., and Xiao, T. (2015). Prognostic role of MicroRNA-126 for survival in malignant tumors: A systematic review and meta-analysis. *Dis. Markers* 2015, 739469.

Liu, W., Hu, K., Zhang, F., Lu, S., Chen, R., Ren, Z., et al. (2021). The prognostic significance of microRNA-221 in hepatocellular carcinoma: An updated meta-analysis. *Int. J. Biol. Markers* 36, 17246008211032689.

Llovet, J. M., Kelley, R. K., Villanueva, A., and Singa, A. G. (2021). Hepatocellular carcinoma. *Nat. Rev. Disease Primers* 7, 6. doi:10.1038/s41572-020-00240-3

Melo, S. A., and Esteller, M. (2011). Dysregulation of microRNAs in cancer: Playing with fire. *FEBS Lett.* 585, 2087–2099. doi:10.1016/j.febslet.2010.08.009

Moeini, A., Cornellà, H., and Villanueva, A. (2012). Emerging signaling pathways in hepatocellular carcinoma. *Liver Cancer* 1, 83–93. doi:10.1159/000342405

Mohamed, A. A., Omar, A. a. A., El-Awady, R. R., Hassan, S. M. A., Eitah, W. M. S., Ahmed, R., et al. (2020). MiR-155 and MiR-665 role as potential non-invasive biomarkers for hepatocellular carcinoma in Egyptian patients with chronic hepatitis C virus infection. *J. Transl. Int. Med.* 8, 32–40.

Noureddin, M., and Rinella, M. E. (2014). Nonalcoholic fatty liver disease, diabetes, obesity, and hepatocellular carcinoma. *Clin Liver Dis.* 19, 361–379. doi:10.1016/j.cld.2015.01.012

Parkin, D. M., Bray, F., Ferlay, J., and Pisani, P. (2002). Global cancer statistics. *Cancer J. Clin.* 55, 74–108.

Patel, M., Shariff, M. I., Ladep, N. G., Thillainayagam, A. V., Thomas, H. C., Khan, S. A., et al. (2012). Hepatocellular carcinoma: Diagnostics and screening. *J. Eval. Clin. Pract.* 18, 335–342. doi:10.1111/j.1365-2753.2010.01599.x

Ravegnini, G., Cargnin, S., Sammarini, G., Zanotti, F., Bermejo, J. L., Hrelia, P., et al. (2019). Prognostic role of miR-221 and miR-222 expression in cancer patients: A systematic review and meta-analysis. *Cancers (Basel)* 11.

Shao, C., Yang, F., Qin, Z., Jing, X., Shu, Y., and Shen, H. (2019). The value of miR-155 as a biomarker for the diagnosis and prognosis of lung cancer: A systematic review with meta-analysis. *BMC Cancer* 19, 1103.

Shimizu, S., Takehara, T., Hikita, H., Kodama, T., Miyagi, T., Hosui, A., et al. (2010). The let-7 family of microRNAs inhibits Bcl-xL expression and potentiates sorafenib-induced apoptosis in human hepatocellular carcinoma. *J. Hepatol.* 52, 698–704.

Singal, A. G., Lampertico, P., and Nahon, P. (2020). Epidemiology and surveillance for hepatocellular carcinoma: New trends. *J. Hepatol.* 72, 250–261. doi:10.1016/j.jhep.2019.08.025

Ting, G., Li, X., Kwon, H. Y., Ding, T., Zhang, Z., Chen, Z., et al. (2020). microRNA-219-5p targets NEK6 to inhibit hepatocellular carcinoma progression. *Am. J. Transl. Res.* 12, 7528–7541.

Vasuri, B., and Wang, G. (2015). MicroRNAs involved with hepatocellular carcinoma (Review). *Oncol. Rep.* 34, 2811–2820. doi:10.3892/or.2015.4275

Vaz, J., Ansari, D., Sasor, A., and Andersson, R. (2015). Sparc: A potential prognostic and therapeutic target in pancreatic cancer. *Pancreas* 44, 1024–1035. doi:10.1097/MPA.0000000000000409

Wu, L. P., Wu, J., Shang, A., Yang, M., Li, L. L., Yu, J., et al. (2018). miR-124 inhibits progression of hepatocarcinoma by targeting KLF4 and promises a novel diagnostic marker. *Artif. Cells Nanomed Biotechnol.* 46, 159–167.

Yang, J. D., and Roberts, L. R. (2010). Hepatocellular carcinoma: A global view. *Nat. Rev. Gastroenterol. Hepatol.* 7, 448–458. doi:10.1038/nrgastro.2010.100

Yang, F. R., Li, H. J., Li, T. T., Zhao, Y. F., Liu, Z. K., and Li, X. R. (2019). Prognostic value of MicroRNA- 15a in human cancers: A meta-analysis and bioinformatics. *Biomed. Res. Int.* 2019, 2063823.

Yang, J., Sheng, Y. Y., Wei, J. W., Gao, X. M., Zhu, Y., Jia, H. L., et al. (2018). MicroRNA-219-5p promotes tumor growth and metastasis of hepatocellular carcinoma by regulating cadherin 1. *Biomed. Res. Int.* 2018, 4793971.

Zhang, J. Y., Chen, J., Xu, Y., Song, N. H., and Yin, C. J. (2014a). Prognostic role of microRNA- 221 in various human malignant neoplasms: A meta-analysis of 20 related studies. *PLoS One* 9, e87606.

Zhang, W. T., Zhang, G. X., and Gao, S. S. (2021). The potential diagnostic accuracy of let-7 family for cancer: A meta-analysis. *Technol. Cancer Res. Treat.* 20, 15330338211033061.

Zhang, Z. Q., Meng, H., Wang, N., Liang, L. N., Liu, L. N., Lu, S. M., et al. (2014b). Serum microRNA 143 and microRNA 215 as potential biomarkers for the diagnosis of chronic hepatitis and hepatocellular carcinoma. *Diagn. Pathol.* 9, 135. doi:10.1186/1746-1596-9-135

Zhou, Z., Lv, J., Wang, J., Yu, H., Lu, H., Yuan, B., et al. (2019). Role of MicroRNA-124 as a prognostic factor in multiple neoplasms: A meta-analysis. *Dis. Markers* 2019, 1654780.

Zhou, J. M., Wang, T., and Zhang, K. H. (2021). AFP-L3 for the diagnosis of early hepatocellular carcinoma: A meta-analysis. *Medicine (Baltimore)* 100 (43), e27673. doi:10.1097/MD.0000000000027673

Zhu, W. J., Yan, Y., Zhang, J. W., Tang, Y. D., and Han, B. (2020). Effect and mechanism of miR-26a- 5p on proliferation and apoptosis of hepatocellular carcinoma cells. *Cancer Manag. Res.* 12, 3013–3022.

Zhuang, L. P., and Meng, Z. Q. (2015). Serum miR-224 reflects stage of hepatocellular carcinoma and predicts survival. *Biomed. Res. Int.* 2015, 731781.

frontiers | Frontiers in Genetics

TYPE Review
PUBLISHED 17 February 2023
DOI 10.3389/fgene.2023.1052731

OPEN ACCESS

EDITED BY
Nadeem Shabir,
Sher-e-Kashmir University of Agricultural Sciences and Technology, India

REVIEWED BY
Alessandro Paolini,
Bambino Gesù Children's Hospital (IRCCS), Italy
Muhammad Nawaz,
University of Gothenburg, Sweden

*CORRESPONDENCE
Faizah Alotaibi,
AlotaibiFai@ksau-hs.edu.sa

SPECIALTY SECTION
This article was submitted to RNA, a section of the journal Frontiers in Genetics

RECEIVED 24 September 2022
ACCEPTED 07 February 2023
PUBLISHED 17 February 2023

CITATION
Alotaibi F (2023), Exosomal microRNAs in cancer: Potential biomarkers and immunotherapeutic targets for immune checkpoint molecules.
Front. Genet. 14:1052731.
doi: 10.3389/fgene.2023.1052731

Exosomal microRNAs in cancer: Potential biomarkers and immunotherapeutic targets for immune checkpoint molecules

Faizah Alotaibi*

College of Science and Health Professions, King Saud bin Abdulaziz University for Health Sciences and King Abdullah International Medical Research Center, Ministry of National Guard Health Affairs, Riyadh, Saudi Arabia

Exosomes are small extracellular vesicles with a lipid bilayer structure secreted from different cell types which can be found in various body fluids including blood, pleural fluid, saliva and urine. They carry different biomolecules including proteins, metabolites, and amino acids such as microRNAs which are small non-coding RNAs that regulate gene expression and promote cell-to-cell communication. One main function of the exosomal miRNAs (exomiRs) is their role in cancer pathogenesis. Alternation in exomiRs expression could indicate disease progression and can regulate cancer growth and facilitate drug response/resistance. It can also influence the tumour microenvironment by controlling important signaling that regulating immune checkpoint molecules leading to activation of T cell anti-tumour immunity. Therefore, they can be used as potential novel cancer biomarkers and innovative immunotherapeutic agents. This review highlights the use of exomiRs as potential reliable biomarkers for cancer diagnosis, treatment response and metastasis. Finally, discuses their potential as immunotherapeutic agents to regulate immune checkpoint molecules and promote T cell anti-tumour immunity.

KEYWORDS

exosomal miRNA, extracellular vesicles (EVs), cancer, small non-coding RNAs (sncRNAs), biomarker, clinical implication, liquid biopsy, immune checkpoint molecules

1 Introduction

Extracellular vesicles (EVs) were initially described by Harding in 1983 (Harding et al., 1983) and later confirmed by Pan in 1985 (Pan et al., 1985). At first, they were known as vehicles for clearance of cellular "waste" which results from cell metabolism with no influence on neighboring cells. This concept, however, switched after the finding of other biomolecules, e.g., amino acids, fatty acid, and nucleic acids including small RNAs particularly microRNA in 2007 (Théry et al., 2002; Valadi et al., 2007). Upon release from cells, they can circulate to the neighboring cells and internalized *via* endocytosis (Larrea et al., 2016) and ultimately result in cell-to-cell communication and contribute to reprogram the recipient cells (Meldolesi, 2018). Thus, exosomal microRNAs (exomiRs) play a major role in intercellular communication to regulate gene expression (Théry, 2011; Kozomara and Griffiths-Jones, 2014). All type of cells including cancer cells can naturally secrete exosomes (Théry et al., 2002) in which can be isolated from different bio-fluids including urine and serum. This secretion is a result of

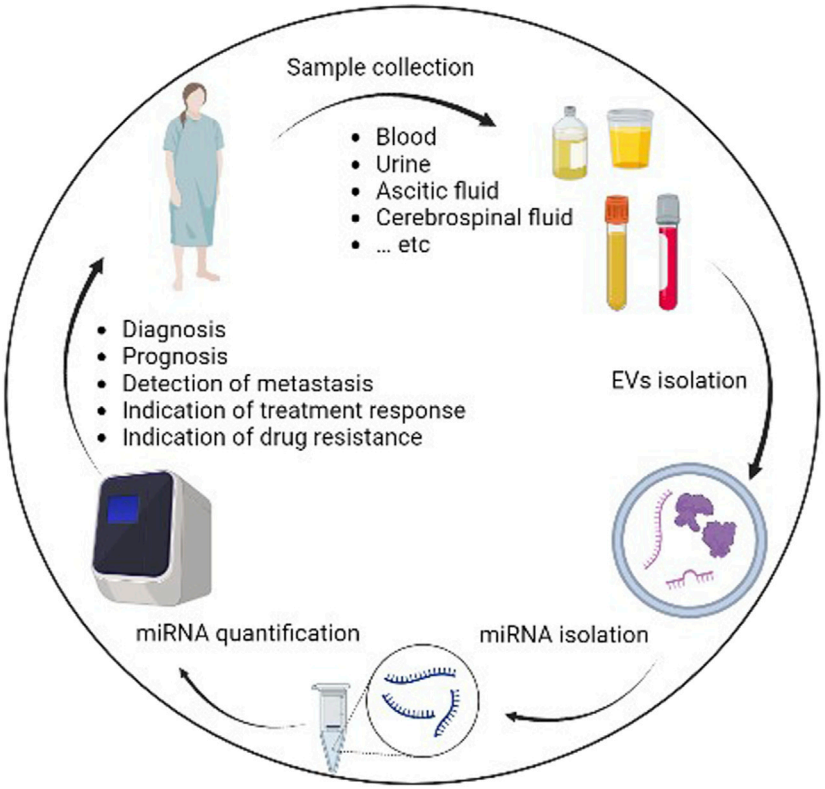

FIGURE 1
Workflow of processing and utilization of exomiRs for cancer clinical implication.

cells undergoing difference condition such as apoptosis/necrosis or chronic inflammation which suggest a possible source of less-invasive method of the so-called "liquid biopsy".

ExomiRs can be isolated from variety of body fluid including blood, saliva, urine, and breast milk (Figure 1) by differential ultracentrifugation (Amorim et al., 2017) which results in separation of exomiRs from contaminated cells, cellular debris and other EVs subtype such as apoptotic bodies and microparticles (Théry et al., 2006). Further techniques based on size exclusion such as chromatography and Optiprep™ density gradient have been used to increase the purity of exomiRs isolation (Boing et al., 2014; Lobb et al., 2015). In 2014, the International Society for EVs has published recommendations for EVs definition and their functions (Lotvall et al., 2014). Protein expression for at least three EV markers (e.g., CD63, CD81 and CD9) is typically used to identify the purity of the sample (Ekström et al., 2022). Furthermore, the use of two techniques (e.g., electron microscopy and nanoparticle tracking analysis) are recommended to illustrate the degree of heterogeneity in the sample (Dragovic et al., 2011; Van der Pol et al., 2014). To help standardize the protocols, EV-TRACK knowledgebase project (Can be access at http://evtrack.org) was developed and conducted by international collaboration from several countries (Van Deun et al., 2017). This helps researchers to add methodological parameters into central repository to quantifies their protocol. It is recommended to follow protocol based on the biofluid resources (Ramirez et al., 2018). For example, when working with blood as a source for the exomiRs, challenges like hemolysis has been shown to decrease the expression of some microRNAs and agitation used to stimulate blood transportation can lead to release of platelets (Ramirez et al., 2018). Another important factor is the storage time which can affect exomiRs yield (Ramirez et al., 2018). Comparison study shows increase amount of exomiRs isolated from the blood after storage for 3 h compared to freshly isolated blood which can be due to platetets-drived EVs (Ramirez et al., 2018).

In cancer, alternation in exomiRs expression is a well-known feature in cancer (Alotaibi, 2021). It can bind to messenger RNA which results in posttranscriptional gene regulation that promote cancer cell processes including progression and metastasis (Lin and Gregory, 2015). This process is critical for carcinogenesis, which help cancer cells thrive in the tumour microenvironment. For example, crosstalk between cancer cell and surrounding cells including immune cells and stromal cells leading to pre-metastatic niche development. Therefore, investigating exomiRs secreted from cancer cells is important to reveal cancer behavior and metastasis and understand their potential role as cancer biomarkers and to develop novel immunotherapeutic agents for cancer. This review describes the use of exomiRs as potential biomarkers for cancer diagnosis/prognosis, treatment response, and cancer metastasis and explore their role as innovative immunotherapeutic agents for cancer.

TABLE 1 List of exomiRs used for cancer diagnosis.

Centralize the miRNAs ID	Pattern of expression	Cancer type	Tumor stage	Body fluid source	References
ExomiR-92	Increased	Colorectal cancer	All stages	Plasma and tissue samples	Ng et al. (2009)
ExomiR-17-5p and exomiR-92a-3p	Increased	Colorectal cancer	Higher clinical stages	Serum	Fu et al. (2018)
ExomiR-17-5p, exomiR-21, exomiR-106a and exomiR-106b	Increased	Gastric cancer	Stages I-IV	Plasma	Tsujiura et al. (2010)
ExomiR-21, exomiR-155, exomiR-210 and exomiR-196a	Increased	Pancreatic adenocarcinoma patients	All stages	Plasma	Wang et al. (2009)
ExomiR-500	Increased	Hepatocellular carcinoma	Not mentioned	Serum	Yamamoto et al. (2009)
ExomiR-184	Increased	Squamous-cell carcinoma of the tongue	Not mentioned	Plasma	Wong et al. (2008)
ExomiR-125a and exomiR-200a	Decreased	Oral squamous-cell carcinoma	Stages I-IV	Saliva	Park et al. (2009)
63 exomiRs	Increased	Non-small-cell lung cancer	Stages I-IV	Serum	(Chen et al., 2008a)
34 exomiRs	Increased	Asymptomatic NSCLC	Early-stage nodule (Ia or Ib)	Serum	Bianchi et al. (2011)
21 exomiRs	Increased	Lung cancer	12–28 before and at the time of diagnosis	Plasma	Boeri et al. (2011)
hsa-miR-212, -214, −205, −210, −203, −191, −192, −146, −155, −21, −106a and -17-3p	Increased	Lung adenocarcinoma	Stages I-IV	Tissues biopsy	Rabinowits et al. (2009)
ExomiR-200-5p, exomiR-379, exomiR-139-5p and exomiR-378a	Increased	Lung adenocarcinoma	Early-stage nodule (Ia or Ib)	Tissue biopsy and plasma	Cazzoli et al. (2013)
ExomiR-141 and other 15 exomiRs	Increased	Prostate cancer	Stage 3 and 4	Serum	Lodes et al. (2009)
ExomiR-21-5p, exomiR-574-3p, and exomiR-141-5p	Increased	Prostate cancer	Not mentioned	Urine	Samsonov et al. (2016)
ExomiR-92, exomiR-93 and exomiR-126	Increased	Epithelial ovarian cancer	Stages I-IV	Serum	Resnick et al. (2009)
ExomiR-21, exomiR-141, exomiR-200a, exomiR-200c, exomiR-200b, exomiR-203, exomiR-205 and exomiR-214)	Increased	Ovarian cancer	Various stages	Serum	Taylor and Gercel-Taylor (2008)
ExomiR-195	Increased	Breast cancer	Stage IV	Serum, plasma, or whole blood	Heneghan et al. (2010)
ExomiR-101 and exomiR-372	Increased	Breast cancer and triple-negative breast cancer	pT1 pT2-4	Serum	Eichelser et al. (2014)
ExomiR-199a-3p	Increased	Pediatric neuroblastoma	Not mentioned	Plasma	Ma et al. (2019)
ExomiR-16	Increased	Pediatric acute lymphoblastic leukemia	Not mentioned	Blood	Kaddar et al. (2009)
ExomiR-21	Increased	Pediatric Hepatoblastoma	Not mentioned	Plasma	Liu et al. (2016b)

(Continued on following page)

TABLE 1 (*Continued*) List of exomiRs used for cancer diagnosis.

Centralize the miRNAs ID	Pattern of expression	Cancer type	Tumor stage	Body fluid source	References
ExomiR-7112-5p, exomiR-885-3p and exomiR-1245a	Increased	Pediatric acute myeloid leukaemia	Risk of disease recurrence	Plasma	Zampini et al. (2017)
ExomiR-25-3p	Increased	Osteosarcoma	Not mentioned	Serum	Fujiwara et al. (2017)
ExomiR-125b	Decreased	Ewing's sarcoma	Metastasis and non-metastasis	Serum	Nie et al. (2015)
ExomiR-21	Increased	Diffuse large B cell lymphoma	Stages I-IV	Serum	Lawrie et al. (2008)
ExomiR-92a	Decreased	Acute leukemias	Not mentioned	Plasma	Tanaka et al. (2009)
ExomiR-148a, exomiR-181a, exomiR-20a, exomiR-221, exomiR-625, and exomiR-9	Increased	Multiple myeloma	Not mentioned	Plasma	Huang et al. (2012a)
ExomiR-32, exomiR-98 and exomiR-374	Decreased	Chronic lymphocytic leukemia	Not mentioned	Blood	Rahimi et al. (2021)
ExomiR-451	Increased	Chronic myelogenous leukemia	Chronic stage	Plasma	Keramati et al. (2021)

2 ExomiRs as novel biomarkers for cancer

Early treatment intervention for cancer can positively impact overall survival and result in desirable treatment outcome (Hiom, 2015). The standard method to confirm diagnosis is usually invasive biopsy of suspected tissue. Although is reliable, such a method can be difficult to perform due to tissue inaccessibility and possible damage to the normal tissue with the risk to stimulate metastasis (Shyamala et al., 2014). Therefore, using less invasive and effective method is important to improve early cancer diagnosis and predict treatment response and metastasis. Changes in levels of exomiRs can be noticed before the patients can develop clear symptoms for cancer and during cancer development (Chen et al., 2008a). Screening variant expression of tissue-specific exomiRs isolated from various body fluids are shown to prove the diagnosis and prognosis of different type of cancer (Table 1). Predict treatment response (Table 2) and metastasis (Table 3).

2.1 Gastrointestinal tumors

In a study of colorectal cancer (CRC), a set of exomiRs including exomiR-92 was significantly overexpressed in plasma and tissue samples (Ng et al., 2009). This study has also suggested that exomiR-92 can be used as potential biomarker to detect colorectal cancer since it was differentially expressed in patients with colorectal cancer compared to gastric cancer (Ng et al., 2009). In another study of CRC patients, there were significant increased in exomiR-92a-3p and exomiR-17-5p levels in serum samples and this increase correlates with the stage and grade of the cancer (Fu et al., 2018) which suggest the value of exomiR not only as diagnostic biomarker but as prognostic biomarker. A study on gastric cancer reported significant levels of exomiR-17-5p, exomiR-21, exomiR-106a and exomiR-106b in plasma from patients with gastric cancer compared to healthy individuals (Tsujiura et al., 2010). Expression analysis of exomiR profile including exomiR-21, exomiR-155, exomiR-210 and exomiR-196a isolated from plasma is shown to be associated with pancreatic adenocarcinoma patients (Wang et al., 2009). ExomiR-210 from plasma was also altered in two independent cohorts with pancreatic cancer (Ho et al., 2010). Increase expression of exomiR-500 was observed in serum of patients with hepatocellular carcinoma (HCC) (Yamamoto et al., 2009). Expression levels of exomiR-184 in plasma were significantly higher in patients with squamous-cell carcinoma of the tongue compared to healthy individuals and its levels decreased significantly after tumour removal (Wong et al., 2008). Although the majority of the studies focused on circulating exomiRs in serum and plasma, further studies have investigated the potential use of exomiRs as diagnostic/prognostic biomarker for cancer in other body fluids. For example, expression levels of exomiR-125a and exomiR-200a in saliva from patients with oral squamous-cell carcinoma were significantly reduced compared to healthy individuals (Park et al., 2009).

Chemotherapy is one of the most common therapeutic approaches to treat cancer. Successful response to initial therapy is often dependent on type of treatment and tumour type and can be identified by disease progression while resistance to drugs often accompanies with recurrence of tumour. The mechanisms of how cancer can resist treatment have been previously identified (Zahreddine and Borden, 2013) and exomiRs mediating intercellular communication have been identified as one of the

TABLE 2 List of exomiRs associated with drug-response.

Centralize the miRNAs ID	Pattern of expression	Cancer type	References
ExomiR-181b	Increased	Better response to 5-fluorouracil in Colorectal cancer	Nakajima et al. (2006)
ExomiR-140 and ExomiR-215	Increased	Resistance to methotrexate, 5-fluorouacil, and Tomudex in human osteosarcoma and colon cancer cells	Song et al. (2009), Song et al. (2010)
ExomiR-19a	Increased	FOLFOX resistance in Advanced Colorectal Cancer Cases	Chen et al. (2013)
ExomiR-155	Increased	Gemcitabine Resistance in Pancreatic Ductal Adenocarcinoma	Mikamori et al. (2017)
ExomiR-34a	Decreased Increased	Docetaxel resistance in castration-resistant prostate cancer Increased sensitivity to sorafenib in hepatocellular carcinoma cell lines	Corcoran et al. (2014) (Yang et al., 2014)
ExomiR-21	Increased	Cisplatin resistance in gastric cancer (In mice)	Zheng et al. (2017)
ExomiR-122	Decreased	Resistance to taxol in liver cancer	Sun et al. (2016)
ExomiR-128b	Loss of expression	Better response to gefitinib in non-small cell lung cancer	Weiss et al. (2008)
ExomiR-21	Increased	Resistant to docetaxel-based chemotherapy in prostate cancer	Zhang et al. (2011a)
ExomiR-9	Increased	Increase sensitivity of ovarian cancer to DNA damaging chemotherapy	Sun et al. (2013)
ExomiR-125 b	Deletion	Better respond to chemotherapy with anthracycline in breast cancer	Climent et al. (2007)
ExomiR-195, ExomiR-455-3p, and ExomiR-10a miR-221	Increased Increased	Temozolomide resistance in glioma	Ujifuku et al. (2010) Yang et al. (2017a)
ExomiR-29a and exomiR-100	Increased	Drug resistance in pediatric acute promyelocytic leukemia	Zhang et al. (2011b)
ExomiR-142-3p and exomiR-17-92	Increased	Glucocorticoid-resistant B cell precursor acute lymphoblastic leukemia	Sakurai et al. (2019)
ExomiR-99a, exomiR-100, and exomiR-125b	Increased	Resistance to daunorubicin and vincristine in pediatric acute lymphoblastic leukemia	Schotte et al. (2011)
ExomiR-142-5p, exomiR-199b, exomiR-217, exomiR-221, and exomiR-365a-3p	Decreased	Tyrosine kinase inhibitors resistance in chronic myelogenous leukemia	Yeh et al. (2016), Jiang et al. (2018), Klümper et al. (2020)
ExomiR-145-3p and exomiR-155	Decreased	Bortezomib resistance in multiple myeloma	Amodio et al. (2019), Wu et al. (2020)
ExomiR-217	Increased	Sensitizes AML to doxorubicin	Xiao et al. (2017)
ExomiR-143	Increased	Enhances chemosensitivity of acute myeloid leukaemia to cytosine arabinoside	Zhang et al. (2020a)
ExomiR-181a/b	Increased	Fludarabine response in chronic lymphocytic leukemia	Zhu et al. (2012)

mechanisms (Maacha et al., 2019). Tumour cells in their microenvironment can exchange genetic materials and mediate intracellular communications through secreted exomiRs which can promote tumour progression (Lin and Gregory, 2015). In CRC study, exomiR-181b was over-expressed in tumour biopsy compared to normal tissues and was associated with response to 5-fluorouracil treatment (Nakajima et al., 2006). Colon cancer cells and human osteosarcoma cells with elevated levels of exomiR-140 and exomiR-215 have been shown resistance to methotrexate, 5-fluorouacil, and Tomudex (Song et al., 2009; Song et al., 2010). FOLFOX chemotherapy is usually giving to patients with advanced CRC as first-line treatment, and half of the patients acquire resistance with no reliable approach to predict resistance. ExomiR-19a was noticed to be upregulated in patients serum with FOLFOX-resistance and further analysis showed that exomiR-19a can predict acquired drug resistance (Chen et al., 2013) which suggest the use of serum exomiR-19a as a potential biomarker to predict resistance in FOLFOX for advanced CRC patients. Gemcitabine (GEM), a common chemotherapy drug used to treat cancer patients, with promising results, but cancer patients often develop resistance after going long-term treatment. Alternation in specific exomiRs level may play a role since long-term administration with GEM has been shown to associate with increase exomiR-155 level which mediate anti-apoptotic activity that led to chemoresistance in pancreatic ductal adenocarcinoma (Mikamori et al., 2017). Therefore, exomiR-155 could predict GEM-resistance and could be used as novel therapeutic target for GEM treatment in pancreatic ductal adenocarcinoma, based on its function as a driver

TABLE 3 List of exomiRs associated with tumour recurrence.

Centralize the miRNAs ID	Pattern of expression	Tumour type	References
ExomiR-106a-5p	Increased	Gastric cancer metastasis	Yuan et al. (2016)
ExomiR-4772-3p	Increased	Recurrence in stage II and III colon cancer	Liu et al. (2016a)
ExomiR-19a	Increased	Recurrence in Colorectal cancer	Matsumura et al. (2015)
ExomiR-3653	Increased	Pancreatic neuroendocrine tumour	Gill et al. (2019)
ExomiR-1307-5p and exomiR-103	Increased	Hepatocellular carcinoma	Fang et al. (2018a), Eun et al. (2020)
ExomiR-1247-3p	Increased	Liver cancer	Fang et al. (2018b)
ExomiR-718	Decreased	Recurrence in hepatocellular carcinoma	Sugimachi et al. (2015)
ExomiR-21	Increased	Esophageal squamous cell cancer	Tanaka et al. (2013)
ExomiR-497-5p	Decreased	Non-small cell lung cancer	Huang et al. (2019)
ExomiR-141, exomiR-146b-3p and exomiR-194	Increased	Recurrence in prostate cancer	Selth et al. (2013)
ExomiR-275	Increased	Recurrence in bone marrow In prostate cancer	Jiang et al. (2022)
ExomiR-148a-3p	Decreased	Lymph node metastasis in ovarian cancer	Gong et al. (2016)
ExomiR-21	Increased	Recurrence in glioma	Shi et al. (2015)
ExomiR-375	Increased	Bone marrow metastases in patients with neuroblastoma	Colletti et al. (2020)

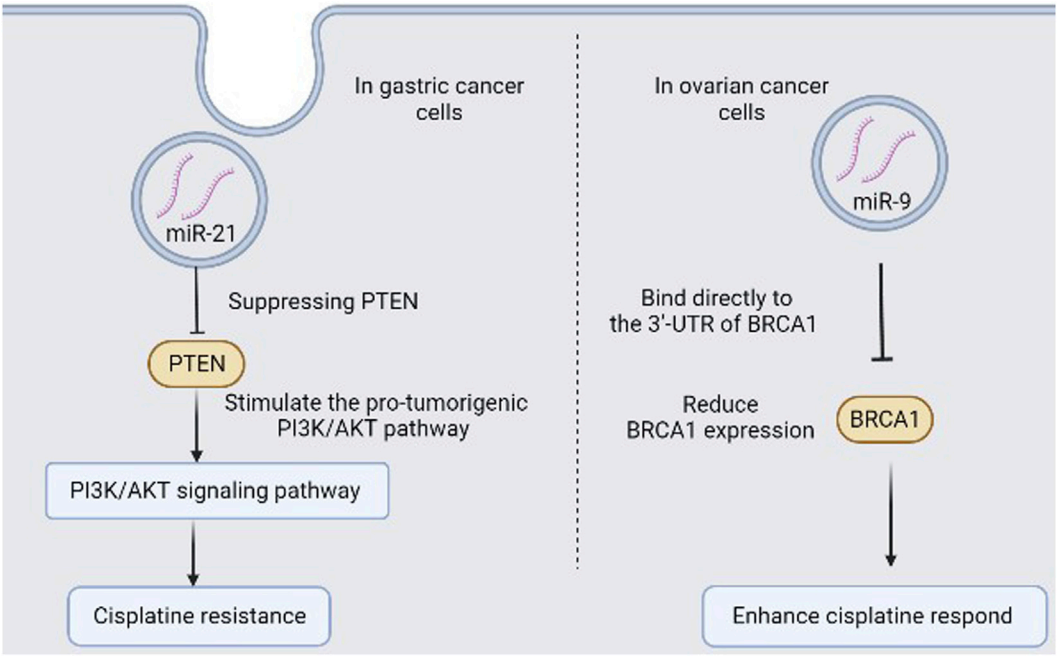

FIGURE 2
Schematic for two examples of exomiRs in drug response/drug resistance in cancer.

of resistance. Docetaxel can induce tumour cell apoptosis through Bcl-2 which can be regulated by exomiR-34a (Corcoran et al., 2014). Increasing exomiR-34a level can reduce cell viability and enhance hepatocellular carcinoma cell lines sensitivity to sorafenib through reduced Bcl-2 expression (Yang et al., 2014). When exomiRs internalized through endocytosis in tumour cells, exomiRs can regulate their response to cell signals (Hannafon and Ding, 2013) and inhibit cell apoptosis by suppressing PTEN and stimulate the

pro-tumorigenic PI3K/AKT pathway (Zheng et al., 2017). Such a process can promote cisplatin resistance (Radisavljevic, 2013) (Figure 2). In addition, elevated level of exomiR-122 in patients could predict better response to taxol as suppressing exomiR-122 can lead to increase septin-9 in liver cancer which correlates with resistance to taxol (Sun et al., 2016). Hence, exomiRs can mediate communication to tumour cells, tumour progression and resistance to drugs (Table 2).

Metastasis can result in tumour recurrence and plays a key role in reducing survival rate (Gandaglia et al., 2015). Currently, there are no approaches to predict recurrence of tumour at any stage of the disease. Several exomiRs shave been shown to associate with different stages of cancer (Calin and Croce, 2006), therefore, they could be used as potential biomarkers to predict recurrence of tumour (Table 3). Increase levels of exomiR-106a-5p in gastric cancer patients is correlated with the potential to promote metastases (Yuan et al., 2016). In colon cancer patients diagnose at stage II and III, exomiR-4772-3p levels have been associated with elevated risk of tumour recurrence and reduced overall survival (Liu et al., 2016a), and a increased expression of exomiR-19a has been associated with tumour recurrence in colorectal cancer (Matsumura et al., 2015). In pancreatic neuroendocrine tumour study, upregulation of exomiR-3653 was associated with high risk of tumour recurrence through interaction with ATRX (Gill et al., 2019). Circulating exomiR-1307-5p was reported to promote tumour metastasis in HCC through promoting epithelial–mesenchymal transition (EMT) (Eun et al., 2020). ExomiR-103 can reduce the integrity of endothelial cell junction and promote the permeability of vessels through targeting of VE-Cadherin and p120-catenin and ZO-1 which results in transendothelial infiltration of HCC cells and promote metastasis (Fang et al., 2018a). Furthermore, increased expression levels of exomiR-1247-3p is associated with lung metastasis in patients with liver cancer (Fang et al., 2018b). HCC recurrence is important factor of therapy such as liver transplantation. Screening exomiR-718 levels in HCC can predict poor prognosis after liver transplantation and HCC recurrence (Sugimachi et al., 2015). Furthermore, in esophageal squamous cell cancer patients, elevated exomiR-21 level is correlated with metastasis (Tanaka et al., 2013).

2.2 Lung cancer

A study examined exomiR-expression profile from serum and found 63 exomiRs to be associated with non-small-cell lung cancer (NSCLC) (Chen et al., 2008a). This study showed that the level of these exomiRs profile differed from serum and blood cells from NSCLC patients while it was the same in healthy individual which suggests that tumour-specific exomiRs in serum were derived from cancer cells. In addition, another board of 34 exomiRs were found in asymptomatic NSCLC patients serum (Bianchi et al., 2011). These reports suggest potential use of exomiRs as non-invasive surrogate diagnostic markers for cancer, potentially of value in screening of asymptomatic populations. A study generated exomiR profile consist of 21 exomiRs analysed from plasma samples collected 12–28 months before lung cancer diagnosis and at the time of detection which suggest a potential diagnosis and prognosis biomarkers for lung cancer (Boeri et al., 2011). Further exomiRs analysis was tested on tissues biopsy took from lung adenocarcinoma patients shows increased levels in panel containing 12 exomiRs including hsa-miR-212, -214, −205, −210, −203, −191, −192, −146, −155, −21, −106a and -17-3p (Rabinowits et al., 2009). A following study used the same approach in screening exomiRs and found similar exomiRs profile in both the tissue biopsy and plasma-derived exosomes from lung adenocarcinoma patients with elevated level of exomiR-200-5p, exomiR-379, exomiR-139-5p and exomiR-378a which suggest a useful biomarker for lung adenocarcinoma (Cazzoli et al., 2013). Loss of exomiR-128b, an EGFR regulator, was associated with better response to gefitinib, an EGFR inhibitor, in patients with relapsed NSCLC (Weiss et al., 2008) and high expression levels of exomiR-21 were found in patients with vertebral column metastasis through increased expression of COX-19 (Guo et al., 2015). NSCLC patients with reduced level of exomiR-497-5p have high chance of metastases (Huang et al., 2019). ExomiR-497-5p can regulate multiple mRNAs including FGF2-encoding mRNAs which can result in migration and invasion (Huang et al., 2019).

2.3 Prostate cancer

A study shows the expression levels of exomiR-141 detected in serum were used to distinguish prostate cancer patients from heathy individuals (Lodes et al., 2009), with other 15 exomiRs including exomiR-16 and exomiR-92a/b were highly expressed in prostate cancer patients (Lodes et al., 2009). In addition, increase levels of exomiR-21-5p, exomiR-141-5p and exomiR-574-3p were also observed in urine samples from patients with prostate cancer (Samsonov et al., 2016). Furthermore, serum exomiR-21 expression levels were associated with resistant to docetaxel-based chemotherapy compared to patients with chemosensitive response in prostate cancer (Zhang et al., 2011a). Prostate cancer patients with increase levels of exomiR-194, exomiR-146b-3p and exomiR-141 have high chance of poor prognosis and recurrence (Selth et al., 2013). Bone metastasis is common in patients with prostate cancer and mediate disease complication (Kfoury et al., 2021). ExomiR-275 derived from prostate cancer has been reported to mediate bone metastasis in prostate cancer patients (Jiang et al., 2022).

2.4 Ovarian and breast cancer

A study on epithelial ovarian cancer found eight exomiRs from serum including exomiR-92, exomiR-93 and exomiR-126 were highly expressed in 19 patients compared to 11 healthy individuals (Resnick et al., 2009). A panel of exomiRs containing exomiR-205, exomiR-214, exomiR-200b, exomiR-203, exomiR-200a, exomiR-200c, exomiR-21 and exomiR-141 were noticed to be escalated in exosomes isolated from patients serum with ovarian cancer (Taylor and Gercel-Taylor, 2008). A prospective analysis showed significant alternation in exomiR-195 in serum, plasma, or whole blood collected from patients with breast cancer (BC) (Heneghan et al., 2010). The serum levels of exomiR-195 was remarkably decreased after tumour removal (Heneghan et al., 2010). Furthermore, BC patents have elevated level of serum

exomiR-101 and exomiR-372 compared to healthy controls (Eichelser et al., 2014) and patients with triple-negative BC have increased level of exomiR-373 increased level of exomiR-373 (Eichelser et al., 2014). This suggests, the use of these exomiRs as potential diagnostic markers for BC.

Increase level of certain exomiRs can enhance sensitivity of many chemotherapy drugs. For instance, exomiR-9 downregulates BRCA1 protein through direct binding to the 3′-UTR of BRCA1 mRNA and reduce the ability of the BRCA complex to repair damage in DNA. Therefore, increase exomiR-9 can suppress DNA damage repair in ovarian cancer and enhance ovarian cancer respond to chemotherapy, such as cisplatin (Figure 2) (Sun et al., 2013). BC patients with genetically deleted chromosome 11q which containing the *miR-125 b* gene often show better respond to chemotherapy with anthracycline (Climent et al., 2007) which suggests a potential association between exomiR-125b dysregulation and response to drugs containing anthracycline in BC patients. Reduced levels of exomiR-148a-3p have been shown to increase chance of tumour metastasis in ovarian cancer (Gong et al., 2016) which suggest the use of exomiR-148a as a potential marker for tumour recurrence and, possibly, tumour invasion and migration in ovarian cancer.

2.5 Neuroblastoma

Patients with recurrent glioma have higher cerebrospinal fluid exomiR-21 levels compared to non-tumour control group, however, no differences were observed in exomiR-21 isolated from serum (Shi et al., 2015). ExomiR-375 has been reported to promote bone marrow metastases in patients with neuroblastoma (NB) (Colletti et al., 2020) by downregulating YAP1 levels which enhance osteogenic differentiation of mesenchymal stromal cells (Colletti et al., 2020). Additional screening of exomiRs in metastatic sites and primary tumour sites is important to enhance prediction of recurrence and metastasis.

First-line treatment for glioma patients is usually temozolomide (TMZ) (Chibbaro et al., 2004), however, there is no reliable approach to predict which patients will be resistance to TMZ. Interestingly, downregulation of exomiR-195, exomiR-455-3p, and exomiR-10a has been associated with acquired TMZ-resistance (Ujifuku et al., 2010). Furthermore, TMZ resistance in glioma cells have been reported to be associated with dysregulation with exomiR-221 level (Yang et al., 2017a). These studies, recommend screening for exomiR-10a, exomiR-122, exomiR-455-3p and exomiR-195 levels before and during TMZ therapy to identify better treatment approach for the patient.

2.6 Pediatric tumours

The non-invasive diagnosis, limited-risk and availability of the exomiRs in the body fluids make them attractive method to diagnose cancer in pediatric patients (Galardi et al., 2019). NB is one of the most common tumour in children with heterogeneous clinical characteristics (Ma et al., 2019). Profile for exomiRs isolated from 17 NB patients plasma have been shown different expression compared to healthy controls (Ma et al., 2019). The significant expression of exomiR-199a-3p was correlated with severity of NB patients (Ma et al., 2019), as it increases proliferation and migration of NB cells *in vitro* (Ma et al., 2019). In another study, high expression levels of exomiR-16 were linked to poor prognosis in childhood acute lymphoblastic leukemia (ALL) (Kaddar et al., 2009).

Another pediatric tumour accounts for 80% of primary tumour liver in young children infant is Hepatoblastoma (HB) (Ranganathan et al., 2020). The expression of exomiR-21 in plasma was higher in HB patients compared to healthy control (Liu et al., 2016b), which makes it a good diagnosis and prognosis biomarker for HB. Further analysis studies of exomiRs profile have shown increased expression of three-miRNA-based expression signature (exomiR-7112-5p, exomiR-885-3p and exomiR-1245a) in plasma of acute myeloid leukaemia patients (AML) (Zampini et al., 2017), increased expression of exomiR-25-3p in serum of osteosarcoma patients (Fujiwara et al., 2017) and decreased expression of exomiR-125b in serum of ewing's sarcoma patients (Nie et al., 2015). These results showed evidence of using exomiRs as a potential diagnostic and prognostic biomarkers for pediatric tumours. In pediatric AML, both exomiR-29a and exomiR-100 were indicator for better response to chemotherapy (Said et al., 2022). Increased expression levels of exomiR-125b were associated with drug resistance in pediatric acute promyelocytic leukemia (Zhang et al., 2011b).

2.7 Hematologic tumours

Alternation in exomiRs expression is potential biomarker not only in solid tumours, but also in non-solid hematologic tumours. For example, increase expression of exomiR-21, exomiR-155, and exomiR-210 was discovered in the serum of diffuse large B cell lymphoma (DLBCL) patients (Lawrie et al., 2008). Moreover, there was a significant decrease of exomiR-92a in plasma collected from patients with acute leukemias compared to healthy individuals (Tanaka et al., 2009). In addition, plasma samples collected from multiple myeloma (MM) patients have elevated levels of exomiR-148a, exomiR-181a, exomiR-20a, exomiR-221, exomiR-625, and exomiR-99b compared to healthy individuals (Huang et al., 2012a). The increased levels of both exomiR-20a and exomiR148a were associated with short relapse-free survival rate (Huang et al., 2012a). The expression profile of exomiR-128a, exomiR-128b, let-7b, exomiR-223 can help distinguish ALL from AML with over 95% accuracy rate (Mi et al., 2007). Alternation expression of exomiR-32, exomiR-98 and exomiR-374 in blood samples is observed in chronic lymphocytic leukemia (CLL) patients (Rahimi et al., 2021). In a chronic myelogenous leukemia (CML) studies, increased levels of exomiR-451 was observed in plasma samples from CML patients in the chronic stage (Keramati et al., 2021) while increased levels of exomiR-126, exomiR-155, and exomiR-222 were observed during blast crisis (Machová Poláková et al., 2011).

Increased expression levels of exomiR-142-3p and the exomiR-17-92 were associated with glucocorticoid-resistant B cell precursor acute lymphoblastic leukemia (Sakurai et al., 2019). Furthermore, resistance to daunorubicin and vincristine in pediatric ALL was

associated with increased expression levels of exomiR-99a, exomiR-100, and exomiR-125b (Schotte et al., 2011).

In CML, tyrosine kinase inhibitors (TKIs) resistance was associated with decreased expression levels of exomiR-142-5p, exomiR-199b, exomiR-217, exomiR-221, and exomiR-365a-3p (Yeh et al., 2016; Jiang et al., 2018; Klümper et al., 2020). In DLBCL studies, upregulation of exomiR-155 and reduced expression levels of exomiR-193b-5p and exomiR-1244 were linked to treatment failure with rituximab plus doxorubicin, cyclophosphamide, prednisone, and vincristine (Iqbal et al., 2015; Bento et al., 2022). Reduced expression levels of both exomiR-145-3p and exomiR-155 were associated with bortezomib resistance in MM (Amodio et al., 2019; Wu et al., 2020). ExomiR-217 sensitizes AML to doxorubicin *via* targeting KRAS (Xiao et al., 2017) while exomiR-143 enhances chemosensitivity of AML to cytosine arabinoside by targeting ATG7-and ATG2B-dependent autophagy (Zhang et al., 2020a). In CLL, fludarabine response was associated with increased expression levels of exomiR-181a/b (Zhu et al., 2012). Another study has shown a role of exomiR-181a in GC resistance in MM cells (Huang et al., 2012b). Elevated expression of exomiR-485-3p increased sensitivity to Top2 inhibitors in CEM/VM-1-5 cells through regulating the NF-YB expression level (Chen et al., 2011). Downregulation of exomiR-451 was associated with Imatinib resistance in CML (Scholl et al., 2012). In patients with refractory AML, downregulation of exomiR-let-7f was associated with Adriamycin resistance (Dai et al., 2014). Plasma levels of let-7a and exomiR-16 were significantly decreased in patients with myelodysplastic syndrome which predict with both progression-free survival and overall survival (Zuo et al., 2011).

3 ExomiRs as immunotherapeutic targets to regulate immune checkpoint molecules

The therapeutic potential of Immune-checkpoint blockade in cancer has improved the overall survival in the last years (Postow et al., 2015). The first checkpoint blockade to receive FDA approval was ipilimumab, which is an antibody that target cytotoxic T-lymphocyte-associated protein 4 (CTLA4) (Hodi et al., 2010). FDA has also approved additional two immune checkpoint blockade antibodies that target programmed cell death protein 1 (PD-1) known as pembrolizumab and nivolumab to treat stage IV melanoma (Robert et al., 2015a; Robert et al., 2015b) and NSCLC (Brahmer et al., 2015; Garon et al., 2015). Although these targeting antibodies have shown promising results in cancer treatment, the systematic administration of these protein-format and murine-origin blocking antibodies can result in undesirable immune-related adverse events (irAEs) (Van Hoecke and Roose, 2019). ExomiRs secreted from cancer cells can regulate stromal cells and promote cancer angiogenesis (Wu et al., 2019). In addition, they play a key role in intercellular transmission of signals that regulate immune checkpoint molecules and influence the function of several immune cells such as dendritic cells and T cells which are important cells in cancer immunotherapy (Huemer et al., 2021). Several exomiRs can regulate the expressions of immune checkpoint molecules, mimicking the therapeutic impact of immune checkpoint blocking antibodies and controlling the irAEs associated with the administration of the blocking antibodies (Van Hoecke and Roose, 2019). Therefore, they have a potential role as immunotherapeutic agents to regulate immune checkpoint molecules expression either as exomiR mimics or exomiR antagonists. The exomiR mimics function to restore the tumour suppressor capabilities of exomiR while the exomiR antagonists serve as inhibitors (Bader et al., 2011).

The first exomiR mimic to enter the clinical trial phase was the use of MRX34, an exomiR-34a mimic (Bader, 2012; Austin, 2013). In AML, exomiR-34a was found to target PD-L1 mRNA and downregulate PD-L1 expression (Wang et al., 2015). In addition, combination therapy of radiotherapy (XRT) and administration of MRX34 result in increased $CD8^+$ T cell infiltration and reduced Treg in NSCLC (Cortez et al., 2016). These results suggest a potential role of exomiR-34a mimic to enhance anti-tumour immunity and reduce tumour growth. Further studies have examined new potential targets for exomiR mimics. For example, exomiR-424 has the ability to supress PD-L1 and CD80 expression, and restores cytotoxic $CD8^+$T cells effector function and improves the survival in ovarian carcinoma mouse model (Xu et al., 2016). The exomiR inhibitors have also shown immunotherapeutic potential. Cobomarsen (MRG105) is an anti-exomiR-155 agent has shown reduce tumour growth when administrated systematically (Van Roosbroeck et al., 2017). Another study of melanoma, adoptive transfer of $CD8^+$ cytotoxic T lymphocytes treated with exomiR-23a inhibitor has shown decreased in tumour growth and increased effector function of $CD8^+$ cytotoxic T lymphocytes (Lin et al., 2014). Furthermore, exomiR-149-3p reduces inhibitory receptors and revised $CD8^+$ T cell exhaustion in breast cancer cells (Zhang et al., 2019), and exomiR-5119 enhance BC immunotherapy through regulation of immune checkpoints in dendritic cells (Zhang et al., 2020b). In addition, exomiR-34a-5p can regulate the expression of PDL-1 in AML (Wang et al., 2015). ExomiR-138-5p can regulate PDL-1 expression in colorectal cancer (Zhao et al., 2016) and regulate PD-1 expression in glioma (Wei et al., 2016). Low expression levels of exomiR-200 in NSCLC cells are associated with increased expression levels of PD-L1 since exomiR-200 have been shown to target 3′UTR of PD-L1 and decreases its expression (Chen et al., 2014). Therefore, NSCLC patients with exomiR-200 low pattern expression may benefit from the use of miR-200 mimics. Furthermore, decrease expression levels of exomiR-197 are associated with increased expression levels of PD-L1 and promote drug resistance and reduced overall survival in patients with NSCLC (Fujita et al., 2015). Thus, treatment with exomiR-197 mimics may benefit patients with PD-L1-positive NSCLC.

CTLA-4 is another important immune checkpoint molecule which can bind to either CD80 or CD86 on antigen presenting cells and result in suppression the effector function of T cell (Teft et al., 2006). CTLA-4 can be regulated by exomiR-138-5p (Wei et al., 2016). *In vivo* treatment of exomiR-138 mimic results in downregulation of CTLA-4, PD-1 and Foxp3 on tumor infiltrating CD4+T cells leading to significant decrease of T reg in glioma mouse model (Wei et al., 2016). In addition, exomiR-424 reduced CD80 expression in dendritic cells and results in CD80/CTLA-4 blockade and increased T cell activity (Xu et al., 2016). Furthermore, T cell immunoglobulin and mucin-domain containing-3 (TIM-3) is expressed on activated T cell and reduces T cell activity by inducing T cell exhaustion and

tolerance (Ferris et al., 2014). In glioma, exomiR-15a/16 knock-out Mice have decreased TIM-3 and PD-1 expression and increased cytokines secretion in tumor-infiltrating $CD8^+$ T cells which result in better overall mice survival (Yang et al., 2017b). These examples show a potential role of targeting exomiRs as immunotherapeutic agents to regulate immune checkpoint molecules and enhance anti-tumour immunity.

4 Conclusion remarks

Treatment to cancer has improved significantly over the past few decades. However, many patients do not benefit from the treatment due to late-stage diagnosis, tumour recurrence and sometime treatment resistance. Therefore, early diagnosis of cancer and reliable biomarkers for cancer recurrence and treatment resistance are critical to determine the best therapeutic approach and to improve overall survival. To develop and identify a sensitive, and less invasive biomarkers for cancer implication, exomiRs should not be ignored. These circulating exomiRs have the potential for new cancer biomarkers due to several characteristic factors. First, oncogenic pathways can be regulated by exomiRs (Sumazin et al., 2011) which can result in tumour development, suppression and can mediate treatment response which makes it good candidate for cancer progression biomarker. The unique expression profiles of exomiRs in tumours helps in providing wide range of information for tumour stage, recurrence and treatment resistance which makes it a good candidate for liquid biopsy without the need for tissue biopsy. The lipid biolayer structure in the exosomal membrane protect exomiRs from degranulation in the biofluid; this protection makes it more desirable compared to other molecules which can be degraded in harsh conditions like extreme temperature and prolong storage (Chen et al., 2008b). The easy accessibility is another reason for their desirable use, exomiRs can be obtained in less-invasive way from liquid biopsy including blood, urine and saliva. The change in exomiRs expression profile observed in these bio-fluid can be seen as early as early stage of tumour (Jiménez-Avalos et al., 2021).

Based on the advantages of exomiRs derived from tumour, it can be used as a potential biomarker for cancer implication as it can predict the growth, spread, recurrence and treatment-resistance of tumours. However, several studies reported unsuccessful validation in using exomiRs as biomarkers for cancer (Sapre et al., 2014; Wan et al., 2014). This could be due to several factors including limited methodologies to access and obtain exomiRs and time of collection and the cancer stage (Mateescu et al., 2017). These studies highlight the significance of incorporating methodological approaches to obtain exomiRs and to ensure the reproducibility of the result in future studies.

The discovery of immune checkpoint blockade as cancer immunotherapy has improved the overall survival significantly, however, new strategies on how to regulate their expression using something other than protein-format and murine-origin antibodies are crucial to avoid undesirable irAE. ExomiRs play a key role in posttranscriptional control of protein expression and therefore, may be of better target since some exomiRs expression levels are associated with expression of immune checkpoint molecules. Further investigations are important to deeply show the effect of exomiRs on cancer biology.

5 Future direction

The variability of cancer lends itself in the growing field of personalized medicine which provide great patient benefit (Verma, 2012). Artificial intelligence (AI) technique is emerging in personalized medicine and biomedical research which include cancer clinical implications including cancer diagnosis, treatment, and the discovery of new potential therapy (Schork, 2019; Elemento et al., 2021). The big data obtained from thousands of studies related to exomiRs in cancer can leverage an opportunity to implement AI in cancer clinical implication and improve cancer diagnosis (Paolini et al., 2022). Together, these computational platforms can provide a new technique in cancer clinical implication and provide a modern approach on the validity of exomiRs signature as biomarker in cancer and immunotherapeutic agents.

Author contributions

FA reviewed the literature, wrote the manuscript and designed the figures and tables.

Acknowledgments

The author would like to thank Prof. James Koropatnick from the departments of Oncology and Pathology, Schulich School of Medicine and Dentistry, University of Western Ontario, London, Ontario, Canada, for all the years of guidance and support.

Conflict of interest

The author declares that the research was conducted in the absence of any commercial or financial relationships that could be construed as a potential conflict of interest.

Publisher's note

References

Alotaibi, F. (2021). Exosomal microRNAs: Potential biomarkers for cancer diagnosis, treatment response and prognosis, in *Role of exosomes in biological communication systems*, 321–336.

Amodio, N., Gallo Cantafio, M. E., Botta, C., Agosti, V., Federico, C., Caracciolo, D., et al. (2019). Replacement of miR-155 elicits tumor suppressive activity and antagonizes bortezomib resistance in multiple myeloma. *Cancers* 11 (2), 236. doi:10.3390/cancers11020236

Amorim, M. G., Valieris, R., Drummond, R. D., Pizzi, M. P., Freitas, V. M., Sinigaglia-Coimbra, R., et al. (2017). A total transcriptome profiling method for plasma-derived extracellular vesicles: Applications for liquid biopsies. *Sci. Rep.* 7 (1), 1–11. doi:10.1038/s41598-017-14264-5

Austin, T. b. M. (2013). First microRNA mimic enters clinic. *Nat. Biotechnol.* 31 (7), 577. doi:10.1038/nbt0713-577

Bader, A., Brown, D., Stoudemire, J., and Lammers, P. (2011). Developing therapeutic microRNAs for cancer. *Gene Ther.* 18 (12), 1121–1126. doi:10.1038/gt.2011.79

Bader, A. G. (2012). miR-34–a microRNA replacement therapy is headed to the clinic. *Front. Genet.* 3, 120. doi:10.3389/fgene.2012.00120

Bento, L., Vogler, O., Sas-Barbeito, A., Muncunill, J., Ros, T., Martinez, J., et al. (2022). Screening for prognostic microRNAs associated with treatment failure in diffuse large B cell lymphoma. *Cancers* 14 (4), 1065. doi:10.3390/cancers14041065

Bianchi, F., Nicassio, F., Marzi, M., Belloni, E., Dall'olio, V., Bernard, L., et al. (2011). A serum circulating miRNA diagnostic test to identify asymptomatic high-risk individuals with early stage lung cancer. *EMBO Mol. Med.* 3 (8), 495–503. doi:10.1002/emmm.201100154

Boeri, M., Verri, C., Conte, D., Roz, L., Modena, P., Facchinetti, F., et al. (2011). MicroRNA signatures in tissues and plasma predict development and prognosis of computed tomography detected lung cancer. *Proc. Natl. Acad. Sci.* 108 (9), 3713–3718. doi:10.1073/pnas.1100048108

Boing, A., Edwin, V, Anita, E G, Frank, A W C, Auguste, S, Rienk, N, et al. (2014), Single-step isolation of extracellular vesicles by size-exclusion chromatography. J Extracell Vesicles. *J Extracell Vesicles* 8, 3, doi:10.3402/jev.v3.23430

Brahmer, J., Reckamp, K. L., Baas, P., Crino, L., Eberhardt, W. E. E., Poddubskaya, E., et al. (2015). Nivolumab versus docetaxel in advanced squamous-cell non–small-cell lung cancer. *N. Engl. J. Med.* 373 (2), 123–135. doi:10.1056/NEJMoa1504627

Calin, G. A., and Croce, C. M. (2006). MicroRNA signatures in human cancers. *Nat. Rev. cancer* 6 (11), 857–866. doi:10.1038/nrc1997

Cazzoli, R., Buttitta, F., Di Nicola, M., Malatesta, S., Marchetti, A., Rom, W. N., et al. (2013). microRNAs derived from circulating exosomes as noninvasive biomarkers for screening and diagnosing lung cancer. *J. Thorac. Oncol.* 8 (9), 1156–1162. doi:10.1097/JTO.0b013e318299ac32

Chen, C.-F., He, X., Arslan, A. D., Mo, Y. Y., Reinhold, W. C., Pommier, Y., et al. (2011). Novel regulation of nuclear factor-YB by miR-485-3p affects the expression of DNA topoisomerase IIα and drug responsiveness. *Mol. Pharmacol.* 79 (4), 735–741. doi:10.1124/mol.110.069633

Chen, L., Gibbons, D. L., Goswami, S., Cortez, M. A., Ahn, Y. H., Byers, L. A., et al. (2014). Metastasis is regulated via microRNA-200/ZEB1 axis control of tumour cell PD-L1 expression and intratumoral immunosuppression. *Nat. Commun.* 5 (1), 5241. doi:10.1038/ncomms6241

Chen, Q., Xia, H. W., Ge, X. J., Zhang, Y. C., Tang, Q. L., and Bi, F. (2013). Serum miR-19a predicts resistance to FOLFOX chemotherapy in advanced colorectal cancer cases. *Asian Pac. J. Cancer Prev.* 14 (12), 7421–7426. doi:10.7314/apjcp.2013.14.12.7421

Chen, X., Ba, Y., Ma, L., Cai, X., Yin, Y., Wang, K., et al. (2008). Characterization of microRNAs in serum: A novel class of biomarkers for diagnosis of cancer and other diseases. *Cell Res.* 18 (10), 997–1006. doi:10.1038/cr.2008.282

Chen, X., Ba, Y., Ma, L., Cai, X., Yin, Y., Wang, K., et al. (2008). Characterization of microRNAs in serum: A novel class of biomarkers for diagnosis of cancer and other diseases. *Cell Res.* 18 (10), 997–1006. doi:10.1038/cr.2008.282

Chibbaro, S., Benvenuti, L., Caprio, A., Carnesecchi, S., Pulera, F., Faggionato, F., et al. (2004). Temozolomide as first-line agent in treating high-grade gliomas: Phase II study. *J. neuro-oncology* 67 (1-2), 77–81. doi:10.1023/b:neon.0000021728.36747.93

Climent, J., Dimitrow, P., Fridlyand, J., Palacios, J., Siebert, R., Albertson, D. G., et al. (2007). Deletion of chromosome 11q predicts response to anthracycline-based chemotherapy in early breast cancer. *Cancer Res.* 67 (2), 818–826. doi:10.1158/0008-5472.CAN-06-3307

Colletti, M., Tomao, L., Galardi, A., Paolini, A., Di Paolo, V., De Stefanis, C., et al. (2020). Neuroblastoma-secreted exosomes carrying miR-375 promote osteogenic differentiation of bone-marrow mesenchymal stromal cells. *J. Extracell. vesicles* 9 (1), 1774144. doi:10.1080/20013078.2020.1774144

Corcoran, C., Rani, S., and O'Driscoll, L. (2014). miR-34a is an intracellular and exosomal predictive biomarker for response to docetaxel with clinical relevance to prostate cancer progression. *Prostate* 74 (13), 1320–1334. doi:10.1002/pros.22848

Cortez, M. A., Ivan, C., Valdecanas, D., Wang, X., Peltier, H. J., Ye, Y., et al. (2016). PDL1 Regulation by p53 via miR-34. *J. Natl. Cancer Inst.* 108 (1), djv303. doi:10.1093/jnci/djv303

Dai, C.-W., Bai, Q. W., Zhang, G. S., Cao, Y. X., Shen, J. K., Pei, M. F., et al. (2014). MicroRNA let-7f is down-regulated in patients with refractory acute myeloid leukemia and is involved in chemotherapy resistance of adriamycin-resistant leukemic cells. *Leukemia Lymphoma* 55 (7), 1645–1648. doi:10.3109/10428194.2013.847936

Dragovic, R. A., Gardiner, C., Brooks, A. S., Tannetta, D. S., Ferguson, D. J. P., Hole, P., et al. (2011). Sizing and phenotyping of cellular vesicles using Nanoparticle Tracking Analysis. *Nanomedicine Nanotechnol. Biol. Med.* 7 (6), 780–788. doi:10.1016/j.nano.2011.04.003

Eichelser, C., Stuckrath, I., Muller, V., Milde-Langosch, K., Wikman, H., Pantel, K., et al. (2014). Increased serum levels of circulating exosomal microRNA-373 in receptor-negative breast cancer patients. *Oncotarget* 5 (20), 9650–9663. doi:10.18632/oncotarget.2520

Ekström, K., Crescitelli, R., Petursson, H. I., Johansson, J., Lasser, C., and Olofsson Bagge, R. (2022). Characterization of surface markers on extracellular vesicles isolated from lymphatic exudate from patients with breast cancer. *BMC cancer* 22 (1), 50–17. doi:10.1186/s12885-021-08870-w

Elemento, O., Leslie, C., Lundin, J., and Tourassi, G. (2021). Artificial intelligence in cancer research, diagnosis and therapy. *Nat. Rev. Cancer* 21 (12), 747–752. doi:10.1038/s41568-021-00399-1

Eun, J. W., Seo, C. W., Baek, G. O., Yoon, M. G., Ahn, H. R., Son, J. A., et al. (2020). Circulating exosomal MicroRNA-1307-5p as a predictor for metastasis in patients with hepatocellular carcinoma. *Cancers* 12 (12), 3819. doi:10.3390/cancers12123819

Fang, J. H., Zhang, Z. J., Shang, L. R., Luo, Y. W., Lin, Y. F., Yuan, Y., et al. (2018). Hepatoma cell-secreted exosomal microRNA-103 increases vascular permeability and promotes metastasis by targeting junction proteins. *Hepatology* 68 (4), 1459–1475. doi:10.1002/hep.29920

Fang, T., Lv, H., Lv, G., Li, T., Wang, C., Han, Q., et al. (2018). Tumor-derived exosomal miR-1247-3p induces cancer-associated fibroblast activation to foster lung metastasis of liver cancer. *Nat. Commun.* 9 (1), 191. doi:10.1038/s41467-017-02583-0

Ferris, R. L., Lu, B., and Kane, L. P. (2014). Too much of a good thing? Tim-3 and TCR signaling in T cell exhaustion. *J. Immunol.* 193 (4), 1525–1530. doi:10.4049/jimmunol.1400557

Fu, F., Jiang, W., Zhou, L., and Chen, Z. (2018). Circulating exosomal miR-17-5p and miR-92a-3p predict pathologic stage and grade of colorectal cancer. *Transl. Oncol.* 11 (2), 221–232. doi:10.1016/j.tranon.2017.12.012

Fujita, Y., Yagishita, S., Hagiwara, K., Yoshioka, Y., Kosaka, N., Takeshita, F., et al. (2015). The clinical relevance of the miR-197/CKS1B/STAT3-mediated PD-L1 network in chemoresistant non-small-cell lung cancer. *Mol. Ther.* 23 (4), 717–727. doi:10.1038/mt.2015.10

Fujiwara, T., Uotani, K., Yoshida, A., Morita, T., Nezu, Y., Kobayashi, E., et al. (2017). Clinical significance of circulating miR-25-3p as a novel diagnostic and prognostic biomarker in osteosarcoma. *Oncotarget* 8 (20), 33375–33392. doi:10.18632/oncotarget.16498

Galardi, A., Colletti, M., Di Paolo, V., Vitullo, P., Antonetti, L., Russo, I., et al. (2019). Exosomal MiRNAs in pediatric cancers. *Int. J. Mol. Sci.* 20 (18), 4600. doi:10.3390/ijms20184600

Gandaglia, G., Karakiewicz, P. I., Briganti, A., Passoni, N. M., Schiffmann, J., Trudeau, V., et al. (2015). Impact of the site of metastases on survival in patients with metastatic prostate cancer. *Eur. Urol.* 68 (2), 325–334. doi:10.1016/j.eururo.2014.07.020

Garon, E. B., Rizvi, N. A., Hui, R., Leighl, N., Balmanoukian, A. S., Eder, J. P., et al. (2015). Pembrolizumab for the treatment of non–small-cell lung cancer. *N. Engl. J. Med.* 372 (21), 2018–2028. doi:10.1056/NEJMoa1501824

Gill, P., Kim, E., Chua, T. C., Clifton-Bligh, R. J., Nahm, C. B., Mittal, A., et al. (2019). MiRNA-3653 is a potential tissue biomarker for increased metastatic risk in pancreatic neuroendocrine tumours. *Endocr. Pathol.* 30, 128–133. doi:10.1007/s12022-019-9570-y

Gong, L., Wang, C., Gao, Y., and Wang, J. (2016). Decreased expression of microRNA-148a predicts poor prognosis in ovarian cancer and associates with tumor growth and metastasis. *Biomed. Pharmacother.* 83, 58–63. doi:10.1016/j.biopha.2016.05.049

Guo, Q., Zhang, H., Zhang, L., He, Y., Weng, S., Dong, Z., et al. (2015). MicroRNA-21 regulates non-small cell lung cancer cell proliferation by affecting cell apoptosis via COX-19. *Int. J. Clin. Exp. Med.* 8 (6), 8835–8841.

Hannafon, B. N., and Ding, W.-Q. (2013). Intercellular communication by exosome-derived microRNAs in cancer. *Int. J. Mol. Sci.* 14 (7), 14240–14269. doi:10.3390/ijms140714240

Harding, C., Heuser, J., and Stahl, P. (1983). Receptor-mediated endocytosis of transferrin and recycling of the transferrin receptor in rat reticulocytes. *J. Cell Biol.* 97 (2), 329–339. doi:10.1083/jcb.97.2.329

Heneghan, H. M., Miller, N., Lowery, A. J., Sweeney, K. J., Newell, J., and Kerin, M. J. (2010). Circulating microRNAs as novel minimally invasive biomarkers for breast cancer. *Ann. Surg.* 251 (3), 499–505. doi:10.1097/SLA.0b013e3181cc939f

Hiom, S. (2015). Diagnosing cancer earlier: Reviewing the evidence for improving cancer survival. *Br. J. Cancer* 112, S1–S5. Nature Publishing Group. doi:10.1038/bjc.2015.23

Ho, A. S., Huang, X., Cao, H., Christman-Skieller, C., Bennewith, K., Le, Q. T., et al. (2010). Circulating miR-210 as a novel hypoxia marker in pancreatic cancer. *Transl. Oncol.* 3 (2), 109–113. doi:10.1593/tlo.09256

Hodi, F. S., O'Day, S. J., McDermott, D. F., Weber, R. W., Sosman, J. A., Haanen, J. B., et al. (2010). Improved survival with ipilimumab in patients with metastatic melanoma. *N. Engl. J. Med.* 363 (8), 711–723. doi:10.1056/NEJMoa1003466

Huang, J.-j., Yu, J., Li, J. y., Liu, Y. t., and Zhong, R. q. (2012). Circulating microRNA expression is associated with genetic subtype and survival of multiple myeloma. *Med. Oncol.* 29, 2402–2408. doi:10.1007/s12032-012-0210-3

Huang, X., Wang, L., and Liu, W. (2019). MicroRNA-497-5p inhibits proliferation and invasion of non-small cell lung cancer by regulating FGF2. *Oncol. Lett.* 17 (3), 3425–3431. doi:10.3892/ol.2019.9954

Huang, X., Yang, M., and Jin, J. (2012). Triptolide enhances the sensitivity of multiple myeloma cells to dexamethasone via microRNAs. *Leukemia lymphoma* 53 (6), 1188–1195. doi:10.3109/10428194.2011.638069

Huemer, F., Leisch, M., Geisberger, R., Zaborsky, N., and Greil, R. (2021). miRNA-based therapeutics in the era of immune-checkpoint inhibitors. *Pharmaceuticals* 14 (2), 89. doi:10.3390/ph14020089

Iqbal, J., Shen, Y., Huang, X., Liu, Y., Wake, L., Liu, C., et al. (2015). Global microRNA expression profiling uncovers molecular markers for classification and prognosis in aggressive B-cell lymphoma. *J. Am. Soc. Hematol.* 125 (7), 1137–1145. doi:10.1182/blood-2014-04-566778

Jiang, Q., Tan, X. P., Zhang, C. H., Li, Z. Y., Xu, Y., et al. (2022). Non-coding RNAs of extracellular vesicles: Key players in organ-specific metastasis and clinical implications. *Cancers* 14 (22), 5693. doi:10.3390/cancers14225693

Jiang, X., Cheng, Y., Hu, C., Zhang, A., Ren, Y., and Xu, X. (2018). MicroRNA-221 sensitizes chronic myeloid leukemia cells to imatinib by targeting STAT5. *Leukemia lymphoma* 60, 1709–1720. doi:10.1080/10428194.2018.1543875

Jiménez-Avalos, J. A., Fernández-Macías, J. C., and González-Palomo, A. K. (2021). Circulating exosomal MicroRNAs: New non-invasive biomarkers of non-communicable disease. *Mol. Biol. Rep.* 48 (1), 961–967. doi:10.1007/s11033-020-06050-w

Kaddar, T., Chien, W. W., Bertrand, Y., Pages, M. P., Rouault, J. P., Salles, G., et al. (2009). Prognostic value of miR-16 expression in childhood acute lymphoblastic leukemia relationships to normal and malignant lymphocyte proliferation. *Leukemia Res.* 33 (9), 1217–1223. doi:10.1016/j.leukres.2008.12.015

Keramati, F., Jafarian, A., Soltani, A., Javandoost, E., Mollaei, M., and Fallah, P. (2021). Circulating miRNAs can serve as potential diagnostic biomarkers in chronic myelogenous leukemia patients. *Leukemia Res. Rep.* 16, 100257. doi:10.1016/j.lrr.2021.100257

Kfoury, Y., Baryawno, N., Severe, N., Mei, S., Gustafsson, K., Hirz, T., et al. (2021). Human prostate cancer bone metastases have an actionable immunosuppressive microenvironment. *Cancer Cell* 39 (11), 1464–1478. e8. doi:10.1016/j.ccell.2021.09.005

Klümper, T., Bruckmueller, H., Diewock, T., Kaehler, M., Haenisch, S., Pott, C., et al. (2020). Expression differences of miR-142-5p between treatment-naïve chronic myeloid leukemia patients responding and non-responding to imatinib therapy suggest a link to oncogenic ABL2, SRI, cKIT and MCL1 signaling pathways critical for development of therapy resistance. *Exp. Hematol. Oncol.* 9 (1), 26–15. doi:10.1186/s40164-020-00183-1

Kozomara, A., and Griffiths-Jones, S. (2014). miRBase: annotating high confidence microRNAs using deep sequencing data. *Nucleic acids Res.* 42 (D1), D68–D73. doi:10.1093/nar/gkt1181

Larrea, E., Sole, C., Manterola, L., Goicoechea, I., Armesto, M., Arestin, M., et al. (2016). New concepts in cancer biomarkers: Circulating miRNAs in liquid biopsies. *Int. J. Mol. Sci.* 17 (5), 627. doi:10.3390/ijms17050627

Lawrie, C. H., Gal, S., Dunlop, H. M., Pushkaran, B., Liggins, A. P., Pulford, K., et al. (2008). Detection of elevated levels of tumour-associated microRNAs in serum of patients with diffuse large B-cell lymphoma. *Br. J. Haematol.* 141 (5), 672–675. doi:10.1111/j.1365-2141.2008.07077.x

Lin, R., Chen, L., Chen, G., Hu, C., Jiang, S., Sevilla, J., et al. (2014). Targeting miR-23a in CD8+ cytotoxic T lymphocytes prevents tumor-dependent immunosuppression. *J. Clin. investigation* 124 (12), 5352–5367. doi:10.1172/JCI76561

Lin, S., and Gregory, R. I. (2015). MicroRNA biogenesis pathways in cancer. *Nat. Rev. cancer* 15 (6), 321–333. doi:10.1038/nrc3932

Liu, C., Eng, C., Shen, J., Lu, Y., Takata, Y., Mehdizadeh, A., et al. (2016). Serum exosomal miR-4772-3p is a predictor of tumor recurrence in stage II and III colon cancer. *Oncotarget* 7 (46), 76250–76260. doi:10.18632/oncotarget.12841

Liu, W., Chen, S., and Liu, B. (2016). Diagnostic and prognostic values of serum exosomal microRNA-21 in children with hepatoblastoma: A Chinese population-based study. *Pediatr. Surg. Int.* 32 (11), 1059–1065. doi:10.1007/s00383-016-3960-8

Lobb, R. J., Becker, M., Wen, S. W., Wong, C. S. F., Wiegmans, A. P., Leimgruber, A., et al. (2015). Optimized exosome isolation protocol for cell culture supernatant and human plasma. *J. Extracell. vesicles* 4 (1), 27031. doi:10.3402/jev.v4.27031

Lodes, M. J., Caraballo, M., Suciu, D., Munro, S., Kumar, A., and Anderson, B. (2009). Detection of cancer with serum miRNAs on an oligonucleotide microarray. *PloS one* 4 (7), e6229. doi:10.1371/journal.pone.0006229

Lotvall, J., Hill, A. F., Hochberg, F., Buzas, E. I., Di Vizio, D., Gardiner, C., et al. (2014). Minimal experimental requirements for definition of extracellular vesicles and their functions: A position statement from the international society for extracellular vesicles. *J. Extracell. Vesicles* 3 (26913), 26913. doi:10.3402/jev.v3.26913

Ma, J., Xu, M., Yin, M., Hong, J., Chen, H., Gao, Y., et al. (2019). Exosomal hsa-miR199a-3p promotes proliferation and migration in neuroblastoma. *Front. Oncol.* 9, 459. doi:10.3389/fonc.2019.00459

Maacha, S., Bhat, A. A., Jimenez, L., Raza, A., Haris, M., Uddin, S., et al. (2019). Extracellular vesicles-mediated intercellular communication: Roles in the tumor microenvironment and anti-cancer drug resistance. *Mol. cancer* 18 (1), 55. doi:10.1186/s12943-019-0965-7

Machová Poláková, K., Lopotova, T., Klamova, H., Burda, P., Trněny, M., Stopka, T., et al. (2011). Expression patterns of microRNAs associated with CML phases and their disease related targets. *Mol. cancer* 10 (1), 41–13. doi:10.1186/1476-4598-10-41

Mateescu, B., Kowal, E. J. K., van Balkom, B. W. M., Bartel, S., Bhattacharyya, S. N., Buzas, E. I., et al. (2017). Obstacles and opportunities in the functional analysis of extracellular vesicle RNA–an ISEV position paper. *J. Extracell. vesicles* 6 (1), 1286095. doi:10.1080/20013078.2017.1286095

Matsumura, T., Sugimachi, K., Iinuma, H., Takahashi, Y., Kurashige, J., Sawada, G., et al. (2015). Exosomal microRNA in serum is a novel biomarker of recurrence in human colorectal cancer. *Br. J. cancer* 113 (2), 275–281. doi:10.1038/bjc.2015.201

Meldolesi, J. (2018). Exosomes and ectosomes in intercellular communication. *Curr. Biol.* 28 (8), R435–R444. doi:10.1016/j.cub.2018.01.059

Mi, S., Lu, J., Sun, M., Li, Z., Zhang, H., Neilly, M. B., et al. (2007). MicroRNA expression signatures accurately discriminate acute lymphoblastic leukemia from acute myeloid leukemia. *Proc. Natl. Acad. Sci.* 104 (50), 19971–19976. doi:10.1073/pnas.0709313104

Mikamori, M., Yamada, D., Eguchi, H., Hasegawa, S., Kishimoto, T., Tomimaru, Y., et al. (2017). MicroRNA-155 controls exosome synthesis and promotes gemcitabine resistance in pancreatic ductal adenocarcinoma. *Sci. Rep.* 7, 42339. doi:10.1038/srep42339

Nakajima, G., Hayashi, K., Xi, Y., Kudo, K., Uchida, K., Takasaki, K., et al. (2006). Non-coding microRNAs hsa-let-7g and hsa-miR-181b are associated with chemoresponse to S-1 in colon cancer. *Cancer genomics & proteomics* 3 (5), 317–324.

Ng, E. K., Chong, W. W. S., Jin, H., Lam, E. K. Y., Shin, V. Y., Yu, J., et al. (2009). Differential expression of microRNAs in plasma of patients with colorectal cancer: A potential marker for colorectal cancer screening. *Gut* 58 (10), 1375–1381. doi:10.1136/gut.2008.167817

Nie, C., Ren, W. H., Ma, Y., Xi, J. S., and Han, B. (2015). Circulating miR-125b as a biomarker of Ewing's sarcoma in Chinese children. *Genet. Mol. Res.* 14, 1904919049–1904919056. doi:10.4238/2015.December.29.12

Pan, B.-T., Teng, K., Wu, C., Adam, M., and Johnstone, R. M. (1985). Electron microscopic evidence for externalization of the transferrin receptor in vesicular form in sheep reticulocytes. *J. Cell Biol.* 101 (3), 942–948. doi:10.1083/jcb.101.3.942

Paolini, A., Baldassarre, A., Bruno, S. P., Felli, C., Muzi, C., Ahmadi Badi, S., et al. (2022). Improving the diagnostic potential of extracellular miRNAs coupled to multiomics data by exploiting the power of artificial intelligence. *Front. Microbiol.* 13, 888414. doi:10.3389/fmicb.2022.888414

Park, N. J., Zhou, H., Elashoff, D., Henson, B. S., Kastratovic, D. A., Abemayor, E., et al. (2009). Salivary microRNA: Discovery, characterization, and clinical utility for oral cancer detection. *Clin. Cancer Res.* 15 (17), 5473–5477. doi:10.1158/1078-0432.CCR-09-0736

Postow, M. A., Callahan, M. K., and Wolchok, J. D. (2015). Immune checkpoint blockade in cancer therapy. *J. Clin. Oncol.* 33 (17), 1974–1982. doi:10.1200/JCO.2014.59.4358

Rabinowits, G., Gercel-Taylor, C., Day, J. M., Taylor, D. D., and Kloecker, G. H. (2009). Exosomal microRNA: A diagnostic marker for lung cancer. *Clin. lung cancer* 10 (1), 42–46. doi:10.3816/CLC.2009.n.006

Radisavljevic, Z. (2013). AKT as locus of cancer multidrug resistance and fragility. *J. Cell. physiology* 228 (4), 671–674. doi:10.1002/jcp.24176

Rahimi, Z., Ghorbani, Z., Motamed, H., and Jalilian, N. (2021). Aberrant expression profile of miR-32, miR-98 and miR-374 in chronic lymphocytic leukemia. *Leukemia Res.* 111, 106691. doi:10.1016/j.leukres.2021.106691

Ramirez, M. I., Amorim, M. G., Gadelha, C., Milic, I., Welsh, J. A., Freitas, V. M., et al. (2018). Technical challenges of working with extracellular vesicles. *Nanoscale* 10 (3), 881–906. doi:10.1039/c7nr08360b

Ranganathan, S., Lopez-Terrada, D., and Alaggio, R. (2020). Hepatoblastoma and pediatric hepatocellular carcinoma: An update. *Pediatr. Dev. Pathology* 23 (2), 79–95. doi:10.1177/1093526619875228

Resnick, K. E., Alder, H., Hagan, J. P., Richardson, D. L., Croce, C. M., and Cohn, D. E. (2009). The detection of differentially expressed microRNAs from the serum of ovarian cancer patients using a novel real-time PCR platform. *Gynecol. Oncol.* 112 (1), 55–59. doi:10.1016/j.ygyno.2008.08.036

Robert, C., Long, G. V., Brady, B., Dutriaux, C., Maio, M., Mortier, L., et al. (2015). Nivolumab in previously untreated melanoma without BRAF mutation. *N. Engl. J. Med.* 372 (4), 320–330. doi:10.1056/NEJMoa1412082

Robert, C., Schachter, J., Long, G. V., Arance, A., Grob, J. J., Mortier, L., et al. (2015). Pembrolizumab versus ipilimumab in advanced melanoma. *N. Engl. J. Med.* 372 (26), 2521–2532. doi:10.1056/NEJMoa1503093

Said, F., Tantawy, M., Sayed, A., and Ahmed, S. (2022). Clinical significance of MicroRNA-29a and MicroRNA-100 gene expression in pediatric acute myeloid leukemia. *J. Pediatr. Hematology/Oncology* 44 (2), e391–e395. doi:10.1097/MPH.0000000000002168

Sakurai, N., Komada, Y., Hanaki, R., Morimoto, M., Ito, T., Nakato, D., et al. (2019). Role of microRNAs in glucocorticoid-resistant B-cell precursor acute lymphoblastic leukemia. *Oncol. Rep.* 42 (2), 708–716. doi:10.3892/or.2019.7191

Samsonov, R., Shtam, T., Burdakov, V., Glotov, A., Tsyrlina, E., Berstein, L., et al. (2016). Lectin-induced agglutination method of urinary exosomes isolation followed by mi-RNA analysis: Application for prostate cancer diagnostic. *Prostate* 76 (1), 68–79. doi:10.1002/pros.23101

Sapre, N., Hong, M. K. H., Macintyre, G., Lewis, H., Kowalczyk, A., Costello, A. J., et al. (2014). Curated microRNAs in urine and blood fail to validate as predictive biomarkers for high-risk prostate cancer. *PLoS One* 9 (4), e91729. doi:10.1371/journal.pone.0091729

Scholl, V., Hassan, R., and Zalcberg, I. R. (2012). miRNA-451: A putative predictor marker of Imatinib therapy response in chronic myeloid leukemia. *Leukemia Res.* 36 (1), 119–121. doi:10.1016/j.leukres.2011.08.023

Schork, N. J. (2019). "Artificial intelligence and personalized medicine," in *Precision medicine in cancer therapy* (Springer), 265–283.

Schotte, D., De Menezes, R. X., Akbari Moqadam, F., Khankahdani, L. M., Lange-Turenhout, E., Chen, C., et al. (2011). MicroRNA characterize genetic diversity and drug resistance in pediatric acute lymphoblastic leukemia. *haematologica* 96 (5), 703–711. doi:10.3324/haematol.2010.026138

Selth, L., Townley, S. L., Bert, A. G., Stricker, P. D., Sutherland, P. D., Horvath, L. G., et al. (2013). Circulating microRNAs predict biochemical recurrence in prostate cancer patients. *Br. J. cancer* 109 (3), 641–650. doi:10.1038/bjc.2013.369

Shi, R., Wang, P. Y., Li, X. Y., Chen, J. X., Li, Y., Zhang, X. Z., et al. (2015). Exosomal levels of miRNA-21 from cerebrospinal fluids associated with poor prognosis and tumor recurrence of glioma patients. *Oncotarget* 6 (29), 26971–26981. doi:10.18632/oncotarget.4699

Shyamala, K., Girish, H., and Murgod, S. (2014). Risk of tumor cell seeding through biopsy and aspiration cytology. *J. Int. Soc. Prev. Community Dent.* 4 (1), 5–11. doi:10.4103/2231-0762.129446

Song, B., Wang, Y., Titmus, M. A., Botchkina, G., Formentini, A., Kornmann, M., et al. (2010). Molecular mechanism of chemoresistance by miR-215 in osteosarcoma and colon cancer cells. *Mol. cancer* 9 (1), 96. doi:10.1186/1476-4598-9-96

Song, B., Wang, Y., Xi, Y., Kudo, K., Bruheim, S., Botchkina, G. I., et al. (2009). Mechanism of chemoresistance mediated by miR-140 in human osteosarcoma and colon cancer cells. *Oncogene* 28 (46), 4065–4074. doi:10.1038/onc.2009.274

Sugimachi, K., Matsumura, T., Hirata, H., Uchi, R., Ueda, M., Ueo, H., et al. (2015). Identification of a bona fide microRNA biomarker in serum exosomes that predicts hepatocellular carcinoma recurrence after liver transplantation. *Br. J. cancer* 112 (3), 532–538. doi:10.1038/bjc.2014.621

Sumazin, P., Yang, X., Chiu, H. S., Chung, W. J., Iyer, A., Llobet-Navas, D., et al. (2011). An extensive microRNA-mediated network of RNA-RNA interactions regulates established oncogenic pathways in glioblastoma. *Cell* 147 (2), 370–381. doi:10.1016/j.cell.2011.09.041

Sun, C., Li, N., Yang, Z., Zhou, B., He, Y., Weng, D., et al. (2013). miR-9 regulation of BRCA1 and ovarian cancer sensitivity to cisplatin and PARP inhibition. *J. Natl. Cancer Inst.* 105 (22), 1750–1758. doi:10.1093/jnci/djt302

Sun, H.-L., Cui, R., Zhou, J., Teng, K. Y., Hsiao, Y. H., Nakanishi, K., et al. (2016). ERK activation globally downregulates miRNAs through phosphorylating exportin-5. *Cancer Cell* 30 (5), 723–736. doi:10.1016/j.ccell.2016.10.001

Tanaka, M., Oikawa, K., Takanashi, M., Kudo, M., Ohyashiki, J., Ohyashiki, K., et al. (2009). Down-regulation of miR-92 in human plasma is a novel marker for acute leukemia patients. *PloS one* 4 (5), e5532. doi:10.1371/journal.pone.0005532

Tanaka, Y., Kamohara, H., Kinoshita, K., Kurashige, J., Ishimoto, T., Iwatsuki, M., et al. (2013). Clinical impact of serum exosomal microRNA-21 as a clinical biomarker in human esophageal squamous cell carcinoma. *Cancer* 119 (6), 1159–1167. doi:10.1002/cncr.27895

Taylor, D. D., and Gercel-Taylor, C. (2008). MicroRNA signatures of tumor-derived exosomes as diagnostic biomarkers of ovarian cancer. *Gynecol. Oncol.* 110 (1), 13–21. doi:10.1016/j.ygyno.2008.04.033

Teft, W. A., Kirchhof, M. G., and Madrenas, J. (2006). A molecular perspective of CTLA-4 function. *Annu. Rev. Immunol.* 24, 65–97. doi:10.1146/annurev.immunol.24.021605.090535

Théry, C., Amigorena, S., Raposo, G., and Clayton, A. (2006). Isolation and characterization of exosomes from cell culture supernatants and biological fluids. *Curr. Protoc. Cell Biol.* 30 (1), Unit 3.22–3.22. 29. doi:10.1002/0471143030.cb0322s30

Théry, C. (2011). Exosomes: Secreted vesicles and intercellular communications. *F1000 Biol. Rep.* 3, 15. doi:10.3410/B3-15

Théry, C., Zitvogel, L., and Amigorena, S. (2002). Exosomes: Composition, biogenesis and function. *Nat. Rev. Immunol.* 2 (8), 569–579. doi:10.1038/nri855

Tsujiura, M., Ichikawa, D., Komatsu, S., Shiozaki, A., Takeshita, H., Kosuga, T., et al. (2010). Circulating microRNAs in plasma of patients with gastric cancers. *Br. J. cancer* 102 (7), 1174–1179. doi:10.1038/sj.bjc.6605608

Ujifuku, K., Mitsutake, N., Takakura, S., Matsuse, M., Saenko, V., Suzuki, K., et al. (2010). MiR-195, miR-455-3p and miR-10a* are implicated in acquired temozolomide resistance in glioblastoma multiforme cells. *Cancer Lett.* 296 (2), 241–248. doi:10.1016/j.canlet.2010.04.013

Valadi, H., Ekstrom, K., Bossios, A., Sjostrand, M., Lee, J. J., and Lotvall, J. O. (2007). Exosome-mediated transfer of mRNAs and microRNAs is a novel mechanism of genetic exchange between cells. *Nat. Cell Biol.* 9 (6), 654–659. doi:10.1038/ncb1596

Van der Pol, E., Coumans, F. A. W., Grootemaat, A. E., Gardiner, C., Sargent, I. L., Harrison, P., et al. (2014). Particle size distribution of exosomes and microvesicles determined by transmission electron microscopy, flow cytometry, nanoparticle tracking analysis, and resistive pulse sensing. *J. Thrombosis Haemostasis* 12 (7), 1182–1192. doi:10.1111/jth.12602

Van Deun, J., Mestdagh, P., Agostinis, P., Akay, O., Anand, S., et al. (2017). EV-TRACK: Transparent reporting and centralizing knowledge in extracellular vesicle research. *Nat. methods* 14 (3), 228–232. doi:10.1038/nmeth.4185

Van Hoecke, L., and Roose, K. (2019). How mRNA therapeutics are entering the monoclonal antibody field. *J. Transl. Med.* 17 (1), 54. doi:10.1186/s12967-019-1804-8

Van Roosbroeck, K., Fanini, F., Setoyama, T., Ivan, C., Rodriguez-Aguayo, C., Fuentes-Mattei, E., et al. (2017). Combining anti-miR-155 with chemotherapy for the treatment of lung cancers. *Clin. Cancer Res.* 23 (11), 2891–2904. doi:10.1158/1078-0432.CCR-16-1025

Verma, M. (2012). Personalized medicine and cancer. *J. personalized Med.* 2 (1), 1–14. doi:10.3390/jpm2010001

Wan, Y.-W., Mach, C. M., Allen, G. I., Anderson, M. L., and Liu, Z. (2014). On the reproducibility of TCGA ovarian cancer microRNA profiles. *PloS one* 9 (1), e87782. doi:10.1371/journal.pone.0087782

Wang, J., Chen, J., Chang, P., LeBlanc, A., Li, D., Abbruzzesse, J. L., et al. (2009). MicroRNAs in plasma of pancreatic ductal adenocarcinoma patients as novel blood-based biomarkers of disease. *Cancer Prev. Res.* 2 (9), 807–813. doi:10.1158/1940-6207.CAPR-09-0094

Wang, X., Li, J., Dong, K., Lin, F., Long, M., Ouyang, Y., et al. (2015). Tumor suppressor miR-34a targets PD-L1 and functions as a potential immunotherapeutic target in acute myeloid leukemia. *Cell. Signal.* 27 (3), 443–452. doi:10.1016/j.cellsig.2014.12.003

Wei, J., Nduom, E. K., Kong, L. Y., Hashimoto, Y., Xu, S., Gabrusiewicz, K., et al. (2016). MiR-138 exerts anti-glioma efficacy by targeting immune checkpoints. *Neuro-oncology* 18 (5), 639–648. doi:10.1093/neuonc/nov292

Weiss, G., Bemis, L. T., Nakajima, E., Sugita, M., Birks, D. K., Robinson, W. A., et al. (2008). EGFR regulation by microRNA in lung cancer: Correlation with clinical response and survival to gefitinib and EGFR expression in cell lines. *Ann. Oncol.* 19 (6), 1053–1059. doi:10.1093/annonc/mdn006

Wong, T.-S., Liu, X. B., Wong, B. Y. H., Ng, R. W. M., Yuen, A. P. W., and Wei, W. I. (2008). Mature miR-184 as potential oncogenic microRNA of squamous cell carcinoma of tongue. *Clin. Cancer Res.* 14 (9), 2588–2592. doi:10.1158/1078-0432.CCR-07-0666

Wu, F., Li, F., Lin, X., Xu, F., Cui, R. R., Zhong, J. Y., et al. (2019). Exosomes increased angiogenesis in papillary thyroid cancer microenvironment. *Endocrine-Related Cancer* 26 (5), 525–538. doi:10.1530/ERC-19-0008

Wu, H., Liu, C., Yang, Q., Xin, C., Du, J., Sun, F., et al. (2020). MIR145-3p promotes autophagy and enhances bortezomib sensitivity in multiple myeloma by targeting HDAC4. *Autophagy* 16 (4), 683–697. doi:10.1080/15548627.2019.1635380

Xiao, Y., Deng, T., Su, C., and Shang, Z. (2017). MicroRNA 217 inhibits cell proliferation and enhances chemosensitivity to doxorubicin in acute myeloid leukemia by targeting KRAS. *Oncol. Lett.* 13 (6), 4986–4994. doi:10.3892/ol.2017.6076

Xu, S., Tao, Z., Hai, B., Liang, H., Shi, Y., Wang, T., et al. (2016). miR-424 (322) reverses chemoresistance via T-cell immune response activation by blocking the PD-L1 immune checkpoint. *Nat. Commun.* 7 (1), 11406. doi:10.1038/ncomms11406

Yamamoto, Y., Kosaka, N., Tanaka, M., Koizumi, F., Kanai, Y., Mizutani, T., et al. (2009). MicroRNA-500 as a potential diagnostic marker for hepatocellular carcinoma. *Biomarkers* 14 (7), 529–538. doi:10.3109/13547500903150771

Yang, F., Li, Q. j., Gong, Z. b., Zhou, L., You, N., Wang, S., et al. (2014). MicroRNA-34a targets Bcl-2 and sensitizes human hepatocellular carcinoma cells to sorafenib treatment. *Technol. cancer Res. Treat.* 13 (1), 77–86. doi:10.7785/tcrt.2012.500364

Yang, J.-K., Tong, J., Jing, S. Y., Fan, B., Wang, F., et al. (2017). Exosomal miR-221 targets DNM3 to induce tumor progression and temozolomide resistance in glioma. *J. neuro-oncology* 131 (2), 255–265. doi:10.1007/s11060-016-2308-5

Yang, J., Liu, R., Deng, Y., Qian, J., Lu, Z., Wang, Y., et al. (2017). MiR-15a/16 deficiency enhances anti-tumor immunity of glioma-infiltrating CD8+ T cells through targeting mTOR. *Int. J. cancer* 141 (10), 2082–2092. doi:10.1002/ijc.30912

Yeh, C.-H., Moles, R., and Nicot, C. (2016). Clinical significance of microRNAs in chronic and acute human leukemia. *Mol. cancer* 15 (1), 37–16. doi:10.1186/s12943-016-0518-2

Yuan, R., Wang, G., Xu, Z., Zhao, H., Chen, H., Han, Y., et al. (2016). Up-regulated circulating miR-106a by DNA methylation promised a potential diagnostic and prognostic marker for gastric cancer. *Anti-Cancer Agents Med. Chem. Former. Curr. Med. Chemistry-Anti-Cancer Agents)* 16 (9), 1093–1100. doi:10.2174/1871520615666150716110657

Zahreddine, H., and Borden, K. (2013). Mechanisms and insights into drug resistance in cancer. *Front. Pharmacol.* 4, 28. doi:10.3389/fphar.2013.00028

Zampini, M., Bisio, V., Leszl, A., Putti, M. C., Menna, G., Rizzari, C., et al. (2017). A three-miRNA-based expression signature at diagnosis can predict occurrence of relapse in children with t (8; 21) RUNX1-RUNX1T1 acute myeloid leukaemia. *Br. J. Haematol.* 183 (2), 298–301. doi:10.1111/bjh.14950

Zhang, H., Kang, J., Liu, L., Chen, L., Ren, S., and Tao, Y. (2020). MicroRNA-143 sensitizes acute myeloid leukemia cells to cytarabine via targeting ATG7-and ATG2B-dependent autophagy. *Aging (Albany NY)* 12 (20), 20111–20126. doi:10.18632/aging.103614

Zhang, H., Luo, X. Q., Feng, D. D., Zhang, X. J., Wu, J., Zheng, Y. S., et al. (2011). Upregulation of microRNA-125b contributes to leukemogenesis and increases drug resistance in pediatric acute promyelocytic leukemia. *Mol. cancer* 10, 108–113. doi:10.1186/1476-4598-10-108

Zhang, H. L., Yang, L. F., Zhu, Y., Yao, X. D., Zhang, S. L., Dai, B., et al. (2011). Serum miRNA-21: Elevated levels in patients with metastatic hormone-refractory prostate cancer and potential predictive factor for the efficacy of docetaxel-based chemotherapy. *Prostate* 71 (3), 326–331. doi:10.1002/pros.21246

Zhang, M., Gao, D., Shi, Y., Wang, Y., Joshi, R., Yu, Q., et al. (2019). miR-149-3p reverses CD8+ T-cell exhaustion by reducing inhibitory receptors and promoting cytokine secretion in breast cancer cells. *Open Biol.* 9 (10), 190061. doi:10.1098/rsob.190061

Zhang, M., Shi, Y., Zhang, Y., Wang, Y., Alotaibi, F., Qiu, L., et al. (2020). miRNA-5119 regulates immune checkpoints in dendritic cells to enhance breast cancer immunotherapy. *Cancer Immunol. Immunother.* 69, 951–967. doi:10.1007/s00262-020-02507-w

Zhao, L., Yu, H., Yi, S., Peng, X., Xiao, Z., et al. (2016). The tumor suppressor miR-138-5p targets PD-L1 in colorectal cancer. *Oncotarget* 7 (29), 45370–45384. doi:10.18632/oncotarget.9659

Zheng, P., Chen, L., Yuan, X., Luo, Q., Liu, Y., Xie, G., et al. (2017). Exosomal transfer of tumor-associated macrophage-derived miR-21 confers cisplatin resistance in gastric cancer cells. *J. Exp. Clin. Cancer Res.* 36 (1), 53. doi:10.1186/s13046-017-0528-y

Zhu, D.-X., Zhu, W., Fang, C., Fan, L., Zou, Z. J., Wang, Y. H., et al. (2012). miR-181a/b significantly enhances drug sensitivity in chronic lymphocytic leukemia cells via targeting multiple anti-apoptosis genes. *Carcinogenesis* 33 (7), 1294–1301. doi:10.1093/carcin/bgs179

Zuo, Z., Calin, G. A., de Paula, H. M., Medeiros, L. J., Fernandez, M. H., Shimizu, M., et al. (2011). Circulating microRNAs let-7a and miR-16 predict progression-free survival and overall survival in patients with myelodysplastic syndrome. *Blood, J. Am. Soc. Hematol.* 118 (2), 413–415. doi:10.1182/blood-2011-01-330704

Frontiers in Genetics

Highlights genetic and genomic inquiry relating to all domains of life

The most cited genetics and heredity journal, which advances our understanding of genes from humans to plants and other model organisms. It highlights developments in the function and variability of the genome, and the use of genomic tools.

Discover the latest Research Topics

See more →

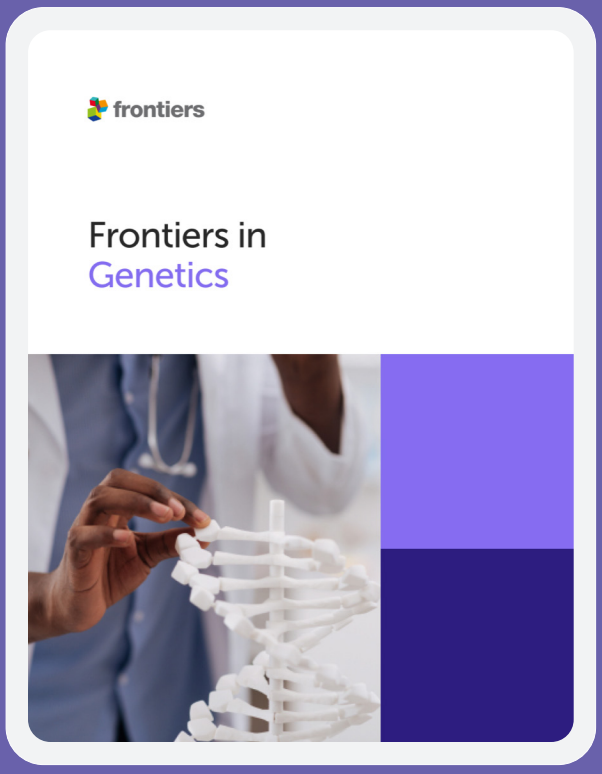

Frontiers

Avenue du Tribunal-Fédéral 34
1005 Lausanne, Switzerland
frontiersin.org

Contact us

+41 (0)21 510 17 00
frontiersin.org/about/contact